
Science
19 December 2008 | $10
Breakthrough of the Year
Reprogramming Cells
AAAS

Volume 322, Issue 5909

COVER

A metaphorical USB cable transmitting genetic information to "reprogram" cells symbolizes the Breakthrough of the Year for 2008. Advances in the burgeoning field of cellular reprogramming have brought scientists closer to the goal of using stem cells to better understand and someday treat disease. See the special section beginning on page 1766.

Image: Chris Bickel

DEPARTMENTS

EDITORIAL

SPECIAL SECTION

Breakthrough of the Year

WINNER

RUNNERS-UP

OTHER FEATURES

>> Editorial p. 1757; for related online content, see p. 1751 or go to www.sciencemag.org/btoy2008/

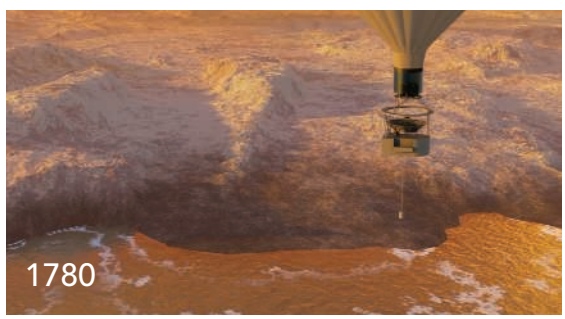

NEWS OF THE WEEK

NEWS FOCUS

CONTENTS continued >>

Published by AAAS

SCIENCE EXPRESS

www.sciencexpress.org

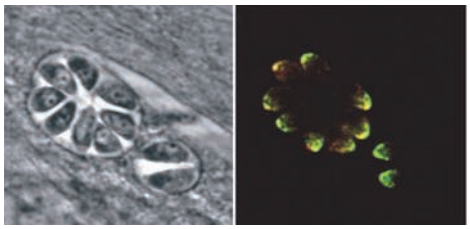

LETTERS

TECHNICAL COMMENT ABSTRACTS

BOOKS *ET AL.*

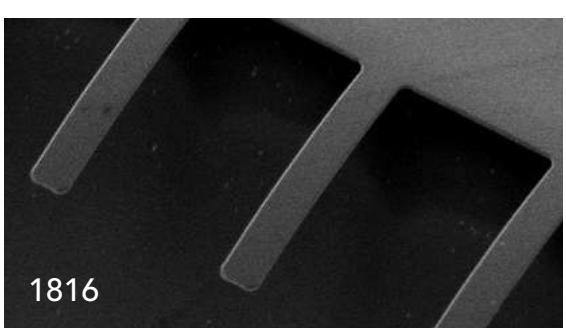

EDUCATION FORUM

POLICY FORUM

PERSPECTIVES

REVIEW

REPORTS

CONTENTS continued >>

REPORTS *CONTINUED...*

1835

AAAS
ADVANCING SCIENCE, SERVING SOCIETY

SCIENCE (ISSN 0036-8075) is published weekly on Friday, except the last week in December, by the American Association for the Advancement of Science, 1200 New York Avenue, NW, Washington, DC 20005. Periodicals Mail postage (publication No. 484460) paid at Washington, DC, and additional mailing offices.

Domestic individual membership and subscription (51 issues): $144 ($74 allocated to subscription). Domestic institutional subscription (51 issues): $770; Foreign postage extra: Mexico, Caribbean (surface mail) $55; other countries (air assist delivery) $85. First class, airmail, student, and emeritus rates on request. Canadian rates with GST available upon request, GST #1254 88122. Publications Mail Agreement Number 1069624. SCIENCE is printed on 30 percent post-consumer recycled paper. **Printed in the U.S.A.**

Change of address: Allow 4 weeks, giving old and new addresses and 8-digit account number. **Postmaster:** Send change of address to AAAS, P.O. Box 96178, Washington, DC 20090–6178. **Single-copy sales:** $10.00 current issue, $15.00 back issue prepaid includes surface postage; bulk rates on request. **Authorization to photocopy** material for internal or personal use under circumstances not falling within the fair use provisions of the Copyright Act is granted by AAAS to libraries and other users registered with the Copyright Clearance Center (CCC) Transactional Reporting Service, provided that $20.00 per article is paid directly to CCC, 222 Rosewood Drive, Danvers, MA 01923. *Science* is indexed in the *Reader's Guide to Periodical Literature* and in several specialized indexes.

Printed on 30% post-consumer recycled paper.

CONTENTS continued **>>**

SCIENCE**NOW**

www.sciencenow.org

HIGHLIGHTS FROM OUR DAILY NEWS COVERAGE

Is That You, Seabiscuit?
A horse can peg another's identity by whinny alone.

Ancient Battlefield Hints at Roman Persistence
2000-year-old site suggests Romans returned to area of massive defeat.

Revenge of the Nerds
Intelligence marks a man as a good match.

Science in translation.

SCIENCE **CAREERS**

www.sciencecareers.org/career_development

FREE CAREER RESOURCES FOR SCIENTISTS

Programs Aim to Train Translational Scientists
B. Vastag
New Ph.D. programs in translational medicine provide basic science training and clinical experience.

A Young Scientist at the Forefront of Cell Reprogramming
E. Pain
Curiosity, boldness, and single-mindedness won Austrian scientist Konrad Hochedlinger a place in cell reprogramming, *Science*'s Breakthrough of the Year for 2008.
>> Breakthrough of the Year section p. 1766 and www.sciencemag.org/btoy2008/

Tooling Up: The ABCs of Transitioning to Leadership
D. Jensen
"Activator," "behavior," and "consequence" are key concepts in this simple management theory.

From the Archives: Translational Research Careers
K. Travis
Translational researchers are pushing a fundamental change in the way science has operated for decades.

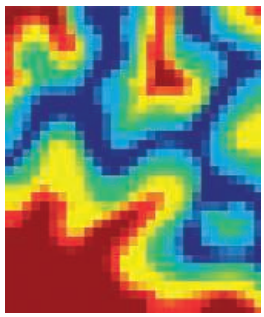

Visualizing gene expression dynamics.

SCIENCE **SIGNALING**

www.sciencesignaling.org

THE SIGNAL TRANSDUCTION KNOWLEDGE ENVIRONMENT

MEETING REPORT: Ontologies of Cellular Networks
R. Arp and B. Smith
A meeting of philosophers and biologists reveals the great diversity in ideas about how pathway information can be organized.

PODCAST
J. F. Foley and A. M. VanHook
Binding of CD3ε subunits to plasma membrane lipids blocks T cell receptor signaling.

NETWATCH: GEDI, the Gene Expression Dynamics Inspector
Convert microarray data into visual portraits to identify genes that share dynamic expression profiles; in Bioinformatics Resources.

NETWATCH: NIH VideoCasting and Podcasting
Watch live and archived NIH-sponsored events; in Web Broadcasts.

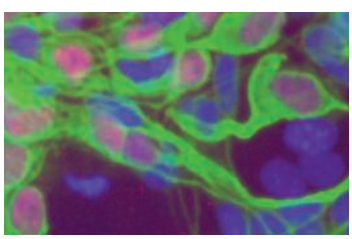

SCIENCE **ONLINE FEATURE**

VIDEO: 2008 Breakthrough of the Year
An introduction to some of the work that led studies in reprogramming cells to be tagged the top scientific story for 2008.
>> Breakthrough of the Year section p. 1766 and www.sciencemag.org/btoy2008/

SCIENCE**PODCAST**

www.sciencemag.org/multimedia/podcast

FREE WEEKLY SHOW

Download the 19 December *Science* Podcast to hear about the breakthroughs and breakdown of the year as well as areas to watch in 2009.

CREDITS: (*SCIENCE SIGNALING*) CHRIS BICKEL; (*SCIENCE CAREERS*) UNIVERSITY OF ROCHESTER MEDICAL CENTER

Separate individual or institutional subscriptions to these products may be required for full-text access.

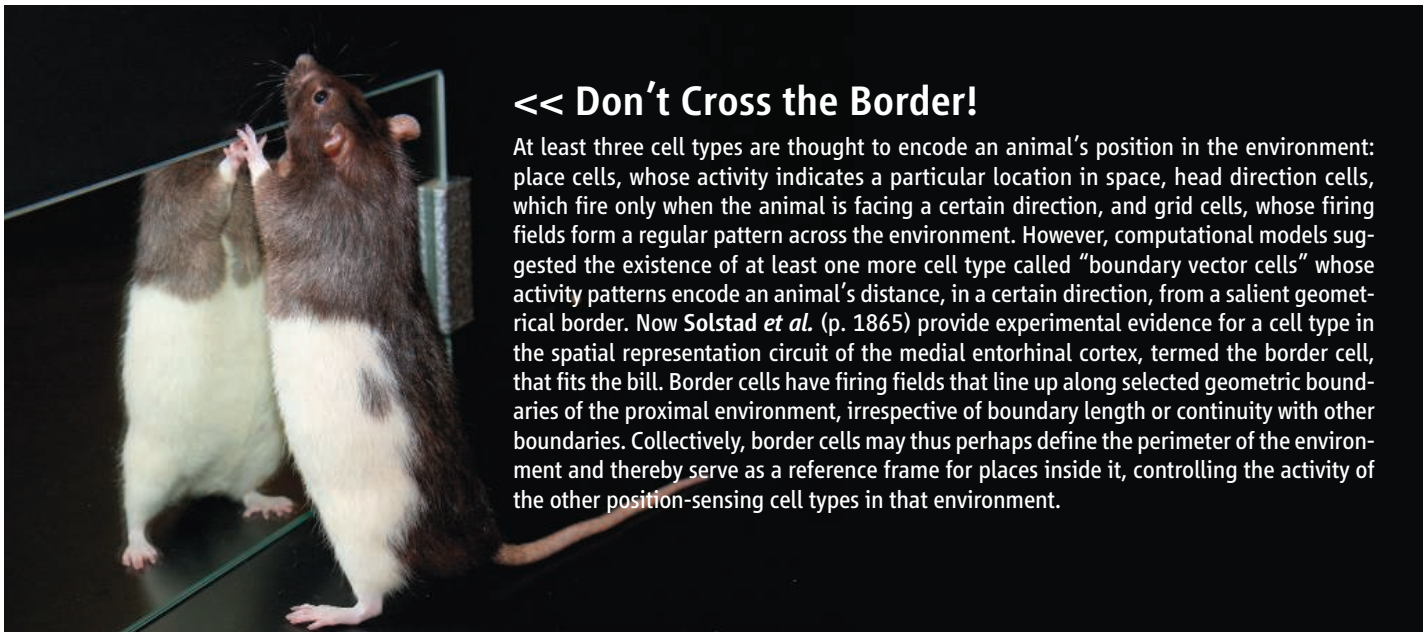

<< Don't Cross the Border!

At least three cell types are thought to encode an animal's position in the environment: place cells, whose activity indicates a particular location in space, head direction cells, which fire only when the animal is facing a certain direction, and grid cells, whose firing fields form a regular pattern across the environment. However, computational models suggested the existence of at least one more cell type called "boundary vector cells" whose activity patterns encode an animal's distance, in a certain direction, from a salient geometrical border. Now **Solstad *et al.*** (p. 1865) provide experimental evidence for a cell type in the spatial representation circuit of the medial entorhinal cortex, termed the border cell, that fits the bill. Border cells have firing fields that line up along selected geometric boundaries of the proximal environment, irrespective of boundary length or continuity with other boundaries. Collectively, border cells may thus perhaps define the perimeter of the environment and thereby serve as a reference frame for places inside it, controlling the activity of the other position-sensing cell types in that environment.

Cellular Reprogramming

After fertilization of the egg its daughter cells progress through embryonic, fetal, and adult stages, taking various pathways to specify the myriad differentiated cell types of an organism. Although these pathways are generally viewed as one-way and irreversible, recent studies report "reprogramming" methods by which a cell is converted to another cell type. **Gurdon and Melton** (p. 1811) review the history and lay out the current understanding of, and future prospects for, cellular reprogramming as seen in somatic cell nuclear transfer, cell fusion, the generation of induced pluripotent cells, and direct cellular reprogramming.

Glass in the Making

A challenge to identifying materials that will form glassy solids is to find properties in the melt state that would indicate that the material will not crystallize on cooling. **Li *et al.*** (p. 1816) describe a method to measure the density changes during crystallization in thin films for a range of copper-zirconium alloys and compare these findings with the maxima in the critical thickness for forming a glass via rapid quenching. A match between the peaks in density and glass-forming ability was observed. The finding of three sets of matching peaks conflicts with existing models on glass formation, which can only account for one set of matching peaks.

Pre-Crystal Clusters

It is very hard to study the earliest stages of crystallization, when nuclei form from the stable clustering of a sufficient number of atoms, molecules or ions. **Gebauer *et al.*** (p. 1819; see the Perspective by **Meldrum and Sear**) present data that imply that calcium carbonate forms stable neutral ion clusters prior to nucleation. These clusters form prior to the formation of an amorphous calcium carbonate phase, which had been thought of as the precursor material used by organisms to grow large, complex single crystals. These findings have implications not only for the understanding of the crystallization of calcium carbonate, but also for the better understanding of the mass transport of calcium carbonate in the formation of scales, biological deposits, and sediments.

Paternal Parenting

Paternal care of eggs and hatchlings is a common feature of birds. This breeding system has not been thought of as being of ancient origin in birds, but instead has been thought to be a derived feature. However, **Varricchio *et al.*** (p. 1826; see the Perspective by **Prum**) present data that support the hypothesis that this breeding system arose in theropod dinosaur ancestors of birds, before the origin of birds and flight. Fossil data on clutch sizes and bone histology show that several groups of Cretaceous dinosaurs share features in common with modern birds that use male-only care systems, suggesting that paternal care has a deep evolutionary history in the vertebrate phylum.

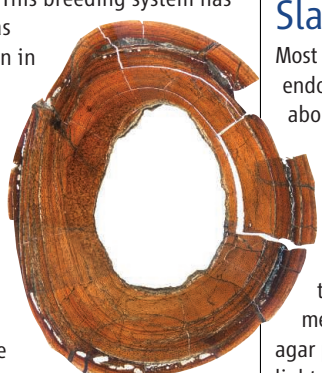

Martian Minerals

Most orbital and rover data has indicated that early Mars' was a fairly acidic environment; large areas of carbonate minerals have not been found in either the older or younger terrains. **Ehlmann *et al.*** (p. 1828) now report the detection of some carbonate minerals using a spectrometer on the Mars Reconnaissance Orbiter. The carbonate minerals are closely associated with abundant clay minerals in this area, implying that weathering of the crust here was by neutral or alkaline waters and that any later alterations by acidic weathering were insufficient to dissolve the carbonate minerals.

Slave to the Rhythm

Most organisms, from bacteria to humans, harbor endogenous clocks that cycle with a period of about 24 hours. These clocks function within individual cells and comprise regulatory feedback loops of transcriptional and post-translational processes. Plants are thought to use a circadian clock consisting of three light-sensitive, interlocked transcription-translation feedback loops. Because experiments have generally used plants grown on agar plates—where the roots are exposed to light—the fact that a different circadian clock operates in plant roots has been obscured. By growing plants hydroponically with the roots in darkness, **James *et al.*** (p. 1832) discovered that

Continued on page 1755

CREDITS (TOP TO BOTTOM): RAYMOND SKJERPENG/NOWEGIAN UNIVERSITY OF SCIENCE AND TECHNOLOGY; DAVID VARRICCHIO

Continued from page 1753

the root circadian clock is a stripped down version of the clock that operates in the shoots, operating on only one of the feedback loops and regulating only a small number of genes. In roots, two of the feedback loops are inactivated in that two clock components (CCA1 and LHY) do not regulate gene expression like they do in shoots. However, the shoot and root clocks are synchronized under normal day/night conditions, possibly by circulating metabolic signals, making the root clock essentially a "slave" to the shoot clock.

Leaf-Shape Control

Each plant leaf emerges from a single primordium, but the shape of the resulting leaves can range from a simple oval to a complex formation of subdivisions—leaflets, with edges that can be lobed or serrated. **Blein *et al.*** (p. 1835) looked at the molecular controls guiding leaf development. The NAM/CUC (NO APICAL MERISTEM/CUP-SHAPED COTYLEDON) genes, which function as transcription factors involved in establishing boundaries, were cloned from a variety of plants and their expression patterns manipulated. Across a wide range of different plants, localized expression of the NAM/CUC genes in leaflet primordia was required for the formation of subdivided leaves, and reductions in these boundary gene expression levels generated fewer and fused leaflets.

Forever Young?

Gamma-globin, a constituent of fetal hemoglobin, is normally expressed during fetal development. After birth, fetal hemoglobin expression is down-regulated when expression of the adult variant, β-globin, rises. Reliance of the adult on β-globin is not a problem, unless genetic defects disrupt the structure or function of β-globin, as is the case with some thalassemias and with sickle cell anemia. In such cases, the fetal variant, γ-globin, could potentially function as a replacement, except the γ-globin gene has usually been turned off by the process of globin gene switching. **Sankaran *et al.*** (p. 1839, published online 4 December; see the Perspective by **Michelson**) now show that the *BCL11A* gene, which encodes a putative transcription factor implicated in globin gene control, seems to function as a repressor of γ-globin gene expression. Use of small RNAs to knock down *BCL11A* expression in cultured erythroid cells resulted in increased γ-globin expression. Thus, *BCL11A* represents a target for interventions to treat sickle cell anemia and some thalassemias.

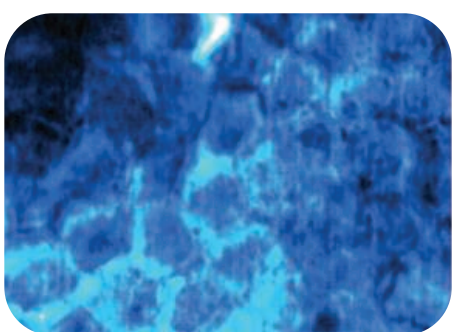

CREDIT: FREUDIGER *ET AL.*

Looking at Lipids

A method for label-free microscopy of fatty acids, drugs, and metabolites in live cells and tissues would be useful for a variety of biomedical, developmental, and cell biological studies. Characteristic Raman scattering frequencies provide signatures for various chemical bonds; however, imaging methods based on Raman scattering have been limited by low sensitivity and high nonresonant backgrounds. **Freudiger *et al.*** (p. 1857) now report a three-dimensional imaging technique based on stimulated Raman scattering that achieves background-free chemical contrast with relatively high sensitivity. They apply the method to image lipids in living cells and tissues, and to monitor drug delivery through the epidermis.

Unhealthy Competition

Hematopoietic progenitor cells (HPCs), the cells that ensure the body is supplied with healthy blood cells throughout life, reside within a specific bone marrow microenvironment, or "niche," that regulates their survival, growth, and differentiation. **Colmone *et al.*** (p. 1861) explored the impact of leukemia on normal HPC niches by applying real-time in vivo imaging methods to mouse leukemia models. Leukemic cells were found to create a malignant niche that out-competes normal niches in attracting HPCs. This competition leads both to a reduction in the number of HPCs and to disruption of HPC function, as evidenced by failure of the cells to mobilize into the circulation in response to cytokine stimulation. These effects were mediated in part by stem cell factor, a chemoattractant secreted by the leukemic cells. Thus, therapeutic inhibition of stem cell factor may be a valuable way to increase hematopoietic reserves in patients with leukemia.

Bruce Alberts is Editor-in-Chief of *Science*.

Celebrating a Year of *Science*

IN THIS FINAL ISSUE OF THE YEAR, *SCIENCE* CONTINUES A TRADITION BY PRESENTING OUR selections for the 10 major scientific breakthroughs of 2008. At the top of the list: the rapidly expanding field of cell reprogramming, which began with a seminal discovery in 2006 and this year reached the stage where much new knowledge of both fundamental and applied significance is being harvested. And the runner-up: the first direct observations of planets orbiting distant Sun-like stars.

A planet 100 light years away is about 10^{15} kilometers from Earth, and a cell spans only about 10^{-5} meter. Thus, our top two breakthroughs of the year represent a difference of 10^{23} in scale, a breathtaking illustration of the tremendous reach of science.

The breakthroughs described on p. 1766 reveal other important aspects of science. One is the powerful way that new technologies promote its advance. The scientists who achieved each of this year's breakthroughs exploited techniques and instrumentation that were unimaginable when I began my life as a scientist in the 1960s. To mention only a few: computational speeds and methods, detectors, telescopes, DNA sequencers, and recombinant DNA technologies. These new technologies are created from the knowledge of the natural world generated by previous scientific and technical advances. Therefore, the more we know, the more we can discover, and the pace of scientific discovery constantly accelerates.

The breakthroughs also illustrate that in science, the unknowns are unending. It seems that there will always be mysteries to challenge scientists, because each new finding raises a new set of unanswered questions about the universe. For example, some investigators have recently been able to reprogram adult human cells in culture to produce cells that carry the alterations known to cause a variety of diseases. Others have been able to transform one type of adult cell to another in a living animal. But the conversion frequencies are very low (usually only 1 cell in 10,000 can be reprogrammed). Thus, embedded in the reprogramming breakthrough are critical new questions: What are the factors that currently limit cell reprogramming, and how can they be overcome so that large numbers of cells can be induced to reprogram, rather than a tiny minority?

And there are always surprises. As scientists develop sensitive tests to probe the properties of the reprogrammed cells derived from induced pluripotent stem cells, they are finding subtle differences from the same types of cells created by a more natural and controversial route from embryonic stem cells. These discoveries add new questions to the unending list of those that remain to be solved.

This year there was no contest for the top breakdown: the frightening financial meltdown. In the past decade, more than half of the graduates of Yale, Princeton, and Harvard who did not go directly to professional schools chose a career in the finance industry or in management consulting. It seems likely that this distribution will now change. Many more of our most talented young people may decide to tackle the urgent problems in energy, environment, health, and education—perhaps a silver lining on a very dark cloud.

On the very bright side, our breakthroughs provide wonderful examples of the beauty of scientific understandings. The physicist Richard Feynman had a gift for explaining this elegance. As he said, "The world looks so different after learning science. For example, trees are made of air, primarily. When they are burned, they go back to air, and in the flaming heat is released the flaming heat of the sun which was bound in to convert the air into tree . . . These things are beautiful things, and the content of science is wonderfully full of them. They are very inspiring, and they can be used to inspire others."

As you read about the new understandings gained in 2008, be inspired—in fact, you might try to envision each of them as a special form of poetry.

– Bruce Alberts

10.1126/science.1169562

Published by AAAS

EDITED BY GILBERT CHIN AND JAKE YESTON

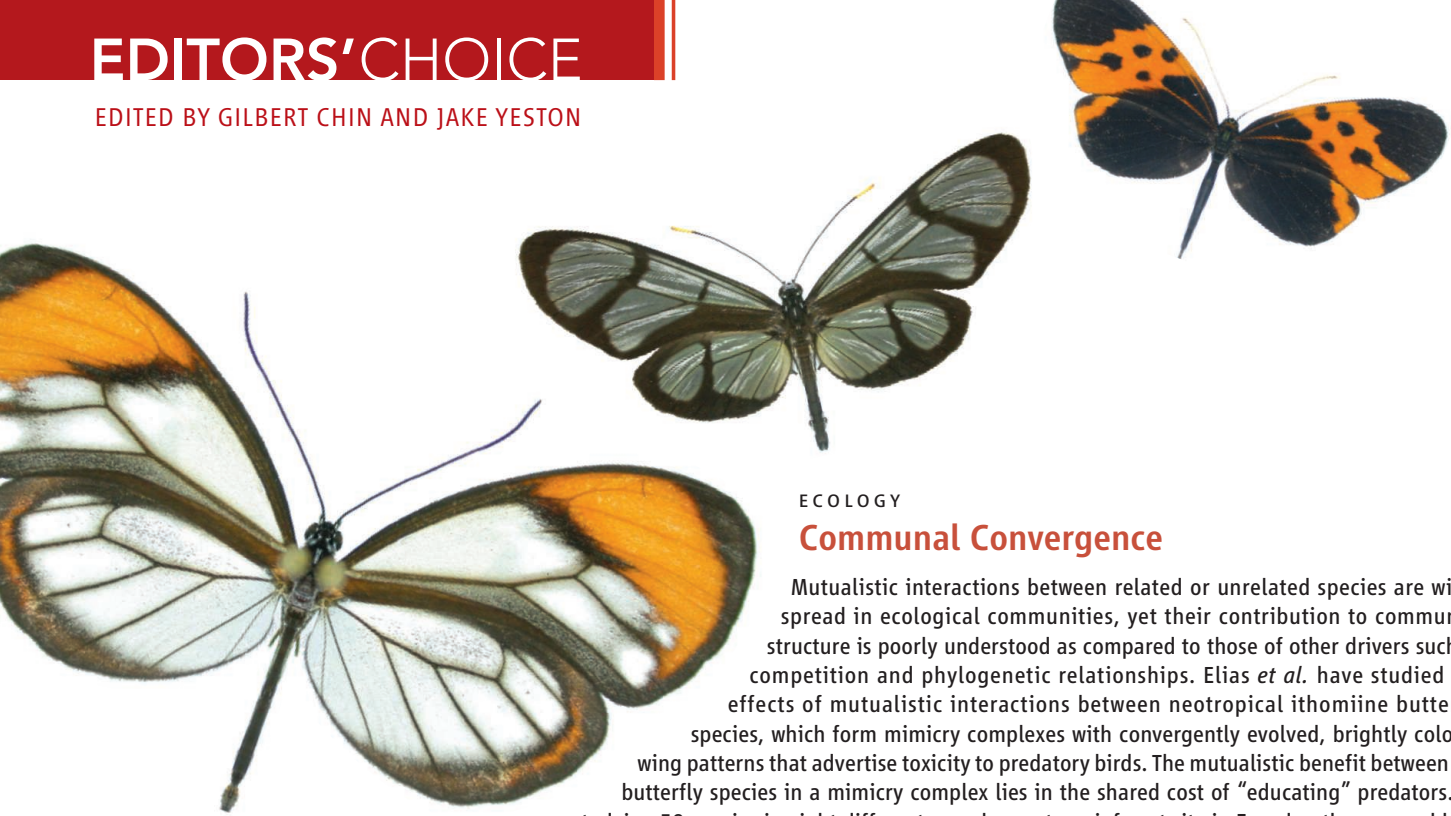

ECOLOGY

Communal Convergence

Mutualistic interactions between related or unrelated species are widespread in ecological communities, yet their contribution to community structure is poorly understood as compared to those of other drivers such as competition and phylogenetic relationships. Elias *et al.* have studied the effects of mutualistic interactions between neotropical ithomiine butterfly species, which form mimicry complexes with convergently evolved, brightly colored wing patterns that advertise toxicity to predatory birds. The mutualistic benefit between the butterfly species in a mimicry complex lies in the shared cost of "educating" predators. By studying 58 species in eight different complexes at a rainforest site in Ecuador, they were able to tease apart the relative effects of competition, phylogeny, and mutualism and showed that the adaptive benefits of mimicry drive increased ecological similarity between species—the opposite, in fact, from the effects of competition on community composition. — AMS

PLoS Biol. **6**, e300 (2008).

BIOMEDICINE

Deadly Exposure

In the Northern Hemisphere, winter is coming; so too are the seasonal episodes of cold and flu. With such a wide range of viruses causing a multitude of human and animal diseases, there remains a lucrative market for drugs that can target multiple classes of viruses and hence boost the current armory of antiviral therapies. The challenge is to develop therapies that are specific, yet avoid stimulating drug resistance.

When viruses hijack intracellular machinery in order to replicate, they alter the infected host cells, making them more visible to the immune system or to specific drugs. Phosphatidylserine is an abundant phospholipid that is actively maintained on the inner side of the plasma membrane, but under certain conditions the asymmetrical localization of this and other aminophospholipids is lost. Soares *et al.* reasoned that infected cells might also expose hidden lipids, which could be used as drug targets. Indeed, they found that four different viruses, including influenza A, induced infected cells to expose phosphatidylserine on their outer surfaces, which could then be recognized by the mouse/human chimeric antibody bavituximab. Animals that had been infected with lethal doses of Pichinde virus or cytomegalovirus were saved by bavituximab treatment, which caused cytotoxicity of virus-infected cells. — HP*

Nat. Med. **14**, 1357 (2008).

*Helen Pickersgill is a locum editor in *Science*'s editorial department.

PHYSIOLOGY

Cockroach Strategies

Household cockroaches, which in northern climes are most often *Periplaneta americana* or *Blattella germanica*, are much maligned as pests despite their fascinating neurobiology. They are also survivors par excellence—as anyone who has tried to swat one well knows, the cockroach skitters away in some unexpected direction and disappears out of sight. The choice of escape trajectory must be sufficiently variable so that a predator cannot learn to predict which way the prey will run. Yet the range of potential trajectories should also exclude, in a nonrandom manner, running toward the source of danger. Domenici *et al.* determined which bearing cockroaches chose by recording multiple escape trajectories of five *P. americana* individuals in response to a wind stimulus (perhaps somewhat similar to the bow wave of a rapidly approaching rolled-up newspaper). They found that the wily little insects first turned away, and then raced along one of four preferred trajectories, of approximately 90°, 120°, 150°, and 180° relative to the stimulus, and that these results were representative of the experimental cockroach colony (86 residents). Radial coordinate analysis of previously published escape data revealed similar, though not identical, preferred escape trajectories. Though these routes are not random and are limited in number, they clearly suffice for the cockroach to live another day. — GR

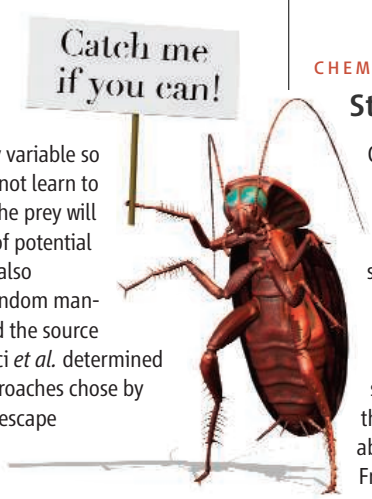

Curr. Biol. **18**, 1792 (2008).

CHEMISTRY

Straight-Ahead Synthesis

One regrettably common source of inefficiency in the synthesis of complex organic molecules is the need to apply successive oxidation-reduction cycles. In principle, a synthesis could proceed by preparing fragments of the molecule in more or less final form and then linking them together in the proper order. In practice, however, this strategy often leaves dangling groups in the wrong orientation or fails to provide reliable linkage sites at intermediate stages. Fragments incorporated into the partial

CREDITS (TOP TO BOTTOM): ELIAS *ET AL.*, *PLOS BIOL.* **6**, E300 (2008); JUPITER IMAGES

Published by AAAS

framework must then be modified, often through redox transformations, to facilitate further assembly, after which they must somehow be retransformed into their previous, proper state. Nicewicz *et al.* have skirted this dilemma in the assembly of the intricately oxygenated core of zaragozic acid C. Taking advantage of a silyl glyoxylate reagent that can self-couple by acting successively as an electrophile and nucleophile, the authors built up the core through several straightforward carbon-carbon bond-forming steps. They could then complete the overall construction of the molecule with minimal application of redox modifications, highlighting the potential of the approach for general synthetic efficiency. — JSY

J. Am. Chem. Soc. 10.1021/ja808347q (2008).

MICROBIOLOGY

Of Migrations and Variations

Once it was thought that *Mycobacterium tuberculosis* was genetically uniform. However, global surveys of clinical samples have shown that like other human-specific pathogens, it has a marked biogeography. Hershberg *et al.* have compared 90 genes in over 100 strains of the tuberculosis bacterium and established that the geographic variation has arisen as a consequence of human migrations over the millennia—first by land out of Africa 50,000 years ago and then by sea back to Africa over the past few centuries—and subsequent genetic drift rather than immune selection. In the apparent absence of purifying selection, many of the mutations are retained and result in nonsynonymous changes in amino acids, which are likely to have functional effects. It is not clear how *M. tuberculosis* tolerates the potentially deleterious consequences of genetic drift, but this cryptic variation needs to be taken into account in vaccine and drug design. — CA

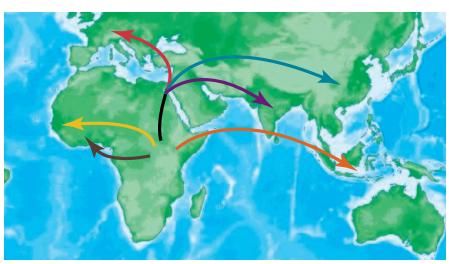

Phylogenetic dispersion to Europe (red), China (blue), and India (purple).

CREDIT: ADAPTED FROM HERSHBERG *ET AL.*, *PLOS BIOL.* 6, E311 (2008)

PLoS Biol. **6**, e311 (2008).

SIGNAL TRANSDUCTION

Suntanned to Death

Cells with DNA damage caused by ultraviolet radiation can become cancerous. Normally, cells damaged by excessive exposure to sunlight are eliminated when they undergo programmed cell death or apoptosis. The protein kinase Rho-associated kinase (ROCK) has been implicated in promoting apoptosis in various cell types. To explore how it might do so, Ongusaha *et al.* identified proteins that preferentially associated with ROCK in cultured human embryonic kidney cells that had been exposed to radiation. One such protein was c-Jun N-terminal kinase (JNK)–interacting protein 3 (JIP3), a scaffold protein that regulates the activity of JNK, a protein kinase that can promote apoptosis. ROCK phosphorylated JNK in vitro, and pharmacological inhibition of ROCK in cultured cells blocked the association of JIP3 with ROCK and also the phosphorylation of JIP3 in response to irradiation. Epidermal cells from $ROCK^{+/-}$ mice, which have about half the normal amount of ROCK, showed decreased phosphorylation of JNK and decreased apoptosis after exposure to ultraviolet radiation. Thus, the authors propose that signaling from ROCK to JNK through JIP3 may constitute an important part of the cell death pathway that gets rid of damaged skin cells and protects organisms from skin cancer. — LBR

Sci. Signal. **1**, ra14 (2008).

GEOLOGY

Volcanic Vetting

Two major extinctions, at the end of the Permian and end of the Cretaceous, appear to have been coincident with massive volcanic eruptions, of the Siberian and Deccan flood basalts respectively. Two studies provide tighter constraints on these associations, the duration of these events, and their potential climatic consequences. Reichow *et al.* provide new Ar-Ar dates on the main eruption of the Siberian flood basalts. The data imply that the eruptions occurred in less than 2 million years, and perhaps a few hundred thousand years, beginning shortly before the extinction (about 250 million years ago) and extending into it. Chenet *et al.* analyzed paleomagnetic data through individual flows in the upper part of the thick Deccan sequence. Their data show that many separate flows have the same paleomagnetic direction, implying that they erupted together in a time shorter than the inferred drift of the orientation of Earth's magnetic field. Four thick packages of flows may have each erupted in as little as a few decades, and the 1200-m section sampled, containing some soil layers, may have formed in less than 100,000 years. Such rates would have emitted copious amounts of sulfur dioxide. — BH

Earth Planet. Sci. Lett. 10.1016/j.epsl.2008.09.030 (2008); *J. Geophys. Res.* **113**, B04101 (2008).

www.sciencemag.org

Science

1200 New York Avenue, NW
Washington, DC 20005
Editorial: 202-326-6550, FAX 202-289-7562
News: 202-326-6581, FAX 202-371-9227
Bateman House, 82-88 Hills Road
Cambridge, UK CB2 1LQ
+44 (0) 1223 326500, FAX +44 (0) 1223 326501

Subscription Services For change of address, missing issues, new orders and renewals, and payment questions: 866-434-AAAS (2227) or 202-326-6417, FAX 202-842-1065. Mailing addresses: AAAS, P.O. Box 96178, Washington, DC 20090-6178 or AAAS Member Services, 1200 New York Avenue, NW, Washington, DC 20005

Institutional Site Licenses please call 202-326-6755 for any questions or information

Reprints: Author Inquiries 800-635-7181
Commercial Inquiries 803-359-4578

Permissions 202-326-7074, FAX 202-682-0816

Member Benefits AAAS/Barnes&Noble.com bookstore www.aaas.org/bn; AAAS Online Store www.apisource.com/aaas/ code MKB6; AAAS Travels: Betchart Expeditions 800-252-4910; Apple Store www.apple/eppstore/aaas; Bank of America MasterCard 1-800-833-6262 priority code FAA3YU; Cold Spring Harbor Laboratory Press Publications www.cshlpress.com/affiliates/aaas.htm; GEICO Auto Insurance www.geico.com/landingpage/go51.htm?logo=17624; Hertz 800-654-2200 CDP#343457; Office Depot https://bsd.officedepot.com/portalLogin.do; Seabury & Smith Life Insurance 800-424-9883; Subaru VIP Program 202-326-6417; VIP Moving Services www.vipmayflower.com/domestic/index.html; Other Benefits: AAAS Member Services 202-326-6417 or www.aaasmember.org.

science_editors@aaas.org	(for general editorial queries)
science_letters@aaas.org	(for queries about letters)
science_reviews@aaas.org	(for returning manuscript reviews)
science_bookrevs@aaas.org	(for book review queries)

Published by the American Association for the Advancement of Science (AAAS), *Science* serves its readers as a forum for the presentation and discussion of important issues related to the advancement of science, including the presentation of minority or conflicting points of view, rather than by publishing only material on which a consensus has been reached. Accordingly, all articles published in *Science*—including editorials, news and comment, and book reviews—are signed and reflect the individual views of the authors and not official points of view adopted by AAAS or the institutions with which the authors are affiliated.

AAAS was founded in 1848 and incorporated in 1874. Its mission is to advance science, engineering, and innovation throughout the world for the benefit of all people. The goals of the association are to: enhance communication among scientists, engineers, and the public; promote and defend the integrity of science and its use; strengthen support for the science and technology enterprise; provide a voice for science on societal issues; promote the responsible use of science in public policy; strengthen and diversify the science and technology workforce; foster education in science and technology for everyone; increase public engagement with science and technology; and advance international cooperation in science.

Information for Authors
See pages 634 and 635 of the 1 February 2008 issue or access www.sciencemag.org/about/authors

EDITOR-IN-CHIEF **Bruce Alberts**
EXECUTIVE EDITOR **Monica M. Bradford**
DEPUTY EDITORS **R. Brooks Hanson, Barbara R. Jasny, Katrina L. Kelner**
NEWS EDITOR **Colin Norman**

Editorial supervisory senior editor Phillip D. Szuromi; **senior editor/perspectives** Lisa D. Chong; **senior editors** Gilbert J. Chin, Pamela J. Hines, Paula A. Kiberstis (Boston), Marc S. Lavine (Toronto), Beverly A. Purnell, L. Bryan Ray, Guy Riddihough, H. Jesse Smith, Valda Vinson; **associate editors** Kristen L. Mueller, Jake S. Yeston, Laura M. Zahn; **online editor** Stewart Wills; **associate online editors** Robert Frederick, Tara S. Marathe; **web content developer** Martyn Green; **book review editor** Sherman J. Suter; **associate letters editor** Jennifer Sills; **editorial manager** Cara Tate; **senior copy editors** Jeffrey E. Cook, Cynthia Howe, Harry Jach, Barbara P. Ordway, Trista Wagoner; **copy editors** Chris Filiatreau, Lauren Kmec; **editorial coordinators** Carolyn Kyle, Beverly Shields; **publications assistants** Ramatoulaye Diop, Joi S. Granger, Jeffrey Hearn, Lisa Johnson, Scott Miller, Jerry Richardson, Jennifer A. Seibert, Brian White, Anita Wynn; **editorial assistants** Carlos L. Durham, Emily Guise, Patricia M. Moore; **executive assistant** Sylvia S. Kihara; **administrative support** Maryrose Madrid

News deputy news editors Robert Coontz, Eliot Marshall, Jeffrey Mervis, Leslie Roberts; **contributing editors** Elizabeth Culotta, Polly Shulman; **news writers** Yudhijit Bhattacharjee, Adrian Cho, Jennifer Couzin, David Grimm, Constance Holden, Jocelyn Kaiser, Richard A. Kerr, Eli Kintisch, Andrew Lawler (New England), Greg Miller, Elizabeth Pennisi, Robert F. Service (Pacific NW), Erik Stokstad; **intern** Rachel Zelkowitz; **contributing correspondents** Jon Cohen (San Diego, CA), Daniel Ferber, Ann Gibbons, Robert Koenig, Mitch Leslie, Charles C. Mann, Virginia Morell, Evelyn Strauss, Gary Taubes; **copy editors** Linda B. Felaco, Melvin Gatling, Melissa Raimondi; **administrative support** Scherraine Mack, Fannie Groom; **bureaus** New England: 207-549-7755, San Diego, CA: 760-942-3252, FAX 760-942-4979, Pacific Northwest: 503-963-1940

Production director James Landry; **senior manager** Wendy K. Shank; **assistant manager** Rebecca Doshi; **senior specialists** Steve Forrester, Chris Redwood; **specialist** Anthony Rosen; **Preflight director** David M. Tompkins; **manager** Marcus Spiegler

Art director Yael Kats; **associate art director** Laura Creveling; **illustrators** Chris Bickel, Katharine Sutliff; **senior art associates** Holly Bishop, Preston Huey, Nayomi Kevitiyagala; **art associate** Jessica Newfield; **photo editor** Leslie Blizard

***Science* International**

Europe (science@science-int.co.uk) **editorial: international managing editor** Andrew M. Sugden; **senior editor/perspectives** Julia Fahrenkamp-Uppenbrink; **senior editors** Caroline Ash, Stella M. Hurtley, Ian S. Osborne, Peter Stern; **associate editor** Maria Cruz; **editorial support** Deborah Dennison, Rachel Roberts, Alice Whaley; **administrative support** John Cannell, Janet Clements; **news: europe news editor** John Travis; **deputy news editor** Daniel Clery; **contributing correspondents** Michael Balter (Paris), John Bohannon (Vienna), Martin Enserink (Amsterdam and Paris), Gretchen Vogel (Berlin); **intern** Sara Coelho

Asia Japan Office: Asca Corporation, Eiko Ishioka, Fusako Tamura, 1-8-13, Hirano-cho, Chuo-ku, Osaka-shi, Osaka, 541-0046 Japan; +81 (0) 6 6202 6272, FAX +81 (0) 6 6202 6271; asca@os.gulf.or.jp; **asia news editor** Richard Stone (Beijing: rstone@aaas.org); **contributing correspondents** Dennis Normile (Japan: +81 (0) 3 3391 0630, FAX +81 (0) 3 5936 3531; dnormile@gol.com); Hao Xin (China: +86 (0) 10 6307 4439 or 6307 3676, FAX +86 (0) 10 6307 4358; cindyhao@gmail.com); Pallava Bagla (South Asia: +91 (0) 11 2271 2896; pbagla@vsnl.com)

EXECUTIVE PUBLISHER **Alan I. Leshner**
PUBLISHER **Beth Rosner**

Fulfillment Systems and Operations (membership@aaas.org); **director** Waylon Butler; **senior systems analyst** Jonny Blaker; **customer service supervisor** Pat Butler; **specialists** Latoya Casteel, LaVonda Crawford, Vicki Linton, April Marshall; **data entry supervisor** Cynthia Johnson; **specialists** Eintou Bowden, Tarrika Hill, William Jones

Business Operations and Administration director Deborah Rivera-Wienhold; **assistant director, business operations** Randy Yi; **manager, business analysis** Michael LoBue; **manager, business operations** Jessica Tierney; **financial analysts** Priti Pamnani, Celeste Troxler; **rights and permissions: administrator** Emilie David; **associate** Elizabeth Sandler; **marketing director** Ian King; **marketing manager** Allison Pritchard; **marketing associates** Aimee Aponte, Alison Chandler, Mary Ellen Crowley, Julianne Wielga, Wendy Wise; **international marketing manager** Wendy Sturley; **marketing executive** Jennifer Reeves; **marketing/member services executive** Linda Rusk; **director, site licensing** Tom Ryan; **director, corporate relations** Eileen Bernadette Moran; **publisher relations, eresources specialist** Kiki Forsythe; **senior publisher relations specialist** Catherine Holland; **publisher relations, east coast** Phillip Smith; **publisher relations, west coast** Philip Tsolakidis; **fulfillment supervisor** Iquo Edim; **fulfillment coordinator** Laura Clemens; **electronic media: manager** Lizabeth Harman; **project manager** Trista Snyder; **assistant manager** Lisa Stanford; **senior production specialists** Christopher Coleman, Walter Jones; **production specialists** Nichele Johnston, Kimberly Oster

Advertising director, worldwide ad sales Bill Moran

Product (science_advertising@aaas.org); **midwest/west coast/w. canada** Rick Bongiovanni: 330-405-7080, FAX 330-405-7081; **east coast/e. canada** Laurie Faraday: 508-747-9395, FAX 617-507-8189; **uk/europe/asia** Roger Goncalves: TEL/FAX +41 43 234 1358; **japan** Mashy Yoshikawa: +81 (0) 3 3235 5961, FAX +81 (0) 3 3235 5852; **senior traffic associate** Deiandra Simms

Commercial Editor Sean Sanders: 202-326-6430

Project Director, Outreach Brianna Blaser

Classified (advertise@sciencecareers.org); **inside sales manager: midwest/canada** Daryl Anderson: 202-326-6543; **inside sales representative** Karen Foote: 202-326-6740; **key account manager** Joribah Able; **northeast** Alexis Fleming: 202-326-6578; **southeast** Tina Burks: 202-326-6577; **west** Nicholas Hintibidze: 202-326-6533; **sales coordinators** Rohan Edmonson, Shirley Young; **international: sales manager** Tracy Holmes: +44 (0) 1223 326525, FAX +44 (0) 1223 326532; **sales** Susanne Kharraz, Dan Pennington, Alex Palmer; **sales assistant** Louise Moore; **japan** Mashy Yoshikawa: +81 (0) 3 3235 5961, FAX +81 (0) 3 3235 5852; **advertising production operations manager** Deborah Tompkins; **senior production specialist/graphic designer** Amy Hardcastle; **senior production specialist** Robert Buck; **senior traffic associate** Christine Hall; **publications assistant** Mary Lagnaoui

AAAS Board of Directors retiring president, chair David Baltimore; **president** James J. McCarthy; **president-elect** Peter C. Agre; **treasurer** David E. Shaw; **chief executive officer** Alan I. Leshner; **board** Lynn W. Enquist, Susan M. Fitzpatrick, Alice Gast, Linda P. B. Katehi, Nancy Knowlton, Cherry A. Murray, Thomas D. Pollard, Thomas A. Woolsey

AAAS
ADVANCING SCIENCE, SERVING SOCIETY

Sex and the Beaked Whale

The 14 species of rare beaked whales (genus *Mesoplodon*) sport a wild variety of tusks—some jutting straight up, others curving like scimitar blades from the males' jaws. Scientists have long puzzled over the remarkable diversity. Now an analysis of the whales' DNA suggests that it's all about sex.

When conservation geneticist C. Scott Baker of Oregon State University, Newport, and colleagues drew up the first molecular phylogenetic tree for *Mesoplodon*, they were surprised to find that species with similarly shaped tusks are not closely related, as had been thought. Nor do closely related species have similar tusks. The pattern is typical of diversification driven by sexual selection, they report in this month's *Systematic Biology*.

Until now, the only mammals known to have undergone speciation as a result of sexual selection were ungulates with horns and hooves. Just as stags use their horns to fight for females, male beaked whales rake each other with their tusks, says lead author Merel Dalebout, an evolutionary biologist at the University of New South Wales, Kensington, in Australia. "Certain tusks may be shaped better for hitting harder or for sneaky attacks. … Those males win the fights and the females, and then their tusk shape spreads through the population."

CREDITS (TOP TO BOTTOM): NAN HAUSER, CENTER FOR CETACEAN RESEARCH AND CONSERVATION; MICHAEL TARR; MAX PLANCK SOCIETY

Red Fellas, Green Gals

Men are colored like Mars, but women are greenish—and the difference may help explain how people perceive *la difference*, researchers at Brown University say.

Cognitive scientist Michael Tarr and grad student Adrian Nestor made the discovery by averaging mug shots of 200 white males and females into a single androgynous face. They then obscured it further with randomly placed red and green pixels.

Three volunteers looked at 20,000 different versions of the image—some redder, others greener—and told the researchers which sex they thought each face represented. The result: Faces with green pixels were tagged as female and those with more red pixels as male. The color of the cheekbones, nose, and sides of the mouth were particularly important to decisions, says Tarr, whose paper is in press in *Psychological Science*.

Marlene Behrmann, a psychologist at Carnegie Mellon University in Pittsburgh, Pennsylvania, says the fact that people subconsciously recognize the red-green distinction "means there is something evolutionarily and ecologically important about color that extends even into the human central nervous system."

Max Planck Turns Blue

It seemed like a good idea at the time. For a special issue on China, *MaxPlanckForschung*—the quarterly magazine of Germany's Max Planck Society—asked a designer to find a nice Chinese poem for the cover image. The text, drawn from a photo database, turned out to be anything but. It included turns of phrase such as: "*Beauties from the north who have a distinguished air of elegance and allure / Young housewives having figures that will turn you on. …* "

"You can find similar language on houses of prostitution all over Hong Kong," says Victor Mair, a professor of Chinese language and linguistics at the University of Pennsylvania who posted a translation on a linguistics blog.

Reactions in China ranged from amusement to outrage. The Max Planck Society immediately apologized, saying in a statement that "it has now emerged that the text contains deeper levels of meaning, which are not immediately accessible to a non-native speaker." Well, not exactly, says Mair. "It's impossible anyone who knows even 2 or 3 years of Chinese would be fooled," he says. "The language is veiled, but it's not that veiled." The journal is playing it safe now: The cover image online and in the forthcoming English edition will be graced with the title of a book by a 17th century Catholic priest.

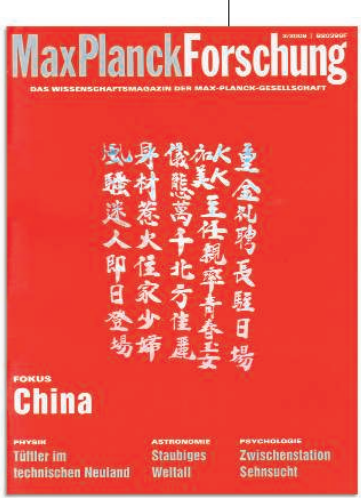

The Starling Has Landed

Whereas jokers wonder about chickens crossing the road, scientists ponder why starling flocks land. The answer is, apparently, because everyone in the flock wants to.

The speed, agility, and cohesion of starling flocks are both beautiful and puzzling. István Daruka of Eötvös University in Budapest designed a digital flock of 200 starlings to model the rapid shift from foraging flight to landing. The model, based on field observations, describes the starlings as independently moving points in space, each with a ranking of "landing intent" that can vary from zero (the bird doesn't want to land) to one (the bird definitely wants to land).

The results, published this month in the *Proceedings of the Royal Society B*, show that a single starling decides to land when the average landing intent of nearby birds—presumably signaled by body language—crosses a critical threshold. Mathematician Andrew Wood of the University of York in the U.K. says most models of complex biological systems do not consistently account for individual reactions to objects, in this case neighboring birds. "It is very welcome to see this work addressing this directly," he says.

Published by AAAS

Montagnier, Chermann, and Barré-Sinoussi in a 1984 photo.

FACE OFFS

NO THANKS. Robert Gallo isn't the only one who feels he was passed over for this year's Nobel Prize for discovering the AIDS virus (*Science*, 10 October, p. 174). Instead of accepting an invitation from his former colleagues Luc Montagnier and Françoise Barré-Sinoussi to accompany them to Stockholm to pick up their award, French virologist Jean-Claude Chermann hosted a lunch for journalists in Paris to explain why he should have shared in the glory.

Chermann, now the scientific director of a French biotech, was a lab leader at the Pasteur Institute and Barré-Sinoussi's boss when they isolated the virus in 1983; Montagnier headed the division. Chermann "taught Barré-Sinoussi everything she knew" and was instrumental in the discovery, says Bernard Le Grelle, a financial consultant who has set up a support committee for his slighted friend.

Some scientists agree. "I don't understand how you can give the prize to her but not to him," says Dutch virologist Jaap Goudsmit, who was in close contact with the Pasteur group at the time. French President Nicolas Sarkozy, who received Chermann at the Elysée Palace on 28 October, has also hailed him as a "co-discoverer." But as Le Grelle discovered during two teleconferences with Stockholm, the Nobel Committee never changes its mind.

MOVERS

A HUMBLE START. The Institute of Science and Technology (IST) Austria has named a computer scientist with global work experience as its first president. Thomas Henzinger of the École Polytechnique Fédérale de Lausanne (EPFL) in Switzerland will take the helm of the new graduate school on the outskirts of Vienna in September 2009.

Henzinger, 46, grew up in Austria but spent most of his career in the United States before joining EPFL in 2004. Henzinger says IST will start small, with about a dozen faculty appointments, "so we shouldn't have any illusions of immediate grandeur." But the ability to have "a biologist sitting next to a computer scientist next to a physicist" should encourage creative collaborations, he says.

The presidential search was initially a source of embarrassment for the school after its first announced choice, neuroscientist Tobias Bonhoeffer, decided not to accept the job, citing personal reasons (*Science*, 25 July, p. 471). Henzinger sees the job as an opportunity he couldn't pass up: "The institute is really starting from scratch. Such things happen once in a lifetime, if ever."

DEATHS

MEMORABLE. He was one of the most famous figures in neuroscience, yet few people knew his name. Henry Gustav Molaison, better known as the patient H.M., died 2 December in Windsor Locks, Connecticut, at age 82.

In 1953, Molaison had much of the medial temporal lobes of his brain removed to relieve severe epilepsy. The experimental procedure rendered him unable to form new memories but left older memories intact. As a cooperative subject for more than half a century, he helped researchers unravel the neural basis of memory, says neuroscientist Suzanne Corkin of the Massachusetts Institute of Technology in Cambridge, who began working with him in 1962 as a graduate student. One key insight was that different kinds of memory depend on different parts of the brain. "He was a very nice man, … soft-spoken, polite, and he had a good sense of humor," says Corkin, whose almost daily interactions with Molaison led him to believe they had met in high school.

H.M.'s contributions to science won't end with his death. Researchers led by Jacopo Annese of the University of California, San Diego, have already begun work to preserve his donated brain and create an interactive 3D reconstruction. Annese hopes it will be available online by next summer.

Got a tip for this page? E-mail people@aaas.org

Rising Stars >>

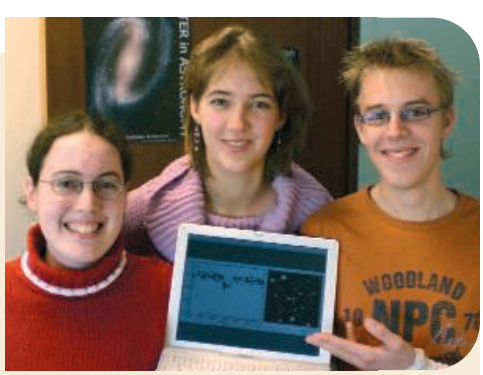

BEGINNER'S LUCK. An undergraduate astronomy project over spring break at Leiden University in the Netherlands has produced otherworldly results for Francis Vuijsje, Meta de Hoon, and Remco van der Burg (left to right in photo).

Their assignment was to develop a search algorithm to detect periodic dimmings in a database of stellar brightness measurements. But when they tested the algorithm by linking PCs in vacant faculty offices for enhanced computing power, they discovered what appeared to be an extrasolar planet.

Their work was confirmed later in the year by the European Very Large Telescope in Chile, which revealed the planet to be five times as massive as Jupiter and orbiting the hottest star ever found to have planets (arxiv.org/abs/0812.0599). "I never thought they would actually find something," says Ignas Snellen, the students' adviser.

The students have christened the planet ReMeFra after their first names, although its official designation is OGLE2-TR-L9b. It's unclear whether the students will pursue careers in the field of exoplanets. Says Vuijsje: "Astronomy has so many interesting topics."

CREDITS (TOP TO BOTTOM): AFP/GETTY IMAGES; SOURCE: FAMILY OF HENRY GUSTAV MOLAISON; LEIDEN UNIVERSITY

Breakthrough of the Year

Reprogramming Cells

By inserting genes that turn back a cell's developmental clock, researchers are gaining insights into disease and the biology of how a cell decides its fate

THIS YEAR, SCIENTISTS ACHIEVED A LONG-SOUGHT FEAT OF CELLULAR alchemy. They took skin cells from patients suffering from a variety of diseases and reprogrammed them into stem cells. The transformed cells grow and divide in the laboratory, giving researchers new tools to study the cellular processes that underlie the patients' diseases. The achievement could also be an important step on a long path to treating diseases with a patient's own cells.

The feat rests on a genetic trick, first developed in mice and described 2 years ago, in which scientists wipe out a cell's developmental "memory," causing it to return to its pristine embryonic state and then regrow into something else. In 2008, researchers achieved another milestone in cell reprogramming. In an elegant study in live mice, they prompted cells to make the leap directly from one mature cell into another—flouting the usual rule that development of cells is a one-way street. These and other advances in tweaking cells to assume new identities add up to make the now flourishing field of cellular reprogramming *Science*'s Breakthrough of the Year.

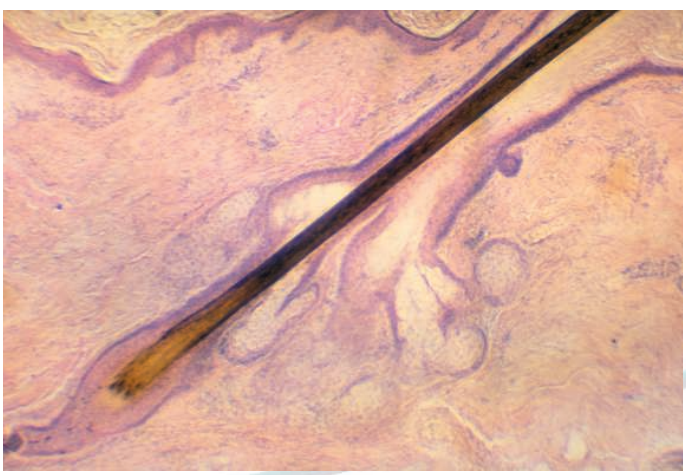

This year's breakthroughs have done much to wipe out memories of a major scandal that erupted 3 years ago, after scientists in South Korea fraudulently claimed to have used somatic cell nuclear transfer—the technique used to clone Dolly the sheep—to generate stem cells from patients suffering from type 1 diabetes, spinal cord injury, and a congenital immune disease. The debacle dealt the field a huge setback; patient-specific stem cells seemed like a distant prospect.

Breakthrough Online

For an expanded version of this section, with references, links, and multimedia, see www.sciencemag.org/btoy2008.

The new developments build on two previous breakthroughs. Ten years ago last month, scientists in Wisconsin announced that they had cultured human embryonic stem (hES) cells—cells with the potential to form any cell type in the body. That power, known as pluripotency, opened up a world of possibilities in developmental biology and medical research, but it came with baggage: Because isolating the cells typically destroys the embryo, the research sparked fierce debates over bioethics. In many countries, including the United States, political decisions limited the work scientists could do with hES cells.

In 2006, Japanese researchers reported that they had found a possible way around the practical and ethical questions surrounding hES cells. By introducing just four genes into mouse tail cells growing in a lab dish, they could produce cells that looked and acted very much like ES cells. They called these cells induced pluripotent stem (iPS) cells. Last year, in a development recognized as the first runner-up in *Science*'s 2007 Breakthrough of the Year issue, the same team and two others in the United States extended the reprogramming technique to human cells. That result opened the floodgates to new research.

Cells, made to order

For nearly a decade, stem cell biologists have sought a way to make long-lived cell lines from patients suffering from hard-to-study diseases. (Most adult cells do not survive culture conditions in the lab, so taking cells of interest directly from patients doesn't work.) This year, two groups achieved that goal. One team derived iPS cell lines from the skin cells of an 82-year-old woman suffering from amyotrophic lateral sclerosis (Lou Gehrig's disease), a degenerative disease that attacks the motor neurons, causing gradual paralysis. The scientists then directed the cells to form neurons and glia, the cells that are most affected by the disease (photos, p. 1767).

Just a week later, another group reported making patient-specific iPS cell lines for 10 different diseases (see table), among them muscular dystrophy, type 1 diabetes, and Down syndrome. Many of these diseases are difficult or impossible to study in animal models; the reprogrammed cells give scientists a new tool for studying the molecular underpinnings of disease. They may also prove useful in screens for potential drugs. Eventually, such techniques might allow scientists to correct genetic defects in the lab dish and then treat patients with their own repaired cells.

Another paper published this year suggests that the reprogramming exit ramp does not have to lead back to an embryonic state but can take a cell directly to a new mature fate. American researchers, working in mice, reprogrammed mature pancreas cells called exocrine cells into beta cells, the cells in the pancreas that produce insulin and are destroyed by type 1 diabetes. The team injected a cocktail of three viruses into the pancreases of adult mice. The viruses primarily infected the exocrine cells, and each one carried a different gene known to play a role in beta cell development. Within days, the treated mice formed insulin-producing cells that looked and acted like bona fide beta cells.

The results are surprising because in living creatures, specialized cells almost never change course, changing, say, from a muscle cell into a lung cell. Such direct reprogramming, however, might be simpler and safer than using pluripotent cells to treat some diseases. The technique might also enable scientists to speed up the lab production of desired cell types, using defined factors to change one type of cultured cell directly into another.

CREDITS (TOP TO BOTTOM): C. BICKEL/*SCIENCE*; LESTER V. BERGMAN/CORBIS

Published by AAAS

Wanted: more breakthroughs

Although researchers made impressive progress in 2008, several more breakthroughs are needed before cellular reprogramming yields its first cure for disease. For reprogramming to be safe enough to use in cell therapy, researchers must find an efficient, reliable way to trigger it. They also want to understand exactly how the process works. Although dozens of labs have used the technique, what is happening inside the reprogrammed cell remains a mystery, and a combination of chance events seems to determine which rare cells end up being reprogrammed. A leading theory is that some of the reprogramming factors first help to loosen up the DNA in a cell's nucleus, making it easier to reactivate turned-off genes. Then the other factors help to set off a cascade of protein signals that give a cell its new identity (see the Review by Gurdon and Melton on p. 1811).

The original reprogramming recipe relies on viruses to insert the reprogramming genes into the infected cell's genome, altering the DNA permanently. Scientists are wary of that approach for a couple of reasons. First, the inserted DNA could interrupt existing genes—for example, those that guard against cancer, leaving the cells likely to form tumors. And although the inserted genes seem to turn off after reprogramming is finished, allowing the cell's own genes to take over, scientists worry that the inserted genes could be reactivated or could have other subtle effects on the cell.

For that reason, labs around the world are working on other ways to trigger reprogramming. This year, they made rapid progress. Several groups found that they could substitute chemicals for some of the inserted genes. Another found that adenoviruses could also do the trick, at least in mouse cells. Adenoviruses, which cause the common cold, do not insert themselves into the genome. The viruses express their genes long enough to reprogram the cells, but as the cells divide, the viruses are diluted down to undetectable levels, leaving reprogrammed cells with their original genomes unchanged. Researchers in Japan showed that rings of DNA called plasmids could also carry the required genes into the cell. The alternatives are much less efficient than the original recipe, however, and most have not yet worked in human cells, which are harder to reprogram than mouse cells.

To be useful, reprogramming also needs to become much more efficient. Most experiments have managed to reprogram fewer than one in 10,000 cells. In what seems to be a lucky break for the field, however, two groups showed this year that the skin cells called keratinocytes are particularly easy to reprogram. Researchers can reprogram roughly 1% of the keratinocytes they treat, and the process takes only 10 days instead of the several weeks that other cells require. Hair follicles (photo, p. 1766) are a rich source of keratinocytes, and researchers in California and Spain showed that they could efficiently derive personalized cell lines from cells taken from a single human hair plucked from the scalp—an even easier source of cells than cutting out a piece of skin.

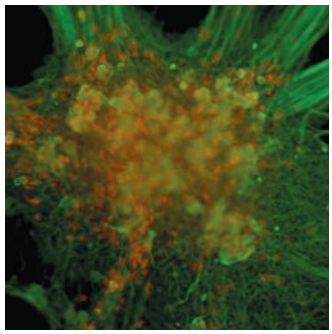

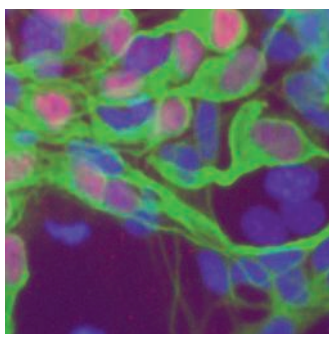

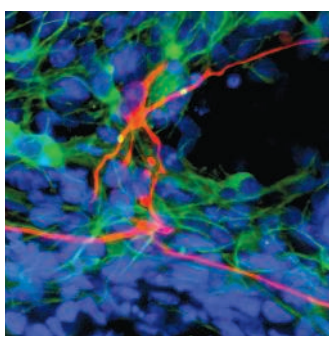

Finally, reprogramming needs better quality control. This year, an American group took a major step in that direction by making cells in which the reprogramming genes could be turned on by the addition of the antibiotic doxycycline. They then used the reprogrammed cells to generate "second generation" iPS cells that are genetically identical—each contains the same viral inserts. These cells will allow scientists to study the process of reprogramming for the first time under standardized conditions and should help to reveal the biochemical processes that enable an adult cell to take an exit ramp from its one-way path of development.

A thorough understanding of reprogramming is not enough, however. Ten years after the discovery of human ES cells, scientists are still working on standardizing procedures for coaxing pluripotent cells to become mature tissue. It's a critical problem: Stray pluripotent cells used in therapies could trigger dangerous tumors. And even though scientists can easily prompt pluripotent cells to become beating heart cells in a lab dish, no one has yet perfected a way to get such cells to integrate into the body's tissues to replace or repair their diseased counterparts. But researchers are moving faster down the highway of discovery than many had expected or dared to hope. **–GRETCHEN VOGEL**

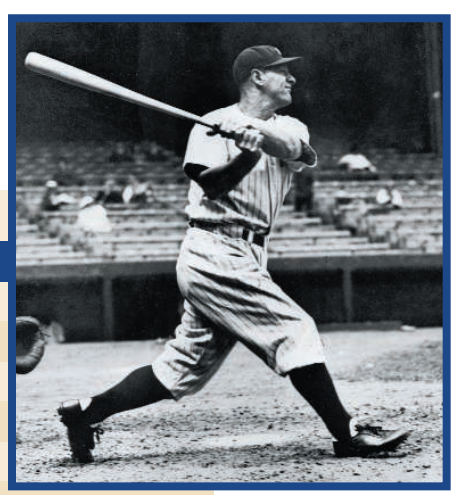

Diseases With Patient-Specific iPS Cell Lines

Amyotrophic Lateral Sclerosis (Lou Gehrig's disease)
ADA-SCID
Gaucher disease type III
Duchenne muscular dystrophy
Becker muscular dystrophy
Down syndrome
Parkinson's disease
Juvenile diabetes mellitus
Shwachman-Bodian-Diamond syndrome
Huntington disease
Lesch-Nyhan syndrome (carrier)

CREDITS (TOP TO BOTTOM): DIMOS *ET AL.* (GROUP OF THREE); C. BICKEL/*SCIENCE*; JERRY COOKE/SPORTS ILLUSTRATED/GETTY IMAGES

Published by AAAS

Seeing Exoplanets

SEEING MIGHT BE BELIEVING, BUT FOR SCIENTISTS BELIEF RARELY depends on seeing. The right squiggles coming out of an instrument are usually enough to confirm that they have caught their quarry, however infinitesimal, insubstantial, or bizarre. Astronomers searching for planets circling other stars, however, may have been getting just a tad impatient with their progress toward their ultimate goal: recognizing a habitable, even an inhabited, planet beyond our own solar system. For that, they'll need to see their target. But all exoplanet detections had been of the squiggly variety.

Now, astronomers have seen exoplanets for the first time—a half-dozen candidates have been announced in the past few months. To some, the new observations may simply have replaced squiggles with dots. But the faint pinpricks of light from far-off worlds have captured the public's imagination and will give astronomers new clues to what those distant planets are made of and how they were formed. Key to these direct detections have been big telescopes and the latest technology to pick out a vanishingly faint planet from its host star's overwhelming glare.

Previous, indirect detections of more than 300 exoplanets had provided breakthroughs of their own. For 13 years, astronomers have been finding exoplanets using ground-based telescopes to monitor the subtle wobble a planet gravitationally induces in its star. This workhorse radial-velocity technique is especially useful for finding massive "hot Jupiters" searingly close to their star. No light is seen from the planet, however. Another method, called microlensing—in which a planet's gravity momentarily brightens a background star by bending its passing light—is particularly good for detecting planets more distant from their stars and in principle could spot lightweights with masses down to that of Earth. But microlensing is a one-off event; once the fleeting alignment with the star is over, no sign of the planet will ever be seen again.

If a planet happens to orbit across the face of its star as viewed from Earth, however, the repeated tiny dimming of the total light of the star plus the planet can reveal the presence of the planet. At the same time, starlight passing through the outer planetary atmosphere can reveal clues about composition. Already, water, methane, and—just last month—carbon dioxide have been detected in transiting exoplanets. Those compounds, plus molecular oxygen, are the key markers of an inhabited planet. But only hot Jupiters—unlikely abodes of life—are liable to transit their stars and be detected using current technology.

That leaves direct detection. The chore is simple enough: Separate the light from a planet from the light of its nearby star. The hitch is that the star is millions of times brighter than any planet, and Earth's turbulent atmosphere churns the light of star and planet together. To solve the latter problem, astronomers can move their telescopes above the atmosphere to Earth orbit. Or they can correct the incoming telescopic image using so-called adaptive optics, in which precisely controlled warping of a mirror many times a second straightens out distorted light. Coping with the vast difference in brightness between planet and star requires a coronagraph in the telescope to physically block out the star or "virtual coronagraph" software to remove starlight from the image. It also helps to search for very young and therefore still hot planets at infrared wavelengths, in which case the star-planet contrast will be much smaller.

With more than 5 years of observations using the latest technology, astronomers are suddenly busting down the doors to announce candidates for directly detected exoplanets. Published last month, the most secure—and surely the most stunning—are three objects orbiting a star called HR 8799, 128 light-years from Earth. Judged to have five to 10 times the mass of Jupiter, they orbit at least 24 to 68 times farther from their star than Earth orbits from the sun. That makes them among the most massive exoplanets discovered and by far the most distant from their star. New detection techniques typically start by finding such oddballs. These are giving theorists fits; they don't see how planets could have formed that far out.

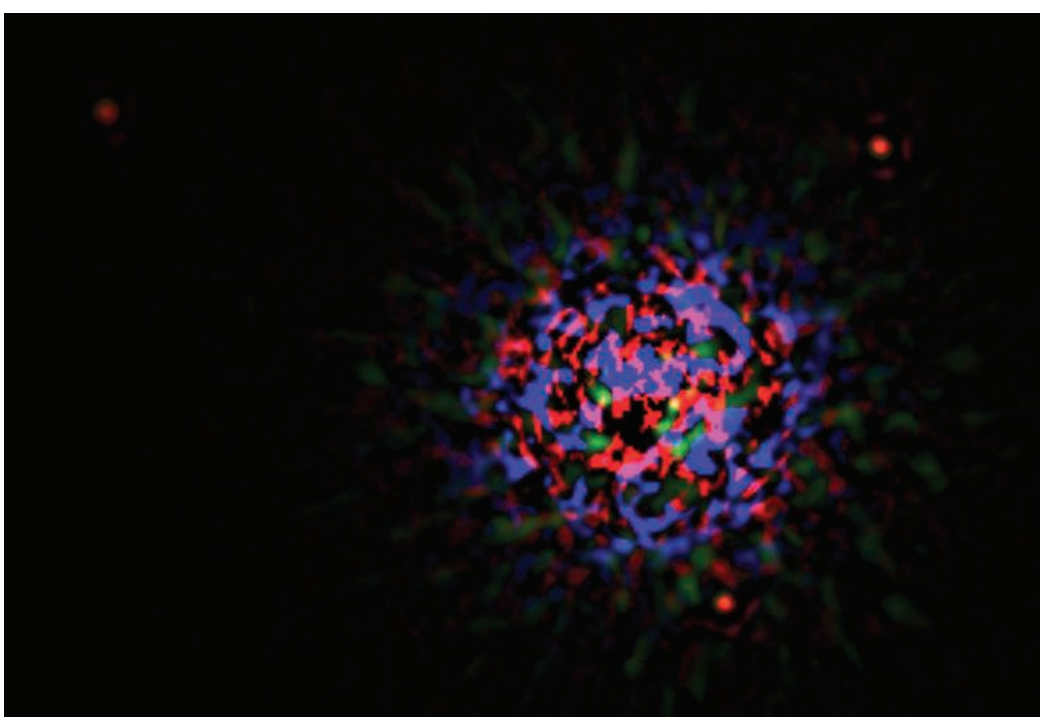

Other direct detections came one per star. Last month, another group also reported detecting a planet of roughly three Jupiter masses orbiting the star Fomalhaut, one of the brightest stars in the sky. A third group announced a single candidate exoplanet last September but must await confirmation that it is orbiting the star rather than just passing through. And a fourth group announced late last month what would be—at eight times the sun-Earth distance from its star—the imaged planet closest to its star.

Astronomers are already starting to analyze the light of some of the new finds for clues to their physical and chemical nature. That should keep planetary formation theorists busy. The chance to directly study potentially inhabited planets is further off. Imaging Earth-like exoplanets in Earth-like orbits is probably still decades and certainly billions of dollars away.

CREDIT: CHRISTIAN MAROIS/NRC HERZBERG INSTITUTE OF ASTROPHYSICS

PHENOMENON OF THE YEAR:
EUROPEAN BIG SCIENCE

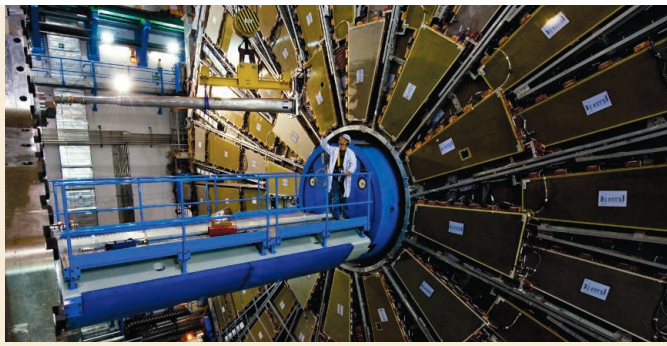

IN SEPTEMBER, WHEN THE FIRST BEAMS circulated through the Large Hadron Collider (LHC), Europe's giant particle accelerator near Geneva, Switzerland, media outlets were quick to name a winner. "Europe leaps ahead on physics frontier" ran a story on MSNBC.com, and a blog trumpeted "LHC a sure sign that Europe is the center of physics." The electrical fault that put the LHC out of action just days after its inauguration didn't change the overall picture.

That success was bittersweet for U.S. particle physicists, whose own machine, the Superconducting Super Collider, was canceled in 1993. By most objective measures, U.S. research still leads the world, but in their ability to pool resources in the pursuit of "big science," European nations are showing increasing ambition and success.

CERN is the model of a pan-European laboratory. Formed in 1953 to help rebuild postwar European science and encourage international cooperation, the facility became a guiding light for European particle physics and spurred other fields to follow suit. The next few decades saw the creation of the Institut Laue-Langevin neutron source, the European Molecular Biology Laboratory, the European Space Agency, the European Southern Observatory, the Joint European Torus, and the European Synchrotron Radiation Facility (ESRF). But after the agreement to build ESRF in 1984, the enthusiasm for joint European ventures faded.

That situation has changed this decade, however. First off, the European Union (E.U.) decided that it wanted to host ITER, the worldwide reactor project that aims to prove nuclear fusion as a viable power source. During much of 2004 and 2005, the E.U. was locked in a staring match with Japan over whose site should take the honor. Determined shuttle diplomacy and a face-saving formula put together by E.U. officials finally paid off, and ITER is now under construction at Cadarache in southern France. Such is Europe's confidence in the project that when Congress zeroed out the U.S. contribution to ITER from its 2008 budget, managers in Cadarache barely broke step.

The E.U. didn't stop there. In 2002, it created the European Strategy Forum on Research Infrastructures (ESFRI), which set about drawing up a list of projects worthy of E.U. support. The ESFRI Roadmap, published in October 2006, lists 35 projects, which include a database on population aging and a neutrino observatory on the Mediterranean seabed. The E.U. didn't have money to build the projects. But it did have money to support design studies and asked all the Roadmap's nominated projects to apply—and nearly all of them did. The aim of the cash is to "get the projects to a point where a political decision can be made" on whether to build, says materials scientist John Wood of Imperial College London, who was chair of ESFRI at the time.

The ESFRI Roadmap and E.U. infrastructure funding have given a number of projects a major push toward becoming reality. This year, the European XFEL, an x-ray light source, and the Facility for Antiproton and Ion Research, both in Germany, have enlisted international partners for construction, and both expect to sign conventions by early next year. The European Spallation Source, proposed in the early 1990s, now has three sites vying to host it, and a decision—in part brokered by ESFRI—is expected this month. A final design for the *Aurora Borealis*, a groundbreaking polar research ship, was also released this month. And this autumn, groups of European astronomers and astroparticle physicists have published their own road maps, listing potentially world-leading instruments such as the European Extremely Large Telescope and the Cherenkov Telescope Array. "I'm absolutely staggered at how influential [the Roadmap] has been," says Wood.

As this issue went to press, ESFRI was about to release a revised road map, updating its original effort and including some fields that were omitted before. European scientists are eager to see where it leads.

–DANIEL CLERY

Cancer Genes

RESEARCHERS THIS YEAR TURNED A SEARCHLIGHT ON THE ERRANT DNA that leads tumor cells to grow out of control. These studies are revealing the entire genetic landscape of specific human cancers, providing new avenues for diagnosis and treatment.

Tumor cells are typically riddled with genetic mistakes that disrupt key cell pathways, removing the brakes on cell division. Thanks to the completion of the human genome and cheaper sequencing, researchers can now systematically survey many genes in cancer cells for changes that earlier methods missed. Results from the first of these so-called cancer genome projects came out 2 years ago, and the output ramped up in 2008.

Leading the list were reports on pancreatic cancer and glioblastoma, the deadliest cancers. By sequencing hundreds or thousands of genes, researchers fingered dozens of mutations, both known and new. For example, a new cancer gene called *IDH1* appeared in a sizable 12% of samples from glioma brain tumors. A separate glioma study revealed hints as to why some patients' tumors develop drug resistance. Other studies winnowed out abnormal DNA in lung adenocarcinoma tumors and acute myeloid leukemia.

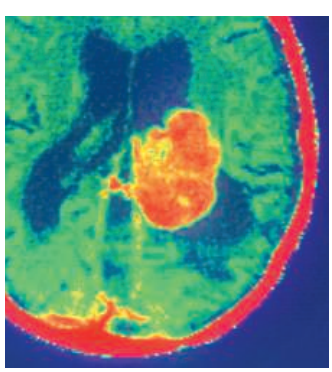

The expanding catalog of cancer genes reveals an exciting but sobering complexity, suggesting that treatments that target biological pathways are a better bet than "silver bullet" drugs aimed at a single gene. Genome projects for at least 10 more cancers are in the works.

CREDITS (TOP TO BOTTOM): CERN; DAN MCCOY/GETTY IMAGES

Published by AAAS

New High-Temperature Superconductors

4

PHYSICISTS DISCOVERED A SECOND FAMILY OF HIGH-TEMPERATURE superconductors, materials that carry electricity without resistance at temperatures inexplicably far above absolute zero. The advance deepened the biggest mystery in condensed-matter physics.

In February, a group in Japan reported the first material, fluorine-doped lanthanum iron arsenic oxide ($LaFeAsO_{(1-x)}F_x$), which is superconducting up to a "critical temperature" of 26 kelvin. Within 3 months, four groups in China had replaced the lanthanum with elements such as praseodymium and samarium and driven the temperature for resistance-free flow up to 55 kelvin. Others have since found compounds with different crystal structures and have bumped the critical temperature up to 56 kelvin.

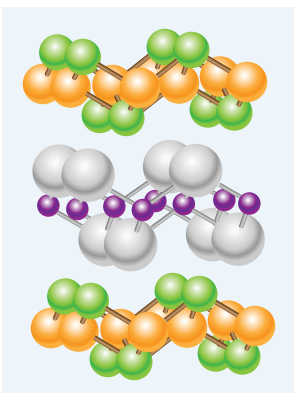

For a critical temperature, that's not so hot. The record is 138 kelvin for members of the other family of high-temperature superconductors, the copper-and-oxygen, or "cuprate," compounds discovered in 1986. Still, the iron-based materials have created a stir, in part because they might help solve the enduring mystery of how the cuprates work. The $64,000 question is whether the two families work the same way. So far, evidence points in both directions.

Watching Proteins at Work

5

AFTER STUDYING PROTEINS FOR MORE THAN A CENTURY, BIOCHEMISTS pushed the boundaries of watching the molecules in action—and received surprises at every turn.

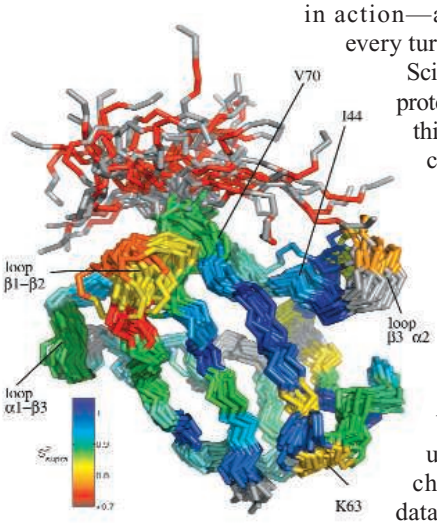

Scientists have long debated how proteins bind to their targets. Most think the shape of a target molecule forces a protein to wiggle into a complementary profile. But it's also possible that proteins in solution wiggle among many slightly different conformations until one finds its target. Computational biologists in Germany and the United States offered bold new support for that upstart idea when they crunched extensive experimental data and showed how one long-studied protein seems to dance among dozens of conformations. In another surprise, a U.S. team tracked individual proteins and found that a single random molecular event can switch a bacterial cell from one metabolic state to another.

Zooming out to the large scale, proteomics researchers in Germany simultaneously monitored the abundance of up to 6000 proteins in yeast cells and quantified how the expression of individual proteins differed between two different cell types. Their technique could lead to new insights into development and disease. Finally, proteomics researchers in Sweden revealed that different tissues in the body likely get their unique characteristics by controlling not which proteins are expressed but how much of each gets made.

Water to Burn

6

RENEWABLE ENERGY SOURCES, SUCH AS WIND AND SOLAR POWER, have plenty going for them. They're abundant and carbon-free, and their prices are dropping. But they're part-timers. Even when the sun is shining and the wind is blowing, there is no good way to store excess electricity on an industrial scale. Researchers in the United States reported this year that they've developed a new catalyst that could begin to change that picture.

The catalyst, a mixture of cobalt and phosphorus, uses electricity to split water into hydrogen and oxygen. Hydrogen can then be burned or fed to fuel cells that recombine it with oxygen to produce electricity. Researchers have known for decades that precious metals such as platinum will split water. But platinum's rarity and high cost make it impractical for large-scale use. The cobalt version isn't all the way there yet, either—it still works too slowly for industrial use—but just getting a cheap and abundant metal to do the job is a key step. Now, if researchers can speed it up, on-again-off-again renewables could have a future as fuels that can be used anywhere at any time.

SCORECARD

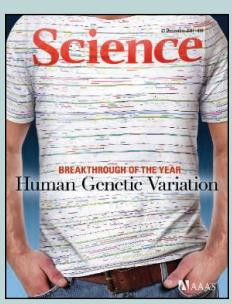

Rating last year's Areas to Watch

(For this year's predictions, see page 1773.)

A smashing start

The Large Hadron Collider came on smoothly in just a few hours, in keeping with *Science*'s observation that the European particle physics lab, CERN, has a knack for getting new machines running quickly. Nine days later, the enormous particle smasher wrecked so bad that it will be down until summer, fulfilling *Science*'s warning that a mishap could take the machine out of action for months.

Micromanagers

MicroRNA work surged in 2008, as efforts to use the molecules to understand and modify disease edged forward. The first successful microRNA manipulation in primates lowered cholesterol in African green monkeys, and the molecules slowed virus replication in ailing mice. Companies are rushing to

CREDITS (TOP TO BOTTOM): ADAPTED FROM M. JOHANNES, *PHYSICS* 1, 28 (2008), ILLUSTRATION BY ALAN STONEBRAKER; JUPITERIMAGES (ARROWS); LANGE *ET AL.*

Published by AAAS

7 The Video Embryo

THE DANCE OF CELLS AS A FERTILIZED EGG BECOMES AN ORGANISM IS at the center of developmental biology. But most microscopes allow only partial glimpses of the process. This year, scientists observed the ballet in unprecedented detail, recording and analyzing movies that traced the movements of the roughly 16,000 cells that make up the zebrafish embryo by the end of its first day of development.

Researchers in Germany made the movies with a new microscope they designed. It uses a laser beam to scan through a living specimen, capturing real-time images and avoiding the bleaching and light damage that have usually limited such videos to just a few hours. The researchers then used massive computing power to analyze and visualize the recorded movements. They also ran the movies backward to trace the origin of cells that form specific tissues, such as the retina. A movie of a well-known mutant strain of fish revealed for the first time exactly what goes wrong as the embryo develops.

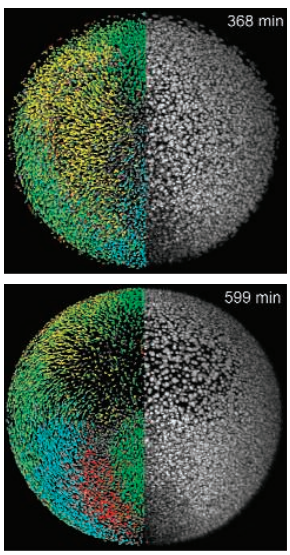

The zebrafish movies are freely available on the Internet, and the developers say they hope the Web site will develop into a full-blown virtual embryo—a sort of developmental biology YouTube with contributions from labs around the world.

8 Fat of a Different Color

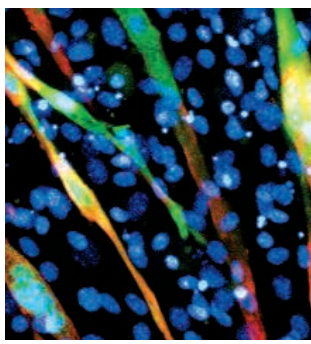

THIS YEAR, RESEARCHERS FINALLY UNCOVERED the mysterious roots of so-called brown fat. Hardly blubber, the energy-using tissue turns out to be one step away from muscle.

Anatomists first noted the distinction between our two fat types more than 400 years ago. White fat is the energy-caching padding that vexes doctors and dieters. If white fat is a quilt, brown fat is an electric blanket. Thanks to plentiful mitochondria, it burns fat molecules to generate heat that warms the body.

Scientists long assumed that both fat varieties developed from the same kind of progenitor cell. Then a team led by U.S. scientists discovered that they could morph brown fat into muscle and vice versa. The researchers knew that the gene *PRDM16* spurs specialization of brown fat. So when they turned down *PRDM16* in brown-fat precursor cells, they expected white fat cells to result.

Instead, the cells stretched out into tube-shaped muscle cells that could even twitch. Reflecting their altered identity, the cells switched off a raft of genes characteristic of brown fat and switched on genes typical of muscle. Coercing cells that had already begun differentiating into muscle to fashion *PRDM16* triggered the reverse transformation, yielding brown fat. Using a technique called lineage tracing, the researchers identified the descendants of the muscle cell clan in mice. They included muscle and brown fat cells but not white fat cells.

The discoveries could mark a step toward antiobesity treatments that melt away bad white fat, either by firing up existing fat-burning brown cells in the body or by transplanting new ones.

develop microRNA-based therapies—but coaxing microRNAs to combat disease is slow going, and safety concerns remain.

Cell to order

Despite high hopes, humanmade microbes are not yet in reach. Researchers did customize cell-signaling circuits in live cells and are exploring new ways of building genomes from scratch. One research group synthesized an entire bacterial genome but has yet to incorporate it into a cell. And designing microbes to make biofuels remains a pipe dream.

Paleogenomics

It was a scramble to get enough sequence done, but a very rough genome of the Neandertal is almost in hand. Along the way, the sequencing team has obtained the complete sequence of Neandertal mitochondrial DNA, finding a few key differences between us and them. Two groups unraveled the mitochondrial genome of extinct cave bears. And sequencing 70% of the woolly mammoth genome prompted speculation about cloning this beast to bring it back to life.

Multiferroics

Multiple electronic, magnetic, and structural behaviors give these materials the potential to carry out both logic and memory functions, now handled separately by semiconductors and metals. Researchers reported steady improvements in performance. Novel multiferroics can change their stripes near room temperature and in low magnetic fields, both important developments for real-world applications. But progress remains muted in turning these materials into complex circuitry.

Megamicrobes

Metagenomics is in full swing, with several key surveys of microbial and viral diversity completed this year in environments as varied as microbial mats, subsurface ecosystems, and the mammalian gut. In addition, DNA sequences from nearly 200 genomes of bacteria associated with humans are finished, and hundreds more are in the pipeline. In October, groups from around the world formed the International Human Microbiome Consortium to study the role the human microbiome plays in health and disease.

New light on neural circuits

This year's Nobel Prize in chemistry honored scientists who turned a luminescent protein from jellyfish into a powerful tool for imaging cells. Building on that work, neuroscientists can now tag neurons with myriad colors to study their connections. And light-sensitive proteins from algae have made it possible to control neural firing with laser pulses. Such methods have great potential for unraveling the function of neural circuits. This year saw steady progress, and the bigger breakthroughs we predicted can't be far off.

CREDITS (TOP TO BOTTOM): PATRICK SEALE AND BRUCE M. SPIEGELMAN; KELLER *ET AL.*

Published by AAAS

BREAKDOWN OF THE YEAR: **FINANCIAL MELTDOWN**

THE SALES SLUMP THAT BECAME A CREDIT crunch and then a global financial crisis this fall will leave a big smudge in the economics record for 2008. Panic hit the stock market in October, engulfed investment companies, and even threatened to pull down the giant General Motors Co. The full scope of the breakdown isn't clear yet.

Luckily, scientific research did not take a direct hit, but scientists are feeling the consequences like everyone else, and research budgets could get caught in the fallout next year. In the United States, the drop in stock values deflated private endowments—some by 15% to 25% over a few months. Retirement accounts withered. Meanwhile, programs funded by endowments began to cut back (*Science*, 7 November, p. 841). The Smithsonian Institution acknowledged in its first public board meeting in November that its endowment was down 21% over a 4-month period and that it would need to tighten its $1 billion budget. Like many, it has delayed announcing hard cuts.

Companies that need capital to advance new technologies will be pinched, and some will go under. New energy projects seem likely to be delayed. In the biomedical area, a recent report by the Biotechnology Industry Organization in Washington, D.C., noted that 38% of its smaller public companies are on track to burn through their cash reserves in a year.

State-funded hospitals and universities are cutting employees and putting off new facilities as state revenues decline. The California state university system, responding to the governor's budget, has threatened to cut student enrollment by 10,000, or 2.1%, next year. Private schools are being affected, too. President Drew Faust announced a 22% drop in Harvard's endowment, along with potential delays in the new Allston campus and research area. The Massachusetts Institute of Technology plans to reduce spending by 10% to 15%, said MIT President Susan Hockfield. Federal spending on research has not changed, but President-elect Barack Obama and Congress have not yet tackled the 2009 budget.

In this murky landscape, there is at least one fixed point: the official starting date of the crisis. According to Federal Reserve Board Chairman Ben Bernanke, the cascade began in August 2007 with a general price collapse in U.S. real estate. Houses went unsold; owners walked away from mortgages; companies holding the mortgages began to default on obligations; a huge firm that insured against such defaults, AIG, ran out of funds and was saved by the government. Five high-flying U.S. investment banks with mortgage-related investments quit the investment field—four to become ordinary commercial banks and one to disappear (Lehman Brothers). Governments in North America, Europe, and Asia are now pumping hundreds of billions of dollars into private companies in an attempt to restore the economy's pulse.

What caused the crash? Bernanke and other Fed economists describe it as the natural end of an "asset bubble," an irrational run-up in values. Whether it's labeled as optimism or greed, the appetite for growth got out of hand, and the financial models that underpinned some investment strategies broke down. Some say the remedy is to increase controls on finance and enable more scrutiny of private funds. One school of economists argues that the solution is to create models that steer investors away from bad risks by relying less on "rational" economic principles and more on observed human behavior (*Science*, 12 December, p. 1624). The debates are just warming up and will occupy analysts of the 2008 crash for years to come. **–ELIOT MARSHALL**

Proton's Mass 'Predicted'

STARTING FROM A THEORETICAL DESCRIPTION OF ITS INNARDS, physicists precisely calculated the mass of the proton and other particles made of quarks and gluons. The numbers aren't new; experimenters have been able to weigh the proton for nearly a century. But the new results show that physicists can at last make accurate calculations of the ultracomplex strong force that binds quarks.

In simplest terms, the proton comprises three quarks with gluons zipping between them to convey the strong force. Thanks to the uncertainties of quantum mechanics, however, myriad gluons and quark-antiquark pairs flit into and out of existence within a proton in a frenzy that's nearly impossible to analyze but that produces 95% of the particle's mass.

To simplify matters, theorists from France, Germany, and Hungary took an approach known as "lattice quantum chromodynamics." They modeled continuous space and time as a four-dimensional array of points—the lattice—and confined the quarks to the points and the gluons to the links between them. Using supercomputers, they reckoned the masses of

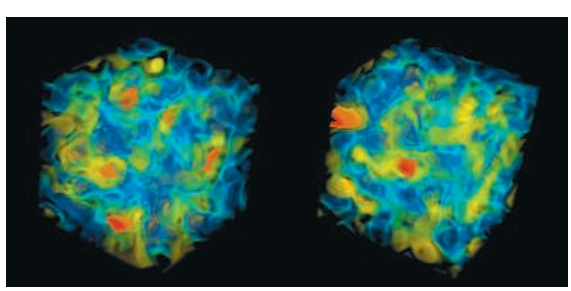

CREDITS (TOP TO BOTTOM): SPENCER PLATT/GETTY IMAGES; TAKU IZUBUCHI, STANIMIRE TOMOV AND MICHAEL MCGUIGAN

Published by AAAS

the proton and other particles to a precision of about 2%—a tenth of the uncertainties a decade ago—as they reported in November.

In 2003, others reported equally precise calculations of more-esoteric quantities. But by calculating the familiar proton mass, the new work signals more broadly that physicists finally have a handle on the strong force.

10 Sequencing Bonanza

NEW GENOME-SEQUENCING TECHNOLOGIES that are much faster and cheaper than the approach used to decipher the first human genome are driving a boom in sequencing.

This year, using "sequencing by synthesis" technology from 454 Sequencing, which "grows" fluorescently labeled DNA on microscopic beads, researchers produced the mitochondrial genomes of extinct cave bears and of a Neandertal, and 70% of the genome of a woolly mammoth.

A preliminary draft of the full Neandertal genome is in the works. Another new technology, developed by Solexa (now part of Illumina), made its debut in the scientific literature with the descriptions of the first genomes of an Asian, an African, and a cancer patient, shedding new light on early human migrations and candidate genes that may underlie malignancies. Illumina's technology sequences DNA in massively parallel reactions on glass plates. A proof-of-concept paper by Pacific Biosciences, a company that sequences single DNA molecules, provided an exciting glimpse of even faster sequencing. Now the goal is to make it more accurate.

Costs continue to drop; at least one company boasts that genomes for $5000 are in reach. **–THE NEWS STAFF**

CREDITS (BOTH): JUPITERIMAGES

AREAS TO WATCH

Plant genomics. Maize got the U.S. government behind deciphering plant DNA. In 2009, expect to see the analysis of its genome published, along with a bumper harvest of DNA sequences from other plants: crops such as soybean and foxtail millet; biofuels plants; monkey flower, much studied by ecologists; and a primitive plant called a lycopod. Several fruits are in the works, and other projects are gaining momentum. And to understand genetic variation, hundreds of strains of the model plant *Arabidopsis* are being sequenced.

Ocean fizz. Acidification of the oceans driven by rising atmospheric carbon dioxide continues apace. The falling pH is bad news for sea creatures, from coral reefs to microscopic plankton. But the looming threat has yet to gain a poster child the likes of global warming's polar bear. Look for a rising tide of studies confirming the pervasive detrimental effects of ocean acidification, although whether more science will grab the public's attention is problematic.

Neuroscience in court. Scientists and legal scholars cringed this year when an Indian court convicted a woman of murdering her fiancé, citing electroencephalograms that purportedly revealed neural activity indicating "experiential knowledge" of the crime. Although images of anatomical abnormalities in the brain have previously been introduced as mitigating evidence during sentencing, the use of methods that measure brain activity is far more controversial. Even so, at least two companies now offer lie-detection services based on functional magnetic resonance imaging. Ready or not, neuroscience appears poised to have its day in court.

Road to Copenhagen. A 12-day international climate summit in November 2009 marks the deadline for countries to set a successor for the Kyoto treaty, which expires in 2012. Can the United States, China, and India agree to binding targets tough enough to mitigate global warming? Will the agreement include funding for developing nations to adopt Western energy technologies and adapt to a warming world? President-elect Barack Obama has pledged that the United States will take a leading role in the talks and will push for a mandatory system. But with the world economy reeling and oil prices low, he'll face a tough crowd in the U.S. Senate, where lawmakers from coal and car states will want to block any deal that doesn't provide maximum leeway.

Darkness visible. Are particles of exotic dark matter annihilating each other in the heavens to produce high-energy cosmic rays? This year, the orbiting PAMELA particle detector and the ATIC balloon experiment reported possible signs of such annihilations. Next year, PAMELA should test the consistency of its result and ATIC's, and NASA's Fermi Gamma-ray Space Telescope, launched this June, will look for photons from dark-matter annihilations. Still, don't expect the stuff to be lured into the light by next December.

Defining species. In the 200th anniversary of Darwin's birth and the 150th of his *On the Origin of Species*, expect more clues about genes that split species into two. In 2008, researchers discovered several sources of genetic incompatibilities that prevent successful reproduction in animals as varied as nematodes and mice. Thanks to advances in genetics, gene sequencing, and protein surveying, they expect to find more and more of such "speciation genes" in coming months.

Tevatron's triumph. Researchers in Switzerland will be scrambling to get the gargantuan Large Hadron Collider up and smashing particles. But the real drama should unfold at the Fermi National Accelerator Laboratory in Batavia, Illinois, where next year the Tevatron Collider should have produced just enough data to reveal signs of the Higgs boson—if its mass is as low as indirect evidence suggests. Don't be surprised to hear shouts of "Eureka!" if not next year then in 2010, when all of next year's data are analyzed.

Published by AAAS

Front-line malaria drug faltering?
1776

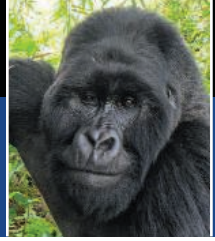

Gorillas caught in Congo crossfire
1778

THE TRANSITION

Nobelist Gets Energy Portfolio, Raising Hopes and Expectations

Standing alongside President-elect Barack Obama this week in Chicago, a visibly nervous Steven Chu might have appeared to be a nerdy scientist out of place in the political spotlight. But make no mistake: Chu has a clear vision of where he wants to go and the determination to get there. His commitment to excellence underpinned his work on trapping supercooled atoms that led to the 1997 Nobel Prize in physics. It also drove him to abandon a comfortable academic career and embrace the challenge of reducing the world's carbon footprint as director of Lawrence Berkeley National Laboratory (LBNL). But it may be on the tennis court where the work ethic of the new secretary of energy nominee is most visible.

While colleagues at a 1998 optics conference in Hawaii partook of the luxury accommodations, the slight, trim physicist, then 50, spent hours testing various rackets with the hotel's tennis pro and practicing his serve before his first match. "He was demanding, like 'Get up, Bambi,' " laughs Mark Cardillo, his assigned partner. "Once he goes after something, nothing is going to stop him," says Galina Khitrova of the University of Arizona, Tucson.

So far, little has. If approved by the Senate, which has given no indication that it would do otherwise, Chu would become the first career scientist to run the $24 billion agency. He'll be carrying on his back the hopes of U.S. researchers to jump-start stagnating science budgets at the Department of Energy (DOE) and retain U.S. leadership in the face of rising overseas competition. The curmudgeonly commentator for the American Physical Society, Robert Park, called the choice a "perfect call."

DOE is a mission agency with four distinct portfolios (see graph); Chu has been tapped to beef up its role in science and energy. "In Steve Chu, we have a Nobel Prize–winning scientist who understands that technology and innovation are the cornerstones of our climate solutions," said Vice President-elect Joe Biden when introducing him this week. Obama went even further in explaining the significance of Chu's nomination. "His appointment should send a signal to all that my Administration will value science, we will make decisions based on the facts, and we understand that the facts demand bold action."

It's a challenge commensurate with Chu's demanding standards. The nation desperately needs new low-cost technologies like solar power, better transmission lines for wind power, and successful large-scale demonstration projects for carbon capture from coal combustion or underground CO_2 storage. Although Congress has indicated a willingness to provide basic physical science with double-digit annual funding increases, lawmakers have repeatedly failed to seal the deal when faced with competing budgetary priorities.

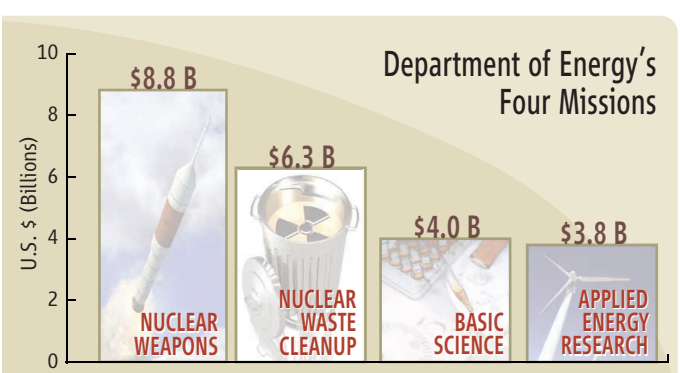

Out of many, one. One big challenge for Steven Chu will be to unite the disparate activities of the Department of Energy.

Raised by Chinese immigrants in Garden City, New York, Chu says he was more free-thinking than studious until his undergraduate days at the University of Rochester in New York state. In graduate school, he bounced from theoretical astrophysics to whimsical tests to find the frequency sensitivity of the human ear. Once he wedded his creativity with his ambition, however, his career took off, first at AT&T Bell Labs and then at Stanford University.

STEVEN CHU, 60

- Director, Lawrence Berkeley National Lab
- Professor of Physics, Professor of Molecular and Cell Biology at UC Berkeley
- Stanford University, 1987-2004
- AT&T Bell Labs, 1978-1987
- Ph.D. in physics, University of California, Berkeley, 1976.
- 1997 Nobel Prize in physics

But being a successful academic scientist wasn't enough. Chu says it was the "sobering" scale of the climate challenge that drew him to accept an offer in 2004 to direct the 4000-person, $650 million Berkeley lab. There he led efforts to partner with BP on a $500 million energy biosciences institute (*Science*, 9 February 2007, pp. 747 and 784) and win a competition for an interdisciplinary $135 million bioenergy research center funded by DOE (*Science*, 25 April 2008, p. 478). Chemist Nathan Lewis of the California Institute of Technology in Pasadena, a partner under Chu's umbrella renewable-energy research program, called Helios, says Chu's ability to understand and cooperate with researchers across a variety of fields will serve him well as he seeks to coordinate research across the sprawling DOE system. "He knows he doesn't have to do it all," says Lewis.

Chu's commitment to interdisciplinary research was underscored at Stanford, where

CREDITS (TOP TO BOTTOM): LAWRENCE BERKELEY NATIONAL LAB; PHOTOS.COM

Published by AAAS

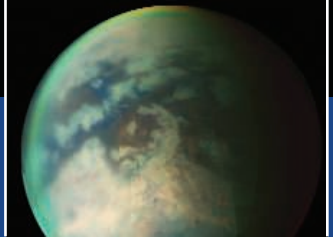

NASA's $3 billion choice
1780

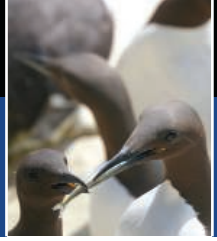

Seabirds and the junk-food hypothesis
1786

he joined three other professors to found the school's Bio-X program, which supports biological research directed at health, energy, and environmental needs. A major challenge for the next energy secretary will be demonstrating to industry that large-scale carbon sequestration facilities can work. Earlier this year, DOE canceled plans to build a $1.8 billion demonstration facility called FutureGen, opting for an approach that involves smaller test facilities. Obama's team has so far signaled that it likes the more modest approach. Although Chu has not made his preferences clear, he wrote in a report last year by the world's science academies that demonstration projects often get "insufficient attention from those who are or have been engaged in funding the R&D phase."

Obama transition team member Elgie Holstein has said that Obama wants to focus "more activities in the basic sciences on the energy problem." Chu has a track record at LBNL of inspiring scientists to do that; Lewis and chemist Paul Alivisatos are among several top scientists who have followed Chu's lead and shifted their research into areas directly applicable to renewable energy. Chu is also the intellectual father of an idea to make DOE science more innovative and nimble through a miniagency called the Advanced Research Projects Agency–Energy (ARPA-E). Congress authorized spending $300 million last year on ARPA-E and "such sums as necessary in 2009 and 2010" in legislation championed by Representative Bart Gordon (D–TN), chair of the House science committee. But so far Congress has not appropriated any money for it, and the Bush Administration views the new agency as needless bureaucracy, an issue on which Chu clashed with DOE headquarters behind the scenes. (Indeed, presidential science adviser John Marburger may have had such encounters in mind when he told *Science* that Chu will need to hire assistants with "strong personalities to interact productively with a highly self-confident Nobel laureate.")

Meanwhile, physical scientists are hoping Chu's impeccable scientific pedigree will heal a wounded U.S. physics enterprise, which has fallen behind European colleagues in particle physics and could face thousands of layoffs across DOE's 21 national laboratories unless the budget picture brightens. "Having been a basic researcher for most of his life," says Lewis, Chu knows "you never know where the big discoveries are going to come from."

But with money tight in Washington, Chu will need to show considerable political prowess to revitalize DOE. Although a regular visitor to Washington over the past 4 years, he lacks the vast network and insider knowledge possessed by Carol Browner, a former head of the Environmental Protection Agency under President Clinton, whom Obama has named as his White House czar for energy, climate, and the environment. Her relationship with Chu and influence over DOE research has yet to be explained.

This time, it seems, it's going to take guile as well as sweat for Chu to walk off the court a champion. **–ELI KINTISCH**

CREDIT: MEL EVANS/AP PHOTO

Obama's Choice to Direct EPA Is Applauded

President-elect Barack Obama's pick to head the Environmental Protection Agency (EPA), Lisa Jackson, has spent 20 years as an environmental officer at the state and national levels. She'll need every bit of that experience to revive an agency demoralized by the actions of Bush Administration appointees, say scientists and environmental activists who welcomed this week's announcement.

A 16-year veteran of EPA's Superfund site remediation program before taking the top environmental job for the state of New Jersey, Jackson holds a master's degree in chemical engineering. "She will be an outstanding administrator, committed to defending the integrity of the science on which EPA regulations must be based," says David Michaels, a research professor of environmental and occupational health at George Washington University (GWU) in Washington, D.C.

That combination of skills and ethics is badly needed at EPA, say Michaels and other scientists. Kathryn Mahaffey, who left EPA this summer for GWU after 15 years of studying the risk to humans from exposure to pollutants, says that she was instructed in 2005 by a political appointee to "go back and recalculate" her results on blood mercury levels among U.S. women. Political interference has grown so serious, she says, that outside scientists "aren't sure what scientific publications coming out of EPA they really should have confidence in."

Familiar environment. Lisa Jackson has been nominated to lead EPA, an agency where she spent 16 years as a regulator.

One issue awaiting the next EPA administrator is whether the agency will regulate carbon emissions under the Clean Air Act. Although the U.S. Supreme Court told EPA in 2007 to reexamine its opposition to doing so, agency Administrator Stephen Johnson said this summer that "the Clean Air Act is the wrong tool for the job" (*Science*, 18 July, p. 324). An aide to Obama said during the campaign that Obama would instruct EPA to regulate carbon under the act if Congress didn't adopt a cap-and-trade system in the next 18 months. Another Bush Administration policy opposed by many environmentalists—to deny California and other states a waiver to tighten auto emission standards—could be reversed by the new EPA administrator.

As head of New Jersey's EPA, Jackson developed a plan to slash the state's carbon emissions and worked with other Northeast states on a regional program to do the same. Dena Mottola Jaborska, executive director of Environment New Jersey, an advocacy group, credits Jackson with making the state "a leader on global warming." At the same time, some groups have criticized Jackson for making inadequate progress on cleaning up toxic waste sites. This month, she became chief of staff to Governor Jon Corzine. If confirmed by the Senate, Jackson, 46, would become the first African-American to lead EPA. **–LILA GUTERMAN**

Lila Guterman is a science writer in Washington, D.C.

MALARIA

Signs of Drug Resistance Rattle Experts, Trigger Bold Plan

NEW ORLEANS, LOUISIANA— "A catastrophic scenario," one researcher calls it. "A global disaster," predicts another, contemplating what could happen if malaria parasites worldwide developed resistance against the new artemisinin-based combination therapies (ACTs) that have become the gold standard. Large parts of the world would have no drugs to fall back on, and malaria cases and deaths could soar, erasing hope that the world might be on the eve of a huge reduction in the disease. Yet resistance against ACTs is precisely what now seems to be developing in western Cambodia, along the Thai border, according to several studies presented here last week at the annual meeting of the American Society of Tropical Medicine and Hygiene (ASTMH).

The data have given new urgency to an audacious proposal hatched last year to eliminate malaria entirely from the areas where resistance seems to arise. Experts are gathering this week in Phnom Penh to discuss the plan's implementation, which will be coordinated by the World Health Organization (WHO). The Bill and Melinda Gates Foundation plans to bankroll the effort, says WHO malaria expert Pascal Ringwald.

Scientists still don't fully understand the extent and nature of the problem, stresses Nicholas White of Mahidol University in Bangkok, who has a study about it coming out soon. The main phenomenon researchers have documented so far is a delay in clearing the parasites from the blood of some patients on artemisinin drugs. Most researchers prefer to say that the parasite is now "tolerant" rather than resistant to the drug. Still, says White, the data are worrisome.

Cambodia's western border has long been the cradle of antimalarial drug resistance: Chloroquine, sulphadoxine-pyrimethamine, and mefloquine all met their match there before becoming useless elsewhere in the world. Scientists believe this may have to do with the misuse of drugs there and the widespread availability of underdose and counterfeit therapies. From Cambodia, gem miners and other migrants have carried resistant parasites to other Southeast Asian countries.

In the case of ACTs, Cambodia has another problem. These combination treatments rely on an artemisinin derivative for their powerful punch and contain a second drug to make it more difficult for the parasite to become resistant. In Cambodia, however, many artemisinin monotherapies are on the market.

On the border. To prevent resistance to ACTs, a massive malaria-elimination campaign is planned along the Thai-Cambodian border (map), where this picture of a malaria patient and his wife was taken.

Nailing down resistance is harder than it might seem. Treatment failures in individual patients—of which there have been several reports in the past 10 years—don't always signal resistance. Sometimes patients don't get better because their blood levels of the drug are too low, for instance. Testing parasites' sensitivity by exposing them to drugs in the test tube is possible, but the results are hard to interpret. Scientists have not yet found unequivocal genetic markers of resistance to artemisinin derivatives, either.

Partly as a result of such problems, malaria scientists have been skeptical of early reports about resistance. When Harald Noedl, then at the U.S. Army Medical Component of the Armed Forces Research Institute of the Medical Sciences in Bangkok, presented resistance data at an ASTMH meeting in Atlanta 2 years ago, he was "attacked," says Ringwald, who had trouble publishing data on the topic himself. "People didn't want to believe it," he says.

Two years later, new data have accumulated and the skepticism has largely dissipated, says Dyann Wirth of Harvard University. In a paper published in last week's issue of *The New England Journal of Medicine*, for instance, Noedl—who is now at the Medical University of Vienna—reports that out of 60 patients from western Cambodia treated with artesunate, two had delayed parasite clearance, with times of 133 and 95 hours, compared with the average of 59 hours. Both had adequate drug levels in their blood.

The new containment plan calls for eliminating malaria from the areas where tolerance has been found and greatly reducing transmission in a large surrounding area (see map). The plan, to be carried out by national malaria-control agencies in Cambodia and Thailand with support from various research institutes, includes rapid and widespread treatment with ACTs, improved mosquito control, the distribution of long-lasting insecticide-impregnated bed nets, a ban on monotherapies in Cambodia (they are already rare in Thailand), and an information campaign. Whether the plan can succeed is unclear, but "it's worth the investment," says Wirth.

Another type of response is also in the works. At the ASTMH meeting, scientists launched the Worldwide Antimalarial Resistance Network (WWARN), a global database that will collect information on resistance in vivo and in vitro, drug levels in patients' blood, and molecular markers. Based at Oxford University in the United Kingdom, the network will be led by Philippe Guérin, an epidemiologist currently working for Doctors Without Borders. WWARN is in the late stages of negotiating a Gates Foundation grant.

Resistance data tend to languish on desks and in drawers for years while they await publication, says Guérin. In exchange for rapid reporting, WWARN will offer scientists statistical help in analyzing the numbers and perhaps even tools for producing a standard manuscript. WWARN also hopes to bring harmony to the myriad ways to test for resistance. "We really need data shared in real time," says Philip Rosenthal of the University of California, San Francisco, who predicts scientists will cooperate. But, he adds, standardizing methods to test for resistance will be a challenge. **–MARTIN ENSERINK**

CREDITS: (PHOTO) APICHART WEERAWONG/REUTERS; (MAP DATA) WHO REGIONAL OFFICE FOR THE WESTERN PACIFIC

Published by AAAS

NUCLEAR PHYSICS

DOE Picks Michigan State Lab for Rare-Isotope Accelerator

A relatively small university lab has beat out a much larger national lab in the competition to host a $550 million accelerator facility for nuclear physics. The U.S. Department of Energy (DOE) announced last week that it would build the Facility for Rare Isotope Beams (FRIB) at the National Superconducting Cyclotron Laboratory (NSCL) at Michigan State University (MSU) in East Lansing instead of at its own Argonne National Laboratory in Illinois. Many had expected Argonne's superior infrastructure and $530 million budget to give it a decisive edge.

The MSU proposal "started out as a long shot," admits C. Konrad Gelbke, director of NSCL, whose $20-million-a-year budget is provided by the U.S. National Science Foundation. "But I always felt very optimistic that if you presented the case in a very open and honest way, it would all level out in the end." Argonne officials said in a statement that they were "disappointed" and noted that "much of the science for FRIB was developed here at the laboratory."

FRIB will serve as a source of exotic and fleeting radioactive nuclei. The heart of the machine will consist of a 400-meter-long high-intensity linear accelerator that can accelerate a nucleus of any weight from hydrogen to uranium. Those nuclei will smash into and through targets to make beams of exotic isotopes, which will then be used to refine existing theories of nuclear structure, probe fundamental symmetries of nature, and help unravel the processes in stellar explosions that presumably produce half the elements heavier than iron. FRIB would pump out beams at least 1000 times more intense than those currently produced at NSCL.

The site selection "was not the easiest of decisions," says Eugene Henry, DOE's acting associate director for nuclear physics. Henry declined to discuss the details of the two proposals but noted that MSU had offered to pay some of the construction costs. The university has committed to chipping in $94 million, says MSU spokesperson Terry Denbow. He did not say how the money would be raised.

DOE also had more confidence in MSU's spending plan, says Donald Levy, vice president for research and for national laboratories at the University of Chicago in Illinois, which contracts with DOE to run Argonne. "The budget part of their proposal was deemed to be more reliable than ours," Levy says, in part because MSU's budget included more "contingency" money to cover possible cost overruns.

Some observers have misgivings about building a large facility at such a small lab. "[T]he scale of the project was more appropriate for one of the existing DOE laboratories," says Burton Richter, a particle physicist and former director of DOE's SLAC National Accelerator Laboratory in Menlo Park, California. But Richard Casten, a nuclear physicist at Yale University, says he's sure that NSCL is up to the task: "I have no worries about that at all."

Many scientists are just glad that the project, originally proposed in the late 1990s, is making progress. "We are happy that the decision has been made and that the excellent team at Michigan State has been chosen," says Witold Nazarewicz, a nuclear theorist at the University of Tennessee, Knoxville. Researchers hope to start detailed design work next year and to have the machine built and running in about a decade.

–ADRIAN CHO

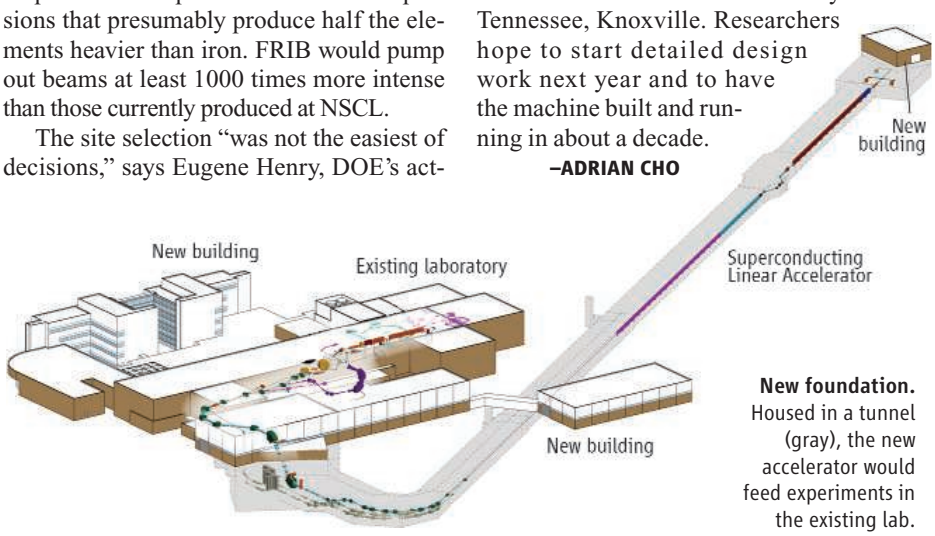

CREDIT: MICHIGAN STATE UNIVERSITY

New foundation. Housed in a tunnel (gray), the new accelerator would feed experiments in the existing lab.

The Road to Copenhagen Begins

International climate negotiators made few important decisions at talks that concluded last week in Poznań, Poland. But activists remain optimistic about reaching an agreement on a post-Kyoto plan next December in Copenhagen (see p. 1773). Attendees created an international fund to help poor nations adapt to changing climates, and a number of developing countries announced new commitments to reduce their emissions. Brazil promised a 70% decrease in deforestation, for example, and Mexico pledged to halve its emissions by 2050. Negotiators also left open the possibility of creating a system to award credits to efforts to curb deforestation. –ELI KINTISCH

Aussie Schools Welcome Cash

Despite the current economic downturn, the Australian government has delivered on promised funds and provided $388 million to 11 universities to boost their ailing infrastructure. Recipients of the funding, set aside last year after a hefty surplus (*Science*, 18 May 2007, p. 968), include the University of Sydney, which received $64 million to establish the Centre for Obesity, Diabetes and Cardiovascular Disease; the University of Melbourne, which received $60 million to establish the Peter Doherty Institute for Infection and Immunity; and Monash University in Melbourne, which won $60 million to establish a New Horizons Centre devoted to collaborations between engineering and science.

–ELIZABETH FINKEL

Mouse Genome Bonanza

A $4.4 million project to sequence the DNA of 17 strains of mice will make these animals more useful for tracking down genes and assessing genetic risks for human diseases. Over the next 3 years, the Wellcome Trust Sanger Institute in Hinxton, U.K., will generate up to 3 trillion bases of mouse DNA, using new low-cost and high-speed sequencing methods, to compile fairly complete genomes of the most commonly used mouse strains. Those strains include those used to make knockout mice, the parent strains for lines used in studies of diseases such as diabetes, obesity, and asthma, and eight strains that are the starting points for the development of 1000 new inbred lines. Partners include the U.K. Medical Research Council, the Juvenile Diabetes Research Foundation, the Wellcome Trust and MRC genetics labs, the European Bioinformatics Institute, and the Jackson Laboratory.

–ELIZABETH PENNISI

Published by AAAS

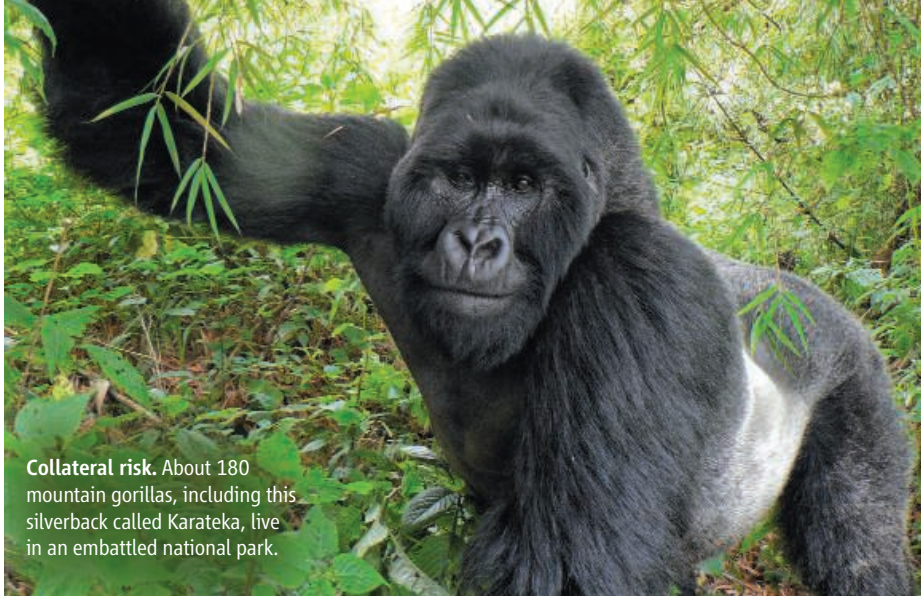

Collateral risk. About 180 mountain gorillas, including this silverback called Karateka, live in an embattled national park.

ENDANGERED SPECIES

Rangers Assess Toll of Congo Conflict On Threatened Mountain Gorillas

In the wake of severe fighting in Virunga National Park in the Democratic Republic of the Congo (D.R.C.), worried rangers began a painstaking census late last month of the park's highly endangered mountain gorillas, nearly a third of the world's known population. "It is imperative to find out the gorillas' status," says the park's director, Emmanuel de Merode, who is leading the census.

Violence in eastern D.R.C. worsened in October when government troops and allied militias clashed with rebels inside the 7800-square-kilometer park, which is Africa's oldest. About 400 park rangers and their families withdrew into temporary refugee status in a camp near the town of Goma.

After an agreement was reached to allow most rangers to return to the park in late November, de Merode—a Ph.D. anthropologist who became the park's director in August—organized a census to find out whether any gorillas succumbed. Last year, he says, nine of the park's approximately 180 gorillas were killed: one for its meat; one in a botched trafficking attempt; and seven "vindictive killings," possibly by a corrupt army faction involved in illegal logging.

The census, expected to be completed by year's end, is focused on the park's 72 or so human-"habituated" gorillas, which rangers can track and recognize. "We identify the habituated gorillas primarily by unique wrinkles on their noses, which can be recorded as signatures," de Merode told *Science*. Each morning, trackers follow forest trails to find a gorilla group; survey teams then try to identify all its members. Tragically, the habituated animals are "the most vulnerable," de Merode says, partly because they "are closest to the forest's edge" and are less fearful of humans.

The nose-count approach has some technical weaknesses: It accurately counts only the habituated animals, about one-third of mountain gorillas in the park, and it depends on the trained eyes of certain rangers. "The fate of the unhabituated groups is unknown" in such nose-counts, says primatologist Martha M. Robbins of the Max Planck Institute for Evolutionary Anthropology in Leipzig, Germany. "Once the area is stable, it will be important to do a census of the entire region so we can get an estimate on the entire population."

The densely populated and ethnically diverse eastern D.R.C. has been volatile for decades. Famed gorilla researcher Dian Fossey fled violence in the D.R.C. (then called Zaire) in 1967 to set up her Karisoke Research Center across the border in Rwanda; ever since then, researchers have tended to shun the D.R.C. in favor of outposts in adjacent countries. Although long-term gorilla research is ongoing at Karisoke and in Uganda, there has been a dearth of scientific studies on the D.R.C. side of the border. "The region has been too insecure" in the past decade, says Robbins, who worked at Karisoke before establishing the first long-term field study of mountain gorillas in Bwindi Impenetrable National Park in Uganda.

Hot zone. Rebels occupy the gorilla sector of the Virunga National Park; other militias have entered from Rwanda.

The danger and lack of resources have so far impeded a more accurate count using techniques such as a "genetic census." It involves a simultaneous sweep of the entire habitat by trackers who find gorilla tracks, identify nest sites, and collect fecal samples from which DNA is later analyzed to genotype every individual gorilla. So far, scientists have conducted a full genetic census of mountain gorillas only at the Bwindi park. In 2006, that census found evidence of 302 animals, 34 fewer than estimated using traditional methods.

Max Planck anthropologist Damien Caillaud, who studies the influence of habitat characteristics on the Bwindi mountain gorillas' social system, says the genetic census there "allows us not only to count the individuals but also to know their sex, the relatedness among individuals, … and the dispersal patterns."

A 2003 census using traditional methods of the entire three-country Virunga Volcanoes area—funded by seven gorilla research and conservation groups—set the region's total population at 380 gorillas, including the 180 to 200 on the D.R.C. side. Together with the 300 or so mountain gorillas in nearby but separate Bwindi, that puts the total known population of the primates at nearly 700.

Although the D.R.C. rangers have now reentered Virunga park, the conflict continues, with some armed rebels entering from Rwanda. Whereas the major armed groups have outposts within the park's borders, a rebel group controls the gorilla area (Mikeno sector) in the park's southern region. As of last week, park rangers had fully surveyed two of the six habituated gorilla groups and found that new infants had increased their numbers. "The results so far have been pretty positive," says de Merode, "but that can change."

Robbins adds that the rangers "have risked their lives and worked through extremely difficult conditions to help protect the gorillas." Researchers and conservationists alike hope that the wild inhabitants of Virunga park will make it safely to 2009, which has been declared the "Year of the Gorilla." **–ROBERT KOENIG**

Published by AAAS

SCIENCE POLICY

Report Faults U.S. Strategy for Nanotoxicology Research

The U.S. government lacks an effective plan for ensuring the safety of nanotechnology, a new report by the National Research Council (NRC) concludes. The report, released last week, finds that the current plan for coordinating federal research on environmental, health, and safety (EHS) risks of nanotechnology amounts to an ad hoc collection of research priorities from the 25 federal agencies that make up the U.S. National Nanotechnology Initiative (NNI), which coordinates federal nanotech programs. What's needed, it argues, are an overall vision and a plan for how to get there and to come up with the money to do so.

"The current plan catalogs nano-risk research across several federal agencies, but it does not present an overarching research strategy needed to gain public acceptance and realize the promise of nanotechnology," says David Eaton, an environmental and occupational health scientist at the University of Washington, Seattle, who chaired the committee that wrote the report.

The NRC report marks new movement in what has been a long-running tug of war between the Bush Administration and its critics in Congress, academia, and nongovernmental organizations over how best to ensure nanotechnology's safety. Administration officials have maintained that the agencies funding the research—such as the National Institutes of Health and the Environmental Protection Agency—are best qualified to set their priorities and budgets to ensure nanotech safety. Critics counter that a point person is needed to ensure that coordination takes place. The House Science and Technology Committee passed a bill earlier this year reauthorizing NNI and pushing much of the critics' agenda. But the Administration opposed installing a nano overseer, among other things. The bill was shunted aside by the election and the economic chaos this fall and never came to a vote.

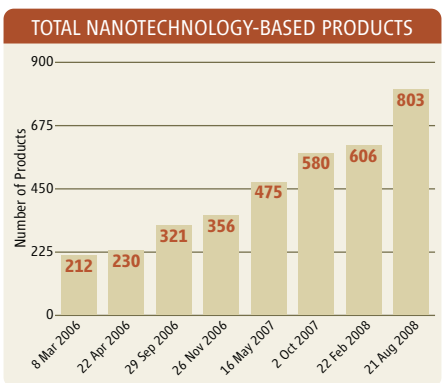

Steady climb. New products containing nanomaterials continue to rise, despite unknowns.

The new report is something of a vindication, says Andrew Maynard, chief scientist at the Woodrow Wilson International Center for Scholars' Project on Emerging Nanotechnologies in Washington, D.C. "It shows we haven't been out on a limb for the last few years," Maynard says. Maynard has long criticized coordination of EHS research under NNI and served on the NRC panel that wrote the report. "Now the government needs to decide who needs to do what risk research and where the money is going to come from."

The current report does not assess the potential toxicity of nanomaterials, which are now found in more than 800 commercial products. Rather, last year, the U.S. National Nanotechnology Coordination Office (NNCO), which oversees day-to-day coordination of nanotechnology programs between U.S. federal agencies, asked NRC to evaluate its current EHS research strategy. A statement from NNCO called the development of a broader national strategy "a worthy goal." However, it says the report's call for reengineering how the federal government oversees NNI "was not within the scope of the NRC panel review, and would require extensive review and analysis and Congressional oversight."

The back and forth will resume next year. Bart Gordon (D–TN), who chairs the House Science and Technology Committee, said last week that he will reintroduce the bill to reauthorize NNI, which will again put these issues front and center. The key will be whether the new Obama Administration sides with its predecessors or with their critics.

–ROBERT F. SERVICE

CREDIT: ADAPTED FROM GRAPHIC BY WOODROW WILSON INTERNATIONAL CENTER FOR SCHOLARS' PROJECT ON EMERGING NANOTECHNOLOGIES

From the *Science* Policy Blog

Last month, *Science* launched a policy blog, *Science*Insider, providing news and analysis on science policy around the world. Postings include breaking news covered more in depth in the magazine as well as news that doesn't appear in print:

Museum layoffs prompt backlash. Archaeologists around the world are condemning the University of Pennsylvania Museum of Archaeology and Anthropology for planning to lay off 18 researchers, in particular one of the world's leading archaeobotanists, Naomi Miller, who has been in the field for 30 years. News of the layoffs, announced late last month, has ricocheted through the global archaeology community.… Director Richard Hodges says the museum will find money to retain the scholars …

Scientists seeking stimulus. A collection of U.S. research universities is making the case for science to be included in legislation aimed at reviving the moribund economy. In a letter to President-elect Barack Obama, the 62-member Association of American Universities (AAU) proposes $2.7 billion in immediate spending on academic buildings, scientific equipment, and young researchers. AAU joins a long line of interest groups hoping to tap into an economic stimulus package …

Bioethics guidance from Rome. The Vatican has issued a new document addressing the morality of various developments in biotechnology, including in vitro fertilization, germ-line gene therapy, and so-called altered nuclear transfer (ANT). *Dignitas Personae*, issued at a Vatican press conference 12 December, is mainly a clarification of previously known positions. It does take a cautious line on ANT, which at least one Catholic bishop had endorsed. The technique was developed to find a way to produce stem cells from cloning without ever producing a viable embryo. Scientists have attempted to inactivate certain genes required for embryo development so that instead of producing an embryo, they produce disorganized cells—which nevertheless can be used to make stem cell lines. The document, however, takes a dim view of the effort …

For the full postings and more, go to blogs.sciencemag.org/scienceinsider.

Published by AAAS

Europa vs. Titan

Planetary scientists are in the final stretch of a first-time competition designed to get the most science for the buck from the next big planetary mission while avoiding the fiscal debacles of the past

TEMPE, ARIZONA—Frances Bagenal wants to get back to the outer solar system, but that will take some doing. It will be at least 20 years before an instrument-laden robot can slip into orbit around Saturn's Titan, a deceptively Earth-like moon lashed by liquefied natural gas storms, or around Jupiter's Europa with its potentially inhabited, ice-covered ocean. And the trip will likely cost a good $3 billion, money that is only getting scarcer at NASA.

So Bagenal and her colleagues in the community of outer planets scientists are submitting themselves to a unique, two-stage selection process for the next major mission to the outer planets: a winner-takes-all competition to deliver the best science at the best price.

"Usually, a committee of graybeards meets and decides" which multibillion-dollar mission NASA will fly next, says Bagenal, a space physicist at the University of Colorado, Boulder, and the outgoing chair of NASA's Outer Planets Assessment Group. In the past, the broader planetary community was pretty much left out of the final decision-making, and there was nothing competitive about it. Now, for the first time, independent study teams of scientists and engineers have taken their best shots at designing missions to the Jupiter or Saturn system and pitted them head-to-head.

"I think that's healthy," says Bagenal. "Each team has had to hone its arguments [even though] it means not everyone gets their favorite instrument on board." In the process, scientists are having "to stand up and be responsible for the costs so we don't get a shock down the road," she says. The novel approach will culminate late next month in the selection of a single mission.

Obsolescence

NASA's foray into community-based competition of the biggest missions came after discoveries in the outer solar system made the latest formal prioritization of future missions outdated. The so-called decadal survey from a committee of the National Research Council in 2002 (*Science*, 19 July 2002, p. 317) had just two missions to the outer planets among its 13 priorities for the decade 2003 to 2013: the relatively modest Juno mission to Jupiter itself to be flown in 2011 and a so-called flagship mission to Jupiter's Europa. Flagship missions are NASA's most expensive, running well above $1 billion apiece. The Europa mission gained that status after the Jupiter-orbiting Galileo found signs in 1997 of an ocean beneath kilometers of ice on Europa, raising the prospect of life. And the prospect of life, the decadal survey made plain, was the mission's prime driver.

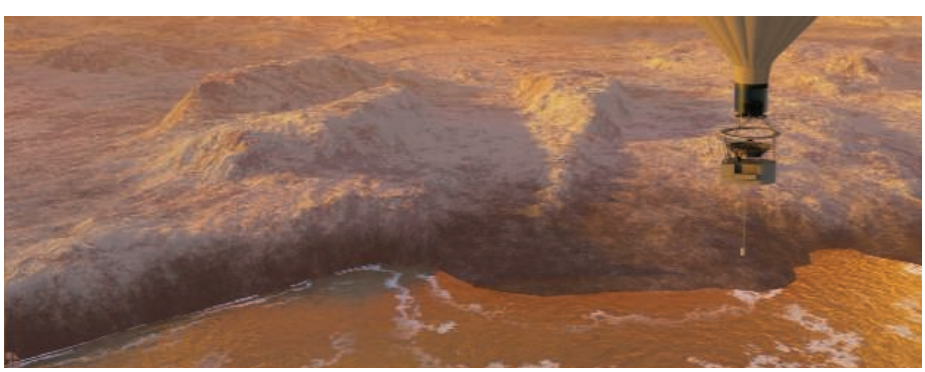

Ambitious. One proposed joint NASA-ESA mission would send an orbiter, a splashdown lander, and this nuclear-fired hot-air balloon to Titan, land of natural-gas lakes and icy ground dirtied with organic goo.

But astrobiology soon beckoned from other quarters around Jupiter and Saturn. In 2005, NASA's Cassini spacecraft, the outer planets flagship following Galileo, discovered a huge plume of ice-laden water vapor spewing from an overheated south pole region of Saturn's little moon Enceladus. Again, liquid water might lurk beneath the icy surface. And in 2005, beneath the haze of Titan, Cassini and its European Space Agency (ESA) Huygens lander found a profoundly frigid but eerily Earth-like world. Earth-like, that is, if you substitute liquefied natural gas for liquid water, water ice for rock, and dark organic gunk for soil. The astrobiology angle came with the gunk. Given its complex origins in Titan's upper atmosphere, it should bear a strong resemblance to the primordial organic matter that came together to begin life on Earth.

Enticing new targets were cropping up, but the next decadal survey was not due out for years, and the prospect of getting to Europa was fading fast. Engineers had long struggled with designing a practical mission. "Each and every one of [the missions studied] was unimplementable," says James Green, director of the planetary science division at NASA Headquarters in Washington, D.C. Jupiter's intense radiation belts threatened to fry the electronics of any spacecraft that lingered in Europa's vicinity for more than a few weeks.

So NASA decided to go to the outer planets community for more possibilities. In 2007, in a process reminiscent of open competitions for missions a fifth the size (*Science*, 23 July 2004, p. 467), four groups of about a dozen scientists and engineers each were given half a year to work up missions to orbit one of four outer planet satellites: Titan, Europa, Enceladus, and Jupiter's moon Ganymede.

CREDITS (TOP TO BOTTOM): NASA/JPL/UNIVERSITY OF ARIZONA; NASA/JPL AND ESA

Published by AAAS

A frigid mystery. Titan (false color) somehow mimics Earth's complexity despite extreme cold.

Two missions eventually survived this head-to-head competition, with NASA Headquarters judging. The latest radiation-hardened electronics made Europa look more practical. And Titan came through, in part, because it "offers a deeper and broader science yield than Enceladus would," suggests outer planets astronomer Heidi Hammel of the Space Science Institute in Boulder, Colorado. What Titan lacks as a potential abode for life, she says, it makes up for with both prelife organic chemistry and fascinating atmospheric and geologic processes.

Enceladus lost out. It "was at a disadvantage," explains engineer Amy Simon-Miller of NASA's Goddard Space Flight Center in Greenbelt, Maryland. "We had to start from scratch," as no one had ever studied going into orbit around Enceladus. Enceladus has so little gravity and orbits so deep in Saturn's powerful "gravity well" that getting into Enceladus's orbit with any affordable propulsion system seemed impractical. Ganymede, on the other hand, was accessible but lacked both astrobiological interest and Titan's bevy of active geological, geophysical, and hydrologic processes, notes outer planets researcher Torrence Johnson of NASA's Jet Propulsion Laboratory in Pasadena, California. In addition, "things have shifted from a total astrobiology focus to more of the wonders of exploration," he says, making Titan's geocomplexity all the more attractive.

Neck and neck

The four were eventually down to two, and those were about to come up against some fiscal rigor. First, S. Alan Stern—NASA associate administrator for space science at the time—imposed a skimpy $2.1 billion limit on the next outer planets flagship mission. Stern's dollar ceiling "was very healthy," says Bagenal. "It made people prioritize, be really ruthless."

Meanwhile, money problems began to loom with NASA's Mars Science Laboratory (MSL), the behemoth rover scheduled to launch in October 2009. MSL's increasingly public problems finally forced a 2-year launch delay earlier this month (*Science*, 12 December, p. 1618). The cost overrun totaled as much as $800 million over the $1.6 billion set in 2006 when NASA committed to the mission. "We have to be careful we don't go down that path," Bagenal said at a meeting of her assessment group here last month.

As it happened, the path for the next outer planets flagship mission took a sharp turn when Stern left NASA this past March and was replaced by Edward Weiler (*Science*, 4 April, p. 31). Parallel studies of missions to Titan and to Europa had been under way since February. NASA study teams had merged with ESA teams to design joint, multicraft missions, but the NASA teams had stuck to Stern's price cap. Weiler wanted alternatives. He did ask for a core option costing $2.1 billion or less, but he added a "full decadal science" option delivering all the science in the decadal survey at whatever cost and an option hitting the "sweet spot" in between, where the science return on the dollar would be maximized. He gave the teams several more months to come up with their proposals.

The flagship-on-the-cheap NASA core missions did not fare well. At the Tempe meeting, after final reports were submitted, NASA outer planets program manager Curt Niebur confirmed that the core option "just wasn't compelling enough to invest $2 billion."

Sweet spots, on the other hand, were more palatable. The Europa orbiter team started with the half-dozen instruments onboard in their $2.1 billion core option and added instruments one by one. The total cost rose slowly until they reached the 13th instrument, the mass of which required a bigger, much more expensive rocket. The sweet spot of $3.0 billion had just been passed. The Titan orbiter team took a somewhat different approach to calculating their sweet spot, but it came out to $2.5 billion. The Cadillac missions fell well out of the running.

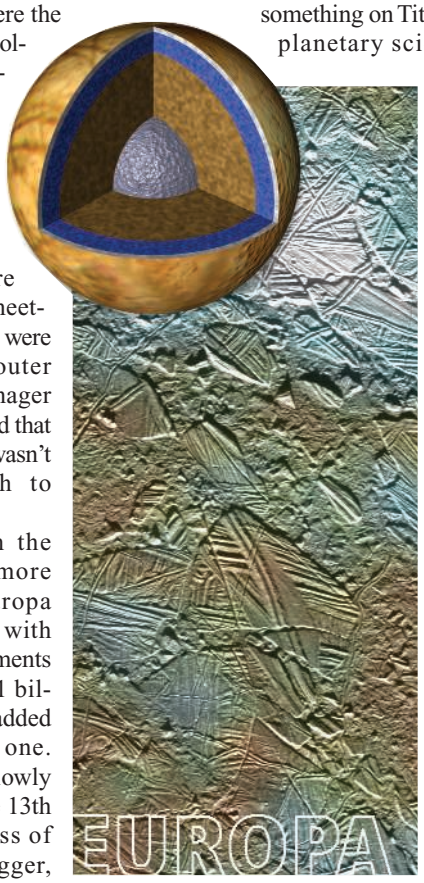

Looking deep. Another proposed joint NASA-ESA mission would probe Europa's ice shell (white in diagram) overlying an ocean (blue) to see whether the ice (above, enhanced color) has ever been breached.

Ready, set, ...

At the Tempe meeting, Ronald Greeley of Arizona State University, Tempe, NASA co-chair of the joint science definition team, declared that "the Europa Jupiter System Mission is essentially ready to go. Of course, the key driver is exobiology." And the theme of the proposed joint mission to the Jupiter system is the emergence of possibly habitable worlds. Both the NASA and the ESA spacecraft—to be launched in 2020 on separate rockets carrying a dozen instruments each—would first orbit Jupiter, probing its magnetosphere and flying by all four moons. NASA's would then enter Europa orbit to probe the ice shell with radar, size up the interior by gauging the ice's tidal flexing, and survey the geology and chemistry of the surface for signs that ocean water ever makes it to the exterior. Meanwhile, the ESA spacecraft would orbit Ganymede.

The Titan team's pitch is broader. "There's something on Titan for virtually all aspects of planetary science," was how Jonathan Lunine of the University of Arizona, Tucson, NASA co-chair of the Titan Saturn System Mission (TSSM) science team, described it. The mission would investigate how Titan functions as a system, determine how far prebiotic chemistry has developed, and continue exploring Enceladus with a series of flybys. A single rocket would deliver three craft: the NASA orbiter; ESA's lander targeted for a splashdown in one of Titan's larger liquid methane-ethane lakes; and an ESA nuclear-fired hot-air balloon that would circle the moon near its equator. "The technologies are ambitious, novel, and imaginative," said Athena Coustenis of the Paris Observatory in Meudon, France, and the TSSM team. "This is the way we need to go."

That will be up to NASA's Weiler and ESA's science head David Southwood. By the end of January, they will jointly select one mission to proceed. They are likely to be balancing the technological ambition of the Titan balloon and the 9-year travel time to Saturn against a science focus on Europa. After that, though, both NASA and ESA have years of maneuvering for funds ahead. NASA will need to navigate around the fallout from MSL; ESA will have to compete its outer planets mission against two astrophysics projects, and both must overcome budgetary woes from the financial crisis. As Green said, an outer planets flagship mission "is not a done deal."

–RICHARD A. KERR

CREDITS: NASA/JPL

PROFILE: ZACK BOOTH SIMPSON

An Artist Develops a New Image—With Aid of Bacteria

After dropping out of high school, Zack Booth Simpson became a video game programmer. Now he's at a university working with cutting-edge synthetic biology labs

Nearly 5 years ago, molecular biologist Edward Marcotte recalls, a high school dropout walked into his office at the University of Texas (UT), Austin, to talk shop. Despite the visitor's unconventional background, which included a stint as a video game programmer, Marcotte says that Zack Booth Simpson "won me over instantaneously. He was so clearly intelligent." They ended up talking for hours on topics such as Marcotte's use of data mining to extract information about the protein networks that control cellular functions.

That was just the beginning. Simpson now has a part-time paid position as a fellow at the university's Center for Systems and Synthetic Biology, where he's shared his expertise and ideas with several labs. His publication record, which includes coauthoring a paper in *Nature* and a chapter in a newly released book on synthetic cells, would make some postdocs envious. "He's jumped right into the top level of research," says Marcotte, who contributes some of his lab funds to Simpson's salary. "It wouldn't be exaggerating to say Zack changed some research directions in my lab—for example, stimulating my interests in synthetic biology and cell-to-cell variability." He can "span a variety of disciplines with relative ease, and he brings fresh and interdisciplinary perspectives to each field," adds Andrew Ellington, another UT Austin molecular biologist who's worked with Simpson for almost as long. Not bad for someone who was once held back by dyslexia and considers science his hobby.

More than 20 years after dropping out of high school during his junior year, Simpson, now 38, says his only regret was "not leaving earlier." He was bored, and teachers weren't helping him overcome his dyslexia. Without intending to, he managed on his own to surmount the reading disability by "geeking out" on computer manuals. Meticulously deciphering something he found interesting did what dull reading assignments couldn't, he says. His parents had divorced by the time he decided to quit school, and his mother, a landscape architect, backed his decision. "She thought I'd figure out my own way in the world."

She was right. After starting out as a "junior programmer" at a database company, by age 23 he'd worked his way up to director of technology at the Austin-based video game maker Origin Systems, which crafted bigsellers such as Wing Commander and Ultima. Then, like almost everyone else in the 1990s, Simpson and some friends started their own company. However, the inauspiciously named Titanic Entertainment went under after releasing only one game, NetStorm. It reportedly sold only 13,500 copies, although one Internet forum later tabbed it as "The Best Game of All Time that Nobody Bought." The lesson from the company's failure, he says, was that "I liked learning things more than I liked doing things."

It wasn't long before he was doing something else, collaborating with artists, engineers, and computer scientists on a series of interactive exhibits called Mine Control. The art installations have appeared everywhere from science museums to department stores, and in such far-flung locations as Norway, Mexico, and Ecuador.

Even children can fool around with Mine Control without alarming museum staff because what the children "handle"—light—can't break. Many of the exhibits use detectors Simpson developed to track a viewer's shadow, helping create the illusion of manipulating images that come from computer-controlled projectors. In one of the simplest exhibits, you stand in front of a screen on which multicolored sand appears to tumble from above. Hold out your hand, and the sand piles up in your palm's shadow on the screen. Many of the pieces have scientific themes, letting you tug and bend a Slinky-like RNA molecule, for example. Simpson's favorite, called Moderation, meshes the visual style of Japanese anime with an ecological message. How fast you walk around a pool projected onto the floor determines whether the virtual plants and other life that sprout in your footsteps thrive or die out. Walk too fast, and the virtual ecosystem dies out.

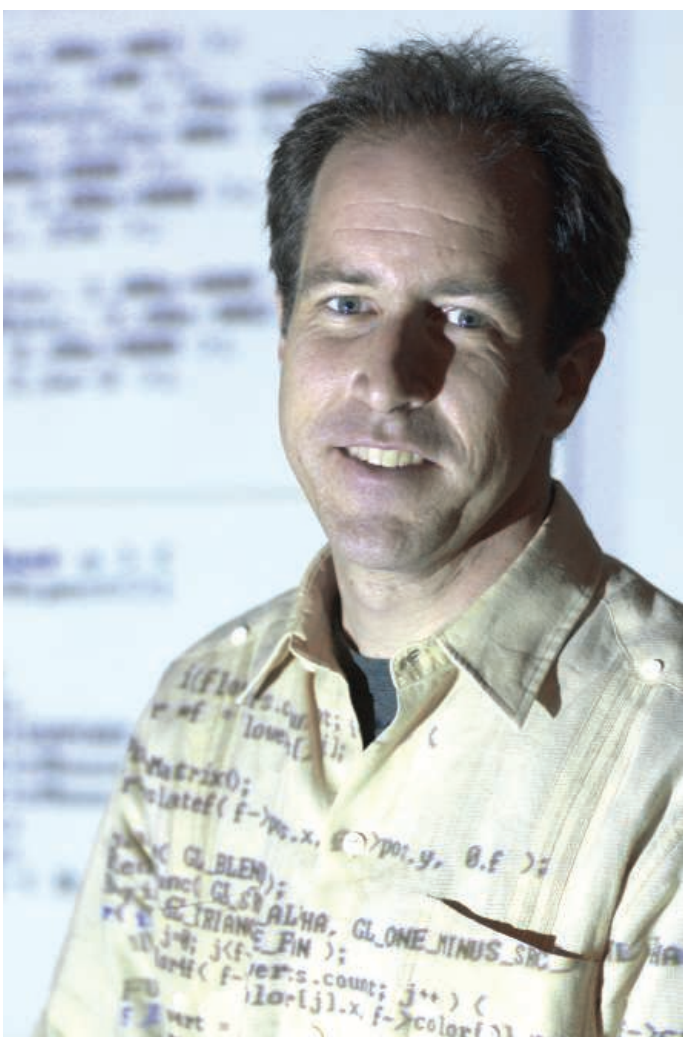

CREDIT: KEVIN GLINER

Bacterial snapshots

Although Simpson has lived just a few blocks from the UT campus in Austin for most of his adult life, he didn't try to forge a formal connection with the school until, after one-too-many conversations about the finer points of thermodynamics with his girlfriend, she recommended he find more nerd buddies. That inspired

Published by AAAS

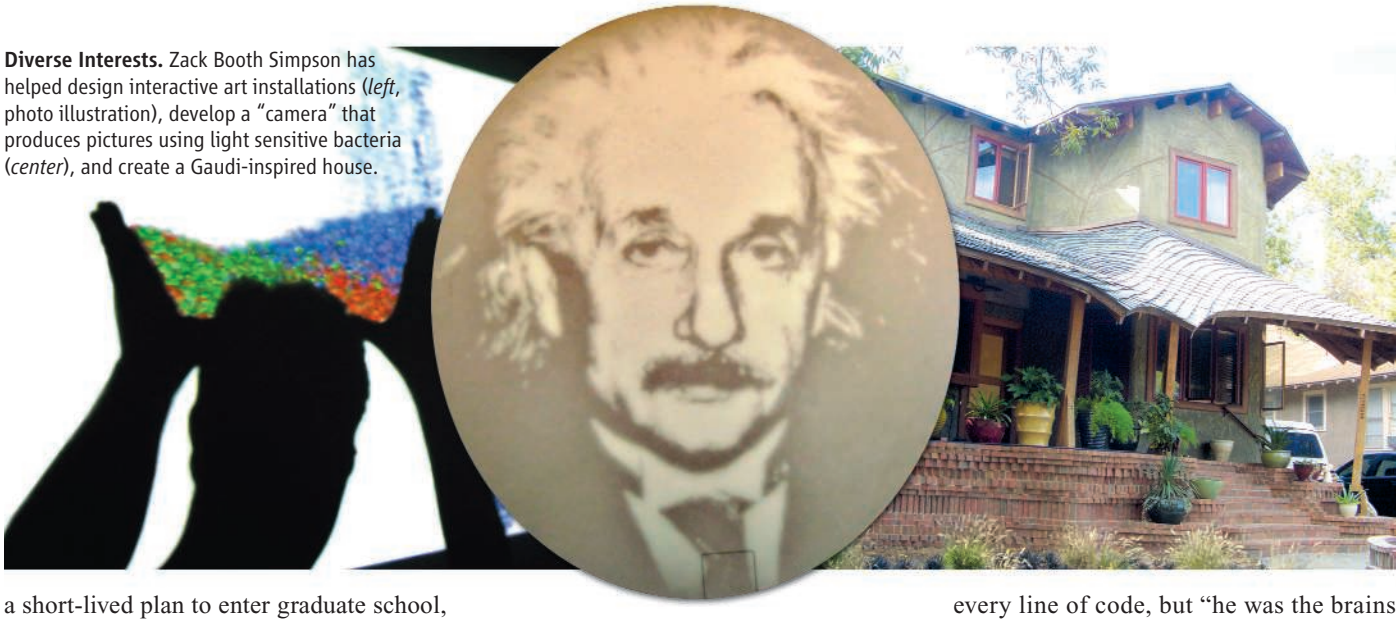

Diverse Interests. Zack Booth Simpson has helped design interactive art installations (*left*, photo illustration), develop a "camera" that produces pictures using light sensitive bacteria (*center*), and create a Gaudi-inspired house.

CREDITS: MINE CONTROL; JEFFREY TABOR AND MATTHEW GOOD/UNIVERSITY OF CALIFORNIA, SAN FRANCISCO; ZACK BOOTH SIMPSON

a short-lived plan to enter graduate school, which Simpson scuttled after learning that he'd first have to complete a high school equivalency program and an undergrad degree. Instead, he paid a visit to Marcotte.

Simpson arrived in time to help students working with Marcotte, Ellington, and colleagues devise a showstopping demonstration for the 2004 international Genetically Engineered Machine (iGEM) competition, a synthetic biology extravaganza in Cambridge, Massachusetts. The goal of this first-of-its-kind meeting was for teams of undergraduates to construct biological machines capable of performing some interesting task. Because he understood computational problems so well, Simpson's role was to urge everyone in the Austin labs to think big, recalls Ellington: "He was putting forward all these grand ideas for what molecules could do, and we were saying, no, no, maybe, no."

One of Simpson's big ideas was to use bacteria as an edge detector. Finding the boundary between objects is a standard task in image analysis and something software can achieve. But duplicating the feat biologically wasn't feasible, given the rapidly approaching iGEM deadline. So the team decided to focus on the project's first step: bacterial photography, in which microbes act like the light-capturing pixels on the sensor of a digital camera.

Simpson provided the concept, but the UT Austin team still needed tricked-up bacteria. There, they got lucky, says Marcotte. They learned that chemical engineer Christopher Voigt of the University of California, San Francisco (UCSF), and colleagues had created the perfect biopixel: a genetically modified bacterium that fashions black pigment in the dark but not in the light. A layer of the bacteria can take a picture with pretty good resolution—they are clearer than some photos from cell phone cameras—though the exposure times required are measured in hours rather than in fractions of a second, as they are for most conventional photographs. The UCSF and UT Austin teams joined forces and showed off their shutterbugs at the competition and in a 2005 *Nature* paper of which Simpson was a co-author.

The biological edge detector was next. Simpson explains that this project required engineering more astute bacteria than what were needed for photography. In an edge detector, a microbe not only has to determine whether it's in the light or dark but also has to know the status of its neighbors. Jeffrey Tabor, who was part of the biofilm team and is now a postdoc at UCSF, and colleagues have now built this device and plan to submit a paper describing it. Bacteria won't be replacing electronics anytime soon, Simpson says. But the two projects provide simple and striking examples of computation with cells rather than microchips. In the future, he says, researchers might build on the similarities between computers and life to create machines with capabilities of living things—repairing themselves if they break, for example, or growing from simpler structures.

Emulating Gaudi

Another scientist to benefit from Simpson's computational smarts is UT Austin biochemist Kenneth Johnson. Simpson helped program enzyme kinetics software now sold by the chemical instrument company Johnson founded. Simpson's contribution, the biochemist says, was applying his background in art and computer gaming to provide the software with intuitive controls and easy-to-understand output. Simpson didn't write every line of code, but "he was the brains behind what we did," Johnson says.

Simpson splits his time about 50–50 between his art—which brings in most of his income—and his scientific work. Those dual interests intersect in his fascination with "how processes beget shape." That fascination shows in the house he recently built in Austin, parts of which reveal the influence of the Spanish architect Antonio Gaudi. Although he wasn't a scientist, Gaudi scrutinized natural forms—not to copy them but to understand "the processes that made those shapes and use that as inspiration," Simpson says. For example, Gaudi designed pillars that branch like a tree or stand at an angle. A year in Barcelona, Spain, home of many of the architect's famous buildings, fed Simpson's love for that style, and Gaudiesque touches in his Austin home include the undulating eaves over the porch and the staircase, which was inspired by a dead, hollowed-out tree Simpson once saw. It's the kind of house that strangers stop by to photograph, says John Davis, an electrical engineering professor at UT Austin who has collaborated with Simpson scientifically and artistically.

Cynics might dismiss Simpson as a science dilettante. And he admits that he lacks the deep knowledge of someone who's been immersed for years in the biological literature. But Simpson believes that he compensates with a breadth of knowledge, from fields as diverse as economics and ecology, that allows him to see new ways to analyze a problem.

Ellington adds that Simpson's success suggests that there's room for more people in science who follow their own paths. "People who take charge of their education are unique, and that is unfortunate," he says. "We need more people like Zack who learn for the fun of it."

–MITCH LESLIE

Shortfalls in Electron Production Dim Hopes for MEG Solar Cells

Four years ago, researchers were delighted to discover that light-absorbing nanoparticles could readily generate more than one electron for every photon of light they absorb. Those extra charges, they hoped, would sharply increase the electrical output of future solar cells. But at the meeting, several teams reported setbacks in reaching that goal.

In typical solar cells, when a semiconductor such as silicon absorbs a photon of light with the right amount of energy, it generates an exciton: an electron paired to a positively charged electron vacancy called a hole. The solar cell then separates those opposite charges and collects them at the electrodes. In 2004, researchers led by Victor Klimov of the Los Alamos National Laboratory in New Mexico reported that when lead sulfide (PbS) nanocrystals were hit with high-energy photons from a laser, they could generate up to seven excitons. Other groups jumped in and found a similar multiple exciton generation (MEG) effect in a variety of other nanocrystals, including cadmium selenide (CdSe) and silicon.

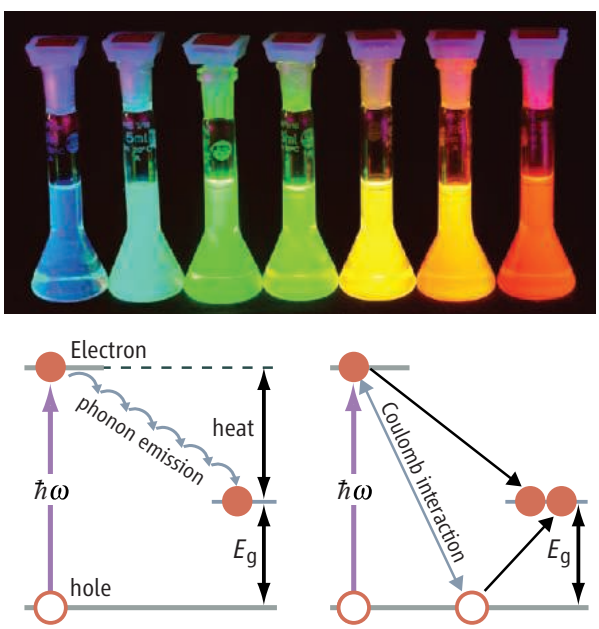

Whither MEG? When semiconductors absorb high-energy photons, they typically create an excited electron (*left*). In nanocrystals (*top*), MEG uses leftover energy to excite more electrons (*right*).

Then doubts began to creep in. Last year, Moungi Bawendi, a chemist at the Massachusetts Institute of Technology in Cambridge, and his Ph.D. student Gautham Nair reported that when they used a different technique, they spotted only a negligible MEG effect in CdSe nanocrystals, a result they later extended to PbS and lead selenide (PbSe). This year, a Dutch group that had previously reported a sharp increase in MEG in indium arsenide nanocrystals reported it couldn't reproduce the result. "The more results that came in, the more controversy there was," Klimov says.

At the meeting, John McGuire, a post-doctoral assistant from Klimov's group, reported new evidence that MEG in nanocrystals is far weaker than originally thought. In contrast to the 700% initially reported, the new Los Alamos results suggest the increase is likely about 40%, only slightly higher than the 25% increase seen by Bawendi's group. The upshot, both Bawendi and Klimov agree, is bad news. "These numbers at this point are not of practical use for solar energy," Bawendi says.

So what changed? Klimov says that for their current experiment, the results of which were also published online 12 November in *Accounts of Chemical Research*, the Los Alamos team stirred the samples to keep the nanoparticles from absorbing more than one photon at a time—a potential source of false-positive results.

Hope for a strong MEG effect isn't entirely lost, Klimov says. In some samples, the MEG effect was more than three times as high as in other samples. Synthetic differences between samples may have left some with surfaces that enhance the effect, he says—and if so, researchers may learn to engineer particles to optimize it.

Even if a large MEG turns out to be real, however, two separate teams found that getting those charges out of the nanocrystals won't be easy. Randy Ellingson of the National Renewable Energy Laboratory (NREL) in Golden, Colorado, reported that his group had made simple solar cells containing a layer of PbSe nanocrystals, with electrodes above and below. Creating the nanocrystals leaves them decorated with organic groups around the outside. When they are put straight into the films, the crystallites are too far apart to pass charges to the electrodes, where they can be sent through a circuit to do work. So in their current study, Ellingson and his team treated their nanocrystals with hydrazine, which shortened the organic groups and allowed the nanocrystals to sit closer to one another. The solar cells worked. But spectroscopic studies suggested that the hydrazine treatment killed the MEG effect.

Meanwhile, Byung-Ryool Hyun, a graduate student in Frank Wise's group at Cornell University, reported another challenge in getting charges out of PbS. In this case, the nanocrystals were linked to titanium dioxide (TiO_2) nanoparticles. When electrons are generated in the nanoparticles, they should move readily to the TiO_2. But Hyun reported that electrons moved so slowly that the charges typically recombined with holes and gave up their energy before the TiO_2 could snag them.

So is this the end of the road for MEG? Arthur Nozik, who has helped lead the MEG effort at NREL, says he hopes not. "It's kind of a messy situation," he says. He's hopeful that further research will reveal ways to produce a large MEG effect. For now, however, hopes are dimming for MEG solar cells.

Protein Chip Promises Cheaper Diagnostics

Ever since recent advances made it possible to study thousands of genes and proteins at once, researchers have dreamed of nipping diseases in the bud by spotting telltale proteins with simple blood tests. So far, that vision remains a long way off. Few individual proteins in blood and tissues have proven to be conclusive indicators of disease. Even if they were, clinical lab tests that measure proteins don't come cheap. Standard diagnostic panels can cost $50 each or more. At that price, scanning millions of patients for dozens or more proteins would cost a fortune. But new glass and plastic microfluidic chips could begin to change that equation.

At the meeting, James Heath, a chemist at the California Institute of Technology

Graphene Recipe Yields Carbon Cornucopia >>

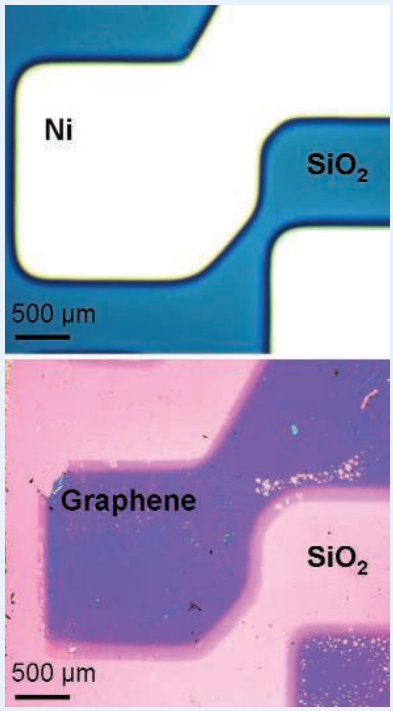

Film star. Graphene is prized for its electrical properties. Now, researchers can make sheets of the atomically thin material and pattern them for devices.

The hottest material in physics these days is graphene, sheets of carbon just a single atom thick. Graphene is flexible yet harder than diamond. It conducts electricity faster at room temperature than anything else. And it's nearly transparent, a handy property for devices such as solar cells and displays that need to let light through. The only trouble is that people have been able to make only small flakes of the stuff—until now.

At the meeting, Alfonso Reina Cecco, a graduate student in chemist Jing Kong's lab at the Massachusetts Institute of Technology (MIT) in Cambridge, reported that he and several colleagues have come up with a cheap, easy way to grow high-quality graphene films and then transfer them wherever they want. "That's a big deal," says Andre Geim, a physicist at the University of Manchester, U.K., who first reported making graphene (*Science*, 22 October 2004, p. 666). "It promises wafers [of graphene]. That changes everything." It opens the door both to better ways of exploring the new physics of atomically thin materials and to potential applications.

To create the first graphene sheets in 2004, Geim peeled single layers of graphene off chunks of graphite with clear tape. But that low-tech approach would be hard to scale up for industrial use. Researchers at the Georgia Institute of Technology in Atlanta came closer in 2004 by growing graphene films atop a substrate made of silicon carbide. But silicon carbide is expensive and must be processed in an ultra-high vacuum, which also raises the cost.

At the meeting, Cecco reported that the MIT team had done away with the silicon carbide. Instead, they deposited a film of nickel atop a standard silicon wafer. They then used a conventional film-growing technique known as chemical vapor deposition to add graphene in either a single sheet or a stack of a few sheets.

To transfer their graphene sheets to another surface, the MIT team coated it with a polymer known as PMMA, then etched away the silicon and the nickel after that, leaving only the graphene on the polymer film. Finally, they covered the newly reexposed graphene surface with glass and then dissolved away the PMMA. By initially patterning the nickel layer, Cecco and his MIT colleagues also showed that they could make graphene films in arbitrary patterns, such as those typically used to make electronic devices. The same day Cecco gave his talk, a paper on the topic was published online in *Nano Letters*.

This ability to pattern and place graphene wherever it's needed, Geim says, will only increase the amount of research done with the material, ensuring that it will stay among the hottest materials in physics. **–R.F.S.**

(Caltech) in Pasadena, reported that his team has made microfluidic chips that can detect and quantify levels of a dozen different proteins in blood plasma simultaneously. What is more, the test needs only a single drop of blood, which it can analyze in less than 10 minutes. Because such chips are cheap and easy to manufacture, they could drop the lab costs to just pennies per test, Heath says.

"If we can develop simple devices [for finding disease markers in plasma], that could be a big development for global health," says Samir Hanash, a proteomics expert at the Fred Hutchinson Cancer Research Center in Seattle, Washington. Still, even though this new device makes strides toward that goal, he cautions that proving the device can work reliably under a wide range of conditions remains a distant prospect.

In coming up with their new chip, Heath's team combined recent innovations in microfluidic chips and DNA arrays, both of which have been advancing rapidly in recent years. The Caltech researchers used standard microfluidic chip-patterning techniques to carve a series of large and small channels in a thin polymer film. Then they bonded the film to a glass slide patterned with 12 strips of antibodies to specific proteins. The resulting device separates blood plasma from whole blood cells, then steers the plasma and the proteins it contains over the antibody arrays for analysis. Fluorescence analysis then reveals any proteins bound to the array, creating a bar-code readout of which proteins are present from each blood sample. When different concentrations of the same antibodies are placed on different strips, the chips can also determine the abundance of target proteins as well.

Using their new chip, the members of the Caltech team showed that they could sort 22 cancer patients into different groups based on which of 12 different proteins associated with cancer were in their blood. Heath says he and his colleagues have formed a company in hopes of commercializing the technology.

–ROBERT F. SERVICE

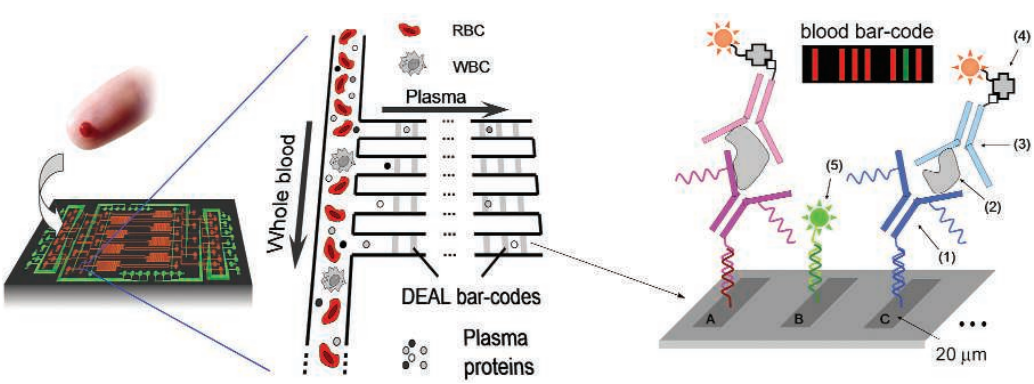

Quick scan. A new biochip analyzes a single drop of blood plasma for up to a dozen different protein indicators of disease. Because the new chips are cheap and fast, they could revolutionize medical diagnostics.

Published by AAAS

Low-fat sprat. As their prey becomes leaner, North Sea guillemots may go hungry.

MARINE MAMMALS

Does 'Junk Food' Threaten Marine Predators in Northern Seas?

Some fish-eating birds and mammals have full bellies but poor diets, say biologists puzzling over declines among these high-latitude marine predators

In 2004, ecologist Sarah Wanless was observing a colony of guillemots on the Isle of May off the coast of southeast Scotland. These diving seabirds were having a terrible breeding season in the United Kingdom, and some colonies hatched no chicks at all. But Wanless could see that parent birds were catching as many fish as ever, if not more. "We couldn't work out what was going wrong," she said. The light dawned when she and her colleagues measured the fat and protein in the fish being caught, mostly sprat, a member of the herring family. Compared with previous years, the amount of energy a hungry guillemot received from a 10-centimeter sprat plunged in 2004, dropping from 55 kilojoules to 12 kilojoules. "They were largely water," Wanless says.

Wanless concludes that the guillemots (*Uria aalge*) were suffering from a diet of what some ecologists have called marine "junk food." They hypothesize that in some cases, marine predators' prey is being replaced by less nutritious species or, like the sprat, becoming leaner. Human junk food is fatty fare, but for these high-latitude birds and mammals it is the opposite—food without enough fat and energy to sustain them.

The highest-profile possible victim of marine junk food is the endangered Steller sea lion, which has seen a massive decline in its Alaskan population. But some researchers say the sea lion data point to suspects such as overfishing rather than junk food (*Science*, 4 April, p. 44). Among northern seabirds, however, researchers are finding multiple examples of struggling populations eating low-quality diets. The details vary among species, but a growing consensus holds that this is one result of climate-driven changes to food webs, which are disrupted as northern seas warm. "Until recently, we were preoccupied with how much food there was, and where. But what the food is can also be crucial," says Wanless, who works at the Centre for Ecology and Hydrology in Edinburgh, U.K.

Birth of an idea

The junk-food hypothesis, as it's become known to the chagrin of some of the researchers working on it, was born in the early 1990s. John Piatt, a seabird ecologist at the U.S. Geological Survey Alaska Science Center in Anchorage, noticed that some colonies of common murres—the American name for guillemots—in the Gulf of Alaska had not recovered as expected from the 1989 *Exxon Valdez* oil spill. Piatt knew that murres and other seabirds were eating mainly juvenile walleye pollock. But gut content data from the early 1970s showed that they had been eating mostly capelin, an oily fish in the smelt family. A gram of capelin can contain up to twice as many calories as a gram of pollock, a lean white fish related to cod. In experiments using captive chicks of a variety of seabird species, those fed oily fish gained weight much more quickly than those fed pollock. Piatt thought this dietary shift might explain the murre's decline.

But what drove that shift? In the mid-1970s, before the spill, capelin numbers plunged while pollock's surged, as reflected in the catch brought up by research trawlers and the growth of the pollock fishery. This also coincided with a flip in a climate cycle called the Pacific Decadal Oscillation (PDO), which warmed the ocean surface off western Alaska by about 1°C in the space of a few months in late 1976. Except for a cool spell between 1998 and 2002, and another that began in late 2007 and which is as yet too brief to call a reversal, that region of water has been relatively warm ever since. The mid-1970s flip is also around the time when numbers of Steller sea lions in western Alaska began to plummet; in the early 1990s, marine biologist Dayton Alverson of Natural Resources Consultants Inc. in Seattle, Washington, independently wondered whether a switch from eating oily fish to pollock was the cause. In 1991, bird and mammal researchers, including both Alverson and Piatt, met to review seabird declines. At the meeting, seabird ecologist Scott Hatch, also of the Alaska Science Center, says he coined the phrase "junk-food hypothesis."

To test the idea, in 2000, marine-mammal researchers Andrew Trites and David Rosen of the University of British Columbia in Vancouver, Canada, fed captive sea lions either pollock or herring. Adults could survive on pollock, they found, but yearlings could not eat enough to sustain themselves. The animals needed to eat more than 20% of their own body weight in pollock each day, but their stomach capacity only allowed them to consume 17% to 18%. "We gave animals as much pollock as they would eat, and they were losing weight," Trites says. The fact that the Steller sea lion population has actually

Down, down, down. In Scotland, the total abundance of 13 species of breeding seabirds has been dropping since the 1980s.

CREDITS: MIKE HARRIS; SOURCE: THE SCOTTISH GOVERNMENT

Published by AAAS

increased in southeast Alaska, where the PDO shows the opposite pattern, also tends to confirm the junk-food/climate hypothesis.

But some sea lion experts aren't convinced. "Lab work suggests the juveniles are most vulnerable to low-quality prey," says Lowell Fritz of the National Marine Fisheries Service in Seattle. "But we're not seeing that result currently in the field. We should have seen starving animals, but we didn't—we just saw them not there." Fritz thinks the sea lions were more likely hammered by deliberate shooting and by-catch in fisheries. He also thinks the PDO's effects on fish have been overstated. "I'm not convinced you can see any links [to ocean conditions] beyond the phytoplankton. I'm not seeing a direct link to fish."

Trites says that perhaps juvenile sea lions are scarce because adult females adapted to a low-fat diet by spacing out breeding. Looking at the condition of adult females might settle the question, but those studies haven't been permitted because of animal-welfare concerns. Although they seek to do more studies, Trites and Fritz agree that the cause of the sea lions' original decline may never be known.

The ultimate junk food

As researchers puzzle over Alaska's sea lions, other scientists report that the Baltic Sea has also shifted ecological regimes, at least in part thanks to humans. In the late 1980s, there was a boom in the sprat population, triggered by a combination of warming seas and heavy fishing of the sprat's main predator, cod. This abundance of small, oily fish ought to have been good news for the sea's guillemots, but in fact chick weights dropped through the 1990s, before recovering as cod stocks have regrown, says marine ecologist Henrik Österblom of the Stockholm Resilience Centre. "We thought that because sprat increased, that chick condition would improve. Instead we found the opposite," he says. The North Sea also experienced large ecological changes in the late 1980s, leading to the bad breeding season Wanless observed in 2004, the worst on record, according to the U.K. government's Seabird Monitoring Programme.

The changes to Baltic sprat are some of the best field evidence for the junk-food hypothesis: As the number of sprat went up, the nutritional worth of each fish in the crowded population went down, say Österblom and his colleagues. This matters to guillemots, because they deliver one fish at a time to their chick, "so what that fish contains is incredibly important," says Österblom.

In the past 5 years, the menu for North Sea birds has become even less promising. For reasons that aren't understood, large numbers of snake pipefish, a relative of seahorses, have appeared in these predator's diets. The pipefish have tough skins and are virtually fat-free: "It's the ultimate in junk food," says Wanless. British birders have spotted starving kittiwake chicks—a marine gull that usually eats oily sand eels—surrounded by the corpses of uneaten pipefish.

A junk-food diet can increase mortality in more roundabout ways. In 2004, for the first time, Wanless saw a pair of guillemot parents fishing at the same time, leaving their chick unattended. This atypical behavior has increased year-on-year, and last September, she and her colleagues revealed its consequences in *Biology Letters*: A growing number of chicks are being killed by their adult neighbors in the colony. Malnourishment has more subtle effects, too: A team including Piatt found that kittiwakes reared on low-fat fish in captivity showed higher levels of stress hormone and cognitive deficits. "We measure things that we can, such as growth rate, but hidden behind this could be physiological stresses that put birds at a disadvantage," he says.

At risk. Researchers still debate whether "junk food" led to the decline of the endangered Steller sea lion or whether overfishing is to blame.

CREDIT: A. W. TRITES/UBC MARINE MAMMAL RESEARCH UNIT

In the North Sea, bad breeding seasons for birds are becoming more common (see graph). This summer, the U.K.'s Royal Society for the Protection of Birds reported that "virtually no" chicks fledged from some kittiwake and tern colonies. The main cause is thought to be changes to fish populations due to fishing and the effects of global warming on fishes' planktonic food species, because the North Sea is now 1.5°C warmer than it was 40 years ago. The warming has resulted in a 70% drop in the populations of a tiny crustacean called *Calanus finmarchicus*, thought to be the main food of sprat and sand eels, as well as a rise in the numbers of a warm-water relative, *C. helgolandicus*, which contains much less fat and so is junk food for the fish. So the spread of *C. helgolandicus* makes these fish both fewer in number and leaner.

In another twist, *C. finmarchicus* itself may have become junk food for other seabirds: Its range has shifted north by about 1600 kilometers, and it is now displacing the even larger and fattier *Calanus* species that support vast colonies of little auk, a crustacean-eating relative of the guillemot, in Greenland and Norway. In the long run, little auk numbers might decline and those of fish-eating birds such as guillemot might start to increase in these areas, says seabird ecologist Morten Frederiksen of the University of Aarhus in Denmark. "We might be seeing the whole system shifting north, with junk food–related problems developing at the northern and southern boundaries of the climate zones."

These studies show that "junk food" takes different forms and has different consequences for various species. So does it make sense to group the effects on North Sea guillemots with those on North Pacific sea lions? Seabird ecologist Robert Furness of the University of Glasgow in the U.K. has his doubts. "The junk-food hypothesis is an attractive term but a bit misleading," he says. "Each ecosystem is unique." In his view, simple issues of food quantity—such as the current low sand eel populations in the North Sea—will most often be the critical determinant of predators' health. Frederiksen adds that researchers aren't yet sure how to separate the effects of quantity from those of quality: "Working out how much the problems are a junk-food issue and how much is lack of food is difficult."

But Trites argues that there is an overarching message. "People have to realize that not all fish were created equal," he says. Should that message hit home, the only thing left to fix will be the name. Trites thinks a better analogy for predators' woes is a diet of celery. Piatt agrees: "Junk food is very fatty," he says. For animals, "it's the lean cuisine that's the problem."

–JOHN WHITFIELD

John Whitfield is a London science writer.

Land art
1791

Research grant allocation process
1797

LETTERS | BOOKS | POLICY FORUM | EDUCATION FORUM | PERSPECTIVES

LETTERS

edited by Jennifer Sills

Making Waves with the Clean Water Act

THE LETTER OF R. E. DODGE *ET AL*., "A CALL TO ACTION FOR CORAL REEFS" (10 OCTOBER, P. 189), lists actions needed to reverse the decline of coral reefs. Although a primary management tool in nearshore environments, marine protected areas (MPAs) are not designed to protect coral reefs from land-based activities or threats that originate outside MPA boundaries (*1*).

In contrast, the objective of the U.S. Clean Water Act (PL 92-500, Sec. 101, 33 U.S.C. 1251) is to "restore and maintain the … biological integrity of the Nation's waters" for all "territorial seas … measured from the line of ordinary low water … and extending seaward a distance of three miles" [Sec. 502, 33 U.S.C. 1362(8)]. Under the Clean Water Act, and with approval of the U.S. Environmental Protection Agency (EPA), states and territories could define biological thresholds for reef condition as part of their water quality standards. Although thresholds have been defined for coral reefs (e.g., coral cover is greater than 10%), states and territories have yet to adopt them as biological criteria (*2*). Failure to meet defined criteria can trigger regulatory actions to support restoration.

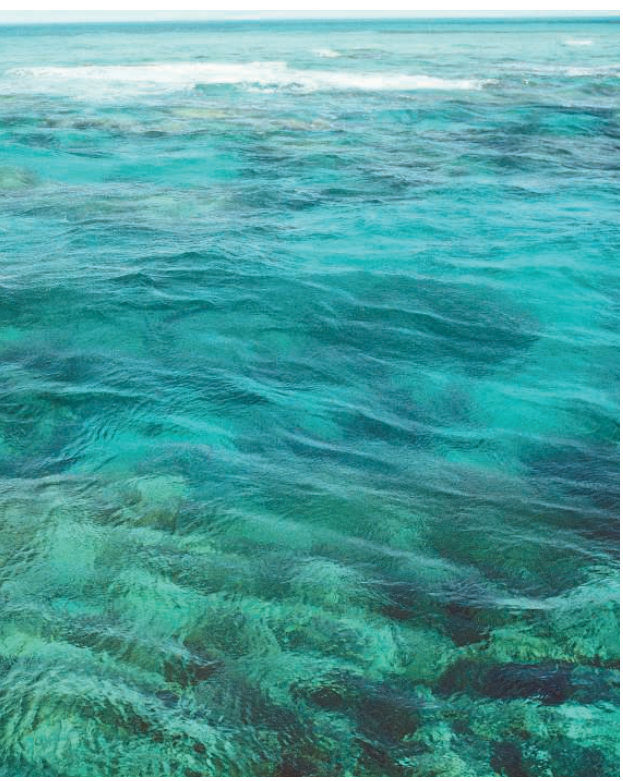

So why has the Clean Water Act never been used specifically to protect coral reefs? Many scientists and managers still mistakenly associate the Clean Water Act with a narrow focus on end-of-pipe chemical contaminants (*3*), but the law actually calls for reduction of all human actions that degrade water resources. Recently, EPA and the states have embraced assessments of fish, invertebrates, and plants as measures of environmental condition (*4*).

Actions taken under the Clean Water Act have vastly improved freshwater and estuarine environments (*5*); similar actions can answer Dodge *et al*.'s call to conserve reefs and nearshore environments. Successful use of the Clean Water Act and biological criteria in U.S. jurisdictions could provide a template for countries with analogous legislation.

LESKA S. FORE,[1]* JAMES R. KARR,[2] WILLIAM S. FISHER,[3] WAYNE S. DAVIS[4]

[1]Statistical Design, 136 NW 40th Street, Seattle, WA 98107, USA. [2]190 Cascadia Loop, Sequim, WA 98382, USA. [3]U.S. Environmental Protection Agency, Office of Research and Development, 1 Sabine Island Drive, Gulf Breeze, FL 32561, USA. [4]U.S. Environmental Protection Agency, Office of Environmental Information, 701 Mapes Road, Fort Meade, MD 20755, USA.

*To whom correspondence should be addressed. E-mail: leska@seanet.com

References

1. B. S. Halpern, *Ecol. Appl.* **13**, S117 (2003).
2. Healthy Reefs Initiative, *Report Card for the Mesoamerican Reef: An Evaluation of Ecosystem Health* (Healthy Reefs for Healthy People, 2008); www.healthyreefs.org/Report_Card/Report_2008/Report_2008index.html.
3. R. H. Richmond *et al*., *BioScience* **57,** 598 (2007).
4. J. R. Karr, C. O. Yoder, *J. Environ. Eng.* **130**, 594 (2004).
5. T. P. Simon, Ed., *Biological Response Signatures: Indicator Patterns Using Aquatic Communities* (CRC Press, Boca Raton, FL, 2002).

The State of Global Hunger

WITH THE PASSING OF ANOTHER WORLD DAY Against Hunger (on 30 October), it is time to take stock of the state of global hunger. Sadly, Millennium goals are still far from being reached, and over 800 million people suffer from malnutrition in the world. The latest core health indicators from the World Health Organization show that many countries still have high rates of chronic malnutrition (>30%) and under-five mortality (>20%) (*1*). Humanitarian aid is insufficient and is hindered even more by wars, political instability, dictatorships, and corruption.

There are two major obstacles to collecting food aid from developed countries. One is cost: World Food Programme activities are extremely expensive. The other is motivation: People only think to donate during emergencies such as wars and tsunamis, when in fact aid is needed at all times.

I have two suggestions that may help us move in the right direction. First, to avoid increases in the price of basic food, the Food and Agriculture Organization should buy low-cost arable lands for agriculture production and use the food grown to help populations suffering from hunger. Second, to provide aid more consistently, Western countries that produce surpluses should send extra food to the World Food Programme for distribution. For instance, in Spain in 2007 there were thousands of tons of surplus oranges that were not harvested (*2*–*4*). It is wrong to limit agricultural productivity when there are millions of people dying of hunger in other countries.

JUAN SASTRE

President of Alimentos Mundi and Department of Physiology, School of Pharmacy, University of Valencia, Avenida Vicente Andrés Estellés s/n, 46100 Burjassot (Valencia), Spain. E-mail: juan.sastre@uv.es

Published by AAAS

Origins of paternal care

1799

Ethical limits of robot use

1800

References

1. World Health Organization, *World Health Statistics Report* (WHO, Geneva, Switzerland, 2008); www.who.int/whosis/whostat/en/.
2. V. Alapont, "Las soluciones ante la crisis citrícolas no satisfacen a nadie," *Valencia Fruits*, No. 2.289, S. L. Sucro, Ed. (Valencia, Spain, 16 January 2007), p. 3.
3. A. Alonso, "Desorientación," *Valencia Fruits*, No. 2.290, S. L. Sucro, Ed. (Valencia, Spain, 23 January 2007), p. 4.
4. Asociación Valenciana de Agricultores (AVA-ASAJA), "La crisis citrícola desencadena una oleada de movilizaciones en toda la Comunitat," *Agricultores y Ganaderos* **161**, 6 (2007).

Bird Brains Key to the Functions of Sleep

IN THEIR LETTER "A BIRD'S EYE VIEW OF SLEEP" (24 October, p. 527), N. C. Rattenborg *et al*. argue that birds "provide a largely untapped opportunity to determine the functions of these [sleep] states in mammals." We wholeheartedly agree that birds make excellent model organisms for the study of sleep. However, these authors seem unaware of the fact that the opportunity has in fact been seized, with fascinating results.

Recently, Low and colleagues (*1*) demonstrated that the structure of sleep in zebra finches is remarkably similar to that of mammals. It has become apparent that sleep plays an important part in avian learning and memory. Working with zebra finches, Dave and Margoliash found "replay" of neuronal activity during sleep that was similar to activity observed when the bird was singing (*2*). In addition, Deregnaucourt *et al*. showed that sleep influences song acquisition in young zebra finches (*3*). Further advances were made in the other major avian memory paradigm, imprinting in domestic chicks. Work from Gabriel Horn's laboratory (*4*) has revealed that a period of sleep immediately after imprinting training is necessary for memory consolidation. In both of these avian paradigms, the neural substrate of memory has been localized—an issue that is still contentious in most mammalian models (*5*). Thus, research on birds has already made considerable advances when it comes to unraveling the functions of sleep.

SHARON M. H. GOBES AND JOHAN J. BOLHUIS*

Department of Behavioural Biology, Utrecht University, Padualaan 8, 3584 CH Utrecht, Netherlands.

*To whom correspondence should be addressed. E-mail: j.j.bolhuis@uu.nl

References

1. P. S. Low *et al.*, *Proc. Natl. Acad. Sci. U.S.A.* **105**, 9081 (2008).
2. A. S. Dave, D. Margoliash, *Science* **290**, 812 (2000).
3. S. Deregnaucourt *et al*., *Nature* **433**, 7027 (2005).
4. C. Jackson *et al*., *Curr. Biol*. **18**, 393 (2008).
5. J. J. Bolhuis, M. Gahr, *Nat. Rev. Neurosci*. **7**, 347 (2006).

Old Seeds Coming in from the Cold

S. SALLON AND COLLEAGUES ("GERMINATION, genetics, and growth of an ancient date seed," Brevia, 13 June, p. 1464) reported the successful germination and growth of a 2000-year-old date seed excavated from underneath a Herodian fortress near the Dead Sea. On the basis of radiocarbon dating of additional seeds recovered from the same excavation as well as seed remains recovered when repotting the palm seedling, S. Sallon *et al.* claimed to have found the oldest seed with the ability to germinate.

However, Sallon *et al*. overlooked a report on a considerably older germinable seed, published in *Science* more than 40 years ago (*1*) [although the paper did appear in the bibliography of one work cited by Sallon *et al*.: Shen-Miller *et al.* (*2*)]. Porsild and co-workers convincingly showed that a seed of the arctic lupine (*Lupinus arcticus*), stored in a lemming burrow since the Pleistocene, could still be germinated. These authors estimated that the seed was at least 10,000 years old, based on the stratigraphic inference of the overlaying frozen silt deposit. Analogous to the dry climate that conserved the date seed, frozen ground provides excellent storage conditions to retain seed viability.

FELIX GUGERLI

Ecological Genetics and Evolution, WSL Swiss Federal Research Institute, 8903 Birmensdorf, Switzerland. E-mail: gugerli@wsl.ch

References

1. A. E. Porsild, C. R. Harington, G. A. Mulligan, *Science* **158**, 113 (1967).
2. J. Shen-Miller, M. B. Mudgett, J. W. Schopf, S. Clarke, R. Berger, *Am. J. Bot.* **82**, 1367 (1995).

Response

GUGERLI CLAIMS THAT ARCTIC LUPINE (*Lupinus arcticus*) are the oldest seeds to be germinated. Much controversy exists over reports of extreme seed longevity under "natural" conditions (as opposed to ex situ storage and conservation of seeds in gene banks). Claims that have been viewed skeptically include alleged viability of ancient cereal grains from Pharonic tombs (*1*); *Chenopodium album* and *Spergula arvensis* from a 1700-year-old site in Denmark (*2*); *Nelunbo nucifera* seeds associated with a 3000-year-old canoe near Tokyo (*3*); and, most extreme, *Lupinus arcticus* seeds retrieved from rodent burrows allegedly dating to the Late Pleistocene period (*4*). In all of these reports, seed dating relied on their association with archaeological artifacts, circumstantial evidence that makes the claims extremely questionable (*1*, *5*–*8*).

The age attribution of the arctic lupine seeds, unearthed 3 to 6 meters below the surface of frozen silt during 1955 mining operations in the Canadian Yukon, was based partly on the identification of a rodent skull also found in the burrow. The modern relative of the *Dicrostoyx groenlandicus* rodent species is apparently found in cooler regions, and the authors assumed that the overlying silt had been frozen during an unspecified geophysical catastrophe. The supporting radiocarbon date of 14,860 ± 840 relates to the nest and remains of an Arctic ground squirrel recovered from burrows similarly buried under permafrost in central Alaska (*9*, *10*).

Without radiocarbon dating of any of the two dozen arctic lupine seeds recovered from the burrows, unequivocal evidence for the contemporaneity of the seeds is lacking. In our Brevia, the claim for germi-

Letters to the Editor

Letters (~300 words) discuss material published in *Science* in the previous 3 months or issues of general interest. They can be submitted through the Web (www.submit2science.org) or by regular mail (1200 New York Ave., NW, Washington, DC 20005, USA). Letters are not acknowledged upon receipt, nor are authors generally consulted before publication. Whether published in full or in part, letters are subject to editing for clarity and space.

CREDIT: JUPITER IMAGES

nating a 2000-year-old date seed was based on direct radiocarbon dating of seed coat fragments from the seed itself and indirectly on two ungerminated date seeds from the same archaeological site and locus. Therefore, although we have not claimed that this is the oldest viable seed, it is the oldest seed in which germination has been documented based on validated direct radiocarbon evidence.

SARAH SALLON,[1]* YUVAL COHEN,[2] MARKUS EGLI,[3] ELAINE SOLOWEY,[4] MORDECHAI KISLEV,[5] ORIT SIMCHONI[5]

[1]Louis Borick Natural Medicine Research Center, Hadassah Hospital, Jerusalem 91120, Israel. [2]Department of Fruit Tree Sciences, Agricultural Research Organization, Volcani Research Center, Israel. [3]Radio-Carbon Laboratory, Department of Geography, University of Zurich, Winterthurerstrasse 190, Zurich, Switzerland. [4]Arava Institute of the Environment, Kibbutz Ketura, 88840, Israel. [5]Mina and Everard Goodman Faculty of Life Sciences, Bar-Ilan University, Ramat-Gan, Israel.

*To whom correspondence should be addressed. E-mail: ssallon@hadassah.org.il

References

1. D. A. Priestly, *Seed Ageing: Implications for Seed Storage and Persistence in the Soil* (Comstock Associates, Ithaca, NY, 1986).
2. S. Odum, *Dansk Botanisk Arkiv* **24**, 1 (1965).
3. H. Goodwin, E. H. Willis, *Radiocarbon* **6**, 132 (1964).
4. A. E. Porsild, C. R. Harington, G. A. Mulligan, *Science* **158**, 113 (1967).
5. J. D. Bewley, M. Black, in *Seeds Physiology and Development* (Plenum, New York, 1994), pp. 388–392.
6. H. Godwin, *Nature* **220**, 708 (1968).
7. J. D. Bewley, M. Black, *Viability, Dormancy, and Environmental Control*, vol. 2 of *Physiology and Biochemistry of Seeds in Relation to Germination* (Springer-Verlag, New York, 1982).
8. M. I. Daws, J. Davies, E. Vaes, R. van Gelder, R. H. Pritchard, *Seed Sci. Res.* **17**, 73 (2007).
9. C. A. Repenning, D. M. Hopkins, M. Rubin, *Arctic* **17**, 176 (1964).
10. T. L. Pewe, D. M. Hopkins, J. L. Giddings, in *The Quarternary of the United States*, H. E. Wright, D. G. Frey, Eds. (Princeton Univ. Press, Princeton, NJ, 1965), pp. 355–374.

CORRECTIONS AND CLARIFICATIONS

Editorial: "Scientists and human rights" by L. Rubenstein and M. Younis (28 November, p. 1303). Leonard Rubenstein is a Jennings Randolph Senior Fellow at the United States Institute of Peace, not a Randolph Jennings Senior Fellow as originally printed.

Reports: "Measurement of the distribution of site enhancements in surface-enhanced Raman scattering" by Y. Fang *et al*. (18 July, p. 388). The term $d\eta$ was inadvertently left off the right side of Eq. 4. The correct equation should read

$$P(\eta)\,d\eta = \frac{A}{\eta^{1.75}} \exp\left(\frac{-\eta^{0.25}}{A'}\right) d\eta$$

We thank M.-W. Shao and G. Shao for bringing this to our attention.

Reports: "Declining wild salmon populations in relation to parasites from farm salmon" by M. Krkošek *et al*. (14 December 2007, p. 1772). This correction summarizes small changes to the statistical results written in the main text of the Report on the effects of sea lice infestations on pink salmon population dynamics. Small changes have also been made to data set S1 and tables S2 and S3 in the Supporting Online Material. The changes to the statistical results do not affect the conclusions of the report.

The changes arise due to revisions of 11 escapement estimates for exposed populations that were not present in the original data provided to the authors by the Canadian Department of Fisheries and Oceans. The changes have been confirmed by Brian Riddell, Division Head, Salmon Assessment and Freshwater Ecosystems, Pacific Biological Station, Fisheries and Oceans Canada.

Population growth rates. The population growth rate r was estimated from the Ricker model for four groups of data. There are small changes to the point estimates of r as well as the 95% confidence intervals. The changes are summarized in Table 1. The associated estimate of b for density-dependent mortality has changed from its original value of 0.64 to its corrected value of 0.65.

Population viability analysis. In this section, a population viability analysis was applied to pink salmon populations in the Broughton Archipelago during sea lice infestation years. Small changes to the results are summarized in Table 2.

Louse-induced salmon mortality. The Ricker model was extended to test whether including louse-induced mortality of wild pink salmon improved the fit of the model. The analysis consisted of estimating a parameter a. The point estimate for the parameter has changed from 0.89 to 0.90. The 95% credible intervals for the parameter a from the analysis using the unconstrained data changed from 0.46 to 1.34 in the original analysis to 0.47 to 1.34 using the corrected data set.

Reports: "Evolution of scleractinian corals inferred from molecular systematics" by S. L. Romano and S. R. Palumbi (2 February 1996, p. 640). In Note 14, the coral-specific primer 16Sc-H was erroneously described as 5′-AACAGCGCAATAACGTTTGAGAG-3′. It should have been reported as being in the 3′-5′ direction, that is, 5′-CTCTCAAACGTTATTGCGCTGTT-3′.

Point estimates and 95% confidence intervals for the population growth rate *r* from the Ricker model fit to grouped pink salmon escapement data.

Data set used	Group	*r*	95% confidence interval (CI)
Original	Unexposed	0.62	0.55 to 0.69
	Exposed pre-lice	0.68	0.46 to 0.90
	Exposed infested	–1.17	–1.71 to –0.59
	Exposed fallow	2.50*	1.28 to 3.62*
Corrected	Unexposed	0.63	0.56 to 0.70
	Exposed pre-lice	0.70	0.47 to 0.92
	Exposed infested	–1.16	–1.68 to –0.62
	Exposed fallow	2.63	1.39 to 3.78

*Results shown as reported in the paper. This should actually read $r = 2.63$ with 95% CI of 1.38 to 3.77.

Table 1.

Population viability analysis of Broughton Archipelago pink salmon populations subjected to sea lice infestations.

Data set used		
Original	Population growth rate	–1.17
	Variance of environmental stochasticity	1.92
	Mean time to 99% collapse	3.9 (95% CI 3.7 to 4.2)
Corrected	Population growth rate	–1.16
	Variance of environmental stochasticity	1.90
	Mean time to 99% collapse	4.0 (95% CI 3.7 to 4.2)

Table 2.

TECHNICAL COMMENT ABSTRACTS

COMMENT ON "Declining Wild Salmon Populations in Relation to Parasites from Farm Salmon"

Brian E. Riddell, Richard J. Beamish, Laura J. Richards, John R. Candy

Krkošek *et al*. (Reports, 14 December 2007, p. 1772) claimed that sea lice spread from salmon farms placed wild pink salmon populations "on a trajectory toward rapid local extinction." Their prediction is inconsistent with observed pink salmon returns and overstates the risks from sea lice and salmon farming.

Full text at www.sciencemag.org/cgi/content/full/322/5909/1790b

RESPONSE TO COMMENT ON "Declining Wild Salmon Populations in Relation to Parasites from Farm Salmon"

Martin Krkošek, Jennifer S. Ford, Alexandra Morton, Subhash Lele, Mark A. Lewis

We evaluated the effect of sea lice (*Lepeophtheirus salmonis*) infestations on wild pink salmon (*Oncorhynchus gorbuscha*) populations in the Broughton Archipelago, British Columbia. Riddell *et al*. suggest that we ignored factors and selectively used data. Here, we clarify misunderstandings and provide analysis to test the strength of our conclusions.

Full text at www.sciencemag.org/cgi/content/full/322/5909/1790c

Comment on "Declining Wild Salmon Populations in Relation to Parasites from Farm Salmon"

Brian E. Riddell,* Richard J. Beamish, Laura J. Richards, John R. Candy

Krkošek *et al*. (Reports, 14 December 2007, p. 1772) claimed that sea lice spread from salmon farms placed wild pink salmon populations "on a trajectory toward rapid local extinction." Their prediction is inconsistent with observed pink salmon returns and overstates the risks from sea lice and salmon farming.

Krkošek *et al*. (*1*) reported that sea lice (*Lepeophtheirus salmonis*) spread from salmon farms in the Broughton Archipelago (BA), British Columbia, Canada, have placed wild pink salmon (*Oncorhynchus gorbuscha*) populations "on a trajectory toward rapid local extinction" and that "a 99% collapse in pink salmon population abundance is expected in four salmon generations." Their conclusions follow directly from their data selection process. Specifically, they defined the sea lice exposure period to begin in 2000 [$n_i(t-2)$], the year with the historic highest escapement of pink salmon in the BA; they excluded the 2004 pink salmon return; they excluded the Glendale River pink population, the largest producer of pink salmon in the BA; and they attributed all differences in wild pink salmon mortality between exposed and unexposed populations to sea lice infection, ignoring other potential sources of between-year variation in survival.

Fisheries and Oceans Canada, Pacific Biological Station, 3190 Hammond Bay Road, Nanaimo, BC V9T 6N7, Canada.

*To whom correspondence should be addressed. E-mail: brian.e.riddell@dfo-mpo.gc.ca

Pink salmon have a fixed age at maturity of 2 years, resulting in discrete (i.e., isolated) returns or lines in even- and odd-numbered calendar years. In the BA, the two lines differ substantially in abundance and trend (Fig. 1). Even-year pink salmon reached historic high returns in 2000 but then dropped to record low returns in 2002 (*2*). The odd-year line for the seven streams analyzed in (*1*) (Fig. 1B) had been declining since the early 1980s. Returns to the excluded Glendale River exhibited an inverse pattern increasing sharply until 2001. The Glendale population then declined to about 160,000 spawning adults in 2003 and increased slightly in 2005 and 2007.

Krkošek *et al*.'s prediction of rapid extinction only holds if the exposure period is defined to begin in 2000, the year of highest abundance, and returns after 2002 and 2003 are misrepresented. In particular, they excluded data for the 2004 pink return, based on their belief that it was aided by "nonrandom management action" (fallowing of the salmon farms during spring 2003) and cited (*3*) as justification. However, the argument in (*3*) is that the strong 2004 return reflected exceptional ocean survival for pink salmon over the entire life cycle, not just the out-migration period. Inclusion of 2004 data (and updating the data with preliminary 2007 returns) would have slowed the rate of decline in Krkosek *et al*.'s analysis but not the downward trend in pink abundance since 2000. The latter is fully determined by their choice to begin the exposure period in 2000.

Krkošek *et al*. excluded pink salmon returns to the Glendale River as an artificially enhanced river but chose to include returns to the enhanced Kakweiken River. The Glendale River dominates pink production in the BA, accounting for up to 90% of pink salmon returns in odd years and 40 to 70% in even years. Juvenile pink salmon originating from the Glendale River would constitute the majority of juvenile salmon passing salmon farms in the BA and would be as susceptible to infection as other populations. In fact, an alternative explanation for the declines reported in (*1*) is competition from the Glendale population, which could also limit the productivity and recovery of interacting populations, as suggested for other areas (*4*).

Krkošek *et al*. further suggested that mortality of pink salmon due to sea lice is "commonly over 80%." Sea lice were estimated to account for most natural mortality in 2002, 2003, and 2005 [table 1 in (*1*)]. This mortality would occur within 60 days of ocean entry, whereas pink salmon rear in the ocean for another 16 months before returning. All British Columbia species of salmon that entered the sea during spring 2005 suffered exceptionally poor marine survival. This fate was shared by pink salmon populations from the "unexposed" region, as demonstrated by the large negative deviations for 2006 in figure 2 in (*1*). Although sea lice infection may be one cause of juvenile mortality, other mortality factors that could exacerbate or compensate for early juvenile mortality should also be considered, particularly those that could have differed between the exposed and unexposed regions. In such ecological studies, the possibility of ecological pseudoreplication is difficult to avoid and should not be ignored.

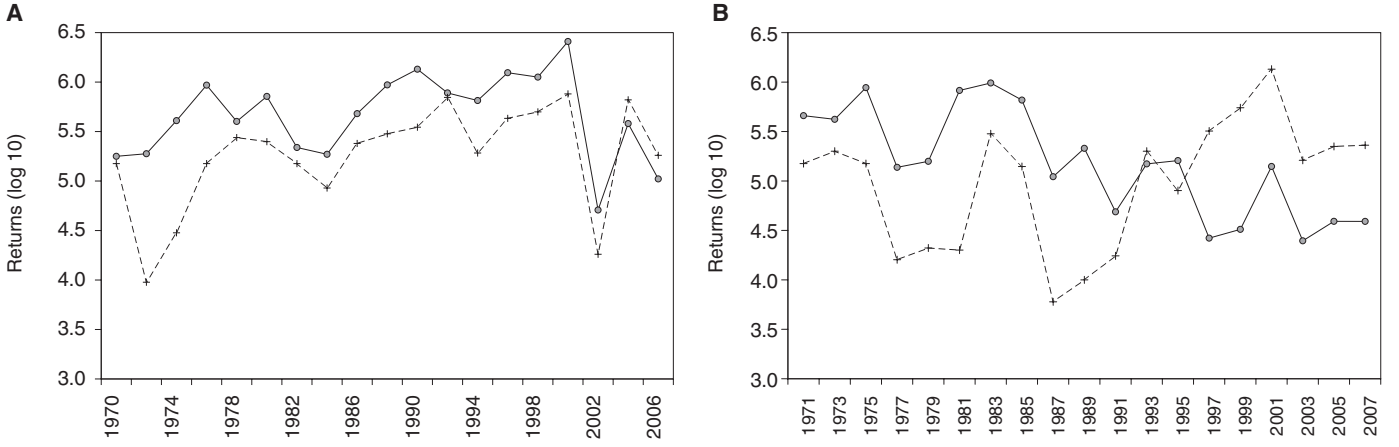

Fig. 1. Time series of pink salmon returns (total estimated number of spawners) to the BA streams included in Krkosek *et al*. (circles and solid line) and to the Glendale River (crosses and dashed line). (**A**) Even year only for adult return years 1970 to 2006. (**B**) Odd years only for adult return years 1971 to 2007. Returns are presented in a log 10 scale because of the large range of return abundances (*6*).

Krkošek *et al*.'s statements of extinctions and 99% loss of production are erroneous. They examined a subset of the BA streams but excluded the largest pink salmon production system. Their conclusions should have been kept in the context of the subset they selected. They could refer to extirpation of production from some streams but not extinction of pink salmon in the BA. Although a loss of production from some streams is undesirable, that loss is replaceable. The BA includes a large mix of small streams to large glacial river systems, but there is no detectable genetic difference between populations within even- and odd-year lines (*5*). Consequently, core populations within lines can recolonize streams that have been extirpated without loss of genetic diversity. Further, intervention by human manipulations can deliberately enhance such exchanges and are frequently conducted for Pacific salmon.

Krkošek *et al*. overstated the risks to wild pink salmon from sea lice and salmon farming. Furthermore, their predictions are inconsistent with recent observations of pink salmon returns to the Broughton Archipelago. Their alarming statements of extinction of pink salmon in the BA are only possible with highly selective use of the available data and extrapolation of their results to all pink salmon in the BA. In assessing and managing pink salmon in the BA, all potential impacts on the productivity of these pink populations, including sea lice, should be acknowledged in developing an effective management strategy.

References and Notes

1. M. Krkošek *et al*., *Science* **318**, 1772 (2007).
2. Pacific Fisheries Resource Conservation Council, 2002 Advisory: The Protection of Broughton Archipelago Pink Salmon Stocks; available from www.fish.bc.ca/files/SalmonAquaculture-Broughton-Advisory_2002_0_CompleteR_20.pdf.
3. R.]. Beamish *et al*., *ICES J. Mar. Sci.* **63**, 1326 (2006).
4. R. Hilborn, D. Eggers, *Trans. Am. Fish. Soc.* **129**, 333 (2000).
5. Data from the Department of Fisheries and Oceans, Canada; available from www.pac.dfo-mpo.gc.ca/sci/mgl/data_e.htm.
6. Data available as supporting material on *Science* Online.

Supporting Online Material

www.sciencemag.org/cgi/content/full/322/5909/1790b/DC1
Tables S1 and S2

11 February 2008; accepted 9 September 2008
10.1126/science.1156341

Response to Comment on "Declining Wild Salmon Populations in Relation to Parasites from Farm Salmon"

Martin Krkošek,[1,2]*† Jennifer S. Ford,[3] Alexandra Morton,[4] Subhash Lele,[1] Mark A. Lewis[1,2]

We evaluated the effect of sea lice (*Lepeophtheirus salmonis*) infestations on wild pink salmon (*Oncorhynchus gorbuscha*) populations in the Broughton Archipelago, British Columbia. Riddell *et al*. suggest that we ignored factors and selectively used data. Here, we clarify misunderstandings and provide analysis to test the strength of our conclusions.

We agree with Riddell *et al*. (*1*) that many factors affect salmon survival. In our study of the effects of sea lice, we controlled for nonlouse factors, using the stochastic Ricker model in a comparative analysis (*2*). The model accounts for density-dependent mortality and environmental variation in survival (*3*), two mortality factors not associated with sea lice. We applied the model comparatively to exposed pre-infestation, exposed infested, and unexposed populations. The exposed pre-infestation and unexposed populations share many factors affecting pink salmon population dynamics, evidenced by similar population growth rates (*2*) and synchronous population dynamics (*4*). The main difference between unexposed populations and exposed populations is that the former did not experience infestations (*5*, *6*), whereas the latter experienced a series of infestations (*5*, *7*, *8*). Because the exposed infested populations have a depressed population growth rate (r), this indicates that sea lice infestations have driven the difference in r between exposed and unexposed populations. Further inclusion of sea lice abundance estimates improved the model fit and showed that increased louse abundance is associated with lower survival (*2*).

The spatial time series data we analyzed have temporal and spatial correlation, raising the issue of pseudoreplication and its impact on statistical inference. We controlled for temporal correlation, using parametric bootstrapping of the stochastic Ricker model to generate confidence intervals for r (*3*). Spatial correlation is known for salmon populations but occurs at a large scale that encompasses both exposed and unexposed populations, indicating synchronous regional environmental variation (*4*). An appropriate statistical analysis in this situation follows a matched case-control design in epidemiology (*9*), where subjects experiencing the same environmental variation are divided into a treatment group (exposed populations) and control group (unexposed populations). After conditioning on the shared common environmental variation, the spatial replicates can be considered independent observations on differences in population growth rate between exposed and unexposed populations. The crucial result is that growth rate r is similar for control and treatment groups before infestations and then declines significantly for the exposed group during infestations but not the unexposed group (Table 1). A potential flaw in this analysis is that the assignment to control and treatment groups was not random but rather was based on proximity to salmon farms and sea lice infestation. Although the assumption of common environmental variation is well supported, it is not impossible that a nonlouse factor changed systematically in a negative way for exposed populations but not for unexposed populations during infestation years. However, neither Riddell *et al*. (*1*) nor we have been able to identify such a confounding factor. Furthermore, the estimated effect of sea lice is consistent with predictions from other independent analyses that established and quantified the underlying mechanisms of transmission and mortality (*8*, *10*).

Riddell *et al*. suggest that it was inappropriate to exclude the 2004 data from our analysis. These data were not excluded but rather were assigned to a separate "fallow" category in accordance with the management intervention. In spring 2003, the provincial and federal governments implemented the Pink Salmon Action Plan, which involved fallowing the primary migration route we identified in (*2*). This constitutes a major management intervention that had not been conducted before or replicated since. The fallowing management action was associated with a significant reduction in *L. salmonis* abundance in 2003 (*11*) and high marine survival for that cohort (*12*) (Table 1). Contrary to Riddell *et al*.'s interpretation, our analysis estimated the survival for pink salmon over their entire life cycle, not just the early out-migration period. Further fallowing interventions may help restore pink salmon, but the fallow treatment needs replication before its effects can be robustly assessed.

Riddell *et al*. (*1*) argue that the beginning of the infestation period (2001 out-migration and 2002 return) is confounded by high spawner abundance in 2000. We agree that density-dependent mortality likely contributed to the 2002 collapse, and we controlled for this in our analysis by using a density-dependent population growth model. The Ricker model shows that pink salmon are commonly in the overcompensation range where high spawner abundance leads to low returns (Fig. 1). Even in the absence of sea louse infestation, the Ricker curve predicts a drop from an average of 2.6 times historical abundance in 2000 to a mean of 0.78 times historical abundance in 2002, a decline by a factor of 3.3. The observed mean abundance in 2002 was 0.085 times historical abundance, which is a decline by a factor of 31, indicating that a density-independent factor was the primary cause of the collapse. Riddell *et al*. (*1*) are incorrect that our results depend on setting 2000 as the start of the infestation period. Annual survival during all the infestation years was mostly negative (Table 2), and excluding the 2000 to 2002 collapses from the data yields an estimated five generations to reach 99% loss (r = –0.85; 95% CI: –1.48 to –0.25 for exposed populations during infestation years), as opposed to four generations, as estimated in our original report (*2*).

Riddell *et al*. (*1*) are concerned that excluding the Glendale but including the Kakweiken in the analysis may affect the results. This criticism has already been addressed and shown to have no effect on the results (*13*). Following the method in (*2*), with Glendale included, the population

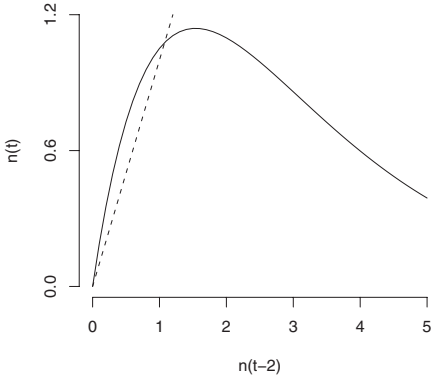

Fig. 1. Plot of the Ricker map $n(t) = n(t-2)\exp[r - bn(t-2)]$ parameterized by pre-infestation (1970 to 2001) escapement data for Broughton Archipelago pink salmon [$n(t)$ is an escapement estimate in year t normalized by its time-series mean (*2*)]. The dotted line is the 1:1 line showing the carrying capacity at the intersection with the Ricker curve. Overcompensation occurs where the curve has negative slope, indicating that high spawner abundance leads to low returns. Comparison with figure 3 in (*2*) shows that pink salmon were commonly in the overcompensatory regime, including the exposed infested group.

[1]Centre for Mathematical Biology, Department of Mathematical and Statistical Sciences, University of Alberta, Edmonton, AB, Canada. [2]Department of Biological Sciences, University of Alberta, Edmonton, AB, Canada. [3]Ecology Action Centre, Halifax, NS, Canada. [4]Salmon Coast Field Station, Simoom Sound, BC, Canada.

*To whom correspondence should be addressed. E-mail: mkrkosek@ualberta.ca

†Present address: School of Aquatic and Fishery Sciences, University of Washington, Seattle, WA 98105, USA.

Table 1. Point estimates and 95% confidence intervals for the population growth rate, *r*, of pink salmon for exposed and unexposed populations before and during the sea lice infestations and the fallow. Small deviation in estimates from those in the corrected results (*16*, *17*) are due to dividing the unexposed populations into Before Infestations, During Infestations, and Fallow groups in the model fits to get the point estimates of the parameters and also due to stochasticity in the bootstrap simulations to get the confidence intervals.

	Before infestations	During infestations	Fallow
Exposed	0.70 (0.49, 0.91)	−1.16 (−1.66, −0.60)	2.63 (1.39, 3.79)
Unexposed	0.63 (0.55, 0.70)	0.78 (0.50, 1.08)	−0.05 (−0.59, 0.62)

Table 2. Annual survival estimates, $\ln[n(t)/n(t-2)]$ per pink salmon population in the Broughton Archipelago during 2002 to 2006.

River	2002	2003	2004*	2005	2006
Ahta	−4.48	−3.16	3.40	1.05	−2.73
Kakweiken	−5.03	−1.93	2.46	0.75	−0.55
Kingcome	−3.79	−1.08	2.63	−1.94	−1.93
Wakeman	−2.54	1.02	0.86	−3.65	−1.55
Viner	−0.51	−2.10	1.57	−1.05	−3.02
Lull	−6.73	−5.31	4.28	3.55	−3.16
Ahnuhati	−4.11	0.40	2.82	−0.01	−2.54
Glendale	−3.73	−2.12	3.59	0.32	−1.29
Average	−3.87	−1.79	2.70	−0.12	−2.10

*This year corresponds to the pink salmon cohort whose juvenile out-migration occurred during the fallow year 2003.

growth rate for Broughton pink salmon populations during the sea lice infestations is –1.00 (95% CI: –1.52 to –0.52), and without Glendale and Kakweiken, the population growth rate is –1.23 (95% CI: –1.80 to –0.62). The population growth rate for Broughton pink salmon populations during the infestations as reported in our paper is r = –1.17 (95% CI: –1.71 to –0.59).

Riddell *et al*. (*1*) also suggest that competition with fish from the Glendale spawning channel contributed to declines in other Broughton pink salmon populations. Unfortunately, they provide no quantitative support for this hypothesis and fail to explain why it is apparent in only half the data (odd but not even years in their figure 1) and only in pre-infestation years. Figure 2 in (*2*) shows that the marked decline in pink salmon during the infestations is unprecedented. Figure 1 in Riddell *et al*. (*1*) indicates the Glendale populations fluctuated synchronously with the other populations in response to the infestations. If their hypothesis were correct, the Glendale populations would have fluctuated opposite to—not synchronously with—the other populations. The common factors that explain recent differences in the fluctuations of pink salmon abundance in the Broughton Archipelago relative to unexposed populations are the sea lice infestations and the fallow treatment.

Riddell *et al*. (*1*) argue from a genetic basis that extirpation of exposed pink salmon populations is acceptable because recolonization could come from other populations in the Broughton Archipelago. Our statistical sample for the Broughton Archipelago was 14 pink salmon populations. The statistical population—and hence the scope of inference—in our analysis is all the Broughton Archipelago pink salmon populations subjected to the infestations. This includes populations that are similarly exposed but excluded from analysis because of enhancement (Glendale) or many missing data points (several rivers). The conclusion that sea lice infestations have depressed wild pink salmon in the Broughton Archipelago applies generally to populations in the Broughton Archipelago (the statistical population), not only to the populations in the analysis (the statistical sample). Should populations be lost, colonization must come from outside the Broughton rather than populations within it; recovery would be more greatly compromised by genetic loss than Riddell *et al*. have suggested.

Referring to extirpation rather than local extinction implies that recovery is possible. This is not the case under a regime of infestations and negative population growth rates; extant populations will be lost and recovery efforts will fail. Riddell *et al*. supply encouraging news that 2007 escapement estimates indicate improved survival. This is only inconsistent with our analysis if 2006 infestations remained unchanged from recent non-fallow years, but Riddell *et al*. provide no supporting data. The impacts of salmon aquaculture on sympatric wild salmon stocks are now known to be widespread (*14*), and solutions are possible given sufficient political will (*15*). Our analysis indicates a critical sea lice threshold of $r^*/\alpha = 1.3$ motile lice per juvenile pink salmon, below which population declines can be reversed (*2*). We agree with Riddell *et al*. that management needs to consider many factors affecting wild salmon. Prevention of sea lice infestations of wild juvenile salmon is a management and policy option that may help restore wild salmon.

References and Notes

1. B. E. Riddell, R. J. Beamish, L. J. Richards, J. R. Candy, *Science* **322**, 1790 (2008); www.sciencemag.org/cgi/content/full/322/5909/1790b.
2. M. Krkošek *et al*., *Science* **318**, 1772 (2007).
3. B. Dennis, M. L. Taper, *Ecol. Monogr.* **64**, 205 (1994).
4. B. J. Pyper, F. J. Mueter, R. M. Peterman, D. J. Blackbourn, C. C. Wood, *Can. J. Fish. Aquat. Sci.* **58**, 1501 (2001).
5. A. Morton, R. Routledge, C. Peet, A. Ladwig, *Can. J. Fish. Aquat. Sci.* **61**, 147 (2004).
6. C. R. Peet, thesis, University of Victoria (2007).
7. A. B. Morton, R. Williams, *Can. Field Nat.* **117**, 634 (2003).
8. M. Krkošek, M. A. Lewis, A. Morton, L. N. Frazer, J. P. Volpe, *Proc. Natl. Acad. Sci. U.S.A.* **103**, 15506 (2006).
9. K. J. Rothman, *Modern Epidemiology* (Little Brown, Boston, 1986).
10. M. Krkošek *et al*., *Proc. R. Soc. London B Biol. Sci.* **274**, 3141 (2007).
11. A. Morton, R. D. Routledge, R. Williams, *N. Am. J. Fish. Manage.* **25**, 811 (2005).
12. R. J. Beamish *et al*., *ICES J. Mar. Sci.* **63**, 1326 (2006).
13. M. Krkošek *et al*., *Rev. Fish. Sci.* **16**, 413 (2008).
14. J. S. Ford, R. A. Myers, *PLoS Biol.* **6**, e33 (2008).
15. A. A. Rosenberg, *Nature* **451**, 23 (2008).
16. Corrections and Clarifications, Reports, Krkošek *et al*., *Science* **322**, 1790 (2008).
17. See revised supporting online material for (*2*) at www.sciencemag.org/cgi/content/full/318/5857/1772/DC1.

18. Funding came from the Natural Science and Engineering Research Council of Canada, the Canadian Mathematics of Information Technology and Complex Systems National Centre of Excellence Network on Biological Invasions and Dispersal Research (with nonacademic participants including the David Suzuki Foundation, Canadian Sablefish Association, Wilderness Tourism Association, Watershed Watch Salmon Society, and Finest at Sea), the National Geographic Society, Tides Canada, a University of Alberta Bill Shostak Wildlife Award, the Lenfest Ocean Program, Census of Marine Life, and a Canada Research Chair.

10 March 2008; accepted 16 September 2008
10.1126/science.1156578

ENVIRONMENTAL ART

Hejira in a Jetta

Mary Parrish

In the summer of 2004, city slicker and "recovering art historian" Erin Hogan jumped—short "urban haircut," titanium German designer glasses, and all—into her black Volkswagen Jetta to search for meaning in land art of the western United States. Three weeks away from the el trains, straight edges, and cacophony of Chicago were a challenge for Hogan (now the public affairs director for the Art Institute of Chicago). Blending a humorous travelogue and serious musings, in *Spiral Jetta* she winds her car and the reader through the complexities of 1970s earthworks and contemporary aesthetics via a varied landscape of people, places, and art.

Spiral Jetta
A Road Trip Through the Land Art of the American West
by Erin Hogan
University of Chicago Press, Chicago, 2008. 188 pp. $20. ISBN 9780226348452.

***Spiral Jetta* in 2005.** The lake level and algae populations have fluctuated since Smithson constructed the work.

Land artists took their work out of museums and galleries to integrate it with the geological settings of some of the most remote areas in the United States. Their creations merge art with the natural world, harnessing an ever-changing mixed media of available light, shadow, color, mud, rock, and possibly manmade materials. The monumental forms absorb inevitable and happenstance changes (such as salt accretion and erosion), which become integral parts of the works. (Some land artists made provisions to preserve their works' original forms, and discussions concerning the conservation of other pieces is ongoing.)

Hogan's first destination is the salt flats of Great Salt Lake near Rozel Point, Utah. When the artist Robert Smithson "went looking for red" in the late 1960s, he found it there. Due to the lack of fresh water and the presence of salt-tolerant red algae and bacteria, the lake was then "bleeding scarlet streaks … pumping into ruby currents … a flaming chromosphere (*1*). On the site, Smithson built his 1500-feet-by-15-feet *Spiral Jetty* (1970).

After viewing *Spiral Jetty*, the author travels to Michael Heizer's *Double Negative* (1970) and Walter De Maria's *Lightning Field* (1977). Along the way, she tries to visit Nancy Holt's *Sun Tunnels* (1976) and James Turrell's still unfinished *Roden Crater* (1972–), but fails to find either. She also describes her reactions to the geology of Arches National Park in Utah; the nearby tourist attraction Hole n" the Rock (a 5000-square-foot house artist-taxidermist Albert Christensen dug into a huge rock between 1945 and 1957); the "dream" and "nightmare" of the bordertown of Juárez, Chihuahua; and Donald Judd's Chinati galleries in Marfa, Texas.

In between her accounts of getting lost, drinking cheap beer in cowboy bars with local characters, and other misadventures along the road, Hogan introduces the heady philosophies of a number of modern and contemporary artists and art critics (including Barnett Newman, Michael Kimmelman, and Michael Fried) as well as her own thoughts and impressions. She is great at keeping the reader's attention: two pages of art philosophy; ten pages of fun.

Hogan loves land art but nonetheless wrestles with its implications. She wonders, "Would *Roden Crater* offer a radically different experience than one could have, say, attentively camping?" At one point, she openly declares, "Everything I had seen so far bordered on the preposterous." She asks whether art is, as Dadaist Marcel Duchamp asserted, whatever we say it is.

In the high desert of western New Mexico, Hogan finds the aesthetic experience she had hoped to encounter. She beautifully describes the effects—seen especially at sunrise and sunset—of color, light, and shadow on the 400 carefully constructed stainless steel poles that form De Maria's 1-mile-by-1-km *Lightning Field*. That work, at least for a few moments, turned off the critic in the author while she stood in awe of the art.

References
1. R. Smithson, in *Robert Smithson: Spiral Jetty*, L. Cooke, K. Kelly, Eds. (Dia Art Foundation, New York, and Univ. California Press, Berkeley, 2005).

10.1126/science.1168820

The Lightning Field. Kenneth Baker. Yale University Press, New Haven, CT, 2008. 166 pp. $35, £16. ISBN 9780300138948.
This monograph comprises two essays on Walter De Maria's 1977 masterpiece by the *San Francisco Chronicle*'s art critic. The first—written for the Dia Art Foundation (which financed and owns *The Lightning Field*) in 1978 but abandoned after the esoteric and highly reclusive artist found it too descriptive—is presented as a "period artifact." Beginning in 1994, Baker returned to the site four times, in different seasons, to deepen his experience of the work. He finished a second manuscript in the summer of 2001, but 9/11 and its aftermath led to substantial revisions. The result is a sobering collection of reflections thematically linked to Baker's personal reactions to "one of the profoundest of American artworks." **–Mary Parrish**

The reviewer is at the Department of Paleobiology, National Museum of Natural History, Smithsonian Institution, Washington, DC 20013–7012, USA. E-mail: parrishm@si.edu

CREDIT: FINNEGAN MARSH

THEATER

To Make Aire Dance

Robert Boyle reckoned that to be a credible scientist one had to be a good Christian gentleman, because experimental science relies on trust in its practitioners and faith in the integrity of its demonstration. Adriano Shaplin's *The Tragedy of Thomas Hobbes* presents the story of the revolution in thought that culminated in the founding of Britain's Royal Society by Boyle and his collaborators. The play sets pure reason, promulgated by the philosopher Thomas Hobbes, against the disinterested experimentation conducted by Boyle as opposing ways of exploring the ways the world works. Shaplin's treatment reveals the breaking waves of real and cultural conflict at work in the British Isles the middle of the 17th century: the transitions of the civil wars that started in England in 1642 and continued past Oliver Cromwell's death in 1658 to the restoration of the monarchy in 1660 under Charles II.

The Tragedy of Thomas Hobbes
by Adriano Shaplin
Royal Shakespeare Theatre, Wilton's Music Hall, London.

This history play is a spectacular windmill of ideas, and although it works less well as a piece of theatre it makes for provoking entertainment. Fortunately Shaplin (an American playwright and artistic director of the award-winning company Riot Group) and historian of science Simon Schaffer (University of Cambridge) were on hand at the Royal Society on 20 November 2008 to guide us through the action (*1*). Meanwhile, a performance of the play by the Royal Shakespeare Company (which, with the Massachusetts Institute of Technology, commissioned the work) was running in London's East End at Wilton's Music Hall. Some of the most provocative aspects of Schaffer and Shaplin's conversation were their references to the modern practice of science. Their heterodox ideas might be bread and butter for historians or sociologists, but practicing scientists are unlikely to feel comfortable seeing themselves in the same light as these authors see Boyle and the early Royal Society.

First up, Schaffer was keen to reveal the parallels between theatrical performance and scientific performance. Most directly, he suggested that public demonstrations of experiments may have been replacements for the theatrical performances that had been abolished during the Puritan interregnum. Perhaps Shaplin's modern play leaves a chaotic sensation because it works in the same way as one of Boyle's experimental demonstrations. Thus the play objectively generates a mass of data unbound by Hobbesian reasoning. The trouble is that it takes a lot of reasoning to stitch large amounts of data together to produce a useful history—even as it does to produce a useful genome or a useful Higgs boson.

The forerunners of the Royal Society were initially members of the "invisible college" of natural philosophers, who gathered in the 1640s to discuss Francis Bacon's ideas. They, as modern scientists are now, were trapped by an ever-pressing need for funds, hence their continual and oftentimes desperate seeking of patronage, any sort of patronage. By 1660, they managed to wrest a Royal Charter from Charles II. But they found no financial backing from him—being a party animal, Charles was spent up. Money is why Boyle was so important.

Against Hobbes. Hooke (Jack Laskey) and Boyle (Amanda Hadingue).

The other major protagonist, Hobbes, was notorious for being an atheist. After the 1651 publication of his *Leviathan*, Hobbes was kicked out of Charles's exiled court in France. He fled to Cromwell's England, where his authoritarian ideas were less anathema. Schaffer drew attention to the fact that Hobbes's views had been formed during a period of terrifying war and dislocation. Shaplin's script interprets the effect of civil disorder on Hobbes by depicting him as a seeker of rigid certainty. He has Hobbes saying, "A real philosopher instantly Knows, he doesn't do poking." For Hobbes, Boyle's experiments, which went wrong more often than they went right, were a confidence trick. Hobbes was only too aware of the manipulation and spin prevalent in politically tumultuous times, and he believed this true of the experimental demonstrations as well. The trouble with Hobbes's method of unfalsifiable reasoning is that it depended on being clever to remain credible. Shaplin shows Hobbes's knowledge under persistent bombardment by pamphlet, primarily from John Wallis (another member of the invisible college), who derided Hobbes for his lack of talent in mathematics.

By contrast, Boyle had it all. Boyle's family owned land in Ireland. The wealth from this property funded Boyle's laboratory and allowed him to think independently of any patron, to form democratic collaborations and discussion groups, to buy knowledge and expertise no matter the price, and, importantly, to be able to afford to acknowledge mistakes and bear the cost of repeating and redesigning experiments. It all sounds like very modern science. Shaplin's Boyle comments, "if a fact is over-turned, it vanishes, It never was a fact. I've noticed knowledge hangs around, it hangs on men." The difficulty for modern scientists, as Schaffer pointed out, is that Boyle saw doing an experiment as a way of revealing God's design and thus a way to increase faith. For him, one had to be a Christian filled with humility to be a good experimentalist.

Most important, Boyle's wealth allowed him to buy Robert Hooke. In Shaplin's play, the handover of the young Hooke from John Wilkins's sphere of control to Boyle's symbolically takes place during an auction of Descartes's work. At the time, Boyle viewed Descartes in the same light as he viewed atheists; he did not want to be tempted from Bacon's way. Hooke was mighty clever. His cleverness allowed him to emerge from an obscure cleric's family on the Isle of Wight to become curator of experiments at the Royal Society. He was an energetic and industrious

polymath, sampling everything from microscopy and evolution to architecture. This breadth of vision was also his undoing.

In the final twist, Shaplin brings on Isaac Newton as Hooke's nemesis. Newton derided Hooke as a "mere smatterer" and was probably responsible for trying to erase Hooke's record. Newton's jealousy best explains why there is no surviving portrait of Hooke and why so little survives of Hooke's ideas on evolution and many other topics. And so the play comes full circle: Hobbes's absolutist reasoning being replaced by Hooke and Boyle's democratic experimental approach, only for that to be usurped by Newton's autocracy in the fully fledged Royal Society.

I loved the show—the acting is wonderful and the crumbling Music Hall venue with its vertical set provides a suitably dusty atmosphere for Restoration London—but not so many were as enthusiastic as I was. Charles II (played by Arsher Ali) as a Russell Brand–style vulgarian, complete with fluffy detachable head piece, did offer a frisson. Shaplin's stipulation that Boyle must be played by a woman has a lucky manifestation in Amanda Hadingue, who closely resembles Boyle's portraits and has the suitably fastidious demeanor of the sickly man. (Shaplin explained that the purpose of having a woman play the part was to emphasise Boyle's special character: his collaborative instincts and his disengagement from the prevailing masculine brawling.) Jack Laskey is particularly good as the energetic and engaging Hooke. Unfortunately, Will Sharpe as Newton does not project dark enough foreboding and his soliloquy makes for a collapse rather than a finale. But, and it is a big but, despite the performance's many pleasures, the audience was left largely mystified, sometimes sleeping. The play is truly a mass of facts that fall and drift hypnotically like confetti. Unless theaters hand out copies of Steven Shapin and Schaffer's *Leviathan and the Air Pump* (*2*) as a study aid, the director Elizabeth Freestone and the playwright should have reined in the text, slapped a stronger structure on the story, and given the performance an emotional heart. I hate to fault a play that so rumbustiously turns over so many brilliant ideas. Go and see *The Tragedy of Thomas Hobbes* if you get a chance, but be prepared.

–Caroline Ash

References and Notes

1. A Webcast of the conversation between Shaplin and Schaffer at the Royal Society event is archived at http://royalsociety.tv (look under the history of science offerings).
2. S. Shapin, S. Schaffer, *Leviathan and the Air Pump: Hobbes, Boyle, and the Experimental Life* (Princeton Univ. Press, Princeton, NJ, 1985); reviewed by T. L. Hankins, *Science* **232**, 1040 (1986).

10.1126/science.1168875

BROWSINGS

Audubon: Early Drawings. Richard Rhodes, Scott V. Edwards, and Leslie A. Morris. Harvard University Press, Cambridge, MA, 2008. Boxed, 292 pp. $125, £92.95, €112.50. ISBN 9780674031029.

These 116 early Audubons from the collections of Harvard University provide a perspective on the development of the artist's mature style. In accordance with established ornithological presentation of the time, most of the birds are stiffly posed in profile with little or no background. Some drawings, however, show their subjects in action [e.g., the whip-poor-will, *Caprimulgus vociferus*, in flight (1812), right] or include details of diet or habitat—approaches Audubon took to portray specimens as "drawn from Nature" in his monumental *The Birds of America*. The watercolors and pastels of the European species were executed in France in 1805 and 1806, and those of the North American birds date from 1805 to 1821. The captions discuss when and where Audubon collected the specimens. Morris, Rhodes, and Edwards contribute essays on the history of the drawings, the artist's life, and his science.

Albatross: Their World, Their Ways. Tui De Roy, Mark Jones, and Julian Fitter. Firefly, Toronto, 2008. 240 pp. $49.95, C$49.95. ISBN 9781554074150. Christopher Helm, London. £35. ISBN 9780713688122.

Renowned for their mastery of marine air and wide-ranging trips over the oceans, albatrosses may spend 95% of their long lives (which can extend beyond 60 years) riding the winds and waves. Being birds, the adults must return to land to nest and hatch the single large egg that they produce every other year. Traveling on a 13-m sailboat, natural history writer-photographers De Roy and Jones observed nearly all the albatross species at breeding sites. De Roy's descriptions of their visits to these usually wild and remote islands and her striking images (below, *Thalassarche impavida* at its only nesting site, on Campbell Island) fill the first half of the book. A second section presents expert essays on albatross biology and conservation issues. The book concludes with short accounts of each of the 22 species, in which Fitter summarizes taxonomy, identification, population, distribution, breeding, food, and threats.

CREDITS: (TOP) JOHN JAMES AUDUBON/COURTESY HARVARD UNIVERSITY PRESS; (BOTTOM) TUI DE ROY/COURTESY FIREFLY BOOKS

Nature's Beloved Son: Rediscovering John Muir's Botanical Legacy. Bonnie J. Gisel and Stephen J. Joseph (photographer). Heyday, Berkeley, CA, 2008. 280 pp. $45. ISBN 9781597141062.
A plant press was among the few possessions Muir carried on his "thousand-mile walk" from Kentucky to the Gulf of Mexico in the fall of 1867. His collections from that journey have since disappeared, but specimens from earlier trips in Wisconsin, Ontario, and Indiana and later excursions in California, Alaska, and the southern states are now scattered among several herbaria and archives. In this volume, environmental historian Gisel traces the importance of Muir's "eternal fondness for plants" through his life and work. Her text incorporates numerous short samples of his correspondence and writings, and it is enhanced with examples of his field sketches. Joseph's 95 artistic, enhanced digital prints highlight a selection of Muir's botanical specimens (right, bent grass, *Agrostis exarata*, collected near Yosemite in 1875).

The Buzz About Bees: Biology of a Superorganism. Jürgen Tautz; photographs by Helga R. Heilmann; David C. Sandeman, translator. Springer, Berlin, 2008. 298 pp. $39.95, £23. ISBN 9783540787273.
Whereas bee colonies were once seen as perfect societies of selfless workers and drones ruled by a queen, Tautz presents them as a self-organized, complex adaptive system that he considers "a mammal in many bodies." This comprehensive introduction to honeybee biology (originally published as *Phänomen Honigbiene*) explores such topics as how bees obtain and communicate information about flowers, "whole-animal gametes," and the comb's contributions to the sociophysiology of the colony. The author has been honored for making research accessible to the public, and his lucid text will reward lay readers, apiarists, students, and professional biologists alike. The book is profusely illustrated with Heilmann's spectacular photos, which capture the full range of bee activities—including some, such as the living chains formed where combs are being built or repaired (bottom left), whose function remains unknown.

A Field Guide to Surreal Botany. Janet Chui and Jason Erik Lundberg, Eds. Two Cranes, Singapore, 2008. Paper, 76 pp. $12, Sg$14. ISBN 9789810810177.
With its delicate illustrations, Latin names, notes on ecology and life cycle, and seemingly aged paper, this appears to be an old-fashioned botanical treatise. What makes the imagined species so much fun is the extent of the details, which draw the reader into plausible descriptions that suddenly take a turn to the bizarre. It is hard to pick a favorite, but contenders include the kvetching aspen (the only known tree with a mating cry, which resembles the call of a stilter's jay), the wind melon (which can levitate), the twilight luon-sibir (which has an "abyss-probability" center), and the bone garden (bottom right, also known as Adam's ribcage). The small book is a bit of lunacy sure to appeal to slightly twisted plant lovers.

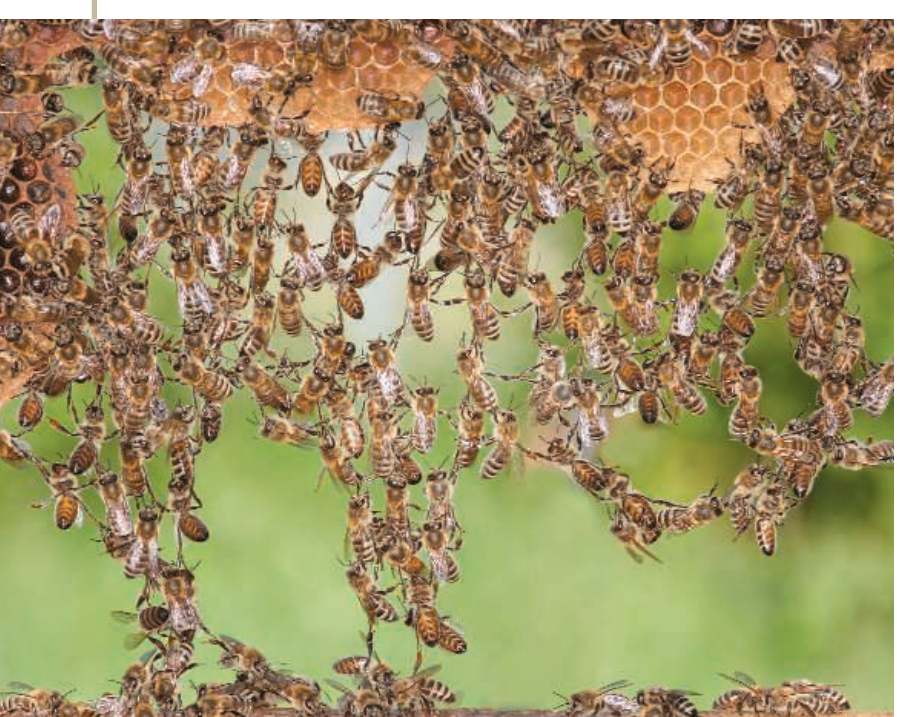

CREDITS: (TOP) STEPHEN J. JOSEPH/COURTESY HEYDAY BOOKS; (BOTTOM LEFT) HELGA R. HEILMANN/WÜRZBURG BEEGROUP; (BOTTOM RIGHT) JANET CHUI/COURTESY TWO CRANES PRESS

Published by AAAS

THE PIPELINE

Science Faculty with Education Specialties

Career dynamics for science faculty with interests in education point the way for developing this nascent career specialty.

S. D. Bush,[1]* N. J. Pelaez,[2]* J. A. Rudd,[3]*† M. T. Stevens,[4]* K. D. Tanner,[5]* K. S. Williams[6]*

Globally, efforts to improve science education continue (*1*, *2*). In the United States, primary and secondary (K–12) science education lags on international assessments and struggles to sustain qualified K–12 science teachers and to prepare the next generation of scientists and engineers (*2*). At U.S. colleges and universities, more than half of entering science majors leave the sciences, most (90%) complaining of ineffective teaching (*3*). Of those who remain in science, 74% express the same complaint (*3*). Further work is needed within specific science disciplines on how students most effectively learn that discipline (*4*). To address K–12 science education, undergraduate science education, and discipline-specific science education research, one approach is seeding university science departments with Science Faculty with Education Specialties (SFES), scientists who take on specialized science education roles within their discipline (*5*).

We present data on SFES in science departments throughout the 23-campus California State University (CSU) system (*6*), the largest U.S. university system (annual enrollment ~450,000 students). The CSU's primary missions are undergraduate, master's-level graduate, and K–12 teacher education. CSU undergraduates are among the top one-third of their high-school graduating classes. The 23 campuses include institutions that differ substantially in their founding dates, settings, student populations, enrollment sizes, and levels of research orientation. We investigated SFES numbers, characteristics, training, professional activities, and persistence.

We identified, with the aid of deans, 156 CSU faculty as SFES and invited all 156 to complete a 111-question survey (*7*), which we had face-validated using non-CSU faculty. Between December 2007 and January 2008, 103 of the invitees responded (66% response rate), representing 20 of the 23 campuses. We collected data anonymously and excluded surveys that were incomplete ($n = 12$), submitted by lecturers or non–tenure-track science faculty ($n = 10$), or lacked informed consent ($n = 3$). Of the remaining 78 survey respondents, 59 individuals self-identified as SFES, and 19 as not SFES. Our further analyses followed only the 59 tenured/tenure-track science faculty who self-identified as SFES.

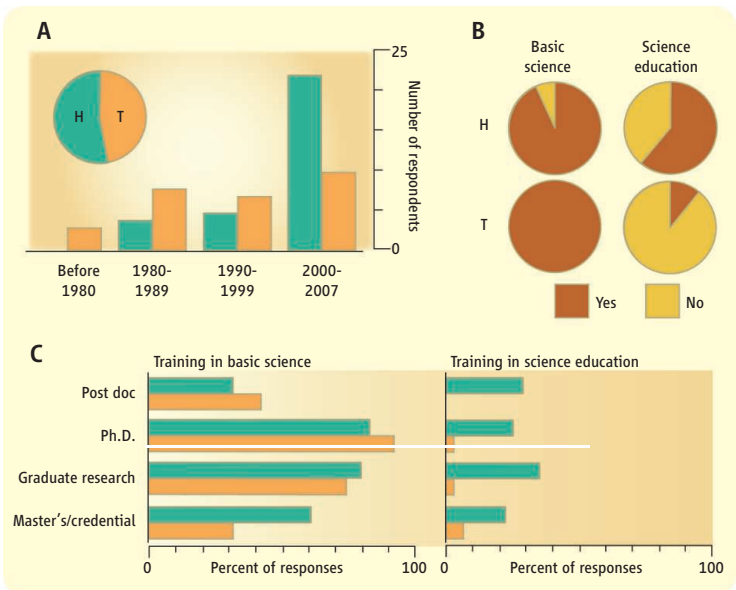

Hiring and formal training. (**A**) The pie chart inset shows the proportion of two SFES types, hired-SFES (H) ($n = 31$) and transitioned-SFES (T) ($n = 28$). The distribution of hire dates for hired-SFES and transitioned-SFES is shown with bars. (**B** and **C**) The proportions with formal training in basic science and/or science education and the types of formal training reported.

Characteristics and Training

These 59 SFES represented four science disciplines [biology (34%), chemistry (24%), geoscience (14%), and physics (25%)], as well as science faculty in centers for science and math education housed in Colleges of Science (3%). They were 46% female, 81% white, across tenure-track faculty ranks (28% assistant, 31% associate, and 41% full professors), and trained extensively as researchers in basic science. We completed Pearson's chi-square and McNemar's tests to compare subpopulations of SFES and to make inferences ($P < 0.05$).

SFES include two subpopulations, those specifically hired as SFES (hired-SFES; $n = 31$, 53%) and those who transitioned to SFES roles (transitioned-SFES; $n = 28$, 47%) from their initial faculty roles [see (A) in chart, left]. Transitioned-SFES had hiring dates beginning in 1970, and hired-SFES had dates beginning in 1987 (see chart, left). More hired-SFES were hired after 2000 than in all previous years combined. Transitioned-SFES (17.9% assistant, 28.6% associate, 53.6% full) tended to hold higher faculty ranks than hired-SFES (41.9% assistant, 35.5% associate, 22.6% full; $\chi^2 = 6.8$, df = 1; $P = 0.033$). Half of transitioned-SFES (50.0%), but only a few hired-SFES (9.7%), had tenure before entering SFES roles ($\chi^2 = 11.6$, df = 1; $P = 0.001$).

Both groups had similar and extensive formal training in basic science [see (B) in chart, above], but more hired-SFES (61%; $\chi^2 = 12.7$, df = 1; $P = 0.001$) had formal training in science education than did transitioned-SFES (11%) [see (C) in chart, above]. Although SFES may have various types of training experiences, we defined formal training as post-baccalaureate training, including degrees, teaching credentials, graduate level research, and/or postdoctoral research. Of note, both groups have substantial proportions of individuals lacking these types of formal training in science education.

Professional Activities and Endurance

Examination of the professional activities for which SFES sought funding revealed that they were undertaking efforts in the three key science education arenas of K–12 science education, undergraduate science education, and

[1]California Polytechnic State University, San Luis Obispo, San Luis Obispo, CA 93407, USA. [2]Purdue University, West Lafayette, IN 47907, USA. [3]California State University, Los Angeles, Los Angeles, CA 90032, USA. [4]California State University, Stanislaus, Turlock, CA 95382, USA. [5]San Francisco State University, San Francisco, CA 94132, USA. [6]San Diego State University, San Diego, CA 92182, USA.

*All authors contributed equally to this work.

†Author for correspondence. E-mail: jrudd@calstatela.edu

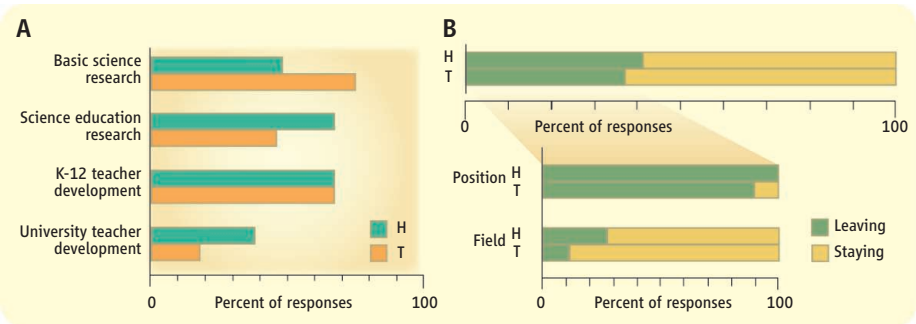

Activities and satisfaction. (**A**) The percentages of those who sought funding for scholarly activities in four areas. (**B**) (Top) The percentage of SFES ($n = 56$; three nonresponders) who were seriously considering leaving their job. (Bottom) Their inclination to leave the position ($n = 21$; one nonresponder) and/or field ($n = 20$; two nonresponders).

discipline-based science education research, as well as continuing basic science research [see (A) in chart, above]. More transitioned-SFES (75%; $\chi^2 = 4.4$, df = 1; $P = 0.036$) pursued basic science research funding compared with hired-SFES (48%), whereas more hired-SFES (68%; $\chi^2 = 2.7$, df = 1; $P = 0.098$) applied for science education research funding compared with transitioned-SFES (46%). Both groups applied at equal rates (68%) for funding to support K–12 teacher development. SFES pursued funding for university teacher development the least, although twice the percentage of hired-SFES (39%; $\chi^2 = 3.1$, df = 1; $P = 0.077$) did so compared with transitioned-SFES (18%). Overall, 41% of respondents had obtained total external funding exceeding $500,000, including 15% who had received total external funding of over $1,000,000.

For their professional activities, most SFES (71%) reported spending "about the same amount" of time on teaching as did their non-SFES department faculty. Nearly all SFES (90%) perceived soliciting external grant funding and publishing peer-reviewed articles as being "essential for obtaining tenure and/or promotion." Fewer than 10% of SFES perceived an equivalent academic infrastructure—undergraduate or graduate courses and degree programs within their science departments—supporting scholarship in science education as compared with supporting scholarship in basic science. Of those with departmental graduate programs, most SFES (79%) reported having less access to graduate student researchers than non-SFES science faculty had. Furthermore, 34% of SFES reported being the only SFES in their department.

Almost 40% of the 59 SFES were "seriously considering leaving" their current jobs [see (B) in chart above], including 41% of hired-SFES and 37% of transitioned-SFES. Of those who specified, nearly all (95%) were considering leaving their particular position. Some (20%) were considering leaving the field entirely [see (B) in chart above]. Results of McNemar's test ($\chi^2 = 13.1$, df = 1; $P < 0.001$) imply most SFES are dedicated to and invested in the field of science education, but find themselves in faculty appointments that they find professionally unacceptable. Although similar proportions of hired-SFES and transitioned-SFES were considering leaving, analysis of open-ended item responses revealed differences. Hired-SFES most commonly reported that they were considering leaving because their science education efforts were not valued or understood. Transitioned-SFES, in contrast, reported being overworked and burned out.

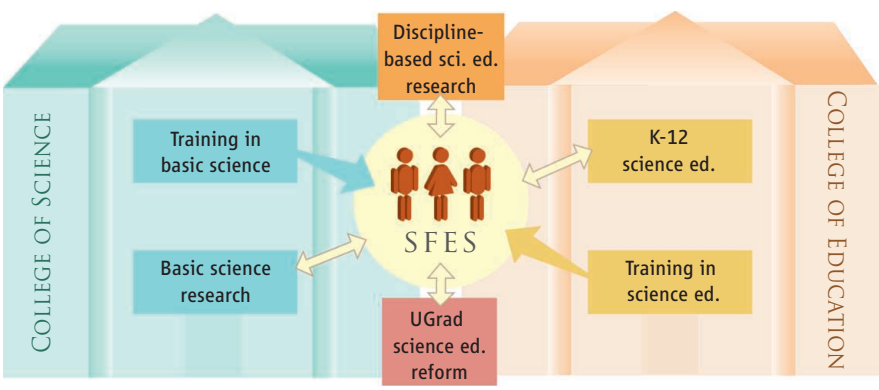

Conclusions

SFES occupy tenured or tenure-track faculty positions across all science disciplines, at all faculty ranks, and across the wide variety of campuses within the CSU. SFES are engaged broadly in science education as well as in basic science research. Hired-SFES and transitioned-SFES share similarities, but show four statistically significant differences. Greater proportions of hired-SFES are untenured faculty, are recent hires, and have formal post-baccalaureate training in science education. A greater proportion of transitioned-SFES sought basic science research funding. As a whole, SFES pursue funding for science education and basic science research and do not simply occupy teaching positions, as most report teaching about the same amount as their non-SFES colleagues. Our results quantify increased rates of hiring for SFES but also suggest potentially high attrition from these positions.

The SFES model appears both promising and challenging (see diagram, left). SFES in university and college science departments have the potential to drive science education reform at K–12 and postsecondary institutions. Our data suggest that science education would benefit from (i) increased training opportunities to develop SFES, (ii) reduced professional isolation for SFES, and (iii) improved academic infrastructure to support SFES research and professional activities. Attention to the issues raised by SFES in this study would likely strengthen the impact of SFES on K–12 science education, undergraduate science education, and science education research within the disciplines.

References and Notes

1. Organization for Economic Cooperation and Development (OECD), *PISA 2006: Science Competencies for Tomorrow's World* (OECD Publication 39725224, Paris, 2007); www.pisa.oecd.org/dataoecd/ 15/13/39725224. pdf.
2. National Academy of Sciences, National Academy of Engineering, Institute of Medicine, *Rising Above the Gathering Storm: Energizing and Employing America for a Brighter Economic Future* (National Academies Press, Washington, DC, 2007; http://books.nap.edu/catalog/11463.html).
3. E. Seymour, N. Hewitt, *Talking About Leaving: Why Undergraduates Leave the Sciences* (Westview Press, Boulder, CO, 1997).
4. Center for Education, National Academies, *Workshop on Education Research Positions in STEM Disciplinary Departments*, Washington, DC, 5 December 2005 (National Academies Press, Washington, DC, 2005); http://www7.nationalacademies.org/cfe/STEM_Disciplines_Agenda.html.
5. S. D. Bush *et al.*, *CBE Life Sci. Educ.* **5**, 297 (2006).
6. California State University, *2008 Facts About the 23 Campuses of the CSU*, www.calstate.edu/PA/2008Facts/index.shtml.
7. Materials and methods are available as supporting material on *Science* Online.
8. The following CSU Deans provided funding: S. Axler, P. Bailey, J. Bruner, S. Maloy, and G. Novak. M.T.S. received the Naraghi Faculty Research Enhancement Grant.

Supporting Online Material

www.sciencemag.org/cgi/content/full/322/5909/1795/DC1

10.1126/science.1162072

CREDIT: NATHALIE CARY

RESEARCH FUNDING

Politics and Funding in the U.S. Public Biomedical R&D System

Research grant allocations can be affected by appropriations committee representation.

Deepak Hegde[1]* and David C. Mowery[2]

Federal funding for biomedical R&D through the National Institutes of Health has grown from $8.3 billion in FY1984 to $28.7 billion in FY2008 (*1*, *2*). The NIH supports half of all federal nondefense R&D and more than 60% of federally funded research in American universities (*3*). The agency awards funds to research performers based on "peer review" but the decisions are not insulated from political influence.

How do congressional appropriations committee members influence the allocation of federal funding for biomedical research? We investigated this question by studying congressional appropriations bills and appropriations committee meeting reports covering the 20 fiscal years between 1984 and 2003. During every year of this period, the director of the NIH negotiated with the Department of Health and Human Services and the Office of Management and Budget within the Executive Office of the President to craft a budget request for the NIH that was consistent with White House priorities. The NIH's budget is considered by the Appropriations Committees of the House and Senate. In the House Appropriations Committee (HAC), the NIH budget request is handled by the Labor, Health and Human Services, and Education and Related Agencies Subcommittee (LHHE). A similarly named subcommittee of the Senate Appropriations Committee (SAC) evaluates the NIH budget request in that chamber. The LHHE subcommittees consider the NIH budget request, amend the funding requests in the presidential budget, and "mark up" the appropriations bills, sometimes specifically for institutes and centers at the NIH, that are ultimately reported to the House and Senate by each chamber's appropriations committee.

The subcommittee meeting reports that accompany the appropriations bills to the floor contain additional detail and guidance on the allocation and disbursement of appropriated funds by the NIH. Transfers affecting the level of support may involve (i) reallocation for NIH funding among the agency's institutes and centers, (ii) subcommittee support for specific fields of biomedical research associated with particular diseases, and (iii) project-level transfers that reallocate funding among particular lines of research and/or research projects within a given disease field. (See Supporting Online Material for examples).

To test whether these reallocations are affected by representation on the relevant appropriations subcommittees and committees, we analyzed data on the amount of NIH peer-reviewed grants received by 8310 "extramural" biomedical research institutions for every congressional NIH appropriations bill during the 1984–2003 period (*4*, *5*). The primary data were drawn from the NIH's "Consolidated Grant Applicant File" (CGAF) database, which contains a record of every research proposal for which a grant was made by the NIH. We matched these data to the number of appropriations committee and LHHE subcommittee members from the state that was home to each NIH grant recipient during the corresponding appropriations year. Hence, for example, the House and Senate appropriations committee composition data for the 107th Congress (years 2001 and 2002) are matched to the NIH grants made during the years 2002 and 2003. During 1984–2003, the HAC had 57 to 64 members, 12 to 17 of whom were assigned to the LHHE subcommittees; the Senate Appropriations Committee had 28 to 29 members, 13 to 15 of whom sat on the corresponding LHHEs. During that period, 11 to 15 states were represented in the LHHE subcommittee of each chamber (*5*).

We estimated a "pooled least squares" regression to analyze the influence of committee membership on the amount of NIH peer-reviewed grants received by performers (i.e., we estimated the effect of membership on the size of grants, conditioned on the institution's receiving grants during the time period) (*5*). A challenge in identifying the causal impact of committee membership is controlling for other "unobserved" attributes of research performers, such as their previous success in obtaining grants, size, or location in states with a high demand for public biomedical resources, which may be correlated with both committee representation and receipts of NIH awards. We used research-performer "fixed effects" regression models in order to control for such confounders. In additional robustness tests, we estimated the effects of members' exit from their subcommittee positions on the NIH grants received by research performers in their states (*5*).

ESTIMATES OF APPROPRIATIONS COMMITTEE MEMBERSHIP EFFECTS

Congress year	Total political effect (B$)	Total allocations (B$)	Political effect as % of total
1983–84	0.57 (0.31)	8.46	6.74 (3.66)
1985–86	0.68 (0.38)	10.45	6.50 (3.63)
1987–88	0.81 (0.45)	12.80	6.33 (3.51)
1989–90	0.91 (0.5)	14.95	6.09 (3.34)
1991–92	1.01 (0.56)	16.81	6.01 (3.33)
1993–94	1.18 (0.66)	18.73	6.30 (3.52)
1995–96	0.74 (0.44)	20.43	3.62 (2.15)
1997–98	0.69 (0.42)	24.24	2.85 (1.73)
1999–00	1.13 (0.67)	30.44	3.71 (2.20)
2001–02	1.66 (0.99)	37.35	4.44 (2.65)

Additional research benefits, 97th to 107th Congress. First column, estimates ($P < 0.01$) of the effects of House and Senate appropriations committee representatives (from "pooled least squares" regressions in table S1) on the receipts of represented research performers to calculate the additional amounts received by performers in the states of committee members, ceteris paribus. The second column reports the total extramural peer-reviewed allocations made by the NIH during the corresponding Congress (covering two fiscal years). Figures in parentheses indicate 95% confidence intervals around the estimates (*5*). B$, billions of dollars.

[1]Walter A. Haas School of Business, University of California at Berkeley, Berkeley, CA 94720, USA. [2]Walter A. Haas School of Business, University of California at Berkeley, Berkeley, CA 94720 and National Bureau of Economic Research, Cambridge, MA 02138, USA.

*Author for correspondence. E-mail: hegde@haas.berkeley.edu

Published by AAAS

NIH directors at a hearing of the Senate Subcommittee on Labor, Health, and Human Services, and Education Appropriations for the FY 2003 budget.

Each additional member on the House subcommittee that deals with NIH appropriations (the "LHHE" subcommittee of the HAC) was associated with a 5.9% ($P < 0.01$) increase in NIH funding for institutions in their state (*5*, *6*) (tables S1 and S2). LHHE senators and non-LHHE House appropriations committee members did not have a statistically significant (at $P < 0.01$) impact on funding for research performers in their states (*7, 8*), with one exception. New York Senator Alfonse D'Amato, a member of the SAC from 1983 to 1994, significantly increased NIH funding for performers in New York State.

We estimated that the distribution of $1.7 billion of the $37.4 billion awarded by the NIH to extramural performers in the years 2002 and 2003 (appropriated during the congressional year 2001–2002) was influenced by representation on the HAC-LHHE subcommittee (*5*) (see table on page 1797 and table S2).

Do some types of research performer benefit more than others from subcommittee representation? We found that an additional HAC-LHHE member increased NIH funding for public universities in the member's state by 8.8% ($P < 0.01$) and grants to small businesses by 10.3% ($P < 0.01$). HAC subcommittee membership had no statistically significant effect (at $P < 0.01$) on grants to private universities, large firms, or other nonprofit institutions (*5*) (table S3).

R-series grants or awards for research projects make up the largest category of activities funded by the NIH (about 60% of the total NIH extramural grants). They fund research projects rather than programs. HAC-LHHE membership increased performers' R-series awards by 4.4% ($P < 0.02$) during this period (*5*) (table S4).

R-series grants are further divided into several subcategories; R01 is the traditional research grant supporting research initiated by investigators associated with research institutions. Research institutions typically are responsible for providing facilities necessary to conduct the research proposed by the investigator and are accountable for the grant funds. R03 or "Small Research Grants" support small research projects such as pilot or feasibility studies and secondary analysis of existing data. R41 to R44 are associated with the Small Business Innovation Research and Technology Transfer grants (SBIR and STTR), and so on. "P-series" awards can be P01 grants to support multidisciplinary or multifaceted research programs that have a focused theme. Estimates of the returns to representation on these more finely specified grant types (R01, R03, R41 to 44, and P01) suggest that HAC-LHHE members do not significantly affect allocations within any one of these classes, but that the effects appear in the overall funding amounts received by represented performers. This result is consistent with an avoidance by political representatives of direct interference with peer review of individual proposals, while influencing the institutional allocation of research funds (*5*, *9*) (table S4).

In an extension of our baseline model, we tested the extent to which an R&D performer's historical strength in specific research fields mediates the influence of subcommittee membership on its NIH funding (*5*) (table S5). Our estimates indicate that House LHHE representation increases NIH funding for research performers in the lowest two quartiles of grant recipients within any biomedical field by an average of 3.6 ($P < 0.02$) to 6.4% ($P < 0.01$). Performers in the top quartile, however, did not receive significantly larger allocations than otherwise comparable but unrepresented performers.

The congressional "power of the purse" is mandated by the Constitution. Political oversight of NIH funding decisions provides an important mechanism for public input into scientific judgments concerning health-research needs. Nevertheless, the exercise of such influence clearly mediates the effects of rigorous peer review. Moreover, the channels through which such influence operates may be more complex than directives contained in appropriations bills. We hope that our findings will spark a clearer debate over the extent and effects of political involvement in the resource allocations of the largest single source of federal civilian R&D spending.

References and Notes

1. Figures represent budget authority in constant FY2008 dollars (*2*).
2. *Historical Data on Federal R&D, FY 1976–2009* (AAAS, Washington, DC, 2008); www.aaas.org/spp/rd/hist09p2.pdf.
3. National Science Foundation, Division of Science Resources Statistics, Survey of Research and Development Expenditures at Universities and Colleges (NSF, Washington, DC. 2006); www.nsf.gov/statistics/nsf08300/pdf/nsf08300.pdf.
4. We utilized those research performers with observations and/or variation in at least two time periods. Those performers that received NIH grants once or twice during the period of our study received less than 13% of the total grant amount allocated by the NIH during 1984–2003, and the mean size of these grants was less than half the mean size for performers that were represented in our data set more than twice. Our estimates capture the effect of subcommittee representation on the size of grants for grant recipients. The presence of a "new grant effect" will not alter our results on the influence of appropriations committee representation unless we believe that applicants of new grants and additional grants differently affect the probability or number of representatives on the committee (which does not seem plausible).
5. Further information, including background, construction of the data set, the empirical model, results, and estimates, as well as examples, are provided in the supporting online material available in *Science* Online.
6. D. Hegde, *J. Law Econ.* (in press) contains additional robustness checks that investigate the endogeneity of LHHE representation and grant receipts, and various related results.
7. This result may reflect the tendency for senators, who serve on many more committees and subcommittees, not to specialize in analyzing and influencing appropriations for individual agencies to the same extent as House appropriations committee members. See, for instance, (*8*).
8. R. F. Fenno, *Power of the Purse: Appropriations Politics in Congress* (Little, Brown, Boston, 1966).
9. NIH, *Activity Codes, Organizational Codes, and Definitions Used in Extramural Programs* (NIH, Bethesda, MD, July 2007), http://grants.nih.gov/grants/funding/ac.pdf
10. D.H. and D.C.M. acknowledge support from the Bradley Foundation and the NSF (Cooperative Agreement 0531184), respectively.

Supporting Online Material

www.sciencemag.org/cgi/content/full/322/5909/1797/DC1

10.1126/science.1158562

EVOLUTION

Who's Your Daddy?

The male-only nest care system of some birds may have its evolutionary origins in theropod dinosaur behavior.

Richard O. Prum

The recognition that birds are theropod dinosaurs has redefined the science of ornithology as extant dinosaur biology (*1*). The placement of birds in a detailed evolutionary context has led to exciting discoveries about the commonalities birds share with their dinosaur ancestors, including feathers (*2*) and possibly flight (*3*). Insights have been gained into both the origins of avian biology and the natural history of some of the most charismatic dinosaurs—the meat-eating, bipedal theropods. The dividends continue with the report by Varricchio *et al.* on page 1826 of this issue (*4*), in which the authors show that fatherhood in theropods was about more than just looking macho and gnashing teeth.

Parental care in theropod dinosaurs. Fossil evidence has shown that theropod dinosaurs such as *Oviraptor* cared for their young (**left**) (*6*). Based on a new analysis, Varricchio *et al.* (*4*) hypothesize that it was male theropods who provided the care, similar to living birds at the base of the avian phylogeny, including ostriches (*Struthio camelus*) (**middle**) and highland tinamous (*Nothocercus bonapartei*) (**right**).

Biological views of dinosaur parenting have evolved a lot over the past century. In 1924, Osborn named a Cretaceous theropod *Oviraptor*, or "egg seizer," because it had been fossilized "in the very act of robbing [a] dinosaur egg nest" (*5*). In 1995, new specimens showed that *Oviraptor* was not stealing those eggs, but caring for them and possibly even brooding them (see the figure, left panel) (*6*). Now, Varricchio *et al.* (*4*) present compelling evidence from three theropods closely related to birds—*Troodon*, *Oviraptor*, and *Citipati*—that the individuals caring for those clutches of eggs were males. Because the basal lineage of living birds, or the earliest branch in the avian phylogenetic tree, also has predominantly male-only nest care, their discovery may have uncovered the dinosaurian origins of the breeding biology of living birds.

Varricchio *et al.* use two lines of evidence to support their revolutionary conclusion. First, they compared clutch volumes to adult body sizes for a sample of living archosaurs—the group of reptiles that includes crocodilians, birds, and other dinosaurs. They found that *Troodon*, *Oviraptor*, and *Citipati* have larger clutch volumes for their body sizes than most of the more than 400 extant species of birds and crocodilians examined, but that their clutch volumes closely match the expected values for birds with exclusively male parental care. Clutch volumes can evolve to be larger in species without maternal care, because females may have more resources to devote to eggs if they provide no care and because a "clutch" may be composed of eggs from multiple females. Second, Varricchio *et al.* took advantage of a distinctive feature of avian reproductive physiology to determine the sex of the dinosaurs from their bones. Many female birds lay down a distinctive layer of spongy, medullary bone inside their long bones during reproduction (*7*). Recent observations of medullary bone in the theropod *Tyrannosaurus rex* as well as in basal birds (*7*) indicate that female *Troodon*, *Oviraptor*, and *Citipati* should also exhibit medullary bone. Varricchio *et al.* show that the *Troodon*, *Oviraptor*, and *Citipati* individuals fossilized at nests lacked medullary bone, independently supporting the conclusion that they were males.

Over 90% of living birds have biparental care. A small group of species have exclusively female care, but less than 100 species of living birds have exclusively male parental care (*8*). In these species, males build the nest, incubate the eggs, and raise the young, whereas females mate with multiple males and lay their eggs in multiple nests, which may or may not be within a defended territory. The birds with the most consistent pattern of male nest care are the basal lineage of living birds, called Paleognathes, which include the flightless ostrich, emu, cassowary, kiwi, and rhea, and the flying neotropical tinamous (*9*) (see the figure, right panel).

Some behavioral ecologists have hypothesized that male-only parental care was the original breeding system of living birds (*8*), and the basal phylogenetic position of Paleognathes has been used to support this hypothesis (*10*). In the absence of any data on parental care in extinct dinosaurs, however, phylogenetic systematists have argued that female-only parental care, found both in birds and crocodilians, was the primitive breeding system of birds (*11*). Most recently, Wesołowski (*12*) argued against the theropod origin of avian breeding behavior while reiterating the male-care-first hypothesis. In a result that is sure to surprise both

Department of Ecology and Evolutionary Biology and Peabody Museum of Natural History, Post Office Box 208105, Yale University, New Haven, CT 06520, USA. E-mail: richard.prum@yale.edu

camps, Varricchio *et al.* show that the theropod origin of avian breeding behavior is consistent with male parental care as the primitive breeding system of birds, thus resolving the conflict between ecological and phylogenetic ornithologists.

These researchers have an excellent track record of establishing details of extinct theropod biology that have changed our views of the origins of avian biology. In 1997, Varricchio *et al*. (*13*) proposed that *Troodon* laid their eggs two at a time and that the uniquely avian behavior of laying the clutch of eggs over a series of days evolved in theropods before the origin of birds or flight. This bold idea was dramatically confirmed in 2005 with a discovery of an oviraptoran fossil with a pair of shelled eggs inside her pelvis (*14*).

According to the new hypothesis (*4*), the parental behaviors of living Paleognathes (like the cassowary) and extinct theropods (like *Oviraptor*) are homologous, and their breeding systems remained unchanged since their common ancestry. But could male parental care have evolved independently in Paleognathes and Cretaceous dinosaurs? There are many lineages between the Paleognathes and the oviraptorans and troodontids (including the huge, flightless, colonial diver *Hesperornis*, the pigeon-sized *Confuciusornis* with elongate ornamental tail feathers, and the archetypal *Archaeopteryx*). Many of these creatures seem so similar in ecology to various modern birds with biparental care that it is tempting to think that their breeding biology should also be similar. However, Varricchio *et al*.'s hypothesis may be supported by the observation that the male-only parental care system has resisted evolutionary change. Most Paleognathes have retained this breeding system, despite substantial ecological radiation, since before the K/T boundary over 65 million years ago (*15*, *16*). Thus, there may be substantial constraints to evolving female incubation if her female ancestors have not done so for tens of millions of years before her.

In the absence of a coherent hypothesis for the origin of birds during the greater part of the 20th century, most evolutionary explanations of avian biology focused on how unique birds are (*1*). Scientists are now identifying the dinosaurian origins of many of the formerly unique features of birds. Are there limits to ornithological revelations that the theropod origin of birds will yield? It seems not. Focused research and lucky paleontological discoveries may someday uncover the theropod origin of bird song, avian respiration, and more.

References

1. R. O. Prum, *Auk* **119**, 1 (2002).
2. R. O. Prum, A. H. Brush, *Quart. Rev. Biol.* **77**, 261 (2002).
3. X. Xu *et al.*, *Nature* **421**, 335 (2003).
4. D. J. Varricchio *et al.*, *Science* **322**, 1826 (2008).
5. H. F. Osborn, *Am. Mus. Nov.* **144**, 1 (1924).
6. M. A. Norell, J. M. Clark, L. Chiappe, D. Dashzeveg, *Nature* **378**, 774 (1995).
7. M. H. Schweitzer, J. L. Wittemeyer, J. R. Horner, *Science* **308**, 1456 (2005).
8. J. D. Ligon, *The Evolution of Avian Breeding Systems* (Oxford Univ. Press, Oxford, 1999).
9. S. J. J. F. Davies, *Ratites and Tinamous* (Oxford Univ. Press, Oxford, 2001).
10. T. Wesołowski, *Am. Nat.* **143**, 39 (1994).
11. B. S. Tullberg, M. Ah-King, H. Temrin, *Philos. Trans. R. Soc. B* **357**, 251 (2002).
12. T. Wesołowski, *Behav. Ecol.* **15**, 520 (2004).
13. D. J. Varricchio, F. Jackson, J. J. Borkowski, J. R. Horner, *Nature* **385**, 247 (1997).
14. T. Sato, Y. Cheng, X. Wu, D. K. Zelenitsky, Y. Hsiao, *Science* **308**, 375 (2005).
15. J. Clarke *et al.*, *Nature* **433**, 305 (2005).
16. J. W. Brown *et al.*, *BMC Biol.* **6**, 6 (2008).

10.1126/science.1168808

COMPUTER SCIENCE

The Ethical Frontiers of Robotics

The use of robots to care for the young and the old, and as autonomous agents on the battlefield, raises ethical issues.

Noel Sharkey

Robots have been used in laboratories and factories for many years, but their uses are changing fast. Since the turn of the century, sales of professional and personal service robots have risen sharply and are estimated to total ~5.5 million in 2008. This number, which far outstrips the 1 million operational industrial robots on the planet, is estimated to reach 11.5 million by 2011 (*1*). Service robots are good at dull, dangerous, and dirty work, such as cleaning sewers or windows and performing domestic duties in the home. They harvest fruit, pump gasoline, assist doctors and surgeons, dispose of bombs, and even entertain us. Yet the use of service robots poses unanticipated risks and ethical problems. Two main areas of potential ethical risk are considered here: the care of children and the elderly, and the development of autonomous robot weapons by the military.

The widespread availability of service robots has resulted from several developments that allowed robots to become mobile, interactive machines. Artificial intelligence has not met its early promise of truly intelligent machines, but researchers in the emerging field of human-robot interaction have implemented artificial intelligence techniques for the expression of emotion, language interaction, speech perception, and face recognition (*2*, *3*).

Sophisticated control algorithms have been developed (*4*) and have been combined with advances in sensor technology, nanotechnology, materials science, mechanical engineering, and high-speed miniaturized computing. With the prices of robot manufacture falling—robots were 80% cheaper in 2006 than they were in 1990—service robots are set to enter our lives in unprecedented numbers.

In the area of personal-care robots, Japanese and South Korean companies have developed child-minding robots that have facilities for video-game playing, conducting verbal quiz games, speech recognition, face recognition, and conversation. Mobility and semiautonomous function are ideal for visual and auditory monitoring; radio-frequency identification tags provide alerts when children move out of range. The robots can be controlled by mobile phone or from a window on a PC that allows input from camera "eyes" and remote talking from caregivers.

Research on child-minding robots in the United States (*5*) using the Sony Qurio and large-scale testing by NEC in Japan with their PaPeRo have demonstrated close bonding and attachment by children, who, in most cases, prefer a robot to a teddy bear. Short-term exposure can provide an enjoyable and entertaining experience that creates interest and curiosity. In the same way, television and computer games may be used by parents as an entertainment or distraction for short periods. They do not provide care and the children still need human attention. However, because of the physical safety that robot minders provide, children could be left without human contact for many hours a day or perhaps for several days, and the possible psychological impact of the varying degrees of social isolation on development is unknown.

Department of Computer Science, University of Sheffield, Sheffield S1 4DP, UK. E-mail: noel@dcs.shef.ac.uk

What would happen if a parent were to leave a child in the safe hands of a future robot caregiver almost exclusively? The truth is that we do not know what the effects of the long-term exposure of infants would be. We cannot conduct controlled experiments on children to find out the consequences of long-term bonding with a robot, but we can get some indication from early psychological work on maternal deprivation and attachment. Studies of early development in monkeys have shown that severe social dysfunction occurs in infant animals allowed to develop attachments only to inanimate surrogates (*6*).

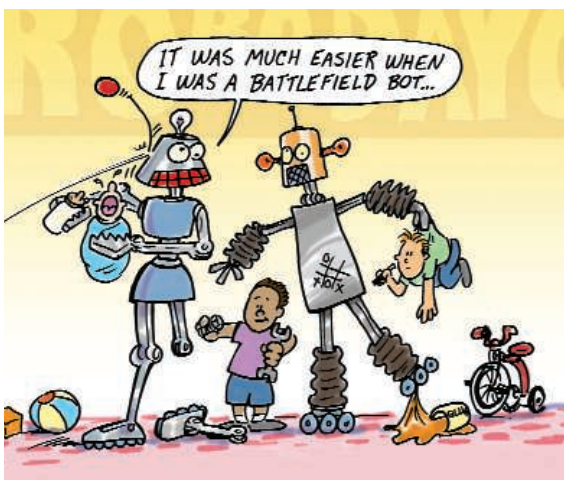

CREDIT: JOE SUTLIFF

Despite these potential problems, no international or national legislation or policy guidelines exist except in terms of negligence, which has not yet been tested in court for robot surrogates and may be difficult to prove in the home (relative to cases of physical abuse). There is no guidance from any international Nanny code of ethics, nor even from the U.N. Convention on the Rights of Children (*7*) except by inference. There is a vital need for public discussion to decide the limits of robot use before the industry and busy parents make the decision themselves.

At the other end of the age spectrum, the relative increase in many countries in the population of the elderly relative to available younger caregivers has spurred the development of sophisticated elder-care robots. Examples include the Secom "My Spoon" automatic feeding robot, the Sanyo electric bathtub robot that automatically washes and rinses, and the Mitsubishi Wakamura robot for monitoring, delivering messages, and reminding about medicine. These robots can help the elderly to maintain independence in their own homes (*8*), but their presence could lead to the risk of leaving the elderly in the exclusive care of machines. The elderly need the human contact that is often only provided by caregivers and people performing day-to-day tasks for them (*9*).

Robot companions such as Paro the seal are marketed as pets because they are soft and cuddly and are designed to imitate some of the features of pets, such as purring when touched—they are exploiting human zoomorphism. They are being touted as a solution to the contact problem, but these are still toys that do not alleviate elder isolation, even if they may relieve some of the guilt felt by relatives or society in general about this problem. The success of these robots may stem from people being systematically deluded about the real nature of their relation to the devices (*10*, *11*).

A different set of ethical issues is raised by the use of robots in military applications. Coalition military forces in Iraq and Afghanistan have deployed more than 5000 mobile robots. Most are used for surveillance or bomb disposal, but some, like the Talon SWORD and MAARS, are heavily armed for use in combat, although there have been no reports of lethality yet. The semi-autonomous unmanned combat air vehicles, such as the MQ1 Predator and MQ9 Reapers, carry Hellfire missiles and bombs that have been involved in many strikes against insurgent targets that have resulted in the deaths of many innocents, including children.

Currently, all these weapons have a human in the loop to decide when to apply lethal force. However, there are plans to create robots that can autonomously locate targets and destroy them without human intervention (*12*)—a high-priority agenda item for all the U.S. armed services (*13*, *14*). Ground-based unmanned autonomous vehicles (UAVs) such as DARPA's Unmanned Ground Combat Vehicle (the PerceptOR Integration System) are already being created (*15*). The military contractor, BAE Systems, has "completed a flying trial which, for the first time, demonstrated the coordinated control of multiple UAVs autonomously completing a series of tasks" (*16*). These developments fit with a major goal of the Future Combat Systems project, with estimated costs to exceed $230 billion, to use robots as force multipliers; one soldier can be a nexus for initiating large-scale ground (*17*) and aerial robot attacks (*13*). Robot autonomy is required because one soldier cannot control several robots.

The ethical problems arise because no computational system can discriminate between combatants and innocents in a close-contact encounter. Computer programs require a clear definition of a noncombatant, but none is available. The 1944 Geneva Convention suggests common sense, while the 1977 Protocol 1 update defines a civilian as someone who is not a combatant (*18*). Even with a definition, sensing systems are inadequate for the discrimination challenge, particularly in urban insurgency warfare. These complexities are difficult to resolve even for experienced troops in the field. No computational inference systems yet exist that could deal with the huge number of circumstances where lethal force is inappropriate. These systems should not be confused with smart bombs or submunitions that require accurate human targeting.

Robots for care and for war represent just two of many ethically problematic areas that will soon arise from the rapid increase and spreading diversity of robotics applications. Scientists and engineers working in robotics must be mindful of the potential dangers of their work, and public and international discussion is vital in order to set policy guidelines for ethical and safe application before the guidelines set themselves.

References and Notes

1. IFR Statistical Department, *World Robotics Report 2008* (www.worldrobotics.org).
2. C. Breazeal, *Robot. Auton. Sys.* **42**, 167 (2003).
3. T. Fong, I. Nourbakhsh, K. Dautenhahn, *Robot. Auton. Sys.* **42**, 143 (2003).
4. R. A. Brooks, *IEEE J. Robot. Automat.* **2**, 14 (1986).
5. F. Tanaka, A. Cicourel, J. R. Movellan, *Proc. Natl. Acad. Sci. U.S.A.* **194**, 46 (2007).
6. D. Blum, *Love at Goon Park: Harry Harlow and the Science of Affection* (Wiley, Chichester, UK, 2003).
7. Convention on the Rights of the Child, adopted and opened for signature, ratification, and accession by U.N. General Assembly Resolution 44/25, 20 November 1989.
8. J. Forlizzi, C. DiSalvo, F. Gemperle, *Hum. Comput. Interact.* **19**, 25 (2004).
9. R. Sparrow, L. Sparrow, *Minds Machines* **16**, 141 (2004).
10. R. Sparrow, *Ethics Inform. Technol.* **4**, 305 (2002).
11. N. E. Sharkey, A. J. C. Sharkey, *Artif. Intell. Rev.* **25**, 9 (2007).
12. N. E. Sharkey, *IEEE Intell. Sys.* **23**, 14 (July–August 2008).
13. U.S. Department of Defense, *Unmanned Systems Roadmap 2007–2032* (10 December 2007).
14. National Research Council, Committee on Autonomous Vehicles in Support of Naval Operations, *Autonomous Vehicles in Support of Naval Operation* (National Academies Press, Washington, DC, 2005).
15. Fox News, "Pentagon's 'Crusher' Robot Vehicle Nearly Ready to Go," 27 February 2008 (www.foxnews.com/story/0,2933,332755,00.html).
16. United Press International, "BAE Systems Tech Boosts Robot UAV's IQ," Industry Briefing, 26 February 2008 (http://bae-systems-news.newslib.com/story/3951-3226462).
17. U.S. Department of Defense, LSD (AT&L) *Defense Systems/Land Warfare and Munitions 3090, Joint Robotics Program Master Plan FY2005* (2005).
18. Protocol 1 Additional to the Geneva Conventions, 1977 (Article 50).

19. Supported by a fellowship from the Engineering and Physical Sciences Research Council, UK.

10.1126/science.1164582

MATERIALS SCIENCE

Now You See Them

Can new results on calcium carbonate nucleation be reconciled with classical nucleation theory?

Fiona C. Meldrum[1] and Richard P. Sear[2]

Crystallization lies at the heart of many natural and technological processes, from the production of pharmaceuticals and nanomaterials to the formation of bones and teeth, frost heave, and scale deposition. Crucial features of these crystals, such as lattice orientation, particle size, and size distribution, are defined by conditions during the earliest stages of precipitation—at nucleation. Yet, nucleation from solution is poorly understood, because experimental studies of nucleation are highly challenging (*1*). Recent studies have highlighted the possible role of clusters in nucleus formation (*2*, *3*). On page 1819 of this issue, Gebauer *et al.* provide support for this thesis (*4*) by demonstrating the presence of large, well-defined clusters before nucleation of one of the phases of calcium carbonate. Crystallization appears to proceed through aggregation of these clusters. The results challenge the conventional picture of crystal nucleation.

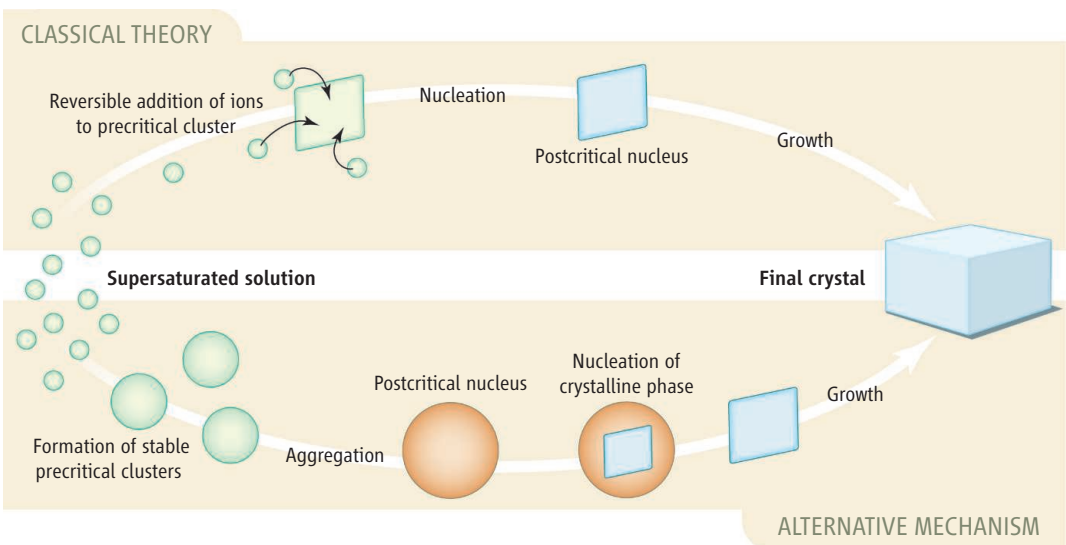

How do crystals nucleate? According to classical nucleation theory, calcium carbonate nucleation proceeds by addition of ions to a single cluster (**top**). Gebauer *et al.* now suggest a different mechanism, in which nucleation of ACC occurs by aggregation of stable, amorphous, precritical clusters (**bottom**). The nucleated ACC phase subsequently crystallizes to generate the final stable crystal product.

Classical nucleation theory provides a simple understanding of how crystals nucleate. Nucleation is often slow because of a free-energy barrier originating from the interface between the nucleus and its surroundings. The theory assumes that nuclei grow one molecule at a time (see the figure, top). As the nuclei grow, their Gibbs free energy increases, until a free-energy maximum is reached at the critical size. At least in simple systems such as argon, critical nuclei are expected to persist for microseconds or less, making them virtually impossible to observe. Beyond the critical size, the nuclei are stable and release energy during growth.

In their investigation of calcium carbonate nucleation, Gebauer *et al*. observe long-lived precritical clusters, about 2 nm in diameter, and suggest that they grow by colliding and coalescing. These results are clearly in contrast to the picture of nucleation presented by classical nucleation theory. The theory assumes that the structure of the nucleus is like a piece of the bulk phase and that its surface has the same interfacial tension as a bulk phase. However, if stable, precritical clusters are to exist, they must lie in a free-energy minimum. Such a minimum would only occur if the classical theory's assumptions are wrong, perhaps because the structure of the clusters is different from that of the bulk.

The possible structure of the precritical calcium carbonate clusters is open to speculation. If the ions are present in a bulk crystal lattice, then it is surprising that the clusters of about 70 ions neither shrink nor grow. Alternatively, the structures may be ordered but differ from that of the bulk phase, thus retarding growth. Modeling has shown that small ordered clusters of argon atoms are not just chunks cut from the bulk lattice but form different structures, such as icosahedra, which are incompatible with growth to fill space (*5*). In the case of argon, the true bulk phase nucleates on these ordered clusters, rendering them transient. However, calcium carbonate solutions are considerably more complex, so that nucleation of the true bulk phase from an ordered nanoparticle may be more difficult. Calcium carbonate is highly polymorphic in that it can exist in six different crystal structures. The first polymorph formed after nucleation is often amorphous calcium carbonate (ACC), which subsequently crystallizes (*6*, *7*). ACC has no long-range order, but it often has short-range structural order that appears to determine the lattice structure after crystallization (*8*). The most likely scenario is therefore that the precritical clusters are themselves amorphous or of low structural order. However, if they are amorphous, it is again unclear why they neither dissolve nor grow.

There is one system in which clusters and their contribution to the nucleation of the bulk phase have been extensively studied, and where we have at least a basic understanding of their behavior: water droplets in Earth's atmosphere (*9*). These droplets range in size from a few nanometers to tens of nanometers. They are stabilized by other species (such as sulfuric acid) that are both highly water-soluble and nonvolatile, so that they partition strongly into the nanometer-scale droplets. These ions provide an osmotic pressure inside the droplets that prevents their evaporating, even when the air is undersaturated with water vapor. Dusek *et al.* have shown that the super-

[1]School of Chemistry, University of Bristol, Cantock's Close, Bristol BS8 1TS, UK. E-mail: fiona.meldrum@bristol.ac.uk [2]Department of Physics, University of Surrey, Guildford GU2 7XH, UK. E-mail: r.sear@surrey.ac.uk

Published by AAAS

saturation at which nucleation occurs is determined largely by the size of the nanodroplets present (*10*).

Could the precritical clusters observed by Gebauer *et al.* also be the result of stabilization of calcium carbonate clusters by another species present as an impurity? This mechanism would provide a basis for stabilizing precritical clusters in a free-energy minimum and does not contradict classical nucleation theory. Such impurities are ubiquitous and virtually impossible to eliminate from any solution. The results of Gebauer *et al.* may thus reflect the mechanism of nucleation of calcium carbonate in "real" systems. Nucleation could then occur by coalescence of the precritical clusters to give ACC, which will subsequently crystallize to a more stable crystalline polymorph. The latter mechanism is consistent with the observations of Gebauer *et al*., who show that ACC is the first phase precipitated after nucleation.

The idea that nucleation of calcium carbonate may proceed via an aggregation mechanism is highly topical. The past decade has seen great progress in understanding crystallization processes, and it is now well recognized that single-crystal growth (as distinct from nucleation) often occurs via the aggregation of small precursor units rather than by addition of ions or molecules to a nucleus (*11*). Cluster species have also been observed before nucleation in saturated solutions of compounds such as sodium chloride (*2*), urea (*12*), and glycine (*3*), and there have been suggestions that clustering can determine which polymorph is formed (*13*). However, none of these even remotely approach the size or stability of the clusters observed by Gebauer *et al.* Further investigation of precritical clusters and their role in the crystallization of calcium carbonate, and indeed other compounds, is eagerly anticipated.

References

1. R. P. Sear, *J. Phys. Cond. Matter* **19**, 033101 (2007).
2. S. A. Hassan, *Phys. Rev. E* **77**, 031501 (2008).
3. C. E. Hughes, S. Hamad, K. D. M. Harris, C. R. A. Catlow, P. C. Griffiths, *Faraday Discuss.* **136**, 71 (2007).
4. D. Gebauer, A. Völkel, H. Cölfen, *Science* **322**, 1819 (2008).
5. F. Baletto, R. Ferrando, *Rev. Mod. Phys.* **77**, 371 (2005).
6. S. E. Wolf, J. Leiterer, M. Kappl, F. Emmerling, W. Tremel, *J. Am. Chem. Soc.* **130**, 12342 (2008).
7. J. R. Clarkson, T. J. Price, C. J. Adams, *J. Chem. Soc. Faraday Trans*. **88**, 243 (1992).
8. R. S. K. Lam, J. M. Charnock, A. Lennie, F. C. Meldrum, *CrystEngComm* **9**, 1226 (2007).
9. J. Seinfeld, S. N. Pandis, *Atmospheric Chemistry and Physics* (Wiley-Interscience, New York, 1998).
10. U. Dusek *et al.*, *Science* **312**, 1375 (2006).
11. H. Cölfen, M. Antonietti, *Mesocrystals and Nonclassical Crystallization* (Wiley, Chippenham, UK, 2008).
12. R. C. Burton *et al.*, *Crystal Growth Des.* **8**, 1559 (2008).
13. R. A. Chiarella *et al.*, *Faraday Discuss.* **136**, 179 (2007).

10.1126/science.1167221

DEVELOPMENTAL BIOLOGY

From Genetic Association to Genetic Switch

Human genetic studies have led to the identification of a transcriptional regulator that could serve as a therapeutic target for adult hemoglobin disorders.

Alan M. Michelson

Deciphering the sequence of the human genome and the subsequent cataloging of common human DNA sequence variation marked a paradigm shift in human genetics. These resources, together with advances in cost-effective genotyping technologies, enabled the design of genome-wide association studies for the unbiased discovery of commonly occurring DNA sequence variations called single-nucleotide polymorphisms (SNPs) that are preferentially associated with a disease or other clinical trait (*1*). Although genome-wide association studies have uncovered disease-associated SNPs, identifying actual disease-causing variants—and gaining deep insights into how those variants generate the underlying molecular pathophysiology—have so far yielded only modest results. This has led to criticisms of the genome-wide association approach for investigating the etiologies of common diseases (*2*). However, this assessment may be premature. On page 1839 of this issue, Sankaran *et al*. (*3*) show how genome-wide association findings can lead to a detailed understanding of disease mechanisms and be used to ascertain novel therapeutic targets.

Previous genome-wide association studies conducted in independent populations have identified SNPs in three chromosomal loci that are associated with varying expression levels of human fetal hemoglobin (HbF) (*4*–*6*). HbF is a clinically important quantitative trait because elevated concentrations reduce the severity of sickle cell disease and β-thalassemia, disorders caused by different mutations in the human β-globin gene (*7*). Normally, HbF predominates in the fetus but declines to very low amounts postnatally due to repression and activation of the γ-globin and β-globin genes, respectively. The "switch" that controls these reciprocal changes in globin gene expression has been intensively investigated, but the molecular basis of this developmental process remains largely unknown. As reported by Sankaran *et al.*, functional studies motivated by recent HbF genome-wide association findings have provided a major breakthrough in understanding the hemoglobin switching problem.

One of the SNPs associated with elevated HbF expression is found in an intron (noncoding region) of the *BCL11A* gene on human chromosome 2 (see the figure). *BCL11A* encodes a protein that represses transcription in the B lymphoid lineage (*8*).

Sankaran *et al.* hypothesized that BCL11A might repress expression of the γ-globin gene, with expression or activity of this repressor correlating inversely with HbF production both during normal development and in individuals of different genotypes at the *BCL11A* locus. They first determined that BCL11A is expressed as two long isoforms, encoded by alternatively spliced messenger RNAs (mRNAs), in primary adult erythroblasts. By contrast, only shorter variants of BCL11A are found in human embryonic erythroleukemia cells and in primary human fetal liver cells, both of which express high amounts of HbF. Moreover, the genotype at the *BCL11A* SNP that affects HbF production influences expression of mRNAs encoding the long isoforms in lymphoblastoid cell lines: High expression of *BCL11A* mRNA corresponds to homozygosity for the allele associated with low HbF production; low mRNA expression corresponds to homozygosity for the allele associated with high HbF production; and SNP heterozygotes express intermediate amounts of mRNA (see the figure). If the association between the *BCL11A* SNP and the expression level of this gene in lymphoblas-

National Heart, Lung and Blood Institute, National Institutes of Health, 31 Center Drive, Bethesda, MD 20892, USA. E-mail: michelsonam@mail.nih.gov

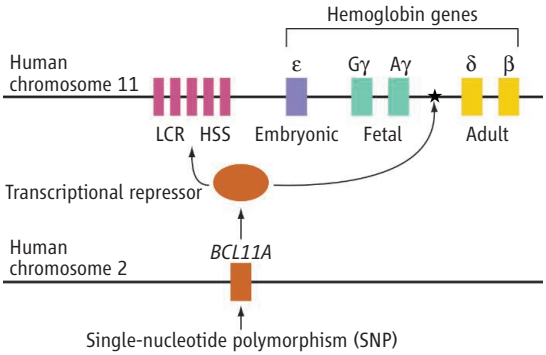

Expression		*BCL11A* SNP
Fetal hemoglobin	*BCL11A*	
Low	High	GG (homozygous)
High	Low	AA (homozygous)

From SNP to mechanism and potential therapy. Hemoglobin genes on human chromosome 11 are differentially expressed in the embryo, fetus, and adult. A SNP in the *BCL11A* gene is associated with varying amounts of fetal hemoglobin in human populations. Because there is an inverse correlation between *BCL11A* and fetal hemoglobin expression, inhibiting BCL11A is a potential therapy for adult hemoglobinopathies. LCR HSS: locus control region hypersensitive sites. The asterisk indicates a DNA region that, when deleted, is associated with increased fetal hemoglobin production.

toid cell lines also applies to erythroid cells, then the causative SNP either has a non–tissue-specific effect on transcription, or it acts at the posttranscriptional level, an issue that remains to be resolved.

Although the results are consistent with the long isoforms of BCL11A functioning to suppress HbF production in a dose-dependent manner, they do not distinguish between a direct effect on γ-globin gene expression and an indirect effect on the kinetics of erythropoiesis that might cause cells containing HbF to be overproduced (*9*). Additional findings of Sankaran *et al.* argue strongly in favor of the former model. For example, BCL11A was found to interact with multiple components of the nucleosome remodeling and histone deacetylase (NuRD) complex, which functions in transcriptional repression (*10*), as well as with GATA-1 and FOG-1, the major activating transcription factor and cofactor, respectively, of the erythroid lineage (*11*). Further, RNA interference specific for *BCL11A* in primary erythroid progenitors increased γ-globin mRNA expression and HbF production without inducing a generalized effect on cellular differentiation or altering expression of known globin gene transcription factors. Finally, chromatin immunoprecipitation revealed that BCL11A binds to multiple regions within the human β-globin locus that control silencing of the γ-globin gene (*7*).

Thus, BCL11A plays an important role in fetal-to-adult hemoglobin switching during normal erythropoiesis, and its expression in adult erythroid cells affects the amount of HbF produced. This raises questions about what controls the stage-specific shift between the long and short BCL11A isoforms, and the molecular mechanism by which BCL11A represses γ-globin gene expression. It is also not clear which genetic variant in *BCL11A* sets the expression level of this gene, nor how it functions in this capacity. Higher-resolution studies of BCL11A chromatin occupancy, functional characterization of the putative cis-regulatory elements containing these binding sites, and sequencing of the entire region of BCL11A that is in linkage disequilibrium with the SNP used to discover its relevance to HbF expression are needed to address these questions.

The findings of Sankaran *et al.* also have potential consequences for developing new therapies to treat sickle cell disease and other hemoglobinopathies. The inverse correlation between BCL11A and HbF expression, combined with the known ameliorative effect of HbF on the pathophysiology of sickle cell disease and β-thalassemia, suggests that inhibition of BCL11A expression or function could be an effective treatment for these disorders. The study also illustrates that, when experiments are appropriately designed, the initial findings of genome-wide association studies can be successfully followed up at a functional level.

References

1. T. A. Manolio, L. D. Brooks, F. S. Collins, *J. Clin. Invest.* **118**, 1590 (2008).
2. W. Bodmer, C. Bonilla, *Nat. Genet.* **40**, 695 (2008).
3. V. G. Sankaran *et al.*, *Science* **322**, 1839 (2008); published online 4 December 2008 (10.1126/science.1165409).
4. G. Lettre *et al.*, *Proc. Natl. Acad. Sci. U.S.A.* **105**, 11869 (2008).
5. S. Menzel *et al.*, *Nat. Genet.* **39**, 1197 (2007).
6. M. Uda *et al.*, *Proc. Natl. Acad. Sci. U.S.A.* **105**, 1620 (2008).
7. A. Bank, *Blood* **107**, 435 (2006).
8. H. Liu *et al.*, *Mol. Cancer* **5**, 18 (2006).
9. D. R. Higgs, W. G. Wood, *Proc. Natl. Acad. Sci. U.S.A.* **105**, 11595 (2008).
10. S. A. Denslow, P. A. Wade, *Oncogene* **26**, 5433 (2007).
11. R. K. Patient, J. D. McGhee, *Curr. Opin. Genet. Dev.* **12**, 416 (2002).

10.1126/science.1169216

TRANSCRIPTION

Gene Expression—Where to Start?

Stephen Buratowski

Transcription just got noisier with the discovery of short RNAs that are synthesized at or near DNA regions that also initiate full-length RNAs.

To convert the encoded genetic information from eukaryotic DNA into proteins, base sequences of genes are first transcribed into RNA by RNA polymerase II. To produce functional RNA molecules, dozens of accessory factors are needed to define the proper locations for RNA polymerase II to begin and end transcription. Although we have some basic knowledge about how these factors work, it is still not possible to take a eukaryotic genome sequence and accurately predict what RNA species it will produce. Recent efforts to map and sequence "transcriptomes" have only increased the challenge by revealing a much more complex set of RNAs than expected, including many that do not produce proteins. The latest surprise, described in four papers in this issue (*1*–*4*), is a new class of transcripts that initiate near the expected transcription start sites upstream of protein-encoding sequences. However, these RNAs are short, present at low abundance, and often occur in the direction opposite to that of the protein-coding region (see the figure). It remains to be seen whether these RNAs have a function, but their existence challenges our simplistic models about how the DNA sequences known as "promoters" define transcription start sites.

In current textbook models, promoters comprise two interacting parts. Basal promoter elements bind accessory transcription initiation factors that position RNA polymerase II in the right place and direction. Enhancer elements bind regulatory factors

Department of Biological Chemistry and Molecular Pharmacology, Harvard Medical School, 240 Longwood Avenue, Boston, MA 02115, USA. E-mail: steveb@hms.harvard.edu

that specify the physiological conditions or cell types where the gene will be expressed. The enhancer and basal promoter complexes functionally and physically interact to determine how often an RNA transcript is produced. The problem with this model is that enhancers can work over large distances of DNA in both directions, whereas basal elements are made up of short, low-complexity sequences (such as the TATA element) that appear frequently by chance. Transcription would likely initiate promiscuously throughout the genome without some way to suppress most transcription start sites.

The major mechanism for suppressing widespread transcription is to sequester potential transcription start sites by wrapping most of the genome in nucleosomes, subunits of chromatin in which DNA is coiled around histone proteins (*5*). Indeed, "real" transcription start sites are typically found in nucleosome-free regions generated by DNA sequences intrinsically resistant to nucleosome wrapping or by targeted modification and removal of nucleosomes to expose the underlying promoter sequences (*6*). Because transcription by RNA polymerase II through protein-coding sequences requires nucleosome displacement, eukaryotic cells even have mechanisms to quickly replace repressive nucleosomes in the wake of RNA polymerase II. Loss of this repression leads to cryptic RNAs initiating within transcribed regions (*7*). Therefore, functional eukaryotic promoters not only must attract RNA polymerase II, but also evade nucleosomal repression.

So what are we to make of these new, promoter-associated transcripts? The simplest view is that they arise from random, weak basal promoter elements that escape suppression. This idea is supported by the fact that the new RNAs are largely derived from DNA in nucleosome-free regions. Interestingly, Preker *et al.* (*3*) show that noneukaryotic DNA placed next to a strong mammalian promoter will also produce short divergent transcripts, indicating minimal sequence specificity. He *et al.* (*2*) also report antisense transcription—the synthesis of RNA complementary to the protein-coding RNA—initiating near 3′ ends of genes, another region that often has reduced nucleosome occupancy.

Although "backward" transcripts are less abundant than the "forward" (coding, full-length) transcripts produced by nearby transcription start sites, a clear correlation in their expression suggests that both types of RNAs respond to the same inducers of gene expression. Interestingly, the new papers find similar amounts of RNA polymerase II associated with the upstream and downstream transcription start sites. The mystery is why RNA polymerase II traveling in one direction can produce RNAs thousands of nucleotides long, whereas polymerases moving in the opposite direction don't get very far. However, as noted by Core *et al.* (*1*), even at many of the transcription start sites that produce full-length RNAs, much of the RNA polymerase II that starts at the promoter does not effectively make it to the end of the gene. The RNA polymerase II molecules that accumulate near promoters are often referred to as "paused," but it is unclear whether they await a positive signal to continue elongating (synthesizing RNA) or instead quickly terminate transcription soon after initiation. In either case, it appears that a rate-limiting step is escape of RNA polymerase II into processive, long-range elongation.

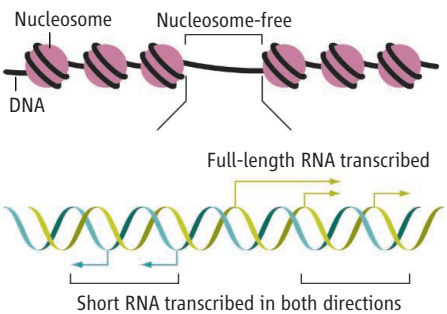

Promoter-associated transcripts. Transcription start sites and transcripts are represented as bent arrows. Short transcripts synthesized in both directions are now described (*1*–*4*).

Even if the short promoter-associated RNAs simply result from incomplete suppression of cryptic initiation, it would be a mistake to assume that there is no associated function. The RNAs produced from these unanticipated transcription start sites may have some undiscovered role, but it is perhaps more likely that the act of transcription itself affects expression of the nearby gene. As suggested by several of the new papers, this could be mediated by transcription-coupled changes in the DNA topology or local chromatin structure. Recent studies in yeast have uncovered interesting regulatory relationships between closely spaced transcription start sites. In the case of the *SER3* gene, RNA polymerase II initiating at an upstream transcription start site reads through the *SER3* promoter to repress synthesis of the full-length messenger RNA (mRNA) (*8*). At several genes involved in nucleotide biosynthesis, the concentration of available nucleotides influences the choice between several possible transcription start sites. Although a subset of these is used when the cell needs full-length mRNA, the other transcription start sites produce short noncoding transcripts (*9*). In yeast, these and other cryptic unstable transcripts use an alternative transcription termination pathway that preferentially acts during early elongation (*10*, *11*). This pathway targets cryptic unstable transcripts for rapid degradation by a complex of nucleases called the exosome. Interestingly, Preker *et al.* report that the mammalian promoter-associated RNAs are also exosome substrates, contributing to their lower levels.

As complete transcriptomes of cells are cataloged at increasingly finer levels of detail, the hope is that we will be able to discern the rules that determine where RNAs are made and how they are processed. However, we should remain open to the idea that expression of the genome may be rather sloppy, with many (perhaps even most) (*12*) initiation events generating nonproductive transcripts that are rapidly degraded. This "noise" could provide abundant raw material for evolution. A cryptic transcription start site upstream of the "correct" initiation site might produce an RNA with additional protein-coding sequence or altered translation efficiency. A minor transcription start site within a gene could produce a truncated protein variant that is targeted to a different subcellular location. If any of these events provide some selective advantage, over the course of time, the cryptic transcription start site could become an alternative one and eventually the real transcription start site. If a low amount of bidirectional transcription around transcription start sites were harmful, cells probably would have evolved additional mechanisms for further suppression. The prevalent nature of the short promoter-associated transcripts suggests that their synthesis may serve some functional role, but this remains to be proven.

References

1. L. J. Core, J. J. Waterfall, J. T. Lis, *Science* **322**, 1845 (2008); published online 4 December 2008 (10.1126/science.1162228).
2. Y. He, B. Vogelstein, V. E. Velculescu, N. Papadopoulos, K. W. Kinzler, *Science* **322**, 1855 (2008); published online 4 December 2008 (10.1126/science.1163853).
3. P. Preker *et al.*, *Science* **322**, 1851 (2008) published online 4 December 2008 (10.1126/science.1164096).
4. A. C. Seila *et al.*, *Science* **322**, 1849 (2008); published online 4 December 2008 (10.1126/science.1162253).
5. K. Struhl, *Cell* **98**, 1 (1999).
6. B. Li, M. Carey, J. L. Workman, *Cell* **128**, 707 (2007).
7. V. Cheung *et al.*, *PLoS Biol.* **6**, e277 (2008).
8. J. A. Martens, L. Laprade, F. Winston, *Nature* **429**, 571 (2004).
9. B. Dichtl, *Mol. Cell* **31**, 617 (2008).
10. S. Lykke-Andersen, T. H. Jensen, *Nat. Struct. Mol. Biol.* **13**, 860 (2006).
11. L. Vasiljeva, M. Kim, H. Mutschler, S. Buratowski, A. Meinhart, *Nat. Struct. Mol. Biol.* **15**, 795 (2008).
12. K. Struhl, *Nat. Struct. Mol. Biol.* **14**, 103 (2007).

10.1126/science.1168805

SCIENCE POLICY

Despite Financial Crisis, Dramatic Shift Expected in U.S. S&T Policy

U.S. President-elect Barack Obama will face profound budget constraints, but still should be able to take significant action on a range of critical science and technology issues within months after he takes office, policy experts said at a recent AAAS seminar.

Obama could expand embryonic stem cell research and smooth visa policies that have frustrated foreign scientists and students coming to the United States. He has committed the U.S. to taking a lead role in crafting a replacement for the Kyoto Protocols on global climate change. And while unprecedented budget deficits are looming, he could use a massive public works program to launch new energy and environmental initiatives.

"It's definitely a bit of a mixed message," said Albert H. Teich, director of Science and Policy Programs at AAAS. "The deficit will limit discretionary spending, but experts also have pointed out the value of investments in research especially in alternative energy and green technology and in education and their potential role in the much-discussed stimulus package."

The science-related challenges and choices confronting the incoming administration were a central theme of the annual AAAS Leadership Seminar on Science and Technology Policy, which convened in Washington, D.C., from 17 to 21 November. The seminar was attended by 34 professionals from academia, business, research centers, nongovernmental organizations, and foreign embassies, and they got deep insight from experts well-versed in the issues and inner workings of the nation's capital.

The seminar reflected AAAS's close engagement with the presidential campaign and transition. Earlier this year, the association helped lead an effort to bring the candidates together for a debate on science and technology. When the candidates were unavailable, it backed Scientists and Engineers for America as the group organized a pair of debates on health and energy policy featuring representatives from the campaigns of Obama and Senator John McCain.

In the days before the election, AAAS joined nearly 180 organizations in urging the next president to appoint a White House science adviser with Cabinet rank by Inauguration Day.

U.S. President-elect Barack Obama.

And as President George W. Bush has prepared to leave office, AAAS wrote letters urging the administration not to weaken the scientific process underlying the Endangered Species Act and to use the best possible science in setting climate change policy.

The week-long Leadership Seminar explored issues ranging from the workings of Congress to research and development funding, the space program and the troubled U.S. visa system. But with the historic election just concluded, much of the discussion turned on the new administration's plans for science and technology.

The consensus, though cautiously optimistic, was hardly rosy, given the state of the economy.

Obama has made it clear that he sees the connection between science and many of the challenges confronting the nation. In addition to a science adviser, he's likely to appoint a chief technology officer, said author and political analyst Norman Ornstein.

Obama could act quickly on embryonic stem cell research, said Rachel Levinson, who served under the past three presidents as assistant director for life sciences in the Office of Science and Technology Policy. "I think that President Obama will release an executive order within 48 hours of his inauguration lifting the ban on federal funds for embryonic stem cell research," predicted Levinson, who now works on special projects and research initiatives for Arizona State University.

Other initiatives may be constrained by the financial crisis, experts said. After a record $455 billion U.S. deficit for fiscal 2008, the deficit could soar past $1 trillion for 2009, said Kei Koizumi, director of the AAAS R&D Budget and Policy Program. But hidden in the crisis is an opportunity, said Ornstein. There is bipartisan support for a fiscal stimulus bill—perhaps hundreds of billions of dollars.

"It's going to be all stimulus, all the time," Ornstein quipped. "The Cialis version of government awaits us, and it'll last more than 4 hours. All of that leads to an imperative for action."

R&D might not be a target for stimulus-funds—green research could take 10 years to pay dividends, said Greg Ip, U.S. economic editor for *The Economist*. But, noted Ornstein, there could be an infusion of investment for such projects as electricity grid improvement, wind power, and infrastructure upgrades.

Obama's advisers have indicated that he plans to move quickly on energy efficiency. If Congress and the new president approve a cap-and-trade system, the sale of pollution permits could generate billions more for green investments.

But several speakers at the Leadership Seminar said that education will be crucial to the energy and climate efforts.

"We need to communicate honestly to the public both the difficult challenges of bringing about a revolutionary transformation of the global energy system and the absolute necessity of starting that transformation as quickly as possible," said Bob Simon, staff director of the U.S. Senate Committee on Energy and Natural Resources. "It is a tough challenge that cannot be put off."

ON-CALL SCIENTISTS

New AAAS Rights Project Aims for Global Impact

During the war in Bosnia and Herzegovina a decade ago, forensic pathologist Yvonne Milewski investigated mass graves in the region, identifying victims for families devastated by the conflict and compiling evidence of war crimes for a United Nations tribunal. The experience showed her how scientific skills "might be utilized in a different context within human rights organizations," said Milewski, chief medical examiner in Suffolk County, N.Y.

With the help of a new AAAS initiative that connects scientists with human rights organizations in need of scientific expertise, Milewski's

DAVID KATZ/OBAMA FOR AMERICA

Published by AAAS

experience might be duplicated around the world. "On-call" Scientists is a new project of the AAAS Science and Human Rights Program which links scientists who can provide vital technical assistance to the organizations that promote, monitor, and protect human rights in the United States and abroad.

Since the launch of the database in late October, 87 scientists and engineers with expertise ranging from parasites to electrical engineering have signed up. The volunteers include early-career and veteran scientists, and they hail from Canada, Germany, India, Italy, Morocco, New Zealand, Nigeria, Spain, Sweden, Switzerland, the Netherlands, the United Kingdom, and the United States.

While human rights organizations can benefit from the *pro bono* consultations, scientists and engineers may also find that their work with the human rights community can reveal new applications for their knowledge, said program Director Mona Younis.

"Both scientists and human rights activists care about impact," said Younis. "Through these relationships, human rights practitioners should see their efforts enhanced and scientists will see new opportunities to make a difference."

The "On-call" project was unveiled at a seminar held 23 October at AAAS headquarters in Washington, D.C., which highlighted the collaboration of Milewski and other scientists who have worked with human rights organizations on issues from prisoners' health care in the U.S. to genocide in Darfur.

Younis encouraged scientists and engineers from all disciplines to consider volunteering "even if their profession is so specialized that they can't imagine a possible application to human rights." At a minimum, she said, scientists of all backgrounds can help organizations integrate the scientific method into their data collection and analysis.

The project is supported by the AAAS Science and Human Rights Coalition, a formal network of scientific associations, professional societies, and science academies that will begin its official work at a free public conference in Washington, D.C., on 14 to 16 January 2009. Along with promoting stronger working ties between the science and human rights communities, the Coalition [http://shr.aaas.org/scisocs/] will address the human rights of scientists under threat and research ethics.

—Benjamin Somers and Becky Ham

CLIMATE POLICY

Game Turns Policy-Makers To Climate Players

Policy-makers tested the tools of greenhouse gas reduction last month with a game that challenges players to build a portfolio of strategies that would flatten carbon emission levels and forestall the worst effects of global warming over the next 50 years.

More than 80 congressional staff members, embassy personnel, and others participated in the Stabilization Wedge Game developed by Princeton researchers and presented at the 20 November briefing for the Congressional Research and Development Caucus. The Capitol Hill event was sponsored by AAAS's Center for Science, Technology, and Congress.

After 15 minutes of lively discussion, many of the participants had settled on a few key options: double the fuel efficiency of cars, boost the capacity of electrical and nuclear power plants, halt the destruction of carbon-storing forests, and gradually replace coal-based energy with wind and solar power projects.

The choices are all feasible with current technology, said Roberta Hotinski, a Princeton science communicator who presented the Wedge Game at the briefing. But, she said, each of the strategies presents serious challenges: They're expensive, resources might be lacking, and they could have profound social consequences.

The game is an outgrowth of a 2004 *Science* paper by Steve Pacala and Robert Socolow, in which the researchers suggest eight main strategies or "wedges" of greenhouse gas reduction or storage to cut projected carbon emissions by 8 billion tons per year until 2055. Without these reductions, the amount of atmospheric carbon dioxide could be tripled from its pre-industrial levels by the end of the century, said Hotinski.

Adam Rosenberg, a staff member on the House Science Committee who played the game at the briefing, said his team was inspired to include new items such as geothermal energy in its wedge portfolio. "I found it to be an interesting exercise," he said. "Several of us had certainly been looking at these energy issues for a long time, but this really helped you gauge where other players' priorities were."

James A. "Jae" Edmonds, chief scientist at the Pacific Northwest National Laboratory's Global Change Research Institute who also spoke at the briefing, said cost looms especially large as a challenge for implementing some of these strategies. For instance, the cost of carbon stabilization would jump significantly if developing countries delay in adopting emission reductions, he noted.

The event was the second congressional briefing on climate change sponsored this year by the AAAS Center for Science, Technology, and Congress, which has tracked climate change proposals in the 110th Congress as part of its ongoing legislative analysis.

—Harvey Leifert and Becky Ham

ANNUAL MEETING

Scientists Convene in Chicago to Explore Earth's Past and Future

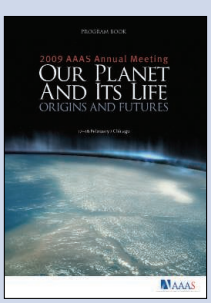

The 2009 calendar features an array of important science anniversaries, including the 200th anniversary of the birth of Charles Darwin, and the 150th anniversaries of the publication of his book *On the Origin of Species by Means of Natural Selection,* the first commercial oil well, and the discovery of carbon dioxide as a greenhouse gas.

As the 176th AAAS Annual Meeting convenes in Chicago next February under the banner, "Our Planet and Its Life: Origins and Futures," these milestones are more than memories. Instead, their implications reverberate throughout science today. At this year's meeting, the top scientists and engineers from more than 50 countries will discuss cutting-edge research from a full range of disciplines, including high-energy physics, sustainability, nanotechnology, infectious disease, social and economic networks, genomics, neuroscience, science diplomacy, and other fields.

Often described as "the Olympics of science conferences," the AAAS Annual Meeting offers attendees a chance to explore their own and other fields, as well as the broader connections between science and the rest of society. There will be nearly 175 symposia, seminars, and career development workshops. Speakers include renowned cosmologist Lord Martin Rees, physicist and energy visionary Amory Lovins, and evolutionary biologist Sean Carroll, who will discuss the latest research on the origins of life on Earth, the search for new energy sources and international scientific collaborations between developed and developing nations.

The staff of *Science, Science*NOW, and AAAS's award-winning *Science Update* radio program will provide extensive coverage from Chicago in news reports, podcasts, and blogs. The AAAS Annual Meeting News Blog on www.aaas.org also will provide extensive coverage of symposia and briefings, along with links to U.S. and international news stories from the meeting.

For registration and other information about the 2009 AAAS Annual Meeting, see www.aaas.org/meetings.

—Becky Ham

AAAS Members Elected as Fellows

In November, the AAAS Council elected 486 members as Fellows of AAAS. These individuals will be recognized for their contributions to science and technology at the Fellows Forum to be held on 14 February 2009 during the AAAS Annual Meeting in Chicago. The new Fellows will receive a certificate and a blue and gold rosette as a symbol of their distinguished accomplishments. Presented by section affiliation, they are:

Section on Agriculture, Food, and Renewable Resources

Carol R. Buell, Michigan State University • Thomas J. Burr, Cornell University/N.Y. State Agricultural Experiment Station • S. K. De Datta, Virginia Tech • James J. Elser, Arizona State University • Louise P. Fortmann, University of California, Berkeley • Jianying (Jay) Gan, University of California, Riverside • Nancy B. Grimm, Arizona State University • Leon V. Kochian, USDA Agricultural Research Service • Schuyler S. Korban, University of Illinois • J. K. Ladha, International Rice Research Institute • Alan McHughen, University of California, Riverside • Kenneth J. Moore, Iowa State University • M. Susan Moran, USDA Southwest Watershed Research Center • Andrew H. Paterson, University of Georgia • Prem S. Paul, University of Nebraska, Lincoln • Michael J. Sadowsky, University of Minnesota • Gary Stacey, University of Missouri • Judith S. Stern, University of California, Davis • Steven H. Strauss, Oregon State University • Deon D. Stuthman, University of Minnesota • Michael J. Vepraskas, North Carolina State University • Paddy L.W. Wiesenfeld, Center for Food Safety and Applied Nutrition, FDA • Roger Wyse, Burrill & Company • Shyu-Dong Yeh, National Chung-Hsing University • Jizhong Zhou, University of Oklahoma

Section on Anthropology

Susan C. Anton, New York University • Claude Bouchard, Louisiana State University • Daniel E. Brown, University of Hawaii • Marian Dagosto, Northwestern University • Robert G. Elston, University of Nevada • Carol R. Ember, Yale University • Charles F. Hildebolt, Mallinckrodt Institute of Radiology • Stephen A. Kowalewski, University of Georgia • Steven R. Leigh, University of Illinois, Urbana-Champaign • Jeffrey K. McKee, Ohio State University • James J. McKenna, University of Notre Dame • J. Michael Plavcan, University of Arkansas • Matthew J. Ravosa, University of Missouri • Audrey Smedley, Virginia Commonwealth University • David G. Smith, University of California, Davis

Section on Astronomy

Charles Alcock, Harvard-Smithsonian Center for Astrophysics • Marcia Bartusiak, Massachusetts Institute of Technology • James S. Bullock, University of California, Irvine • Jack O. Burns, University of Colorado, Boulder • Harriet Dinerstein, University of Texas, Austin • Andrew P. Gould, Ohio State University • Chris Kochanek, Ohio State University • Karen Kwitter, Williams College • Harry Y. McSween, University of Tennessee, Knoxville

Section on Atmospheric and Hydrospheric Sciences

Michael A. Celia, Princeton University • L. Ruby Leung, Pacific Northwest National Laboratory • Alan Robock, Rutgers University • John Walsh, University of Alaska, Fairbanks

Section on Biological Sciences

Warren G. Abrahamson, Bucknell University • David S. Adams, Worcester Polytechnic Institute • Jeffrey M. Becker, University of Tennessee, Knoxville • Darwin Berg, University of California, San Diego • Mark D. Bertness, Brown University • Timothy Block, Drexel University College of Medicine • James U. Bowie, University of California, Los Angeles • Jeffrey D. Brawn, University of Illinois, Urbana-Champaign • H. Jane Brockman, University of Florida • Garry R. Buettner, University of Iowa • Joanna Burger, Rutgers University • Michael Castellini, University of Alaska, Fairbanks • Avis H. Cohen, University of Maryland • Karen C. Cone, University of Missouri • Peter S. Curtis, Ohio State University • Prescott L. Deininger, Tulane University Medical Center • Dean DellaPenna, Michigan State University • Jennifer A. Doudna, University of California, Berkeley • Dale E. Edmondson, Emory University School of Medicine • Rebecca A. Efroymson, Oak Ridge National Laboratory • Daphne J. Fairbairn, University of California, Riverside • Christopher B. Field, Carnegie Institution for Science • Denise A. Galloway, Fred Hutchinson Cancer Research Center • Susan M. Gasser, Friedrich Miescher Institute for Biomedical Research • Brandon S. Gaut, University of California, Irvine • Susan A. Gerbi, Brown University • David M. Gilbert, Florida State University • Myron F. Goodman, University of Southern California • Howard D. Grimes, Washington State University • Michael D. Griswold, Washington State University • Louis J. Gross, University of Tennessee, Knoxville • Lorraine J. Gudas, Weill Medical College, Cornell University • Christine Guthrie, University of California, San Francisco • Tsonwin Hai, Ohio State University • Michael Hampsey, University of Medicine and Dentistry of New Jersey • Jo Handelsman, University of Wisconsin, Madison • Paul J. Hanson, Oak Ridge National Laboratory • J. Daniel Hare, University of California, Riverside • Denham Harman, University of Nebraska Medical Center • Randall E. Harris, Ohio State University • Caroline S. Harwood, University of Washington • James W. Hicks, University of California, Irvine • James M. Hill, Louisiana State University Eye Center • Alan G. Hinnebusch, Laboratory of Gene Regulation and Development, NIH • William K. Holloman, Weill Medical College, Cornell University • Anita K. Hopper, Ohio State University • Yue-ie C. Hsing, Institute of Plant and Microbial Biology • Feng Sheng Hu, University of Illinois, Urbana-Champaign • Peter Jackson, Stanford University School of Medicine • Kenneth A. Jacobson, University of North Carolina School of Medicine • Theodore S. Jardetzky, Stanford School of Medicine • Marshall W. Johnson, University of California, Riverside • H. Ronald Kaback, UCLA, David Geffen School of Medicine • Debra A. Kendall, University of Connecticut • Bruce S. Klein, University of Wisconsin • Daniel J. Klionsky, University of Michigan • Douglas E. Koshland, Carnegie Institution for Science • Sudhir Kumar, Arizona State University • Arthur D. Lander, University of California, Irvine • Jennifer Lippincott-Schwartz, National Institute of Child Health and Human Development, NIH • R. Michael Liskay, Oregon Health & Science University • Jun O. Liu, Johns Hopkins University School of Medicine • Carol J. Lovatt, University of California, Riverside • Terry Magnuson, University of North Carolina, Chapel Hill • Russell L. Malmberg, University of Georgia • James L. Manley, Columbia University • Therese A. Markow, University of Arizona • Mark Q. Martindale, University of Hawaii, Manoa • Bruce McClure, University of Missouri • Bruce McKee, University of Tennessee, Knoxville • Mark A. McPeek, Dartmouth College • Marvin L. Meistrich, University of Texas, M.D. Anderson Cancer Center • Barbara J. Meyer, University of California, Berkeley • Thomas G. Mitchell, Duke University Medical Center • Michelle Momany, University of Georgia • Peter Mombaerts, Max Planck Institute of Biophysics • Timothy A. Mousseau, University of South Carolina • Laurence D. Mueller, University of California, Irvine • Joseph H. Nadaeu, Case Western Reserve University • Jeremy Nathans, Johns Hopkins University School of Medicine • Eugene A. Nothnagel, University of California, Riverside • Stephen G. Oliver, University of Cambridge • Baldomero Olivera, University of Utah • Luis F. Parada, University of Texas, Southwestern Medical Center • Nipam H. Patel, University of California, Berkeley • Norbert Perrimon, Harvard Medical School • Craig S. Pikaard, Washington University, St. Louis • Daryl R. Pring, University of Florida • Douglas D. Randall, University of Missouri • Anjana Rao, Harvard Medical School • Jeffrey V. Ravetch, Rockefeller University • Susan E. Riechert, University of Tennessee, Knoxville • Michael R. Rose, University of California, Irvine • Paul B. Rothman, University of Iowa Carver College of Medicine • Rodney Rothstein, Columbia University Medical Center • Joan Ruderman, Harvard Medical School • Immo Erich Scheffler, University of California, San Diego • John C. Schimenti, College of Veterinary Medicine Cornell University • John F. Sheridan, Ohio State University • Neil H. Shubin, University of Chicago • Howard A. Shuman, Columbia University Medical Center • Barry D. Shur, Emory University • Robert H. Silverman, Cleveland Clinic Lerner Research Institute • Daniel Simberloff, University of Tennessee, Knoxville • Gerald R. Smith, Fred Hutchinson Cancer Research Center • Didier Y.R. Stainier,

University of California, San Francisco School of Medicine • Oswald Steward, University of California, Irvine • Jeffry Stock, Princeton University • Michael R. Strand, University of Georgia • Adam P. Summers, University of California, Irvine • Venkatesan Sundaresan, University of California, Davis • Betsy M. Sutherland, Brookhaven National Laboratory • Gabor Szabo, University of Virginia • Waclaw Szybalski, University of Wisconsin, Madison • Jordan J.N. Tang, Oklahoma Medical Research Foundation • Susan S. Taylor, University of California, San Diego • Carl S. Thummel, University of Utah School of Medicine • Lydia Villa-Komaroff, Cytonome, Inc. • Geoffrey M. Wahl, The Salk Institute • Graham C. Walker, Massachusetts Institute of Technology • Johannes Walter, Harvard Medical School • Nancy C. Walworth, University of Medicine and Dentistry of New Jersey • Gregory W. Warr, Hollings Marine Laboratory • Michael R. Waterman, Vanderbilt University School of Medicine • Patrick J. Weatherhead, University of Illinois, Urbana-Champaign • Alan M. Weiner, University of Washington • George M. Weinstock, Washington University School of Medicine • Richard K. Wilson, Washington University School of Medicine • Samuel H. Wilson, National Institute of Environmental Health Sciences, NIH • Jeffrey Wilusz, Colorado State University • Eckard A.F. Wimmer, Stony Brook University School of Medicine • Marc S. Wold, University of Iowa Carver College of Medicine • John L. Woolford, Carnegie Mellon University • Michael J. Yarus, University of Colorado, Boulder

Section on Chemistry

Mark M. Banaszak Holl, University of Michigan • Bridgette A. Barry, Georgia Institute of Technology • Ugo Bertocci, National Institute of Standards and Technology • Robert G. Bryant, University of Virginia • Carol J. Burns, Los Alamos National Laboratory • Mark J. Cardillo, The Camille and Henry Dreyfus Foundation, Inc. • Arup Chakraborty, Massachusetts Institute of Technology • Shirley Chiang, University of California, Davis • Jean Chmielewski, Purdue University • Mukund S. Chorghade, Chorghade Enterprises • Robert S. Coleman, Ohio State University • Michael E. Coltrin, Sandia National Laboratories • Phillip Crews, University of California, Santa Cruz • Mattanjah S. de Vries, University of California, Santa Barbara • Gautam R. Desiraju, University of Hyderabad • Michael Dupuis, Pacific Northwest National Laboratory • William J. Evans, University of California, Irvine • William Fenical, University of California, San Diego • Graham R. Fleming, University of California, Berkeley • Maria Flytzani-Stephanopoulos, Tufts University • Cynthia M. Friend, Harvard University • David W. Grainger, University of Utah • Nancy R. Gray, Gordon Research Conferences • Zhibin Guan, University of California, Irvine • P. Jeffrey Hay, Los Alamos National Laboratory • George W. Kabalka, University of Tennessee, Knoxville • William H. Kirchhoff, National Institute of Standards and Technology • Dilip P. Kondepudi, Wake Forest University • George A. Kraus, Iowa State University • Clark R. Landis, University of Wisconsin, Madison • Cynthia K. Larive, University of California, Riverside • Timothy P. Lodge, University of Minnesota • Jianpeng Ma, Baylor College of Medicine • Surya K. Mallapragada, Iowa State University • Mark Maroncelli, Pennsylvania State University • Susan Marqusee, University of California, Berkeley • Rachel W. Martin, University of California, Irvine • Pradip Mascharak, University of California, Santa Cruz • Joel S. Miller, University of Utah • Thomas A. Moore, Arizona State University • Catherine J. Murphy, University of South Carolina • Peter Nordlander, Rice University • Eric Oldfield, University of Illinois, Urbana-Champaign • Stanley M. Parsons, University of California, Santa Barbara • Charles H.F. Peden, Pacific Northwest National Laboratory • B. Montgomery Pettitt, University of Houston • Frank M. Raushel, Texas A&M University • Jack Saltiel, Florida State University • Charles R. Sanders, Vanderbilt University • H. Bernhard Schlegel, Wayne State University • Andreas K. Schmid, National Center for Electron Microscopy • Klaus Schmidt-Rohr, Iowa State University • Lynn F. Schneemeyer, Rutgers University • Susannah L. Scott, University of California, Santa Barbara • David H. Sherman, University of Michigan • Gary Sulikowski, Vanderbilt University • Elizabeth C. Theil, University of California, Berkeley • James J. Valentini, Columbia University • Tom Vogt, University of South Carolina • J. Herbert Waite, University of California, Santa Barbara • Mark E. Welker, Wake Forest University • Michael Widom, Carnegie Mellon University • David A. Wink, National Cancer Institute, NIH • Huan-Xiang Zhou, Florida State University

Section on Dentistry and Oral Health Sciences

Irma Thesleff, University of Helsinki

Section on Education

Donald L. Correll, Lawrence Livermore National Laboratory • Elson S. Floyd, Washington State University • Michael W. Klymkowsky, University of Colorado, Boulder • David D. Kumar, Florida Atlantic University • Wolff-Michael Roth, University of Victoria • Mike U. Smith, Mercer University School of Medicine • Conrad L. Stanitski, Franklin and Marshall College

Section on Engineering

Hojjat Adeli, Ohio State University • D. Grant Allen, University of Toronto • Braden R. Allenby, Arizona State University • Radhakisan S. Baheti, National Science Foundation • Issa Batarseh, University of Central Florida • Richard D. Braatz, University of Illinois, Urbana-Champaign • Cynthia J. Bruckner-Lea, Pacific Northwest National Laboratory • Douglas C. Cameron, Khosla Ventures • Jie Chen, University of California, Riverside • J. Gary Eden, University of Illinois • Said Elghobashi, University of California, Irvine • Harold B. Finger, Retired • Charles W. Forsberg, Massachusetts Institute of Technology • Brendan J. Frey, University of Toronto • Yury Gogotsi, Drexel University • Yassin A. Hassan, Texas A&M University • J. David Irwin, Auburn University • Fadi J. Kurdahi, University of California, Irvine • Thomas R. Kurfess, Clemson University • Terence G. Langdon, University of Southern California • Gary S. May, Georgia Institute of Technology • Chia-Hsiang Menq, Ohio State University • Edward I. Moses, Lawrence Livermore National Laboratory • Nitin P. Padture, Ohio State University • Mary Jane Phillips, University of Toronto • Sarah A. Rajala, Mississippi State University • Danny Reible, University of Texas, Austin • Rebecca Richards-Kortum, Rice University • Sudipta Seal, University of Central Florida • Kamalesh K. Sirkar, New Jersey Institute of Technology • Eswaran Subrahmanian, Carnegie Mellon University • Yong Wang, Pacific Northwest National Laboratory • Peter A. Wilderer, European Academy of Sciences and Arts • Jimmy Xu, Brown University • Yushan Yan, University of California, Riverside • Christopher Yip, University of Toronto • Xiang Zhang, Nanoscale Science and Engineering Center

Section on General Interest in Science and Engineering

Kenneth R. Fulton, National Academy of Sciences • Charles P. Gerba, University of Arizona • Michael A. Keller, Stanford University • John Kelley, University of Alaska, Fairbanks • Andrea E. Messer, Pennsylvania State University • David Perlman, San Francisco Chronicle • Joseph J. Romm, Center for Energy and Climate Solutions

Section on Geology and Geography

Patrick J. Bartlein, University of Oregon • Oliver A. Chadwick, University of California, Santa Barbara • Patricia Gober, Arizona State University • Edward Landing, New York State Museum • Jian Lin, Woods Hole Oceanographic Institute • Kam-Biu Liu, Louisiana State University • Shih-Lung Shaw, University of Tennessee, Knoxville • David A. Siegel, University of California, Santa Barbara • Thomas T. Veblen, University of Colorado, Boulder • Dawn J. Wright, Oregon State University

Section on History and Philosophy of Science

Angela Creager, Princeton University • Richard Creath, Arizona State University • David H. DeVorkin, National Air and Space Museum • Alan Touwaide, Smithsonian National Museum of Natural History

Section on Industrial Science and Technology

Orlando Auciello, Argonne National Laboratory • Richard R. Burgess, University of Wisconsin, Madison • Franco Cerrina, University of Wisconsin, Madison • Charles A. Eckert, Georgia Institute of Technology • John A. Rogers, University of Illinois, Urbana-Champaign

Section on Information, Computing, and Communication

Chandrajit Bajaj, University of Texas, Austin • Pierre Baldi, University of California, Irvine •

Steven E. Brenner, University of California, Berkeley • Alan Kay, Viewpoints Research Institute • Daniel E. Koditschek, University of Pennsylvania • Dexter Kozen, Cornell University • Douglas B. Lenat, Cycorp, Inc. • K.J. Ray Liu, University of Maryland • Darrell D.E. Long, University of California, Santa Cruz • Tom M. Mitchell, Carnegie Mellon University • Mart Molle, University of California, Riverside • Thomas P. Moran, IBM Almaden Research Center • Aristides A.G. Requicha, University of Southern California • Ravi Sandhu, University of Texas, San Antonio • Peter Scheuermann, Northwestern University • Shashi Shekhar, University of Minnesota • Venkatramanan S. Subrahmanian, University of Maryland • Leslie G. Valiant, Harvard University

Section on Linguistics and Language Science
Sally McConnell-Ginet, Cornell University • Betty Tuller, Florida Atlantic University

Section on Mathematics
Walter Craig, McMaster University • Robert J. Daverman, University of Tennessee, Knoxville • Richard Durrett, Cornell University • Alexander Nagel, University of Wisconsin • Jacob Rubinstein, Technion-Israel Institute of Technology • William Y. Velez, University of Arizona

Section on Medical Sciences
Michael Bevan, University of Washington • Bruce R. Blazar, University of Minnesota • Ernest C. Borden, Cleveland Clinic • Michael B. Brenner, Brigham and Women's Hospital • Paolo Casali, University of California, Irvine • Webster K. Cavenee, Ludwig Institute for Cancer Research • Cecilia Cheng-Mayer, Aaron Diamond AIDS Research Center • Bruce D. Cheson, Georgetown University Hospital • David E. Clapham, Boston Children's Hospital • Steven S. Clinton, Ohio State University • Shu Man Fu, University of Virginia • Barbara C. Furie, Beth Israel Deaconess Medical Center • Martha L. Gray, Massachusetts Institute of Technology • Martin S. Hirsch, Partners AIDS Research Center • Rebecca D Jackson, Ohio State University • Kuan-Teh Jeang, National Institute of Allergy and Infectious Diseases, NIH • Eric Kodish, Cleveland Clinic • Steven L. Kunkel, University of Michigan Medical School • Thomas Kupper, Brigham and Women's Hospital • Paul A. Luciw, University of California, Davis • George K. Michalopoulos, University of Pittsburgh School of Medicine • Elizabeth G. Nabel, National Heart, Lung, and Blood Institute, NIH • Gary Nabel, National Institute of Allergy and Infectious Diseases, NIH • Daniel Ory, Washington University School of Medicine • Guy H. Palmer, Washington State University • Yvonne Paterson, University of Pennsylvania School of Medicine • Alan R. Saltiel, University of Michigan • Jean Elise Schaffer, Washington University School of Medicine • Bryan K. Slinker, Washington State University • Joseph G. Sodroski, Dana-Farber Cancer Institute • Sarah Spiegel, Virginia Commonwealth University School of Medicine • John W. Sweetenham, Cleveland Clinic • Megan Sykes, Massachusetts General Hospital • Snorri S. Thorgeirsson, National Cancer Institute • Li-Huei Tsai, Picower Institute for Learning and Memory • Stephen J. Weiss, University of Michigan • Susan R. Weiss, University of Pennsylvania School of Medicine • Irving Weissman, Stanford University • Judith M. White, University of Virginia • William T.C. Yuh, Ohio State University

Section on Neuroscience
Laurence F. Abbott, Columbia University College of Physicians and Surgeons • Michael A. Arbib, University of Southern California • Jocelyne Bachevalier, Emory University • David M. Berson, Brown University • Sarah W. Bottjer, University of Southern California • Paul Brehm, Oregon Health & Science University • Ted Dawson, Johns Hopkins University School of Medicine • John P. Donoghue, Brown University • Gerald Fischbach, Columbia University • Charles G. Glabe, University of California, Irvine • Michael E. Goldberg, Columbia University College of Physicians and Surgeons • Andrea C. Gore, University of Texas, Austin • Fritz A. Henn, Brookhaven National Laboratory • Allen S. Levine, University of Minnesota • Robert C. Malenka, Stanford University School of Medicine • Herbert Needleman, University of Pittsburgh School of Medicine • Diane K. O'Dowd, University of California, Irvine • Dale Purves, Duke University • Jochen Schacht, University of Michigan • Sangram S. Sisodia, University of Chicago • Mriganka Sur, Massachusetts Institute of Technology • J. David Sweatt, University of Alabama, Birmingham • Gary L. Wenk, Ohio State University • Phyllis M. Wise, University of Washington • Jerrel L. Yakel, National Institute of Environmental Health Sciences, NIH

Section on Pharmaceutical Sciences
Robert Diasio, Mayo Clinic Cancer Center • Rodney J.Y. Ho, University of Washington • James P. Kehrer, Washington State University College of Pharmacy • Lois D. Lehman-McKeeman, Bristol-Myers Squibb Company • Daniel C. Liebler, Vanderbilt University School of Medicine • Craig C. Malbon, State University of New York, Stony Brook • Enrico Mihich, Roswell Park Cancer Institute • Charles D. Smith, Medical University of South Carolina

Section on Physics
Zhores I. Alferov, Ioffe Physico-Technical Institute • Ani Aprahamian, University of Notre Dame • Donald R. Baer, Pacific Northwest National Laboratory • Jonathan Bagger, Johns Hopkins University • William A. Bardeen, Fermi National Accelerator Laboratory • Pushpa Bhat, Fermi National Accelerator Laboratory • Carlton M. Caves, University of New Mexico • Robert A. Eisenstein, Santa Fe Alliance for Science • Rodolfo Gambini, Instituto de Fisica • Howard Gordon, Brookhaven National Laboratory • David L. Griscom, Impact Glass Research International • Nicholas J. Hadley, University of Maryland • Mikhail V. Kovalchuk, Russian Research Center Kurchatov Institute • Prem Kumar, Northwestern University • James E. Lovelock, Consultant • Fabio Marchesoni, Universita di Camerino • Douglas L. Mills, University of California, Irvine • Earl W. Plummer, University of Tennessee, Knoxville • Serban Protopopescu, Brookhaven National Laboratory • Thomas R. Roser, Brookhaven National Laboratory • Qimiao Si, Rice University • Jerry A. Simmons, Sandia National Laboratories • Henry W. Sobel, University of California, Irvine • John C.H. Spence, Arizona State University • Maria Spiropulu, European Organization for Nuclear Research • Daniel L. Stein, New York University • Jeffrey Y. Tsao, Sandia National Laboratories • Stephan von Molnar, Florida State University • Samuel A. Werner, University of Missouri • Steven R. White, University of California, Irvine • Miguel J. Yacaman, University of Texas, San Antonio • Michael S. Zisman, Lawrence Berkeley National Laboratory

Section on Psychology
Martin S. Banks, University of California, Berkeley • Lisa Feldman Barrett, Boston College • Steven J. Breckler, American Psychological Association • Eliot A. Brenowitz, University of Washington • Nathan Fox, University of Maryland • John D.E. Gabrieli, Massachusetts Institute of Technology • Barbara Landau, Johns Hopkins University • Douglas L. Medin, Northwestern University • Laura-Ann Petitto, University of Toronto • Linda P. Spear, Binghamton University

Section on Social, Economic, and Political Sciences
Kenneth Bollen, University of North Carolina • Steven Brint, University of California, Riverside • Craig Calhoun, Social Science Research Council • Arthur G. Cosby, Mississippi State University • Samuel Gubins, Annual Review • James J. Heckman, University of Chicago • Philip S. Khoury, Massachusetts Institute of Technology • Jan E. Stets, University of California, Riverside

Section on Societal Impacts of Science and Engineering
Albert Carnesale, University of California, Los Angeles • Rochelle Anne Diamond, California Institute of Technology • Gerald L. Epstein, Center for Strategic and International Studies • Kevin Finneran, National Academy of Sciences • William S. Hammack, University of Illinois, Urbana-Champaign • James E. Katz, Rutgers University • Susan M. Wolf, University of Minnesota Law School

Section on Statistics
Mark Becker, University of South Carolina • Bernie Devlin, University of Pittsburgh School of Medicine • Xuming He, University of Illinois • George P. McCabe, Purdue University • George C. Roussas, University of California, Davis • Thomas J. Santner, Ohio State University • Leland Wilkinson, SYSTAT Inc. • Bin Yu, University of California, Berkeley

Nuclear Reprogramming in Cells

J. B. Gurdon[1] and D. A. Melton[2]

Nuclear reprogramming describes a switch in gene expression of one kind of cell to that of another unrelated cell type. Early studies in frog cloning provided some of the first experimental evidence for reprogramming. Subsequent procedures included mammalian somatic cell nuclear transfer, cell fusion, induction of pluripotency by ectopic gene expression, and direct reprogramming. Through these methods it becomes possible to derive one kind of specialized cell (such as a brain cell) from another, more accessible, tissue (such as skin) in the same individual. This has potential applications for cell replacement without the immunosuppression treatments that are required when cells are transferred between genetically different individuals. This article provides some background to this field, a discussion of mechanisms and efficiency, and comments on prospects for future nuclear reprogramming research.

As a fertilized egg develops into an adult organism, specialized cells are formed by a one-way process, and they become increasingly, and normally irreversibly, committed to their fate. A skin cell does not naturally turn into, or give rise to, a brain cell, nor does an intestine cell generate a heart cell. Nevertheless, there are certain experimental procedures that enable just these kinds of changes to take place. They entail nuclear reprogramming, a term that describes a switch in nuclear gene expression of one kind of cell to that of an embryo or other cell type. This process is of interest for three reasons. First, identifying how reprogramming takes place can help us understand how cell differentiation and specialized gene expression are normally maintained. Second, nuclear reprogramming represents a first major step in cell-replacement therapy, in which defective cells are replaced by normal cells of the same or a related kind but derived from a different cell type. Eventually, it may be possible to derive replacement heart, pancreas, or other types of cells from the skin of the same individual, thereby avoiding the need for immunosuppression. Third, nuclear reprogramming enables the culture of lines of cells from diseased tissues, and hence allows us to analyze the nature of the disease and to screen for therapeutic drugs. We review these procedures, discuss the mechanisms that may be involved, and comment on prospects in this field.

Nuclear Transfer to Eggs and Oocytes

The earliest evidence for the experimental reversal of cell differentiation came from the transplantation of a viable cell nucleus into an enucleated frog egg. Briggs and King (*1*) first succeeded in producing normal swimming tadpoles of *Rana pipiens* by transplanting the nuclei of embryo (blastula) cells. They found, however, that the transfer of nuclei from slightly older (gastrula) embryos resulted only in abnormal development and concluded that cell differentiation was likely to involve irreversible nuclear changes (*2*). Soon after this, similar experiments were carried out with eggs of the South African frog *Xenopus laevis* (*3*). In due course, it was found that even when *Xenopus* nuclei were transplanted from fully differentiated cells, in this case from the intestinal epithelium of feeding tadpoles, entirely normal and fertile male and female frogs were obtained (*4*). These results led to the conclusion that the process of cell differentiation can be fully reversed and does not require irreversible nuclear changes; it involves changes in nuclear gene expression but not in gene content. Therefore, although cells become stably and functionally very different from each other during development, their genome stays the same in all cells (with the exception of antibody-producing cells) and therefore retains the potential to form any cell type.

The next major advance in this field came with the production of a normal adult sheep (Dolly) by transplanting the nuclei of cultured mammary gland cells derived from an adult sheep to enucleated sheep eggs (*5*). This and later work (*6*) showed that it is possible to completely reverse the process of mammalian cell differentiation using nuclei from an adult mammal, and this suggests that this same procedure might work with humans. An important step in this direction has recently been taken by the generation of monkey embryonic stem (ES) cells from the nuclei of adult monkey cells. These proliferation- and differentiation-competent cells were derived from blastocysts grown after transplanting nuclei from adult monkey cells to enucleated monkey eggs (*7*). It is therefore likely that human eggs contain the components required to reverse the differentiation of adult human somatic cells.

Efficiency

The gold standard for the completeness of reprogramming by eggs has been described as the formation of a fertile adult animal containing functional cells of every kind (termed totipotency). However, as far as therapy is concerned, we do not regard totipotency or even pluripotency (the formation of many but not all cell types) (Fig. 1A) as a necessary attribute. It would not, for example, be therapeutically useful to supply a patient with spinal cord injury with replacement cells of every kind. In the case of somatic cell nuclear transfer, it is important to determine the efficiency of obtaining a particular differentiated cell type by using the transplanted nucleus of an entirely unrelated cell type. It has been shown that the success of nuclear reprogramming decreases as donor cells become more differentiated (*3*, *8*) (Fig. 2). The frog experiments include the results of serial nuclear transfers (transplanting nuclei from a nuclear transplant embryo to another set of enucleated eggs) and grafts (transplanting nuclei from a nuclear transplant embryo to host embryos reared from fertilized eggs) to produce the conclusion that about 30% of intestinal epithelium cell nuclei can generate functional muscle and nerve cells (*9*). In mammals, cells of a nuclear transplant blastocyst can be used to derive ES cells, whose differentiation capacity is tested by transplanting these cells to normal host embryos. The frequency with which a normal adult is obtained from the nucleus of a specialized cell is usually 1 to 2%, as compared with about 30% from embryo nuclei (*10*).

Because of the ethical concerns about obtaining human unfertilized eggs, animal eggs such as those of cows, mice, or rabbits might be used to generate ES cells from transplanted human somatic nuclei. Nuclear transfers between different strains or subspecies are just as successful as those within a species; however, eggs produced by transfers between very different species such as human and mouse, cow, or pig generally die before the 32-cell stage (*10*). So far, there is no confirmed evidence that proliferating ES cells can be obtained from such distant combinations, including human nuclei in monkey cytoplasm.

Mechanism

An appeal of using eggs to reprogram nuclei is that eggs have the natural ability to reprogram highly specialized sperm nuclei with 100% efficiency. Another advantage of this procedure is that it does not require a permanent genetic change to the transplanted nucleus or to the resulting reprogrammed cells. Therefore, it is important to discover the mechanisms involved and ask, how is successful reprogramming achieved, and what makes the process frequently unsuccessful even when eggs are used?

The mechanism of nuclear reprogramming by eggs (in second meiotic metaphase) has been explored by the use of oocytes (female germline cells in first meiotic prophase and immediate progenitors of eggs). Multiple mammalian somatic nuclei transplanted to the germinal vesicle of an oocyte are directly reprogrammed to transcribe stem-cell marker genes, including *Oct4*, *Nanog*, and *Sox2* (Fig. 1B). Nuclear reprogramming by oocytes does not yield new cells but, in

[1]Wellcome Trust/Cancer Research UK Gurdon Institute and Department of Zoology, University of Cambridge, Cambridge CB2 12N, UK. [2]Molecular and Cellular Biology, Harvard/Howard Hughes Medical Institute (HHMI), Cambridge, MA 02138, USA.

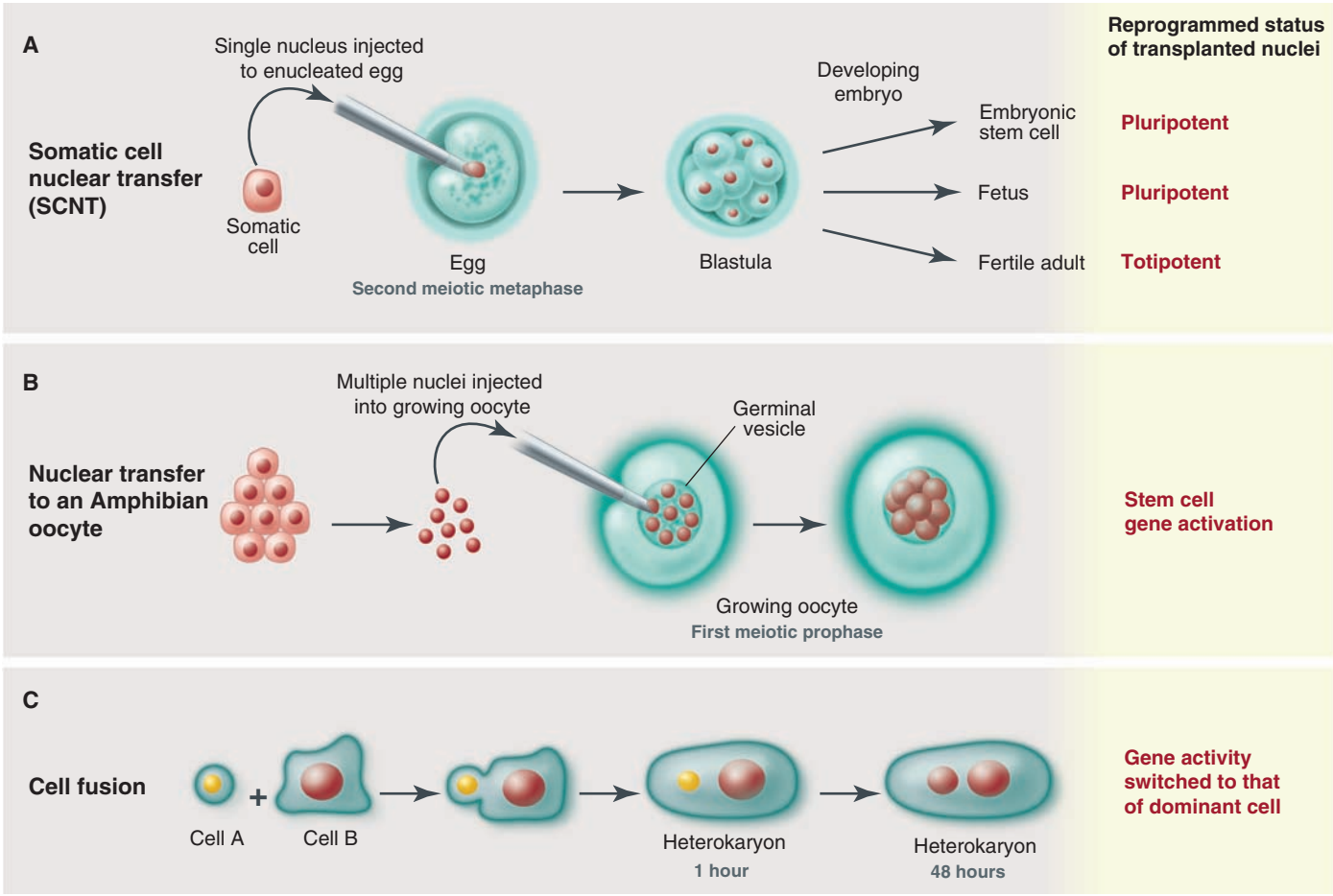

Fig. 1. Designs of nuclear transfer experiments (**A**) to unfertilized eggs (second meiotic metaphase) of frogs or mammals or (**B**) to first meiotic frog oocytes. (A) and (B) show the transfer of somatic cell nuclei. (**C**) Design of cell fusion experiments.

contrast to eggs, takes place without cell division and does not need protein synthesis. Mechanisms accompanying this reprogramming include (i) a massive volume increase of 30 times in transferred nuclei and chromatin decondensation (Fig. 3, A and B), due in part to an oocyte histone chaperone nucleoplasmin (*11*, *12*); (ii) the removal of differentiation marks, such as DNA methylation (*13*) and histone modifications; and (iii) chromatin protein exchange, especially of the oocyte-specific linker histone H1 by the oocyte-specific histone variants B4 or H1foo (*14*). The general principle here seems to be that, during their formation, oocytes (and hence eggs) acquire very high concentrations of certain proteins that are responsible for the above effects. If egg proteins can be exchanged in seconds or minutes for those in transplanted somatic nuclei [as suggested by most fluorescence recovery after photobleaching experiments (*15*)], complete reprogramming should always take place.

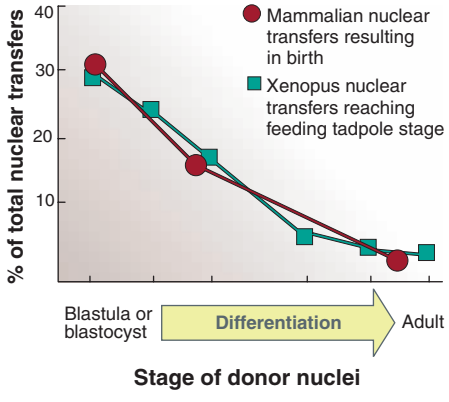

Fig. 2. Nuclear transfer success decreases as donor cells differentiate (*3*, *8*).

This concept of rapid exchange does not, however, agree with the fact that eggs are often unsuccessful in fully reprogramming somatic nuclei. If the rapid exchange of chromosomal proteins referred to above applies to all those components of an egg that normally reprogram sperm nuclei after fertilization, there would be time in frogs, and even more in mammals, for transplanted somatic nuclei to be fully reprogrammed before the first egg division (24 hours in mammals). This often does not happen. One reason may be that transplanted nuclei carry an epigenetic memory of their gene expression in their donor cells. For example, nuclei taken from muscle cells sometimes continue to strongly express muscle genes in neural and other non-muscle cells of an embryo obtained by nuclear transfer. This may be caused by the incorporation of an abundant egg histone variant (H3.3) into the chromatin of daughters of transplanted nuclei (*16*). The incorporation of the H3.3 histone is thought to prevent reprogramming and so to preserve a memory of previous gene expression.

Cell Fusion and Cell Extracts

It is possible to fuse two somatic cells and to use a cell-division inhibitor to ensure that the two nuclei remain separate (Fig. 1C). In these heterokaryons, the dominant cell, usually the larger and more actively dividing partner, imposes its own pattern of gene expression on the other partner. Examples include the fusion of an erythrocyte with a growing cultured cell or of a human liver cell with a multinucleate muscle cell (*17*, *18*). If enucleated cytoplasms of one kind of somatic cell (cytoplasts) are fused to another cell, they also impose gene expression of their original cell type on the incoming nucleus. However, these fused cells do not proliferate well, and therefore are not likely to be of therapeutic value.

Some important conclusions can be drawn from these experiments (*19*, *20*). One is that reprogrammed gene expression is commonly preceded by nuclear swelling and chromatin

decondensation, such as in nuclear transfers to eggs and oocytes (Fig. 3). Another is that new gene expression does not depend on the extinction of donor cell–specific gene expression, nor on cell division; therefore, neither of these is a necessary part of reprogramming. The third conclusion is that differentiated cells (as well as embryo cells) contain regulatory molecules that can redirect gene expression in the nuclei of other cells. When the recipient cell is very large, such as an egg or myotube (100 or so muscle cells fused into one large syncytial cell), it is understandable that its own programming molecules can override a much smaller supply of regulatory molecules introduced by the incoming nucleus or cell (Fig. 4). These molecules probably have a role in normal (non-nuclear transfer) conditions by ensuring that cells and their daughters do not escape from their lineage or change cell type; in other words, cells seem to continually self-reprogram themselves and their daughters to remain in the same lineage.

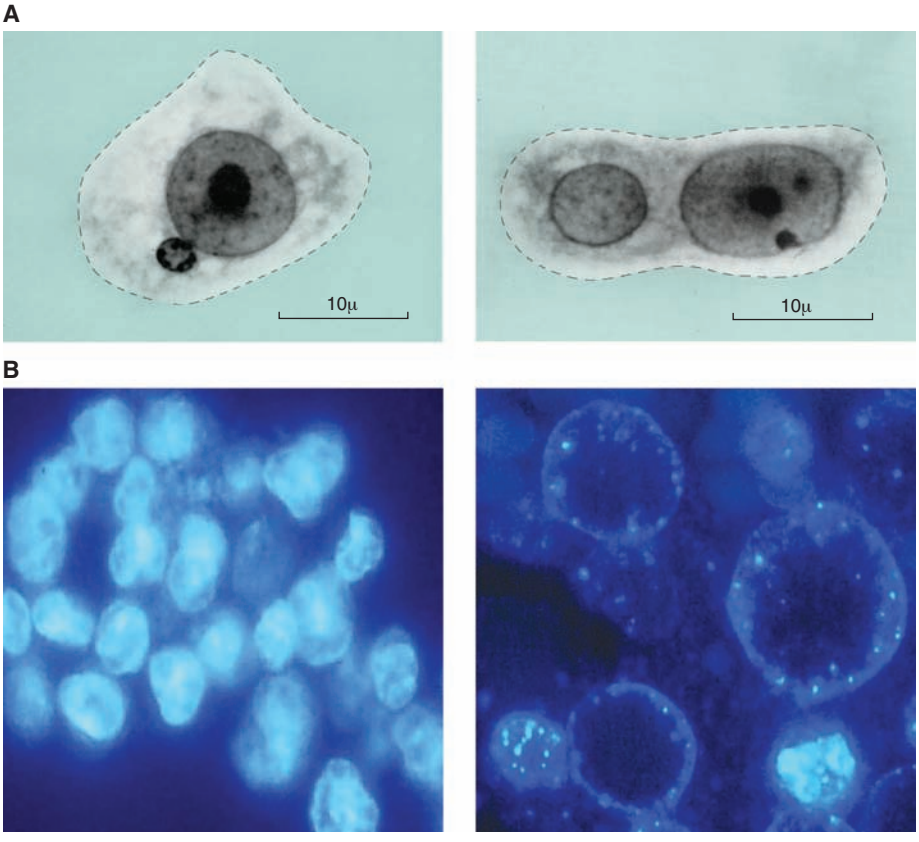

Fig. 3. Nuclei enlarge and chromatin decondenses during nuclear reprogramming. (**A**) A chick erythrocyte 1 hour (left) and 2 days (right) after fusion to a human HeLa cell (*17*). The dotted lines indicate the outside of the fused hybrid cells. The smaller nucleus is that of the chick erythrocyte. [Adapted with permission from (*17*)] (**B**) Mouse ES cell nuclei immediately (left) and 2 days (right) after injection into an amphibian oocyte germinal vesicle (*9*). The injected nuclei have enlarged about 30 times in volume.

Induced Pluripotency

A spectacular advance in this field came when Takahashi and Yamanaka (*21*) discovered that viral transfection of four genes (*Oct 3/4*, *Sox2*, *c-Myc*, and *KLF4*) into an adult mouse fibroblast population can lead to the appearance of some cells with the characteristics of ES cells. After further selection for the expression of *Nanog*, in addition to the first four genes, the resulting stem cells were shown to enter all cell lineages when transplanted to immunotolerant host embryos; hence, they are pluripotent and termed induced pluripotent cells, or iPS cells. iPS cells from human somatic cells require the same set of factors used in mice (above) (*22*) or the combination of *Oct4*, *Sox3*, *Nanog*, and *lin28* (*23*). These procedures have now been confirmed and extended. iPS cells have been obtained from differentiated stomach and liver cells (Fig. 5, arrow B) (*24*) and can be obtained even if Myc, which can induce cancer, is omitted (*25*, *26*). The resulting stem cells do not appear to be substantially different from ES cells and may eventually provide a suitable source of different cell types for patient-specific cell replacement therapy in humans and of disease-specific cell lines to test potential therapeutic agents, but only after methods are developed to eliminate the concern of genome integration by the associated viral vectors. Recent work provides a step in this direction by showing that stable viral integration is not required to generate iPS cells when nonintegrating adenoviruses or plasmids are used (*27*, *28*, *29*).

The mechanism by which iPS cells arise after the introduction of transcription factors to a differentiated somatic cell is not clear. Because in the first experiments these cells arose at such a low rate (10^{-4} to 10^{-3} of the transfected cell population), and because the treated cell population needs to proliferate in the continuing presence of the factors for nearly 2 weeks, the provenance of the occasional iPS cell is difficult to analyze. In some cases, the pluripotent state may need to be stabilized by the suppression of differentiation processes. Possible mechanisms have been reviewed (*30*, *31*).

Lineage Switching

The possibility of redirecting cell differentiation by overexpression of genes was suggested many years ago by Weintraub with the identification of the "master gene," *MyoD* (*32*). The overexpression of this one gene, which encoded a muscle-specific transcription factor, was sufficient to make a range of nonmuscle cell types switch into muscle. However, in other muscle-unrelated cells, the myogenic conversion was temporary, or not observed. Selection for *MyoD* expression is needed for a number of cell cycles before a muscle phenotype is established. When it has been, *MyoD* autoactivates its own continuing transcription, and exogenous overexpression of *MyoD* is no longer required.

Switches in cell type have also been successfully achieved with several other cell types, notably the blood-forming cell lineage, by overexpressing key transcription factors, the balance of which can activate or repress genes determining cell fate (*33*, *34*). In these cases (Fig. 5, arrow C), the process may possibly involve a reversion to a less differentiated state, a kind of dedifferentiation, before the new cell type is formed. As with MyoD, overexpressing cells are selected in culture for many cell divisions before the new cell type is established.

A recent development in this area is the direct conversion of exocrine cells of the pancreas into endocrine β cells (Fig. 5, arrow D) (*29*). In this case, three transcription factors normally required for β-pancreas differentiation, namely Pdx1, Ngn3, and MafA, are provided by adenovirus transfection, and up to 20% of the transfected exocrine cells switch to insulin-producing β cells. The adenoviruses carrying the overexpressed genes do not need to be integrated into the exocrine cell genomes, and gene overexpression is needed only temporarily. Moreover, this lineage switch does not appear to require cell division. This direct lineage switching, and the iPS formation pioneered by Yamanaka, provide a general strategy for changing cell fates, whereby one can aim to discover the set of transcription factors that can turn one cell type into another.

Protein-DNA Interactions and Fleeting Access

Two basic characteristics of cell differentiation influence our understanding of nuclear reprogramming. One is that every cell seems to express

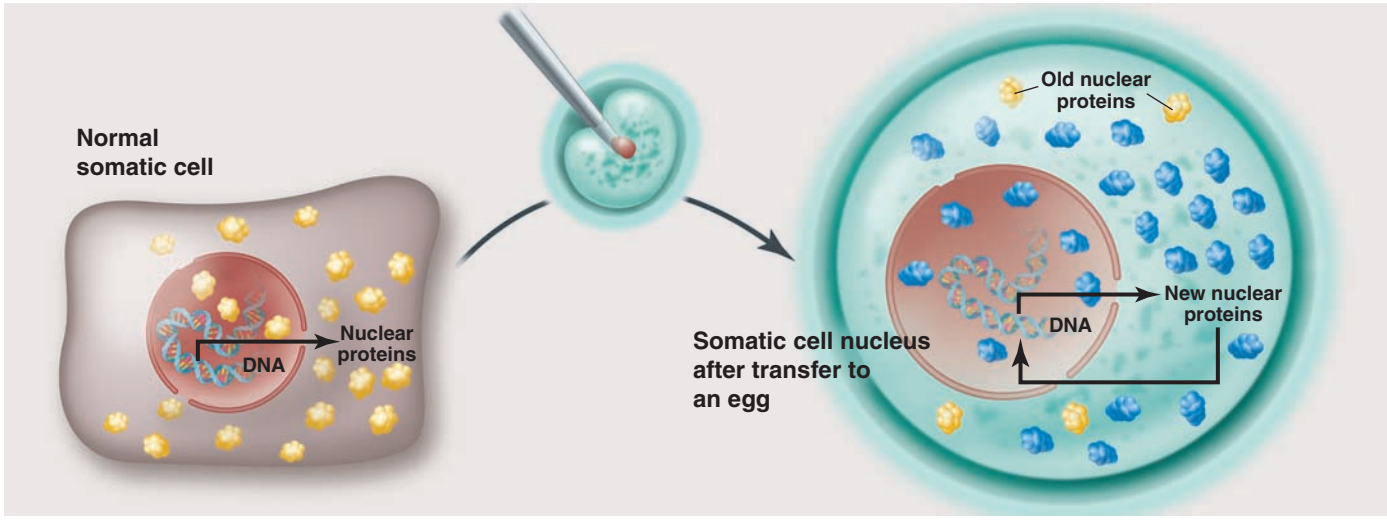

Fig. 4. Chromosomal protein exchange in a normal cell (**left**) or after nuclear transfer to an egg or oocyte (**right**). Yellow indicates donor-cell nuclear proteins that maintain gene expression. Blue indicates egg nuclear proteins that replace somatic proteins lost by dilution and that induce new gene expression.

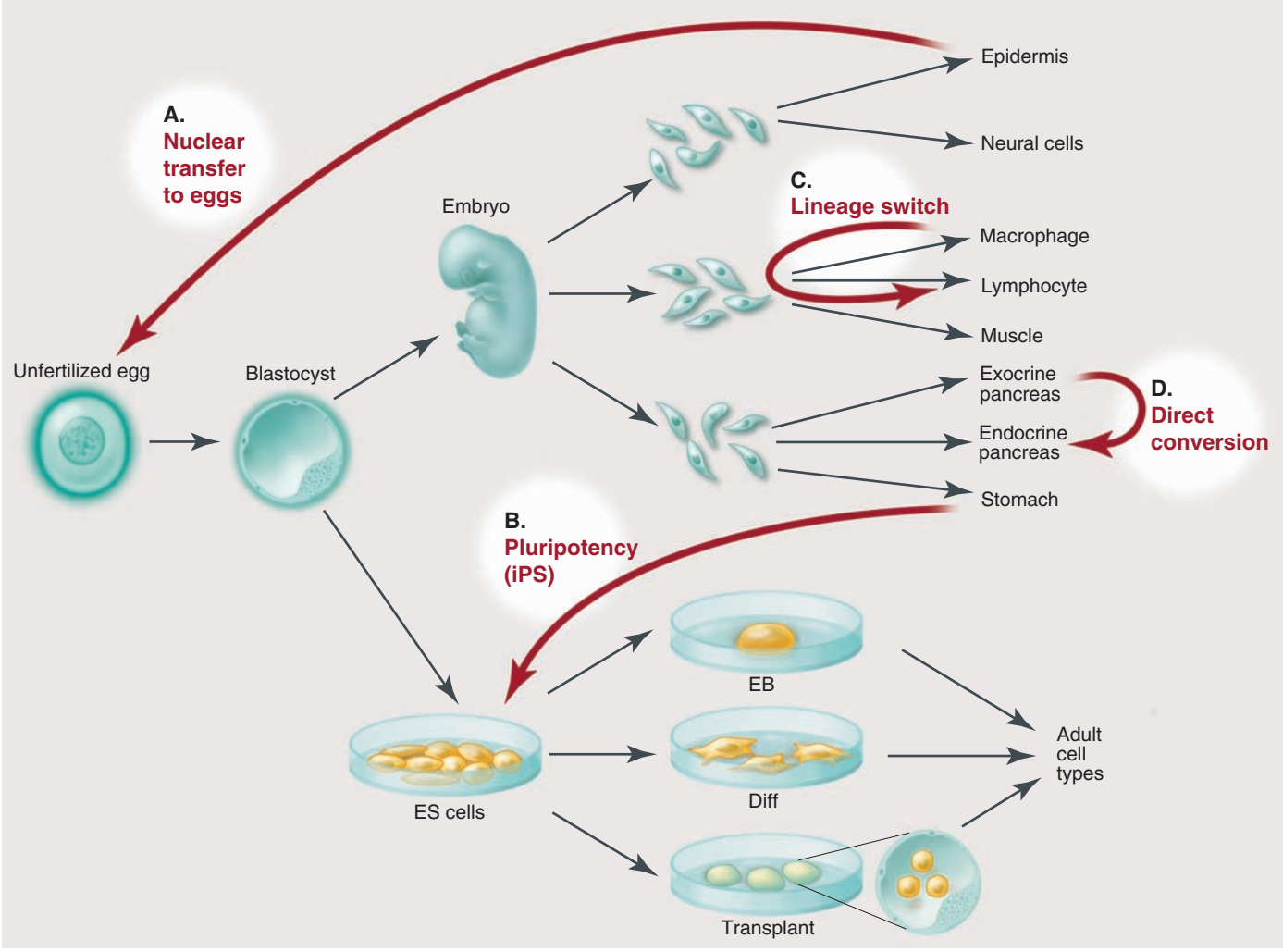

Fig. 5. Four experimental routes for nuclear reprogramming. Blue components represent the normal process of cell differentiation during development from a fertilized egg to adult cells or tissues. Red arrows represent nuclear reprogramming (**A**) by nuclear transfer to eggs, (**B**) by induced pluripotency iPS, (**C**) by lineage switching back to a branch point and out again in a different direction, and (**D**) by direct conversion. The lower part of the figure shows reprogramming by the generation of ES cells; these can be aggregated into an embryoid body (EB), made to differentiate in culture (diff), or transplanted to a blastocyst. In each case, various types of adult cells can be formed.

those genes whose products determine its state of differentiation, a conclusion especially clear from cell-fusion experiments (*19*, *20*). Thus, a muscle cell will maintain by autoactivation a high enough content of MyoD, for example, to continually program itself to be a muscle cell (Fig. 4). The larger the cell, and/or the more embryonic it is, the greater abundance it will have of self-reprogramming molecules. Therefore, eggs will be particularly effective without added factors.

A second characteristic of all nuclear reprogramming experiments is that the experimental resetting of gene expression becomes increasingly difficult as cells become more differentiated (Fig. 2). The differentiated state becomes more firmly established as cells embark on their terminal pathways and shut down inappropriate lineages. To understand the basis of this is a major challenge in this field, and much informative work has already been done on DNA and histone modifications (*35*). A general hypothesis is the idea of "fleeting access." We propose that combinations of DNA binding or chromosomal proteins become increasingly tightly associated with the regulatory regions of inactive genes. Even though most proteins are thought to dissociate from DNA at frequent intervals of seconds or a few minutes (*15*), and in a few instances for longer (*36*), a multicomponent complex as a whole may have a very long dwell time on inactive genes. It will be a very rare event for a sufficient number of individual proteins in a complex to dissociate from a chromosome at the same time for a gene region to be accessible to reprogramming factors. In embryonic cells, most genes (and in differentiated cells, the active genes) will be in a decondensed configuration with relatively short dwell times for multicomponent complexes.

According to this view, the probability of reprogramming taking place in nuclear transfer, cell fusion, iPS, and lineage-switching experiments would depend on the statistical access frequency of gene regulatory regions together with the duration and concentration of transcription or other regulatory factors. Large cells such as eggs or myotubes with a high content of factors would be especially successful at reprogramming, as would any cell with an experimentally enhanced content of factors. A major advance in the future will be to understand why the nuclei of differentiated cells are reprogrammed so much less well than those of embryonic cells. This will probably require an explanation of chromatin decondensation.

The Future

Will the mechanism of reprogramming be the same in nuclear transfer to eggs, iPS experiments, and lineage switching? Probably not. The concept of fleeting access will be the same, but the actual reprogramming molecules will be different. We already know that eggs have very high concentrations of certain molecules such as nucleoplasmin and histones B4 and H3.3. The eventual identification of egg-reprogramming molecules may well be able to enhance the efficiency of the iPS and lineage-switching routes for adult cells.

The future value of reprogrammed cells is of two kinds. One is to create long-lasting cell lines from patients with genetic diseases, in order to test potentially useful drugs or other treatments (*37*, *38*). The other is to provide replacement cells for patients. To be therapeutically beneficial, replacement cells will probably need (i) to be provided in sufficient numbers; (ii) to carry out their function, even though they are not normally integrated into host tissues; and (iii) to be able to produce the correct amount of their product.

A human adult has about 10^{15} cells, and the liver contains about 10^{14} cells. To create this number of cells starting from a 10^{-4} success rate of deriving iPS cells from skin would require an enormous number of cell divisions in culture, although the prolonged culture of ES-like cells provides a valuable amplification step. However, many parts of the human body need a far smaller number of cells to improve function. An example is the human eye retina, in which only 10^5 cells could be of therapeutic benefit.

Will introduced cells be useful even if not "properly" integrated into the host? Most organs consist of a complex arrangement of several different cell types. The pancreas, for example, contains exocrine (acinar) cells, ductal cells, and at least four kinds of hormone-secreting cells in the endocrine islet. Replacement endocrine cells can provide useful therapeutic benefit even if not incorporated into the normal complex pancreas cell configuration (*29*). In some cases, introduced cells can have functionally beneficial effects, even if indirectly (*39*, *40*). It is not yet clear whether introduced cells will be correctly regulated to produce the desired amount of product.

Looking ahead, alternative routes to cell replacement may emerge. One is to avoid the need to transfect genes into cells if the right combinations of small molecules that can easily enter cells can be found (*41*). It may also be increasingly fruitful to find populations of naturally dividing cells in adult organs so that these cells in their naturally less-specialized state can be expanded and differentiated in culture before implantation. A future objective, in our view, is to aim for unipotency and oligopotency (the generation of only one or a few cell types) rather than pluripotency (the potential to differentiate into any of the three germ layers) and certainly not totipotency (the potential to differentiate into all embryonic and extra-embryonic cell types) (Fig. 5). Likewise, we would much prefer to be able to create new cells by switching normal cells from a closely related lineage than by going back to totipotency and then narrowing down the differentiation options from a wide range. For replacement therapy, totipotency and germline transmission are not desirable criteria or objectives. An oligopotent state with limited differentiation potential is likely to be much safer and more useful from a therapeutic point of view.

References and Notes

1. R. Briggs, T. J. King, *Proc. Natl. Acad. Sci. U.S.A.* **38**, 455 (1952).
2. R. Briggs, T. J. King, *J. Morphol.* **100**, 269 (1957).
3. J. B. Gurdon, *J. Embryol. Exp. Morphol.* **10**, 622 (1962).
4. J. B. Gurdon, V. Uehlinger, *Nature* **210**, 1240 (1966).
5. I. Wilmut *et al.*, *Nature* **419**, 583 (2002).
6. K. Eggan *et al.*, *Nature* **428**, 44 (2004).
7. J. A. Byrne *et al.*, *Nature* **450**, 497 (2007).
8. X. Yang, S. L. Smith, X. C. Tian, H. A. Lewin, J. P. Renard, *Nat. Genet.* **39**, 295 (2007).
9. J. B. Gurdon, *Annu. Rev. Cell Dev. Biol.* **22**, 1 (2006).
10. T. Tecirlioglu, J. Guo, A. Trounson, *Stem Cell Rev.* **2**, 277 (2006).
11. A. Philpott, G. H. Leno, R. A. Laskey, *Cell* **65**, 569 (1991).
12. H. Tamada *et al.*, *Mol. Cell. Biol.* **26**, 1259 (2006).
13. G. Barreto *et al.*, *Nature* **445**, 671 (2007).
14. H. Saeki *et al.*, *Proc. Natl. Acad. Sci. U.S.A.* **102**, 5697 (2005).
15. F. Catez *et al.*, *Mol. Cell. Biol.* **24**, 4321 (2004).
16. R. K. Ng, J. B. Gurdon, *Nat. Cell Biol.* **10**, 102 (2008).
17. H. Harris, *J. Cell Sci.* **2**, 23 (1967).
18. J. Pomerantz, H. M. Blau, *Nat. Cell Biol.* **6**, 810 (2004).
19. R. Terranova, C. F. Pereira, C. Du Roure, M. Merkenschlager, A. G. Fisher, *J. Cell Sci.* **119**, 2065 (2006).
20. D. W. Han *et al.*, *Stem Cells* **26**, 445 (2008).
21. K. Takahashi, S. Yamanaka, *Cell* **126**, 663 (2006).
22. K. Takahashi *et al.*, *Cell* **131**, 861 (2007).
23. J. Yu *et al.*, *Science* **318**, 1917 (2007).
24. T. Aoi *et al.*, *Science* **321**, 699 (2008).
25. K. Okita, T. Ichisaka, S. Yamanaka, *Nature* **448**, 313 (2007).
26. M. Wernig, A. Meissner, J. P. Cassady, R. Jaenisch, *Cell Stem Cell* **2**, 10 (2008).
27. M. Stadtfeld, M. Nagaya, J. Utikal, G. Weir, K. Hochedlinger, *Science* **322**, 945 (2008); published online 25 September 2008 (10.1126/science.1162494).
28. K. Okita, M. Nakagawa, H. Hyenjong, T. Ichisaka, S. Yamanaka, *Science* **322**, 949 (2008); published online 9 October 2008 (10.1126/science.1164270).
29. Q. Zhou, J. Brown, A. Kanarek, J. Rajagopal, D. A. Melton, *Nature* **455**, 627 (2008).
30. S. Yamanaka, *Cell Stem Cell* **1**, 39 (2007).
31. R. Jaenisch, R. Young, *Cell* **132**, 567 (2008).
32. H. Weintraub *et al.*, *Proc. Natl. Acad. Sci. U.S.A.* **86**, 5434 (1989).
33. H. Xie, M. Ye, R. Feng, T. Graf, *Cell* **117**, 663 (2004).
34. S. H. Orkin, L. I. Zon, *Cell* **132**, 631 (2008).
35. T. Kouzarides, *Cell* **128**, 693 (2007).
36. J. Yao, K. M. Munson, W. W. Webb, J. T. Lis, *Nature* **442**, 1050 (2006).
37. I.-H. Park *et al.*, *Cell* **134**, 877 (2008).
38. J. T. Dimos *et al.*, *Science* **321**, 1218 (2008).
39. N. Lowry *et al.*, *Exp. Neurol.* **209**, 510 (2008).
40. M. Wernig *et al.*, *Proc. Natl. Acad. Sci. U.S.A.* **105**, 5856 (2008).
41. Y. Xu, Y. Shi, S. Ding, *Nature* **453**, 338 (2008).

42. J.B.G. thanks the Wellcome Trust (UK) and the European Commission Cells into Organs for support. D.A.M. is an HHMI investigator and is supported in part by the Harvard Stem Cell Institute and NIH. J.B.G. serves on the Harvard Stem Cell Institute Advisory Board.

10.1126/science.1160810

Matching Glass-Forming Ability with the Density of the Amorphous Phase

Y. Li,[1,2]* Q. Guo,[1,2] J. A. Kalb,[1,3]† C. V. Thompson[1,3]*

The density of the amorphous phase of metals is generally thought to be related to glass formation, but this correlation has not been demonstrated experimentally to date. In this work, systematic deflection measurements using microcantilevers and a combinatorial deposition method show a correlation between glass-forming ability and the density change upon crystallization over a broad compositional range in the copper-zirconium binary system. Distinct peaks in the density of the amorphous phase were found to correlate with specific maxima in the critical thickness for glass formation. Our findings provide quantitative data for the development of structural models of liquids that are readily quenched to the amorphous state. The experimental method developed in this work can facilitate the search for new glass-forming alloys.

Metallic glasses are amorphous metals that do not have a structure with long-range atomic order like crystalline materials do, but have pronounced short- and medium-range order at the atomic scale. Because of their very different properties as compared to those of their crystalline counterparts, metallic glasses are very promising materials for future structural, chemical, and magnetic applications (*1*, *2*). The packing density of the amorphous phase is a key consideration in studying the formation of metallic glasses (*2*–*5*). A liquid of high packing density (*6*–*8*) has a low free volume content and a correspondingly low atomic mobility (*9*–*11*). Upon quenching, such a liquid is expected to have a strong kinetic constraint on nucleation and the subsequent growth of crystals. This has been the basis for recent theoretical studies (*12*, *13*) of structural models of metallic glasses, in which a correlation between compositions having especially dense packing and compositions that are known to quench to the glassy state at relatively low cooling rates was sought, but not obtained. Earlier studies of the density of glasses, based on the Archimedes method, have been mostly limited to relatively narrow compositional ranges of ternary and quaternary alloys with large critical sample sizes for glass formation (*14*–*16*), and no correlation between density and the ease of glass formation has been demonstrated.

We have developed a method for the measurement of density changes, using microfabricated Si-rich silicon nitride (SiN) cantilevers (*17*). Owing to the small size and close spacing of the cantilevers, the deposition of alloy films with compositions that varied in a controlled way from cantilever to cantilever allowed a combinatorial approach to measurements of density changes for a broad range of compositions, with high compositional resolution. This process is schematically illustrated in fig. S1. Heating-induced crystallization of the initially amorphous Cu-Zr films causes an increase in density (a decrease in volume) that causes an upward deflection of the cantilevers, as a result of the tensile elastic mismatch strain developed at the interface between the film and the cantilever. By measuring the magnitude of the cantilever tip deflection after crystallization, the corresponding density change in the film can be determined as a function of composition. Results obtained in this way were compared with the critical thicknesses for glass formation determined with the wedge-casting technique (fig. S3). The effective cooling rate in these wedge-casting experiments is uniform for all compositions tested, and the critical thickness for glass formation can serve as a consistent measure of glass-forming ability. A binary alloy system is particularly suitable for this study because of the relatively simple variation in composition. The Cu-Zr system was selected, in which glass formation has been extensively studied, particularly in the compositional range of the current study, from $Cu_{47}Zr_{53}$ to $Cu_{68}Zr_{32}$ (*18*–*21*).

Freestanding, low-stress, SiN microcantilevers 216 ± 3 nm thick were fabricated with standard microfabrication techniques (*17*). Cu-Zr films with thicknesses of 128 ± 4 nm were sputter-deposited on the cantilevers by means of separate elemental sources. The deposition ranges of the two sources overlapped, but the two deposition fluxes varied over the surface of the wafer, so that the composition of the films deposited on a row of cantilevers varied monotonically from Zr-rich to Cu-rich [a schematic illustration of the experimental configuration can be found in the supporting online material (SOM)]. To avoid oxidation of the film during annealing, a thin (15 ± 5 nm) Pt capping layer was sputter-deposited on top of all the cantilevers. The final structure of the cantilever is schematically shown in Fig. 1. The film composition was determined by energy-dispersive x-ray spectroscopy (EDX), with an error estimated to be within 1.0 atomic %. X-ray diffraction (XRD) analysis was carried out at different locations along the row of cantilevers, and the as-deposited structure of the film was confirmed to be fully amorphous everywhere. Samples were then annealed in a furnace at 600°C for 5 min, in a vacuum of 5×10^{-5} torr. This led to complete crystallization of the Cu-Zr films (*22*), as determined by post-annealing XRD analysis. The upward deflections of the microcantilevers were measured by correlating the focus conditions with measurements of the *z*-axis displacement of the objective lens in an optical microscope.

The as-fabricated stress-free SiN cantilevers had near-zero curvature. After deposition of the amorphous Cu-Zr films, the cantilevers curved downward (Fig. 2A), indicating that the as-deposited films were subject to a compressive

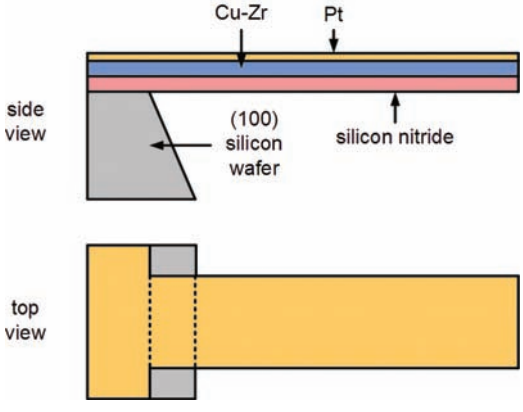

Fig. 1. Layer structure of a microcantilever with a fixed support (side view). A thin film of amorphous Cu-Zr (thickness 128 ± 4 nm) was deposited on the SiN (thickness 216 ± 3 nm). A thin Pt capping layer (thickness 15 ± 5 nm) was used to prevent oxidation of the Cu-Zr film during annealing. The thicknesses of the layers are not drawn to scale.

[1]Singapore–Massachusetts Institute of Technology (MIT) Alliance, 4 Engineering Drive 3, Singapore 117576. [2]Department of Materials Science and Engineering, National University of Singapore, 7 Engineering Drive 1, Singapore 117576. [3]Department of Materials Science and Engineering, MIT, Cambridge, MA 02139, USA.

†Present address: Intel Corporation, Santa Clara, CA 95054, USA.

*To whom correspondence should be addressed. E-mail: mseliy@nus.edu.sg (Y.L.); cthomp@mit.edu (C.V.T.)

residual deposition stress. Observation of residual compressive stress is not uncommon for vapor-deposited amorphous films (*23*, *24*). When these samples are heated, the residual stress will be relaxed before crystallization occurs. This relaxation will result in a return to the original (near-zero) curvature of the cantilevers. Upon crystallization, the cantilevers deflect upward (Fig. 2B) with uniform radius of curvature *r*, resulting in a vertical tip deflection δ, as shown in Fig. 2C. By measuring δ, the density change upon crystallization $(\rho_c - \rho_a)/\rho_a$ (>0) can be calculated, where ρ_a and ρ_c are the densities of the amorphous and crystalline phases, respectively. Details of this calculation can be found in (*17*) and the SOM (section 3), which includes fig. S2, which defines other important geometric characteristics of the bent beam.

For wedge-casting experiments, Cu-Zr alloys in the same composition range were prepared by arc-melting pure Zr (99.98%) and Cu (99.999%) and casting them in wedge-shaped molds. The critical thickness for glass formation was measured for each composition by optical microscopy of the wedge cross-sections. The critical thickness corresponds to the minimum cooling rate at which a glass will form, and is used as a measure of the ease of glass formation.

Figure 3A shows $(\rho_c - \rho_a)/\rho_a$. There are three local minima: 2.64 ± 0.02% at $Cu_{50.6}Zr_{49.4}$, 2.88 ± 0.02% at $Cu_{56.6}Zr_{43.4}$, and 2.52 ± 0.02% at $Cu_{63.1}Zr_{36.9}$. The overall range for the density change is 2.5 to 4.5%, which is typical for binary metallic glasses (*3*, *25*). The measured changes in deflection are related to several phenomena which include, but are not limited to, crystallization alone. For example, we have assumed that that the residual deposition stresses are fully relaxed before crystallization, and that pre-crystallization structural relaxation does not significantly contribute to the observed stress changes. It should also be noted that the densities of our vapor-deposited films may be systematically lower than those of glasses formed by liquid quenching, owing to the high effective quench rate of vapor deposition. Although these effects could possibly change the calculated absolute magnitudes of the volume changes, the general trend shown in Fig. 3A (three peaks in the density change) is likely to remain unchanged.

The critical thickness for glass formation determined from the wedge-casting experiments (Fig. 3B) follows the trend seen for the density change, with a smaller density change corresponding to larger critical thicknesses (and therefore to easier glass formation). The three maxima of 1.14 ± 0.04 mm at $Cu_{50}Zr_{50}$, 1.02 ± 0.04 mm at $Cu_{56}Zr_{44}$, and 1.14 ± 0.04 mm at $Cu_{64}Zr_{36}$ match the minima in the density change. These thicknesses match previously reported values (*19*–*21*).

The quench rate from a liquid that is required to produce a glass rather than a crystalline solid is a complex function of the interplay between kinetic constraints and the thermodynamic quantities that drive crystallization. The ease of glass formation is often found to correlate with small thermodynamic driving forces for crystallization (*26*), kinetic constraints on crystal nucleation and/or growth (*27*, *28*), and high viscosity in the undercooled liquid regime (*26*, *29*). Quite a number of parameters based on these considerations have been proposed to evaluate the glass-forming ability of metallic alloys. However, none of the parameters can be used to provide a complete explanation for all three of the peaks in the critical thickness shown in Fig. 3B. For example, Turnbull's widely used criterion that the ease of glass formation correlates with a high reduced glass transition temperature T_{rg} (= T_g/T_l, where T_g is the glass transition temperature and T_l is the liquidus temperature) (*27*), can only be correlated with the peak corresponding to the eutectic composition $Cu_{56}Zr_{44}$. On the other hand, if we rely solely on the thermodynamic driving force for crystallization as an indicator, the peak at $Cu_{50}Zr_{50}$ would not be expected, because intermetallic crystalline compound formation at $Cu_{50}Zr_{50}$ should be much more energetically favored over glass formation as compared to adjacent compositions. The one-to-one match between the minima in the density change and the peaks of the critical thickness in Fig. 3 indicates that a small density change upon crystallization is a more fundamental factor in determining the ease of glass formation.

As previously reported by Mukherjee *et al.* (*3*), a liquid with a high density, as compared to its crystalline counterpart, has a lower content of free volume and a higher viscosity at its melting temperature. The volume change upon crystallization was correlated with the viscosity in accordance with the Cohen-Grest free volume theory (*6*–*8*). This would then result in a larger critical thickness measured in wedge-casting

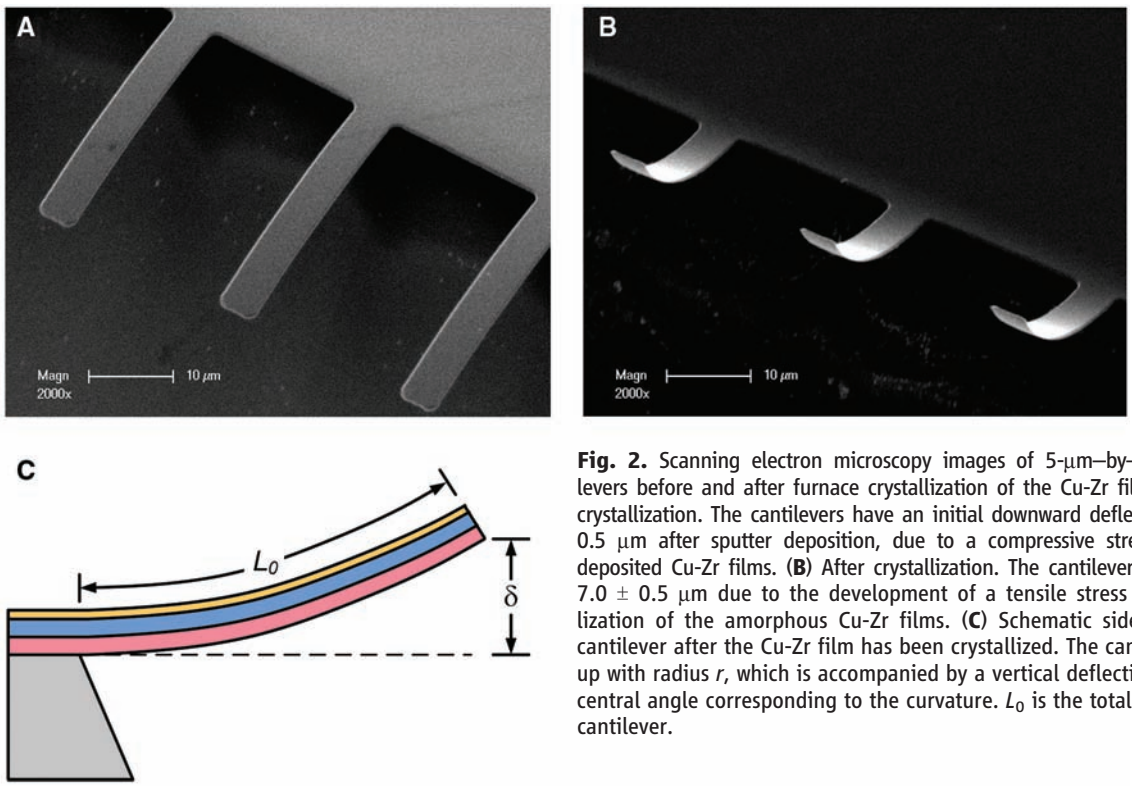

Fig. 2. Scanning electron microscopy images of 5-μm–by–30-μm cantilevers before and after furnace crystallization of the Cu-Zr film. (**A**) Before crystallization. The cantilevers have an initial downward deflection of 3.0 ± 0.5 μm after sputter deposition, due to a compressive stress in the as-deposited Cu-Zr films. (**B**) After crystallization. The cantilevers curve up by 7.0 ± 0.5 μm due to the development of a tensile stress upon crystallization of the amorphous Cu-Zr films. (**C**) Schematic side view of the cantilever after the Cu-Zr film has been crystallized. The cantilever curves up with radius *r*, which is accompanied by a vertical deflection δ. α is the central angle corresponding to the curvature. L_0 is the total length of the cantilever.

experiments. The correlation between the density change and the critical thickness shown in Fig. 3 is consistent with this argument, although no direct measurements of viscosity have been made in this study.

Figure 4 shows the density of the amorphous phase (ρ_a) as a function of alloying composition, as obtained by subtracting the measured density change upon crystallization from the density of the equilibrium crystalline state. Also shown are previously measured densities for a few compositions of Cu-Zr metallic glasses taken from (*25, 30–32*).

Consistent with the trend shown in Fig. 3, there are three peaks in ρ_a at the compositions corresponding to density-change minima. Although their magnitudes relative to the density baseline are only on the order of 1% higher, their correlation with glass-forming ability is established, suggesting a strong effect of density maxima. A successful structural model of metallic glasses must account for the three distinct compositions with correlated maxima in the density of the amorphous phase and minima in the cooling rate required to form a glass. Unfortunately, it seems that none of the existing models have these capabilities. For example, the dense-random-packing model leads to the expectation of only one peak, at $Cu_{65}Zr_{35}$ (*33*), whereas the efficient-cluster-packing model (*12*) predicts only two densely packed structures at $Cu_{18.0}Zr_{82.0}$ (for Cu-centered cluster packing) and $Cu_{90.9}Zr_{9.1}$ (for Zr-centered cluster packing), respectively. The Ma model (*13*) applies to alloys of low solute contents and is therefore not applicable to the $Cu_{50}Zr_{50}$ case, and the Egami-Waseda topological model (*34*) only gives the minimum solute concentration needed for glass formation, which is 10.8 atomic % for Zr and 20.8 atomic % for Cu in the Cu-Zr system. Therefore, although all of these models are fundamentally based on the dense packing concept, they cannot fully explain the correlation between the density and structure of metallic glasses and the ease of glass formation. Owing to the relatively small magnitudes of the density maxima, we speculate that they are related to a change in the short-range atomic order in the amorphous phase.

We have developed and demonstrated an effective and efficient combinatorial method for the investigation of the compositional dependence of the density change upon crystallization, over broad compositional ranges with high resolution. Using the Cu-Zr binary system, we have shown that there is a clear correlation between the density change and the glass-forming ability, which is consistent with models that suggest that glass formation correlates with reduced diffusivity in the glassy state. Moreover, the three density peaks for the amorphous phase suggested by this work not only correlate with the ease of glass formation but are also unexpectedly and unexplainably sharp. Our results provide evidence for the dense packing phenomenon in metallic glasses and provide new data to prompt improved modeling of their structures. The experimental methodology adopted in this work can be applied to other binary systems and more complex multicomponent systems, providing a new tool for broad investigations of the properties of glass-forming alloy systems, as well as for the search for new glass-forming alloys.

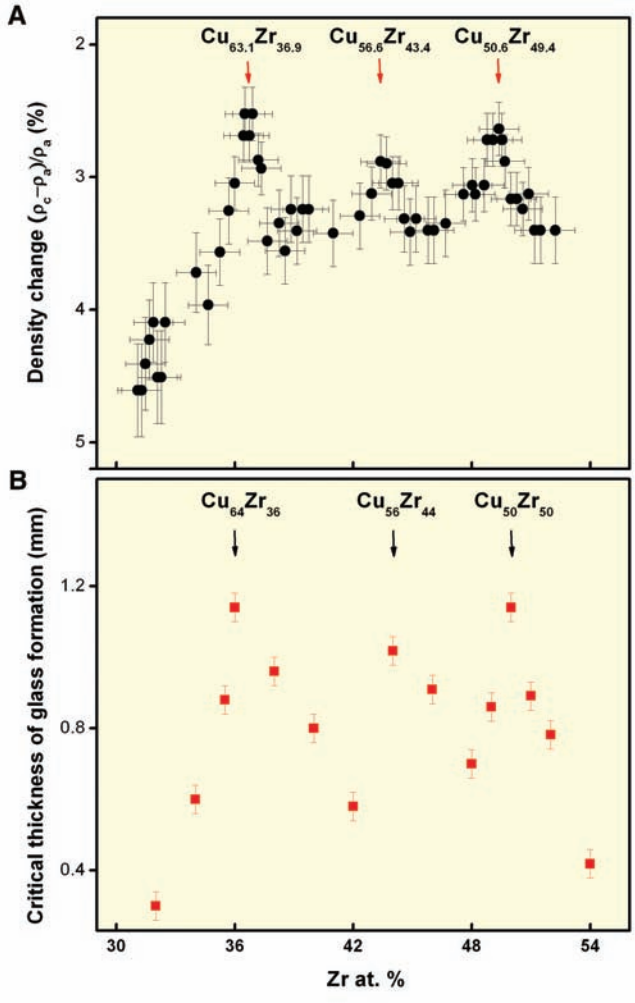

Fig. 3. Density change upon crystallization $(\rho_c - \rho_a)/\rho_a$ (**A**), and the critical thickness for glass formation (**B**) versus Zr content (atomic %). The density change axis is inverted, to make the two plots more directly comparable. The error of the composition measurement (A) is estimated to be ±1.0 atomic %. In the wedge-casting experiments (B), the error of the critical thickness measurement is ±0.04 mm, and the variation of the composition can be controlled within ±0.05 atomic %

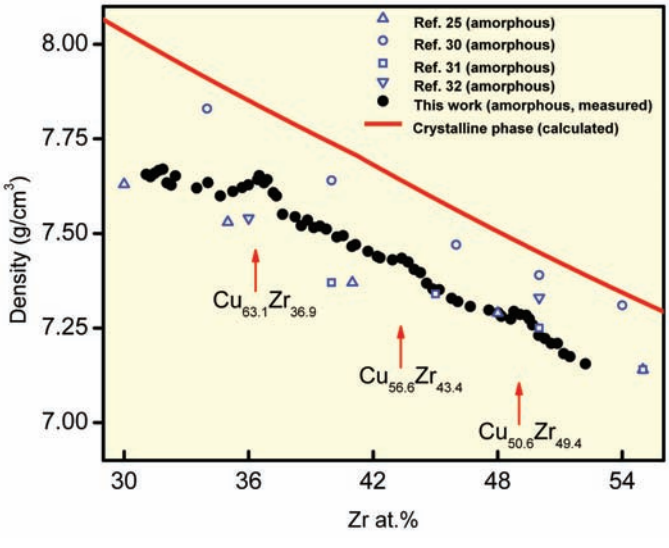

Fig. 4. Density plot for different compositions in the binary Cu-Zr system. The density of the crystalline phase (estimated from the equilibrium phase diagram using the lever rule), the density of the amorphous phase (estimated from the density change upon crystallization in the present study and the density of the crystalline phase), and density data for Cu-Zr metallic glasses reported in the literature (*25*, *30–32*) are shown.

References and Notes

1. A. Inoue, N. Nishiyama, *Mater. Res. Bull.* **32**, 651 (2007).
2. A. L. Greer, E. Ma, *Mater. Res. Bull.* **32**, 611 (2007).
3. S. Mukherjee, J. Schroers, Z. Zhou, W. L. Johnson, W.-K. Rhim, *Acta Mater.* **52**, 3689 (2004).
4. A. R. Yavari, *Phys. Lett.* **95A**, 165 (1983).
5. A. R. Yavari, A. Inoue, *Mater. Res. Soc. Symp. Proc.* **554**, 21 (1999).

6. D. Turnbull, M. H. Cohen, *J. Chem. Phys.* **34**, 120 (1961).
7. D. Turnbull, M. H. Cohen, *J. Chem. Phys.* **52**, 3038 (1970).
8. M. H. Cohen, G. S. Grest, *Phys. Rev. B* **20**, 1077 (1979).
9. D. B. Miracle, W. S. Sanders, O. N. Senkov, *Philos. Mag.* **83**, 2409 (2003).
10. T. Egami, *J. Alloy. Comp.* **434-435**, 110 (2007).
11. F. Faupel *et al.*, *Rev. Mod. Phys.* **75**, 237 (2003).
12. D. B. Miracle, *Acta Mater.* **54**, 4317 (2006).
13. H. W. Sheng, W. K. Luo, F. M. Alamgir, J. M. Bai, E. Ma, *Nature* **439**, 419 (2006).
14. X. Hu, S. C. Ng, Y. P. Feng, Y. Li, *Phys. Rev. B* **64**, 172201 (2001).
15. A. Inoue, T. Negishi, H. M. Kimura, T. Zhang, A. R. Yavari, *Mater. Trans. Jpn. Inst. Metals* **39**, 318 (1998).
16. T. D. Shen, Y. He, R. B. Schwarz, *J. Mater. Res.* **14**, 2107 (1999).
17. J. A. Kalb *et al.*, *J. Microelectromech. Syst.* **17**, 1094 (2008).
18. D. Xu, B. Lohwongwatana, G. Duan, W. L. Johnson, C. Garland, *Acta Mater.* **52**, 2621 (2004).
19. M. B. Tang, D. Q. Zhao, M. X. Pan, W. H. Wang, *Chin. Phys. Lett.* **21**, 901 (2004).
20. D. Wang *et al.*, *Appl. Phys. Lett.* **84**, 4029 (2004).
21. A. Inoue, W. Zhang, *Mater. Trans. Jpn. Inst. Metals* **45**, 584 (2004).
22. N. Mattern *et al.*, *J. Non-Cryst. Solids* **354**, 1054 (2008).
23. J. A. Floro *et al.*, *J. Appl. Phys.* **89**, 4886 (2001).
24. S. G. Mayr, K. Samwer, *Phys. Rev. Lett.* **87**, 036105 (2001).
25. Z. Altounian, G. H. Tu, J. O. Strom-Olsen, *J. Appl. Phys.* **53**, 4755 (1982).
26. B. Busch, J. Schroers, W. H. Wang, *Mater. Res. Bull.* **32**, 620 (2007).
27. D. Turnbull, *Contemp. Phys.* **10**, 473 (1969).
28. D. Ma, H. Tan, D. Wang, Y. Li, E. Ma, *Appl. Phys. Lett.* **86**, 191906 (2005).
29. S. Mukherjee, J. Schroers, W. K. Rhim, W. L. Johnson, *Phys. Rev. Lett.* **94**, 245501 (2005).
30. Y. Calvayrac, J. P. Chevalier, M. Harmelin, A. Quivy, J. Bigot, *Philos. Mag. B* **48**, 323 (1983).
31. Z. Altounian, J. O. Strom-Olsen, *Phys. Rev. B* **27**, 4149 (1983).
32. L. A. Davis, C.-P. Chou, L. E. Tanner, R. Ray, *Scripta Met.* **10**, 937 (1976).
33. J. C. Lee *et al.*, *J. Mater. Res.* **22**, 3087 (2007).
34. T. Egami, Y. Waseda, *J. Non-Cryst. Solids* **64**, 113 (1984).

35. Q.G. acknowledges the Singapore-MIT Alliance for a graduate student fellowship and J.A.K. acknowledges partial financial support from the Alexander-von-Humboldt Foundation. We thank C. Sow for help with optical microscopy and G. Chen for help with the furnace annealing experiments.

Supporting Online Material

www.sciencemag.org/cgi/content/full/322/5909/1816/DC1
Materials and Methods
Figs. S1 to S3
References

10 July 2008; accepted 18 November 2008
10.1126/science.1163062

Stable Prenucleation Calcium Carbonate Clusters

Denis Gebauer, Antje Völkel, Helmut Cölfen*

Calcium carbonate forms scales, geological deposits, biominerals, and ocean sediments. Huge amounts of carbon dioxide are retained as carbonate ions, and calcium ions represent a major contribution to water hardness. Despite its relevance, little is known about the precipitation mechanism of calcium carbonate, and specified complex crystal structures challenge the classical view on nucleation considering the formation of metastable ion clusters. We demonstrate that dissolved calcium carbonate in fact contains stable prenucleation ion clusters forming even in undersaturated solution. The cluster formation can be characterized by means of equilibrium thermodynamics, applying a multiple-binding model, which allows for structural preformation. Stable clusters are the relevant species in calcium carbonate nucleation. Such mechanisms may also be important for the crystallization of other minerals.

Calcium carbonate has great scientific relevance in biomineralization and geosciences, forming enormous scales of biological (reefs and ocean sediments) and geological origin, which bind a huge amount of CO_2 and affect the chemistry of ocean water (*1*) and, with it, Earth's atmosphere and climate. Scale formation (incrustation) also affects daily life, industry, and technology and can require the addition of scale inhibitors to laundry detergents and household cleaners and in many industrial applications. Scale formation also lowers the efficiency of heating and cooling devices and can result in machine damage. $CaCO_3$ provides a model system for nucleation and crystallization analysis of minerals for classical (*2*) and nonclassical crystallization (*3*) and has been studied for more than a century. Nevertheless, little is known about the very early stages of its crystallization, that is, the prenucleation stage. Amorphous calcium carbonate (ACC) is identified as a postnucleation-stage precursor phase in calcium carbonate mineralization (*4*, *5*), in bio- (*6*) and biomimetic mineralization (*7*), and liquid precursors have been identified in some cases (*8*). There is growing evidence that different species of ACC exist, that is, where the amorphous phase shows a specific short-range order that corresponds to the long-range order of the particular crystalline polymorph (*9*–*11*). Besides stable biogenic species, ACC occurs as a transient precursor phase in biomineralization. Precursor species that form still earlier than ACC or liquid precursors—that is, directly after ion contact and before nucleation occurs—have been postulated (*12*) and suggested through modeling approaches (*13*).

In the classical picture, nucleation is considered to take place in a solution of ions that has become supersaturated, leading to the nucleation of the solid phase by stochastic solute clustering, and the earliest crystal precursor is considered to be a cluster of critical size (*14*, *15*). Because of the stochastic formation mechanism, such metastable clusters are a rare species. In contrast, there is increasing evidence that small polymeric species and stable clusters play a dominant role in the prenucleation stage of biomineralization and the formation of organic nanoparticles (*16*, *17*). Such soluble species have been reported for the polycondensation of silicic acid (*18*), precipitation of aluminum oxyhydroxide (*19*), and aqueous solutions of hydrated ions of the transition metals iron, chromium, uranium, molybdenum, and tungsten (*20*). In the above examples, the prenucleation cluster formation is a polymerization-like event, because the chemical bonds formed are mostly covalent (silica) to partly ionic (transition metals). For nonpolymerizing ionic crystals, solute clustering has been reported only for highly soluble compounds such as citric acid, urea, sodium nitrate, and potassium sulfate (*21*) and in supersaturated solutions (*22*). Cluster formation for low concentrations, that is, undersaturated and slightly supersaturated ionic solutions, has not been reported, and even advanced data analysis like induction time statistics do not allow for the accurate observation of all subcritical species present in a dilute system (*23*, *24*).

Our experiments are based on the measurement of Ca^{2+} concentrations at constant pH values, facilitating a quantitative determination of all species present at the different stages of crystallization while the supersaturation slowly evolves. This is achieved by slow addition of dilute calcium chloride solution into dilute carbonate buffer to induce supersaturation, causing nucleation and precipitation of calcium carbonate. The experimental set-up is described in detail in supporting online material (SOM) section 1 (fig. S1). The increase in calcium ions is shown for a single experiment at pH = 9.25 (Fig. 1A). The red line reflects the amount of calcium ions added. However, the amount of free calcium ions detected by the calcium ion selective electrode (black line) increases considerably slower straight from the beginning of the experiment; that is, a distinct part of free calcium ions disappears due to binding. The prenucleation-stage time development is linear, indicating that the calcium binding behavior in under- and supersaturated stages of the prenucleation stage is equal. Once a critical point is reached, nucleation occurs and the amount of free calcium ions drops

Max Planck Institute of Colloids and Interfaces, Research Campus Golm, Am Mühlenberg 1, D-14424 Potsdam, Germany.

*To whom correspondence should be addressed. E-mail: coelfen@mpikg.mpg.de

to a value that corresponds to the particular solubility concentration of the precipitated phase according to a typical LaMer diagram (*25*).

Measurements of the time development of the amount of free calcium ions for five pH levels within an interval from 9.00 to 10.0 show good reproducibility (fig. S2). The pH range investigated is rather limited because the fraction of carbonate ions in the buffer is very low below a pH of 9.00 and hinders precipitation of calcium carbonate, while concurrent precipitation of calcium hydroxide occurs at pH values that are too high. The differences between the averages of measured free amounts and the dosed amount of calcium ions give the averaged amount of bound calcium ions (Fig. 1B). The dotted red line represents 100% binding of dosed calcium ions. Both in the prenucleation stage (i.e., before the sigmoid increase of the amount of bound calcium) and in the postnucleation stage, an increasing tendency for calcium binding with increasing pH is observed. The increasing binding tendency is based on the higher fraction of carbonate ions in the carbonate buffer at higher pH (SOM section 2.1 and fig. S3). Solid calcium carbonate, like any solid, has an activity of 1 by definition. Thus, the dissolution equilibrium is characterized by the ion product of calcium and carbonate ions, giving the solubility constant. To maintain the solubility constant, which, however, slightly differs for the phases precipitated in different pH ranges, the solubility concentration of calcium ions is specifically lower at higher concentrations of carbonate (higher pH). In this way, the binding of calcium ions in solid calcium carbonate increases with increasing pH. Similar binding of calcium ions is observed in the prenucleation stage. About 35% of added calcium ions are bound at pH = 9.00 (~4% carbonate ions in the buffer equilibrium), whereas ~75% of added calcium ions are bound at pH = 10.0 (~25% carbonate ions in the buffer equilibrium). This shows that calcium binding during the prenucleation stage depends on the carbonate concentration, that is, calcium carbonate clusters form. It is important to note that these clusters form in both the undersaturated and supersaturated stages (Fig. 1A). An activity of 1 cannot be assigned to clusters, because they have to be considered as solutes. Basically, this is the reason for the linear increase in free calcium ions during the prenucleation stage in contrast to the postnucleation stage (Fig. 1A). After nucleation, further added calcium is consumed by the growth of particles of constant activity, giving rise to a constant solubility concentration. In the prenucleation stage, further added calcium ions are consumed by the increasing activity of clusters. The increasing fraction of carbonate ions in the buffer at higher pH promotes cluster formation and in this way increases calcium binding (principle of LeChatelier). This is evidence that calcium carbonate clusters of the prenucleation stage form on the basis of equilibrium thermodynamics. These clusters are thermodynamically stable and not metastable as classically considered, because an equilibrium constant of cluster formation exists, which corresponds to a minimum in Gibbs energy (Fig. 2).

Indeed, the binding of carbonate ions in the clusters can be quantitatively evaluated by constant pH titration. The binding of carbonate ions in the clusters (and in particles after nucleation) requires titration with dilute NaOH to maintain constant pH (SOM section 2.1 and fig. S4). Analyses show that calcium binding (Fig. 1B) is congruent to carbonate binding within experimental accuracy at all pH values investigated (SOM section 2.2 and fig. S5), that is, the formed clusters are neutral on average. The thermodynamics of cluster formation cannot be quantitatively characterized assuming the equilibrium $z \times Ca^{2+} + z \times CO_3^{2-} \rightleftharpoons [CaCO_3]_z$, because an excess of variables remains unknown, that is, the number of ions combined in clusters (z), the equilibrium constant of cluster formation, and the clusters' ($[CaCO_3]_{z,aq}$) activity. Such equilibrium is valid for all concentrations of calcium and carbonate ions; thus, clusters form in the undersaturated stage (Fig. 1A) and most likely also in the presence of solid calcium carbonate, and the solubility product of calcium carbonate may account for a low concentration of clusters in the presence of solid $CaCO_3$.

The prenucleation-stage clusters can be independently detected by means of analytical ultracentrifugation (AUC) (SOM section 2.3, fig. S6, and table S1). The clusters cannot be detected in the undersaturated stage of the experiments, while their existence is evidenced by potential

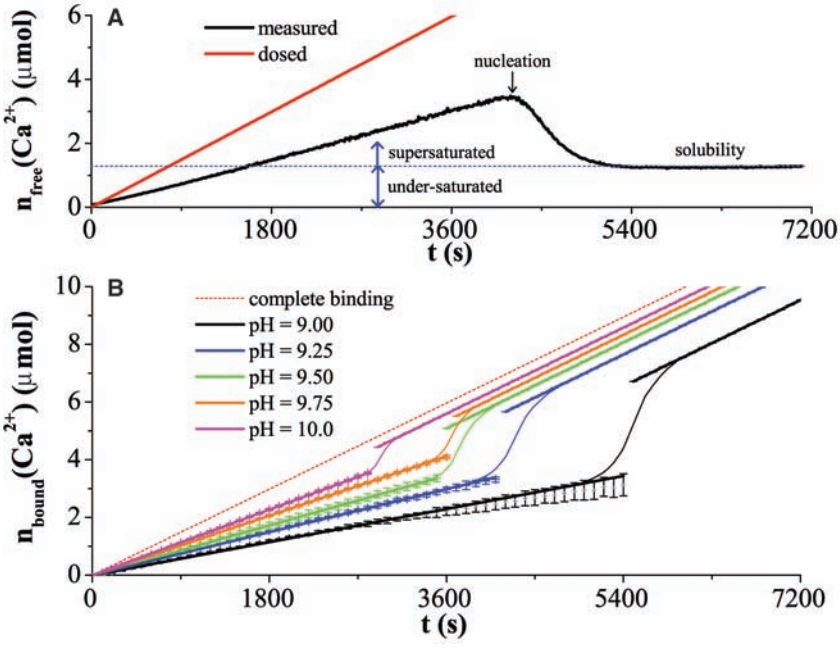

Fig. 1. (**A**) Development of the free calcium ions measured by the calcium ion selective electrode (black line) at pH = 9.25 in comparison with the dosed amount of calcium ions (red line). The solubility concentration of the precipitated phase defines the undersaturated and supersaturated stages of the prenucleation stage. Already in undersaturated solution, calcium ions are bound. (**B**) Averaged amount of bound calcium ions as calculated from the difference between the measured amount of free calcium ions and the dosed amount of calcium ions shown in (A) for five pH levels. The arithmetic average of a sample of three measurements is calculated in the prenucleation stage and the postnucleation stage. Averaging during nucleation is not appropriate, and the particular developments are indicated by fine lines. Error bars depict ±1 SD of a sample of three measurements; the center of the error bars gives the arithmetic average of the particular data points (see also fig. S2).

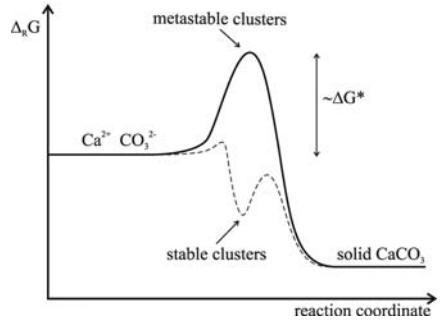

Fig. 2. Schematic illustration of the free reaction enthalpy $\Delta_R G$ versus the reaction coordinate. In the classical view (bold line), metastable clusters form and nucleation occurs when the critical nucleation enthalpy ΔG^* is overcome. In fact, stable clusters (dashed line) are formed with an activation barrier negligible compared to thermal energy. The structure and depth of the indicated minimum remain unknown, as well as the height of the activation barrier for nucleation.

measurements and constant pH titration (Fig. 1). Proximately, the cluster concentration is too low for detection by AUC in this stage. A cluster species with a hydrodynamic diameter of ~2 nm can be detected with good statistical significance in the supersaturated stage and close to nucleation. This size corresponds to roughly 70 calcium and carbonate ions combined in single clusters on average. A second, larger cluster species (hydrodynamic diameter ~4 nm) can be detected, too, although with low statistical relevance. In fact, an even larger cluster species (hydrodynamic diameter ~5 to 6 nm) can be detected in the early postnucleation stage. The smaller cluster species cannot be detected anymore after nucleation; however, the concentration of these species may be too low for detection. These findings suggest that nucleation takes place through cluster aggregation.

The cluster equilibrium can be quantitatively characterized by means of a multiple-binding model usually applied in protein/ligand binding equilibria (*26*) (SOM section 2.4 and figs. S7 to S10). The derived binding parameters are pH-dependent and relate to the binding strength in clusters. This pH-dependent change of binding strength (fig. S11) gives a possible basis for structural preformation and the nucleation of different ACC species discussed above, which later transform into the particular crystalline polymorph. ACC is initially nucleated as revealed by polarized light microscopy (fig. S12), and the analysis of the time development of ion products (Fig. 3) shows that, in fact, two different ACC phases are precipitated—a more stable phase (ACC I) at high binding strength in clusters (pH = 9.00 to 9.50) and a less stable phase (ACC II) at low binding strength in clusters (pH = 9.75 to 10.0).

WAXS (wide angle x-ray scattering) analysis of the crystalline particles finally formed at ambient conditions shows that pure calcite (the stable polymorph of calcium carbonate) forms at pH-values corresponding to high binding strength in clusters and that predominantly vaterite (the least stable polymorph) and traces of calcite form at pH-values corresponding to low binding strength in clusters (fig. S13). Both polymorphs finally form in parallel at intermediate binding strength, whereas aragonite (the intermediate stable polymorph) could not be detected. This suggests that ACC I may relate to an amorphous phase exhibiting calcitic short-range order and that ACC II may relate to an amorphous phase exhibiting vateritic short-range order. The solubilities (Fig. 3) show a discrete differentiation of the ACC phases in between pH 9.50 and 9.75, whereas distinct amounts of vaterite are precipitated when the ion product is still dominated by ACC I (pH = 9.40) (fig. S13). In our opinion, both ACC phases are precipitated in parallel at intermediate binding strength, that is, the system is not yet in thermodynamic equilibrium (Gibbs' phase rule). The coexistence may not be resolved by the development of the ion product (Fig. 3) because ACC II may become crystalline fast, and the solubility of ACC I may be covered by ACC II because the solubility is dominated by the most soluble species. This is also true for minimum binding strength (pH = 9.75), at which traces of calcite are still obtained. The correlation between binding strength in clusters and the kind of amorphous phase and polymorph finally formed furthermore suggests that the clusters are direct precursor species of ACC, in which the particular structure may be also preformed. The accurate mechanism, that is, whether the nucleation of different ACC phases is under thermodynamic or kinetic control, remains unknown.

The proposed mechanism of calcium carbonate precipitation allows for early structural preformation during the prenucleation stage conveyed into the postnucleation stage (Fig. 4). The classical view, in contrast, does not facilitate such early structural preformation because ionic solutions form clusters randomly. The classical critical stage is characterized by the stochastic formation of clusters of critical size, which are thermodynamically able to grow without limit but are in fact a rare species. The growth of these clusters is then considered to take place by the addition of single ions, and the formation of different polymorphs is considered to be under thermodynamic or kinetic control. We have shown that prenucleation-stage clusters form on the basis of pH-dependent equilibrium thermodynamics (Fig. 4). The clusters show an average size of ~70 ions (pH = 9.00), which is larger than expected from the classically considered, exponentially decreasing cluster size distribution. A precise cluster size distribution, however, is yet unknown. Also a precise (pH-dependent) cluster structure remains unknown, but it is apparent that prenucleation-stage clusters exhibit "solute character." This means that not surface tension, which is a characteristic property of phase boundaries and is classically attributed to clusters, but hydration energy taking solvent effects into account can be ascribed to clusters. The surface tension characterizing a phase interface establishes when the critical stage is reached, and amorphous $CaCO_3$ is precipitated at first. It remains unknown whether the clusters form critical nuclei that grow classically by single-ion attachment or aggregate and then precipitate and how the precipitation of different ACC phases at different pH values can be explained precisely, because several options exist (Fig. 4). In fact, AUC experiments provide evidence that the clusters are the nucleation-relevant species, because small cluster species cannot be detected after nucleation. In our opinion, nucleation is most probable cluster aggregation, supported by the detection of larger clusters in the early postnucleation stage and close to nucleation by means of AUC. Comparing the classical and novel view,

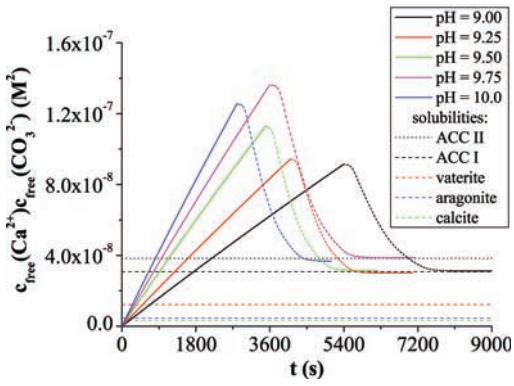

Fig. 3. Time development of the free ion product. Shown are averaged values obtained from a sample of three measurements. Because averaging is not appropriate during nucleation, the particular developments are indicated by dashed lines. We find two different ACC phases with solubility products of ~3.1×10^{-8} M^2 (ACC I) and ~3.8×10^{-8} M^2 (ACC II), corresponding to the pH dependency of the prenucleation cluster equilibrium. Also given are the solubilities of vaterite, aragonite, and calcite (*27*) (SOM section 2.5.)

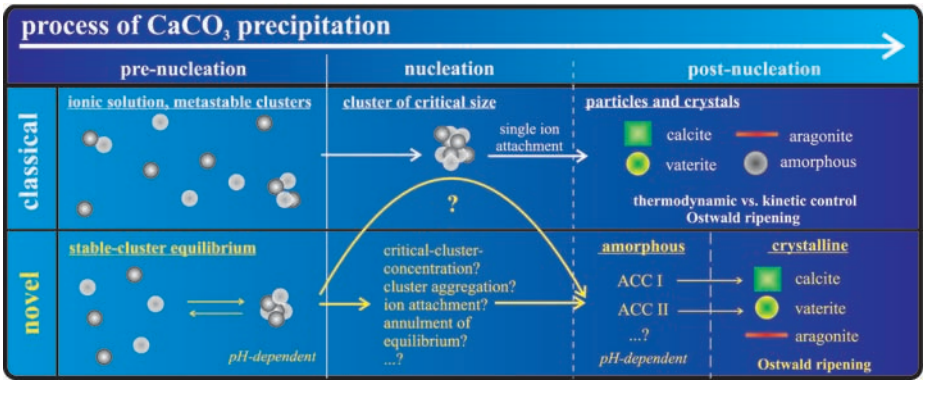

Fig. 4. Schema of the classical and novel view on precipitation (not to scale). Prenucleation-stage calcium carbonate clusters provide an early precursor species of different ACC phases giving rise to an alternative crystallization-reaction channel.

it is furthermore crucial to note that a distinct part of the nucleation driving force given by the change in Gibbs energy is already released by stable cluster formation (SOM section 2.6, fig. S14, and Fig. 2).

Prenucleation-stage cluster formation on the basis of equilibrium thermodynamics can be qualitatively shown also for the biominerals calcium phosphate and calcium oxalate (SOM section 2.7 and fig. S15) and suggests a similar nucleation mechanism for these minerals. The cluster-formation mechanism on the basis of equilibrium thermodynamics can be speculatively explained by entropic solvent effects. The probable release of water molecules from the hydration layer of ions caused by cluster formation may result in an increased number of degrees of freedom of the system. In classical nucleation theories, only enthalpic effects (interaction potentials) are taken into account, and entropic solvent effects are neglected. In the end, a pH-dependent change of ionic hydration layers may explain the pH dependency of cluster-formation thermodynamics.

References and Notes

1. R. E. Zeebe, J. C. Zachos, K. Caldeira, T. Tyrrell, *Science* **321**, 51 (2008).
2. J. J. De Yoreo, P. G. Vekilov, *Rev. Mineral. Geochem.* **54**, 57 (2003).
3. M. Niederberger, H. Cölfen, *Phys. Chem. Chem. Phys.* **8**, 3271 (2006).
4. J. Rieger *et al*., *Faraday Discuss.* **136**, 265 (2007).
5. M. Faatz, F. Gröhn, G. Wegner, *Adv. Mater.* **16**, 996 (2004).
6. L. Addadi, S. Raz, S. Weiner, *Adv. Mater.* **15**, 959 (2003).
7. A. W. Xu, Y. R. Ma, H. Cölfen, *J. Mater. Chem.* **17**, 415 (2007).
8. L. B. Gower, D. J. Odom, *J. Cryst. Growth* **210**, 719 (2000).
9. Y. Politi *et al*., *Adv. Funct. Mater.* **16**, 1289 (2006).
10. R. S. K. Lam, J. M. Charnock, A. Lennie, F. C. Meldrum, *Cryst. Eng. Comm.* **9**, 1226 (2007).
11. B. Hasse, H. Ehrenberg, J. C. Marxen, W. Becker, M. Epple, *Chem. Eur. J.* **6**, 3679 (2000).
12. C. G. Sinn, R. Dimova, M. Antonietti, *Macromolecules* **37**, 3444 (2004).
13. D. Quigley, P. M. Rodger, *J. Chem. Phys.* **128**, 4 (2008).
14. M. Volmer, *Kinetik der Phasenbildung* (Steinkopff, Dresden, 1939).
15. R. Becker, W. Döring, *Annalen Der Physik* **24**, 719 (1935).
16. A. Navrotsky, *Proc. Natl. Acad. Sci. U.S.A.* **101**, 12096 (2004).
17. D. Horn, J. Rieger, *Angew. Chem. Int. Ed.* **40**, 4330 (2001).
18. C. C. Perry, *Biomineralization* **54**, 291 (2003).
19. G. Furrer, B. L. Phillips, K. U. Ulrich, R. Pothig, W. H. Casey, *Science* **297**, 2245 (2002).
20. W. H. Casey, T. W. Swaddle, *Rev. Geophys.* **41**, 1008 (2003).
21. M. A. Larson, J. Garside, *Chem. Eng. Sci.* **41**, 1285 (1986).
22. M. A. Larson, *Adv. Ind. Cryst.* **1991**, 20 (1991).
23. D. Knezic, J. Zaccaro, A. S. Myerson, *J. Phys. Chem. B* **108**, 10672 (2004).
24. A. F. Izmailov, A. S. Myerson, S. Arnold, *J. Cryst. Growth* **196**, 234 (1999).
25. V. K. Lamer, R. H. Dinegar, *J. Am. Chem. Soc.* **72**, 4847 (1950).
26. G. Scatchard, *Ann. N. Y. Acad. Sci.* **51**, 660 (1949).
27. L. Brecevic, A. E. Nielsen, *J. Cryst. Growth* **98**, 504 (1989).

28. Financial support by the German Science Foundation priority program 1117 "Principles of Biomineralization" and the Max Planck Society are gratefully acknowledged. We thank M. Antonietti (MPI) and P. Bowen (Ecole Polytechnique Fédérale de Lausanne, Switzerland) for valuable discussions on the manuscript, A. Verch (MPI) for experimental assistance, and O. Paris and I. Zenke (both MPI) for SAXS analysis. D.G. thanks T. Ketterer and J. Thomas of Deutsche Metrohm for technical assistance.

Supporting Online Material

www.sciencemag.org/cgi/content/full/322/5909/1819/DC1
Materials and Methods
SOM Text
Figs. S1 to S15
Table S1
References

6 August 2008; accepted 12 November 2008
10.1126/science.1164271

Shock-Wave Exploration of the High-Pressure Phases of Carbon

M. D. Knudson,* M. P. Desjarlais, D. H. Dolan

The high–energy density behavior of carbon, particularly in the vicinity of the melt boundary, is of broad scientific interest and of particular interest to those studying planetary astrophysics and inertial confinement fusion. Previous experimental data in the several hundred gigapascal pressure range, particularly near the melt boundary, have only been able to provide data with accuracy capable of qualitative comparison with theory. Here we present shock-wave experiments on carbon (using a magnetically driven flyer-plate technique with an order of magnitude improvement in accuracy) that enable quantitative comparison with theory. This work provides evidence for the existence of a diamond-bc8-liquid triple point on the melt boundary.

The high–energy density behavior of carbon has received increased attention of late, in part due to its relevance to planetary astrophysics. The outer planets, particularly Neptune and Uranus, are thought to contain large quantities of carbon (as much as 10 to 15% of the total planetary mass). The carbon is mostly in the form of methane (*1*) that has been shown to decompose at high pressure and temperature (*2*). The freed carbon may condense in the form of diamond at high pressures and densities within the planet's ice layer (*2*, *3*). Diamond is also being considered as an ablator material for inertial confinement fusion capsules. Consequently, understanding the melt properties of diamond at high pressures and densities achievable through compression by large-amplitude shock waves is paramount for designing capsules and drive-pressure pulse shapes that minimize the possibility of microstructural effects during the implosion phase of the capsule. Such effects could lead to heterogeneities that would seed instabilities capable of quenching the implosion (*4*).

Previous models for carbon based on the chemical picture framework have shown great variation in the diamond melt boundary (*5*–*8*). The melt boundary of diamond has also been explored within the framework of quantum calculations by Grumbach and Martin (*9*, *10*) and Wang *et al*. (*11*). Both groups predicted a maximum in the melt curve for diamond near 500 GPa and ~8000 to 9000 K. More recently, Correa *et al*. (*12*) used ab initio molecular dynamics (AIMD) simulations to explore the phase diagram, considering both the diamond and bc8 solid phases. They also predicted a maximum in the diamond melt curve, in reasonable agreement with Grumbach and Martin (*9*). Furthermore, as can be seen in Fig. 1, Correa *et al*. (*12*) predicted the existence of a diamond-bc8-liquid triple point at ~850 GPa. Romero and Mattson (*13*) used AIMD methods to determine the Hugoniot of carbon, the locus of end states achievable through compression by large-amplitude shock waves (*14*), in the pure solid (diamond) and liquid phases, suggesting that the Hugoniot would enter the pure liquid phase at a pressure above the triple point.

Concurrently, the melt properties of diamond have been explored experimentally with the use of large laser facilities. Using the Omega laser, Bradley *et al*. (*15*) observed a rapid increase of reflectivity with shock velocity that reached saturation at ~1000 GPa. This saturation was interpreted as evidence for the completion of melt along the principal Hugoniot. More recently, groups from Japan (*16*), using the Gekko laser, and France (*17*), using the Laboratoire pour l'Utilisation des Lasers Intenses (LULI) laser, obtained Hugoniot measurements in the pressure ranges of 500 to 2000 GPa and 600 to 1500 GPa, respectively.

The results from these studies largely agree within experimental uncertainty. However, to reach the required energy densities, the laser spot size was a few hundred microns, resulting in a restriction in the sample thickness of

Sandia National Laboratories, Albuquerque, NM 87185, USA.

*To whom correspondence should be addressed. E-mail: mdknuds@sandia.gov

~20 μm to ensure one-dimensional loading, which then resulted in experimental durations of <1 ns and uncertainty of the inferred pressure and density on the Hugoniot of ~5 to 10%. As illustrated in Fig. 2A, this accuracy is not adequate to provide quantitative comparison with theory. Whereas the experimental results obtained at LULI (*17*) suggest a substantial density increase upon melt (and thus a negative slope in the melt curve), its value is not well constrained because of the large experimental uncertainty. Thus, there is still a lack of understanding of the shock response of diamond in the vicinity of the melt boundary.

We present the results of magnetically accelerated flyer-plate experiments on diamond performed at the Sandia Z machine (*18*) over the pressure range of 550 to 1400 GPa. The relatively large lateral area of the flyer plates permitted simultaneous shock loading of multiple samples of several hundred micron thickness, comparable with those typical of gas-gun studies (*19*). Furthermore, the ability to precisely measure an impact velocity in such experiments placed substantial constraints on the particle velocity and thus on the inferred pressure and density. These aspects enabled roughly an order-of-magnitude improvement in accuracy as compared with previous work in this pressure range (*16*, *17*), as illustrated in Fig. 2. Coupled with the reflectivity results of Bradley *et al*. (*15*) and a detailed AIMD study of the Hugoniot response of diamond, these experiments indicate the existence of a diamond-bc8-liquid triple point on the principal Hugoniot of diamond at ~875 GPa and ~6.6 g/cm^3 density.

AIMD calculations for carbon were performed using the Vienna ab initio simulation program, a plane-wave density functional theory code developed at the Technical University of Vienna (*20*–*22*). Initial calculations performed to determine the thermodynamic stability regions for the liquid, diamond, and bc8 phases were largely consistent with those reported by Correa *et al*. (*12*), as shown in Fig. 1 (*23*). This work focused primarily on the determination of the principal Hugoniot, in particular along the melt boundary.

The Rankine-Hugoniot jump conditions (*14*), which are derived by considering conservation of mass, momentum, and energy across a steady propagating shock wave, provide a set of equations relating the initial energy E, volume V, and pressure P, with steady-state, post-shock values

$$(E - E_0) = P/2(V_0 - V) \quad (1)$$

$$P = \rho_0 U_s u_p \quad (2)$$

$$\rho = \rho_0[U_s/(U_s - u_p)] \quad (3)$$

where ρ, U_s, and u_p denote the density, shock velocity, and particle velocity, respectively, and the subscript 0 denotes initial values (P_0 is taken to be zero) (*24*). The first of these equations, derived from the conservation of energy, provides a prescription for the calculation of the Hugoniot. For a given P, an initial estimate is made for the temperature (T), or ρ that would satisfy Eq. 1. On the basis of the resulting AIMD calculation, corrections are made to T or ρ, and the process is repeated. The resulting iteration converges rapidly and provides very accurate Hugoniot states within the framework of the AIMD.

The results of the Hugoniot calculations are shown in Fig. 1. The solid (diamond) Hugoniot is predicted to intersect the melt boundary at ~680 GPa, along the diamond-liquid coexistence curve. In contrast, the liquid Hugoniot is predicted to intersect the melt boundary at ~1040 GPa, along the bc8-liquid coexistence curve. For intermediate pressures, the Hugoniot is predicted to be on the melt boundary, inclusive of the proposed diamond-bc8-liquid triple point. This prediction of the triple point lying within the coexistence region of the Hugoniot raises an interesting question: Is there an experimental observable that could indicate the presence of the triple point along the principal Hugoniot? The answer lies in the compressibility and is directly related to the predicted anomalous diamond-liquid and normal bc8-liquid melt lines, respectively.

Calculations performed within the coexistence region, and in particular around the predicted triple point, are shown in Fig. 3, which illustrates the diamond-liquid and bc8-liquid coexistence regions in the vicinity of the triple point in P-ρ-T space, along with projections in the P-T and P-ρ planes. The predicted Hugoniot is also plotted in this figure. Approaching the triple point from lower pressure, the Hugoniot lies along the diamond-liquid coexistence curve. An increase in pressure corresponds to an increase in the volume fraction of the liquid in the diamond-liquid composition. Because the diamond-liquid melt boundary is predicted to be anomalous in this region, the liquid has a higher ρ than does the diamond-phase solid. This results in a more rapid increase in ρ with P, as illustrated in Figs. 2 and 3. At a pressure just beyond the triple point, the composition of the Hugoniot state changes abruptly to a mixture of

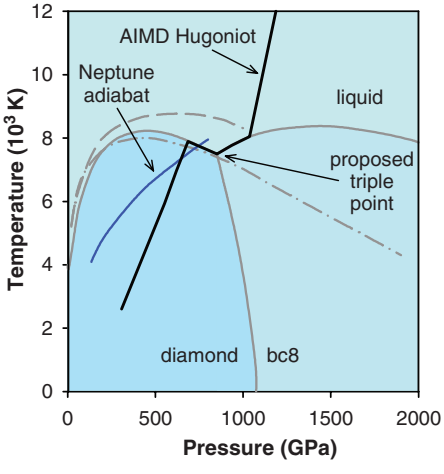

Fig. 1. Phase diagram for high–energy density carbon. Solid gray line, phase boundaries from Correa *et al*. (*12*); dot-dashed gray line, diamond-liquid melt curve from Grumbach and Martin (*9*); dashed gray line, diamond-liquid melt curve from Wang *et al*. (*11*); solid blue line, predicted adiabat for Neptune (Uranus similar) (*28*); solid black line, AIMD Hugoniot from this work.

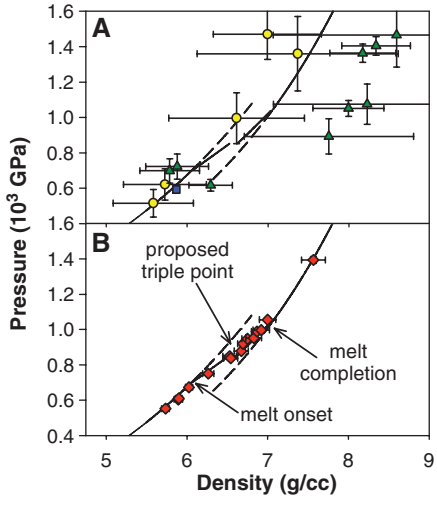

Fig. 2. Diamond P-ρ Hugoniot: (**A**) previous data and (**B**) this work. Solid line, AIMD Hugoniot from this work; dashed line, AIMD metastable solid (diamond) and liquid Hugoniots from this work; yellow circles, Gekko laser (*16*); green triangles, LULI laser (*17*); blue square, Pavlovskii (*29*); red diamonds, this work.

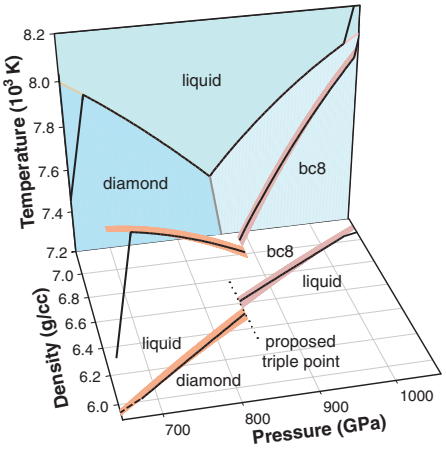

Fig. 3. Coexistence regions and Hugoniot in P-ρ-T space. The Hugoniot (black line) enters the diamond-liquid coexistence region (orange band) from the diamond phase at ~680 GPa (6.02 g/cm^3), reaches the diamond-bc8-liquid triple point at ~850 GPa, and exits the bc8-liquid coexistence region (pink band) at ~1040 GPa (7.04 g/cm^3). The Hugoniot has two solutions at the proposed triple point: (i) a mixture of diamond and liquid (6.52 g/cm^3) and (ii) a mixture of bc8 and liquid (6.62 g/cm^3).

liquid and the bc8 phase of the solid. Again, an increase in P corresponds to an increase in the volume fraction of the liquid. However, in this region the melt boundary is predicted to be normal, and thus the ρ of the liquid is lower than that of the bc8 solid. As a result, ρ increases less rapidly with P, and the Hugoniot increases in stiffness compared with the segment along the diamond-liquid coexistence, as illustrated in Figs. 2 and 3. In addition, a discontinuity is predicted in the Hugoniot at the triple point due to the fact that two solutions to Eq. 1 exist at the triple point: (i) a mixture of diamond and liquid and (ii) a mixture of bc8 and liquid.

Thus, the presence of the triple point within the coexistence region is manifest by the Hugoniot being broken into four distinct segments, each having a different compressibility. In contrast, the absence of the triple point would result in the Hugoniot being broken into three segments. As can be seen in Fig. 2A, the compressibility differences predicted by AIMD for the various segments of the diamond Hugoniot are substantial; the difference in ρ between the metastable extensions of the solid and liquid over this pressure range is >5% on average. However, quantitative comparison with this prediction requires experimental Hugoniot data with greatly improved precision, with respect to previous work in this pressure range (*16*, *17*).

A series of experiments on polycrystalline diamond were performed on the Z machine at Sandia National Laboratories, a pulsed power accelerator capable of producing extremely large current (~20 MA) and magnetic field densities (~10 MG) within a short-circuit, coaxial load geometry. These current and magnetic field densities result in substantial magnetic pressures (in excess of 400 GPa) produced over time scales of a few hundred nanoseconds. The resulting impulse is capable of propelling the outer anode plates of the coaxial load outward at high velocity. With proper shaping of the current pulse and design of the coaxial load geometry, macroscopic metal plates (several square centimeters in lateral area and several hundred microns in thickness) can be launched as flyer plates, to velocities approaching 35 km/s. Moreover, these plates are capable of being used in high-precision equation of state measurements at several hundred gigapascal pressures (*23*, *25*).

A 17–by–40-mm copper flyer plate was magnetically accelerated to peak velocities between 13 and 24 km/s. The relatively large area of the flyer plate was exploited by impacting multiple diamond samples, as shown in Fig. 4A. Each experiment consisted of two quartz or sapphire windows bracketing three polycrystalline diamond samples, each of which were backed by quartz or sapphire windows. In all cases, at least two of the samples were microcrystalline diamonds, which were largely transparent; in some cases, the third sample was nanocrystalline diamond, which was completely opaque. The diamond samples, fabricated using chemical vapor deposition techniques, were nominally 6 mm square in lateral dimensions and 520, 750, and 950 μm in thickness. Actual thickness at the center of each sample was determined to within ~1 to 2 μm from multiple measurements across the surface of the sample with the use of a through-the-lens laser auto focus instrument.

We used a velocity interferometer (*26*) to optically measure velocity via the Doppler shift of light reflecting from a moving surface. A total of 16 diagnostic channels were available for each experiment, enabling multiple, redundant diagnostic channels to be fielded at each sample location. The transparency of the microcrystalline diamond samples allowed for laser light to initially reflect from the copper flyer plate. In these cases, each data record consisted of the velocity of the copper flyer plate over its entire trajectory, enabling the velocity at impact to be determined within ~0.5% (*23*). Also, on the same data record were clear fiducials of the flyer-plate impact with the diamond sample and subsequent transmission of the induced shock wave from the diamond sample into the quartz or sapphire window. This provided a highly accurate transit time through the sample, unaffected by any nonplanarity of impact. Transit times were on the order of 20 to 45 ns, with ~0.4-ns resolution, enabling U_s for each sample to be determined in the range of ~1 to 2% (*23*). In the case of the nanocrystalline samples, the impact time was interpolated from the observed impact time of the transparent samples on either side. This reliance on laterally displaced measurements to infer the transit time resulted in somewhat greater uncertainty in U_s of ~2 to 4%. Because each of the three diamond samples on a given panel was nearly identically loaded, weighted averaging (*27*) could be used to reduce the overall uncertainty in the measured U_s to ~1% or less for most experiments.

Equations 1 to 3 could then be used to determine P and u_p of the diamond in the shocked state, as shown graphically in Fig. 4B. A linear U_s-u_p response for copper, obtained from experimental data, provides a quadratic relation for the P-u_p response of copper (*23*). Given Eq. 2, P in the shocked state of the diamond is constrained to lie along a chord with slope given by $\rho_0 U_s$. The intersection of these two curves provides P and u_p in the shocked state. In this way, u_p was determined to better than 1% in all cases. Given U_s and u_p for diamond, ρ could then be inferred through the use of Eq. 3. Propagation of uncertainties in U_s and u_p resulted in uncer-

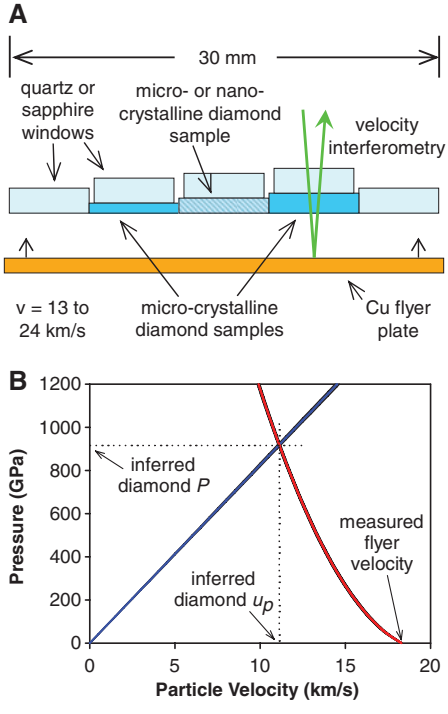

Fig. 4. (**A**) Experimental configuration. The figure is not drawn to scale. (**B**) Graphical impedance matching used to obtain P and u_p in the shocked state. Blue line, chord with slope given by $\rho_0 U_s$; red line, the copper Hugoniot. The uncertainties in the measured flyer velocity, the copper Hugoniot, and the measured diamond shock velocity are represented in the figure by the width of the lines.

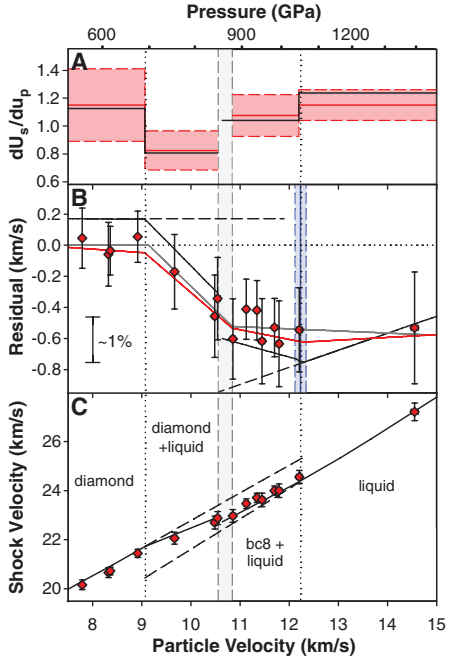

Fig. 5. (**A**) U_s-u_p slopes. Solid (dashed) red line, slope (1σ deviation) of the four segment fit of the U_s-u_p experimental data with breakpoints determined by AIMD; solid black line, slope of the AIMD U_s-u_p Hugoniot; dotted vertical lines, breakpoints corresponding to onset and completion of melt; gray region, bound for the location of the proposed triple point. (**B**) Residual plot of U_s with respect to U_s in the solid (diamond) phase. Symbols, solid, and dashed black lines are as in Fig. 2. The gray and red lines represent three- and four-segment fits, respectively. Rightmost shaded region, u_p corresponding to the saturation in reflectivity observed by Bradley *et al.* (*15*). (**C**) Diamond U_s-u_p Hugoniot. Lines and symbols are as in Fig. 2.

tainties in ρ of ~1%. We performed a total of 15 experiments over the pressure range of 550 to 1400 GPa (45 total diamond samples, 36 microcrystalline, and 9 nanocrystalline). The results of these experiments are shown in Fig. 2B.

Figure 5C shows a comparison of the measured values of U_s-u_p with the AIMD predicted values. The AIMD results suggest a substantial offset between the pure solid (diamond) and liquid branches of the Hugoniot, as illustrated by the metastable extensions shown as dashed lines. The present experimental results are in good agreement with the predicted offset and thus with the gross features of melt predicted by AIMD.

To further explore the melt behavior within the coexistence region, we first considered a three-segment piecewise-linear fit to the data. Such behavior would be consistent with the completion of melt along the diamond-liquid coexistence and would correspond to either (i) the absence of a triple point along the Hugoniot (i.e., the triple point occurs at a pressure higher than that at which completion of melt occurs) or (ii) sluggish kinetics that inhibit a phase transition to the bc8 phase within the time scale of the shock-wave experiments (i.e., the triple point occurs along the Hugoniot but the observed response is nonequilibrium). Either of these scenarios would be manifest as a three-segment Hugoniot through melt.

We followed a two-step fitting process to determine both the most probable locations of the breakpoints and the slope of each individual region while enforcing the continuity of U_s at each of the segment breakpoints (*23*). The resulting fit is shown as a gray line in Fig. 5B, which plots the residual of U_s with respect to the U_s fit for the solid (diamond) phase. As can be seen in the figure, substantial slope changes occur at pressures near ~700 and ~875 GPa.

It is instructive to compare the present results with the previous work of Bradley *et al.* (*15*), in which an abrupt saturation in reflectivity was observed at a U_s of 24.5 km/s. Given the present Hugoniot measurements, this would correspond to P and u_p of 1055 ± 9 GPa and 12.23 ± 0.1 km/s, respectively, as shown by the rightmost shaded region in Fig. 5B. Here, the uncertainties in P and u_p reflect the uncertainty in the U_s-u_p fits of the present data. The present results and those of Bradley *et al.* (*15*) would be inconsistent with completion of melt from the diamond-liquid coexistence. In this scenario, the substantial slope changes in the three-segment fit would suggest the onset and completion of melt at ~700 and ~875 GPa, respectively, whereas the saturation of reflectivity observed by Bradley would suggest the completion of melt at ~1055 GPa, nearly 200 GPa higher than the value predicted from the three-segment fit.

Therefore, we next considered a four-segment piecewise-linear fit to the data, commensurate with the presence of a triple point on the Hugoniot. We again employed a two-step fitting process to determine the most probable breakpoint locations and segment slopes while enforcing continuity of U_s (*23*). The AIMD calculations suggest a discontinuity in U_s-u_p at the triple point (Fig. 5), with an abrupt drop in U_s. However, the magnitude of this drop is <1%. It is not clear that the present data exhibit the necessary accuracy to warrant this level of sophistication. Furthermore, because of the anomalous and normal diamond-liquid and bc8-liquid melt boundaries, respectively, the discontinuity in U_s must be negative; treating the triple point as continuous avoids any unphysical results for the four-segment fit in which a positive discontinuity in U_s occurs.

The resulting four-segment piecewise-linear fit is shown as a red line in Fig. 5B. As can be seen in the figure, substantial slope changes still occur at pressures near ~700 and ~875 GPa. In particular, the inclusion of a fourth segment only influences the fit above ~875 GPa through an additional subtle slope change at a pressure of ~1060 GPa, but otherwise it is quite similar to the three-segment fit. However, this scenario provides a way to reconcile the present results with those of Bradley *et al.* (*15*). The four-segment fit and the Bradley results would suggest the onset and completion of melt at ~700 and ~1060 GPa, respectively. Furthermore, the present results would indicate a substantial slope change within the coexistence region at ~875 GPa, commensurate with the presence of a triple point. Because of the discontinuity in U_s at the triple point, the present data can only constrain the location of the proposed triple point between ~850 to 880 GPa; this corresponds to the pressure range between data points that encompasses the location of the second breakpoint.

Thus, the following picture emerges. The first slope change (at P and ρ of 699 GPa and 6.08 g/cm^3, respectively) corresponds to the onset of melt from the diamond phase. The second slope change (at P and ρ between ~850 to 880 GPa and ~6.53 to 6.67 g/cm^3, respectively) corresponds to a triple point along the solid-melt boundary. The third slope change (at P and ρ of 1064 GPa and 7.01 g/cm^3, respectively), coincident with the saturation of reflectivity observed by Bradley *et al.* (*15*), corresponds to the completion of melt from a solid phase other than diamond.

These values correlate well with the predicted AIMD values for the triple point at P and ρ of 850 GPa and 6.52 to 6.62 g/cm^3, respectively, and are also in quite good agreement with the AIMD predictions of the onset and completion of melt at ~680 GPa and ~1040 GPa, respectively. Also, the magnitudes of the slopes of the four-segment fit are in quite good agreement with those obtained from the AIMD calculations, as illustrated in Fig. 5A. This level of agreement provides a high-fidelity experimental validation of AIMD methods in prediction of the carbon response at these high–energy density conditions, and it also provides evidence for a diamond-bc8-liquid triple point.

References and Notes

1. W. B. Hubbard *et al.*, *Science* **253**, 648 (1991).
2. M. Ross, *Nature* **292**, 435 (1981).
3. L. R. Benedetti *et al.*, *Science* **286**, 100 (1999).
4. J. D. Lindl, *Inertial Confinement Fusion*, *The Quest for Ignition and Energy Gain Using Indirect Drive* (Springer, New York, 1998).
5. M. van Thiel, F. H. Ree, *High Press. Res.* **10**, 607 (1992).
6. A. M. Molodets, M. A. Molodets, S. S. Nabatov, in *Shock Compression of Condensed Matter*, S. C. Schmidt, D. P. Dandekar, J. W. Forbes, Eds. (American Institute of Physics Press, Melville, NY, 1998), pp. 91–94.
7. L. E. Fried, W. H. Howard, *Phys. Rev. B* **61**, 8734 (2000).
8. G. I. Kerley, L. C. Chhabildas, *Sandia National Laboratories Report No. SAND2001-2619* (Sandia National Laboratories, Albuquerque, NM, 2001).
9. M. P. Grumbach, R. M. Martin, *Phys. Rev. B* **54**, 15730 (1996).
10. M. P. Grumbach and R. M. Martin also discussed the bc8 melt line. However, the melt temperature and *dT/dP* were estimated from the Lindemann melt criterion and observations regarding the pressure change observed for the melting of the simple cubic structure, respectively. Ab initio methods were not used in the bc8 melt line determination.
11. X. Wang, S. Scandolo, R. Car, *Phys. Rev. Lett.* **95**, 185701 (2005).
12. A. A. Correa, S. A. Bonev, G. Galli, *Proc. Natl. Acad. Sci. U.S.A.* **103**, 1204 (2006).
13. N. A. Romero, W. D. Mattson, *Phys. Rev. B* **76**, 214113 (2007).
14. G. E. Duvall, R. A. Graham, *Rev. Mod. Phys.* **49**, 523 (1977).
15. D. K. Bradley *et al.*, *Phys. Rev. Lett.* **93**, 195506 (2004).
16. H. Nagao *et al.*, *Phys. Plasmas* **13**, 052705 (2006).
17. S. Brygoo *et al.*, *Nat. Mater.* **6**, 274 (2007).
18. M. K. Matzen, *Phys. Plasmas* **4**, 1519 (1997).
19. A. C. Mitchell, W. J. Nellis, *J. Appl. Phys.* **52**, 3363 (1981).
20. G. Kresse, J. Hafner, *Phys. Rev. B* **47**, 558 (1993).
21. G. Kresse, J. Hafner, *Phys. Rev. B* **49**, 14251 (1994).
22. G. Kresse, J. Furthmuller, *Phys. Rev. B* **54**, 11169 (1996).
23. Materials and methods are available as supporting material on *Science* Online.
24. Longitudinal stress, σ_{xx}, should be used for shock states that remain in the solid phase, as it is possible that the solid state can support shear stresses such that $P \neq \sigma_{xx}$. However, the majority of the data presented here is either in the coexistence region or the pure fluid, in which case the shocked state is expected to be hydrostatic.
25. R. W. Lemke *et al.*, *J. Appl. Phys.* **98**, 073530 (2005).
26. L. M. Barker, R. E. Hollenbach, *J. Appl. Phys.* **43**, 4669 (1972).
27. J. R. Taylor, *An Introduction to Error Analysis* (Univ. Science Books, Sausalito, CA, ed. 2, 1982).
28. W. B. Hubbard, M. Podolak, D. J. Stevenson, in *Neptune and Triton*, D. P. Cruikshank, Ed. (Univ. of Arizona Press, Tucson, AZ, 1995), pp. 109–138.
29. M. N. Pavlovskii, *Sov. Phys. Solid State* **13**, 741 (1971).

30. We would like to acknowledge the crew of the Sandia Z facility for their contributions in the design, fabrication, and assembly of the experiments, as well as the fielding of diagnostics. Sandia is a multiprogram laboratory operated by Sandia Corporation, a Lockheed Martin Company, for the U.S. Department of Energy's National Nuclear Security Administration under contract no. DE-AC04-94AL85000.

Supporting Online Material

www.sciencemag.org/cgi/content/full/322/5909/1822/DC1
Materials and Methods
Figs. S1 to S6
References

25 March 2008; accepted 17 November 2008
10.1126/science.1165278

Avian Paternal Care Had Dinosaur Origin

David J. Varricchio,[1]* Jason R. Moore,[2] Gregory M. Erickson,[3] Mark A. Norell,[4] Frankie D. Jackson,[1] John J. Borkowski[5]

The repeated discovery of adult dinosaurs in close association with egg clutches leads to speculation over the type and extent of care exhibited by these extinct animals for their eggs and young. To assess parental care in Cretaceous troodontid and oviraptorid dinosaurs, we examined clutch volume and the bone histology of brooding adults. In comparison to four archosaur care regressions, the relatively large clutch volumes of *Troodon*, *Oviraptor*, and *Citipati* scale most closely with a bird-paternal care model. Clutch-associated adults lack the maternal and reproductively associated histologic features common to extant archosaurs. Large clutch volumes and a suite of reproductive features shared only with birds favor paternal care, possibly within a polygamous mating system. Paternal care in both troodontids and oviraptorids indicates that this care system evolved before the emergence of birds and represents birds' ancestral condition. In extant birds and over most adult sizes, paternal and biparental care correspond to the largest and smallest relative clutch volumes, respectively.

Avian reproduction differs from that of other vertebrates in the extensive contribution of males to the care of eggs and young. Males participate in parental care in more than 90% of extant bird species (*1*). By comparison, males contribute to parental care in fewer than 5% of mammalian species and even more rarely among extant non-avian reptiles (*1*). The origin of this paternal contribution as well as the overall parental care system in ancestral birds remains controversial (*2*, *3*). Maternal care predominates in crocodilians (the closest living sister taxon to birds), and the two major clades of extant birds use differing parental care systems. Neognathes (i.e., galliforms through passerines) typically exhibit biparental care, with females and males variably sharing incubation and care of the young (*1*–*3*). In contrast, males of nearly all Paleognathes (ratites, tinamous) incubate and care for the young alone (*4*). Cretaceous troodontid and oviraptorid dinosaurs share a close ancestry with birds and display some of their reproductive attributes, including multilayered eggshells, asymmetric eggs, and monoautochronic ovulation (*5*). Additionally, adult *Troodon formosus*, *Oviraptor philoceratops*, and *Citipati osmolskae* have been discovered on top of egg clutches, with some specimens retaining avian-like brooding postures (*5*, *6*). We assessed the parental care system of these dinosaurs with the use of clutch volume–adult body mass models and bone histology data from brooding adults (*7*).

Complete egg clutches for *Troodon* and the oviraptorids contain 22 to 30 large eggs (*7*). Total clutch volumes far exceed those of extant crocodilians, more closely matching those of polygamous ratites with similar adult size (Fig. 1). We generated regression models describing the adult

[1]Department of Earth Sciences, Montana State University, Bozeman, MT 59717, USA. [2]Department of Geology and Geophysics, Texas A&M University, College Station, TX 77843, USA. [3]Department of Biological Science, Florida State University, Tallahassee, FL 32306, USA. [4]Division of Paleontology, American Museum of Natural History, New York, NY 10024, USA. [5]Department of Mathematical Sciences, Montana State University, Bozeman, MT 59717, USA.

*To whom correspondence should be addressed. E-mail: djv@montana.edu

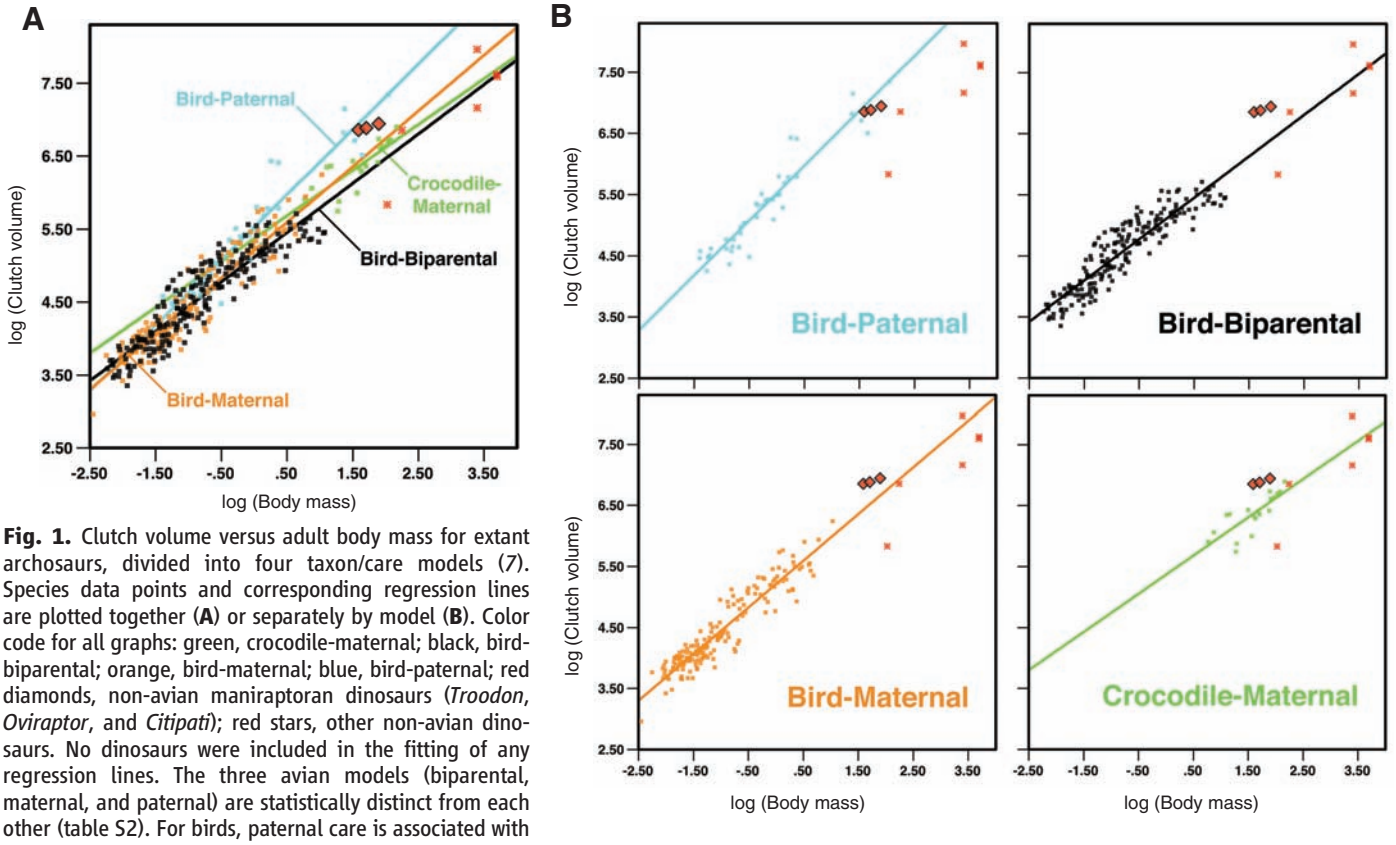

Fig. 1. Clutch volume versus adult body mass for extant archosaurs, divided into four taxon/care models (*7*). Species data points and corresponding regression lines are plotted together (**A**) or separately by model (**B**). Color code for all graphs: green, crocodile-maternal; black, bird-biparental; orange, bird-maternal; blue, bird-paternal; red diamonds, non-avian maniraptoran dinosaurs (*Troodon*, *Oviraptor*, and *Citipati*); red stars, other non-avian dinosaurs. No dinosaurs were included in the fitting of any regression lines. The three avian models (biparental, maternal, and paternal) are statistically distinct from each other (table S2). For birds, paternal care is associated with relatively larger clutch volumes than either biparental or maternal care over most body sizes; biparental care is associated with the smallest relative clutch volumes. The bird-paternal regression most likely accounts for the clutch volume–body mass relationship in *Troodon* and the two oviraptorids.

clutch volume–adult body mass relationships of 433 extant archosaurs (crocodilians and birds) divided into four taxon/care groups: crocodile-maternal, bird-maternal, bird-biparental, and bird-paternal (Fig. 1 and tables S1 and S5). (For this analysis we defined "clutch" as the complete collection of eggs in a nest, regardless of their parentage.) We used corrected Akaike information criterion values (*8*) to assess which taxon/care group regression model best described the data from the three maniraptoran theropods (*7*). Of the four regression models, the dinosaur ratios most closely matched bird-paternal care (Fig. 1) (*7*). Akaike weights for the four models were bird-paternal, 0.45; bird-maternal, 0.24; crocodile-maternal, 0.19; and bird-biparental, 0.12. Thus, clutch volume–adult body mass ratios of these dinosaurs are 1.8, 2.4, and 3.6 times more likely to fit the bird-paternal model than the bird-maternal, crocodile-maternal, and bird-biparental models, respectively (table S4). Although relatively large clutch volumes occur in lepidosaurs with maternal care (*9*–*11*), a lepidosaur-maternal care model is inappropriate for these three non-avian dinosaurs. Maternal care occurs in only a small percentage of extant lepidosaurs (*1*, *12*) and represents a derived condition within the clade (*2*, *13*); further, lepidosaurs produce parchment-like eggshells and generate their clutches en masse, whereas troodontids, oviraptorids, and extant birds share hard-shelled eggs with multilayered microstructure and iterative egg production (*5*, *14*).

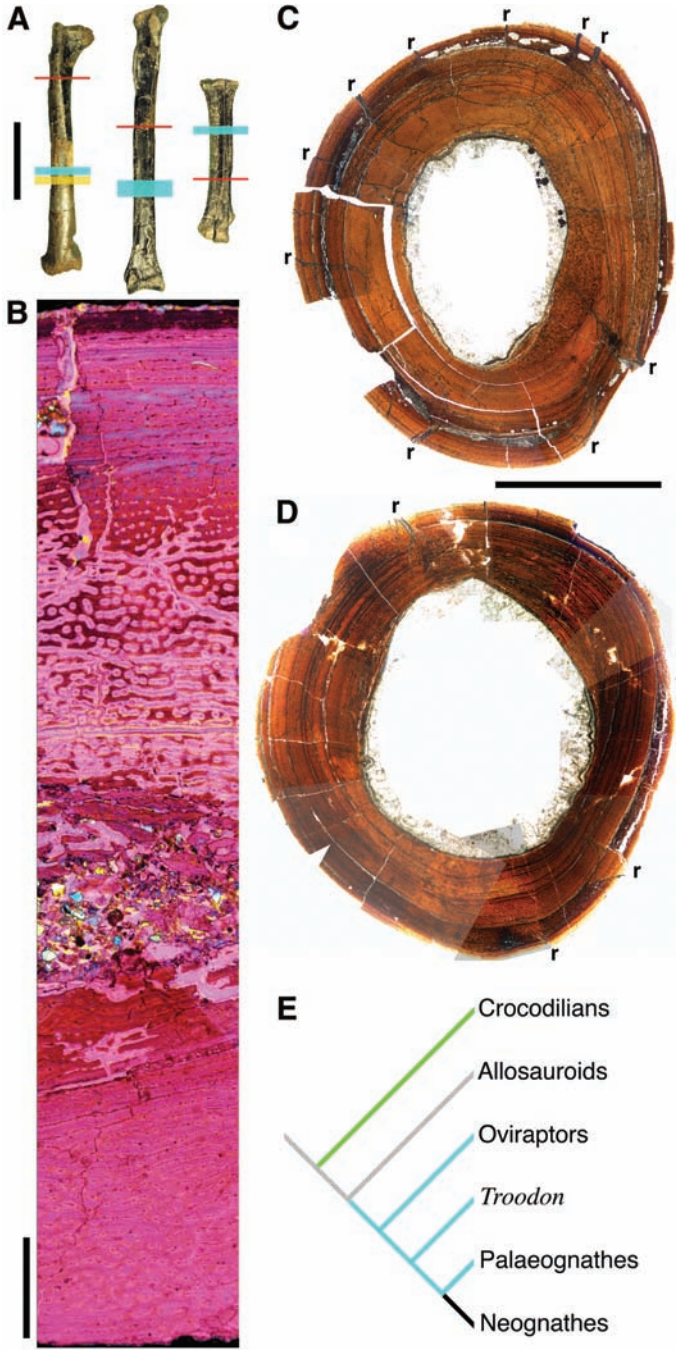

Fig. 2. Bone histology of clutch-associated *Troodon formosus* and *Citipati osmolskae* adults. (**A**) *Troodon* (Museum of the Rockies, MOR 748) right femur, tibia, and metatarsus (from left to right). Histologic examinations were conducted on an incomplete left leg. Color bars indicate relative position of thin-section microscope samples (blue, *Troodon*; yellow, equivalent position of *Citipati* sample) and fracture planes (red, *Troodon*) examined with dissecting scope. Scale bar, 10 cm. (**B**) Cross section of *Citipati* (Institute of Geology, Mongolia, IGM 100/979) femur from endosteum to periosteum (at top) showing fibrolamellar bone with lines of arrested growth, an external fundamental system, and no reproductive-associated tissues. Fractured zone with matrix and bone shards marks the middle of the section. Scale bar, 1 mm. (**C** and **D**) *Troodon* (MOR 748) tibia (C) and femur (D) composite cross sections consisting predominantly of fibrolamellar bone with minor amounts of endosteal lamellar bone. Both lack medullary bone and cortical erosion rooms. Fossil root or fungal traces (r) invade both bones; branching systems with largely micritic fill penetrate the exterior cortex, producing peripheral bands of irregular erosion and dark staining. Root damage, limited in the femur (right side), extends as a nearly complete circumferential band in the tibia. Scale bar, 10 mm. (**E**) Distribution of parental care systems (green, maternal; blue, paternal; black, biparental; gray, equivocal) in modern archosaurs and three clades of non-avian theropod dinosaurs.

Female archosaurs extract substantial amounts of calcium and phosphorus from their skeletal tissues during egg formation (*15*, *16*). Consequently, the long bones of reproductively active crocodilians and possibly the primitive theropod *Syntarsus* (*17*) exhibit extensive resorption cavities within the cortex (*15*). Many birds possess medullary bone, a complex of irregular bone tissue deposited along the interior endosteal surface of long bones (*16*). Although medullary bone is largely resorbed during egg laying, birds can retain some medullary bone days to weeks after ovulation (*16*). Medullary bone was recently reported in the dinosaurs *Tyrannosaurus* (*18*), *Allosaurus*, and *Tenontosaurus* (*19*); each represents a clade more distantly related to birds than either troodontids or oviraptorids (*20*).

Histologic examination (*7*) of femoral, tibial, and metatarsal cross sections from an adult *Troodon* discovered in direct contact with an egg clutch (*5*) revealed minimal secondary remodeling, with no medullary bone or evidence of active bone resorption through the diaphyseal length (Fig. 2, A, C, and D). A distal femur and fibula from an adult *Citipati* specimen found in brooding posture also lack medullary bone or large resorption cavities (Fig. 2B). A variety of additional elements from six other brooding maniraptoran adults (*21*) similarly display no reproductive tissues. If these dinosaurs used long bone tissues as sources of calcium and phosphorus, as in crocodilians, then the absence of resorption cavities implies that the clutch-associated adults were male. If they relied on medullary bone as in birds, the absence of such tissues suggests that these adults were males or postreproductive or nonreproductive females. Some modern birds lack medullary bone, relying instead on dietary intake of minerals for egg production (*22*). Given their proportionately large eggs (*23*) and clutches, this strategy seems unlikely for *Troodon* and oviraptorids in the absence of paternal care (*24*). Thus, histologic examination of *Troodon* and *Citipati* clutch-associated adults provides no evidence to falsify paternal care.

Relatively large clutch volumes like those found in *Troodon* and oviraptorids occur only among extant archosaurs with polygamous mating systems and extensive male care—for example, *Struthio* (ostrich), *Dromaius* (emu), and *Rhea* (*4*). The presence of a paleognath-like reproductive strategy within these non-avian dinosaurs supports an earlier hypothesis that large *Troodon* clutches represent communal nests (*25*).

Large clutch volume–adult body mass ratios do not occur in dinosaurs more distantly related to birds, such as allosauroids (*26*). Troodontids and oviraptorids further differ from other more basal dinosaurs in featuring relatively larger eggs, monoautochronic ovulation, and brooding (*5*, *6*, *23*). Consequently, two factors may have contributed to the evolution of paternal care: (i) increased energy demands of larger, sequentially ovulated eggs, necessitating females to focus strictly on their own feeding and egg laying (*24*, *27*), and (ii) greater thermal incubation needs of embryos, requiring an attendant brooding adult (*28*). Because maternal and biparental care systems occur within extant crocodilians, the nature of parental care within more basal theropods and dinosaurs in general remains ambiguous.

Paternal care in both troodontids and oviraptorids (Fig. 2E) implies that this reproductive system originated before the origin of flight and was primitive for Aves. Biparental care of Neognathes would then represent a derived condition. Although paternal care has previously been suggested as the ancestral condition for extant birds (*3*, *24*, *27*, *29*), it has largely been envisioned as evolving within primitive birds, potentially in conjunction with superprecocial chicks (*24*, *27*). In extant birds, the three parental care strategies correspond to statistically distinct clutch volume–adult body mass relationships (table S2), with paternal care associated with the largest clutches, maternal care with intermediate-size clutches, and biparental care with the smallest clutches for most adult sizes. This suggests a trade-off in parental investment between overall clutch mass and total parental care.

References and Notes

1. T. H. Clutton-Brock, *The Evolution of Parental Care* (Princeton Univ. Press, Princeton, NJ, 1991).
2. B. S. Tullberg, M. Ah-King, H. Temrin, *Philos. Trans. R. Soc. London Ser. B* **357**, 251 (2002).
3. J. D. Ligon, *The Evolution of Avian Breeding Systems* (Oxford Univ. Press, Oxford, 1999).
4. S. J. J. F. Davies, *Ratites and Tinamous* (Oxford Univ. Press, Oxford, 2002).
5. D. J. Varricchio, F. Jackson, J. J. Borkowski, J. R. Horner, *Nature* **385**, 247 (1997).
6. M. A. Norell, J. M. Clark, L. M. Chiappe, D. Dashzeveg, *Nature* **378**, 774 (1995).
7. See supporting material on *Science* Online.
8. H. Motulsky, A. Christopoulos, *Fitting Models to Biological Data Using Linear and Nonlinear Regression* (Oxford Univ. Press, Oxford, 2004).
9. W. R. Branch, R. W. Patterson, *J. Herpetol.* **9**, 243 (1975).
10. L. H. S. Van Mierop, S. M. Barnard, *J. Herpetol.* **10**, 333 (1976).
11. O. Lourdais, T. C. M. Hoffman, D. F. DeNardo, *J. Comp. Physiol. B* **177**, 569 (2007).
12. L. A. Somma, *Smithsonian Herpetological Information Service 81* (1990).
13. R. Shine, in *Biology of the Reptilia*: *Volume 16, Ecology B*, C. Gans, R. B. Huey, Eds. (Liss, New York, 1988), pp. 276–329.
14. D. J. Varricchio, F. D. Jackson, *J. Vertebr. Paleontol.* **24**, 931 (2004).
15. C. S. Wink, R. M. Elsey, *J. Morphol.* **189**, 183 (1986).
16. K. Simkiss, *Calcium in Reproductive Physiology* (Chapman and Hall, London, 1967).
17. A. Chinsamy, *Palaeontol. Afr.* **27**, 77 (1990).
18. M. H. Schweitzer, J. L. Wittmeyer, J. R. Horner, *Science* **308**, 1456 (2005).
19. A. H. Lee, S. Werning, *Proc. Natl. Acad. Sci. U.S.A.* **105**, 582 (2008).
20. P. C. Sereno, *Science* **284**, 2137 (1999).
21. G. M. Erickson, K. C. Rogers, D. J. Varricchio, M. A. Norell, X. Xu, *Biol. Lett.* **3**, 558 (2007).
22. R. Pahl, D. W. Winkler, J. Graveland, B. W. Batterman, *Proc. R. Soc. London Ser. B* **264**, 239 (1997).
23. D. J. Varricchio, F. D. Jackson, in *Feathered Dragons*, P. J. Currie, E. B. Koppelhus, M. A. Shugar, J. L. Wright, Eds. (Indiana Univ. Press, Bloomington, 2004), pp. 215–233.
24. A. Elzanowksi, in *Acta XVIII Congressus Internationalis Ornithologici*, V. D. Ilyichev, V. M. Gavrilov, Eds. (Academy of Sciences of the USSR, Moscow, 1985), pp. 178–183.
25. J. R. Horner, in *Dinosaurs Past and Present, Volume II*, S. J. Czerkas, E. C. Olson, Eds. (Univ. of Washington Press, Seattle, 1987), pp. 51–63.
26. I. Mateus *et al*., *C. R. Acad. Sci. Paris IIA* **325**, 71 (1997).
27. T. Wesolowski, *Am. Nat.* **143**, 39 (1994).
28. S. L. Vehrencamp, *Behav. Ecol.* **11**, 334 (1999).
29. J. Van Rhijn, *Neth. J. Zool.* **34**, 103 (1984).

30. We thank J. Horner, A. Chinsamy-Turan, L. Hall, H. Akashi, J. Rotella, and P. T. Varricchio Sr. Supported by NSF grants EAR-0418649 and DBI-0446224 (G.M.E.).

Supporting Online Material

www.sciencemag.org/cgi/content/full/322/5909/1826/DC1
Materials and Methods
Tables S1 to S5
References

14 July 2008; accepted 14 November 2008
10.1126/science.1163245

Orbital Identification of Carbonate-Bearing Rocks on Mars

Bethany L. Ehlmann,[1] John F. Mustard,[1] Scott L. Murchie,[2] Francois Poulet,[3] Janice L. Bishop,[4] Adrian J. Brown,[4] Wendy M. Calvin,[5] Roger N. Clark,[6] David J. Des Marais,[7] Ralph E. Milliken,[8] Leah H. Roach,[1] Ted L. Roush,[7] Gregg A. Swayze,[6] James J. Wray[9]

Geochemical models for Mars predict carbonate formation during aqueous alteration. Carbonate-bearing rocks had not previously been detected on Mars' surface, but Mars Reconnaissance Orbiter mapping reveals a regional rock layer with near-infrared spectral characteristics that are consistent with the presence of magnesium carbonate in the Nili Fossae region. The carbonate is closely associated with both phyllosilicate-bearing and olivine-rich rock units and probably formed during the Noachian or early Hesperian era from the alteration of olivine by either hydrothermal fluids or near-surface water. The presence of carbonate as well as accompanying clays suggests that waters were neutral to alkaline at the time of its formation and that acidic weathering, proposed to be characteristic of Hesperian Mars, did not destroy these carbonates and thus did not dominate all aqueous environments.

Although telescopic measurements hinted at the presence of carbonate on Mars (*1*–*3*), subsequent orbiting and landed instruments found no large-scale or massive carbonate-bearing rocks (*4*, *5*). Carbonate in veins within Martian meteorites (*6*) and possibly at <5% abundance in Mars dust (*1*, *4*) indicates that it is present as a minor phase. The lack of carbonate-bearing rock outcrops is puzzling in light of evidence for surface water and aqueous alteration, which produced sulfate and phyllosilicate minerals (*5*, *7*). Carbonate is an expected weathering product of water and basalt in an atmosphere with CO_2 (*8*, *9*), and large-scale deposits, which might serve as a reservoir for atmospheric CO_2, were predicted for Mars (*10*). Lack of carbonate among identified alteration minerals has compelled suggestions that either (i) a warmer, wetter early Mars was sustained by greenhouse gases other than CO_2 (*11*, *12*); (ii) liquid water on Mars' surface in contact with its CO_2 atmosphere was not present for long enough to form substantial carbonate (*13*) (thus implying that minerals such as phyllosilicates must have formed in the subsurface); or (iii) formation of carbonate deposits was inhibited or all such deposits were destroyed by acidic aqueous activity (*14*, *15*) or by decomposition (*16*). Here we report the detection of carbonate in a regional-scale rock unit by the Mars Reconnaissance Orbiter's (MRO's) Compact Reconnaissance Imaging Spectrometer for Mars (CRISM) and discuss the implications for the climate and habitability of early Mars.

In targeted mode, CRISM acquires hyperspectral images from 0.4 to 4.0 μm in 544 channels at a spatial resolution of 18 meters per pixel (*17*). In addition to diverse hydrated silicates (*18*), CRISM identified a distinct, mappable

[1]Department of Geological Sciences, Brown University, Providence, RI 02912, USA. [2]Johns Hopkins University/Applied Physics Laboratory, 11100 Johns Hopkins Road, Laurel, MD 20723, USA. [3]Institut d'Astrophysique Spatiale, Université Paris Sud 11, 91405 Orsay, France. [4]SETI Institute and NASA Ames Research Center, 515 North Whisman Road, Mountain View, CA 94043, USA. [5]Department of Geological Sciences and Engineering, University of Nevada, MS 172, 1664 North Virginia Street, Reno, NV 89557, USA. [6]U.S. Geological Survey, MS 964, Box 25046, Denver Federal Center, Denver, CO 80225, USA. [7]NASA Ames Research Center, Mountain View, CA 94043, USA. [8]Jet Propulsion Laboratory, California Institute of Technology, MS 183-301, 4800 Oak Grove Drive, Pasadena, CA 91109, USA. [9]Department of Astronomy, Cornell University, 610 Space Sciences Building, Ithaca, NY 14853, USA.

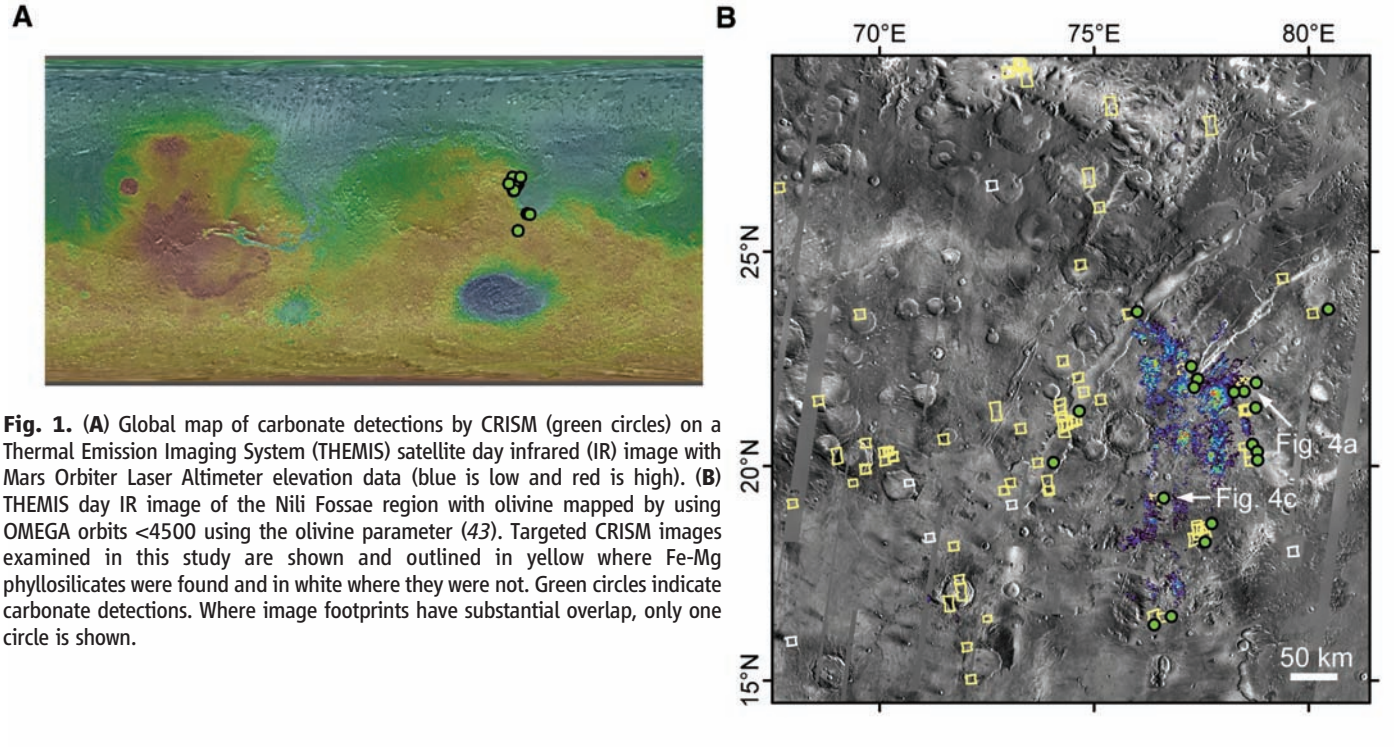

Fig. 1. (**A**) Global map of carbonate detections by CRISM (green circles) on a Thermal Emission Imaging System (THEMIS) satellite day infrared (IR) image with Mars Orbiter Laser Altimeter elevation data (blue is low and red is high). (**B**) THEMIS day IR image of the Nili Fossae region with olivine mapped by using OMEGA orbits <4500 using the olivine parameter (*43*). Targeted CRISM images examined in this study are shown and outlined in yellow where Fe-Mg phyllosilicates were found and in white where they were not. Green circles indicate carbonate detections. Where image footprints have substantial overlap, only one circle is shown.

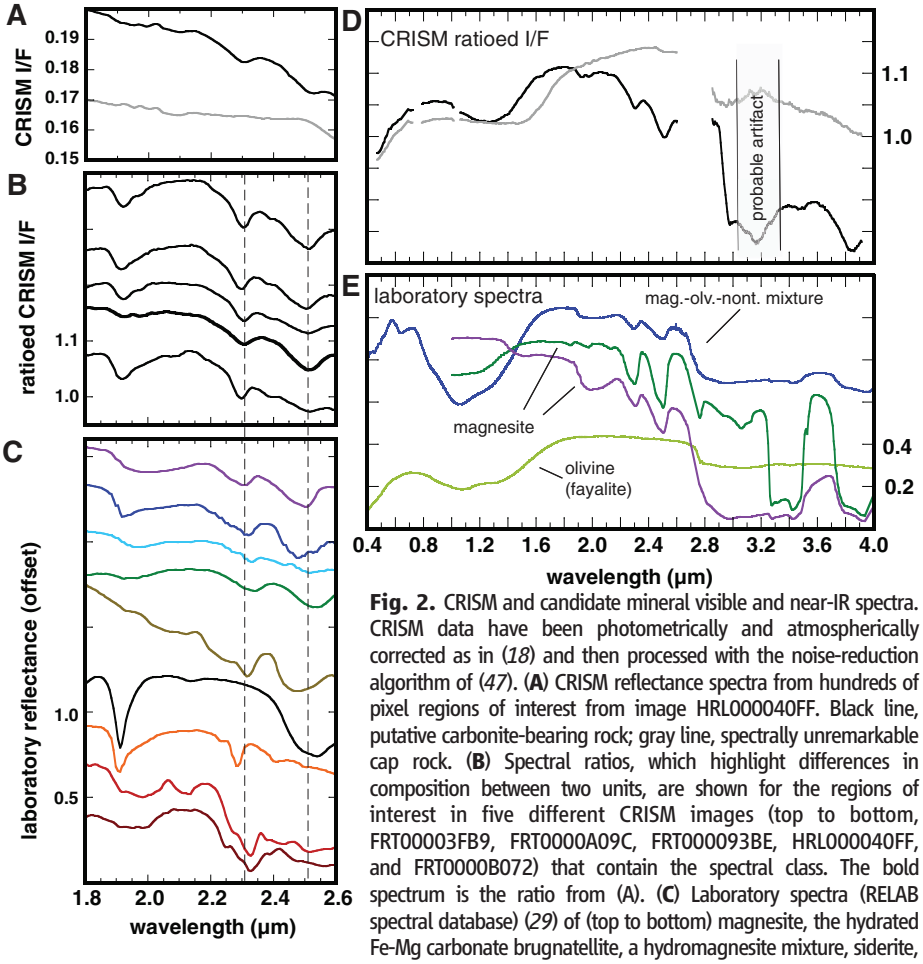

Fig. 2. CRISM and candidate mineral visible and near-IR spectra. CRISM data have been photometrically and atmospherically corrected as in (*18*) and then processed with the noise-reduction algorithm of (*47*). (**A**) CRISM reflectance spectra from hundreds of pixel regions of interest from image HRL000040FF. Black line, putative carbonite-bearing rock; gray line, spectrally unremarkable cap rock. (**B**) Spectral ratios, which highlight differences in composition between two units, are shown for the regions of interest in five different CRISM images (top to bottom, FRT00003FB9, FRT0000A09C, FRT000093BE, HRL000040FF, and FRT0000B072) that contain the spectral class. The bold spectrum is the ratio from (A). (**C**) Laboratory spectra (RELAB spectral database) (*29*) of (top to bottom) magnesite, the hydrated Fe-Mg carbonate brugnatellite, a hydromagnesite mixture, siderite, brucite, the zeolite analcime, nontronite, serpentine, and chlorite. (**D**) CRISM spectral ratios over the full wavelength range, using the same denominator, for terrains from HRL000040FF inferred to be carbonate-bearing (black) and olivine-bearing (gray). (**E**) Laboratory spectra for fayalitic olivine, magnesite, and a mixture of magnesite (80 wt %) and nontronite (5 wt %), sparsely covered with medium-grained olivine sand (15 wt %).

spectral class of hydrated material in the Nili Fossae region and two nearby areas (Fig. 1) for which a match to known mineral reflectance spectra was not initially evident (*19*). This spectral class has a 1.9-μm combination overtone from structural H_2O and also characteristic absorptions at 2.3 and 2.5 μm and a broad 1-μm absorption (Fig. 2). Similar spectra have been obtained with the Observatoire pour la Minéralogie, l'Eau, les Glaces, et l'Activité (OMEGA) imaging spectrometer on Mars Express (*20*).

Mg carbonate is the best candidate to explain the distinctive features of this spectral class. Paired absorptions at 2.3 and 2.5 μm are overtones and combination tones of C-O stretching and bending fundamental vibrations in the mid-infrared (*21*). The wavelength of their minima identifies the major metal cation in the carbonate (Fig. 3) (*21*, *22*). Anhydrous carbonates with mostly Mg exhibit minima at shorter wavelengths (2.30 and 2.50 μm) than those with mostly Ca (2.34 and 2.54 μm) and Fe (2.33 and 2.53 μm) (*22*) and match the spectral class identified by CRISM (Fig. 3). We know of no other mineral spectrum that has all of the properties of this class in terms of band position and width in the 2.0-to-2.6-μm spectral region (Fig. 2, B and C). The overall spectral shape, position, and relative strengths of the 2.3- and 2.5-μm absorption bands are consistent among CRISM spectra (Figs. 2B and 3), which suggests that the distinctive spectral class is generated by the presence of a single phase rather than a mixture of many alteration minerals (*23*). In a mixture, the relative strengths of individual bands would be expected to vary with variation in the relative abundances of the mineral

components. In some CRISM spectra of what we infer to be carbonate-bearing materials (Fig. 2B), intimate or spatial mixing is indicated by a wavelength shift and narrowing at 2.3 μm and broadening at 2.5 μm that is accompanied by the appearance of a weak band at 2.4 μm. These collectively indicate the presence also of iron-magnesium smectite [for example, nontronite (Fig. 2C, orange)], which has been previously identified in the region (*18*–*20*, *24*).

Although the distinctive CRISM spectroscopic signature was recognized in earlier OMEGA (*20*) and CRISM (*19*) observations, a carbonate mineral identification was rejected because the data lacked the strong 3.4- and 3.9-μm overtone absorptions seen in some laboratory data of calcite, other anhydrous carbonates (Fig. 2E, dark green), and their mixtures (*25*). However, we found the highly correlated 2.3- and 2.5-μm bands in many CRISM observations and thus reexamined the 3-to-4-μm region in both CRISM and laboratory data. Absorptions at 3.45 and 3.9 μm in the CRISM spectra are present in terrains with the 2.3/2.5-μm absorptions yet not in terrains lacking those absorptions [Fig. 2D and supporting online material (SOM) text] but are quite subtle and become apparent only after averaging of spectra from hundreds of pixels. Laboratory data show that absorptions from 3 to 4 μm in carbonate are not always strong (Fig. 2E, purple and blue). The presence of water, coatings, or additional minerals can reduce or eliminate these features. In the putative carbonate-bearing spectral class, the presence of a water-bearing phase (or phases) is indicated by 1.9-μm (Fig. 2B) and a deep 3.0-μm absorption (Fig. 2D). Hydrous carbonates (carbonates whose structures incorporate water) frequently have no 3.4- or 3.9-μm bands (*2*, *26*) and are a kinetically favored low-temperature alteration product from solutions with Mg and CO_3 (*9*, *27*, *28*). Strong overtones and fundamentals of water and OH near 3 μm in hydrated phases (for example, hydrous carbonates or clays) when mixed with anhydrous carbonate can subdue the 3-to-4-μm carbonate absorptions [Fig. 2E, blue; magnesite + hydromagnesite in (*21*, *29*)]. Additionally, remote detections in the 3-to-4-μm region are complicated by a thermal emission contribution that reduces band strength (*30*, *31*) and also by instrument effects. CRISM's signal-to-noise ratio is more than four times lower at wavelengths >2.7 μm, and interpretation of that region is additionally complicated by uncorrected out-of-order light (*17*) and a probable detector artifact at 3.18 μm. The combination of subtle absorption features at 3.4 and 3.9 μm and the distinctive 2.3- and 2.5-μm bands is consistent with the presence of carbonate.

The CRISM spectra also display a strong broad band near 1.1 μm, which is generated by electronic transitions of Fe^{2+} (*32*). Magnesite ($MgCO_3$) and siderite ($FeCO_3$) form a complete solid solution, and a strong broad electronic band centered near 1.1 μm is apparent with even <1 weight percent (wt %) iron without changing the position of the 2.3- and 2.5-μm bands (*21*) (Fig. 2E, dark green). Alternatively, the strong 1.1-μm band in the putative CRISM carbonate spectra might result from small amounts of olivine, which is commonly associated with the carbonate as discussed below. Indeed, a laboratory mixture of magnesite (80 wt %), olivine (15 wt %), and the Fe-rich smectite nontronite (5 wt %) produces a spectrum similar to that observed by CRISM (Fig. 2E, blue).

Thousands of CRISM-targeted images sampling Mars' surface have been examined for this phase (*33*). One image in Terra Tyrrhena and two in Libya Montes contain small exposures of carbonate-bearing rocks, but the largest and most clearly defined exposures are in the Nili Fossae region, found to date in 24 CRISM-targeted images (Fig. 1). The Mg carbonate is present in relatively bright rock units exposed over <10 km^2, which allows detection by OMEGA and CRISM but probably precludes definitive detection by the Thermal Emission Spectrometer (TES) with its larger spatial footprint. The carbonate-bearing materials are restricted to Noachian cratered terrain (*34*), and their brightness in nighttime thermal infrared images and morphology in High-Resolution Imaging Science Experiment (HiRISE) images indicates that they occur in lithified deposits. The carbonate is observed in eroded mesa topography around the fossae, rocks exposed on the sides of valleys in the Jezero crater watershed and elsewhere, and sedimentary rocks within Jezero crater (*35*).

The carbonate-bearing rocks are relatively bright-toned and are commonly fractured (Fig. 4). Like the regional smectite and olivine deposits in Nili Fossae (*18*, *36*, *37*), the carbonate-bearing rocks consistently lie stratigraphically beneath an unaltered mafic cap unit (Fig. 4). All CRISM images examined that exhibit carbonate also exhibit Fe-Mg smectite-bearing rock units. In many examples, the carbonate-bearing unit is clearly above the smectite-bearing unit (Fig. 4), although in some cases the relationship is indeterminate and lateral variations between smectite and carbonate create pixels that display mixtures of the phases. In places where both carbonates and aluminum phyllosilicates can be mapped clearly, the carbonate-bearing unit is always stratigraphically lower. The carbonate-bearing unit appears to occupy the same stratigraphic position as other nearby olivine-bearing units (*18*), namely beneath the mafic cap unit but above Fe-Mg smectite-bearing units.

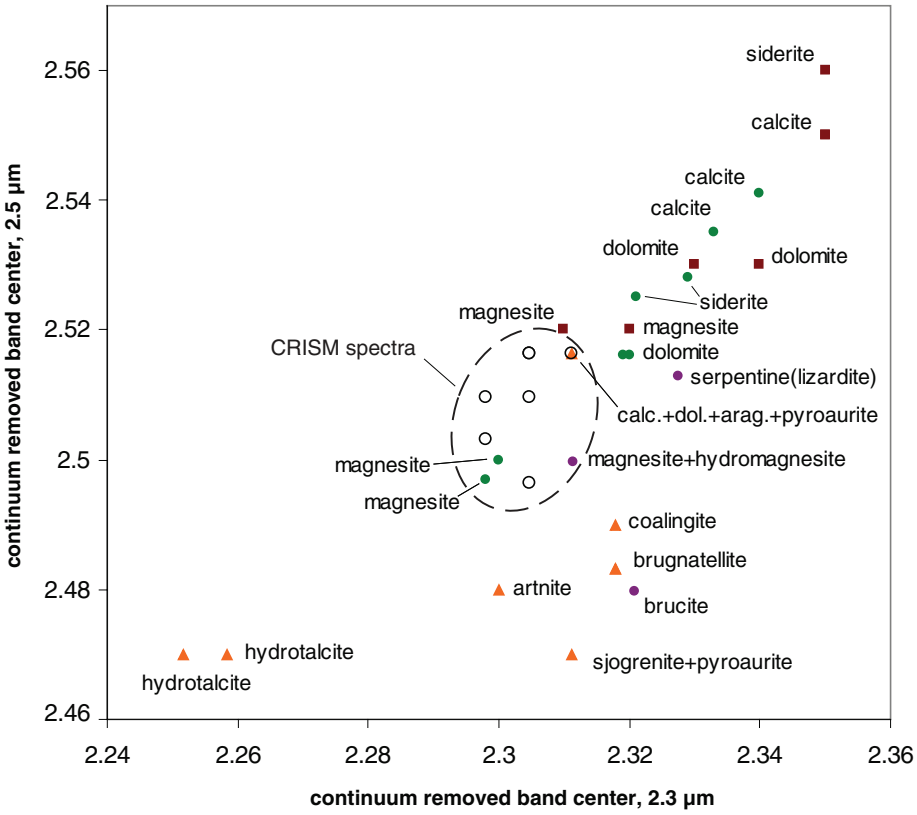

Fig. 3. Scatter plot of continuum-removed absorption band positions for anhydrous carbonates, hydrous carbonates, and other minerals with 2.3- and 2.5-μm absorptions. CRISM data that we identify as magnesite are shown as open circles within the larger dashed circle. Laboratory mineral spectra are shown from Gaffey (green circles) (*22*), Hunt and Salisbury (red squares) (*21*), RELAB spectra measured by E. Cloutis (orange triangles) (RELAB spectral database), and the USGS spectral library (purple circles) (*29*). Band centers of CRISM spectra are known to ±0.01 μm.

Whereas Fe-Mg smectites are found in a broad region extending westward to the Antoniadi basin (*19*), carbonate is restricted to the eastern portion of Nili Fossae (Fig. 1). This area is the most olivine-rich region so far observed on Mars (*38*, *39*) and has numerous valleys and sapping channels, which indicate that extensive surface fluvial activity extended into the early Hesperian (*36*).

We propose two possible formation settings to explain the origin, stratigraphy, and distribution of these carbonate-bearing rocks. First, the carbonate could have formed in the subsurface by groundwater percolating through fractures in the ultramafic rock and altering olivine. This may have occurred at only slightly elevated temperatures, as determined by the geothermal gradient. Alternatively, hot olivine-rich rocks excavated from deep in the crust by the Isidis impact (*37*) or volcanic flows (*39*, *40*) may have been deposited on top of water-bearing phyllosilicate rocks of the Noachian crust and may have initiated local hydrothermal alteration in a zone along the contact. The magnesite thus might occur in veined structures throughout olivine-rich rock, a relationship also observed in some Martian meteorites (*6*). These ultramafic rocks might have been serpentinized; however, CRISM has not yet conclusively identified serpentine.

An alternative explanation is that exposed olivine-rich rocks were weathered at surface ambient temperatures, perhaps during the surface fluvial activity in Nili Fossae that continued after the Isidis impact into the early Hesperian (*36*). The transformation of olivine-rich rocks to magnesite under cold dry conditions on Mars might resemble the weathering of olivine-rich meteorites in Antarctica (*41*), which produces magnesite and iron oxide mineral assemblages as rock rinds and/or coatings. A more water-rich surface-formation scenario would be that carbonate precipitated in shallow ephemeral lakes (*42*) from waters enriched in Mg^{2+} relative to other cations by percolation through ultramafic olivine-bearing rocks. Either scenario implies that surface conditions in the Nili Fossae region were sufficiently wet to cause chemical weathering during the late Noachian or early Hesperian eras.

The Nili Fossae carbonates do not appear to have sequestered large quantities of CO_2. With the possible exception of carbonate in transported sedimentary units within Jezero crater (*35*), we found no evidence of classic bedded sedimentary carbonate rocks resembling those on Earth. Instead, our results are consistent with carbonates having formed in response to specific local conditions. Although olivine is globally distributed on Mars (*43*, *44*), ultramafic rocks and their substantial interaction with water may have been necessary to generate carbonate in sufficient quantities to be detected from orbit at resolutions of tens of meters per pixel. Mg-carbonate–bearing rocks found at Nili Fossae, and perhaps also carbonate present at scales undetectable by CRISM, may contribute to a few percent magnesite in dust indicated by TES (*4*).

The existence of carbonate in rocks on Mars implies that neutral-to-alkaline waters existed at the time of their formation. Such conditions are consistent with those indicated by Fe-Mg smectite formation during the Noachian (*5*, *11*, *24*) but contrast with the acid, low-water-activity conditions thought to prevail over at least some of Mars during later time periods (*5*, *45*). The survival of the Nili Fossae carbonates indicates that they escaped destruction by exposure to acidic conditions, which would have dissolved the carbonate. Because aqueous activity in the Nili Fossae region extended into the Hesperian era (*36*), these carbonate-bearing rock units indicate that not all aqueous crustal environments experienced the acidic sulfate-forming conditions proposed to be characteristic of the planet during the Hesperian era, approximately 3.5 billion years ago (*5*, *46*). Ancient Mars apparently hosted aqueous environments in a variety of geologic settings in which waters ranged from the acidic to the alkaline. Such diversity bodes well for the prospect of past habitable environments on Mars.

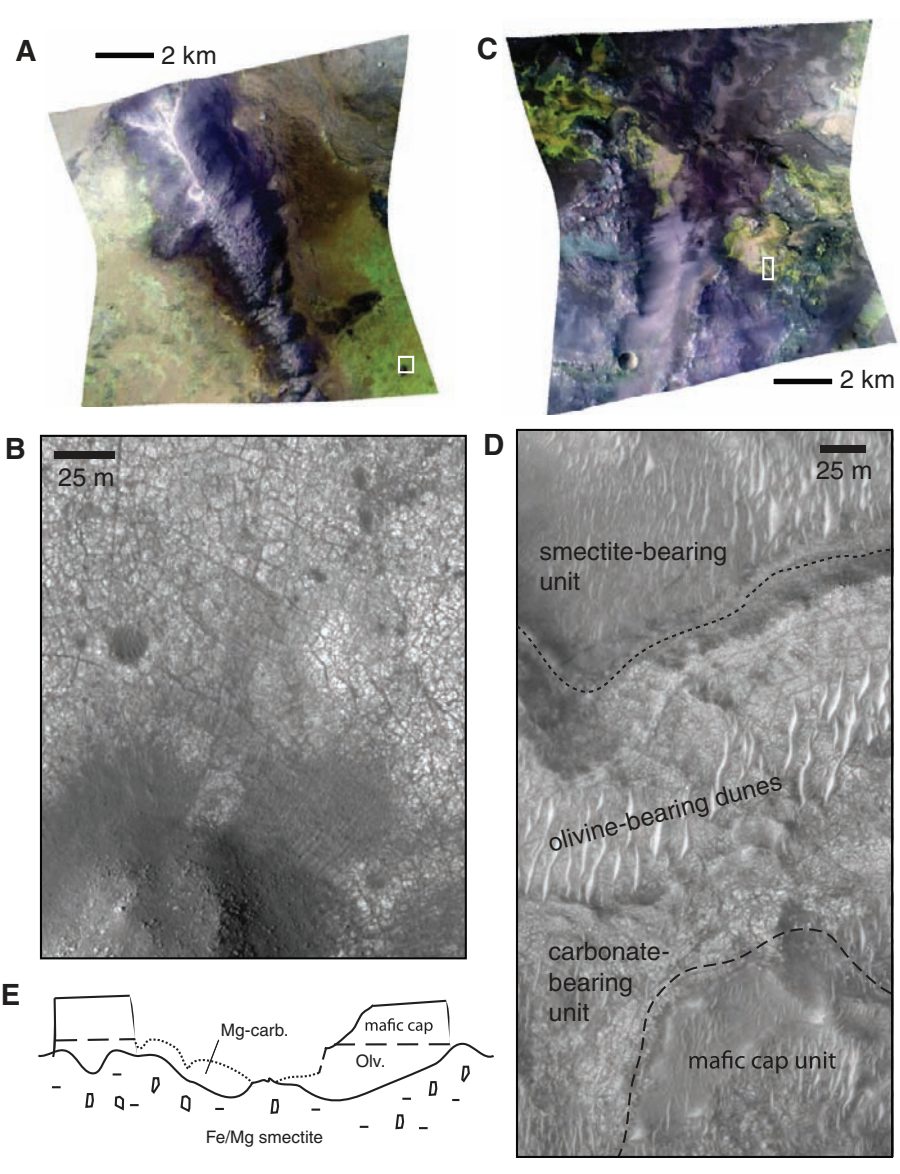

Fig. 4. Geomorphology and stratigraphy of the carbonate-bearing units. (**A**) CRISM false-color composite of FRT0000B072 (R, 2.38 μm; G, 1.80 μm; and B, 1.15 μm) where carbonate is green, olivine is yellow to brown, phyllosilicate is blue, and the mafic cap unit is purple. (**B**) subset of HiRISE PSP_002532_2020 from the white box in (A) showing a mafic knob overlying carbonate-bearing terrain. (**C**) FRT000093BE with colors as in (A). (**D**) Subset of HiRISE PSP_006778_1995 from the white box in (C), which shows the stratigraphy of carbonate-bearing units. (**E**) Schematic stratigraphy of the mineralogic units in the Nili Fossae region (not to scale).

References and Notes

1. J. B. Pollack *et al.*, *J. Geophys. Res.* **95**, 14595 (1990).
2. W. M. Calvin *et al.*, *J. Geophys. Res.* **99**, 14659 (1994).
3. E. Lellouch *et al.*, *Planet. Space Sci.* **48**, 1393 (2000).
4. J. L. Bandfield *et al.*, *Science* **301**, 1084 (2003).
5. J.-P. Bibring *et al.*, *Science* **312**, 400 (2006).
6. J. C. Bridges *et al.*, *Space Sci. Rev.* **96**, 365 (2001).

7. S. W. Squyres *et al*., *Science* **306**, 1698 (2004).
8. J. L. Gooding, *Icarus* **33**, 483 (1978).
9. D. C. Catling, *J. Geophys. Res.* **104**, 16453 (1999).
10. J. B. Pollack *et al*., *Icarus* **71**, 203 (1987).
11. V. Chevrier *et al*., *Nature* **448**, 60 (2007).
12. I. Halevy *et al*., *Science* **318**, 1903 (2007).
13. P. R. Christensen, in *Sixth International Conference on Mars* (Lunar and Planetary Institute, Houston, TX, 2003), abstract 3126.
14. A. G. Fairen *et al*., *Nature* **431**, 423 (2004).
15. M. A. Bullock, J. M. Moore, *Geophys. Res. Lett.* **34**, L19201 (2007).
16. L. M. Mukhin, *Nature* **379**, 141 (1996).
17. S. Murchie *et al*., *J. Geophys. Res.* **112**, E05S03 (2007).
18. J. F. Mustard *et al*., *Nature* **454**, 305 (2008).
19. B. L. Ehlmann *et al*., in *Seventh International Conference on Mars* (Lunar and Planetary Institute, Houston, TX, 2007), abstract 3270.
20. F. Poulet *et al*., in *Seventh International Conference on Mars* (Lunar and Planetary Institute, Houston, TX, 2007), abstract 3170.
21. G. R. Hunt, J. W. Salisbury, *Mod. Geol.* **2**, 23 (1971).
22. S. J. Gaffey, *J. Geophys. Res.* **92**, 1429 (1987).
23. A multicomponent mineral assemblage of approximately constant proportions (for example, brucite + analcime + Fe-Mg smectite + olivine) is a possible alternative explanation for the observed position of the 2.3- and 2.5-μm features and their relative strengths. However, alteration assemblages are typically compositionally variable. Especially over the 10^5 km^2 considered here and in light of the 3.4- and 3.9-μm bands, a fixed-proportion multicomponent mixture is less plausible geologically than a contribution from a single component, namely Mg carbonate.
24. F. Poulet *et al*., *Nature* **438**, 623 (2005).
25. D. Jouglet *et al*., in *Seventh International Conference on Mars*, (Lunar and Planetary Institute, Houston, TX, 2007), abstract 3153.
26. E. A. Cloutis *et al., Lunar Planet Sci. Conf.* **31**, abstract 1152 (2000).
27. M. Hanchen *et al*., *Chem. Eng. Sci.* **63**, 1012 (2008).
28. E. Konigsberger *et al*., *Geochim. Cosmochim. Acta* **63**, 3105 (1999).
29. R. N. Clark *et al*., U.S. Geological Survey (USGS) Digital Spectral Library splib06a, USGS Digital Data Series 231 (USGS, Denver, CO, 2007).
30. C. Wagner, U. Schade, *Icarus* **123**, 256 (1996).
31. D. Blaney, T. McCord, *J. Geophys. Res.* **94**, 10,159 (1989).
32. R. G. Burns, *Mineralogical Applications of Crystal Field Theory* (Cambridge Univ. Press, ed. 2, Cambridge, 1993).
33. Thousands of targeted CRISM images acquired through January 2008 in dust-free terrains were searched by coauthors and team members for this spectral class in the course of ongoing investigations. Additionally, all regions with OMEGA codetections of both olivine and hydration or phyllosilicate were investigated by the coauthors where CRISM images were available. Large Nili Fossae–scale regional carbonate units are unlikely to have been missed. Small outcrops of carbonate-bearing rock may yet be found elsewhere as more high-resolution CRISM data are acquired.
34. R. Greeley, J. E. Guest, "Geological Map of the Eastern Equatorial Region of Mars," *U.S. Geol. Surv. Misc. Inv. Series Map I-1802-B* (1987).
35. B. L. Ehlmann *et al*., *Nat. Geosci.* **1**, 355 (2008).
36. N. Mangold *et al*., *J. Geophys. Res.* **112**, E08S04 (2007).
37. J. F. Mustard *et al*., *J. Geophys. Res.* **112**, E08S03 (2007).
38. T. M. Hoefen *et al*., *Science* **302**, 627 (2003).
39. V. E. Hamilton, P. R. Christensen, *Geology* **33**, 433 (2005).
40. L. Tornabene *et al*., *J. Geophys. Res.*, 10.1029/2007JE002988 (2008).
41. A. J. T. Jull *et al*., *Science* **242**, 417 (1988).
42. V. A. Melezhik *et al*., *Sedimentology* **48**, 379 (2001).
43. F. Poulet *et al*., *J. Geophys. Res.* **112**, E08S02 (2007).
44. W. C. Koeppen, V. E. Hamilton, *J. Geophys. Res.* **113**, E05001 (2008).
45. N. J. Tosca *et al*., *Science* **320**, 1204 (2008).
46. J. A. Hurowitz, S. M. McLennan, *Earth Planet. Sci. Lett.* **260**, 432 (2007).
47. M. Parente, *Lunar and Planet Sci. Conf*. **39**, abstract 2528 (2008).

48. We thank R. Arvidson, R. Morris, N. Mangold, A. Baldridge, J.-P. Bibring, D. Jouglet, A. Fraeman, S. Wiseman, A. McEwen, G. Marzo, P. McGuire, and M. Wyatt for thoughtful discussions during manuscript preparation and E. Cloutis and others who have made quality spectral libraries available and contributed to the building of the NASA/Keck Reflectance Experiment Laboratory (RELAB) spectral database. We are grateful for the ongoing efforts of the MRO science and engineering teams, in particular the CRISM team, which enable these discoveries.

Supporting Online Material

www.sciencemag.org/cgi/content/full/322/5909/1828/DC1
SOM Text
Figs. S1 and S2
Table S1
References

18 August 2008; accepted 3 November 2008
10.1126/science.1164759

The Circadian Clock in *Arabidopsis* Roots Is a Simplified Slave Version of the Clock in Shoots

Allan B. James,[1] José A. Monreal,[1] Gillian A. Nimmo,[1] Ciarán L. Kelly,[1] Pawel Herzyk,[2,3] Gareth I. Jenkins,[1] Hugh G. Nimmo[1]*

The circadian oscillator in eukaryotes consists of several interlocking feedback loops through which the expression of clock genes is controlled. It is generally assumed that all plant cells contain essentially identical and cell-autonomous multiloop clocks. Here, we show that the circadian clock in the roots of mature *Arabidopsis* plants differs markedly from that in the shoots and that the root clock is synchronized by a photosynthesis-related signal from the shoot. Two of the feedback loops of the plant circadian clock are disengaged in roots, because two key clock components, the transcription factors CCA1 and LHY, are able to inhibit gene expression in shoots but not in roots. Thus, the plant clock is organ-specific but not organ-autonomous.

Many organisms have circadian clocks that temporally regulate their physiology and behavior and contribute to fitness (*1*–*3*). The eukaryotic clock involves gene expression feedback loops, with both negative and positive elements, and cytosolic signaling molecules (*4*–*7*). In the model plant *Arabidopsis*, the clock mechanism is thought to include at least three interlocking feedback loops (*5*, *8*, *9*). The central loop comprises two partially redundant MYB domain transcription factors, CIRCADIAN CLOCK ASSOCIATED1 (CCA1) and LATE ELONGATED HYPOCOTYL (LHY), which inhibit expression of a pseudo-response regulator TIMING OF CAB EXPRESSION1 (TOC1) (also known as PSEUDO-RESPONSE REGULATOR1, PRR1), whereas TOC1 activates expression of *CCA1* and *LHY* by an unknown mechanism (*5*, *10*–*12*). In the morning-phased loop, CCA1 and LHY activate the expression of *PSEUDO-RESPONSE REGULATOR7* (*PRR7*) and *PSEUDO-RESPONSE REGULATOR9* (*PRR9*) (*13*, *14*); the evening-phased loop involves TOC1 and GIGANTEA (GI) (see legend to fig. S12 for further information). These conclusions are based on experiments using whole seedlings grown in the presence of sucrose, without consideration of organ specificity. Yet, one major function of the plant clock involves the temporal partitioning of metabolic pathways via the control of output gene expression (*15*), and metabolism is inherently organ-specific. We therefore analyzed the circadian clock separately in shoots and roots of mature, hydroponically grown *Arabidopsis* plants (*16*).

Following transfer of plants from 12 hours light/12 hours dark (LD) to constant light (LL), *LHY* and *CCA1* transcripts continued to oscillate in both shoots and roots for three full cycles, with some damping (Fig. 1A and fig. S1), as determined by quantitative real-time reverse transcription polymerase chain reaction (qPCR). Notably, the period was some 2 hours longer in roots than in shoots; analysis of LHY protein (fig. S2) gave a similar result. *PRR9* and *PRR7* transcripts oscillated in both organs, with the time of peak expression later in roots than in shoots (fig. S3). *TOC1* transcripts in shoots oscillated in LL, in antiphase to those of *CCA1* and *LHY*, as expected. In marked contrast, *TOC1* transcripts in roots dipped slightly during the first subjective day in LL, then remained at a high level without oscillations (Fig. 1B and table S1). In shoots, oscillations in TOC1 protein were detectable for at least two cycles, whereas in roots TOC1 was present, with little variation, for 72

[1]Division of Molecular and Cellular Biology, Faculty of Biomedical and Life Sciences, University of Glasgow, Glasgow G12 8QQ, UK. [2]Division of Integrated Biology, Faculty of Biomedical and Life Sciences, University of Glasgow, Glasgow G12 8QQ, UK. [3]The Sir Henry Wellcome Functional Genomics Facility, Faculty of Biomedical and Life Sciences, University of Glasgow, Glasgow G12 8QQ, UK.

*To whom correspondence should be addressed. E-mail: h.g.nimmo@bio.gla.ac.uk

hours in LL (fig. S2). The differences in *LHY*, *CCA1*, and *TOC1* expression between shoots and roots were also observed with microarray analysis (fig. S4). Furthermore, the other genes implicated in the central oscillator, namely *GI*, *LUX ARRHYTHMO* (*LUX*), *EARLY FLOWERING 3* and *4* (*ELF3* and *ELF4*), and *PSEUDO-RESPONSE REGULATOR 3* and *5* (*PRR3* and *PRR5*), all behaved similarly to *TOC1*; their transcripts oscillated in shoots but not in roots (fig. S5). Analysis of qPCR data for genes in the central clock with the modified cosinor analysis program COSOPT (*17*) confirmed that only *CCA1*, *LHY*, *PRR7*, and *PRR9* behaved rhythmically in roots and that the period in roots was longer than that in shoots (table S1). We also studied expression patterns in constant darkness (DD) (fig. S6). Oscillations in *CCA1* and *LHY* transcripts were detectable in both shoots and roots for three cycles. In shoots, the period was appreciably longer in DD than LL, in accord with Aschoff's rule (*18*), but in roots the periods in LL and DD were similar (tables S1 and S2). In DD, *TOC1* transcripts showed a low amplitude rhythm in shoots, but no clear rhythmic behavior in roots.

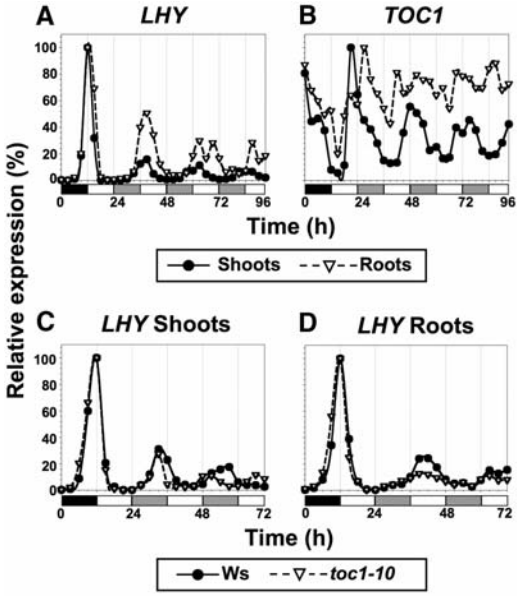

Fig. 1. TOC1 does not contribute to the root clock in constant light. (**A** and **B**) Gene expression in (A) *LHY* and (B) *TOC1* was monitored over 24 hours in LD and then 72 hours in LL in *Arabidopsis* Col-0 by qPCR in shoots and roots. Estimates of period and the probability that the best-fit rhythm has a significant amplitude were made with COSOPT and are given in table S1. (**C** and **D**) *LHY* expression was monitored in (C) shoots and (D) roots in *Arabidopsis* Ws-0 and *Arabidopsis toc1-10* by qPCR over 24 hours in LD and then 48 hours in LL. The levels of *LHY* transcripts in Ws-0 and *toc1-10* were similar. Black bar, dark; white bars, light, day or subjective day; hatched bars, light, subjective night.

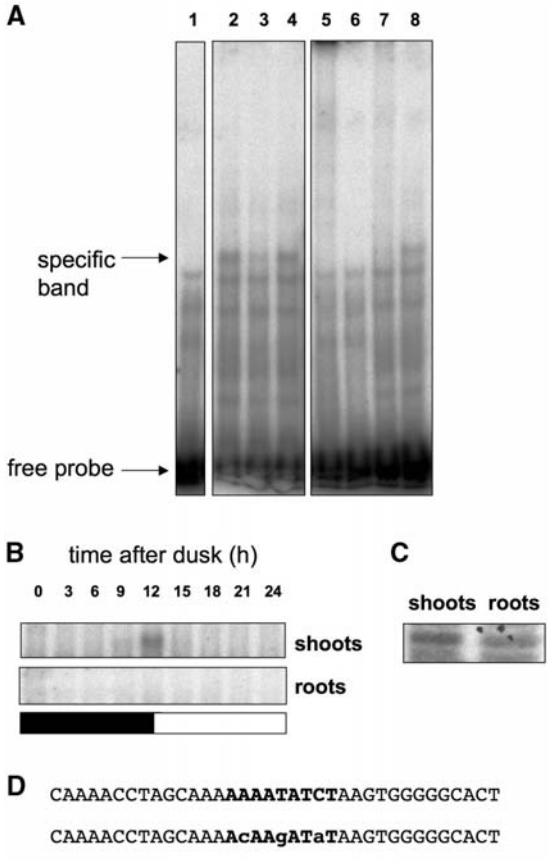

Fig. 2. Shoots, but not roots, contain an EE-binding protein expressed around dawn. (**A**) Specificity of the probe. Lane 1, labeled probe alone; lane 2, labeled probe plus shoot extract prepared at dawn; lane 3, as lane 2 plus unlabeled competitor probe; lane 4, as lane 2 plus unlabeled mutant competitor; lane 5, as lane 1 plus antiserum to LHY diluted 1:100; lane 6, as lane 1 plus antiserum to LHY diluted 1:1000; lane 7, as lane 2 plus antiserum to LHY diluted 1:100; lane 8, as lane 2 plus antiserum to LHY diluted 1:1000. (**B**) EE binding across a diurnal cycle. Shoot and root samples harvested at 3-hour intervals in an LD cycle were incubated with labeled probe. White bar, day; black bar, night. (**C**) LHY doublet bands (see also fig. S10) from shoot and root samples harvested at dawn and prepared for mobility shift analysis are shown by Western blotting. (**D**) Sequences of the probes: top, wild-type *CAT3* EE probe, EE in bold; bottom, mutated probe, the altered bases are in lower case.

These data show that, in roots, the morning-phased loop of the clock operates, but the genes of the central and evening-phased loops are decoupled from oscillations in *CCA1* and *LHY* expression. To determine whether *TOC1* is necessary for the clock in roots, we examined the *toc1-10* null mutant, which has a short-period phenotype in seedlings (*8*). Compared with the wild-type (Ws-0), the *toc1-10* mutation shortens the period of transcript oscillations for both *LHY* (Fig. 1, C and D) and *CCA1* (fig. S1) in shoots, but not in roots. Thus TOC1 does not contribute to the period of the root clock in mature plants. Consistent with previous work on seedlings (*19*), the phase of the circadian rhythm in Ws-0 shoots, as judged by the timing of maximum expression of *LHY*, is earlier than that in Col-0. However, this is not observed in roots, again pointing to a fundamental difference in clock mechanism between the organs. It is surprising that the decoupling of the central and evening-phased loops from the morning-phased loop in roots requires PRR7 and/or PRR9, as both *TOC1* and *GI* transcripts regain rhythmicity in roots of the *prr7, prr9* double mutant (fig. S7).

The evening-phased expression of many *Arabidopsis* genes, including *TOC1*, *GI*, other central clock genes, and many output genes such as *CHALCONE SYNTHASE* (*CHS*), is thought to be caused at least partly by the binding of the morning-expressed proteins CCA1 and/or LHY to evening elements (EEs) (the sequence AAAATATCT) in the promoters of these genes, resulting in inhibition of expression (*15*). We therefore analyzed the expression of output genes regulated by EEs. For those genes expressed in both shoots and roots, transcript abundance in LL was rhythmic in shoots but not in roots (fig. S5), and root transcript levels were much closer to the corresponding peak values in shoots than to the trough values. A previous study using seedlings grown in the light on sucrose (*20*) reported that the *toc1-1* mutation altered the period of *CHS* expression in roots. However, *CHS* is not expressed in mature roots grown hydroponically (fig. S5), and the roots of plants grown in this way evidently differ physiologically from those of light-grown seedlings. For *TOC1* (Fig. 1) and *GI* (not shown), root transcript levels in LL defaulted to the highest level seen in LD cycles. Thus, our data suggest that CCA1 and LHY do not cause EE-mediated inhibition of gene expression in mature roots. This behavior is not confined to *Arabidopsis*, because circadian expression of the soybean protein kinase gene *GmPPCK4* was observed in shoots but not in roots (*21*).

To test the hypothesis that CCA1 and LHY do not cause EE-mediated inhibition of gene

expression in roots, we sought to detect EE-binding proteins using mobility shift assays. We used a 36-bp sequence from the promoter of the *CATALASE3* (*CAT3*) gene in a region that confers evening-phased expression (*22*) (Fig. 2D). Shoot extracts prepared at dawn contained a component able to bind this sequence. Binding was substantially reduced by addition of unlabeled competitor oligonucleotide but not by a mutated competitor (Fig. 2A). No binding was detected with mutated radiolabeled probe. Preincubation of extracts with LHY-specific antiserum prevented binding of the probe (Fig. 2A), but two control antisera had no effect. Antiserum to CCA1 had no effect (not shown), but this does not rule out the involvement of CCA1 in the EE-binding complex; for example, the epitopes recognized by CCA1-specific antiserum might be hidden in a putative CCA1/LHY/DNA complex. Extracts were prepared from shoot and root samples at 3-hour intervals across a normal diurnal cycle. Binding was detected in the shoot samples only around dawn, which matched the expression profile of *CCA1* and *LHY*, but no binding was detected in the root samples (Fig. 2B). The shoot and root samples prepared at dawn contained comparable amounts of LHY protein (Fig. 2C). Thus LHY, alone or in combination with other components, can specifically bind the EE in shoots but not in roots.

We, therefore, predicted that fewer genes would display rhythmicity in roots than in shoots. Indeed, applying COSOPT with the criterion for significant rhythmicity of pMMC-β < 0.05 to microarray data, 13.7% of shoot genes were scored rhythmic, but only 3.2% of root genes. Examples of rhythmic root genes are shown in fig. S8, including the MYB genes *RVE1* and *RVE8* (At5g17300 and At3g09600, respectively). The time of peak expression of these genes, like that of *CCA1* and *LHY*, is delayed in roots relative to shoots, consistent with control by the root-specific clock.

In contrast to LL, the expression profiles of *LHY* and *CCA1* in shoots and roots in LD were exactly in phase (Fig. 3A and fig. S9). *TOC1* transcripts in shoots showed a marked peak around dusk with a later shoulder and a trough during the first half of the day. However, *TOC1* transcripts in roots were relatively steady across most of the diurnal cycle, with a modest 3-fold decline 3 hours into the day, compared with the 20-fold change seen in shoots (Fig. 3B). The abundance of LHY, CCA1 and TOC1 proteins closely followed the transcript abundances (fig. S10). Transcript profiles for *PRR9, PRR7, GI*, and *ELF4* in shoots and roots in LD were also exactly in phase, though *ELF3* transcripts oscillated only in shoots (fig. S9). Thus, the expression of several clock genes is synchronous in shoots and roots in LD but not in LL.

This finding demonstrates that a signal is transmitted between the organs in LD conditions, probably from shoots to roots. It seems unlikely that the signal is direct perception of light by the roots because the expression of *CCA1* and *LHY* commences before dawn in LD cycles. We reasoned that the signal might be related to shoot metabolism. We first tested whether the addition of sucrose to the hydroponic medium could selectively affect the root clock (Fig. 4). Provision of 2.5 mM sucrose at dusk in LD delayed and extended the next expression of *CCA1* and *PRR9* in roots, but not in shoots, and resulted in an expression pattern like that observed in LL (Fig. 4, B and C). A similar effect was observed with *LHY* and with the output gene At1g78600, which encodes a zinc finger protein (Fig. 4D). In contrast, this treatment did not affect the expression of *TOC1* (Fig. 4A) in roots; nor did it have a significant effect on the expression of these genes in shoots (Fig. 4). Provision of palatinose, a nonmetabolizable sucrose analog, had no effect. Thus, exogenous sucrose can prevent the entrainment of the root clock by LD cycles, acting as an anti-zeitgeber for roots. We then showed that 3-(3,4-dichlorophenyl)-1,1-dimethylurea (DCMU), a specific inhibitor of photosynthetic electron transport, progressively disrupts operation of the root clock. It curtails rhythmic expression of *CCA1*, *LHY*, and *PRR9* in roots but does not affect their expression in shoots (fig. S11). Thus, a synchronizing signal between shoots and roots depends on photosynthesis and can be antagonized by sucrose. This signal may result from diurnal fluctuations in the supply of carbohydrate to the roots, although the precise mechanism remains unclear, and the existence of additional signals cannot yet be ruled out.

We draw two main conclusions from this work and propose the scheme shown in fig. S12. First, rhythmic expression of many of the genes associated with the plant circadian clock is not required for circadian rhythmicity in roots. Indeed, in roots, the circadian clock appears to run on only one of the loops in the current model and drives rhythmic expression of only a restricted set of genes. This organ specificity of the clock machinery is achieved through the failure of the MYB protein LHY to complex with DNA and cause EE-mediated inhibition of gene expression in roots. Whether CCA1 is involved in this protein: DNA complex remains to be determined. In mammalian systems, some clock components are dispensable in particular cell types (*23*, *24*), but the plant root clock exhibits an extreme version of organ specificity. Second, the circadian clock is synchronized between shoots and roots only in LD cycles. Contrary to previous thinking (*25*), there must be communication between the clocks of different plant organs. In mammals, restricted food availability can reset the circadian

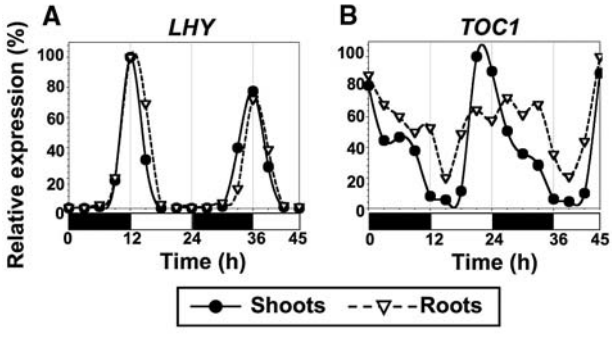

Fig. 3. The shoot and root clocks are synchronized in diurnal cycles. Gene expression in (**A**) *LHY* and (**B**) *TOC1* was monitored over 45 hours in LD in *Arabidopsis* Col-0 by qPCR in shoots and roots. Black bars, dark; white bars, light. The data shown are from one representative experiment. Means and SEM from three replicate experiments are shown in fig. S13.

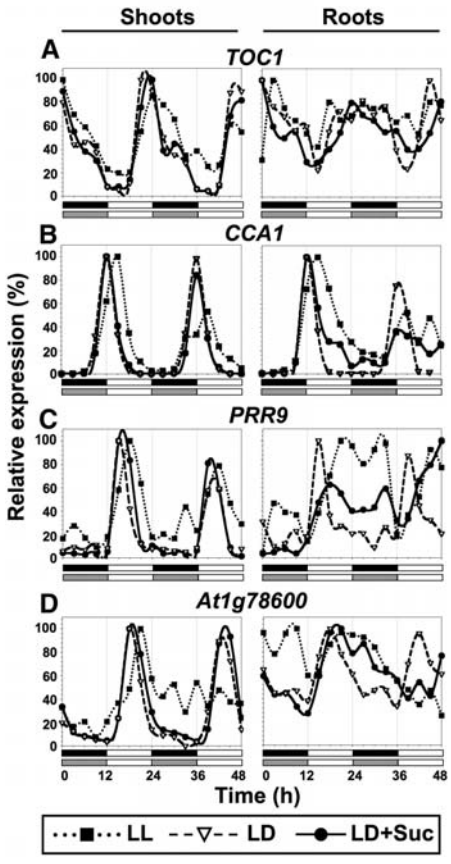

Fig. 4. Sucrose perturbs expression of clock genes in roots but not shoots. Gene expression in (**A**) *TOC1*, (**B**) *CCA1*, (**C**) *PRR9*, and (**D**) At1g78600 was monitored in *Arabidopsis* Col-0 by qPCR over 48 hours in LD, in LL, and in LD after addition of 2.5 mM sucrose to the hydroponic medium at dusk. Black bars, dark; white bars, light, day or subjective day; hatched bars, light, subjective night. The data shown are from one representative experiment. Means and SEM from three replicate experiments are shown in fig. S14.

clock in peripheral tissues, but not the master clock in the suprachiasmatic nucleus (*26*, *27*), and there is increasing evidence of links between diet, metabolism, and the clock (*28*, *29*). Similarly, our data show that in plants a photosynthesis-related signal, possibly sucrose or a derivative, can affect setting of the clock in roots but not in shoots. In summary, the plant clock is organ-specific but not organ-autonomous.

References and Notes

1. J. C. Dunlap, *Cell* **96**, 271 (1999).
2. Y. Ouyang, C. R. Andersson, T. Kondo, S. S. Golden, C. H. Johnson, *Proc. Natl. Acad. Sci. U.S.A.* **95**, 8660 (1998).
3. A. N. Dodd *et al*., *Science* **309**, 630 (2005).
4. S. L. Harmer, S. Panda, S. A. Kay, *Annu. Rev. Cell Dev. Biol.* **17**, 215 (2001).
5. C. R. McClung, *Plant Cell* **18**, 792 (2006).
6. A. N. Dodd *et al*., *Science* **318**, 1789 (2007).
7. J. S. O'Neill, E. S. Maywood, J. E. Chesham, J. S. Takahashi, M. H. Hastings, *Science* **320**, 949 (2008).
8. J. C. W. Locke *et al*., *Mol. Syst. Biol.* **2**, 59 (2006).
9. M. N. Zeilinger, E. M. Farré, S. R. Taylor, S. A. Kay, F. J. Doyle, *Mol. Syst. Biol.* **2**, 58 (2006).
10. D. Alabadi, M. J. Yanovsky, P. Más, S. L. Harmer, S. A. Kay, *Curr. Biol.* **12**, 757 (2002).
11. T. Mizoguchi *et al*., *Dev. Cell* **2**, 629 (2002).
12. D. Alabadi *et al*., *Science* **293**, 880 (2001).
13. E. M. Farré, S. L. Harmer, F. G. Harmon, M. J. Yanovsky, S. A. Kay, *Curr. Biol.* **15**, 47 (2005).
14. P. A. Salome, C. R. McClung, *Plant Cell* **17**, 791 (2005).
15. S. L. Harmer *et al*., *Science* **290**, 2110 (2000).
16. Materials and methods are available in supporting material on *Science* Online.
17. M. Straume, *Methods Enzymol.* **383**, 149 (2004).
18. J. Aschoff, in *Handbook of Behavioural Neurobiology: Biological Rhythms*, J. Aschoff, Ed. (Plenum Press, New York, 1981), pp. 81–94.
19. T. P. Michael *et al*., *Science* **302**, 1049 (2003).
20. S. C. Thain, G. Murtas, J. R. Lynn, R. B. McGrath, A. J. Millar, *Plant Physiol.* **130**, 102 (2002).
21. S. Sullivan, G. I. Jenkins, H. G. Nimmo, *Plant Physiol.* **135**, 2078 (2004).
22. T. P. Michael, C. R. McClung, *Plant Physiol.* **130**, 627 (2002).
23. J. P. DeBruyne *et al*., *Neuron* **50**, 465 (2006).
24. Y. Fan, A. Hida, D. A. Anderson, M. Izumo, C. H. Johnson, *Curr. Biol.* **17**, 1091 (2007).
25. S. C. Thain, A. Hall, A. J. Millar, *Curr. Biol.* **10**, 951 (2000).
26. R. Hara *et al*., *Genes Cells* **6**, 269 (2001).
27. K. A. Stokkan, S. Yamazaki, H. Tei, Y. Sakaki, M. Menaker, *Science* **291**, 490 (2001).
28. L. Yin *et al*., *Science* **318**, 1786 (2007).
29. A. Kohsaka *et al*., *Cell Metab.* **6**, 414 (2007).

30. We thank A. Millar (Edinburgh), S. A. Kay (San Diego), and C. R. McClung (Dartmouth) for *Arabidopsis* lines; I. Carré (Warwick) and E. M. Tobin (Los Angeles) for the LHY- and CCA1-specific antisera, respectively; K. Edwards (Advanced Technologies, Cambridge) for advice on COSOPT; and J. Galbraith (Faculty of Biomedical and Life Sciences, University of Glasgow) for microarray experiments. The work was supported by the Leverhulme Trust. J.A.M. holds a fellowship from the Spanish Ministry of Education and Science.

Supporting Online Material

www.sciencemag.org/cgi/content/full/322/5909/1832/DC1
Materials and Methods
Figs. S1 to S14
Tables S1 to S4
References

5 June 2008; accepted 29 September 2008
10.1126/science.1161403

A Conserved Molecular Framework for Compound Leaf Development

Thomas Blein,[1] Amada Pulido,[1] Aurélie Vialette-Guiraud,[1]* Krisztina Nikovics,[1]† Halima Morin,[1,2] Angela Hay,[3] Ida Elisabeth Johansen,[4] Miltos Tsiantis,[3] Patrick Laufs[1]‡

Diversity in leaf shape is produced by alterations of the margin: for example, deep dissection leads to leaflet formation and less-pronounced incision results in serrations or lobes. By combining gene silencing and mutant analyses in four distantly related eudicot species, we show that reducing the function of *NAM*/*CUC* boundary genes (*NO APICAL MERISTEM* and *CUP-SHAPED COTYLEDON*) leads to a suppression of all marginal outgrowths and to fewer and fused leaflets. We propose that *NAM/CUC* genes promote formation of a boundary domain that delimits leaflets. This domain has a dual role promoting leaflet separation locally and leaflet formation at distance. In this manner, boundaries of compound leaves resemble boundaries functioning during animal development.

Leaves of seed plants can be simple, with a single leaf blade, or compound when divided into distinct leaflets (*1*, *2*). Additionally, margins of both simple and compound leaves can elaborate less-pronounced incisions such as serrations or lobes. Regardless of the final shape, leaves are initiated as simple primordia from the shoot apical meristem. Primordia of compound leaves maintain an organogenic region at their margin from which leaflet primordia emerge (*1*, *2*). Two different pathways have been recruited to promote this organogenic activity during the multiple independent origins of compound leaves in seed plants. One pathway involves expression in the primordia of compound leaves of class 1 homeodomain KNOTTED1–like (KNOXI) transcription factors that were initially identified for their role in maintenance of meristem identity (*3*–*5*). This pathway is active in a wide range of flowering seed plants, including *Solanum lycopersicum* and *Cardamine hirsuta*. A second pathway involving the *UNIFOLIATA* (*UNI*) gene is found in *Pisum sativum*, which does not express *KNOXI* genes in the leaf primordium. *UNI* encodes a member of the LEAFY (LFY) family of transcription factors, initially identified for its role in floral meristem identity (*6*, *7*). Despite progress in understanding what promotes the organogenic potential of compound leaves, the mechanistic basis of leaflet formation and delimitation is less clear. The generation of activity maxima of auxin, a small indolic hormone, is one such mechanism that facilitates initiation and separation of both leaves at the shoot apical meristem and leaflets from the rachis (*8*–*10*). Other key regulators of organ initiation and delimitation are the *NAM*/*CUC3* genes, which are members of a large evolutionarily conserved family of plant transcription factors that are subdivided into *NAM* (*NO APICAL MERISTEM*) and *CUC3* (*CUP-SHAPED COTYLEDON3*) clades (*11*–*14*). They are expressed in the boundary of organ primordia, where they repress growth to allow organ separation (*15*). In addition, they are involved in meristem establishment via their activation of KNOXI expression (*16*).

Because previous work showed that *AtCUC2* is required for *Arabidopsis* leaf serration (*17*), we hypothesized that *NAM*/*CUC3* genes could have a broader role in leaf dissection. To test this hypothesis, we analyzed the function of *NAM*/*CUC3* genes in a selection of five eudicots with compound leaves (*Aquilegia caerulea*, *S. lycopersicum*, *S. tuberosum*, *C. hirsuta*, and *P. sativum*) that show contrasting phylogenetic positions, genetic controls and patterning of leaflet development, dissection of leaflet margins, and leaflet specialization (Fig. 1, A, E, I, M, and R, and fig. S1) (*18*). We cloned 11 *NAM/CUC3* genes from these species, and phylogenetic analysis showed that they group either into *NAM* (*AcNAM*, *SlNAM*, *StNAM*, *PsNAM1*, *PsNAM2*, *ChCUC1*, and *ChCUC2*) or *CUC3* (*AcCUC3*, *StCUC3*, *PsCUC3*, and *ChCUC3*) clades (fig. S2). The *NAM*/*CUC3* genes had a typical expression pattern in the boundary domain at the base of organ primordia, a pattern that is complementary to the cell proliferation marker *HISTONE H4* (fig. S3). This suggested conserved roles in defining boundary and organ separation by local repression of cell proliferation.

To determine whether the *NAM/CUC3* genes have a role in defining compound leaf morphology, we examined their expression during leaf development. A similar expression pattern was

[1]Laboratoire de Biologie Cellulaire, Institut Jean Pierre Bourgin, Institut National de la Recherche Agronomique (INRA), 78026 Versailles Cedex, France. [2]Plateforme de Cytologie et d'Imagerie Végétale, Institut Jean Pierre Bourgin, INRA, 78026 Versailles Cedex, France. [3]Department of Plant Sciences, University of Oxford, South Parks Road, Oxford OX1 3RB, UK. [4]Department of Genetics and Biotechnology, University of Aarhus, Thorvaldsensvej 40, DK-1871 Frederiksberg C, Denmark.

*Present address: Laboratoire de Reproduction et Développement des Plantes, UMR INRA-CNRS-Ecole Normale Supérieure de Lyon, Université de Lyon I, 46 allée d'Italie, 69364 Lyon Cedex 07, France.

†Present address: Unité INSERM U552, Institut Universitaire d'Hématologie, Batiment HAYEM, Hôpital Saint Louis, 1, avenue Claude Vellefaux, 75475 Paris Cedex 10, France.

‡To whom correspondence should be addressed. E-mail: laufs@versailles.inra.fr

observed in all species examined (Fig. 1 and fig. S4). *NAM*/*CUC3* genes were expressed in a narrow strip of cells at the distal boundary of leaflet primordia, whereas no expression was observed in the proximal region (e.g., Fig. 1, B, G, K, N, and U, and fig. S3). *NAM*/*CUC3* expression preceded the actual outgrowth of leaflet primordia (e.g., Fig. 1, F and J, and fig. S3). Given the diversity of the species analyzed here, this conserved *NAM*/*CUC3* gene expression pattern is likely to reflect a fundamental mechanism of leaflet formation. *NAM* genes were also expressed later in association with *A. caerulea* and *S. lycopersicum* leaflet margin dissection (Fig. 1, D and H), as shown for the simple *Arabidopsis thaliana* leaf (*17*).

Next, we undertook a series of functional analyses in *A. caerulea*, *S. lycopersicum*, *P.*

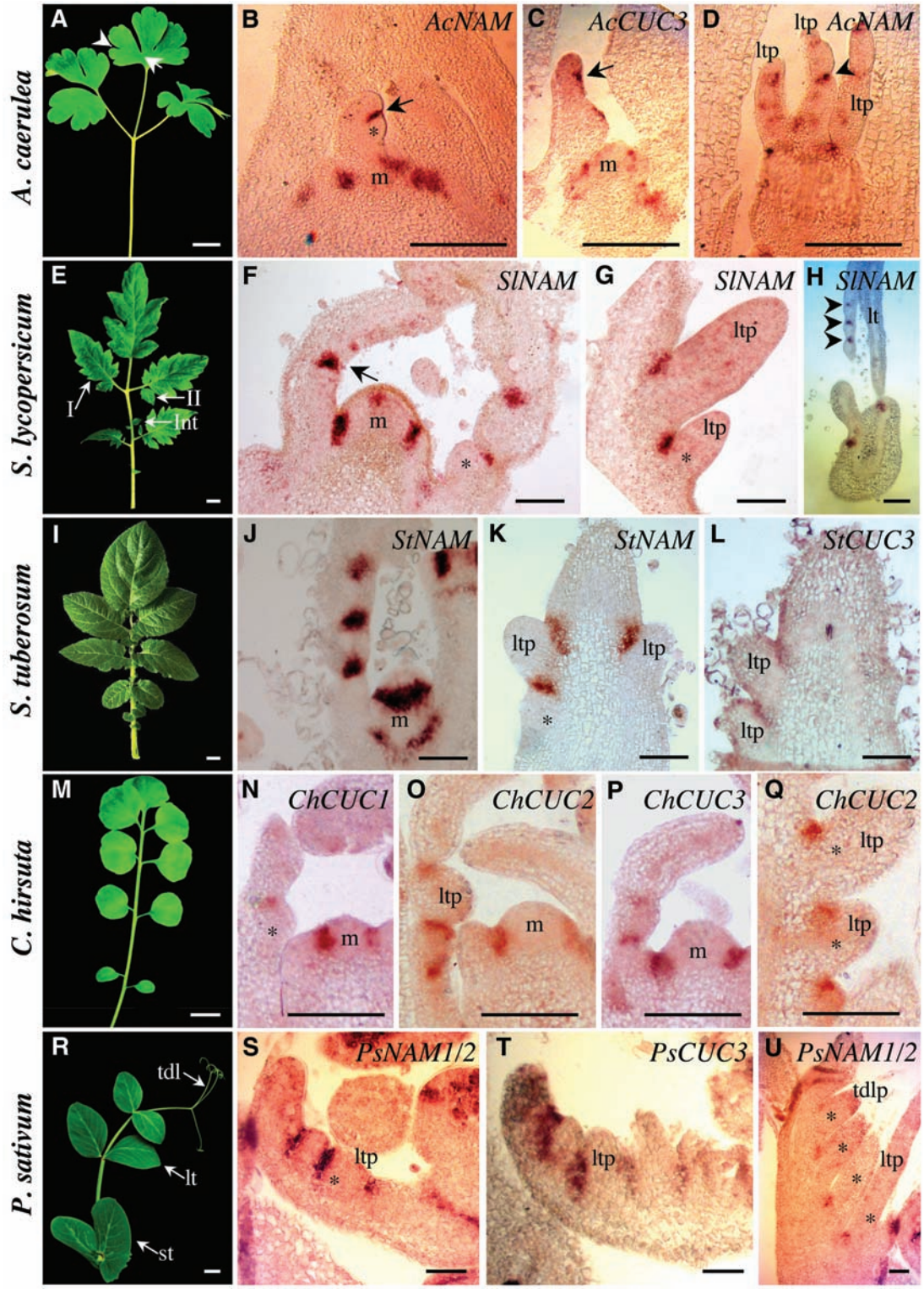

Fig. 1. Leaf shape and expression of the *NAM*/*CUC3* genes during leaf development in eudicots: *A. caerulea* [(A) to (D)], *S. lycopersicum* [(E) to (H)], *S. tuberosum* [(I) to (L)], *C. hirsuta* [(M) to (Q)], and *P. sativum* [(R) to (U)]. (**A**) *A. caerulea* leaf formed by three leaflets subdivided into three majors lobes (arrow), each of which is dissected (arrowhead). (**B** and **C**) In a young leaf primordium, *AcNAM* and *AcCUC3* are expressed in relation to the formation of the leaflet primordia (arrows). *AcNAM* expression is restricted to the distal side of the primordium marked in (B) by an asterisk. (**D**) *AcNAM* expression is coincident with further leaflet primordia (ltp) dissection (arrowhead). (**E**) *S. lycopersicum* leaf formed by primary (I), secondary (II), and intercalary (Int) leaflets that have dissected margins. (**F** and **G**) *SlNAM* expression precedes leaflet outgrowth [arrow in (F)] and marks the distal boundary of young or older leaflet primordia (asterisks). (**H**) *SlNAM* is expressed in relation with the serration of older leaflet (lt) margins (arrowheads). (**I**) *S. tuberosum* leaf formed by primary leaflets with entire leaf margins. (**J** to **L**) *StNAM* and *StCUC3* are expressed during early stages of leaflet initiation (J) and are still detected at later stages [(K) and (L)]. Asterisk in (K) indicates a young leaflet primordium showing *StNAM* expression only on its distal part. (**M**) A rosette leaf of *C. hirsuta* formed by several leaflets that show mild incision of their margins. (**N** to **Q**) *ChCUC1*, *ChCUC2*, and *ChCUC3* are expressed during leaflet initiation and at later stages. *ChCUC* expression is limited to the distal part of young [asterisk in (N)] and older [asterisks in (Q)] primordia. (**R**) *P. sativum* leaf formed by several pairs of proximal leaflets (lt) and distal tendrils (tdl). Leafletlike stipules (st) subtend the leaf. (**S** to **U**) The *PsNAM1/2* and *PsCUC3* genes are expressed during leaflet and tendril primordia development. *PsNAM1/2* is expressed in the distal boundary of young [asterisk in (S)] and older [asterisks in (T)] leaflet primordia. Scale bars indicate 1 cm [(A), (E), (I), (M), and (R)] or 0.1 mm [(B) to (D), (F) to (H), (J) to (L), (N) to (Q), and (S) to (U)].

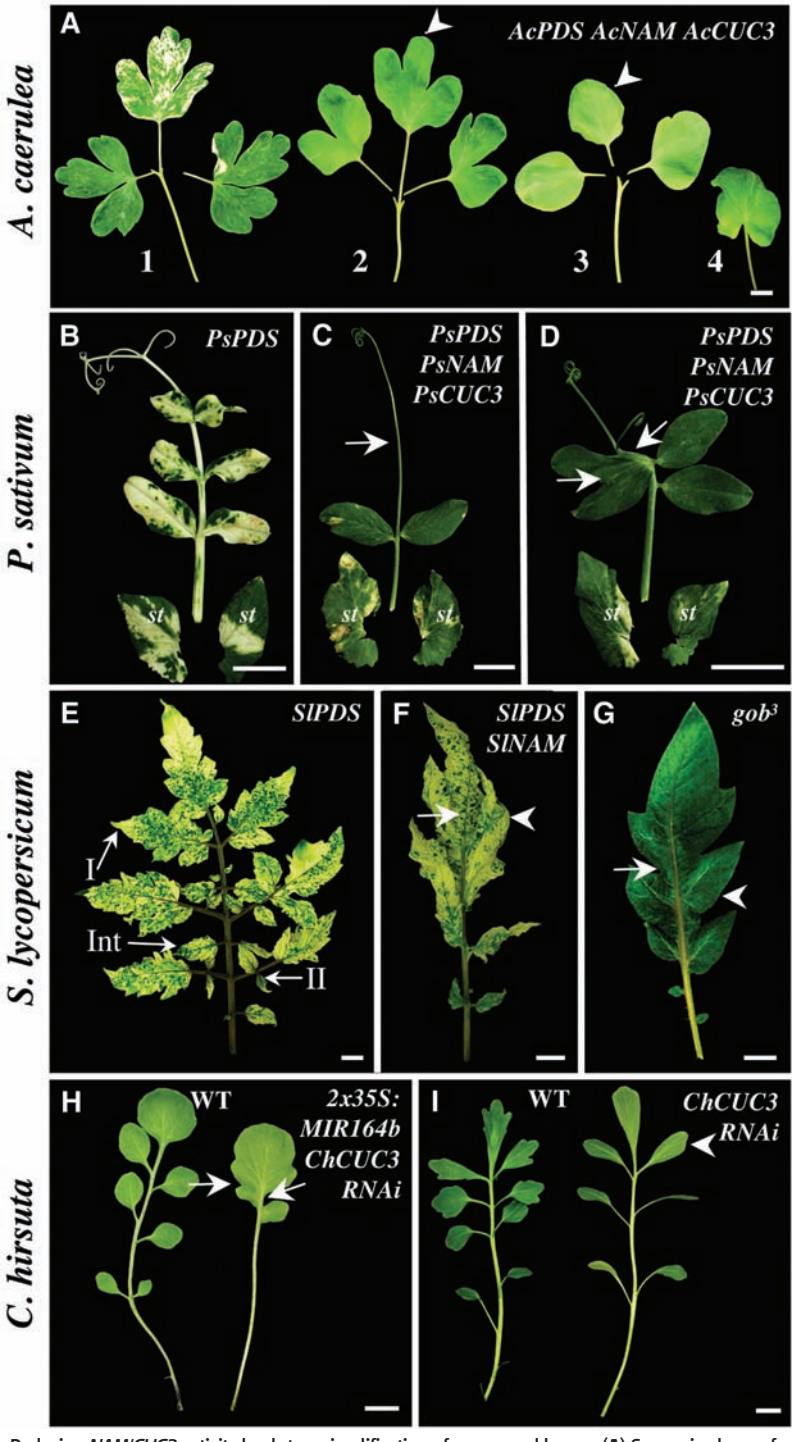

Fig. 2. Reducing *NAM/CUC3* activity leads to a simplification of compound leaves. (**A**) Successive leaves formed on an *A. caerulea* plant silenced for the *AcPDS*, *AcNAM*, and *AcCUC3* genes. Note the progressive smoothening of the leaflet margins from leaf 1 to 3 (arrowheads). At the final stage (leaf 4), corresponding to early silencing, a simple leaf with an entire margin is formed. (**B**) Control leaf of *P. sativum* silenced for *PsPDS* with three pairs of leaflets and three pairs of tendrils subtended by a pair of stipules (st). (**C**) *P. sativum* leaf silenced for *PsPDS*, *PsNAM1/2*, and *PsCUC3* formed by one pair of leaflets and one pair of tendrils separated by a long, organless rachis (arrow). (**D**) *P. sativum* leaf silenced for *PsPDS*, *PsNAM1/2*, and *PsCUC3* showing fusions between leaflets (left arrow) and between a leaflet and the rachis (right arrow). (**E**) Control leaf of *S. lycopersicum* silenced for *SlPDS* showing primary (I), secondary (II), and intercalary (Int) leaflets. (**F**) *S. lycopersicum* leaf silenced for *SlPDS* and *SlNAM* showing smoothed leaf margins (arrowhead), fusions between leaflets (arrow), and fewer leaflets. (**G**) Leaf of *gob*^{3} that harbors a mutation in the *SlNAM* gene and is similar to a *SlNAM*-silenced leaf. (**H**) Rosette leaf number 8 of wild-type (WT) *C. hirsuta* and of a line with reduced *CUC* expression (*2x35S:MIR164b ChCUC3 RNAi*). A reduced number of leaflets leads to a long, leafletless petiole and the fusion of the leaflets (arrows). (**I**) First cauline leaf of WT *C. hirsuta* and of a plant silenced for *ChCUC3* showing fewer and smoothed leaflets (arrowhead). Scale bars, 1 cm.

sativum, and *C. hirsuta* combining three different methods. Down-regulation of *NAM* and/or *CUC3* expression in *A. caerulea*, *P. sativum*, and *S. lycopersicum* by transient virus-induced gene silencing (VIGS) (fig. S5, A, C, and D) led to three specific leaf developmental defects that were never observed in control VIGS experiments (Fig. 2, fig. S6, and tables S1 to S3). First, the extent of serration or lobing at the leaf margin was reduced. Silencing of *SlNAM* was sufficient to produce smooth leaflet margins in *S. lycopersicum* (Fig. 2F and fig. S6), whereas full smoothing of the *A. caerulea* leaf margin required the simultaneous silencing of *AcNAM* and *AcCUC3* (Fig. 2A and fig. S6). Second, all lines silenced for *NAM*/*CUC3* except *A. caerulea* showed fusions of the leaflets with the rachis or between leaflets, and *P. sativum* showed tendril fusions (Fig. 2, D and F, and fig. S6).This indicated that *NAM*/*CUC3* expression at the base of outgrowing leaflets is required for their separation, a function resembling that of organ primordia separation in the meristem. Third, the number of leaflets was reduced. *A. caerulea* silenced for *AcNAM* or *AcNAM*/*AcCUC3* formed a single leaf blade, and fewer leaflets and tendrils were formed in *P. sativum* after *PsNAM1/2* and *PsNAM1/2*/*PsCUC3* silencing (Fig. 2, A, C, and D, and fig. S6). The number of primary leaflets was slightly reduced in *SlNAM*-silenced plants, whereas secondary and intercalary leaflet numbers were highly reduced (Fig. 2F and fig. S6).

The *S. lycopersicum goblet* mutant confirmed the role of the *SlNAM* gene during compound leaf ontogeny. The *goblet* mutant displays developmental defects reminiscent of *nam*/*cuc3* mutants in other plant species (*19*), and sequencing of three *goblet* mutants revealed that each harbored a mutation in the *SlNAM* gene (fig. S7). Leaves regenerated from ectopic meristems of these mutants showed the same morphological defects as *SlNAM*-silenced plants (Fig. 2G).

In *C. hirsuta*, we stably reduced the expression of all three *NAM/CUC3* genes by overexpressing *MIR164b*, which gives rise to mature microRNA164 that directs *ChCUC1* and *ChCUC2* repression, and silencing *ChCUC3* through hairpin-mediated RNA interference (RNAi) (fig. S5B). Individually, *MIR164b* overexpression and *ChCUC3* RNAi led to leaflet fusions and reduced leaflet lobing and number. The severity of these defects was increased in double transgenics (Fig. 2, H and I, and fig. S8).

Altogether, our data revealed a conserved requirement for *NAM/CUC3* genes during leaflet formation, leaflet separation, and margin dissection. In addition, we showed the existence of a morphological continuity from leaf margin to leaflet dissection, which is facilitated at the molecular level by a common underlying mechanism involving *NAM*/*CUC3* genes.

Next, we investigated *NAM/CUC3* gene expression in response to modifications of other regulators of compound leaf development. First, we observed no *NAM/CUC3* expression in the simple leaves of *S. lycopersicum Lanceolate* (*La*)

mutants containing a gain-of-function *TEOSINTE BRANCHED1/CYCLOIDEA/PCF* (*TCP*) *TCP* gene (*20*) and in *P. sativum uni* mutants (fig. S9), consistent with *NAM/CUC3* expression being required for leaflet formation. Second, we analyzed *C. hirsuta* transgenics bearing a *KNOTTED1-GR* fusion (*3*). A 2-day-long activation of the *KNOTTED1-GR* fusion led to increased *ChCUC1-3* expression (Fig. 3A). *ChCUC* activity was required for the induction of ectopic leaflets by *KNOTTED1-GR* (*3*) because they did not form when the *ChCUC* genes were silenced (Fig. 3B).Altogether, these analyses showed that *LA*, *UNI*, and *KNOXI* genes influence *NAM/CUC3* expression, which in turn regulate leaflet formation.

Conversely, we tested whether *NAM/CUC3* genes had an effect on the expression of *KNOXI* and *LFY*-like genes. Accumulation of *KNOXI* (*Tkn1* and *Tkn2* in *S. lycopersicum*) and *LFY*-like (*SlLFY* in *S. lycopersicum* and *UNI* in *P.sativum*) transcripts was reduced in lines silenced for the *NAM/CUC3* genes (Fig. 3, C and D). In line with these results, KNOXI reporter (*ChSTM:GUS*) expression was reduced in the developing leaf of a *C. hirsuta* line with reduced *ChCUC* activity (Fig. 3E). This indicated that *NAM/CUC3* genes are required for proper expression of *KNOXI/LFY*-like genes during compound leaf development. Together, these findings advocate the existence of a feed-forward regulatory loop between *NAM/CUC3* and *KNOXI/LFY*-like genes and indicate that this coordinately regulated expression controls leaflet formation.

We reveal a dual evolutionarily conserved role for *NAM/CUC3* genes during eudicot leaf development (fig. S10). First, *NAM/CUC3* are required to dissect compound leaves into leaflets and leaflet margins into serrations or lobes. This is a local, probably cell-autonomous function of the *NAM/CUC3* genes because they are expressed in the boundary domain. Second, *NAM/CUC3* genes are required for leaflet formation. This is likely to be a non–cell-autonomous effect of *NAM/CUC3* genes. Differences between formation of a leaflet, a lobe, or a serration could depend on different capacities of cells to respond to *NAM/CUC3* expression. For example, factors such as TCP proteins (*20*–*22*) may limit growth and prevent leaflet formation.

In contrast to the *KNOX* and *LFY*-like pathways, whose contributions vary between the compound-leafed eudicots, the requirement for NAM/CUC3 activity during leaflet formation is conserved in all species tested here and is likely to be extensively conserved within eudicots. Our results suggest that species-specific activity of either the *KNOXI* or the *LFY* pathway induces expression of *NAM/CUC3* genes, which are responsible for leaflet formation and maintenance of *KNOXI/LFY* expression through a positive feedback loop.

The dual role of the *NAM/CUC* genes revealed here during leaf development could also exist in the plant apex, where the topology of *NAM/CUC3* expression is similar to that observed during leaflet formation [i.e., they are expressed at the boundary between the meristem and the primordium (*23*)]. It will therefore be interesting to determine whether NAM/CUC3 proteins, in addition to their well-established role in organ separation at the apex, also contribute to the outgrowth of the leaf primordium and whether *NAM/CUC3* action in leaves is mediated by auxin maxima (*8*–*10*). This evolutionarily conserved deployment of both *NAM/CUC3* genes and auxin in both leaf and leaflet formation may reflect the common evolutionary origin of leaves from branched shoots (*10*).

Our results highlight an unexpected role for the interleaflet boundary domain patterned by *NAM/CUC3* genes in directing novel axes of growth that give rise to leaflets. This role is conceptually similar to that of boundary domains acting during animal development (*24*, *25*) and hence provides an example of a common developmental logic operating to sculpt organ form in evolutionary lineages where multicellularity evolved independently.

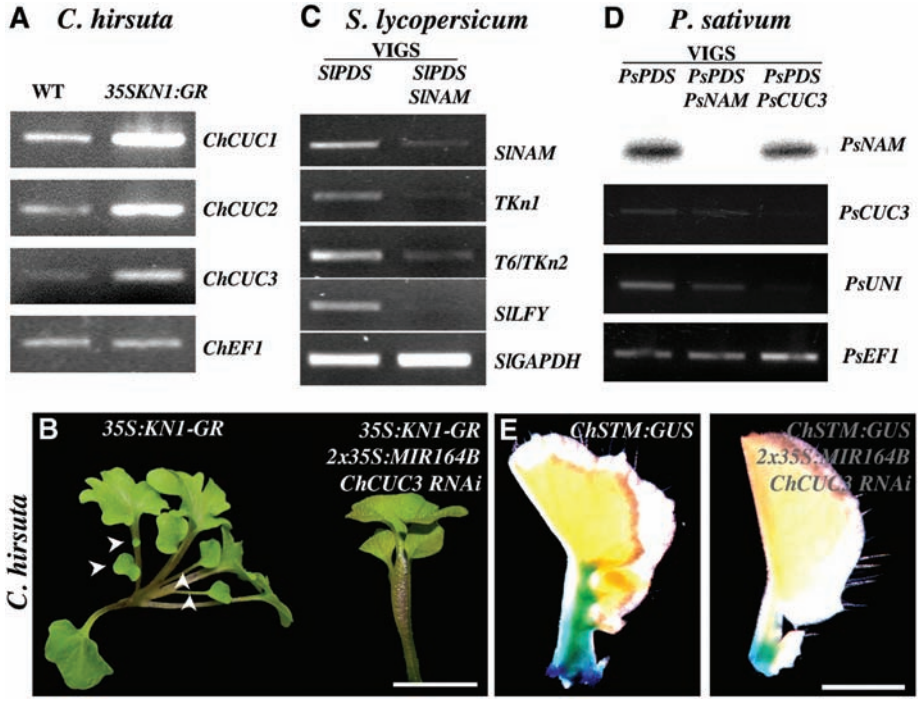

Fig. 3. Interplay between the *NAM/CUC3* genes and other regulators of compound leaf development. (**A**) After 2 days of induction of the *KN1:GR* fusion, the expression of *ChCUC1*, *ChCUC2*, and *ChCUC3* was increased compared with that of WT *C. hirsuta* control plants. *ChEF1* was used as an internal control. (**B**) Upon dexamethasone induction, ectopic leaflets were formed on the primary leaflets in *C. hirsuta* expressing a *KN1-GR* fusion (arrowheads). No ectopic leaflets were formed when the same construct is induced in a background with reduced *ChCUC* activity (*2x35S:MIR164B ChCUC3 RNAi*). (**C**) A reduction of *SlNAM* expression after *SlPDS SlNAM* VIGS was correlated with reduced expression of *SlLFY* and of the two *KNOXI* genes *TKn1* and *T6/TKn2*. *SlGAPDH* was used as an internal control. (**D**) *PsNAM1/2* and *PsCUC3* expression was reduced in plants silenced for *PsPDS PsNAM1/2* or *PsPDS PsCUC3*, respectively, and correlated with lower *UNI* expression. *PsEF1* was used as an internal control. (**E**) The *ChSTM:GUS* reporter was expressed in the petiole and rachis of a WT *C. hirsuta* leaf, and its expression was strongly reduced in a background with reduced *ChCUC* activity (*2x35S:MIR164B ChCUC3 RNAi*). Scale bars, 1 mm in (D) and 1 cm in (E).

References and Notes

1. C. Champagne, N. Sinha, *Development* **131**, 4401 (2004).
2. M. Barkoulas, C. Galinha, S. P. Grigg, M. Tsiantis, *Curr. Opin. Plant Biol.* **10**, 660 (2007).
3. A. Hay, M. Tsiantis, *Nat. Genet.* **38**, 942 (2006).
4. D. Hareven, T. Gutfinger, A. Parnis, Y. Eshed, E. Lifschitz, *Cell* **84**, 735 (1996).
5. G. Bharathan *et al.*, *Science* **296**, 1858 (2002).
6. C. E. Champagne *et al.*, *Plant Cell* **19**, 3369 (2007).
7. J. Hofer *et al.*, *Curr. Biol.* **7**, 581 (1997).
8. D. Reinhardt *et al.*, *Nature* **426**, 255 (2003).
9. M. G. Heisler *et al.*, *Curr. Biol.* **15**, 1899 (2005).
10. M. Barkoulas, A. Hay, E. Kougioumoutzi, M. Tsiantis, *Nat. Genet.* **40**, 1136 (2008).
11. M. Aida, M. Tasaka, *Curr. Opin. Plant Biol.* **9**, 72 (2006).
12. E. Souer, A. van Houwelingen, D. Kloos, J. Mol, R. Koes, *Cell* **85**, 159 (1996).
13. M. Aida, T. Ishida, H. Fukaki, H. Fujisawa, M. Tasaka, *Plant Cell* **9**, 841 (1997).
14. C. W. Vroemen, A. P. Mordhorst, C. Albrecht, M. A. Kwaaitaal, S. C. de Vries, *Plant Cell* **15**, 1563 (2003).
15. S. Breuil-Broyer *et al.*, *Plant J.* **38**, 182 (2004).
16. M. Aida, T. Ishida, M. Tasaka, *Development* **126**, 1563 (1999).
17. K. Nikovics *et al.*, *Plant Cell* **18**, 2929 (2006).
18. Materials and methods are available as supporting material on *Science* Online.
19. A. Brand, N. Shirding, S. Shleizer, N. Ori, *Planta* **226**, 941 (2007).
20. N. Ori *et al.*, *Nat. Genet.* **39**, 787 (2007).
21. J. F. Palatnik *et al.*, *Nature* **425**, 257 (2003).
22. U. Nath, B. C. Crawford, R. Carpenter, E. Coen, *Science* **299**, 1404 (2003).
23. M. Aida, M. Tasaka, *Plant Mol. Biol.* **60**, 915 (2006).

24. K. D. Irvine, C. Rauskolb, *Annu. Rev. Cell Dev. Biol.* **17**, 189 (2001).
25. C. Kiecker, A. Lumsden, *Nat. Rev. Neurosci.* **6**, 553 (2005).
26. This work was partly supported by an Action Concertée Incitative "Jeunes Chercheuses et Jeunes Chercheurs" and the trilateral Génoplante GENOSOME program TRIL-046. T.B. was supported by a Ph.D. fellowship from the Ministère de l'Enseignement Supérieur et de la Recherche, and A.P. was supported by the Fundacíon Española para la Ciencia y la Tecnología (Ministerio de Ciencia e Innovacíon) and the Région Ile-de-France. M.T. is supported by the UK Biotechnology and Biological Sciences Research Council and the Gatsby Charitable Foundation and is the recipient of a European Molecular Biology Organization young investigator award and a Royal Society Wolfson Merit award. A.H. is a recipient of a Royal Society Research Fellowship. The authors thank S. Biemelt, D. Zamir, C. Rameau, J. Hofer, B. Letarnec, C. Navarro, E. Kramer, and the Tomato Genetics Resource Centre for providing material; the Cell Biology Laboratory gardener team for their plant care; J. D. Faure, H. Höfte, J. Hofer, A. Mallory, G. Mouille, J. C. Palauqui, F. Parcy, and C. Rameau for their comments on the manuscript; and N. Ori for discussions and sharing results before publication. Sequences have been deposited in GenBank, accessions FJ435156 to FJ435166.

Supporting Online Material
www.sciencemag.org/cgi/content/full/322/5909/1835/DC1
Materials and Methods
Figs. S1 to S10
Tables S1 to S7
References

19 September 2008; accepted 12 November 2008
10.1126/science.1166168

Human Fetal Hemoglobin Expression Is Regulated by the Developmental Stage-Specific Repressor *BCL11A*

Vijay G. Sankaran,[1,2] Tobias F. Menne,[1] Jian Xu,[1] Thomas E. Akie,[1] Guillaume Lettre,[3,4] Ben Van Handel,[5] Hanna K. A. Mikkola,[5] Joel N. Hirschhorn,[3,4] Alan B. Cantor,[1] Stuart H. Orkin[1,2,6]*

Differences in the amount of fetal hemoglobin (HbF) that persists into adulthood affect the severity of sickle cell disease and the β-thalassemia syndromes. Genetic association studies have identified sequence variants in the gene *BCL11A* that influence HbF levels. Here, we examine *BCL11A* as a potential regulator of HbF expression. The high-HbF *BCL11A* genotype is associated with reduced *BCL11A* expression. Moreover, abundant expression of full-length forms of *BCL11A* is developmentally restricted to adult erythroid cells. Down-regulation of *BCL11A* expression in primary adult erythroid cells leads to robust HbF expression. Consistent with a direct role of *BCL11A* in globin gene regulation, we find that *BCL11A* occupies several discrete sites in the β-globin gene cluster. *BCL11A* emerges as a therapeutic target for reactivation of HbF in β-hemoglobin disorders.

Genome-wide association studies have yielded insights into the genetics of complex diseases and traits (*1*, *2*). In the majority of instances, the functional link between a genetic association and the underlying pathophysiology remains obscure. The level of fetal hemoglobin (HbF) is inherited as a quantitative trait and is of enormous clinical relevance, given its role in ameliorating the severity of the principal hemoglobin disorders, sickle cell disease and β-thalassemia (*3*, *4*). Two recent genome-wide association studies have identified three major loci containing a set of five common single-nucleotide polymorphisms (SNPs) that account for ~20% of the variation in HbF levels (*5*–*7*). Moreover, several of these variants predict the clinical severity of sickle cell disease (*5*), and at least one of these SNPs may also affect clinical outcome in β-thalassemia (*6*). The SNP with the largest effect size is located in the second intron of a gene on chromosome 2, *BCL11A*. Although *BCL11A* has been investigated in the context of lymphocyte development (*8*, *9*), its role in the red blood cell lineage has not been previously assessed.

HbF is a tetramer of two adult α-globin polypeptides and two fetal β-like γ-globin polypeptides. During gestation, the duplicated γ-globin genes constitute the predominant genes transcribed in the β-globin cluster. After birth, γ-globin is replaced by adult β-globin (*4*), a process referred to as the "fetal switch." The molecular mechanisms responsible for this switch have remained largely undefined. Moreover, the extent to which γ-globin gene expression is silenced in adulthood varies among individuals (*5*, *6*). In nonanemic individuals, HbF makes up <1% of total hemoglobin. However, in those with sickle cell disease and β-thalassemia, higher levels of γ-globin expression partially compensate for defective or impaired β-globin gene production, which ameliorates the clinical severity in these diseases. The results of recent genetic association studies provide candidate genes to test for involvement in control of the γ-globin genes. In light of the strong association of SNPs within the *BCL11A* locus with HbF levels in disparate populations (*5*–*7*, *10*), we explore here the hypothesis that the product of the *BCL11A* locus, a multi–zinc finger transcription factor, encodes a stage-specific regulator of HbF expression.

As a first step in seeking how variation at the *BCL11A* locus might relate to γ-globin expression, we examined expression of *BCL11A* in erythroid cells (*11*). In primary adult human erythroid cells, BCL11A is expressed as two major isoforms at the protein and RNA levels (Fig. 1A). These isoforms (designated XL and L) differ only in usage of the 3′ terminal exon and function similarly in other settings (*9*). We have recently fine-mapped the *BCL11A*-HbF association signal to a variant in close linkage disequilibrium (LD) with the SNP rs4671393 (*5*). Because this association has been confirmed in multiple independent European and African diasporic populations, we examined expression of the XL and L isoforms of *BCL11A* as a function of the genotype at rs4671393 in lymphoblastoid cell lines from the HapMap European (CEU) and African (YRI) groups. The utility of this strategy has been shown in prior studies examining the consequences of common genetic variation on gene expression (*12*–*14*). We observed a striking difference in expression for both isoforms between individuals of different SNP genotypes (Fig. 1B). Cells homozygous for the "high-HbF" allele expressed a lower level of *BCL11A* transcripts than those homozygous for the "low-HbF" allele or heterozygous for both alleles. The difference in expression between the "high" and "low" HbF–associated *BCL11A* alleles is 3.5-fold. Hence, relatively modest differences in *BCL11A* expression appear to be associated with changes in HbF expression.

To our surprise, we observed that the embryonic erythroleukemia cell line K562 expressed very little, if any, of the XL and L isoforms but, instead, expressed shorter variant proteins (Fig. 1C). To assess whether the difference between adult erythroblasts and K562 cells reflected developmental stage–specific control of *BCL11A* or the malignant nature of these cells, we examined stage-matched, $CD71^{+}/CD235^{+}$ erythroblasts isolated from adult bone marrow, second-trimester fetal liver (FL), and circulating first-trimester primitive cells. FL and primitive erythroblasts, which both robustly express γ-globin (*15*), expressed predominantly shorter BCL11A variants (Fig. 1C). Although we continue to investigate the structure of these variant proteins, our findings indicate that the *BCL11A* locus is developmentally regulated, such that full-length XL and L isoforms are expressed almost exclusively in adult-stage erythroblasts. Independently, the genetic data strongly argue that the level of XL and L isoforms is influenced by sequence variants in the *BCL11A* gene.

[1]Division of Hematology/Oncology, Children's Hospital Boston, Harvard Stem Cell Institute, Harvard Medical School, Boston, MA 02115, USA. [2]Department of Pediatric Oncology, Dana-Farber Cancer Institute, Boston, MA 02115, USA. [3]Program in Medical and Population Genetics, Broad Institute of MIT and Harvard, Cambridge, MA 02142, USA. [4]Divisions of Genetics and Endocrinology and Program in Genomics, Children's Hospital Boston, Boston, MA 02115, USA. [5]Department of Molecular, Cell, and Developmental Biology, University of California at Los Angeles, Los Angeles, CA 90095, USA. [6]Howard Hughes Medical Institute, Boston, MA 02115, USA.

*To whom correspondence should be addressed. E-mail: stuart_orkin@dfci.harvard.edu

To better understand potential mechanisms through which BCL11A might act in erythroid cells, we characterized interacting proteins. We affinity-tagged versions of BCL11A in mouse erythroleukemia (MEL) cells, adult-type erythroid cells that express exclusively adult globins (*16*) (Fig. 2A). We observed no major global transcriptional changes by microarray analysis when tagged versions of BCL11A were expressed in these cells (fig. S1). After affinity purification of protein complexes containing tagged BCL11A and mass spectrometric peptide sequencing, we identified numerous peptides of BCL11A (*9*), as well as all components of the nucleosome remodeling and histone deacetylase (NuRD)–repressive complex (Fig. 2B). The strong association between BCL11A and the NuRD complex in erythroid cells is consistent with prior observations in B cells and of the homolog BCL11B in T cells (*17*), as well as the presence of an N-terminal motif that recruits the NuRD complex (fig. S2) (*18*, *19*). We also found that the nuclear matrix protein, matrin-3 (*20*), consistently copurified with BCL11A, which may account in part for the localization of BCL11A to the nuclear matrix (*9*) (Fig. 2B). Prior work has shown that the β-globin locus is closely associated with the nuclear matrix until later stages of erythropoeisis, when high-level globin gene transcription occurs (*21*).

Additionally, BCL11A complexes contain peptides derived from GATA-1, the principal erythroid transcription factor (*22*) (Fig. 2B). By immunoprecipitation (IP), we confirmed that GATA-1 specifically associates with BCL11A in erythroid cells (Fig. 2C). Moreover, we found that the GATA-1 cofactor FOG-1 (*23*) specifically associates with BCL11A and confirmed the interaction with NuRD components in erythroid cells (Fig. 2C). Prior work has shown that FOG-1 binds to the NuRD complex (*19*), and our results suggest that BCL11A may synergize with this interaction in the context of specific loci. From size fractionation of erythroid nuclear extracts, we observed considerable overlap between NuRD components and BCL11A in megadalton protein complexes, with less extensive overlap with GATA-1 and FOG-1 (fig. S3). It is possible that only a minor fraction of these factors are bound within the BCL11A and NuRD complexes. Alternatively, in vivo association might be greater, but dissociation of the components of protein complexes occurs during gel filtration. GATA-1 and FOG-1 immunoprecipitated with BCL11A when expressed exogenously in nonerythroid cells, which suggests that these proteins directly interact (Fig. 2, D and E). We used this approach to map the determinants mediating association of GATA-1 with BCL11A to the zinc fingers of GATA-1 (Fig. 2F). Together, the proteomic data indicate that BCL11A binds the NuRD complex along with GATA-1 and FOG-1 in erythroid cells. These associated factors are likely to be critical for the action of BCL11A as a transcriptional repressor in erythroid cells.

Genetic, developmental, and biochemical approaches support a potential role for *BCL11A* in γ-globin gene silencing. To test this hypothesis, we modulated the level of *BCL11A* in primary human erythroid cells. As a cellular system in which to perform experiments, we expanded and differentiated erythroid precursors from purified $CD34^+$ human hematopoietic progenitors. We began by examining the effect of transient introduction of small interfering RNAs (siRNAs) that target *BCL11A* mRNA. When siRNAs were introduced into erythroid progenitors at day 0 of differentiation, 40 to 45% depletion (knockdown) of *BCL11A* mRNA levels was achieved, as assessed on day 4 of differentiation. With this knockdown, we observed a 2.3-fold increase in the level of γ-globin RNA (compared with total β-like globin RNA) on day 7 of differentiation (Fig. 3A). We found that, as these siRNAs were introduced at later time points during erythroid differentiation, induction of the γ-globin gene was observed to be less (with 1.7- and 1.4-fold average γ-globin induction seen by adding siRNAs on days 1 and 2 of differentiation). The results we observed from siRNA knockdown of *BCL11A* could be due to a broad effect on the cellular differentiation state, which has been shown to alter γ-globin expression (*3*) or could reflect more direct action at a limited number of targets, including the γ-globin gene. To distinguish between these possibilities, we performed microarray expression profiling of the cells after knockdown of *BCL11A* and subsequent differentiation. The transcriptional profiles of genes in the quantitative range of the array (which excluded the globins) were remarkably similar between cells on day 7 after treatment with *BCL11A* siRNAs and non-targeting (NT) siRNAs on day 0, with a correlation coefficient (r^2) of 0.9901 for the $\log_2$ normalized intensities (Fig. 3B). The expression of the well-characterized transcriptional regulators of the globin genes, GATA-1, FOG-1, NF-E2, and EKLF (*4*), in this microarray data set, was also comparable between the groups (with all *P* values > 0.05 and average fold changes of <1.1-fold). This observation suggests that the effect of *BCL11A* on γ-globin gene regulation is unlikely to be mediated via an effect on the expression of one of these previously characterized transcriptional regulators. Additionally, the morphology of these two groups of cells was indistinguishable throughout differentiation. Together, these results suggest that knockdown of *BCL11A* affects γ-globin expression without causing global changes in the differentiation state of the cells.

To examine the effects of more persistent reduction in *BCL11A* expression, we utilized lentiviral short hairpin RNA (shRNA)–mediated knockdown of *BCL11A* expression with drug selection of transduced cells (*24*). We chose two independent shRNA constructs. When cells were infected with the two *BCL11A* shRNA lentiviruses and selection was imposed on the initiation of differentiation, we

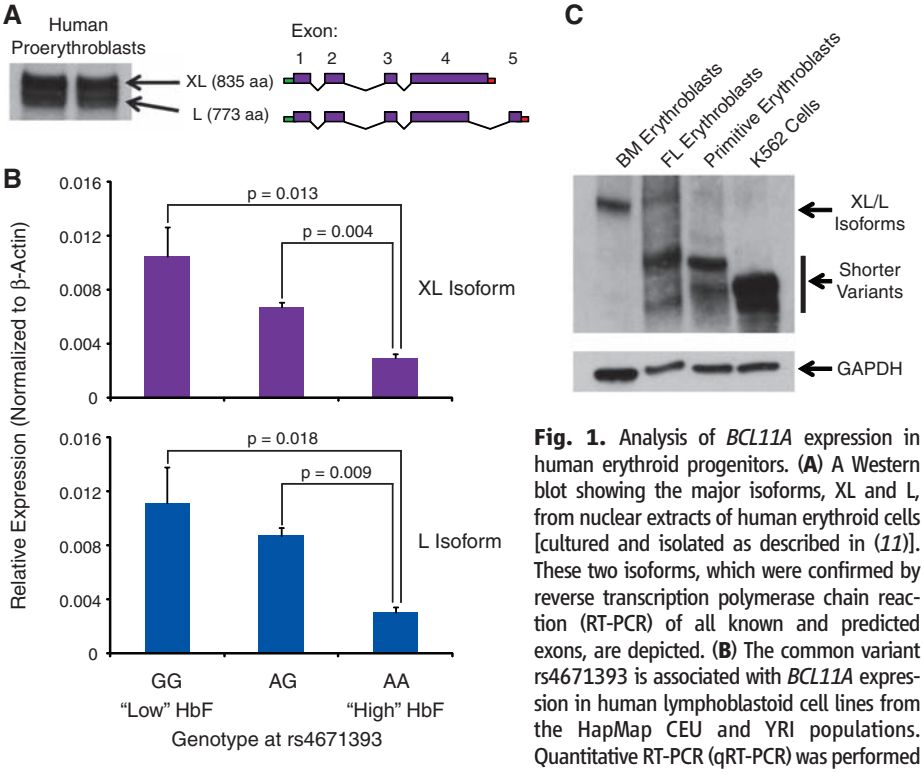

Fig. 1. Analysis of *BCL11A* expression in human erythroid progenitors. (**A**) A Western blot showing the major isoforms, XL and L, from nuclear extracts of human erythroid cells [cultured and isolated as described in (*11*)]. These two isoforms, which were confirmed by reverse transcription polymerase chain reaction (RT-PCR) of all known and predicted exons, are depicted. (**B**) The common variant rs4671393 is associated with *BCL11A* expression in human lymphoblastoid cell lines from the HapMap CEU and YRI populations. Quantitative RT-PCR (qRT-PCR) was performed on RNA from these cell lines and normalized to the level of human β-actin (5, 3, and 3, from left to right). Results are means ± SEM. Significance of differences between genotypes was calculated using the Student's *t* test. (**C**) Western blots of lysates of primary human bone marrow (BM) erythroblasts, second-trimester FL erythroblasts, first-trimester circulating primitive erythroblasts, and K562 cells. Primary human stage–matched erythroblasts were isolated by sorting for the CD235 and CD71 double-positive population. The XL and L bands migrate together here as a result of reduced separation on this blot.

observed an average of 97 and 60% knockdown of BCL11A at the protein level by day 5 of erythroid differentiation (Fig. 3C). No morphological differences between the groups of cells were noted during differentiation, again suggesting that *BCL11A* knockdown did not perturb overall erythroid differentiation (Fig. 3D). The level of γ-globin at day 7 of differentiation was dramatically elevated by 6.5- and 3.5-fold (from an average of 7.4 % in the control to 46.8 and 26%) for the two shRNAs as compared with the control infected cells (Fig. 3E). This robust effect is likely to be the result of elimination of non-transduced cells, as well as the continuous expression of the shRNAs after viral transduction. Induction of γ-globin RNA was accompanied by corresponding levels of mature HbF, as shown by hemoglobin high-performance liquid chromatography (HPLC) and electrophoresis (Fig. 3F and fig. S4). The HPLC revealed that a substantial fraction of the mature hemoglobin in these cells was HbF (with an average level of 35.9 and 23.6%, compared with undetectable levels in the control). On the basis of the differing extents of knockdown of *BCL11A* in the siRNA and shRNA experiments and the concomitant degree of γ-globin induction observed, it appears that BCL11A functions as a molecular rheostat to control silencing of the γ-globin genes.

In principle, *BCL11A* might influence globin gene expression either directly by interacting with cis-regulatory elements within the β-globin cluster or indirectly by affecting cell cycle or other pathways that ultimately impinge on HbF expression. To discriminate between these possibilities, we used chromatin immunoprecipitation (ChIP) in primary human erythroid progenitors. Occupancy of neither the γ- nor β-globin proximal promoters was detected. Rather, we observed robust binding in several other regions of the β-globin cluster (Fig. 4). These include the third hypersensitivity site (HS3) of the locus control region (LCR) (*25*), the region of the high HbF–associated Corfu deletion upstream of the δ-globin gene (*4*), and another region downstream of the Aγ-globin gene that is commonly deleted in certain forms of hereditary persistence of fetal hemoglobin (*4*). Of particular note, all of these cis elements have been suggested to play a role in γ-globin silencing. Our results strongly argue that *BCL11A* acts within the β-globin cluster. A fuller accounting of mechanism will necessitate comprehensive analysis of chromatin occupancy of BCL11A and partner proteins in the β-globin cluster. We speculate that the shorter BCL11A variants present in cells that actively express γ-globin may participate in other aspects of transcriptional regulation within the β-globin cluster. As such, we propose that *BCL11A*, at different levels and in its variant forms, reconfigures the β-globin locus at different development stages.

The molecular studies of globin switching during ontogeny serve as a paradigm for the developmental control of mammalian genes. Our results indicate that *BCL11A* is itself a developmentally regulated and critical modulator of this process. We have shown that silencing of γ-globin gene expression in primary adult human erythroid cells depends on the presence of full-length (XL and L isoforms) *BCL11A*. Our protein data suggest that BCL11A functions in concert with the NuRD-repressor complex, GATA-1, and FOG-1. Of note, inhibitors of histone deacetylases (HDACs) induce some HbF in patients with hemoglobin disorders (*26*). HDAC1 and HDAC2 are both core components of the NuRD complex, and its association with BCL11A suggests that this complex may be the molecular target of these therapies. On the basis of findings of human genetics studies, we postulate that directed down-regulation of *BCL11A* in patients would elevate HbF levels and ameliorate the severity of the major β-hemoglobin disorders (*5*–*7*). As a stage-specific component involved in the silencing of γ-globin expression, *BCL11A*, therefore, emerges as a new therapeutic target for reactivation of HbF in sickle cell disease and the β-thalassemias.

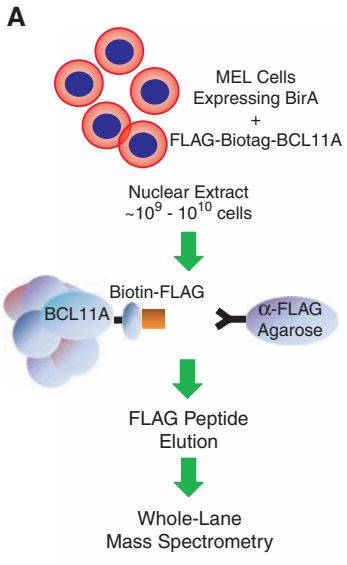

B

Protein	Peptides
BCL11A	29, 49
GATA-1	1, 1
CHD4	16, 10
RBBP4	8, 15
MTA2	6, 18
p66b	5, 16
MTA1	9, 12
p66a	3, 8
HDAC1	11, 11
HDAC2	4, 3
RBBP7	4, 5
MTA3	1, 1
MBD3	5, 3
MATRIN-3	8, 9

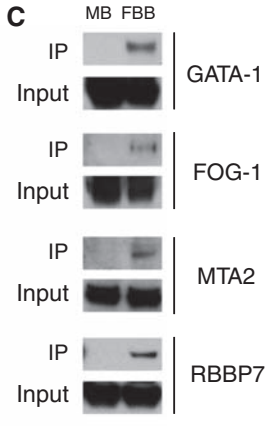

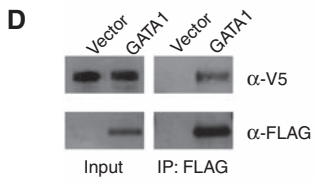

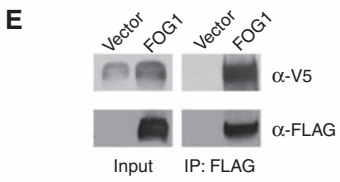

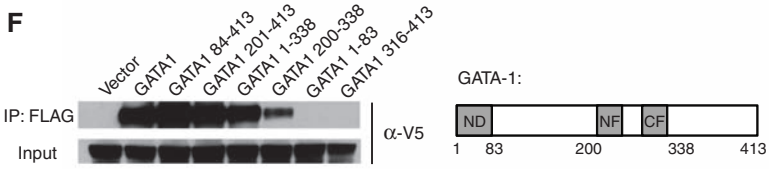

Fig. 2. Proteomic affinity screen identifies BCL11A partner proteins in erythroid cells. (**A**) The scheme used for the affinity-purification in mouse erythroleukemia (MEL) cells is depicted in this diagram. Once FLAG peptide elution was performed, whole-lane mass spectrometry from acrylamide gels was done as described in (*11*). We used a subtractive approach, including a simultaneous pull-down in parental Mel-BirA (MB) cells. (**B**) The results of this subtractive screen are shown with the number of peptides obtained in each trial listed adjacent to the identified protein. The components of the NuRD complex are shown in blue. (**C**) Confirmation of interactions of BCL11A with GATA-1, FOG-1, MTA2, and RBBP7 in erythroid (MEL) cells (FBB is the cell line containing tagged BCL11A). BCL11A interactions with GATA-1 (**D**) and FOG-1 (**E**) could be confirmed by exogenous expression in COS-7 cells by using FLAG-tagged versions of GATA-1 or FOG-1 and V5-tagged versions of BCL11A. (**F**) Using this same strategy in 293T cells, fragments of GATA-1 (all of which show robust expression here) could be used to map the interaction with BCL11A. The structure of GATA-1 is shown on the right side, including the N-terminal domain (ND), the N-terminal zinc finger (NF), and the C-terminal zinc finger (CF).

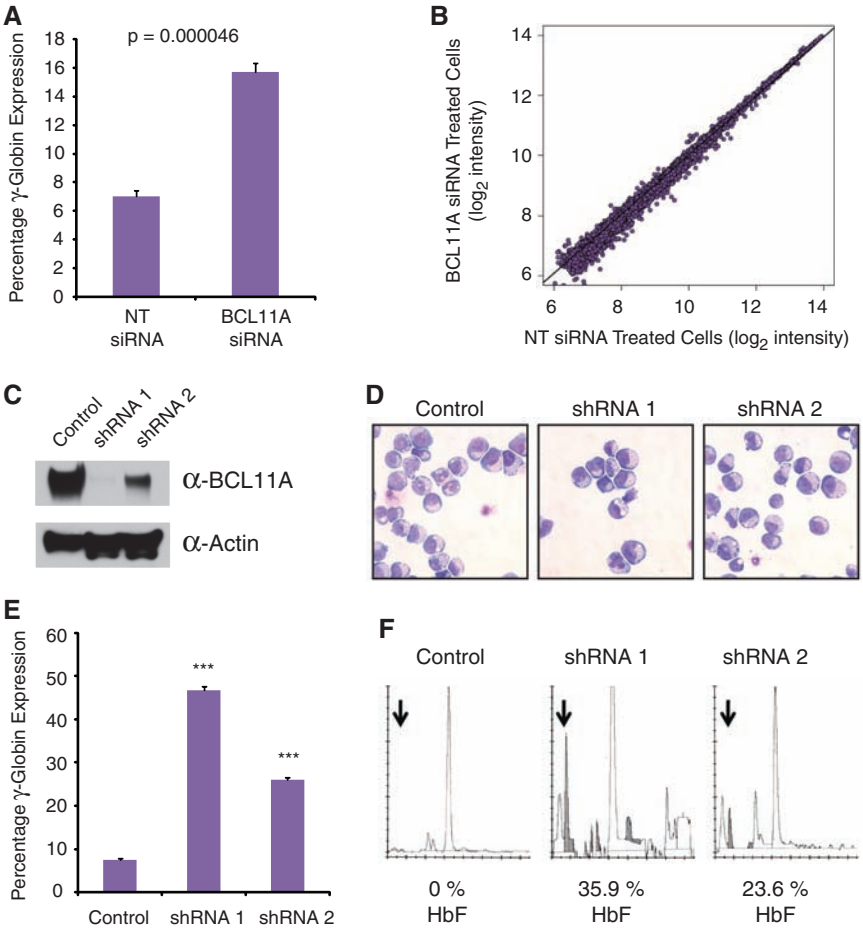

Fig. 3. *BCL11A* acts as a silencer of γ-globin gene expression, based on modulation of *BCL11A* levels. (**A**) siRNA-mediated knockdown of *BCL11A* results in elevations of γ-globin mRNA levels (as a percentage of total β-like globin gene expression) in human erythroid progenitor cells at day 7 of differentiation in comparison with NT control siRNAs. (**B**) Microarray profiling of these cells using the Affymetrix U133 Plus 2.0 array reveals that there is close similarity in the expression profile of NT and *BCL11A* siRNA-treated cells ($r^2 = 0.9901$). Microarray data processing and filtering were performed as described previously (*27*) and in (*11*). (**C**) Lentiviral-mediated shRNA delivery to human erythroid progenitors results in robust knockdown of BCL11A protein. Control samples were infected with lentivirus prepared from the backbone pLKO.1ps vector. (**D**) At day 6 of differentiation, the cells appear to be morphologically indistinguishable; this is also the case at other stages of differentiation. (**E**) The shRNA-mediated knockdown of *BCL11A* results in robust induction of γ-globin mRNA level on day 7 of differentiation (***$P < 10^{-5}$ in comparison with control). (**F**) Hemolysates prepared from cells on day 12 of differentiation show the presence of mature HbF by hemoglobin HPLC. The HbF peaks are labeled with an arrow in each chromatogram, with the first peak corresponding to acetylated HbF (*28*) and the second unmodified HbF. All results are means ± SEM. Statistical significance was calculated using the Student's *t* test.

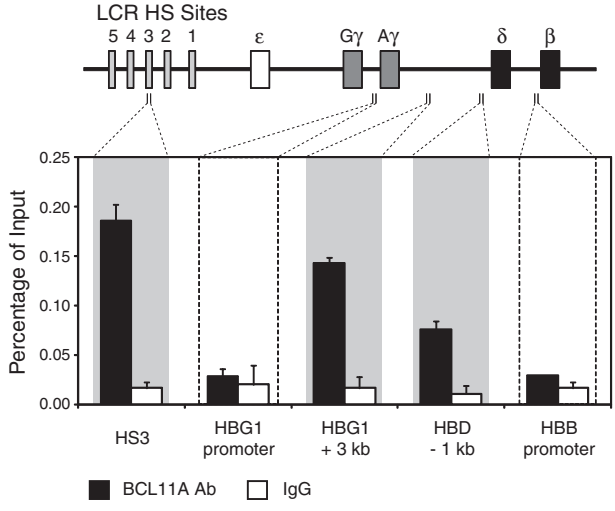

Fig. 4. *BCL11A* occupies discrete regions in the human β-globin locus in adult erythroid progenitors. The human β-globin locus is depicted at the top with regions showing significant binding shaded in gray in the histogram plot below. The results are means ± SD ($n = 3$ per group).

References and Notes

1. M. I. McCarthy *et al.*, *Nat. Rev. Genet.* **9**, 356 (2008).
2. T. A. Manolio, L. D. Brooks, F. S. Collins, *J. Clin. Invest.* **118**, 1590 (2008).
3. G. Stamatoyannopoulos, *Exp. Hematol.* **33**, 259 (2005).
4. A. Bank, *Blood* **107**, 435 (2006).
5. G. Lettre *et al.*, *Proc. Natl. Acad. Sci. U.S.A.* **105**, 11869 (2008).
6. M. Uda *et al.*, *Proc. Natl. Acad. Sci. U.S.A.* **105**, 1620 (2008).
7. S. Menzel *et al.*, *Nat. Genet.* **39**, 1197 (2007).
8. P. Liu *et al.*, *Nat. Immunol.* **4**, 525 (2003).
9. H. Liu *et al.*, *Mol. Cancer* **5**, 18 (2006).
10. A. E. Sedgewick *et al.*, *Blood Cells Mol. Dis.* **41**, 255 (2008).
11. Materials and methods are available as supporting material on *Science* Online.
12. M. F. Moffatt *et al.*, *Nature* **448**, 470 (2007).
13. R. R. Graham *et al.*, *Proc. Natl. Acad. Sci. U.S.A.* **104**, 6758 (2007).
14. H. H. Goring *et al.*, *Nat. Genet.* **39**, 1208 (2007).
15. C. Peschle *et al.*, *Nature* **313**, 235 (1985).
16. T. Papayannopoulou, M. Brice, G. Stamatoyannopoulos, *Cell* **46**, 469 (1986).
17. V. B. Cismasiu *et al.*, *Oncogene* **24**, 6753 (2005).
18. S. M. Lauberth, M. Rauchman, *J. Biol. Chem.* **281**, 23922 (2006).
19. W. Hong *et al.*, *EMBO J.* **24**, 2367 (2005).
20. H. Nakayasu, R. Berezney, *Proc. Natl. Acad. Sci. U.S.A.* **88**, 10312 (1991).
21. T. Ragoczy, M. A. Bender, A. Telling, R. Byron, M. Groudine, *Genes Dev.* **20**, 1447 (2006).
22. S. F. Tsai *et al.*, *Nature* **339**, 446 (1989).
23. A. P. Tsang *et al.*, *Cell* **90**, 109 (1997).
24. J. Moffat *et al.*, *Cell* **124**, 1283 (2006).
25. P. A. Navas *et al.*, *Mol. Cell. Biol.* **18**, 4188 (1998).
26. L. Quek, S. L. Thein, *Br. J. Haematol.* **136**, 353 (2007).
27. V. G. Sankaran, S. H. Orkin, C. R. Walkley, *Genes Dev.* **22**, 463 (2008).
28. R. L. Garlick *et al.*, *J. Biol. Chem.* **256**, 1727 (1981).

29. We thank J. Snow, P. Tucker, G. Ippolito, B. Lee, M. Leid, T. Nakamura, D. Altshuler, E. Choy, and S. Bonakdar for providing reagents and suggestions. We are grateful to D. Nathan and A. Michelson for critical comments; D. Shao, N. Yudanin, and A. Soriano for experimental assistance; and C. Chen and V. Sankaran for assistance with data analysis. This work was supported by grants from the National Heart, Lung, and Blood Institute, NIH (HL32262-26 and HL32259-27), a Center of Excellence in Molecular Hematology Award from the National Institute of Digestive and Kidney Diseases, NIH, and the Howard Hughes Medical Institute. T.F.M. was supported by the Leukaemia Research and Kay Kendall Leukaemia Funds. V.G.S. was supported by a Medical Scientist Training Program grant from the NIH. Array datasets are deposited at Gene Expression Omnibus (accession no. GSE 13285). A patent application related to this work was filed, and V.G.S. and S.H.O. are inventors on this patent.

Supporting Online Material

www.sciencemag.org/cgi/content/full/1165409/DC1
Materials and Methods
Figs. S1 to S4
References

3 September 2008; accepted 12 November 2008
Published online 4 December 2008;
10.1126/science.1165409
Include this information when citing this paper.

CRISPR Interference Limits Horizontal Gene Transfer in Staphylococci by Targeting DNA

Luciano A. Marraffini and Erik J. Sontheimer*

Horizontal gene transfer (HGT) in bacteria and archaea occurs through phage transduction, transformation, or conjugation, and the latter is particularly important for the spread of antibiotic resistance. Clustered, regularly interspaced, short palindromic repeat (CRISPR) loci confer sequence-directed immunity against phages. A clinical isolate of *Staphylococcus epidermidis* harbors a CRISPR spacer that matches the *nickase* gene present in nearly all staphylococcal conjugative plasmids. Here we show that CRISPR interference prevents conjugation and plasmid transformation in *S. epidermidis*. Insertion of a self-splicing intron into *nickase* blocks interference despite the reconstitution of the target sequence in the spliced mRNA, which indicates that the interference machinery targets DNA directly. We conclude that CRISPR loci counteract multiple routes of HGT and can limit the spread of antibiotic resistance in pathogenic bacteria.

Clustered, regularly interspaced, short palindromic repeat (CRISPR) loci are present in ~40% of eubacterial genomes and nearly all archaeal genomes sequenced to date and consist of short (~24 to 48 nucleotides) repeats separated by similarly sized unique spacers (*1*, *2*). They are generally flanked by a set of CRISPR-associated (*cas*) protein-coding genes (*3*–*5*). The CRISPR spacers and repeats are transcribed and processed into small CRISPR RNAs (crRNAs) (*4*, *6*–*8*) that specify acquired immunity against bacteriophage infection by a mechanism that relies on the strict identity between CRISPR spacers and phage targets (*3*, *4*).

The rise of hospital- and community-acquired methicillin- and vancomycin-resistant *Staphylococcus aureus* (MRSA and VRSA, respectively) is directly linked to the horizontal transfer of antibiotic resistance genes by plasmid conjugation (*9*, *10*). *S. aureus* and *S. epidermidis* strains are the most common causes of nosocomial infections (*11*–*13*), and conjugative plasmids can spread from one species to the other. Although the *S. epidermidis* strain American Type Culture Collection (ATCC) 12228 (*14*) lacks CRISPR sequences, the clinically isolated strain RP62a (*15*) contains a CRISPR locus (Fig. 1A and fig. S1A) that includes a spacer (*spc1*) that is homologous to a region of the *nickase* (*nes*) gene found in all sequenced staphylococcal conjugative plasmids (fig. S1B), including those from MRSA and VRSA strains (*9*, *16*, *17*).

To test whether *spc1* prevents plasmid conjugation into *S. epidermidis* RP62a, we disrupted the sequence match by introducing nine silent mutations into the *nes* target in the conjugative plasmid pG0400 (*18*), generating pG0(mut) (Fig. 1B) (*19*). We tested whether both wild-type and mutant pG0400 transferred from *S. aureus* strain RN4220 (*20*) into either of the two *S. epidermidis* strains (Fig. 1D and fig. S1C). Although the conjugation frequency of both plasmids was similar for the CRISPR-negative ATCC 12228 strain, only pG0(mut) was transferred into the CRISPR-positive RP62a strain and with a frequency similar to that of wild-type pG0400 in the control ATCC 12228 strain. These results indicate that CRISPR interference can prevent plasmid conjugation in a manner that is specified by sequence identity between a spacer and a plasmid target sequence.

To test this conclusion more rigorously, and to determine whether the CRISPR sequences themselves are responsible for the observed interference, we deleted the four repeats and three spacers present in the RP62a locus in order to generate the isogenic Δ*crispr* strain LAM104 (Fig. 1A) and tested its ability to act as a recipient for the conjugative transfer of pG0400. Again, wild-type RP62a was refractory to pG0400 transfer, whereas the conjugation efficiency for the LAM104 strain was similar to that obtained for *S. epidermidis* ATCC 12228 (Fig. 1D and fig. S1C). pG0(mut) transfer was similar in both strains. To restore interference in the Δ*crispr* mutant, we transformed LAM104 with plasmid pCRISPR or pCRISPR-L (Fig. 1C). Both of these plasmids contain the RP62a CRISPR repeats and spacers downstream of an isopropyl-β-D-thiogalactopyranoside (IPTG)–inducible pro-

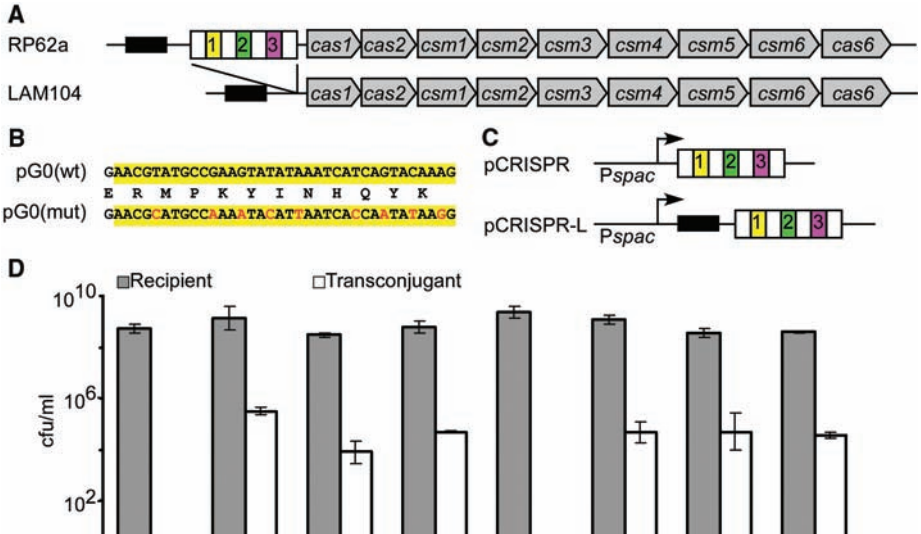

Fig. 1. A CRISPR locus provides immunity against plasmid conjugation in *S. epidermidis*. (**A**) Organization of the RP62a CRISPR locus. Repeats and spacers (colored boxes) are followed by CRISPR-associated genes (*cas1*, *cas2*, and *cas6*) and *cas* subtype *Mycobacterium tuberculosis* genes (*csm1* to *csm6*) (*5*). An AT-rich "leader" sequence precedes the repeat-spacer region (black box). LAM104 is an isogenic Δ*crispr* strain lacking only the repeat and spacer sequences. (**B**) The staphylococcal conjugative plasmid pG0400 *spc1* target sequence [pG0(wt), highlighted in yellow] is shown on the top. This sequence was altered to introduce synonymous mutations to generate pG0(mut), with changes shown in red. (**C**) To restore interference in strain LAM104, two plasmids were introduced: pCRISPR and pCRISPR-L. (**D**) Conjugation was carried out by filter-mating in triplicate; the colony-forming units (CFU) per milliliter values (mean ± SD) obtained for recipients and transconjugants are shown. Recipient strains, complementing plasmids, and donor conjugative plasmids are indicated. Conjugation efficiency (Conj. Eff.) was calculated as the recipients/transconjugants ratio.

Department of Biochemistry, Molecular Biology and Cell Biology, Northwestern University, 2205 Tech Drive, Evanston, IL 60208, USA.

*To whom correspondence should be addressed. E-mail: erik@northwestern.edu

moter, but they differ in the amount of upstream flanking sequence included. The appearance of the *spc1* crRNA in pCRISPR-L–containing LAM104 cells (fig. S2) was IPTG-independent, which indicates that the insert includes a natural CRISPR promoter. pCRISPR-L restored interference in the Δ*crispr* strain, but pCRISPR did not, even in the presence of IPTG (fig. S1D). This suggests a role for the leader sequence (Fig. 1A) or other upstream sequences in cis during CRISPR interference, perhaps for processing of the crRNA precursor by Cascade proteins (*4*). Introduction of pCRISPR-L into strain ATCC 12228 did not alter the conjugation efficiency of pG0400 (fig. S1D) as expected because of the lack of *cas* genes in this strain.

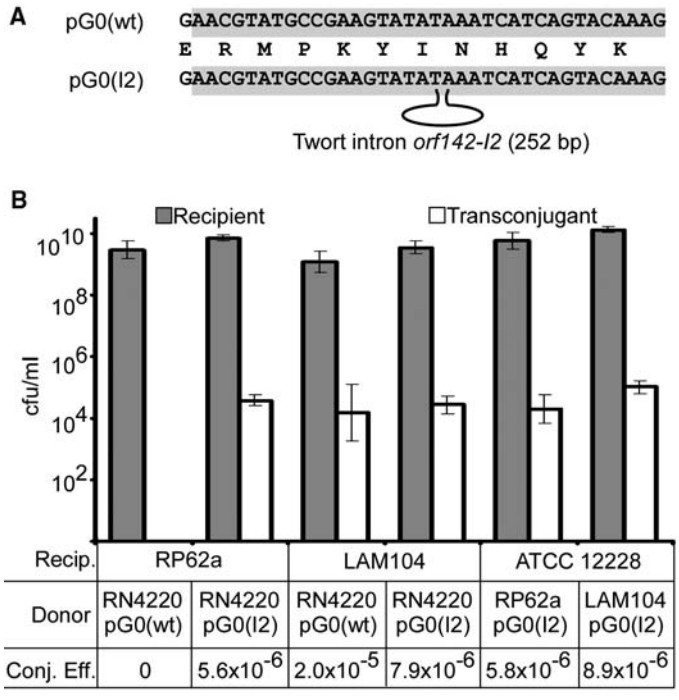

Fig. 2. CRISPR interference requires an intact target sequence in plasmid DNA but not mRNA. (**A**) Disruption of the pG0400 *nes* target sequence with the *orf142-I2* self-splicing intron, generating the conjugative plasmid pG0(I2). (**B**) Conjugation efficiency was measured as in Fig. 1D with RP62a and the Δ*crispr* mutant LAM104 as recipients for pG0(wt) and pG0(I2). To test for interference with spliced *nes* mRNA, RP62a and LAM104 transconjugants were also used as donors of pG0(I2) to *S. epidermidis* ATCC 12228.

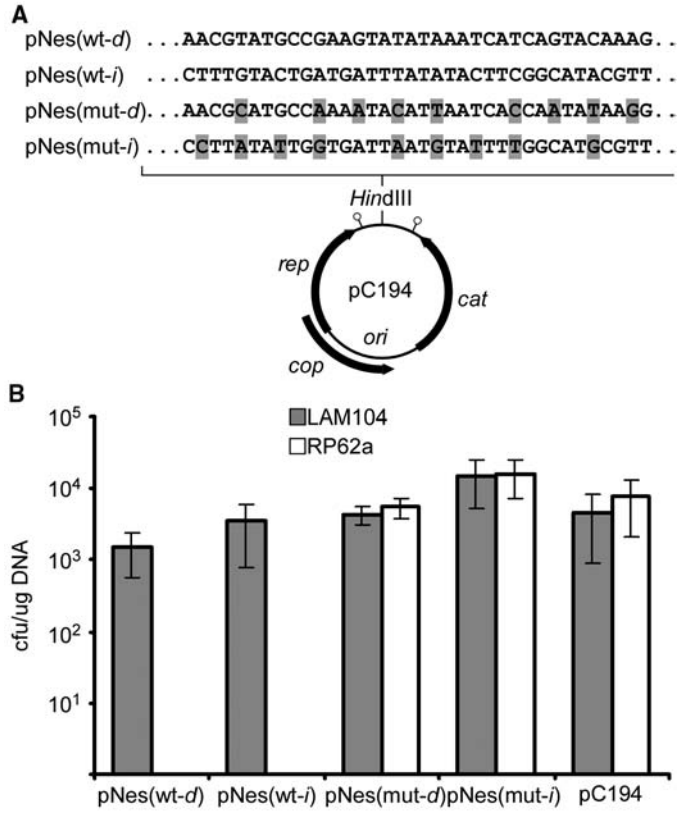

Fig. 3. Plasmid transformation is subject to CRISPR interference. (**A**) Introduction of the wild-type and mutant *nes* target sequences (mutations highlighted in gray) into the plasmid pC194 (*d*, direct insertion; *i*, inverted insertion). The origin of replication (*ori*) and protein-coding genes are indicated. Stem loops denote the *rep* and *cat* transcriptional terminators. (**B**) RP62a and the Δ*crispr* mutant LAM104 were transformed in triplicate, with the plasmids described in (A). Transformation efficiency was calculated as CFU/μg of DNA (mean ± SD).

The nature of the crRNA targeting event (RNA-RNA or RNA-DNA) is not known. The requirement for nickase activity only in the donor cell (*16*) implies that interference with *nes* mRNA and protein expression should block the ability of *S. epidermidis* RP62a to function as a donor. Instead, our data (Fig. 1 and fig. S1) indicate that the CRISPR locus limits the ability of *S. epidermidis* RP62a to act as a plasmid recipient and therefore suggest that *spc1*-directed interference does not target the *nes* transcript. Consistent with this, the orientation of *spc1* leads to the expression of a crRNA that is identical with, rather than complementary to, the *nes* mRNA target sequence, and we have found no evidence for the expression of RNA from the opposite strand (fig. S2) (*4*). Alternatively, the *spc1* crRNA may target the incoming DNA. To test this, we interrupted the target sequence of the pG0400 *nes* gene with the *orf142-I2* self-splicing group I intron from the staphylococcal Twort phage (*21*, *22*). The mutant conjugative plasmid pG0(I2) lacks an intact *spc1* target DNA sequence (Fig. 2A), but the *spc1* target sequence is regenerated in the *nes* mRNA after transcription and rapid splicing. When tested in conjugation assays, pG0(I2) was transferred to wild-type and Δ*crispr* strains with equal efficiencies (Fig. 2B). This observation reflects an evasion of CRISPR activity when the intron is present in the plasmid and therefore indicates that an intact target site is required in the *nes* DNA, but not mRNA, for interference to occur. To confirm that splicing is required for *nes* function, we tested the conjugation of pG0(dI2), a derivative of pG0(I2) containing a three-nucleotide deletion within the intron that inactivates self-splicing (*21*) (fig. S3A). The pG0(dI2) plasmid was unable to transfer to the RP62a strain (fig. S3B), which indicates a lack of nickase activity in the presence of the unspliced intron.

The requirement for *nes* transcription, splicing, and translation in the donor cell during conjugation (*16*), and our ability to obtain RP62a transconjugants with the intron-containing plasmid, allowed us to test the capacity of the CRISPR system to target intact spliced *nes* mRNA by using RP62a as a pG0(I2) donor. pG0(I2) conjugative transfer was just as efficient from RP62a as from the isogenic Δ*crispr* strain LAM104 (Fig. 2), which indicates that spliced functional *nes* mRNA (which must be present for conjugation to occur) is not targeted during CRISPR interference. Reverse transcription polymerase chain reaction assays confirmed the splicing of the *nes* pre-mRNA in RP62a cells carrying pG0(I2) (fig. S3C). Although our observations do not formally exclude an RNA targeting event that is somehow restricted to nascent, transient, unspliced transcripts, they provide strong evidence that DNA rather than mRNA is the likely crRNA target during CRISPR interference.

CRISPR activity against phage and conjugative plasmid DNA molecules suggests that CRISPR systems may also prevent plasmid DNA transformation. We therefore introduced pG0(wt) and pG0(mut) *nes*-target and -flanking sequences (200 base pairs) in either orientation into the staphylococcal plasmid pC194 (*23*), generating pNes(wt) and pNes(mut), respectively (Fig. 3A). Flanking DNA was included in the inserts to ensure the presence of any sequences outside of the target that may contribute to CRISPR interference (*24*). Plasmids were transformed by electroporation into wild-type RP62a and isogenic Δ*crispr* LAM104 strains. pC194 and both pNes(mut) plasmids were transformed into both strains, whereas the pNes(wt) plasmids were transformed only into the Δ*crispr* mutant (Fig. 3B). We also performed pNes(wt)/pNes(mut) mixed transformations of RP62a or LAM104 strains to test interference in an internally controlled fashion. Again, only pNes(mut) plasmids were recovered from RP62a transformants, whereas pNes(wt) and pNes(mut) plasmids were found in LAM104 transformant colonies (fig. S4). It remains to be established whether natural transformation, which involves the uptake of a single DNA strand (*25*), is subject to CRISPR interference. Nonetheless, our experiments suggest that CRISPR systems can counteract multiple routes of plasmid transfer.

These transformation data provide additional evidence that crRNAs target DNA molecules. First, interference occurred regardless of the insert orientation in pNes(wt); this, combined with the lack of compelling evidence for CRISPR-derived double-stranded RNA (fig. S2) (*4*, *6*, *7*), is consistent with *spc1* targeting either DNA strand rather than a unidirectional transcript. Second, the target sites in the pNes(wt) and pNes(mut) plasmids are located between the transcriptional terminators of the *rep* and *cat* genes (Fig. 3A) (*23*, *26*, *27*). This minimizes the likelihood that this region of the plasmid is even transcribed, which is consistent with its dispensability for plasmid maintenance (*23*, *28*).

Altogether, these data provide strong functional evidence that CRISPR interference acts at the DNA level and therefore differs fundamentally from the RNA interference (RNAi) phenomenon observed in eukaryotes and with which CRISPR activity was originally compared (*29*). A DNA targeting mechanism for CRISPR interference implies a means to prevent its action at the encoding CRISPR locus itself, as well as other potential chromosomal loci, such as prophage sequences. Little information exists to suggest how crRNAs would avoid targeting "self" DNA, although the role of flanking sequences during CRISPR interference (*24*) could contribute to target specificity. From a practical standpoint, the ability to direct the specific addressable destruction of DNA that contains any given 24- to 48-nucleotide target sequence could have considerable functional utility, especially if the system can function outside of its native bacterial or archaeal context. Furthermore, our results demonstrate that CRISPR function is not limited to phage defense, but instead encompasses a more general role in the prevention of HGT and the maintenance of genetic identity, as with restriction-modification systems. A primary difference between restriction-modification and CRISPR interference is that the latter can be programmed by a suitable effector crRNA. If CRISPR interference could be manipulated in a clinical setting, it would provide a means to impede the ever-worsening spread of antibiotic resistance genes and virulence factors in staphylococci and other bacterial pathogens.

References and Notes

1. I. Grissa, G. Vergnaud, C. Pourcel, *BMC Bioinformatics* **8**, 172 (2007).
2. R. Sorek, V. Kunin, P. Hugenholtz, *Nat. Rev. Microbiol.* **6**, 181 (2008).
3. R. Barrangou *et al.*, *Science* **315**, 1709 (2007).
4. S. J. Brouns *et al.*, *Science* **321**, 960 (2008).
5. D. H. Haft, J. Selengut, E. F. Mongodin, K. E. Nelson, *PLoS Comput. Biol.* **1**, e60 (2005).
6. T. H. Tang *et al.*, *Proc. Natl. Acad. Sci. U.S.A.* **99**, 7536 (2002).
7. T. H. Tang *et al.*, *Mol. Microbiol.* **55**, 469 (2005).
8. C. Hale, K. Kleppe, R. M. Terns, M. P. Terns, *RNA*, 10.1261/rna.1246808 (2008).
9. L. M. Weigel *et al.*, *Science* **302**, 1569 (2003).
10. E. Y. Furuya, F. D. Lowy, *Nat. Rev. Microbiol.* **4**, 36 (2006).
11. S. M. Lim, S. A. Webb, *Anaesthesia* **60**, 887 (2005).
12. F. D. Lowy, *N. Engl. J. Med.* **339**, 520 (1998).
13. C. von Eiff, G. Peters, C. Heilmann, *Lancet Infect. Dis.* **2**, 677 (2002).
14. Y. Q. Zhang *et al.*, *Mol. Microbiol.* **49**, 1577 (2003).
15. S. R. Gill *et al.*, *J. Bacteriol.* **187**, 2426 (2005).
16. M. W. Climo, V. K. Sharma, G. L. Archer, *J. Bacteriol.* **178**, 4975 (1996).
17. B. A. Diep *et al.*, *Lancet* **367**, 731 (2006).
18. T. M. Morton, J. L. Johnston, J. Patterson, G. L. Archer, *Antimicrob. Agents Chemother.* **39**, 1272 (1995).
19. Materials and methods are available as supporting material on *Science* Online.
20. B. N. Kreiswirth *et al.*, *Nature* **305**, 709 (1983).
21. B. L. Golden, H. Kim, E. Chase, *Nat. Struct. Mol. Biol.* **12**, 82 (2005).
22. M. Landthaler, D. A. Shub, *Proc. Natl. Acad. Sci. U.S.A.* **96**, 7005 (1999).
23. S. Horinouchi, B. Weisblum, *J. Bacteriol.* **150**, 815 (1982).
24. H. Deveau *et al.*, *J. Bacteriol.* **190**, 1390 (2008).
25. I. Chen, D. Dubnau, *Nat. Rev. Microbiol.* **2**, 241 (2004).
26. W. H. Byeon, B. Weisblum, *J. Bacteriol.* **158**, 543 (1984).
27. M. F. Gros, H. te Riele, S. D. Ehrlich, *EMBO J.* **8**, 2711 (1989).
28. M. F. Gros, H. te Riele, S. D. Ehrlich, *EMBO J.* **6**, 3863 (1987).
29. K. S. Makarova, N. V. Grishin, S. A. Shabalina, Y. I. Wolf, E. V. Koonin, *Biol. Direct* **1**, 7 (2006).

30. We are indebted to O. Schneewind (University of Chicago) for reagents and experimental assistance, B. Golden (Purdue University) for *orf142-2* intron constructs and advice, and members of our laboratory for discussions and comments on the manuscript. Results described here are being used in support of a patent filing by Northwestern University. L.A.M. is a fellow of The Jane Coffin Childs Memorial Fund for Medical Research. This work was supported by a grant (GM072830) from NIH to E.J.S.

Supporting Online Material

www.sciencemag.org/cgi/content/full/322/5909/1843/DC1
Materials and Methods
Figs. S1 to S4
Table S1
References

10 September 2008; accepted 14 November 2008
10.1126/science.1165771

Nascent RNA Sequencing Reveals Widespread Pausing and Divergent Initiation at Human Promoters

Leighton J. Core,* Joshua J. Waterfall,* John T. Lis†

RNA polymerases are highly regulated molecular machines. We present a method (global run-on sequencing, GRO-seq) that maps the position, amount, and orientation of transcriptionally engaged RNA polymerases genome-wide. In this method, nuclear run-on RNA molecules are subjected to large-scale parallel sequencing and mapped to the genome. We show that peaks of promoter-proximal polymerase reside on ~30% of human genes, transcription extends beyond pre-messenger RNA 3′ cleavage, and antisense transcription is prevalent. Additionally, most promoters have an engaged polymerase upstream and in an orientation opposite to the annotated gene. This divergent polymerase is associated with active genes but does not elongate effectively beyond the promoter. These results imply that the interplay between polymerases and regulators over broad promoter regions dictates the orientation and efficiency of productive transcription.

Transcription of coding and noncoding RNA molecules by eukaryotic RNA polymerases requires their collaboration with hundreds of transcription factors to direct and control polymerase recruitment, initiation, elongation, and termination. Whole-genome microarrays and ultra-high-throughput sequencing technologies enable efficient mapping of the distribution of transcription factors, nucleosomes, and their modifications, as well as accumulated RNA transcripts throughout genomes (*1*, *2*), thereby providing a global correlation of factors and transcription states. Studies using the chromatin immunoprecipitation assay coupled to genomic DNA microarrays (ChIP-chip) or to high-throughput sequencing (ChIP-seq) indicate that RNA polymerase II (Pol II) is present at disproportionately higher amounts near the 5′ end of many eukaryotic

genes relative to downstream regions (*3*–*6*). However, these techniques cannot determine whether Pol II is simply promoter-bound or engaged in transcription. Small-scale analyses using independent methods have shown that this distribution likely represents transcriptionally engaged Pol II that has accumulated between ~20 and 50 bases downstream of transcription start sites (TSSs) (*5*, *6*), indicating that transcription can be regulated at the stage of elongation as well as the recruitment and initiation stages (*7*). This promoter-proximal pausing or stalling (*8*) is proposed to be an important post-initiation, rate-limiting target for gene regulation (*7*, *9*).

Here, we present a global run-on-sequencing (GRO-seq) assay to map and quantify transcriptionally engaged polymerase density genome-wide. These measurements provide a snapshot of genome-wide transcription and directly evaluate promoter-proximal pausing on all genes. We used nuclear run-on assays (NRO) to extend nascent RNAs that are associated with transcriptionally engaged polymerases under conditions where new initiation is prohibited. To specifically isolate NRO-RNA, we added a ribonucleotide analog [5-bromouridine 5′-triphosphate (BrUTP)] to BrU-tag nascent RNA during the run-on step (fig. S1). The length of the polynucleotide was kept short, and the NRO-RNA was chemically hydrolyzed into short fragments (~100 bases) to facilitate high-resolution mapping of the polymerase origin at the time of assay (*8*). BrU-containing NRO-RNA was triple-selected through immunopurification with an antibody that is specific for this nucleotide analog, resulting in a 10,000-fold enrichment of the NRO-RNA pool that was determined to be >98% pure (*8*). A NRO-cDNA library was then prepared for sequencing from what represents the 5′ end of the fragmented, BrU-incorporated RNA molecule by using the Illumina high-throughput sequencing platform. The origin and the orientation of the RNAs and therefore the associated transcriptionally engaged polymerases were documented genome-wide by mapping the reads to the reference human genome (*8*).

In total, ~2.5×10^7 33–base pair (bp) reads were obtained from two independent replicates (*8*) prepared from primary human lung fibroblast (IMR90) nuclei, of which ~1.1×10^7 (44%) mapped uniquely to the human genome. Most reads (85.8%) align on the coding strand within boundaries of known RefSeq genes, human mRNAs, or expressed sequence tags (fig. S2). The number of transcriptionally active genes was determined by using an experimentally and computationally determined background of 0.04 reads per kilobase (*8*). We found 16,882 (68%) of RefSeq genes to be active ($P < 0.01$) compared with 8438 active genes found by a microarray experiment performed in the same cell line (*3*), reflecting, in part, the added sensitivity of sequencing platforms (*10*). Examination of several large regions shows that GRO-seq can differentiate between transcriptionally active and inactive regions in large chromosomal domains (Fig. 1). In addition, we are able to detect a generally low, but significant ($P < 0.01$ relative to background) amount of antisense transcription for 14,545 genes (58.7% of genes in the genome) (fig. S3).

Aligning the GRO-seq data relative to RefSeq TSSs shows that the density of reads peaks near the TSS in both sense (~50 bp) and antisense (~−250 bp) directions (see below) (Fig. 2A). Alignment of GRO-seq reads to annotated 3′ ends of genes reveals a broad peak that is maximal at about +1.5 kb and can extend greater than 10 kb downstream of polyadenylation (poly-A) sites (Fig. 2B). This peak distance is consistent with previous and recent estimates (*11*, *12*). A small peak followed by a sharp drop off is observed at the site of polyadenylation, likely representing the known 3′ cleavage before polyadenylation of the RNA (*13*).

To identify all genes that show a peak of engaged Pol II that is characteristic of promoter-proximal pausing, we assessed whether each gene showed significant enrichment of read density in the promoter-proximal region relative to the density in the body of each gene (*8*). The ratio of these densities is called the pausing index (*5*, *6*, *8*), and significant pausing indices range from 2 to 10^3 (fig. S4). Within the defined promoter region, 7057 genes have a significant enrichment of GRO-seq reads relative to the body of the gene ($P < 0.01$), representing 28.3% of all genes (41.7% of active genes). Comparison of paused genes to either microarray expression or GRO-seq data revealed four classes of genes: class I, not paused and active; class II, paused and active; class III, paused and not active; and class IV, inactive (not paused and not active) (Fig. 3). Class III was severely depleted when we used GRO-seq to classify gene activity because GRO-seq provides a more sensitive measure of gene activity. Given the low signal at the promoters of the few genes left within this class, they are likely to be classified as active with deeper sequencing. Therefore, the overwhelming majority of genes with a paused polymerase also produce significant transcription throughout the gene, albeit often to quantities not detectable by expression microarrays. A recent comparison of Pol II ChIP-seq data to RNA-seq also supports the view that nearly all genes that are bound by Pol II produce full-length transcripts (*10*).

The density of polymerases within the promoter-proximal region generally correlates with the level of gene activity when all genes (Fig. 4A) or only genes with a paused polymerase are considered (fig. S5). Whereas nearly all paused genes show significant full-length activity by GRO-seq, the pausing index inversely corre-

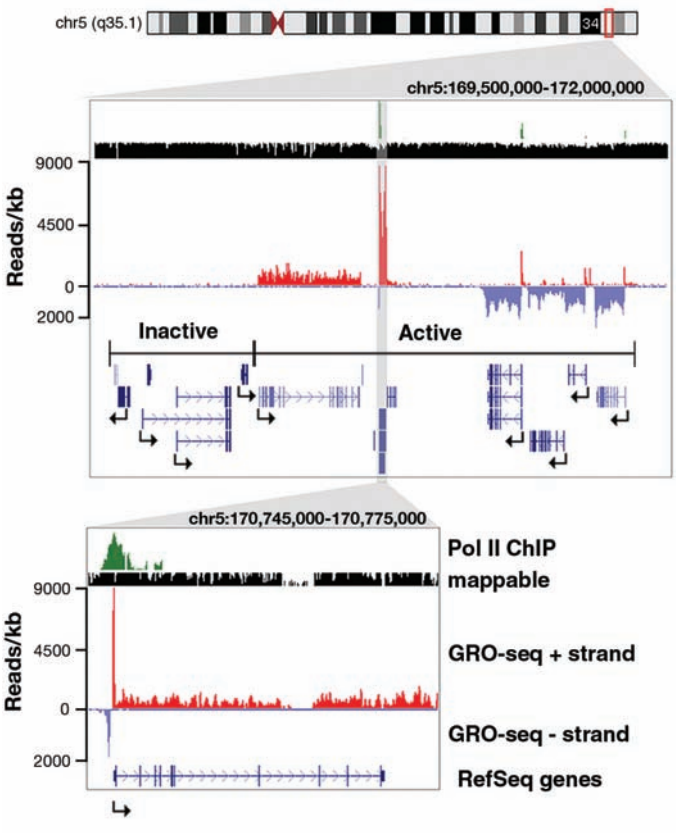

Fig. 1. Sample of GRO-seq data view on the University of California at Santa Cruz (UCSC) genome browser. A 2.5-Mb region on chromosome 5 showing GRO-seq reads aligned to the genome at 1-bp resolution, followed by an up-close view around the *NPM1* gene. Pol II ChIP results (*3*) are shown in green; mappable regions, black; GRO-seq reads on the plus strand (left to right), red; GRO-seq reads on the minus strand (right to left), light blue; RefSeq gene annotations, dark blue.

Department of Molecular Biology and Genetics, Cornell University, Ithaca, NY 14853, USA.

*These authors contributed equally to this work.
†To whom correspondence should be addressed. E-mail: jtl10@cornell.edu

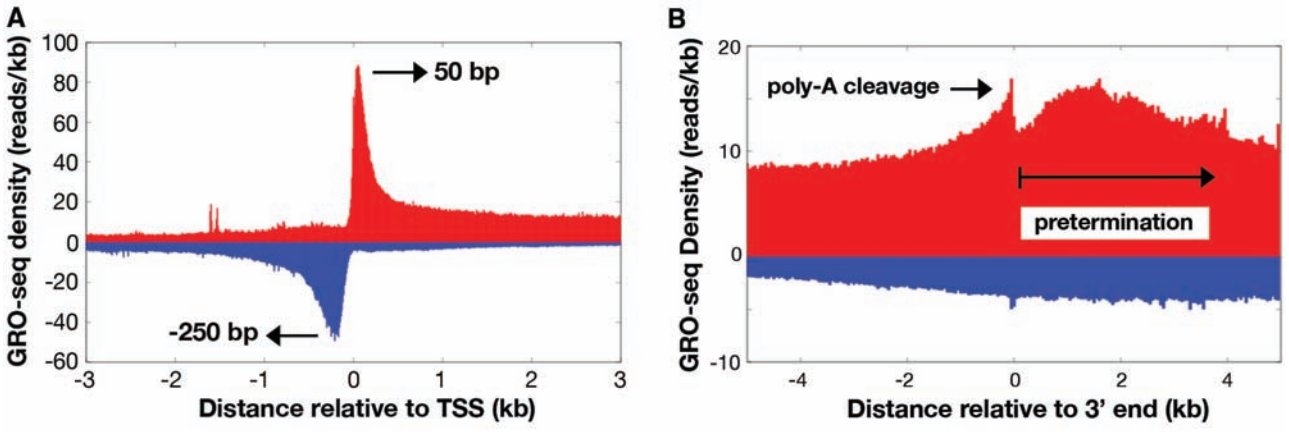

Fig. 2. Alignment of GRO-seq reads to TSSs and 3′ ends. (**A**) GRO-seq reads aligned to Ref-seq TSSs in 10-bp windows in both sense (red) and antisense (blue) directions relative to the direction of gene transcription. (**B**) GRO-seq reads flanking the 3′ ends of genes. The sharp peak coincides with the new 5′ end created after cleavage at the poly-A site. Polymerase density extends considerably downstream before termination.

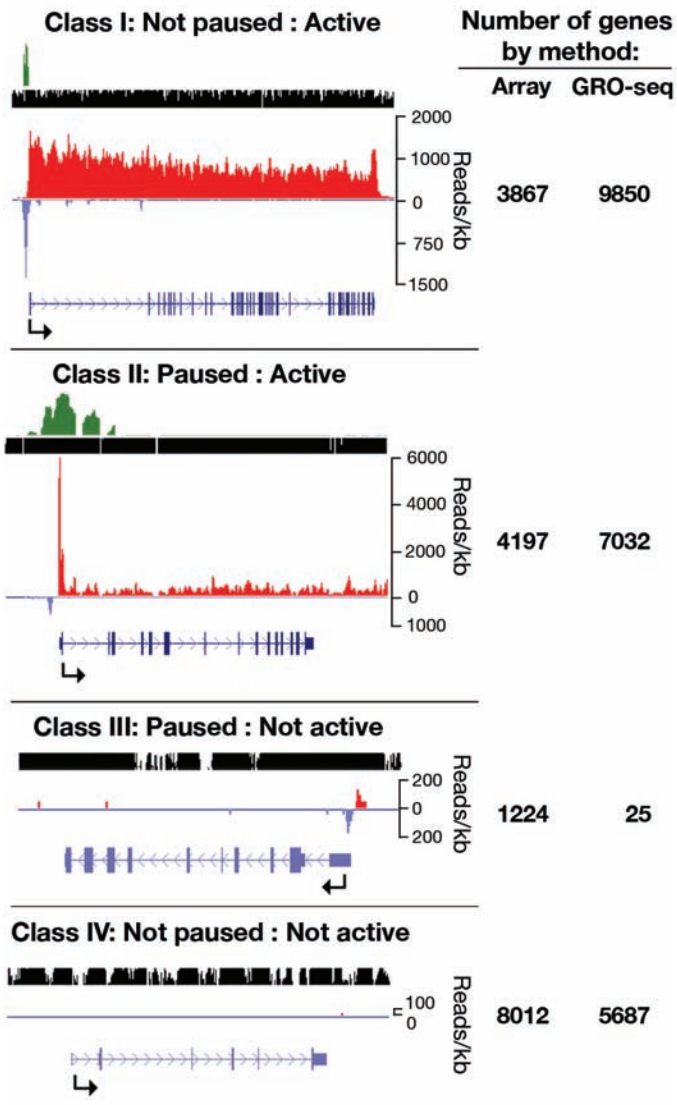

Fig. 3. Comparison of pausing with gene activity. Four classes of genes are found when comparing genes with a paused polymerase and transcription activity either by microarray or GRO-seq density in the downstream portions of genes. An example of each class is shown, with tracks shown in the UCSC genome browser as in Fig. 1. The gene names, pausing index, and *P* value, from top to bottom, respectively, are as follows: *TRIO*, 1.1, 0.62; *FUS*, 41, 2.8×10^{-43}; *IZUMO1*, 410, 7.6×10^{-3}; and *GALP* (which has no reads and therefore no pausing index). The number of genes represented in each class is shown to the right.

lates with gene activity (Fig. 4B). Considering that pausing is observed when Pol II enters a pause site faster than the rate of escape from pausing (*9*), this inverse correlation is consistent with the hypothesis that highly transcribed, but paused genes appear to be controlled, at least in part, by increasing the rate at which Pol II escapes the pause site and enters productive elongation (*8*).

A prominent and unexpected feature of the GRO-seq profiles around TSSs is the robust signal from an upstream, divergent, engaged polymerase. RNAs generated by these divergent polymerases can be identified at low concentrations when small RNAs are isolated from whole cells (*14*). These divergent polymerases cannot be accounted for by the 10% of known bidirectional promoters that are less than 1 kb apart (*15*) (fig. S6). We found that 13,633 genes (55% of all genes, 77% of active genes) display significant divergent transcription within 1 kb upstream of sense-oriented promoter-proximal peaks ($P < 0.001$), indicating that the number of bidirectional promoters exceeds even the highest estimates (*16*, *17*). However, because it appears that the majority of these promoters produce mRNAs in only one direction (see below), we refer to this class of promoters as divergent. Although the top 10% of active genes have, on average, a slightly larger promoter-proximal than divergent peak (Fig. 3D), amounts of divergent transcription generally correlate with both the promoter-proximal signal (fig. S7) and the transcription level of the associated gene (Fig. 4C). Thus, divergent transcription is a mark for most active promoters.

Gene activity, pausing, and divergent transcription correlate with each other and with promoters containing a CpG island. These four characteristics co-occur significantly more often than would be expected by chance ($P < 10^{-52}$) (table S1). Previous mapping of capped mRNA transcripts has shown that at CpG island promoters initiation occurs broadly over hundreds of base pairs (*18*), and GRO-seq shows that polymerases initiate and accumulate on this large class of promoters in both orientations.

Does existing ChIP-chip data (*3*) show any indication of the divergent peak of polymerase? Manual inspection of a number of genes and comparison with composite profiles aligned to TSSs show that the Pol II ChIP peak at promoters

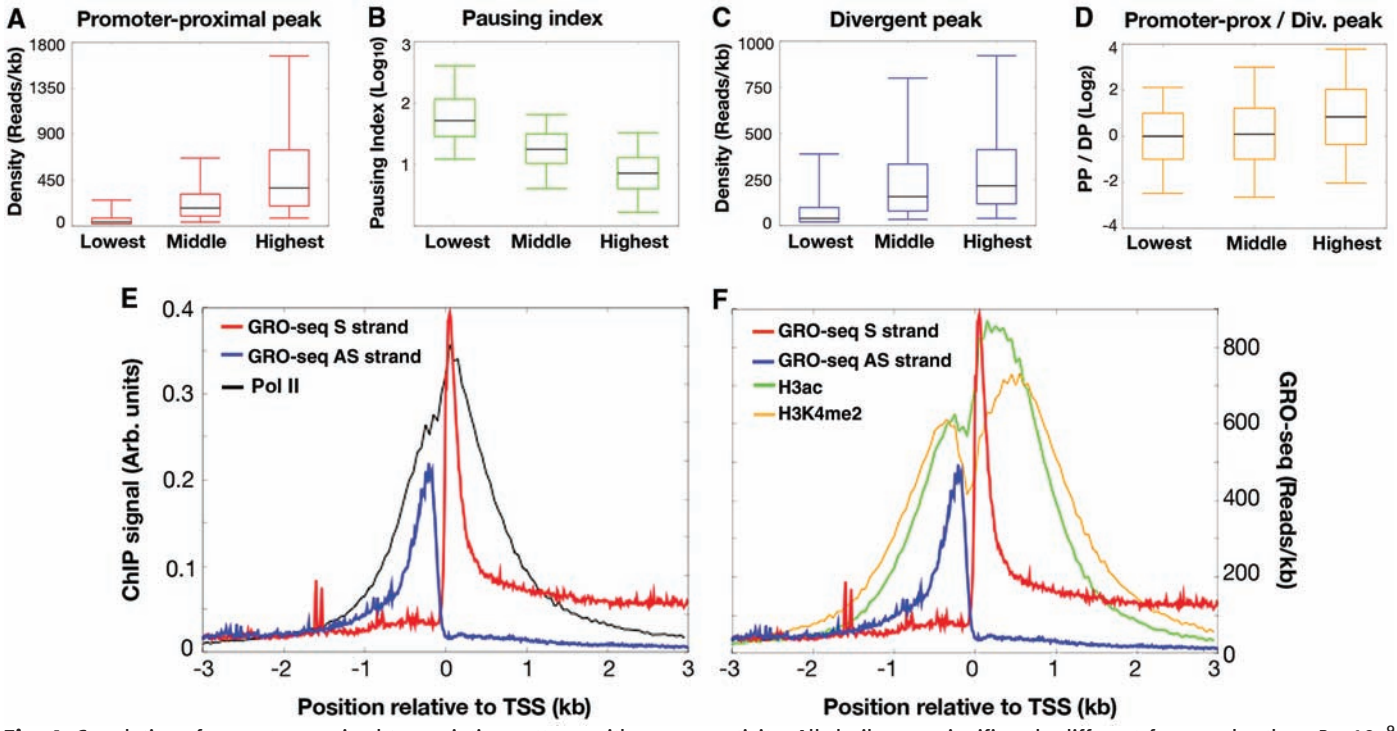

Fig. 4. Correlation of promoter-proximal transcription patterns with gene activity. (**A** to **D**) Box plots (each showing the fifth, 25th, 50th, 75th, and 95th percentiles) that show the relationship of promoter-proximal (PP) sense peaks (red), divergent peaks (DP) (blue), pausing indices (green), and PP/DP ratios (orange) to the top, middle, and bottom deciles of gene activity. All deciles are significantly different from each other: $P < 10^{-9}$ for all comparisons except between the lowest and the middle deciles in (D) ($P < 10^{-3}$). (**E**) ChIP profiles of Pol II and GRO-seq sense (S) and antisense (AS) strand reads aligned to TSSs. (**F**) ChIP profiles of H3ac and H3K4me2 and GRO-seq aligned to TSSs.

is accounted for by the two divergent peaks uncovered by GRO-seq (Figs. 1B and 4E). Higher-resolution ChIP-seq data in different cell lines has identified Pol II molecules upstream of promoters that were proposed to be in the same orientation of the annotated gene; however, these instead are likely to represent the divergent promoters identified by GRO-seq (*10*). Additionally, active promoters are typically marked by histone modifications such as di- and trimethylation of H3-Lys^4 (H3K4me2 and H3K4me3) as well as acetylation of histone H3 and H4 (H3ac and H4ac). These modifications show a bimodal distribution around TSSs, with the trough representing a nucleosome-free region encompassing the TSS (*3*, *4*, *19*). Comparison of available H3ac and H3K4me2 data in this cell line (*3*) with GRO-seq suggests that both upstream and downstream peaks of these histone modifications are associated with active transcription, with each peak of histone modifications being adjacent and downstream of an engaged polymerase (Fig. 4F) (*8*). Other studies have shown that histone modifications associated with transcription elongation (e.g., H3K36me3 and H3K79me3) do not associate in a bimodal fashion around TSSs (*4*, *19*). This and the lack of divergent GRO-seq reads further upstream (fig. S8) indicate that the majority of promoters experience initiation in the upstream direction but that these divergent polymerases do not productively elongate transcripts. Thus, promoters can distinguish polymerase in the forward versus the reverse direction.

We envision several possible functions for divergent transcription. First, the act of transcription itself could be crucial for granting access of transcription factors to control elements that reside upstream of core promoters, possibly by creating a barrier that prevents nucleosomes from obstructing transcription factor binding sites (*20*, *21*). Second, as proposed by Seila *et al.* (*14*), negative supercoiling produced in the wake of transcribing polymerases could facilitate initiation in these regions. Third, these short nascent RNAs could themselves be functional, through either Argonaute-dependent (*22*) or -independent (*23*) pathways. Upcoming challenges will be to decipher whether the widespread transcriptional activity that lies upstream but divergent from the direction of coding genes positively or negatively regulates transcription output and how promoter or unknown DNA elements are designed to distinguish between productive elongation in one direction versus the other.

References and Notes

1. ENCODE Project Consortium *et al.*, *Nature* **447**, 799 (2007).
2. B. Wold, R. M. Myers, *Nat. Methods* **5**, 19 (2008).
3. T. H. Kim *et al.*, *Nature* **436**, 876 (2005).
4. M. G. Guenther, S. S. Levine, L. A. Boyer, R. Jaenisch, R. A. Young, *Cell* **130**, 77 (2007).
5. G. W. Muse *et al.*, *Nat. Genet.* **39**, 1507 (2007).
6. J. Zeitlinger *et al.*, *Nat. Genet.* **39**, 1512 (2007).
7. A. Saunders, L. J. Core, J. T. Lis, *Nat. Rev. Mol. Cell Biol.* **7**, 557 (2006).
8. Materials and methods are available as supporting material on *Science* Online.
9. L. J. Core, J. T. Lis, *Science* **319**, 1791 (2008).
10. M. Sultan *et al.*, *Science* **321**, 956 (2008); published online 3 July 2008 (10.1126/science.1160342).
11. N. J. Proudfoot, *Trends Biochem. Sci.* **14**, 105 (1989).
12. Z. Lian *et al.*, *Genome Res.* **18**, 1224 (2008).
13. N. Proudfoot, *Curr. Opin. Cell Biol.* **16**, 272 (2004).
14. A. C. Seila *et al.*, *Science* **322**, 1849 (2008); published online 4 December 2008 (10.1126/science.1162253).
15. N. D. Trinklein *et al.*, *Genome Res.* **14**, 62 (2004).
16. P. Kapranov *et al.*, *Science* **316**, 1484 (2007); published online 16 May 2007 (10.1126/science.1138341).
17. A. Rada-Iglesias *et al.*, *Genome Res.* **18**, 380 (2008).
18. P. Carninci *et al.*, *Nat. Genet.* **38**, 626 (2006).
19. A. Barski *et al.*, *Cell* **129**, 823 (2007).
20. T. N. Mavrich *et al.*, *Nature* **453**, 358 (2008).
21. D. A. Gilchrist *et al.*, *Genes Dev.* **22**, 1921 (2008).
22. J. Han, D. Kim, K. V. Morris, *Proc. Natl. Acad. Sci. U.S.A.* **104**, 12422 (2007).
23. X. Wang *et al.*, *Nature* **454**, 126 (2008).

24. We gratefully thank C. Haudenschild for advice on construction of our libraries and for performing the initial alignments, Q. Sun and L. Ponnala for aligning the trimmed reads, A. Siepel for computational and statistical discussion, and the members of the Lis lab for suggestions regarding this work. The work was funded by NIH grant GM25232 to J.T.L. The data discussed in this publication have been deposited in National Center for Biotechnology Information's Gene Expression Omnibus under accession number GSE13518. The authors are filing a patent based on the work in this paper.

Supporting Online Material

www.sciencemag.org/cgi/content/full/1162228/DC1
Materials and Methods
SOM Text
Figs. S1 to S26
Tables S1 to S3
References

24 June 2008; accepted 7 November 2008
Published online 4 December 2008;
10.1126/science.1162228
Include this information when citing this paper.

Divergent Transcription from Active Promoters

Amy C. Seila,[1]* J. Mauro Calabrese,[1,2]*† Stuart S. Levine,[3] Gene W. Yeo,[4]‡ Peter B. Rahl,[3] Ryan A. Flynn,[1] Richard A. Young,[2,3] Phillip A. Sharp[1,2]§

Transcription initiation by RNA polymerase II (RNAPII) is thought to occur unidirectionally from most genes. Here, we present evidence of widespread divergent transcription at protein-encoding gene promoters. Transcription start site–associated RNAs (TSSa-RNAs) nonrandomly flank active promoters, with peaks of antisense and sense short RNAs at 250 nucleotides upstream and 50 nucleotides downstream of TSSs, respectively. Northern analysis shows that TSSa-RNAs are subsets of an RNA population 20 to 90 nucleotides in length. Promoter-associated RNAPII and H3K4-trimethylated histones, transcription initiation hallmarks, colocalize at sense and antisense TSSa-RNA positions; however, H3K79-dimethylated histones, characteristic of elongating RNAPII, are only present downstream of TSSs. These results suggest that divergent transcription over short distances is common for active promoters and may help promoter regions maintain a state poised for subsequent regulation.

Transcription of DNA by RNAPII is an orchestrated process subject to regulation at numerous levels: binding of RNAPII to the promoter, transcription initiation, and elongation. These phases and their transitions require concerted action by many protein complexes and are accompanied by changes in local chromatin structure (*1*).

When examining short RNA expression in murine embryonic stem (ES) cells, we noted the presence of ~20 nucleotide (nt)–long RNAs located near the transcription start site (TSS) of protein-encoding genes (*2*). To further investigate these low abundance RNAs, 8.4 million sequence reads were analyzed from several murine short RNA cDNA libraries: 7.3 million were derived from ES cells and 1.1 million from differentiated cell types (*3*, *4*). About 42,000 of these reads, referred to as TSSa-RNAs, uniquely mapped within 1.5 kb of protein-encoding gene TSSs (Fig. 1 and table S1). A single TSS frequently had more than one associated TSSa-RNA (Fig. 1B). TSSa-RNAs were associated with more than half of all mouse genes and were detected in all cell types examined (fig. S1). TSSa-RNAs were also found in ES cells lacking Dicer, an RNase III enzyme necessary for microRNA processing, suggesting that they are not Dicer products (fig. S1F). Sequenced TSSa-RNAs were 16 to 30 nt long, with a mean length of 20 nt (fig. S2).

TSSa-RNAs surround promoters in nonrandom, divergent orientations. Sense TSSa-RNAs map downstream of the associated promoter, overlapping genic transcripts and peaking in abundance between +0 and +50 nt downstream of the TSS. Forty percent of TSSa-RNAs map upstream of the TSS and are oriented in the antisense direction relative to their associated genes, peaking between nucleotides –100 and –300 (Fig. 1A). Sense and antisense TSSa-RNAs associated with overlapping sets of 8115 and 6331 gene promoters, respectively (table S2). This distribution is not dependent on mapping to either head-to-head gene pairs or genes with multiple TSSs, nor is it seen in intergenic regions or at gene 3′ ends (figs. S3 and S4).

A majority (67%) of ES cell genes with two or more TSSa-RNAs have both sense and antisense species; thus, individual TSSs produce both RNA subtypes (fig. S3). Based on their direction and position relative to TSSs, we hypothesize that sense and antisense TSSa-RNAs arise from divergent transcription, defined as nonoverlapping transcription initiation events that proceed in opposite directions from the TSS. Divergent transcription is likely a common feature of mammalian TSSs, given the presence of TSSa-RNAs in all cell types examined in this study.

TSSa-RNAs associate with genes expressed at varying levels in ES cells but were biased toward higher levels of gene expression. TSSa-RNAs were found at the majority of highly and moderately expressed genes (Fig. 2 and fig. S5), and 80% associate with promoters having high CpG dinucleotide frequency (CpG islands) (table S2). Additionally, the number of TSSa-RNA observations per gene correlated positively with gene expression levels, with a notable increase in the sense:antisense ratio found at the highest levels of expression (Fig. 2B). This increase suggests that a fraction of these reads from the most active genes arise from mRNA turnover.

Whereas typical RNAPII transcripts have a bias toward G at their 5′ ends, TSSa-RNAs show a nearly random 5′-nucleotide distribution (*4*, *5*) (table S3). This significant distribution difference suggests that the 5′-most base of the TSSa-RNAs does not represent the initial nucleotide transcribed by RNAPII.

Based on sequencing frequency, ~20 nt TSSa-RNAs are estimated to be present at ~1 molecule per 10 cells (*4*). Therefore, an enrichment procedure was developed to determine the nature of the short RNAs surrounding TSSa-RNA–associated genes. Sequenced 21-nt sense and antisense TSSa-RNAs associated with Ring finger protein 12

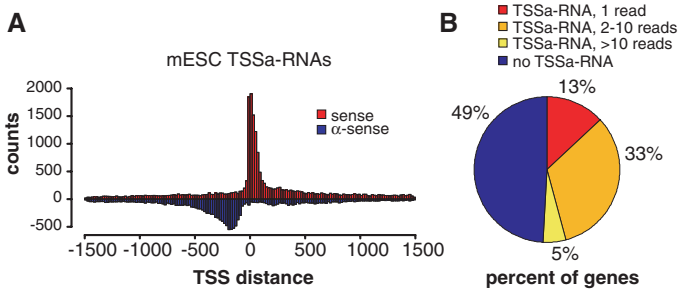

Fig. 1. The distribution of TSSa-RNAs around TSSs shows divergent transcription. (**A**) Histogram of the distance from each TSSa-RNA to all associated gene TSSs (*4*). Counts of TSSa-RNA 5′ positions relative to gene TSSs are binned in 20-nt windows. Red and blue bars represent bins of sense and antisense TSSa-RNAs, respectively. (**B**) Percentage of annotated mouse genes with indicated number of associating TSSa-RNAs.

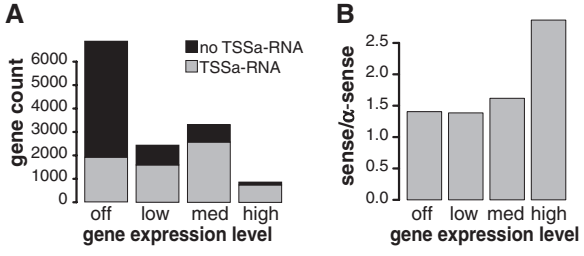

Fig. 2. In ES cells, TSSa-RNA associated genes are primarily expressed. (**A**) ES cell expression data separated into four bins based on Log2 signal intensity. Off, 1 to 4; low, 5 to 8; med, 6 to 12; and high ≥ 13 (*13*). Gene counts for each expression bin are shown. (**B**) Ratio of sense to antisense reads in each expression bin.

[1]Koch Institute, Massachusetts Institute of Technology, Cambridge, MA 02139, USA. [2]Department of Biology, Massachusetts Institute of Technology, Cambridge, MA 02139, USA. [3]Whitehead Institute for Biomedical Research, 9 Cambridge Center, Cambridge, MA 02142, USA. [4]Salk Institute, Crick-Jacobs Center for Theoretical and Computational Biology, 10010 North Torrey Pines Road, La Jolla, CA 92037, USA.

*These authors contributed equally to this work.
†Present address: Department of Genetics and the Carolina Center for Genome Sciences, University of North Carolina, Chapel Hill, NC 27599, USA.
‡Present address: Department of Cellular and Molecular Medicine, University of California, San Diego, CA 92037, USA.
§To whom correspondence should be addressed. E-mail: sharppa@mit.edu

(Rnf12) or Coiled-coil domain containing 52 (Ccdc52) transcripts, respectively, were not detected as unique species in ES cells. Instead, species between 20 and 90 nt were detected at levels estimated to be greater than 10 molecules per cell (*4*) (Fig. 3, B and D). Similar sized fragments were not found in HeLa cell RNA samples using the same sequence probes, demonstrating specificity of the procedure (Fig. 3, B and D). Northern analysis for two other TSSa-RNA–associated genes showed similar results (figs. S6 and S7). We suggest that 20 to 90 nt transcripts are the dominant short RNA species from these promoters and that sequenced TSSa-RNAs represent no more than 10% of promoter-associated transcripts.

To further classify promoters that produce TSSa-RNAs, we examined their local chromatin environment using chromatin immunoprecipitation coupled with DNA sequencing (ChIP-seq) (*3*, *4*). TSSa-RNA–associated promoters are enriched in bound RNAPII and histone H3 lysine 4 trimethylated (H3K4me3) chromatin in ES cells (Fig. 4A). About 90% of TSSa-RNA–associated genes show H3K4me3-modified nucleosomes at their promoters, as compared to ~60% for all mouse genes (Fig. 4A). TSSa-RNA–associated genes also show a ~3-fold enrichment in promoter proximal RNAPII over all genes (Fig. 4A). In contrast, TSSa-RNA–associated genes are depleted of the Polycomb component Suz12, a known transcriptional repressor thought to help maintain pluripotency by repressing developmental regulators (Fig. 4A) (*6*, *7*).

Composite profiles of ChIP-seq data were used to determine RNAPII and histone modification positions relative to TSS, revealing a correlation with sense and antisense TSSa-RNA peaks. In such analyses, the midpoint between the forward and reverse ChIP-seq read maxima defines the average DNA binding site for a factor (Fig. 4B) (*3*). At TSSa-RNA–associated genes, two distinct peaks for RNAPII are detectable with a spacing of several hundred base pairs (Fig. 4, C and D). A sharp RNAPII peak just downstream of the TSS lies directly over the sense TSSa-RNA peak (Fig. 4D). A second RNAPII peak, upstream of the first, is more diffuse but again lies directly over the antisense TSSa-RNA peak (Fig. 4D). The co-occurrence with antisense TSSa-RNAs strongly suggests that the upstream peak of RNAPII is indicative of divergent transcription rather than sense initiation upstream of the TSS, as has been proposed (*8*).

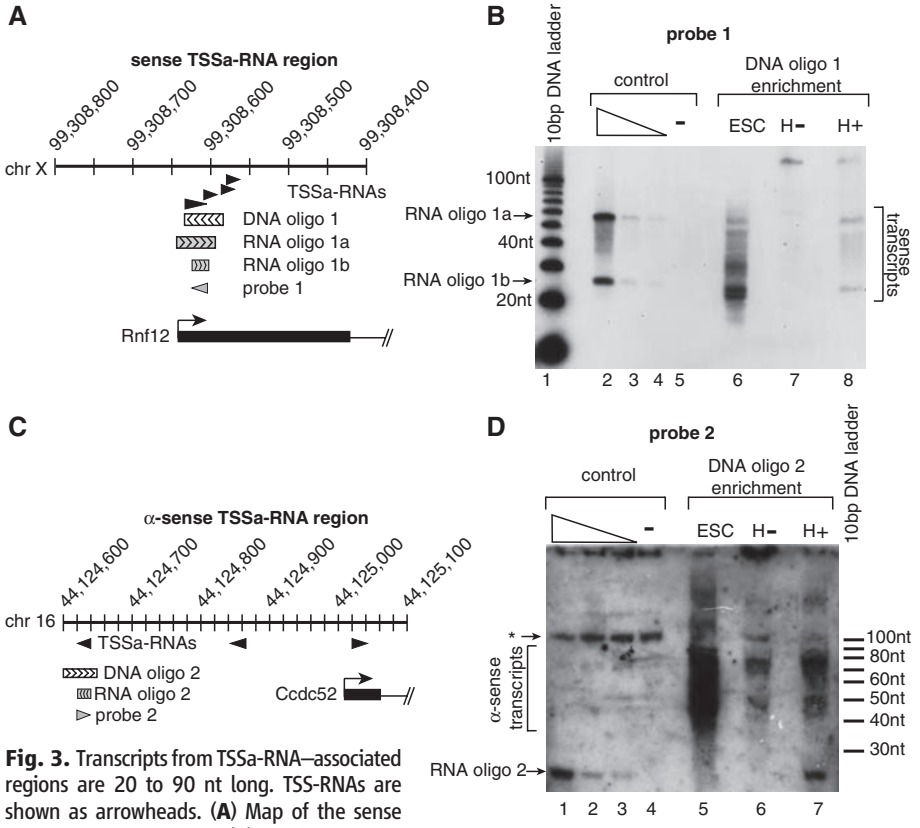

Fig. 3. Transcripts from TSSa-RNA–associated regions are 20 to 90 nt long. TSS-RNAs are shown as arrowheads. (**A**) Map of the sense TSSa-RNA Rnf12 region. (**B**) Northern analysis for Rnf12 sense TSSa-RNA using probe 1 in (A). Lane 1, 10–base pair ladder. Lanes 2 to 5, detection controls with 15, and 1.5, 0.75, and 0 fMol, respectively, of RNA oligo 1a+1b in (A). Lanes 6 to 8, material recovered from ES RNA (ESC), HeLa RNA (H-), and HeLa RNA + 15 fMol RNA oligo 1a+1b (H+), respectively, using DNA oligo 1 in (A). (**C**) Map of the antisense TSSa-RNA Ccdc52 region. (**D**) Northern analysis for the Ccdc52 antisense TSSa-RNA using probe 2 in C. Lanes 1 to 7 are as lanes 2 to 8 in (B), except using RNA oligo 2 for controls and DNA oligo 2 in (C) for enrichment. Bracket marks ESC-specific transcripts; * marks background band.

H3K4me3-modified nucleosome alignment with respect to the TSS shows peaks flanking the TSSa-RNA and RNAPII maxima, consistent with H3K4 methylation at the nucleosomes immediately upstream and downstream of TSSs (Fig. 4, C and D). These flanking peaks suggest that divergently paused RNAPII complexes may recruit H3K4 methyltransferase activity to mark active promoter boundaries. In contrast to the dual peaks of RNAPII and H3K4me3 surrounding TSSs, H3K79me2, a chromatin mark found over RNAPII elongation regions, is solely enriched in the direction of productive transcription (Fig. 4D). These observations suggest that although divergent transcription initiation is widespread, productive elongation by RNAPII occurs primarily unidirectionally, downstream of TSSs.

Sense and antisense TSSa-RNAs with bound RNAPII are found at a large number of mammalian promoters, suggesting that divergent initiation by RNAPII at TSSs is a general feature of transcriptional processes. Supporting this hypothesis, genome-wide nuclear run-on assays by Core *et al*. show that divergent transcripts arise from transcriptionally engaged RNAPII at many genes in human fibroblasts (*9*).

Because TSSa-RNAs do not represent the 5′ end of transcripts, they likely mark regions of RNAPII pausing rather than initiation. Pausing of RNAPII 20 to 50 nt downstream of the TSS has been observed at many genes, most notably *Drosophila* Hsp^{70}, and is thought to maintain a chromatin structure permissive to transcription initiation (*10*, *11*). The results presented here suggest the presence of antisense paused RNAPII upstream of many TSSs. The position of paused, antisense RNAPII centers around 250 nt upstream of the TSS, as inferred by the presence of bound RNAPII and antisense short RNAs colocalizing at this location. Considering that chromatin marks associated with elongating RNAPII are only found downstream of TSSs, it appears that antisense RNAPII frequently does not elongate after TSSa-RNA production (Fig. 4D) (*12*–*14*). This suggests the existence of an undefined mechanism that discriminates between the sense and antisense polymerase for productive elongation.

RNAPII initiation complex polarity at promoters is thought to be established by TFIID/TBP complex binding together with TFIIB (*15*). RNAPII/TFIIF binding and DNA unwinding by the TFIIH helicase then gives rise to the open preinitiation complex (*10*). The prevalence of divergently oriented RNAPII at most promoters suggests a more complex situation. We hypothesize that transcription factors first nucleate a sense-oriented preinitiation complex at the TSS. Transcription by this complex generates at least two signals that could subsequently promote upstream antisense paused polymerase. First, the RNAPII carboxy-terminal domain and other initiation complex components can activate transcription when tethered to DNA, suggesting

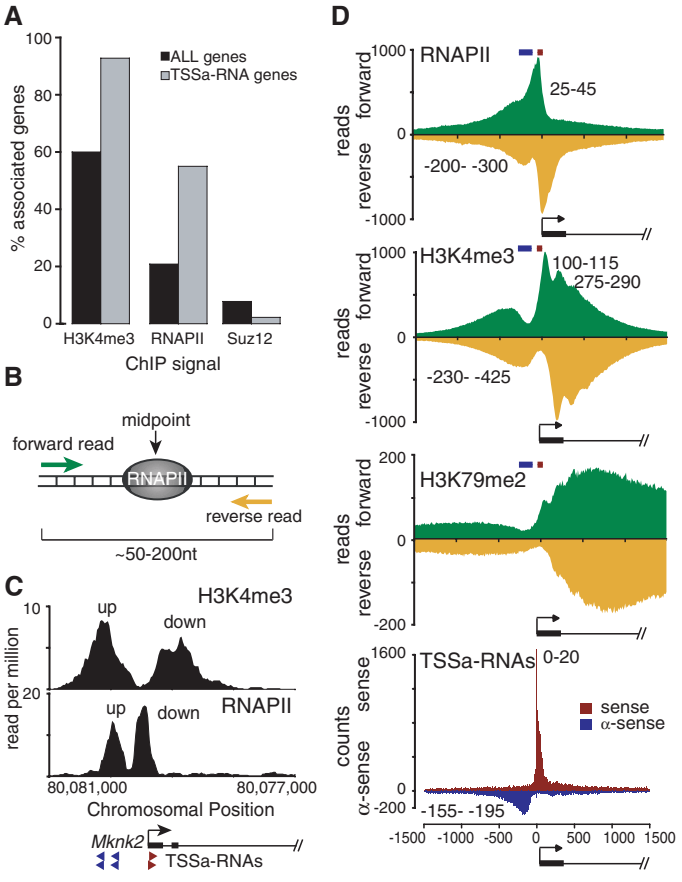

Fig. 4. Relationship between TSSa-RNAs, chromatin structure, and RNAPII. (**A**) Percentage of genes associated with H3K4me3, RNAPII and Suz12. ALL, all mouse genes. *t* test gives $P < 2.2 \times 10^{-16}$ for all marks. (**B**) Schematic of factor binding site mapping using Chip-seq reads. (**C**) Chromosomal position versus enrichment ratio for H3K4me3-modified nucleosomes and RNAPII for representative gene Mknk2. TSSa-RNAs are shown as arrowheads. (**D**) Metagene profiles for forward (green) and reverse (yellow) reads for ChIP-seq data (first three panels) and TSSa-RNAs from the sense (red) and antisense (blue) strand (bottom panel). Panels are aligned at the TSS. The TSS is denoted by the arrow. Black numbers on the profiles define the midpoint between forward and reverse peaks. Red and blue bars above the ChIP-seq profiles represent sense and antisense TSSa-RNA peak maxima.

that the sense complex may promote antisense preinitiation complex formation in the upstream region (*16*). Second, as RNAPII elongates the sense transcript, negative supercoiling of the DNA will occur upstream, perhaps promoting the antisense initiation process (*17*). This divergent transcription could structure chromatin and nascent RNA at the TSS for subsequent regulation.

References and Notes

1. G. Orphanides, D. Reinberg, *Cell* **108**, 439 (2002).
2. J. M. Calabrese, A. C. Seila, G. W. Yeo, P. A. Sharp, *Proc. Natl. Acad. Sci. U.S.A.* **104**, 18097 (2007).
3. A. Marson *et al.*, *Cell* **134**, 521 (2008).
4. Materials and methods are available as supporting material on *Science* Online.
5. P. Carninci *et al.*, *Science* **309**, 1559 (2005).
6. L. A. Boyer *et al.*, *Nature* **441**, 349 (2006).
7. T. I. Lee *et al.*, *Cell* **125**, 301 (2006).
8. M. Sultan *et al.*, *Science* **321**, 956 (2008).
9. L. J. Core, J. J. Waterfall, J. T. Lis, *Science* **322**, 1845 (2008); published online 4 December 2008 (10.1126/science.1162228).
10. A. Saunders, L. J. Core, J. T. Lis, *Nat. Rev. Mol. Cell Biol.* **7**, 557 (2006).
11. D. A. Gilchrist *et al.*, *Genes Dev.* **22**, 1921 (2008).
12. M. G. Guenther, S. S. Levine, L. A. Boyer, R. Jaenisch, R. A. Young, *Cell* **130**, 77 (2007).
13. A. Barski *et al.*, *Cell* **129**, 823 (2007).
14. T. S. Mikkelsen *et al.*, *Nature* **448**, 553 (2007).
15. A. R. Kays, A. Schepartz, *Chem. Biol.* **7**, 601 (2000).
16. H. Xiao, J. T. Lis, H. Xiao, J. Greenblatt, J. D. Friesen, *Nucleic Acids Res.* **22**, 1966 (1994).
17. L. F. Liu, J. C. Wang, *Proc. Natl. Acad. Sci. U.S.A.* **84**, 7024 (1987).

18. We thank G. Zheng, C. Whittaker, S. Hoersch, and A. F. Seila. A.C.S. was supported by NIH postdoctoral fellowship 5-F32-HD051190 and G.W.Y. by the Crick-Jacobs Center for Computational Biology. This work was supported by NIH grants RO1-GM34277 and HG002668, NCI grant PO1-CA42063, and the NCI Cancer Center Support (core) grant P30-CA14051. The data discussed in this publication have been deposited in National Center for Biotechnology Information's Gene Expression Omnibus under accession numbers GSE13483 and GSE12680.

Supporting Online Material

www.sciencemag.org/cgi/content/full/1162253/DC1
Materials and Methods
Figs. S1 to S7
Tables S1 to S5
Data Files
References

24 June 2008; accepted 12 November 2008
Published online 4 December 2008;
10.1126/science.1162253
Include this information when citing this paper.

RNA Exosome Depletion Reveals Transcription Upstream of Active Human Promoters

Pascal Preker,[1] Jesper Nielsen,[2] Susanne Kammler,[1]* Søren Lykke-Andersen,[1] Marianne S. Christensen,[1] Christophe K. Mapendano,[1] Mikkel H. Schierup,[2] Torben Heick Jensen[1]†

Studies have shown that the bulk of eukaryotic genomes is transcribed. Transcriptome maps are frequently updated, but low-abundant transcripts have probably gone unnoticed. To eliminate RNA degradation, we depleted the exonucleolytic RNA exosome from human cells and then subjected the RNA to tiling microarray analysis. This revealed a class of short, polyadenylated and highly unstable RNAs. These promoter upstream transcripts (PROMPTs) are produced ~0.5 to 2.5 kilobases upstream of active transcription start sites. PROMPT transcription occurs in both sense and antisense directions with respect to the downstream gene. In addition, it requires the presence of the gene promoter and is positively correlated with gene activity. We propose that PROMPT transcription is a common characteristic of RNA polymerase II (RNAPII) transcribed genes with a possible regulatory potential.

Recent high-throughput analyses have revealed that >90% of all human DNA is transcribed (*1*). The vast majority of these transcripts are noncoding, thus challenging the classical definition of what constitutes a gene and, by association, a promoter (*2*–*4*). Furthermore, additional short-lived RNAs might have escaped detection. With the aim of identifying such transcripts, we used RNA interference in HeLa cells to deplete hRrp40, a core component of the human 3′ to 5′ exoribonucleolytic exosome, one of the major RNA degradation complexes (fig. S1A) (*5*). This resulted in a severe processing defect of the known exosome substrate 5.8S ribosomal RNA (fig. S1B), demonstrating diminished exosome function. Oligo dT-primed, double-stranded cDNA from cells that had been treated with either a control [enhanced green fluorescent protein (eGFP)] or hRrp40 small interfering RNA (siRNA) was hybridized to an encyclopedia of DNA elements (ENCODE) tiling array, which covers a representative ~1% of the human genome (*1*). Comparison of array data to public gene annotations revealed overall stabilization of mRNAs (exons in Fig. 1A), as expected. RNA from intronic and intergenic regions were largely unaffected, with the exception of a 1.5-kb region immediately upstream of transcription start sites (TSSs) that was stabilized ~1.5-fold on average (Fig. 1A). The relative stabilization of

RNA expressed from a 500-kb region exemplifies this: Four of the five genes in this region display peaks of stabilized RNA upstream of their annotated promoters (Fig. 1B).

To validate these results, we subjected RNA from exosome-depleted versus control cells to oligo dT-primed reverse transcription followed by quantitative polymerase chain reaction (RT-qPCR) analyses of a region upstream of 20 TSSs, all of which confirmed a statistically significant stabilization under hRrp40 knockdown conditions (Fig. 1C and fig. S2A). Depletion of an additional exosome component (hRrp46) resulted in similar levels of stabilization, whereas depletion of other factors involved in RNA turnover (hUpf1, hXrn1, hXrn2, hDcp2, PARN) had no effect (fig. S2B), indicating that promoter upstream transcripts (PROMPTs) are exosome-specific targets. Individual depletion of hRrp6 or hRrp44, the catalytically active exosome subunits, resulted in no or only modest stabilization. Depletion of both, however, caused levels of stabilization comparable to that observed upon depletion of hRrp40 (Fig. 1C and fig. S2A), suggesting that hRrp6 and hRrp44 act redundantly to degrade PROMPTs. This stabilization of PROMPTs in exosome-depleted cells is reminiscent of that of *Saccharomyces cerevisiae* cryptic unstable transcripts that, like PROMPTs, are also transcribed from nongenic regions (*6*).

To overview the average RNA stabilization profile around all 1594 annotated ENCODE TSSs, we aligned array data from the hRrp40 and control knockdown experiments, as well as the ratio of the two, relative to each other (Fig. 2A, top). Because of the different levels of stabilization of exonic and intronic RNA (Fig. 1A), we only considered data derived from exonic sequences downstream of the TSSs (fig. S3). Moreover, because many genes have multiple TSS clusters (i.e., promoters) that may confound analyses, we also aligned array data from 64 selected genes with only one major TSS cluster (low-complexity genes) (Fig. 2A, bottom, and table S1). Both alignments revealed an average RNA stabilization profile over a ~2-kb region upstream of the TSS with a peak around –1 kb (Fig. 2A). In control cells, RNA levels are near background, whereas they are greatly elevated upon hRrp40 depletion. RNA levels in the hRrp40-depleted cells drop to background levels nearing the TSS, indicating that stabilized transcripts are distinct from their neighboring mRNAs. Thus, PROMPTs constitute a class of unstable transcripts, and we refer to the PROMPT-encoding DNA as the "PROMPT region." Short RNAs produced around TSSs have previously been reported, most notably promoter-associated short RNAs, which were on average 0.5 kb on either side of the TSS (*4*). These are, however, physically separate from PROMPTs by several hundred base pairs (fig. S4). In contrast, a few verified PROMPT regions show weak signs of transcriptional activity in other data sets, such as scattered cap analysis of gene expression tags (markers of transcription initiation events) (*7*) and expressed sequence tags unassigned to known genomic features (fig. S5).

We next examined whether PROMPTs were sense or antisense relative to the mRNA produced from the downstream positioned genes. Orientation-specific RT-qPCR performed on RNA from either hRrp40 depleted- or control cells demonstrated that, regardless of directional preference, both sense and antisense transcripts were detectable in PROMPT regions (Fig. 2B). In the presence of actinomycin D, which inhibits spurious synthesis of potential second-strand cDNA artifacts (*8*), this bidirectionality of PROMPTs was still observed (fig. S6). Moreover, both sense and antisense RNAs were stabilized to a similar extent by hRrp40 depletion (Fig. 2B), demonstrating that both species are exosome substrates. When aligning array data to the TSSs of PROMPT regions where either sense or antisense RNA production predominates, they displayed patterns similar to the average PROMPT profile (fig. S7). Taken together, these data suggest a complex pattern of RNA polymerase II (RNAPII) activity in either orientation upstream of individual gene promoters. This observation was supported by nonexhaustive rapid amplification of cDNA ends (RACE) analyses of eight PROMPT regions, which often reveals multiple 5′ and 3′ ends (fig. S8).

To investigate the requirements for transcription upstream of promoters, we transiently transfected HeLa cells with a plasmid containing the

[1]Centre for mRNP Biogenesis and Metabolism, Department of Molecular Biology, C. F. Møllers Alle, Building 1130, Aarhus University, Denmark. [2]Bioinformatics Research Center, C. F. Møllers Alle, Building 1110, Aarhus University, Denmark.

*Present address: Exiqon A/S, Bygstubben 9, 2850 Vedbæk, Denmark.

†To whom correspondence should be addressed. E-mail: thj@mb.au.dk

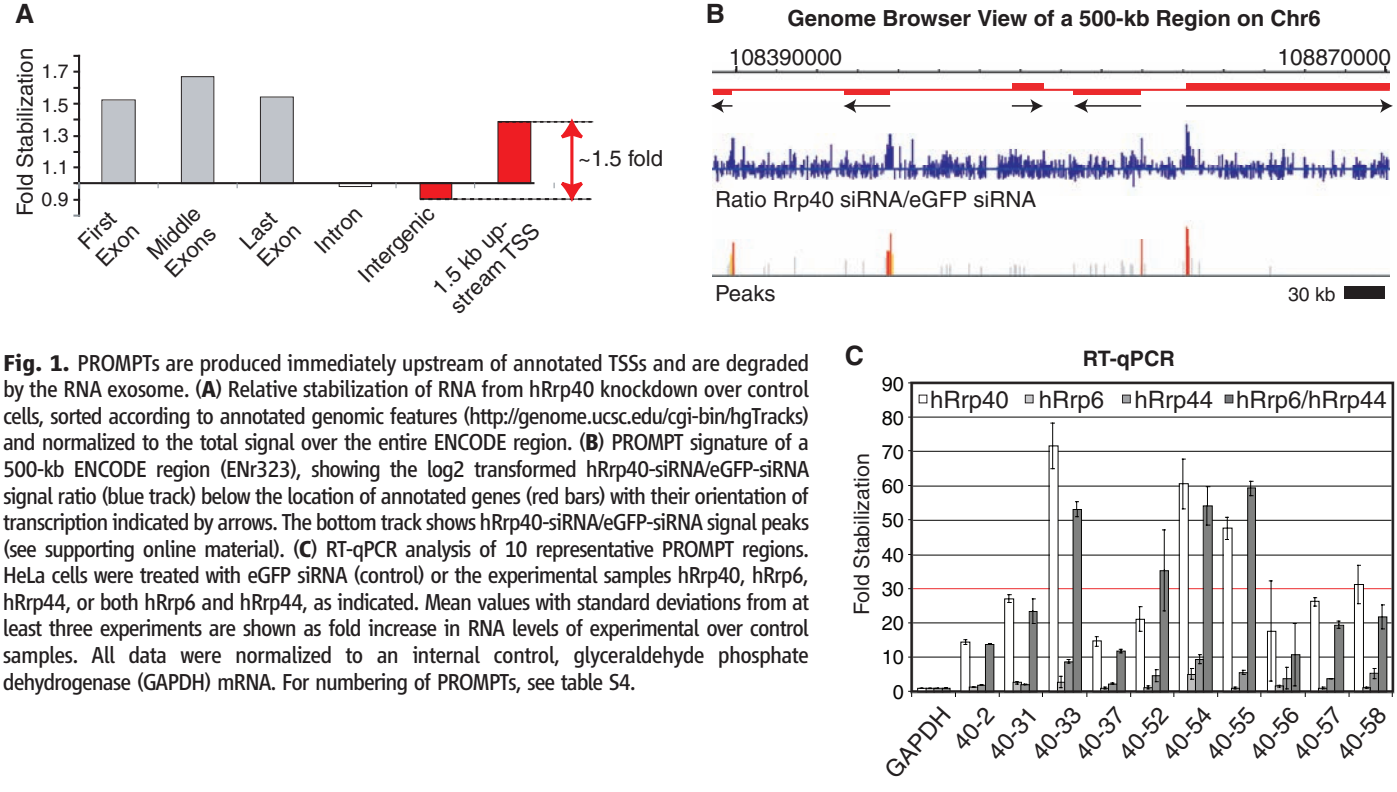

Fig. 1. PROMPTs are produced immediately upstream of annotated TSSs and are degraded by the RNA exosome. (**A**) Relative stabilization of RNA from hRrp40 knockdown over control cells, sorted according to annotated genomic features (http://genome.ucsc.edu/cgi-bin/hgTracks) and normalized to the total signal over the entire ENCODE region. (**B**) PROMPT signature of a 500-kb ENCODE region (ENr323), showing the log2 transformed hRrp40-siRNA/eGFP-siRNA signal ratio (blue track) below the location of annotated genes (red bars) with their orientation of transcription indicated by arrows. The bottom track shows hRrp40-siRNA/eGFP-siRNA signal peaks (see supporting online material). (**C**) RT-qPCR analysis of 10 representative PROMPT regions. HeLa cells were treated with eGFP siRNA (control) or the experimental samples hRrp40, hRrp6, hRrp44, or both hRrp6 and hRrp44, as indicated. Mean values with standard deviations from at least three experiments are shown as fold increase in RNA levels of experimental over control samples. All data were normalized to an internal control, glyceraldehyde phosphate dehydrogenase (GAPDH) mRNA. For numbering of PROMPTs, see table S4.

β-globin gene under control of the strong cytomegalovirus promoter (pCMV) that is preceded by 2.2 kb of bacteriophage λ DNA (Fig. 2C). This resulted in transcript production from the λ DNA, demonstrating that PROMPT-like transcription can be initiated independent of the underlying DNA sequence. Transcripts arising from the λ DNA region cannot be read-through products from transcription around the plasmid because β-globin transcript levels reach background immediately downstream of the transcription termination site. Again, 5′- and 3′-RACE analyses were employed to map some transcription start- and end points, which substantiated the observation of dynamic and complex RNAPII activity in the region (fig. S9). Deletion of the CMV promoter resulted in the concomitant elimination of PROMPT and β-globin gene transcription (Fig. 2C and fig. S9). Thus, the generation of transcripts upstream of an active gene appears to depend on the gene promoter.

To further characterize the transcriptional activity and its origin in PROMPT regions, we compared PROMPT patterns to RNAPII occupancy, transcription factor binding, and chromatin modifications using public data sets generated by the ENCODE project (table S2). In two representative examples, the PROMPT region is covered by markers of active transcription, RNAPII and acetylated histone 3 (H3K9ac), whereas the transcription initiation factor TAF1 peaks at the TSS (Fig. 3A). The generality of this observation was examined by creating composite profiles of the 64 low-complexity regions encompassing PROMPT and TSS sequences. PROMPTs generally overlap with RNAPII, marks of active chromatin, and DNAse hypersensitive sites (*9*, *10*), but not with peaks of transcription initiation factors; e.g., TAF1 or E2F1 (*10*, *11*) (Fig. 3B and fig. S10). Although this reinforces the concept of substantial transcription activity upstream of bona fide genes, the TSS-restricted localization of transcription initiation factors supports our conclusion using CMV/ΔCMV plasmids and argues against the presence of an independent PROMPT promoter.

A link between transcriptional activity in PROMPT and gene regions is further supported by scatter plots showing a strong positive correlation between total average RNAPII chromatin immunoprecipitation (ChIP) signal within the first 1.5 kb up- and downstream of all 1594 ENCODE TSSs (Fig. 4A). This relation is also evident from raw RNA expression data from the hRrp40 depletion experiment (Fig. 4B). With slopes of up to 0.7, these plots indicate that transcription activity in the PROMPT region is comparable to that in the beginning of the gene.

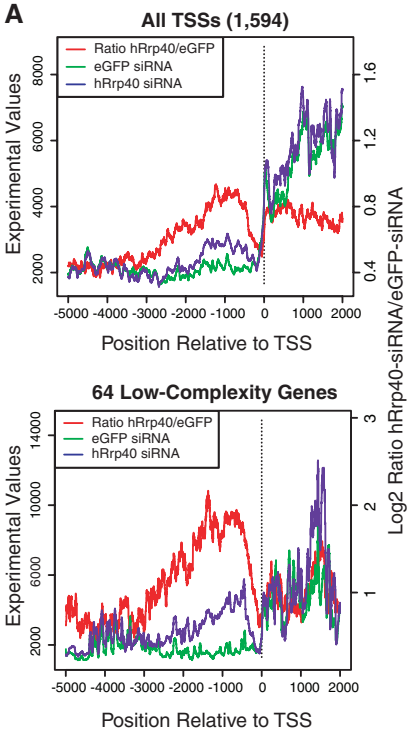

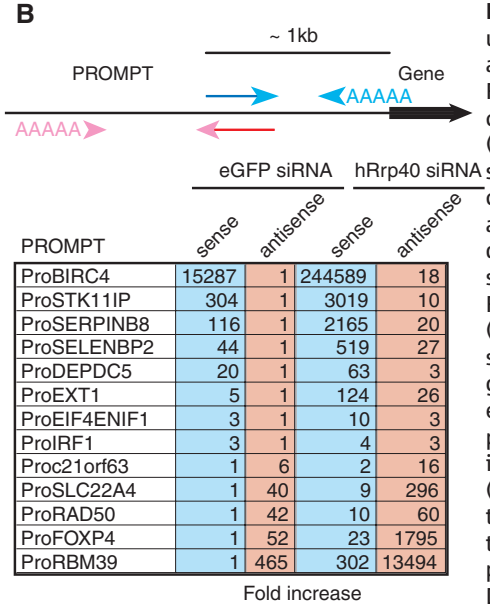

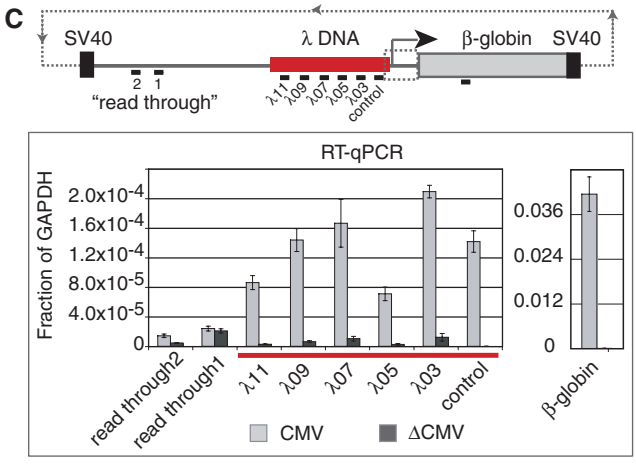

Fig. 2. PROMPT expression maps to 0.5 to 2.5 kb (i) upstream of TSSs, (ii) can occur in both orientations, and (iii) requires the gene promoter. (**A**) Composite RNA profiles upstream of all 1594 (top) or 64 low-complexity (bottom) TSSs. Raw (single-channel) data (smoothened over a 10-bp window) from hRrp40-siRNA treated cells, control (eGFP) siRNA–treated cells, and their ratio are shown as indicated. The left *y* axis denotes values for raw data, and the right *y* axis denotes the log2-transformed ratio of the raw data, scaled to center at zero. Positions in base pairs of RNA signals relative to TSSs are shown on the *x* axes. (**B**) The sense (blue)/antisense (red) directionality of selected PROMPTs was determined by RT-qPCR with gene-specific primers (~1 kb upstream the TSS) in either orientation in combination with a $T_{20}VN$ primer that hybridizes to the 3′ poly(A) tail. Fold increases relative to the lowest value in control cells (set to 1) are plotted. PROMPTs are ordered such that the one with the highest preference for sense transcription is at the top. (**C**) Generation of promoter-upstream transcription in nonhuman DNA. Plasmids containing the β-globin gene under control of a viral promoter (CMV) or its ΔCMV control were transiently transfected into HeLa cells. Both constructs have an insertion of bacteriophage λ DNA (red bar) upstream and a strong SV40 poly(A) site (black box) downstream of the β-globin gene. RNA levels were analyzed by RT-qPCR. Read-through transcription from the β-globin promoter was measured with the use of two amplicons upstream of the λ DNA ("read through"). The "control" amplicon has no complementary sequence in the ΔCMV plasmid. Values on the *y* axis are percentages of GAPDH mRNA levels. The dashed box in the linear plasmid representation (top, not drawn to scale) encloses the region that is deleted in the ΔCMV construct. Mean values with standard deviations ($n = 3$) are shown.

Given their ubiquitous nature, do PROMPTs have a function? A few noncoding RNAs that have been reported to exert regulatory functions are located in potential PROMPT regions (*12*, *13*). Likewise, a noncoding RNA directly upstream of the sphingosine-kinase1 (SPHK1) gene, which affects the methylation status of CpG dinucleotides within its promoter (*13*), is also stabilized in hRrp40 knockdown cells (fig. S11A). It is therefore interesting to note that the methylation level of some CpG dinucleotides within the SPHK1 promoter region is increased upon hRrp40 depletion (fig. S11B). That PROMPTs more generally may affect promoter methylation is further indicated by the finding that for genes with similar expression levels, PROMPT levels are generally higher around promoters with a high CpG score (fig. S11C).

PROMPTs may arise wherever open chromatin presents itself, possibly as the byproduct of an as yet unexplored aspect of the mechanism of gene transcription. Evolution, being an opportunistic force, may then have co-opted at least some of these PROMPTs as part of regulatory mechanisms (fig. S11). One such molecular system could involve the control of CpG (de)methylation, an as of now poorly understood process (*14*). An alternative, but not mutually exclusive, possibility is that PROMPT transcription may have a more general function by providing reservoirs of RNAPII molecules, which can facilitate rapid activation of the downstream gene, and/or by serving to alter chromatin structure. Clearly, the generality of the PROMPT phenomenon hints at a more complex regulatory chromatin structure around the TSS than was previously anticipated.

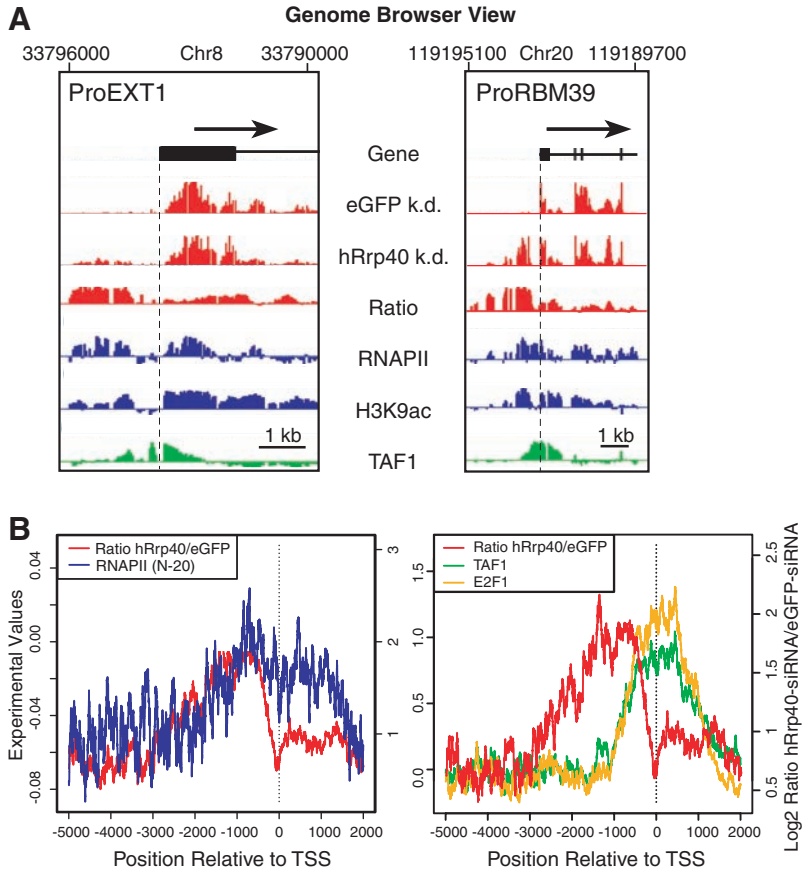

Fig. 3. PROMPT regions are actively transcribed. (**A**) Details of transcript levels from this study compared with previously published ChIP-chip data for PROMPT and 5′ regions of two representative genes. Genomic coordinates are shown on top in numbers of base pairs. (**B**) Composite profiles of RNA stabilization in the PROMPT regions of 64 low-complexity TSSs displayed as in Fig. 2A and compared with the indicated data sets.

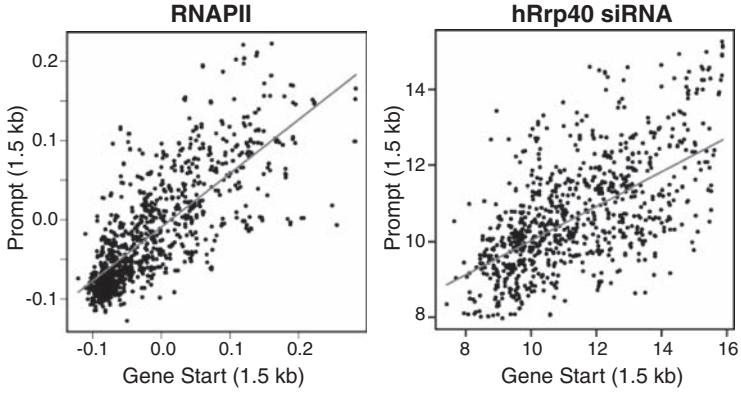

Fig. 4. Overall correlation of PROMPT- and gene-expression levels. (**Left**) Scatter plot of RNAPII distribution as measured by ChIP-chip over all 1594 TSSs in the ENCODE region (data taken from GEO, accession number GSE6391). Data were integrated over 1.5 kb before (*y* axis, "PROMPT") and after (*x* axis, "Gene Start") each TSS and plotted against each other. The slope of the linear regression is 0.68 with a *P* value of $\leq 10^{-300}$ (*t* test, product-moment correlation) and an r^2 value of 0.61 [degrees of freedom (df) = 1511]. (**Right**) Scatter plot of single-channel RNA microarray signals from hRrp40 siRNA-treated cells created as above with the exception that, in the gene, only data corresponding to exonic DNA were used to remove exon/intron biases (fig. S3). Statistical values are slope = 0.45, *P* value < 10^{-137}, and r^2 = 0.39 (df = 1420).

References and Notes

1. E. Birney *et al.*, *Nature* **447**, 799 (2007).
2. M. B. Gerstein *et al.*, *Genome Res.* **17**, 669 (2007).
3. A. Sandelin *et al.*, *Nat. Rev. Genet.* **8**, 424 (2007).
4. P. Kapranov *et al.*, *Science* **316**, 1484 (2007); published online 16 May 2007 (10.1126/science.1138341).
5. Materials and methods are available as supporting material on *Science* Online.
6. F. Wyers *et al.*, *Cell* **121**, 725 (2005).
7. P. Carninci *et al.*, *Nat. Genet.* **38**, 626 (2006).
8. F. Perocchi, Z. Xu, S. Clauder-Munster, L. M. Steinmetz, *Nucleic Acids Res.* **35**, e128 (2007).
9. A. P. Boyle *et al.*, *Cell* **132**, 311 (2008).
10. N. D. Heintzman *et al.*, *Nat. Genet.* **39**, 311 (2007).
11. M. Bieda, X. Xu, M. A. Singer, R. Green, P. J. Farnham, *Genome Res.* **16**, 595 (2006).
12. X. Wang *et al.*, *Nature* **454**, 126 (2008).
13. T. Imamura *et al.*, *Biochem. Biophys. Res. Commun.* **322**, 593 (2004).
14. S. K. Ooi, T. H. Bestor, *Cell* **133**, 1145 (2008).

15. We thank G. Pruijn for antibodies, D. Libri, A. Sandelin, and D. Schubeler for comments on the manuscript, and D. Riishøj and K. Jürgensen for technical assistance. This work was supported by the Danish National Research Foundation and the Danish Natural Science Research Council. Microarray data have been submitted to gene expression omnibus (GEO) at the National Center for Biotechnology Information (http://www.ncbi.nlm.nih.gov/) under accession number GSE12431.

Supporting Online Material

www.sciencemag.org/cgi/content/full/1164096/DC1
Materials and Methods
Figs. S1 to S11
Table S1 to S4
References

1 August 2008; accepted 12 November 2008
Published online 4 December 2008;
10.1126/science.1164096
Include this information when citing this paper.

The Antisense Transcriptomes of Human Cells

Yiping He, Bert Vogelstein, Victor E. Velculescu, Nickolas Papadopoulos,* Kenneth W. Kinzler

Transcription in mammalian cells can be assessed at a genome-wide level, but it has been difficult to reliably determine whether individual transcripts are derived from the plus or minus strands of chromosomes. This distinction can be critical for understanding the relationship between known transcripts (sense) and the complementary antisense transcripts that may regulate them. Here, we describe a technique that can be used to (i) identify the DNA strand of origin for any particular RNA transcript, and (ii) quantify the number of sense and antisense transcripts from expressed genes at a global level. We examined five different human cell types and in each case found evidence for antisense transcripts in 2900 to 6400 human genes. The distribution of antisense transcripts was distinct from that of sense transcripts, was nonrandom across the genome, and differed among cell types. Antisense transcripts thus appear to be a pervasive feature of human cells, which suggests that they are a fundamental component of gene regulation.

The DNA in each normal human cell is virtually identical. The key to cellular differentiation therefore lies in understanding the gene products—transcripts and proteins—that are derived from the genome. For more than a decade, it has been possible to measure the levels of transcripts in a cell at the whole-genome level (*1*). The word "transcriptome" was coined to denote this genome-wide assessment (*2*). However, it has been difficult to determine which of the two strands of the chromosome (plus or minus) serves as the template for transcripts in a global fashion. Sense transcripts of protein-encoding genes produce functional proteins, whereas antisense transcripts are often thought to have a regulatory role (*3*–*7*).

Several unequivocal examples of antisense transcripts, such as those corresponding to imprinted genes, have been described [reviewed in (*3*–*7*)]. However, estimates of the fraction of genes associated with antisense transcripts in mammalian cells vary from less than 2% to more than 70% of the total genes (*8*–*18*). We have developed a technique called asymmetric strand-specific analysis of gene expression (ASSAGE) that allows unambiguous assignment of the DNA strand coding for a transcript. The key to this approach is the treatment of RNA with bisulfite, which changes all cytidine residues to uridine residues. The sequence of a bisulfite-treated RNA molecule can only be matched to one of the two possible DNA template strands (fig. S1). After generating cDNA from bisulfite-treated RNA with reverse transcriptase (RT), sequencing of the reverse transcription polymerase chain reaction (RT-PCR) product can be used to establish whether a particular RNA was transcribed from the plus or minus strand. To identify the DNA strands of origin for the entire transcriptome, we ligate cDNA fragments derived from bisulfite-treated RNA to adapters and then determine the sequence of one end of each fragment through sequencing-by-synthesis. The number and distribution of the sequenced tags provide information about the level of transcription of each gene in the analyzed cell population as well as the strand from which each transcript was derived.

We used ASSAGE to study transcription in normal human peripheral blood mononuclear cells (PBMCs). Several quality controls were performed to evaluate the library of tags derived from this RNA source. First, we calculated the bisulfite conversion efficiency from the sequences of the tags and found that 95% of the C residues in the original RNA had been converted to U residues (*19*). Second, we determined whether the bisulfite treatment altered the distribution of tags by preparing libraries without bisulfite treatment. We found a good correlation between the number of sense tags in a gene derived from ASSAGE data and the number of tags derived from sequencing of DNA synthesized from the same RNA used for ASSAGE without bisulfite treatment from the same cells ($R^2 = 0.59$). We also found a correlation between the relative expression levels determined by ASSAGE and those assessed by hybridization to microarrays [$R^2 = 0.45$ (*19*)].

From the PBMC tag library, 4 million experimental tags could be unambiguously assigned to a specific genomic position in the converted genome (table S1). Of the 4 million tags, 47.5% had the sequence of the plus strand (that is, the template of these transcripts had been the minus strand), and 52.5% had the sequence of the minus strand. This is consistent with the expected equal distribution of sense transcripts from the two strands (*20*). As shown in table S1, 90.3% of the 4 million tags could be assigned to known genes; the remaining tags were in unannotated regions of the genome. The fraction of unannotated tags (9.7%) is consistent with data from other sources indicating the likely existence of actively transcribed genes in human cells that have not yet been discovered or annotated (*6*, *21*–*24*). Of the

Table 1. Classification of genes with respect to antisense tags. We classified only those genes whose sum of distinct sense and antisense tags was 5 or more. S genes contained only sense tags or had a sense/antisense tag ratio of 5 or more; AS genes contained only antisense tags or had a sense/antisense tag ratio of 0.2 or less; SAS genes contained both sense and antisense tags and had a sense/antisense ratio between 0.2 and 5. Samples were derived from the following sources: PBMC, peripheral blood mononuclear cells isolated from a healthy volunteer; Jurkat, a T cell leukemia line; HCT116, a colorectal cancer cell line; MiaPaCa2, a pancreatic cancer line; MRC5, a fibroblast cell line derived from normal lung.

	Cell type									
	PBMC		Jurkat		HCT116		MiaPaCa2		MRC5	
	No. of genes	Fraction	No. of genes	Fraction	No. of genes	Fraction	No. of genes	Fraction	No. of genes	Fraction
All genes										
S genes	10,586	81.60%	9,928	89.60%	11,176	88.00%	9,500	89.50%	10,165	89.30%
AS genes	329	2.50%	240	2.20%	203	1.60%	155	1.50%	212	1.9%
SAS genes	2,061	15.9%	908	8.2%	1,327	10.4%	959	9%	1,002	8.8%
Total	12,976		11,076		12,706		10,614		11,379	
Coding genes										
S genes	10,375	81.30%	9,778	89.50%	10,770	87.60%	9,348	89.40%	10,029	89.20%
AS genes	325	2.50%	239	2.20%	201	1.60%	154	1.50%	210	2%
SAS genes	2,055	16.1%	907	8.3%	1,325	10.8%	959	9.2%	1,000	8.9%
Total	12,755		10,924		12,296		10,461		11,239	
Noncoding genes										
S genes	211	95.50%	150	98.70%	406	99.00%	152	99.30%	136	97.10%
AS genes	4	1.80%	1	0.70%	2	0.50%	1	0.70%	2	1.4%
SAS genes	6	2.7%	1	0.70%	2	0.50%	0	0%	2	1.4%
Total	221		152		410		153		140	

Ludwig Center for Cancer Genetics and Therapeutics and Howard Hughes Medical Institute, Johns Hopkins Kimmel Cancer Center, Baltimore, MD 21231, USA.

*To whom correspondence should be addressed. E-mail: npapado1@jhmi.edu

informative tags in annotated regions, 11% were antisense and 89% were sense (table S1).

We next assessed the expression of each gene by counting the total number of tags matching a gene or by counting tags with identical sequence matching a gene only once (distinct tags). On average, there were three total tags for each distinct tag, but this number varied widely and reflected the level of expression of the corresponding transcript. With respect to antisense transcription, genes could be divided into three main classes. S genes were defined as those with a ≥5:1 ratio of distinct sense tags to distinct antisense tags; AS genes were defined as those with a ≥5:1 ratio of distinct antisense tags to distinct sense tags. The SAS class included the remaining genes, all of which contained both sense and antisense tags. In PBMCs, we identified 329 (2.5%) AS genes, 2061 (15.9%) SAS genes, and 10,586 (81.6%) S genes among the 12,976 Ensembl genes in which at least five distinct tags were observed (Table 1 and table S2). There were 6457 genes in which at least two distinct antisense tags were found.

When normalized by length, there was an obvious concentration of antisense tags in exons relative to the entire genome or to introns ($P < 0.0001$; Fig. 1). Within promoter regions, there was a concentration of antisense tags near the transcription initiation site of the sense transcripts, which gradually tapered off upstream ($P < 0.01$; Fig. 1 and fig. S2). We also found clear differences between the relative distributions of sense and antisense tags, with a higher proportion of antisense tags than sense tags within promoter and terminator regions of genes ($P < 0.0001$; Fig. 1). Examples of the distribution of sense and antisense tags derived from S and AS genes are shown in Fig. 2 and fig. S3. The predicted AS transcripts could be confirmed by ASSAGE using gene-specific primers (fig. S4).

To determine whether the patterns described above were particular to PBMCs, we used ASSAGE to study four additional human cell types. In all cases, the patterns observed—including the proportions of S, AS, and SAS genes—were similar to those in PBMCs (Table 1 and table S1). However, the identity of the S, AS, and SAS genes varied among the cell lines, which suggests that the expression of antisense tags may be regulated in a cell- or tissue-specific manner (fig. S5 and tables S2 and S3). These differences were not related to interexperimental variation, as repeat experiments performed with independently generated ASSAGE libraries from the same RNA sample were highly correlated (fig. S6 and table S2) and differential expression could be confirmed by strand-specific PCR from RNA (fig. S7). In every sample, there was a concentration of both sense and antisense tags within exons (relative to the whole genome or to intronic regions) and a preferential concentration in promoter and terminator regions ($P < 0.01$; figs. S2 and S8).

To determine whether splicing of antisense transcripts occurred, we constructed new libraries from Jurkat and MRC5 cells and determined the sequences of both ends of each cDNA fragment ("paired-end sequencing"). As expected, transcripts levels assessed with this paired-end ASSAGE and the original ASSAGE were highly correlated (fig. S9). The size-selected transcript fragments used to construct these libraries were, on average, ~175 base pairs in length. A cDNA fragment whose ends were located at genomic positions more than 3 times this distance (>600 base pairs apart) would be expected to represent spliced transcripts. By this criterion, more than 20% of sense-strand cDNA fragments were spliced (fig. S10). In contrast, only ~1% of antisense fragments exhibited this spliced pattern. Sequencing of five putative spliced antisense transcripts confirmed the splicing, and comparison with genomic DNA revealed the splice site consensus sequences at the expected locations (figs. S11 and S12).

Our results raise many questions about the genesis and metabolism of antisense transcripts. It has been hypothesized that antisense transcripts are widely and promiscuously expressed, perhaps because of weak promoters distributed throughout the genome [reviewed in (*25*, *26*)]. Our data argue against this hypothesis in human cells: Promiscuous expression would lead to a uniform distribution of antisense tags across the genome, whereas the observed distribution

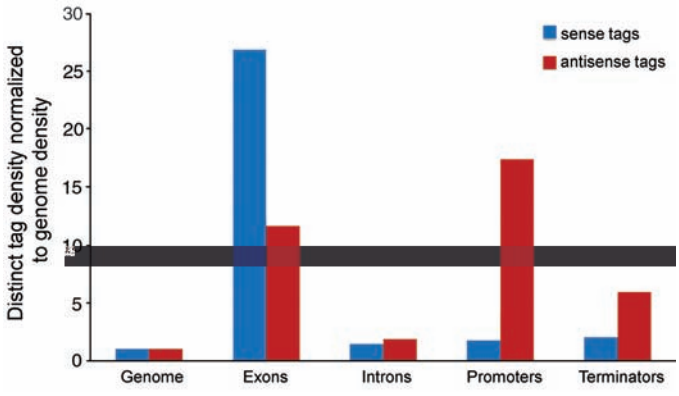

Fig. 1. ASSAGE tag densities in PBMCs. The densities of distinct sense and antisense tags in the indicated regions were normalized to the overall genome tag density. The promoter and terminator regions were defined as the 1 kb of sequence that was upstream or downstream, respectively, of the transcript start and end sites.

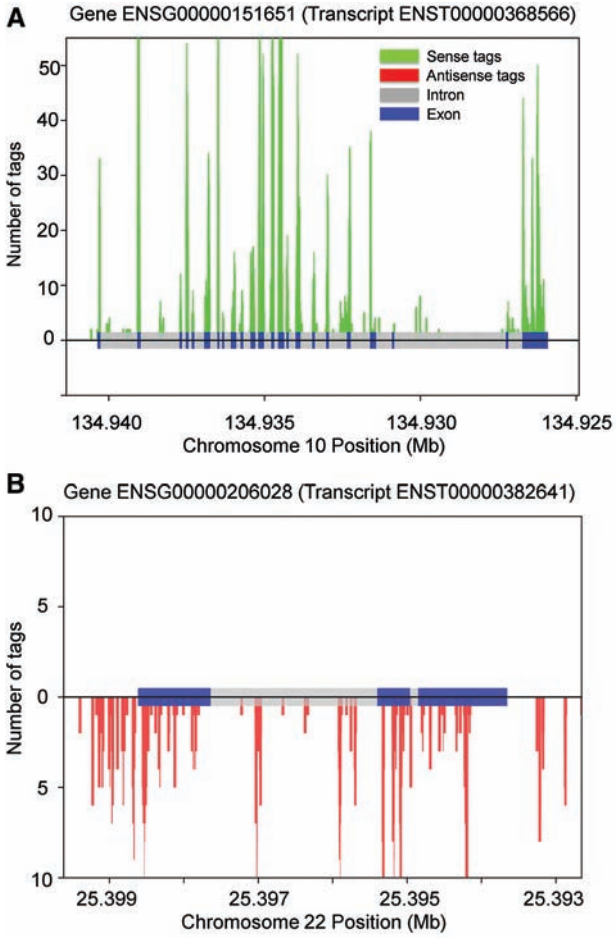

Fig. 2. Tag distribution in the indicated S (**A**) and AS (**B**) genes in PBMCs.

was nonrandom, localized to genes and within particular regions of genes, much like sense transcripts (Fig. 1 and figs. S2 and S8). This distribution is consistent with a model wherein many antisense transcripts initiate and terminate near the terminators and promoters, respectively, of the sense transcripts. Some of the apparent antisense transcripts from a gene on the plus strand could actually be sense transcripts originating from unterminated transcription of a downstream gene on the minus strand (or vice versa). However, this idea is not generally supported because there was a poor correlation between antisense tag density within a gene and the density of sense tags from the closest downstream gene (fig. S13). One explanation for the higher density of antisense tags in transcribed regions is that transcription of the sense transcripts from correct initiation sites would reduce nucleosome density throughout the entire transcribed region, thereby increasing DNA accessibility and hence the likelihood of nonspecific transcription (*26*). This is unlikely, given that genes with high sense tag densities did not generally have high antisense densities. There is substantial evidence that sense transcripts can be negatively regulated by antisense transcripts (*3*–*7*). Such regulation can occur either by transcriptional interference or through posttranscriptional mechanisms involving splicing or RNA-induced silencing complexes (RISCs). Our data support the possibility that antisense-mediated regulation affects a large number of genes.

References and Notes

1. P. O. Brown, D. Botstein, *Nat. Genet.* **21**, 33 (1999).
2. V. E. Velculescu *et al.*, *Cell* **88**, 243 (1997).
3. M. Lapidot, Y. Pilpel, *EMBO Rep.* **7**, 1216 (2006).
4. A. Mazo, J. W. Hodgson, S. Petruk, Y. Sedkov, H. W. Brock, *J. Cell Sci.* **120**, 2755 (2007).
5. J. A. Timmons, L. Good, *Biochem. Soc. Trans.* **34**, 1148 (2006).
6. P. Kapranov, A. T. Willingham, T. R. Gingeras, *Nat. Rev. Genet.* **8**, 413 (2007).
7. O. Yazgan, J. E. Krebs, *Biochem. Cell Biol.* **85**, 484 (2007).
8. J. Chen *et al.*, *Nucleic Acids Res.* **32**, 4812 (2004).
9. M. E. Fahey, T. F. Moore, D. G. Higgins, *Comp. Funct. Genomics* **3**, 244 (2002).
10. B. Lehner, G. Williams, R. D. Campbell, C. M. Sanderson, *Trends Genet.* **18**, 63 (2002).
11. J. Shendure, G. M. Church, *Genome Biol.* **3**, RESEARCH0044 (2002).
12. R. Yelin *et al.*, *Nat. Biotechnol.* **21**, 379 (2003).
13. H. Kiyosawa, I. Yamanaka, N. Osato, S. Kondo, Y. Hayashizaki, *Genome Res.* **13**, 1324 (2003).
14. D. J. Lipman, *Nucleic Acids Res.* **25**, 3580 (1997).
15. G. G. Carmichael, *Nat. Biotechnol.* **21**, 371 (2003).
16. RIKEN Genome Exploration Research Group and Genome Science Group (Genome Network Project Core Group) and FANTOM Consortium, *Science* **309**, 1564 (2005).
17. Y. Okazaki *et al.*, *Nature* **420**, 563 (2002).
18. D. Kampa *et al.*, *Genome Res.* **14**, 331 (2004).
19. See supporting material on *Science* Online.
20. A. J. Simpson, S. J. de Souza, A. A. Camargo, R. R. Brentani, *Comp. Funct. Genomics* **2**, 169 (2001).
21. B. A. Peters *et al.*, *Genome Res.* **17**, 287 (2007).
22. M. Sultan *et al.*, *Science* **321**, 956 (2008); published online 3 July 2008 (10.1126/science.1160342).
23. A. Mortazavi, B. A. Williams, K. McCue, L. Schaeffer, B. Wold, *Nat. Methods* **5**, 621 (2008).
24. J. Q. Wu *et al.*, *Genome Biol.* **9**, R3 (2008).
25. J. M. Johnson, S. Edwards, D. Shoemaker, E. E. Schadt, *Trends Genet.* **21**, 93 (2005).
26. K. Struhl, *Nat. Struct. Mol. Biol.* **14**, 103 (2007).

27. We thank W. Yu for assistance with microarrays. Supported by the Virginia and D. K. Ludwig Fund for Cancer Research and NIH grants CA57345, CA43460, CA62924, and CA121113. Under a licensing agreement between Johns Hopkins University and Genzyme, technologies related to SAGE were licensed to Genzyme for commercial purposes, and B.V., V.E.V., and K.W.K. are entitled to a share of the royalties received by the university from the sales of the licensed technologies. The university and researchers (B.V. and K.W.K.) own Genzyme stock, which is subject to certain restrictions under university policy. The terms of these arrangements are being managed by the university in accordance with its conflict-of-interest policies. There are existing patents for SAGE that have been licensed as disclosed above, and similar patents are likely to be filed for ASSAGE.

Supporting Online Material

www.sciencemag.org/cgi/content/full/1163853/DC1
Materials and Methods
Figs. S1 to S13
Tables S1 to S3
References

26 July 2008; accepted 10 November 2008
Published online 4 December 2008;
10.1126/science.1163853
Include this information when citing this paper.

Label-Free Biomedical Imaging with High Sensitivity by Stimulated Raman Scattering Microscopy

Christian W. Freudiger,[1,2]* Wei Min,[1]* Brian G. Saar,[1] Sijia Lu,[1] Gary R. Holtom,[1] Chengwei He,[3] Jason C. Tsai,[4] Jing X. Kang,[3] X. Sunney Xie[1]†

Label-free chemical contrast is highly desirable in biomedical imaging. Spontaneous Raman microscopy provides specific vibrational signatures of chemical bonds, but is often hindered by low sensitivity. Here we report a three-dimensional multiphoton vibrational imaging technique based on stimulated Raman scattering (SRS). The sensitivity of SRS imaging is significantly greater than that of spontaneous Raman microscopy, which is achieved by implementing high-frequency (megahertz) phase-sensitive detection. SRS microscopy has a major advantage over previous coherent Raman techniques in that it offers background-free and readily interpretable chemical contrast. We show a variety of biomedical applications, such as differentiating distributions of omega-3 fatty acids and saturated lipids in living cells, imaging of brain and skin tissues based on intrinsic lipid contrast, and monitoring drug delivery through the epidermis.

Vibrational microscopies based on infrared absorption and Raman scattering (*1*, *2*) have been used as label-free contrast mechanisms due to characteristic frequencies of various chemical bonds. However, infrared microscopy has limited spatial resolution because of long infrared wavelengths. Spontaneous Raman scattering microscopy, while having higher spatial resolution due to shorter excitation wavelengths, is insensitive and thus often has limited imaging speed. Coherent anti-Stokes Raman scattering (CARS) microscopy offers higher sensitivity than spontaneous Raman microscopy (*3*, *4*). However, a CARS spectrum is different from its corresponding spontaneous Raman spectrum due to a nonresonant background, which complicates spectral assignment, causes difficulties in image interpretation, and limits detection sensitivity.

Here we explore stimulated Raman scattering (SRS) as an imaging contrast mechanism. SRS is analogous (*5*, *6*) to the well-known phenomenon of stimulated emission (*7*) and was first observed in 1962 (*8*). Since then it has been used in many spectroscopic studies (*9*–*12*). In spontaneous Raman scattering, one laser beam at a frequency ω_p illuminates the sample and the signal is generated at the Stokes and anti-Stokes frequencies, ω_S and ω_{AS}, respectively, due to inelastic scattering. In SRS, however, two laser beams at ω_p and ω_S coincide on the sample (Fig. 1A). When the difference frequency, $\Delta\omega = \omega_p - \omega_S$, also called the Raman shift, matches a particular molecular vibrational frequency Ω, amplification of the Raman signal is achieved by virtue of stimulated excitation. Consequently, the intensity of the Stokes beam, I_S, experiences a gain, ΔI_S (stimulated Raman gain, SRG), and the intensity of the pump beam, I_p, experiences a loss, ΔI_p (stimulated Raman loss, SRL), as shown in Fig. 1B. In contrast, when $\Delta\omega$ does not match any vibrational resonance, SRL and SRG cannot occur. Therefore, unlike CARS, SRL and SRG do not exhibit a nonresonant background (*11*).

The intensity of SRG or SRL is described by $\Delta I_S \propto N \times \sigma_{Raman} \times I_p \times I_S$ and $\Delta I_p \propto -N \times$

[1]Department of Chemistry and Chemical Biology, Harvard University, Cambridge, MA 02138, USA. [2]Department of Physics, Harvard University, Cambridge, MA 02138, USA. [3]Department of Medicine, Massachusetts General Hospital and Harvard Medical School, Boston, MA 02114, USA. [4]Pfizer Global Medical, 685 3rd Avenue, MS 1325, New York, NY 10017, USA.

*These authors contributed equally to this work.
†To whom correspondence should be addressed. E-mail: xie@chemistry.harvard.edu

$\sigma_{Raman} \times I_p \times I_S$, where N is the number of molecules in the probe volume and σ_{Raman} is the molecular Raman scattering cross-section (*6*). As in other multiphoton techniques (*3*, *13*), the nonlinearity of SRL and SRG in the overall excitation intensity allows three-dimensional (3D) sectioning. Such nonlinear excitation is typically accomplished by picosecond or femtosecond pulse trains in the near-infrared region.

SRS as a contrast mechanism for microscopy has been recently reported using multiplex detection with a photodiode array in combination with a femtosecond amplified laser system (*14*). Although the amplified laser system generates a large SRS signal, it is not suitable for bioimaging because the excessive peak power causes sample damage (*15*) and the low repetition rate limits the image acquisition speed.

We take a different approach, using high–repetition rate (76 MHz) picosecond pulse trains with more than three orders of magnitude lower peak power. The pump beam for SRL is provided by a synchronously pumped, tunable optical parametric oscillator (OPO), and the Stokes beam is provided by a 1064-nm mode-locked Nd:YVO_4 oscillator. A 7-ps pulse width is chosen because its frequency bandwidth offers optimal spectral resolution (3 cm^{-1}). Under this excitation condition, the small SRL and SRG signals ($\Delta I_p/I_p$ and $\Delta I_S/I_S < 10^{-4}$) are buried in the laser noise. Realizing that laser noise occurs primarily at low frequencies, we implement a high-frequency phase-sensitive detection scheme, as previously used in other applications (*10*, *16*, *17*). For SRL, we modulate the intensity of the Stokes beam at 1.7 MHz and detect the resulting intensity modulation of the pump beam at the same frequency with a lock-in amplifier (Fig. 1C). Similarly, SRG can be measured by modulating the pump beam and detecting the Stokes beam (*18*). With this approach, $\Delta I_p/I_p < 10^{-7}$ can be achieved with a 1-s time constant. To acquire images via beam scanning, we used a 300-μs time constant and a pixel dwell time of 170 μs. It is difficult to incorporate such phase-sensitive detection at radio frequency (MHz) with a multiplex detector such as a diode array. Our approach can detect intensity changes $\Delta I_p/I_p$ and $\Delta I_S/I_S$ four orders of magnitude more sensitive than in the previous report (*14*).

Collinear pump and Stokes beams are focused with a high–numerical aperture (NA) objective (NA = 1.2) onto a common focal spot (Fig. 1D). In SRS, the spatial resolution is diffraction limited and similar to that of two-photon fluorescence. Because SRL and SRG are measured at the same frequencies as those of the input fields, phase matching is automatically fulfilled. This allows deconvolution with a point spread function similar to that of fluorescence microscopy and makes image interpretation simpler than in the case of CARS (*19*).

To detect the pump or Stokes beams in the forward direction, we used a condenser with an NA = 1.35, which is higher than that of the excitation objective, to minimize spurious background due to cross-phase modulation (*20*, *21*). Alternatively, backward (epi) detection is possible in turbid samples because multiple scattering events redirect a considerable portion of the forward-propagating pump and Stokes beams to the backward direction, which can be collected with the same excitation objective lens (*22*). SRL or SRG spectra at a particular position in the sample can be recorded by automated OPO tuning. We detected SRL instead of SRG because the responsitivity of the photodiode used is higher for the pump than for the Stokes beam.

We verified that SRL is linear in both I_p and I_S (*18*). Unlike the CARS signal that is proportional to the square of the concentration, the linear dependence of SRL on analyte concentration (Fig. 1E) allows straightforward quantitative analysis. The detection limit is 50 μM for retinol (Fig. 1E) and 5 mM for methanol solutions (*18*), with average laser power <40 mW (30 MW/cm^2) for each beam. Close to the shot noise limit, this sensitivity corresponds to about 3000 retinol and 300,000 methanol molecules in focus, respectively, which has surpassed the detection limit reported for CARS microscopy (*23*).

We show in Fig. 1F the SRL, spontaneous Raman, and CARS spectra of an isolated Raman peak of *trans*-retinol (*18*). Whereas SRL and spontaneous Raman spectra are nearly identical, the CARS spectrum exhibits a nonresonant background independent of the Raman shift, and spectral distortion because of interference with the background (*24*). Good agreement between the SRL, SRG, and spontaneous Raman spectra is also seen for spectra with multiple peaks (Fig. 1G) (*18*, *25*). Thus, SRS allows simple spectroscopic identification based on the Raman literature, particularly in the "crowded" fingerprint region.

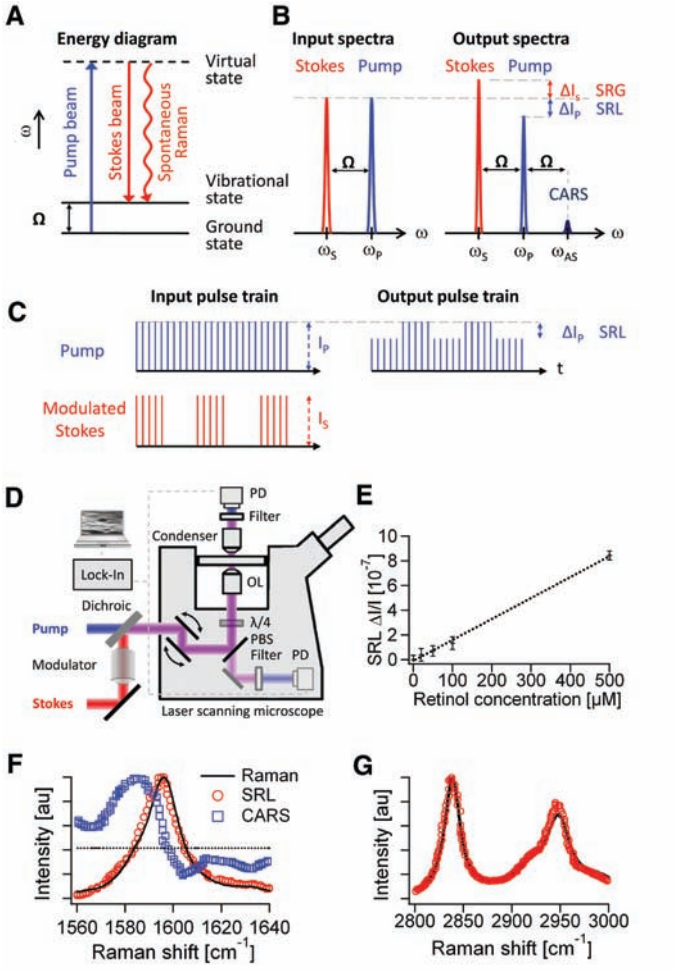

Fig. 1. Principle and design of SRS microscopy. (**A**) Energy diagram for SRS. (**B**) Input and output spectra of SRS. SRS leads to an intensity increase in the Stokes beam (SRG) and an intensity decrease in the pump beam (SRL). Also shown (not to scale) is the CARS signal generated at the anti-Stokes frequency ω_{AS}. (**C**) SRL detection scheme. Stokes beam is modulated at high frequency (MHz), at which the resulting amplitude modulation of the pump beam due to SRL can be detected. (**D**) SRL microscope with both forward and epi detection. The Stokes beam is modulated by an electro-optic modulator. The transmitted or reflected pump beam is filtered and detected by a large-area photodiode (PD). For epi detection, the backscattered beams are collected by the excitation objective lens (OL) and separated from the excitation beams by a combination of a quarter wave plate (λ/4) and polarizing beam splitter (PBS). The SRL is measured by a lock-in amplifier to provide a pixel of the image. Three-dimensional images are obtained by raster-scanning the laser focus across the sample, and microspectroscopy can be performed by automated tuning of the pump wavelength. (**E**) Linear dependence of SRL on concentrations of retinol in ethanol at 1595 cm^{-1}. Modulation depth $\Delta I_p/I_p < 10^{-7}$ can be achieved. Error bars show 1 SD of the signals for a 1-min recording. The detection limit was determined to be 50 μM. (**F**) Agreement of SRL spectrum (red circles) with the spontaneous Raman spectrum (black line) of the Raman peak (1595 cm^{-1}) of 10 mM retinol in ethanol. The distorted CARS spectrum (blue squares) exhibits a typical peak shift, dispersive shape and nonresonant background. (**G**) Agreement of the more complex SRL spectrum of methanol (red circles) with the spontaneous Raman spectrum (black line).

As the first application, we monitored the uptake of omega-3 fatty acids by living human lung cancer cells through SRL imaging and microspectroscopy (Fig. 2). Polyunsaturated omega-3 fatty acids, such as eicosapentaenoic acid (EPA), provide health benefits through mechanisms such as dampening inflammation, lowering blood triglyceride concentrations, and inducing cancer cell apoptosis, but can only be obtained from the diet (*26*). As shown in Fig. 2A, unsaturated fatty acids exhibit a Raman band at 3015 cm^{-1}, attributable to the stretching mode of =C-H bond associated with C=C double bonds (*27*). The intensity of this 3015 cm^{-1} mode is approximately proportional to the number of C=C double bonds in the lipid molecule. In contrast, the 2920cm^{-1} peak intensity is found to be similar for all saturated and unsaturated fatty acids.

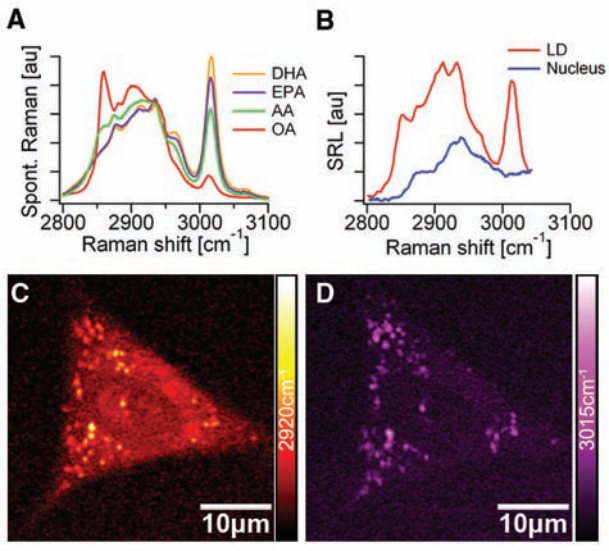

Fig. 2. Omega-3 fatty acid uptake by A549 human lung-cancer cells monitored with SRL microscopy and microspectroscopy. (**A**) Spontaneous Raman spectra of docosahexaenoic acid (DHA, with six C=C bonds), eicosapentaenoic acid (EPA, with five C=C bonds), arachidonic acid (AA, with four C=C bonds), and oleic acid (OA, with a single C=C bond). The strong Raman peak around 3015 cm^{-1} is characteristic of unsaturated fatty acids. (**B**) SRL spectra of a lipid droplet (LD, red line) and a region inside the nucleus (blue line). Unlike the nuclear region, the SRL spectrum of the LD shows good correspondence with the spectra from the pure EPA shown in (A). (**C**) SRL image of a cell at 2920 cm^{-1}. (**D**) SRL image of the same cell at 3015 cm^{-1}. These findings indicate that EPA is taken up by the cells and more strongly enriched in the LDs compared to other cellular organelles.

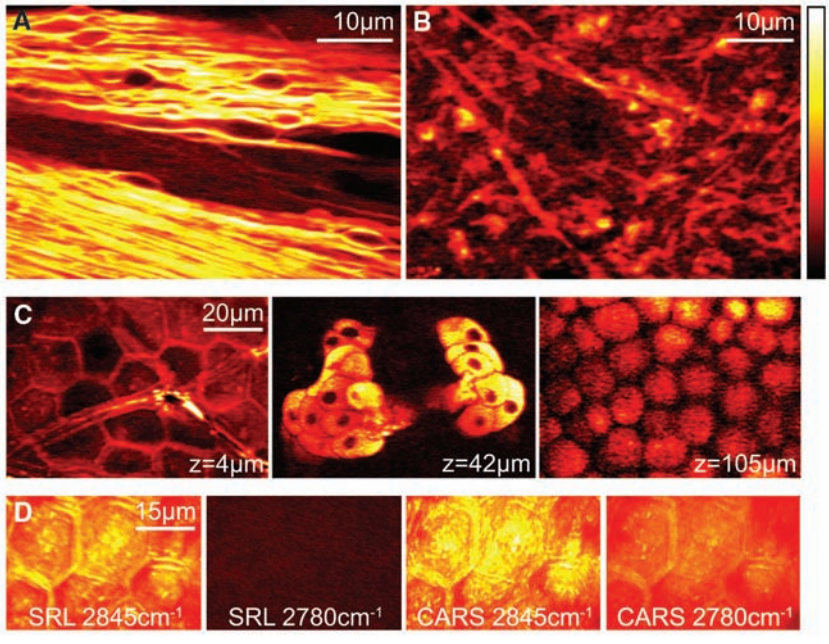

Fig. 3. SRL imaging of fresh mouse tissue. (**A**) Neuron bundles in corpus callosum of mouse brain imaged at 2845 cm^{-1} highlighting myelin sheaths rich in CH_2. See movie in (*18*). (**B**) Epi-detected SRL CH_2 image acquired from thick brain tissue. (**C**) SRL CH_2 images of mouse ear skin in the same area at the indicated depths. From left to right: stratum corneum (4 μm), sebaceous gland (42 μm), and subcutaneous fat layer (105 μm). See movie in (*18*). (**D**) Comparison of SRL and CARS images of stratum corneum on (2845 cm^{-1}) and off (2780 cm^{-1}) the CH_2 resonance. Unlike CARS, SRL has no nonresonant background.

When cells are grown with 25 μM EPA for 24 hours (*18*), lipid droplets (LDs) are visible when imaging at both 2920 cm^{-1} (Fig. 2C) and 3015 cm^{-1} (Fig. 2D) bands. The SRL images show a much stronger signal outside the LDs at 2920 cm^{-1} than at 3015 cm^{-1}, indicating that most of the fatty acids outside the LDs are saturated. In the absence of EPA in the culturing media, the cells have few LDs inside the cytoplasm due to the limited lipid supply (*18*). We also conducted SRL microspectroscopy at specific positions inside the cell to identify the local chemical composition. The nucleus exhibits an SRL spectrum (blue in Fig. 2B) similar to that of the saturated fatty acids, with negligible contribution at 3015 cm^{-1}, whereas the spectrum from the LD has a pronounced 3015 cm^{-1} peak (red in Fig. 2B). No sign of photodamage, such as plasma membrane blebbing (*15*), was observed after repeated images of the same cell. Therefore, we can use SRL spectral imaging and microspectroscopy to follow uptake of unsaturated fatty acids by living cells, opening possibilities to study lipid metabolism and its associated diseases.

Next, we present SRS tissue imaging without staining. Many stains are impossible to apply in vivo. Label-free optical techniques, such as optical coherence tomography and diffusive optical tomography, often do not offer chemical contrast, while autofluorescence is limited to a few chemical species. A strong SRL signal originates from the CH_2 stretching vibration (2845cm^{-1}) of lipids in tissue, especially in the brain, where lipid-rich myelin sheaths surround axons, as was seen in CARS microscopy (*28*). Figure 3A shows forward-detected SRL images of a fiber tract in the corpus callosum of a thin slice of mouse brain. We also demonstrate epi SRL imaging from a ~1-mm-thick slice of mouse brain (Fig. 3B), which clearly reveals individual neurons.

Skin imaging is another application of SRS microscopy. Figure 3C shows three individual SRL sections of mouse skin in the same area but at different depths, all with Δω tuned into 2845cm^{-1} (*18*). This highlights the 3D sectioning capability and subcellular resolution of SRS in tissue. At a depth of 4 μm, the SRL image shows the stratum corneum, which consists of polygonal cells and serves as the main protective layer of the body. This suggests that the intercellular space is rich in lipids. At a depth of 42 μm, lipid-rich sebaceous glands can be identified in the dermis. The nuclei of the gland cells are dark spots due to the lack of lipids. At a depth of 105 μm, the subcutaneous fat layer is clearly visible.

Figure 3D compares on and off vibrational resonance SRL and CARS images of stratum corneum. When Δω is tuned from on-resonance (2845 cm^{-1}) to off-resonance (2780 cm^{-1}) of the

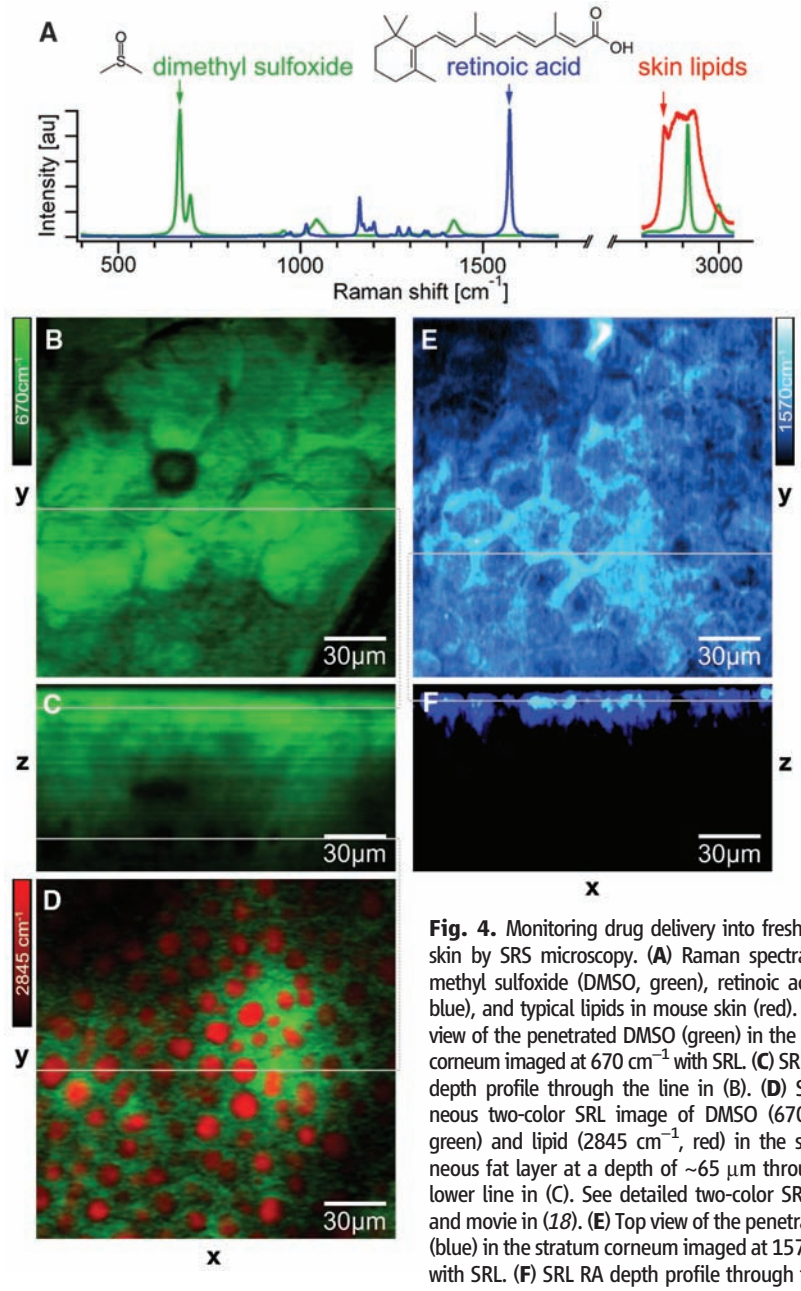

Fig. 4. Monitoring drug delivery into fresh mouse skin by SRS microscopy. (**A**) Raman spectra of dimethyl sulfoxide (DMSO, green), retinoic acid (RA, blue), and typical lipids in mouse skin (red). (**B**) Top view of the penetrated DMSO (green) in the stratum corneum imaged at 670 cm^{-1} with SRL. (**C**) SRL DMSO depth profile through the line in (B). (**D**) Simultaneous two-color SRL image of DMSO (670 cm^{-1}, green) and lipid (2845 cm^{-1}, red) in the subcutaneous fat layer at a depth of ~65 μm through the lower line in (C). See detailed two-color SRL setup and movie in (*18*). (**E**) Top view of the penetrated RA (blue) in the stratum corneum imaged at 1570 cm^{-1} with SRL. (**F**) SRL RA depth profile through the line in (E). SRS allows label-free 3D in situ visualization of two different drug-delivery pathways into the skin.

CH_2 stretching mode, the SRL signal vanishes completely, whereas the nonresonant CARS background still exhibits contrast that complicates image interpretation. We note that tissue autofluorescence does not interfere with the SRS. The absence of the nonresonant background in SRS reflects the major advantage over CARS imaging.

We also show the use of SRS to monitor drug delivery. Fluorescent labels are usually larger than drug molecules and may perturb their transport properties. Although confocal spontaneous Raman microspectroscopy has been used to obtain longitudinal penetration profiles, the lateral distribution is often compromised due to the long pixel dwell times (*29*). Here we show the mapping of the distribution of two compounds: dimethyl sulfoxide (DMSO), a skin-penetration enhancer (*29*); and retinoic acid (RA), which is used to treat acne, wrinkles, photoaging, and acute promyelocytic leukemia (*30*). According to Raman spectra (Fig. 4A), DMSO and RA have isolated vibrational resonances at 670 and 1570 cm^{-1}, respectively.

As a hydrophilic molecule, DMSO penetrates the skin via the protein phase, so the DMSO image in the stratum corneum (Fig. 4B) shows inverse contrast compared to the lipid image in Fig. 3C. A depth profile shows detectable DMSO over more than 60 μm (Fig. 4C), and the hydrophilic interaction with the tissue is confirmed in the subcutaneous fat layer. Simultaneous two-color imaging tuned into lipid and DMSO (*18*) allows us to show that the DMSO is insoluble in the lipid structures (Fig. 4D). In contrast, RA, which is a hydrophobic molecule, penetrates via the lipid-rich intercellular space in the epidermis (Fig. 4, E and F) after ultrasonication of the tissue to enhance delivery (*18*). These results show that SRS offers a new approach for studying pharmacokinetics in situ. As a label-free and sensitive imaging modality, SRS microscopy allows mapping of molecular species in 3D and the ability to follow their dynamics in living cells and organisms based on the wealth of Raman spectroscopy.

References and Notes

1. C. V. Raman, K. S. Krishnan, *Nature* **121**, 711 (1928).
2. G. Turrell, J. Corset, *Raman Microscopy: Developments and Applications* (Academic Press, San Diego, 1996).
3. A. Zumbusch, G. R. Holtom, X. S. Xie, *Phys. Rev. Lett.* **82**, 4142 (1999).
4. C. L. Evans, X. S. Xie, *Annu. Rev. Anal. Chem.* **1**, 27 (2008).
5. N. Bloembergen, *Am. J. Phys.* **35**, 989 (1967).
6. R. W. Boyd, *Nonlinear Optics* (Academic Press, San Diego, 2003).
7. A. Einstein, *Phys. Z.* **18**, 121 (1917).
8. E. J. Woodbury, W. K. Ng, *Proc. Inst. Radio Eng.* **50**, 2367 (1962).
9. A. Owyoung, *Opt. Commun.* **22**, 323 (1977).
10. B. F. Levine, C. V. Shank, J. P. Heritage, *IEEE J. Quantum Electron.* **15**, 1418 (1979).
11. M. D. Levenson, S. S. Kano, *Introduction to Nonlinear Laser Spectroscopy* (Academic Press, San Diego, 1988).
12. P. Kukura, D. W. McCamant, R. A. Mathies, *Annu. Rev. Phys. Chem.* **58**, 461 (2007).
13. W. Denk, J. H. Strickler, W. W. Webb, *Science* **248**, 73 (1990).
14. E. Ploetz, S. Laimgruber, S. Berner, W. Zinth, P. Gilch, *Appl. Phys. B Lasers Opt.* **87**, 389 (2007).
15. Y. Fu, H. F. Wang, R. Y. Shi, J. X. Cheng, *Opt. Exp.* **14**, 3942 (2006).
16. J. Ye, L. S. Ma, J. L. Hall, *J. Opt. Soc. Am. B* **15**, 6 (1998).
17. D. Fu *et al.*, *Opt. Lett.* **32**, 2641 (2007).
18. Methods, additional results, and movies are available as supporting material on *Science* Online
19. E. O. Potma, W. P. de Boeij, D. A. Wiersma, *J. Opt. Soc. Am. B* **17**, 1678 (2000).
20. K. Ekvall *et al.*, *J. Appl. Phys.* **87**, 2340 (2000).
21. Another spurious background signal can arise from two-color two-photon absorption of the pump and Stokes beams. See (*17*).
22. C. L. Evans *et al.*, *Proc. Natl. Acad. Sci. U.S.A.* **102**, 16807 (2005).
23. F. Ganikhanov, C. L. Evans, B. G. Saar, X. S. Xie, *Opt. Lett.* **31**, 1872 (2006).
24. Y. R. Shen, *The Principle of Nonlinear Optics* (Wiley, New Jersey, 2003).
25. Subtle spectral differences between spontaneous Raman spectroscopy and SRS have been predicted theoretically. See (*31*).
26. J. X. Kang, *J. Membr. Biol.* **206**, 165 (2005).
27. C. Heinrich *et al.*, *Opt. Exp.* **16**, 2699 (2008).
28. H. Wang, Y. Fu, P. Zickmund, R. Y. Shi, J. X. Cheng, *Biophys. J.* **89**, 581 (2005).
29. P. J. Caspers *et al.*, *Pharm. Res.* **19**, 1577 (2002).
30. P. C. M. Van De Kerkhof *et al.*, *J. Dermatolog. Treat.* **17**, 198 (2006).
31. P. Kukura, D. W. McCamant, R. A. Mathies, *J. Phys. Chem. A* **108**, 5921 (2004).

32. We thank C. Ackermann and S. Zhang for advice on skin imaging; S. Kesari, X. Xu and the MCB Harvard Mouse Facilities for providing mouse tissue; J. Grice and M. Roberts for the loan of a sonicator; and G. Young, X. Xu, M. Rückel, and P. Sims for helpful discussions. C.W.F. and B.G.S. thank Boehringer Ingelheim Fonds for a Ph.D. Fellowship and the Army Research Office for a National Defense Science and Engineering Graduate Fellowship, respectively. J.X.K. acknowledges support from the NIH (grant CA113605).

The Xie Group is grateful to the U.S. Department of Energy's Basic Energy Sciences program (DE-FG02-07ER15875) for supporting high-sensitivity Raman detection. The instrumentation development was supported by NSF (grant DBI-0649892), NIH Director's Pioneer Award (to X.S.X.), the Bill & Melinda Gates Foundation Gates Foundation, and Pfizer Global Medical. Harvard University has filed a patent application based on this work.

Supporting Online Material

www.sciencemag.org/cgi/content/full/322/5909/1857/DC1
Materials and Methods
Figs. S1 to S6
Movies S1 to S3

10 September 2008; accepted 19 November 2008
10.1126/science.1165758

Leukemic Cells Create Bone Marrow Niches That Disrupt the Behavior of Normal Hematopoietic Progenitor Cells

Angela Colmone, Maria Amorim, Andrea L. Pontier, Sheng Wang, Elizabeth Jablonski, Dorothy A. Sipkins*

The host tissue microenvironment influences malignant cell proliferation and metastasis, but little is known about how tumor-induced changes in the microenvironment affect benign cellular ecosystems. Applying dynamic in vivo imaging to a mouse model, we show that leukemic cell growth disrupts normal hematopoietic progenitor cell (HPC) bone marrow niches and creates abnormal microenvironments that sequester transplanted human $CD34^+$ (HPC-enriched) cells. $CD34^+$ cells in leukemic mice declined in number over time and failed to mobilize into the peripheral circulation in response to cytokine stimulation. Neutralization of stem cell factor (SCF) secreted by leukemic cells inhibited $CD34^+$ cell migration into malignant niches, normalized $CD34^+$ cell numbers, and restored $CD34^+$ cell mobilization in leukemic mice. These data suggest that the tumor microenvironment causes HPC dysfunction by usurping normal HPC niches and that therapeutic inhibition of HPC interaction with tumor niches may help maintain normal progenitor cell function in the setting of malignancy.

Hematopoietic progenitor cells (HPCs) home to and engraft in highly specific bone marrow (BM) microenvironments, or niches, that regulate their survival, proliferation, and differentiation (*1*, *2*). These niches have been defined by the association of particular stromal cell types and by their elaboration or secretion of specific signaling molecules, growth factors, and cytokines (*3*). At least two distinct HPC-supportive niches have been identified in the BM: an osteoblastic niche in which molecules including bone morphogenetic protein, osteopontin, angiopoietin-1, and Notch appear to play important regulatory roles; and a vascular niche that remains to be molecularly defined (*4*–*8*).

Although defects in hematopoiesis are frequently observed in patients with malignant involvement of the BM, the molecular bases of these phenomena, and whether they might reflect perturbations in HPC-supportive niches, are unknown. Suppression of normal hematopoiesis can occur in the setting of relatively low tumor burden and thus does not necessarily reflect anatomic "crowding out" of benign cells.

Using a severe combined immunodeficiency (SCID) mouse xenograft model of Nalm-6 pre-B acute lymphoblastic leukemia (ALL), we have shown that malignant cells metastasize to specific stromal cell–derived factor–1 (SDF-1)–positive vascular niches in the BM that overlap with perivascular HPC niches (*9*). To investigate whether benign and malignant cells compete for niche resources, we used real-time, in vivo confocal and multiphoton microscopy imaging approaches that allowed us to colocalize fluorescently labeled BM antigens with fluorescently labeled human $CD34^+$ cells, which are highly enriched in HPCs, and fluorescent tumor cells (*10*). For intravenous transplant into mice, we harvested $CD34^+$ cells from human cord blood and from the peripheral blood of human donors who had been treated

Department of Medicine, Section of Hematology/Oncology, The University of Chicago, 5841 South Maryland Avenue MC 2115, Chicago, IL 60637, USA.

*To whom correspondence should be addressed: E-mail: dsipkins@medicine.bsd.uchicago.edu

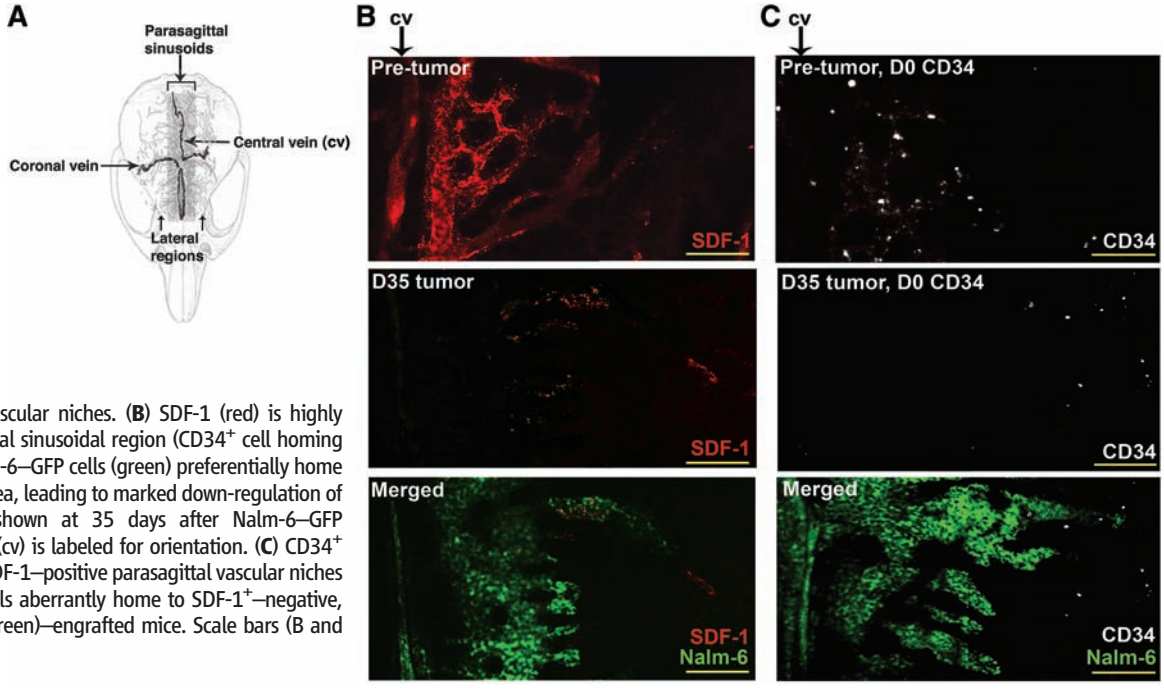

Fig. 1. Leukemia-induced changes in the BM microenvironment disrupt $CD34^+$ cell homing. (**A**) Diagram of mouse calvarial BM vasculature. In control mice, $CD34^+$ cells predominantly home to parasagittal sinusoidal vasculature. A major fraction of $CD34^+$ cells engraft in this parasagittal region after homing, whereas other $CD34^+$ cells migrate to more lateral osteoblastic and vascular niches. (**B**) SDF-1 (red) is highly expressed in the parasagittal sinusoidal region ($CD34^+$ cell homing sites) of control mice. Nalm-6–GFP cells (green) preferentially home to and proliferate in this area, leading to marked down-regulation of SDF-1 expression, here shown at 35 days after Nalm-6–GFP engraftment. Central vein (cv) is labeled for orientation. (**C**) $CD34^+$ cells (white) home to the SDF-1–positive parasagittal vascular niches in control mice. $CD34^+$ cells aberrantly home to $SDF\text{-}1^+$–negative, lateral regions in tumor (green)–engrafted mice. Scale bars (B and C), 250 μm.

with cytokines to stimulate mobilization of HPCs from the BM. Both of these populations are currently used for therapeutic BM transplantation in humans. Serial imaging of individual mice permitted us to observe cellular migration and proliferation in the calvarial BM over multiple time points from initial BM homing of circulating $CD34^+$ cells through long-term $CD34^+$ cell engraftment (12 weeks or more after transplantation) [Fig. 1A and figs. S1 and S2 (*10*)].

SDF-1 is an important chemoattractant for HPC homing to the BM and plays a key role in maintaining hematopoiesis (*11*–*13*). Because SDF-1 expression is up-regulated in regions of hypoxia or inflammation (*14*, *15*), we hypothesized that SDF-1 protein levels would be increased in the tumor niche. Surprisingly, however, when we assessed the mice for BM SDF-1 expression ~1 month after initial Nalm-6–GFP (green fluorescent protein) engraftment, we found that SDF-1 was markedly down-regulated in regions of heavy tumor growth (Fig. 1B and figs. S3 and S4). These areas of extensive tumor proliferation and SDF-1 down-regulation corresponded to typical $CD34^+$ cell homing niches.

Given that leukemic proliferation occurred preferentially within $CD34^+$ cell homing niches and disrupted chemokine SDF-1 expression at these sites, we next examined whether $CD34^+$ cell BM homing was altered in leukemic mice. Nalm-6–GFP leukemic mice versus control mice were engrafted intravenously with purified, fluorescently labeled human $CD34^+$ cells. Whereas in control mice $CD34^+$ cell homing localized to SDF-1–positive parasagittal vascular niches, in leukemic mice $CD34^+$ cell homing was redirected to atypical lateral microenvironments (Fig. 1C and fig. S5). This finding did not reflect an inability of cells to enter parasagittal regions in leukemic mice, because video-rate imaging confirmed that the cells transited freely through parasagittal tumor-associated vasculature [movies S1 and S2 (*10*)]. Furthermore, when $CD34^+$ cells were pretreated with pertussis toxin (an inhibitor of chemokine receptor $G\alpha_i$-mediated signaling) or with AMD3100 (a small-molecule antagonist of the SDF-1 receptor CXCR4), there was no significant decrease in $CD34^+$ cell homing to the BM in tumor mice (figs. S6 and S7). These data suggest that in leukemic mice, $CD34^+$ cells homed to atypical regions through an SDF-1– and chemokine-independent mechanism.

Although $CD34^+$ cells were able to traffic to BM in leukemic mice, our observation that initial homing occurred in abnormal vascular niches raised the possibility that subsequent engraftment would be altered. We therefore performed serial imaging studies of individual mice to assess the intra-BM movement of $CD34^+$ cells. Surprisingly, most $CD34^+$ cells did not remain at sites of initial homing or migrate to other tumor-free niches. Instead, within days, the vast majority of the transplanted cells aberrantly migrated to SDF-1–negative tumor beds, suggesting that the

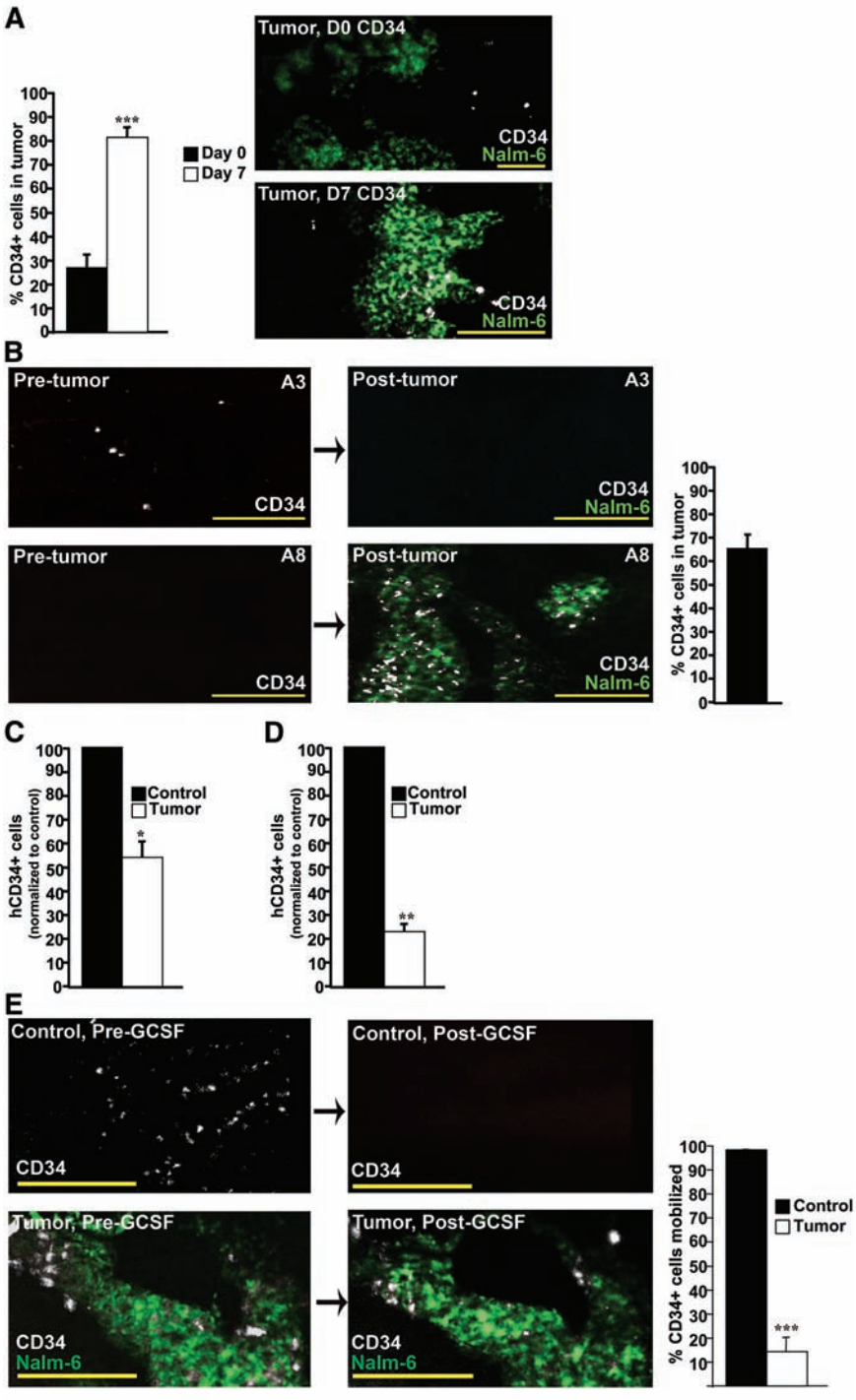

Fig. 2. The malignant microenvironment, or niche, attracts $CD34^+$ cells, but does not maintain $CD34^+$ cell pool size or response to cytokine mobilization. (**A**) Few $CD34^+$ cells colocalize with tumor upon homing to BM (day 0: 25.6 ± 6.7%), yet $CD34^+$ cells migrate into tumor niches over time (day 7: 82.1 ± 4.5%, normalized to total $CD34^+$ cells in BM; $n = 4$ mice, $^{***}P < 0.0001$). (**B**) Serial imaging of mice from 12 to 16 weeks after $CD34^+$ cell (white) transplant reveals that long-term transplanted $CD34^+$ cells abandon normal niches (representative area A3 pretumor) after leukemia (green) engraftment. Conversely, $CD34^+$ cells in leukemic mice migrate to tumor regions (area A8 posttumor) where $CD34^+$ cells do not normally localize. Most of the long-term transplanted $CD34^+$ cells are found within tumor beds (65.9 ± 7%; $n = 6$ mice) in mice imaged ~1 month after tumor engraftment. Tumor involves only 20 to 30% of BM at this time point. (**C** and **D**) Fewer $CD34^+$ cells are harvested from BM of leukemic versus control mice at 7 days (C) [day 7: 55.2 ± 8.5%; $n = 4$ mice (leukemia), $n = 2$ mice (control), $^*P = 0.029$] and 16 weeks (D) (16 weeks: 21.7 ± 3.3%; $n = 4$ (leukemia), $n = 4$ (control), $^{**}P = 0.005$) after $CD34^+$ cell transplant. (**E**) $CD34^+$ cells mobilize from BM upon G-CSF treatment of naïve (98.6 ± 0.2%), but not leukemic (13.8 ± 7%), mice (serial imaging of the same areas; $n = 3$ mice each, leukemia and control, $^{***}P < 0.0005$). Scale bars (A, B, and E), 250 μm.

tumor had created a new malignant niche capable of recruiting CD34$^+$ cells (Fig. 2A).

To determine if the malignant niche could also compete for CD34$^+$ cells previously established in normal BM niches, we introduced Nalm-6–GFP into mice that had been transplanted with CD34$^+$ cells 12 to 16 weeks earlier. One month after tumor engraftment, most CD34$^+$ cells abandoned tumor-free niches for malignant niches (Fig. 2B). To determine if the malignant niche was able to maintain the new resident CD34$^+$ populations, we harvested human CD34$^+$ cells from leukemic and control mice by magnetic bead selection and quantified the cells by flow cytometry. Significantly fewer CD34$^+$ cells (55.2 ± 8.5%) were recovered from leukemic mice 1 week after CD34$^+$ cell transplantation when compared with control mice (Fig. 2C). In long-term CD34$^+$ cell–transplanted mice subsequently engrafted with leukemia, CD34$^+$ cell counts also declined significantly (21.7 ± 3.3%) over time in leukemic versus control mice (Fig. 2D). These data suggest that the malignant niche, although outcompeting native niches for CD34$^+$ cell localization, fails to preserve the CD34$^+$ cell pool size seen in normal mice.

HPCs are routinely collected for autologous or allogeneic transplant by harvest from the peripheral blood after these cells are mobilized out of the BM by treatment of patients with the cytokine granulocyte colony-stimulating factor (G-CSF). However, the presence of residual BM disease is associated with decreased CD34$^+$ cell mobilization into the peripheral circulation after cytokine treatment (*16*). Addition of the investigational agent AMD3100 to enhance mobilization can also fail to yield adequate stem cell numbers (*17*). Although some of this effect may be related to stromal damage from chemo- and radiotherapy, a clear cause for mobilization failure has not been established (*18*). We therefore examined the effect of malignant niche migration in leukemic mice on CD34$^+$ cell mobilization. CD34$^+$ cells engrafted in leukemic mice minimally mobilized in response to a 5-day course of G-CSF compared with controls (Fig. 2E). Mobilization was not enhanced by the addition of AMD3100 (fig. S8).

We next explored the molecular mechanism responsible for CD34$^+$ cell migration into the malignant niche, with the goal of correcting CD34$^+$ cell dysfunction by inhibiting the transit of these cells from normal microenvironments. To investigate the possibility that the malignant cells might be the source of chemoattractants, we performed transwell migration assays with CD34$^+$ cells and conditioned media (CM) from Nalm-6–GFP, primary human ALL, and primary human acute myeloblastic leukemia (AML) cell cultures. Relative to control media, CD34$^+$ cells migrated in significantly greater numbers (by a factor of 3.5) to leukemia CM (Fig. 3A). Addition of SDF-1 to CM had an additive, but not synergistic, effect on migration (fig. S9). We next screened CM by Western blot for molecules with chemotactic activity for CD34$^+$ cells. Among our initial candidates was stem cell

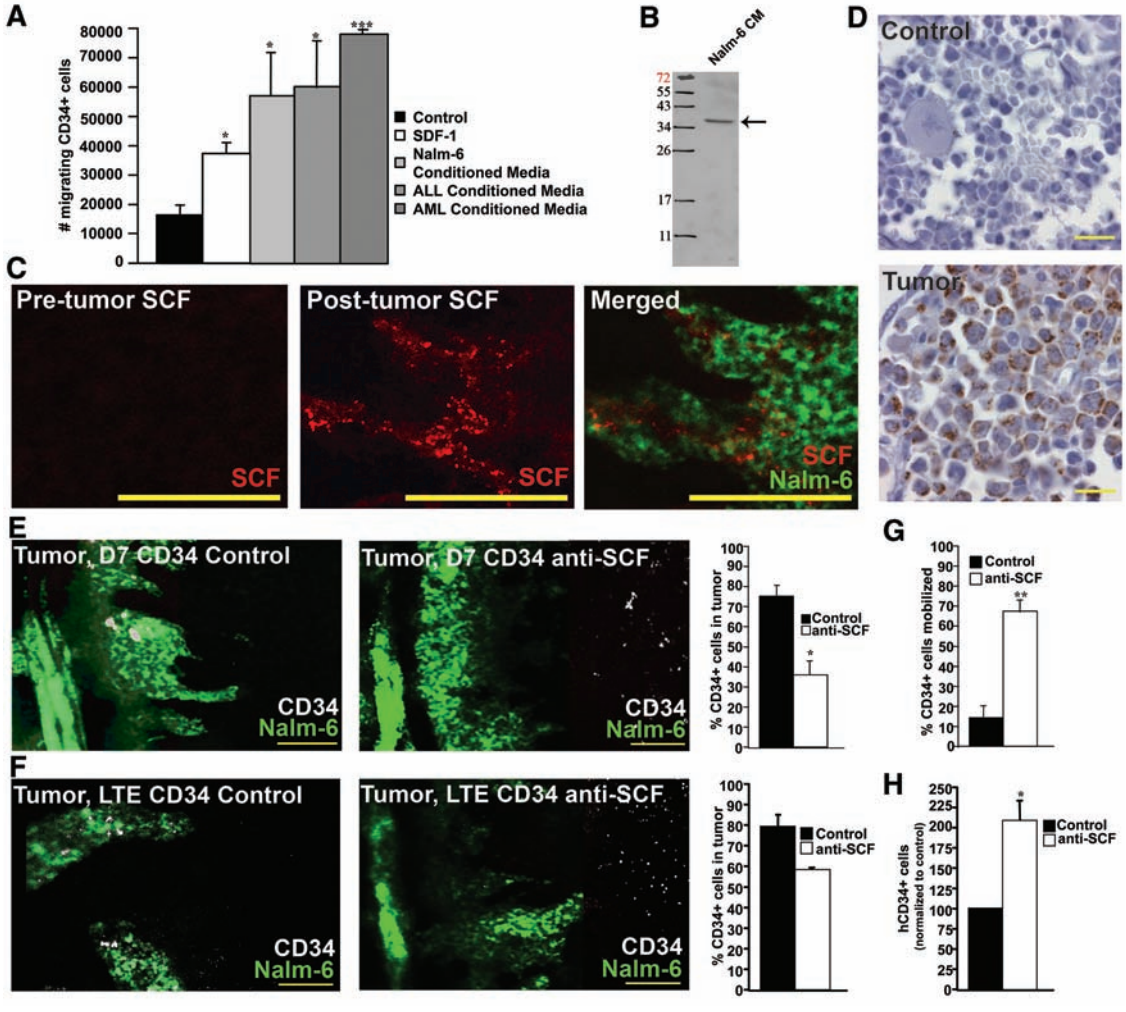

Fig. 3. SCF mediates CD34$^+$ cell migration into the malignant niche, as well as mobilization failure and decrease in CD34$^+$ cell number in leukemic mice. (**A**) CD34$^+$ cells migrate in vitro in response to leukemia-conditioned media (CM). (Control media: 16,137 ± 3799; SDF-1: 37,056 ± 3058; Nalm6-CM: 57,086 ± 14686; ALL-CM: 59,311 ± 17,495; AML-CM: 79,933 ± 933; n = 3 experiments; SDF-1:control, $^*P = 0.0014$; SDF-1:all leukemia-CM, $^*P = 0.009$; SDF-1:Nalm6-CM, $^*P = 0.026$; SDF-1:ALL-CM, $^*P = 0.020$; SDF-1:AML-CM, $^{***}P < 0.0001$). (**B**) SCF protein is secreted by Nalm-6–GFP in vitro. (**C**) In vivo imaging demonstrates increased SCF (red) expression in a tumor (green)–engrafted versus naïve mouse. Scale bars, 250 μm. (**D**) Immunohistochemistry shows hSCF (brown) expression in tumor-engrafted but not control mouse femur. Scale bars, 100 μm. (**E** and **F**) CD34$^+$ cells (white); Nalm-6–GFP (green) (E) Neutralizing treatment with anti-SCF inhibits CD34$^+$ cell migration into tumor 7 days after CD34$^+$ cell transplant into leukemic mice (control: 76.1 ± 5.6%; anti-SCF: 36.7 ± 8.3%; n = 5 mice each, control and anti-SCF, $^*P = 0.008$). Scale bars, 250 μm. (F) Neutralizing anti-SCF inhibits migration of long-term engrafted (LTE) CD34$^+$ cells into the malignant niche. Treatment began 12 weeks after CD34$^+$ cell transplant (at the time of tumor engraftment) and continued for 4 weeks (control: 79.6 ± 6.3%; anti-SCF: 59.3 ± 0.4%; n = 2 mice each, control and anti-SCF). Scale bars, 250 μm. (**G**) Neutralizing anti-SCF restores G-CSF–mediated CD34$^+$ cell mobilization in leukemic mice (control: 13.75 ± 7.0%; anti-SCF: 68.0 ± 6.0%; n = 3 mice each, control and anti-SCF, $^{**}P = 0.004$). (**H**) Seven days after transplant, increased numbers of CD34$^+$ cells were isolated from BM of leukemic mice treated with neutralizing anti-SCF versus control IgG (anti-SCF: 211 ± 23, normalized to control = 100; n = 2 mice each, control and anti-SCF, $^*P = 0.04$).

factor (SCF), an HPC growth factor and chemoattractant believed to play a role in HSC localization to endosteal niches (*19*–*22*). SCF is produced by a wide variety of solid tumors (*23*–*26*). AML cell lines and primary AML cells have been shown to produce SCF RNA transcripts, but expression of SCF by hematologic malignancies is not well defined (*27*). Figure 3B and fig. S10 show that SCF protein is clearly present in leukemia-CM.

To assess whether SCF expression was up-regulated in the leukemic niche in our mouse model, we performed in vivo immunoimaging of control versus Nalm-6–GFP leukemic mice using fluorescently labeled mouse/human cross-reactive antibodies to SCF (anti-SCF). Whereas only a faint SCF signal was detectable at baseline in control mouse calvarial BM, SCF was highly expressed in mice imaged ~1 month after Nalm-6–GFP engraftment (Fig. 3C). Immunohistochemical staining of mouse femurs confirmed that human SCF (hSCF) was present at high abundance in this marrow compartment (Fig. 3D). In addition, Western blotting of control versus leukemic BM showed expression of human SCF protein product (fig. S11). Quantitative reverse transcription–polymerase chain reaction demonstrated a significant decrease in mouse SCF RNA transcript copy numbers, suggesting that leukemic cells constituted the major source of SCF in the malignant microenvironment (fig. S12).

To determine whether $CD34^+$ cell migration into the malignant niche could be prevented by inhibition of SCF activity, we treated Nalm-6–GFP leukemic mice with SCF-neutralizing antibodies beginning 1 day before $CD34^+$ cell engraftment. We found that at 7 days after $CD34^+$ cell engraftment, significantly fewer $CD34^+$ cells had migrated into tumor niches in treated (37%) versus untreated (76%) mice (Fig. 3E). We also treated long-term $CD34^+$ cell–engrafted mice (12 to 16 weeks) with SCF-neutralizing antibodies beginning 1 day before Nalm-6–GFP engraftment and continuing for 30 days. Again, fewer $CD34^+$ cells exited normal niches for the malignant niche compared with the control (Fig. 3F). To determine if prevention of $CD34^+$ cell egress from benign niches also rescued $CD34^+$ cell function in leukemic mice, we administered a 5-day course of G-CSF (to induce $CD34^+$ cell mobilization) to mice that had been treated with SCF-neutralizing antibody, as well as to control immunoglobulin G (IgG)–treated mice. Sixty-eight percent of $CD34^+$ cells in neutralizing antibody–treated mice mobilized in response to cytokine stimulation versus 14% in untreated mice (Fig. 3G). In another set of experiments, leukemic mice were treated with SCF-neutralizing antibody versus control IgG beginning 1 day before transplant of $CD34^+$ cells. Mice were killed after 7 days for $CD34^+$ cell harvest and quantitation. More than twice as many $CD34^+$ cells were obtained from treated mice (Fig. 3H). These data suggest that $CD34^+$ cell pool size could be maintained in leukemic mice by inhibiting $CD34^+$ cell engagement with the malignant niche.

To extend our observations with the Nalm-6 ALL cell line to primary human disease, we performed similar experiments with cells isolated from BM aspirates of ALL or AML patients. Imaging of mice ~8 weeks after engraftment of primary pre-B ALL or AML in nonobese diabetic–severe combined immunodeficiency (NOD-SCID) mice revealed pronounced up-regulation of SCF signal in the calvarial BM (Fig. 4A and fig. S13). $CD34^+$ cells engrafted in these mice exhibited migration into SCF^+ domains similar to that in Nalm-6–GFP leukemic mice (Fig. 4B). $CD34^+$ cells also failed to respond to G-CSF mobilization (Fig. 4C).

Finally, we determined whether changes in SCF expression could be detected in initial diagnostic BM samples from patients with pre-B ALL. Normal BM biopsies (no evidence of disease) and BM biopsies with known ALL involvement were assayed for SCF by immunohistochemistry of paraffin-embedded sections. As seen in representative micrographs in Fig. 4D, basal expression was low in all three normal controls, whereas SCF staining was markedly elevated (by a factor of 2; Fig. 4E) in all seven patient samples.

We have shown that leukemic proliferation in the BM alters the stromal microenvironment and creates malignant niches that outcompete native HPC niches for $CD34^+$ cell engraftment. Normal $CD34^+$ cells engaged by the malignant niche exhibit abnormal behavior. Our data suggest that therapeutic targeting of SCF may increase the hematopoietic reserve and improve outcomes in BM transplantation and autologous stem cell harvest in the setting of hematologic malignancy. The findings from our xenograft model, however, require confirmation in human studies.

Our results raise many questions about the nature of tumor-host interactions: Do leukemic cells reorganize the molecular microenvironment specifically to entrap HPCs, or is the creation of competitive HPC niches a coincidental side effect of leukemic growth? Conceivably, derangements in hematopoiesis and HPC mobilization could impair anti-tumor immune responses. Of note, SCF neutralization did not significantly inhibit Nalm-6 proliferation in our model, and indeed Nalm-6 cells down-regulate their expression of the SCF receptor, KIT, in vivo (fig. S14). These findings, although not definitive, suggest that Nalm-6 SCF production does not principally serve to fuel autocrine tumor growth. Future studies that elucidate the intricacies of these tumor-host interactions are expected to further our understanding of stem and progenitor cell dysfunction in cancer and expose new therapeutic targets.

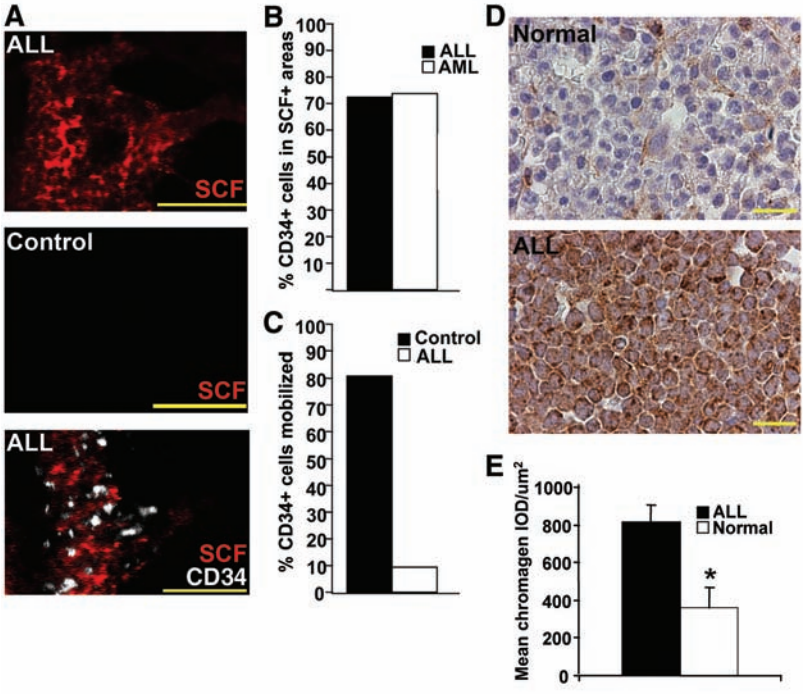

Fig. 4. Primary leukemic cells from patients with ALL and AML create abnormal $CD34^+$ cell niches; human ALL BM biopsies demonstrate marked up-regulation of SCF. (**A**) SCF (red) expression is markedly up-regulated in ALL-engrafted versus control mice. $CD34^+$ cells (white) localize to regions of high SCF expression. Scale bars, 250 μm. (**B**) $CD34^+$ cells migrate into the malignant niche in ALL and AML-engrafted mice (ALL: 72.7%; AML: 73.6%). (**C**) $CD34^+$ cells do not respond to G-CSF mobilization in ALL-engrafted mice (control: 80.4%, ALL: 7.8%). (**D**) Representative micrographs of SCF (brown) immunohistochemical staining in a diagnostic BM biopsy from a patient with pre-B ALL versus a normal BM biopsy. Scale bars, 100 μm. (**E**) Quantitative analysis of SCF immunostaining intensity in ALL versus normal BM biopsies (ALL: 814 ± 88, n = 7 patients; normal: 364 ± 107, n = 3 patients; *P = 0.004).

References and Notes

1. O. Naveiras, G. Q. Daley, *Cell. Mol. Life Sci.* **63**, 760 (2006).
2. H. G. Kopp, S. T. Avecilla, A. T. Hooper, S. Rafii, *Physiology (Bethesda)* **20**, 349 (2005).
3. T. Yin, L. Li, *J. Clin. Invest.* **116**, 1195 (2006).
4. J. Zhang *et al.*, *Nature* **425**, 836 (2003).
5. S. K. Nilsson *et al.*, *Blood* **106**, 1232 (2005).
6. F. Arai *et al.*, *Cell* **118**, 149 (2004).
7. L. M. Calvi *et al.*, *Nature* **425**, 841 (2003).

8. M. J. Kiel, O. H. Yilmaz, T. Iwashita, C. Terhorst, S. J. Morrison, *Cell* **121**, 1109 (2005).
9. D. A. Sipkins *et al.*, *Nature* **435**, 969 (2005).
10. Materials and methods are available as supporting material on *Science* Online.
11. A. Peled *et al.*, *Science* **283**, 845 (1999).
12. T. Lapidot, O. Kollet, *Leukemia* **16**, 1992 (2002).
13. H. E. Broxmeyer, *Curr. Opin. Hematol.* **15**, 49 (2008).
14. D. J. Ceradini *et al.*, *Nat. Med.* **10**, 858 (2004).
15. C. Hitchon *et al.*, *Arthritis Rheum.* **46**, 2587 (2002).
16. B. Nervi, D. C. Link, J. F. DiPersio, *J. Cell. Biochem.* **99**, 690 (2006).
17. G. Calandra *et al.*, *Bone Marrow Transplant.* **41**, 331 (2008).
18. W. Bensinger *et al.*, *J. Clin. Oncol.* **13**, 2547 (1995).
19. N. Okumura *et al.*, *Blood* **87**, 4100 (1996).
20. R. L. Driessen, H. M. Johnston, S. K. Nilsson, *Exp. Hematol.* **31**, 1284 (2003).
21. L. K. Ashman, *Int. J. Biochem. Cell Biol.* **31**, 1037 (1999).
22. S. Sharma *et al.*, *Stem Cells Dev.* **15**, 755 (2006).
23. N. Théou-Anton *et al.*, *Br. J. Cancer* **94**, 1180 (2006).
24. K. A. Giehl, U. Nagele, M. Vokenandt, C. Berking, *J. Cutan. Pathol.* **34**, 7 (2007).
25. G. Bellone *et al.*, *Int. J. Oncol.* **29**, 851 (2006).
26. M. Tao *et al.*, *Cytokine* **12**, 699 (2000).
27. R. Zheng, K. Klang, N. C. Gorin, D. Small, *Leuk. Res.* **28**, 121 (2004).

28. We thank A. Chenn, K. Cohen, L. Godley, and R. Salgia for critical discussions and reading of the manuscript; A. Chenn for assistance with retroviral cell transduction; A. Wickrema for help with CD34$^+$ purification; V. Bindokas for imaging expertise; and S. Gurbuxani for assistance with histopathology interpretation. Supported by a grant from the Illinois Regenerative Medicine Institute (IRMI), an NIH (National Cancer Institute) K08 award (5K08CA112126-02), and an NIH Director's DP2 award (1DP2OD002160-01). A patent application related to this work has been filed by the University of Chicago.

Supporting Online Material

www.sciencemag.org/cgi/content/full/322/5909/1861/DC1
Materials and Methods
Figs. S1 to S13
Movies S1 and S2

7 August 2008; accepted 19 November 2008
10.1126/science.1164390

Representation of Geometric Borders in the Entorhinal Cortex

Trygve Solstad, Charlotte N. Boccara,* Emilio Kropff,* May-Britt Moser, Edvard I. Moser†

We report the existence of an entorhinal cell type that fires when an animal is close to the borders of the proximal environment. The orientation-specific edge-apposing activity of these "border cells" is maintained when the environment is stretched and during testing in enclosures of different size and shape in different rooms. Border cells are relatively sparse, making up less than 10% of the local cell population, but can be found in all layers of the medial entorhinal cortex as well as the adjacent parasubiculum, often intermingled with head-direction cells and grid cells. Border cells may be instrumental in planning trajectories and anchoring grid fields and place fields to a geometric reference frame.

An animal's current position in the environment is encoded by a network of hippocampal and parahippocampal neurons with diverse spatial firing properties. Within this network, at least three cell types contribute to the computation of self-location: place cells, which fire when the animal moves through a particular location in space (*1*–*3*); head-direction cells, which fire when the animal is facing in a certain direction (*4*–*7*); and grid cells, whose multiple sharply localized firing fields form a remarkably regular triangular pattern across the environment (*3*, *7*–*9*). In addition to these cell types, computational models posit the existence of cortical "boundary vector cells," whose activity patterns encode the animal's distance from salient geometric borders (*10*, *11*). Based on predictions from these models, we investigated whether proximity to borders is represented by specific cell types in the entorhinal spatial representation circuit (*12*).

A total of 624 principal cells were recorded from the dorsocaudal quarter of the medial entorhinal cortex (MEC) and adjacent parasubiculum in 13 rats (fig. S1). Neural activity was sampled while these animals foraged in enclosures with moveable walls and barriers. The animals were first tested in a square enclosure (1 m by 1 m or 1.5 m by 1.5 m) with 50-cm-high walls. Many recorded cells were grid cells and head-direction cells (*7*–*9*), but in addition the data included a previously unknown class of entorhinal cells that fired exclusively along one or several walls of the enclosure (Fig. 1 and fig. S2). These cells were identified by computing, for each cell, the difference between the maximal length of a wall touching upon a single firing field and the average distance of the fields from the nearest wall, divided by the sum of those values (*12*). Border scores ranged from –1 for cells with central firing fields to +1 for cells with fields that perfectly lined up along at least one entire wall. "Border cells" were defined as spatially stable cells with border scores above 0.5. A total of 69 cells from 12 animals passed this criterion (Fig. 1 and fig. S2) (*13*). In these cells, 86.0 ± 0.6% of the spikes occurred closer to the walls than to the center of the box per unit of time [mean ± SEM; $t(68) = 17.4$, one-sample t test, $P < 0.001$; expected value 75%]. Only 3.6 ± 1.0% of the

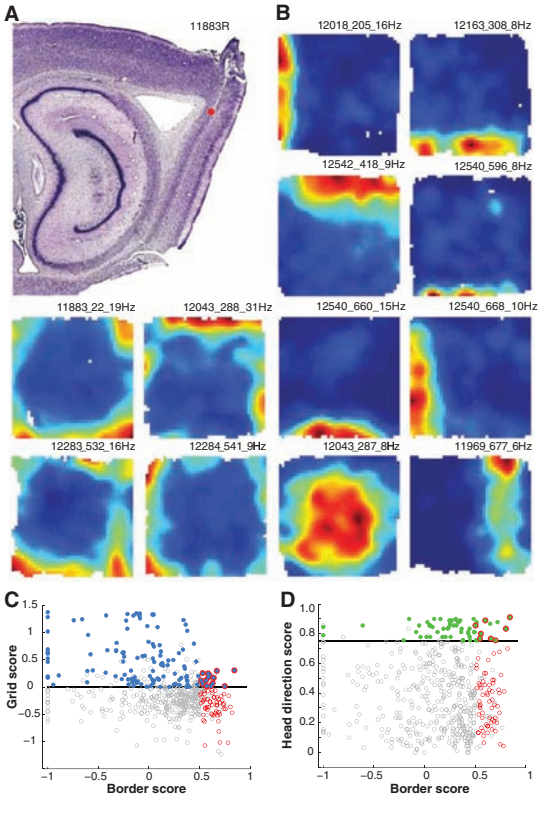

Fig. 1. Examples of border cells in the MEC and adjacent parasubiculum. (**A**) Sagittal Nissl-stained section showing a representative recording location in the MEC (red dot, recording location; rat number and hemisphere (R, right) are indicated; see fig. S1 for all other recording positions). (**B**) Color-coded rate maps for 12 border cells. Red is maximum, dark blue is zero. Pixels not covered are white. Animal numbers (five digits), cell numbers (two or three digits), and peak firing rates are indicated above each panel. Cells 287 and 677 did not pass the criterion for border cells because the fields were located at some distance from the wall; the number of such cells was fewer than 10. See fig. S2 for the complete set of rate maps, trajectories, and directional tuning curves, and representative waveforms and tetrode clusters. (**C** and **D**) Scatter plots showing correlation between border scores and grid scores (C) or head-direction scores (D) (*12*). Each dot in the scatter plot corresponds to one cell (red, border cells; blue, grid cells; green, head-direction cells; gray, cells not passing any criterion, including cells with high spatial or directional scores but low stability; double-colored dots, cells that satisfy criteria for two cell classes). Horizontal lines indicate thresholds for grid and head-direction cells.

Kavli Institute for Systems Neuroscience and Centre for the Biology of Memory, Norwegian University of Science and Technology, 7489 Trondheim, Norway.

*These authors contributed equally to this work.
†To whom correspondence should be addressed. E-mail: edvard.moser@ntnu.no

central area was part of a firing field [expected value 25%; $t(68) = 22.1$, $P < 0.001$]. Fifty-two of the cells fired along a single wall; the remaining 17, mostly from the deep layers of the MEC, had fields along two, three, or four walls (fig. S2A). On average, the border field along the dominant wall covered 75.4 ± 1.8% of the length of the wall. The mean distance between the active bins in the field and the wall was 8.4 ± 0.3% of the box length. An additional set of fewer than 10 cells, excluded by the formal criterion, had fields that were parallel to the box walls but separated by a stripe of inactivity between the walls and the field (Fig. 1B, cells 287 and 677). The activity pattern of the border cells was fundamentally different from that of grid cells and head-direction cells recorded simultaneously on the same tetrodes [Fig. 1, C and D, and supporting online material (SOM) text]. Border cells were found in all layers of the MEC and in the adjacent parasubiculum (fig. S1 and SOM text). Thirty-one of 69 border cells were modulated by the theta rhythm (fig. S3).

If the activity was determined by the walls rather than other localized variables, the cells should continue to fire along their preferred walls after changes in the length of the box, and the mean firing distance from the nearest wall might remain unchanged. This prediction was confirmed for most of the cells that were classified as border cells in the small square enclosure. Extending the 1-m–by–1-m square to a 1-m–by–2-m or 2-m–by–1-m rectangle caused a corresponding extension of the firing field if the field was parallel to the extended wall but not if its long axis was orthogonal to the direction of extension (44 cells; Fig. 2A and fig. S4). The fraction of spikes along the walls per unit of time was not changed [79.9 ± 1.7% in the square and 80.8 ± 1.5% in the rectangles; paired t test, $t(43) = 0.45$]. The proportion of the central area covered by firing fields [5.0 ± 1.0% in the square and 7.9 ± 1.5% in the rectangle; paired t test, $t(43) = 2.3$, $P < 0.05$] remained far below the chance level of 25% [for the rectangle, $t(43) = 11.8$, < 0.001], suggesting that the firing was indeed controlled by the walls of the environment.

Do border cells primarily encode the periphery of the environment or are they tuned to barriers more generally, irrespective of their continuity with the other borders? We recorded the activity of 22 border cells after inserting a discrete wall into the square enclosure (*11*, *12*) (Fig. 2B and figs. S5 and S6). Only cells with fields along a single wall were analyzed (12 cells). When the wall was inserted in parallel with the original firing field, an additional field emerged in the rate map of all cells, although only 9 of the new fields met our selection criteria for quantitative analysis. In all 12 cases, the new field lined up along the inserted wall. The new field and the parent field were always on the same side of the insert relative to the distal room cues (for example, both were on the east side in Fig. 2B). The new field covered 68.7 ± 8.2% of the inserted wall on this side. The coverage of the opposite side (the side that faced the parent field) was 0 in all cases. Reducing the height of the barrier from 50 cm to 5 cm did not abolish the new field as long as the animal's trajectory was impeded (fig. S6; three experiments).

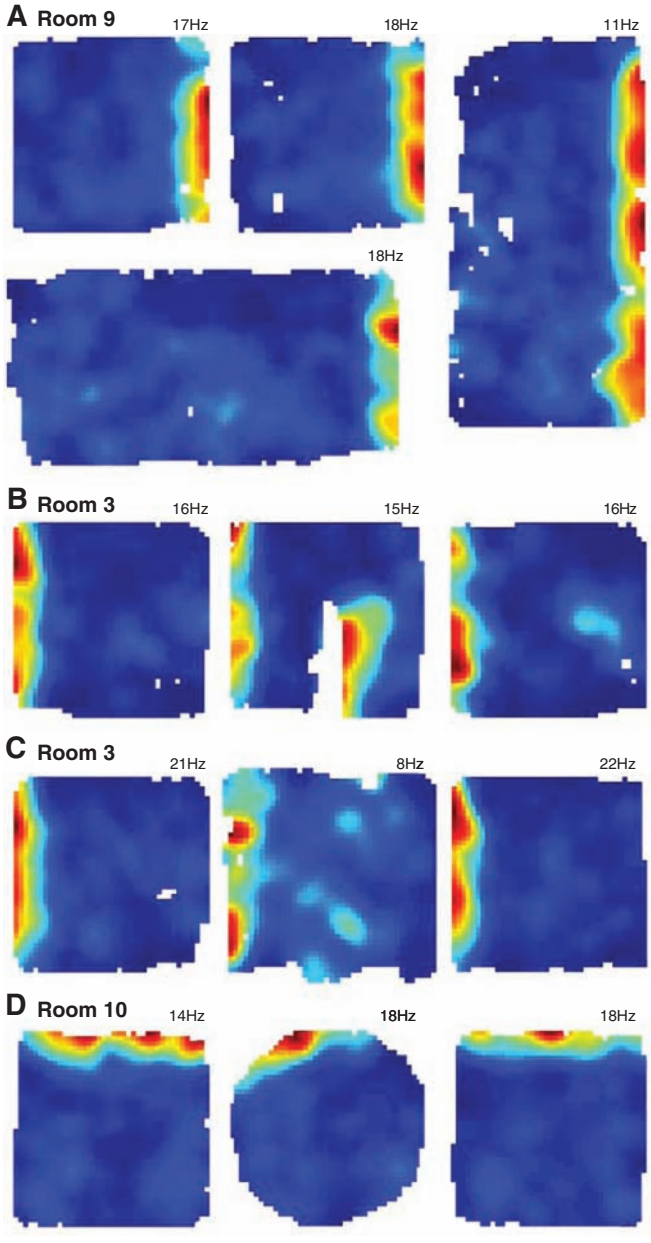

Fig. 2. Border cells express proximity to boundaries in a number of environmental configurations. (**A** to **D**) Color-coded rate maps for a representative border cell in boxes with different geometric configurations (cell 205 of rat 12018). Each panel shows one trial. Symbols are as in Fig. 1B. (A) The border field follows the walls when the square enclosure is stretched to a rectangle. (B) Introducing a discrete wall (white pixels) inside the square causes a new border field to appear (middle panel). The new field has the same orientation relative to distal cues as the original field on the peripheral wall. (C) Border fields persist after removal of the box walls (middle panel). Without walls, the drop along the edges was 60 cm. (D) Preserved firing along borders across rooms and geometrical shapes. All trials in (D) were recorded in a different room than those in (A) to (C). The conditions favor hippocampal global remapping between rooms and rate remapping within rooms (*12*, *16*, *22*) (fig. S9).

To determine whether border cells also respond to boundaries other than walls, the box walls were removed and the animals were tested on the remaining open surface, which now had a 60-cm drop on all four sides. In general, border fields could still be identified (Fig. 2C and figs. S7 and S8). The fraction of spikes along the walls per unit of time was not changed significantly [84.4 ± 1.5% with walls, 80.3 ± 3.1% without walls, $t(9) = 1.8$, $P > 0.10$], although the fraction of the central area that was part of a firing field increased [2.8 ± 2.1% with walls, 11.2 ± 4.1 without walls, $t(9) = 2.5$, $P < 0.05$; expected value 25%, $t(9) = 3.3$, $P < 0.01$]. The persistence of activity along the edges suggests that the cells respond to a variety of borders.

Unlike place cells (*14*, *15*), grid cells and head-direction cells retain their basic activity pattern across environments (*5*, *9*, *16*, *17*). To determine whether border cells are similarly context-independent, we first compared the activity of 27 cells in two different rooms, using square recording boxes in each room. The fraction of spikes along the walls, normalized by dwell times, did not change between the rooms [83.0 ± 1.5% versus 84.7 ± 1.3%; paired t test, $t(26) = 1.41$, $P > 0.15$; Fig. 2, B and C, versus D], nor did the proportion of the central area that was part of a firing field [11.5 ± 4.1% versus 7.5 ± 2.8%; $t(26) = 0.98$, $P > 0.30$]. We also compared the firing patterns of 21 border cells in two differently shaped enclosures, a square and a circle,

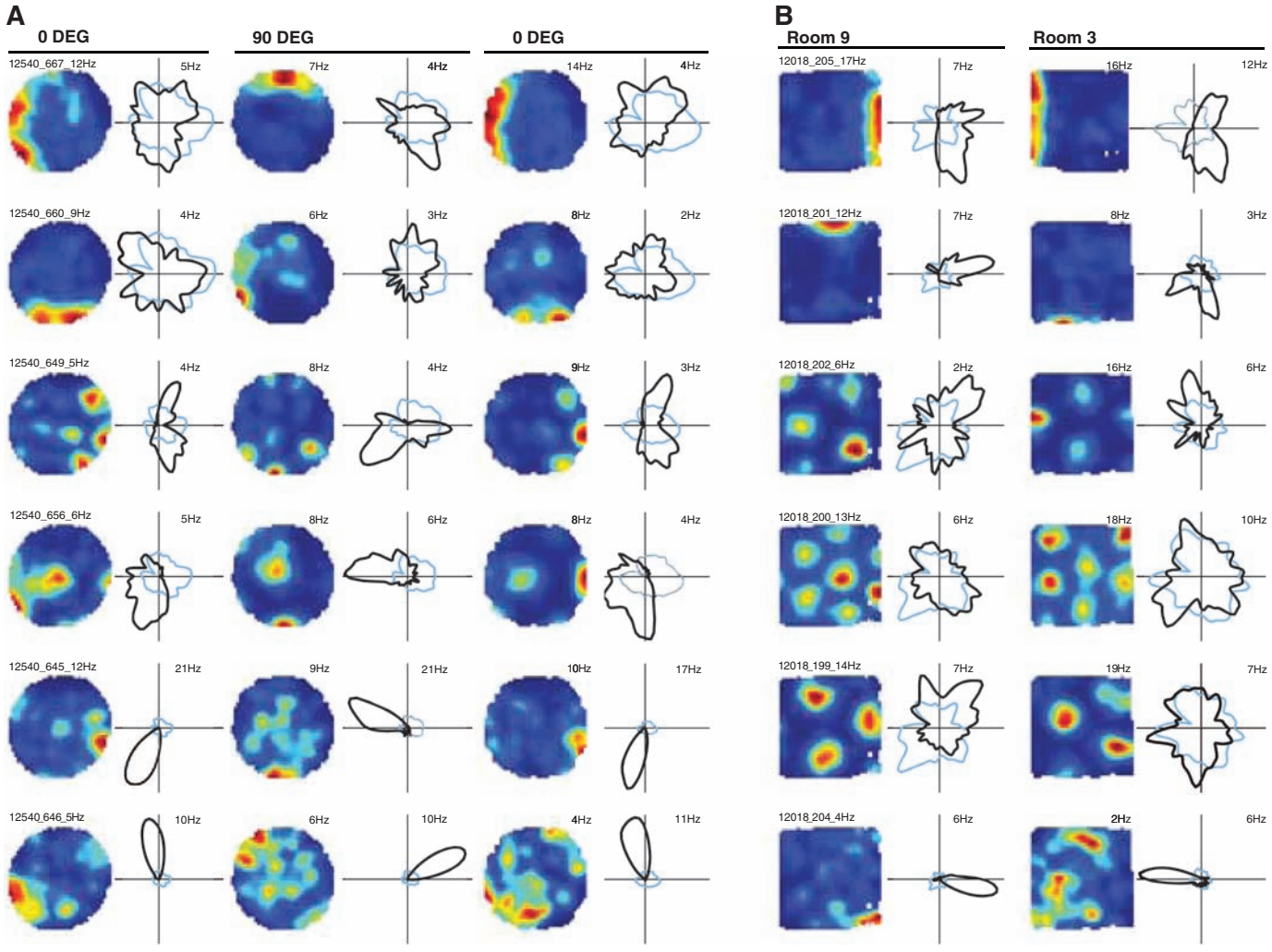

Fig. 3. Border cells, grid cells, and head-direction cells respond coherently to environmental manipulations. (**A**) Rate and head-direction maps for two border cells (top two rows), two grid cells with some head-directional modulation (middle two rows), and two head-direction cells (bottom two rows) recorded simultaneously before and after the rotation of a polarizing cue card (left and right columns, 0°; middle column, 90°). The polar plots show firing rate as a function of head direction (black traces) and the time that the rat faced each direction (blue traces). Peak firing rate is indicated. (**B**) Rate maps and polar plots for two border cells (top two rows), three grid cells (middle three rows), and one head-direction cell (bottom row) in two different rooms. The cells were recorded simultaneously.

in a single room (Fig. 2D and fig. S9). Again, the time-normalized fraction of spikes along the walls was not different [square, 87.1 ± 1.0%; circle, 85.0 ± 1.6%; paired *t* test, $t(20) = 1.67$, $P > 0.10$; Fig. 2D] and the firing fields covered a similar proportion of the central area of the environments [6.1 ± 2.2% and 12.7 ± 4.3; $t(20) = 1.95$, $P > 0.05$]. The persistence of border-related activity across environments, under conditions that often lead to realignment in grid cells and remapping in place cells (*16*) (fig. S8), suggests that the firing of these cells is primarily defined by geometric borders and less by the content of the environment or the training history of the animal.

Does the representation of borders, grid positions, and directions remain coherent across environments? We recorded 10 border cells along with grid cells and head-direction cells in five experiments. When the cue card on the wall of the circle was rotated 90°, simultaneously recorded border cells always rotated in concert (three experiments; pairwise difference in rotation 1°, 1°, and 9°; Fig. 3A). The same was observed with simultaneously recorded border cells and grid cells (mean difference between cell types 0°, 7.2°, and 9.5°; Fig. 3A) and with simultaneously recorded border cells and head-direction cells (mean difference 8.5°, 12.5°, and 13.6°; Fig. 3A; two of these experiments also included grid cells). When the animals were tested in different rooms, differences in the relative orientation of simultaneously recorded border cells were retained; that is, cells with fields on opposite walls in one room also fired along opposite walls in the other room, and their relation to grid cells and head-direction cells remained constant (Fig. 3B).

Taken together, these findings provide evidence for a previously unknown cell type in the spatial representation circuit of the MEC. Border cells have firing fields that line up along selected geometric borders of the proximal environment, irrespective of their length and continuity with other borders. The observation of border cells across all layers of the MEC confirms predictions from computational models that posit the existence of a boundary-responsive cortical cell population upstream of the hippocampus (*10*, *11*, *18*). Given that border cells are distributed widely in the circuit, information about obstacles and borders should be accessible to the majority of the entorhinal grid cells as well as to external target regions involved in path planning (*19*). By defining the perimeter of the environment, border cells may serve as reference frames for place representations within that environment, determining the firing locations of grid cells in the MEC as well as of place cells in the hippocampus and spatially selective cells in other cortical regions (*20*) (SOM text).

References and Notes

1. J. O'Keefe, J. Dostrovsky, *Brain Res.* **34**, 171 (1971).
2. J. O'Keefe, L. Nadel, *The Hippocampus as a Cognitive Map* (Clarendon, Oxford, 1978).

3. E. I. Moser, E. Kropff, M.-B. Moser, *Annu. Rev. Neurosci.* **31**, 69 (2008).
4. J.B. Ranck Jr., in *Electrical Activity of the Archicortex*, G. Buzsáki, C. H. Vanderwolf, Eds. (Akademiai Kiado, Budapest, Hungary, 1985), pp. 217–220.
5. J. S. Taube, R. U. Muller, J. B. Ranck Jr., *J. Neurosci.* **10**, 420 (1990).
6. J. S. Taube, *Annu. Rev. Neurosci.* **30**, 181 (2007).
7. F. Sargolini *et al.*, *Science* **312**, 758 (2006).
8. M. Fyhn, S. Molden, M. P. Witter, E. I. Moser, M.-B. Moser, *Science* **305**, 1258 (2004).
9. T. Hafting, M. Fyhn, S. Molden, M.-B. Moser, E. I. Moser, *Nature* **436**, 801 (2005).
10. T. Hartley, N. Burgess, C. Lever, F. Cacucci, J. O'Keefe, *Hippocampus* **10**, 369 (2000).
11. C. Barry *et al.*, *Rev. Neurosci.* **17**, 71 (2006).
12. Materials and methods are available as supporting material on *Science* Online.
13. The proportion of border cells in the medial entorhinal cell population is overestimated because experiments were often not started on days with no known border cells in the cell sample. The estimates should be taken as an upper limit.
14. E. Bostock, R. U. Muller, J. L. Kubie, *Hippocampus* **1**, 193 (1991).
15. L. L. Colgin, E. I. Moser, M.-B. Moser, *Trends Neurosci.* **31**, 469 (2008).
16. M. Fyhn, T. Hafting, A. Treves, M.-B. Moser, E. I. Moser, *Nature* **446**, 190 (2007).
17. D. Yoganarasimha, X. Yu, J. J. Knierim, *J. Neurosci.* **26**, 622 (2006).
18. A small number of boundary-modulated cells has also been reported downstream of the hippocampus, in the subiculum (*11*), but whether these signals are derived from local neurons or from entorhinal axons [as in (*21*)] has not been established.
19. J. R. Whitlock, R. J. Sutherland, M. P. Witter, M.-B. Moser, E. I. Moser, *Proc. Natl. Acad. Sci. U.S.A.* **105**, 14755 (2008).
20. D. A. Nitz, *Neuron* **49**, 747 (2006).
21. J. K. Leutgeb, S. Leutgeb, M.-B. Moser, E. I. Moser, *Science* **315**, 961 (2007).
22. S. Leutgeb *et al.*, *Science* **309**, 619 (2005).
23. We thank N. Burgess and a number of other colleagues for helpful discussion and suggestions; M. P. Witter for advice about electrode location; M. Fyhn for donating an implanted animal; and A. M. Amundsgård, E. Sjulstad, I. M. F. Hammer, K. Haugen, K. Jenssen, R. Skjerpeng, H. Waade, and T. Åsmul for technical assistance. The work was supported by the Kavli Foundation, the Centre of Excellence scheme of the Norwegian Research Council, and a European Commission Framework 7 project (SPACEBRAIN).

Supporting Online Material

www.sciencemag.org/cgi/content/full/322/5909/1865/DC1
Materials and Methods
SOM Text
Figs. S1 to S12
References

26 September 2008; accepted 10 November 2008
10.1126/science.1166466

New Products Focus: Proteomics

Multiplex Data Software

Milliplex Analyst is original equipment manufacturer's software that is seamlessly integrated with Luminex xPonent software, the system that controls Luminex multiplexed bioassay instruments. Multiplexing is virtually universal in the drug discovery industry and the Luminex system is one of the most commonly used platforms. Milliplex Analyst allows users to analyze multiplex data with accuracy, speed, and efficiency. Data sets can be easily extracted from acquisition or imported as Excel or text files. The software's unique algorithms and analytics allow robust processing of challenging data sets in seconds, with multiple output format options for maximum flexibility. Multiplate data can be analyzed using a variety of curve-fitting options to generate reports that feature fitting parameters and statistics.

Millipore and VigeneTech
For information 800-548-7853
www.millipore.com

Digital Imaging System

The AlphaImager Mini is a compact and economical digital imaging system suitable for routine imaging of fluorescent and colorimetric DNA and protein gels. The Mini's scientific-grade, 1.3-megapixel camera acquires high-resolution images suitable for quantitative downstream analysis. Images are captured using streamlined software, then can be printed directly to any digital or Windows-compatible printer and saved in several standard file formats. The instrument's cabinet offers a large pull-door for sample access and an ultraviolet-shielded viewport in a footprint less than 11 inches by 14 inches. It is compatible with ethidium bromide, SYBR green, Coomassie, silver stain, and more.

Alpha Innotech
For information 510-904-5647
www.alphainnotech.com

Low-Pressure Chromatography Columns

AxiChrom columns for low-pressure chromatography are designed to support the lean-enabling approach to column operation and maintenance. The columns feature "Intelligent Packing," in which preprogrammed and verified packing methods save time and make packing less dependent on the operator. The columns have a novel design with a pivot or swing-out column tube that provides easy access for maintenance. They are easy to prime, operate, and service with interactive guidance from the AxiChrom Master and Unicorn method wizard. AxiChrom columns are available with diameters from 50 mm to 1,000 mm, allowing users to choose the most suitable column size for separations from process development to full-scale production. They are designed to enable predictable scale-up for reproducible results over a range of column diameters and lengths.

GE Healthcare
For information +44-(0)20-7457-2020
www.gehealthcare.com

Proteomics Imaging System

The FLA-9000 is a modular image scanner for proteomic applications in radioisotopic, fluorescent, chemiluminescent, and digitized imaging. The FLA-9000 is designed for customized upgradeability and features a 40 cm by 46 cm scanning area. It is suitable for fluorescence detection of two-dimensional gels by SYPRO Ruby stain and digitization of Coomassie-brilliant-blue–stained or silver-stained samples. It can be configured in three different models. The IP Model is apt for storage phosphor imaging and records image data in a log file format for greater linear accuracy when analyzing images containing the large dynamic range information sets that radioisotopes can generate. The RGB Model is for multispectral two-dimensional gel imaging. It allows researchers to complete scans of samples labeled with Cy3 and Cy5 dyes in a single run. The IR+IP Model, for conducting near infrared and radioisotope imaging, accommodates up to four lasers to scan imaging plates as well as quantum dots and traditional fluorophors that emit in near infrared.

Fujifilm Life Science
For information 866-902-3854
www.fujifilmlifescienceusa.com

Membrane Protein Interactions

Designed to detect novel interaction partners for membrane proteins, the DUALmembrane System can be used to detect pairwise protein interactions, identify novel protein interactions by complementary DNA library screening, investigate ternary complexes, and map interaction domains. The system reliably detects interactions between integral membrane proteins and receptor subunits and co-receptors, as well as membrane-associated proteins and soluble proteins. It is based on the properties of ubiquitin, a small protein modifier that is conserved in all eukaryotes and plays a primary role in protein degradation. The system is available in both kit form and as a custom screening service.

Dualsystems Biotech
For information +41-(0)1-738-50-00
www.dualsystems.com

Cell-Free Protein Expression

New additions to the TNT system include an insect system and an improved bacteria system for cell-free expression of proteins. The recent additions expand a comprehensive offering of tools for cell-free expression of proteins from DNA in a single reaction. The insect lysate system delivers expression at a lower temperature than other systems, which can enhance protein folding and stability and is often preferred for mutagenesis studies. The TNT system is a single-step process that makes use of DNA as a template for the coupled transcription/translation, and saves the user from the need to purify and quantify messenger RNA for in vitro expression. Cell-free protein expression's advantages over cell-based protein expression include time savings and increased yields of functional, soluble, full-length proteins.

Promega
For information 608-274-4330
www.promega.com

Electronically submit your new product description or product literature information! Go to **www.sciencemag.org/products/newproducts.dtl** for more information.

Newly offered instrumentation, apparatus, and laboratory materials of interest to researchers in all disciplines in academic, industrial, and governmental organizations are featured in this space. Emphasis is given to purpose, chief characteristics, and availabilty of products and materials. Endorsement by *Science* or AAAS of any products or materials mentioned is not implied. Additional information may be obtained from the manufacturer or supplier.

Science Careers
Classified Advertising

For full advertising details, go to **ScienceCareers.org** and click **For Advertisers**, or call one of our representatives.

UNITED STATES & CANADA
E-mail: advertise@sciencecareers.org
Fax: 202-289-6742

Joribah Able
Industry – US & Canada
Phone: 202-326-6572

Alexis Fleming
Northeast Academic
Phone: 202-326-6578

Tina Burks
Southeast Academic
Phone: 202-326-6577

Daryl Anderson
Midwest/Canada Academic
Phone: 202-326-6543

Nicholas Hintibidze
West Academic
Phone: 202-326-6533

EUROPE & INTERNATIONAL
E-mail: ads@science-int.co.uk
Fax: +44 (0) 1223 326532

Tracy Holmes
Associate Director, *Science* Careers
Phone: +44 (0) 1223 326525

Alex Palmer
Phone: +44 (0) 1223 326527

Dan Pennington
Phone: +44 (0) 1223 326517

Susanne Kharraz Tavakol
Phone: +44 (0) 1223 326529

Louise Moore
Phone: +44 (0) 1223 326528

JAPAN
Mashy Yoshikawa
Phone: +81 (0) 3 3235 5961
E-mail: myoshikawa@aaas.org

To subscribe to *Science*:
In US/Canada call 202-326-6417 or 1-800-731-4939.
In the rest of the world call +44 (0) 1223 326515.

Science makes every effort to screen its ads for offensive and/or discriminatory language in accordance with US and non-US law. Since we are an international journal, you may see ads from non-US countries that request applications from specific demographic groups. Since US law does not apply to other countries we try to accommodate recruiting practices of other countries. However, we encourage our readers to alert us to any ads that they feel are discriminatory or offensive.

Science Careers
From the journal *Science* AAAS

POSITIONS OPEN

FACULTY POSITION in PLANT SIGNALING MECHANISMS

The University of North Texas (UNT) seeks candidates at the **PROFESSOR** level with an active research program in metabolomics, cell biology, or genetics. Exceptional candidates at the **ASSOCIATE PROFESSOR** level may also be considered. The successful candidate must have a strong record of obtaining extramural funding, and will be an integral part of a new initiative in plant signaling mechanisms targeted by the UNT administration for research cluster support. This faculty-hire will be part of a new four-member group that is being recruited to the University of North Texas over the next three years to enhance research activities in the plant sciences. Exceptional startup funding and salary will be provided. An 80,000 square-foot state-of-the-art Life Sciences Building is being constructed that will house the plant signaling research cluster. Potential interactions exist with plant science researchers at the nearby Samuel Roberts Noble Foundation. Send cover letter with qualifications and research interests and curriculum vitae to: **Dr. Kent Chapman, Plant Signaling Mechanisms Search Committee Chair, University of North Texas, Department of Biological Sciences, 1155 Union Circle #305220, Denton, TX 76203-5017; e-mail: chapman@unt.edu.** Applications will be reviewed beginning February 20, 2009, and will continue until the position is closed. UNT is the largest and most comprehensive University in the north Texas region with 96 undergraduate, 111 Master's, and 50 doctoral degree programs. It is the fourth-largest University in Texas, with nearly 35,000 students and eight straight record increases in annual enrollment. UNT is located in Denton in the vibrant, rapidly expanding Dallas/Fort Worth (DFW) metroplex, with easy access to DFW airport. New research initiatives were announced in September 2008 **(website: http://web3.unt.edu/news/story.cfm?story=11146).** Also see **website: http://www.biol.unt.edu.**

Affirmative Action/ADA/Equal Opportunity Employer.

The Department of Physiology and Developmental Biology at Brigham Young University announces the availability of a permanent (continuing faculty status track) **FACULTY** position. Review of applications will begin February 17, 2009, and continue until the position is filled. Applicants should have a Doctorate degree and postdoctoral experience, with expertise and teaching capability in developmental biology, physiology, pharmacology, cell biology, anatomy, neuroscience, or histology. Candidates must demonstrate a high potential for establishment of an externally funded research program. Send curriculum vitae and one-page statement of research and teaching interests/goals to: **Dr. Allan Judd, Search Committee Chair, Department of Physiology and Developmental Biology, Brigham Young University, Provo, UT 84602. (Telephone: 801-422-3179; fax: 801-422-0700; e-mail: allan_judd@byu.edu.)** Additional information is available at *BYU is an Equal Employment Opportunity Employer. Preference is given to qualified candidates who are members in good standing of the affiliated church, the Church of Jesus Christ of Latter-day Saints.*

ASSISTANT PROFESSOR of BIOLOGY

The Biology Department at Armstrong Atlantic State University, **website: http://www.biology.armstrong.edu,** seeks applications for a tenure-track position in eukaryotic cell/molecular biology. A Ph.D. is required; postdoctoral experience preferred. A second position is also available for an Assistant Professor (renewable up to three years), both beginning August 2009. Review of completed applications will begin on January 5, 2009, and continue until the position is filled. Please visit **website: http://www.hr.armstrong.edu/jobs.htm** for details.

POSITIONS OPEN

POSTDOCTORAL FELLOW
The Center for Cardiovascular Research
Department of Biochemistry and Molecular Biology
Saint Louis University School of Medicine

Saint Louis University, a Catholic, Jesuit institution dedicated to student learning, research, health care, and service, is seeking applicants for a Postdoctoral Fellow in the Edward A. Doisy Department of Biochemistry and Molecular Biology, beginning in the winter of 2009. A Postdoctoral position is now available in the laboratory of **Dr. David Ford.** Successful candidates are expected to have a Ph.D. degree in life or physical sciences with a special emphasis on biochemistry and/or mass spectrometry. Projects using mass spectrometry to research dynamic alterations in lipidomes and signaling pathways in metabolic and cardiovascular diseases are available in the laboratory. NIH standards will be used in setting the pay scale.

Interested candidates must submit a cover letter, application, and current curriculum vitae to **website: http://jobs.slu.edu** (position number 20080680).

Saint Louis University is an Affirmative Action, Equal Opportunity Employer and encourages nominations of an application from women and minorities.

BIOCHEMISTRY and MOLECULAR BIOLOGY FACULTY POSITION
University of California, Los Angeles (UCLA)

The Biochemistry Division of the Department of Chemistry and Biochemistry **(website: http://www.biochemistry.ucla.edu)** is seeking applications for a faculty position. The position may be filled at the **ASSISTANT PROFESSOR** (tenure track) level or at the **ASSOCIATE or FULL PROFESSOR** (tenured) level. We invite outstanding candidates in any area of biochemistry and molecular biology. The new faculty member will be expected to develop a strong and creative research program and contribute to teaching in biochemistry.

Applications should include curriculum vitae, list of publications, a summary of research accomplishments (one to two pages), future research plans (three pages) and two to three reprints of representative publications. Applicants should also arrange to have three letters of reference sent to the address below. To assure consideration, all application materials and letters should be received by January 20, 2009. Please do not send applications by e-mail. All application materials should be sent to: **Chair, Biochemistry Search Committee, c/o Penny Jennings, Department of Chemistry and Biochemistry-UCLA, P.O. Box 951569, Los Angeles, CA 90095-1569.**

The University of California is an Affirmative Action/Equal Opportunity Employer with a strong institutional commitment to the development of a climate that supports equality of opportunity and respect for differences.

POSTDOCTORAL RESEARCH ASSOCIATE POSITION in immunology at Brown University in the Department of Molecular Microbiology and Immunology. A position is available for an individual interested in cytokines and innate immune responses to viral infections. Focus of the project is on regulation of cytokine signaling and the role of signal transducers and activators of transcriptions in shaping cellular responses. The successful candidate must have a Ph.D. or equivalent and experience in immunology. It is preferred that the candidate's research experience focus on signaling.

Review of applications will begin immediately and will continue until the position is filled or the search is closed. Please send curriculum vitae and three references to: **Prof. Christine Biron, Brown University, P.O. Box G-B6, Providence, RI 02912.**

Brown University is an Equal Employment Opportunity/Affirmative Action Employer and encourages applications from minorities and women.

Lead the next generation of drug discovery informatics

Eli Lilly and Company is a leading, innovation-driven pharmaceutical corporation with a firm commitment to help people live longer, healthier and more active lives by making breakthroughs in medicines and treatments.

To find the next generation of drugs, we know we need to use next generation technologies and employ the best of the biopharmaceutical industry.

The Integrative Computational Sciences (ICS) group at Lilly Singapore Centre for Drug Discovery (LSCDD), provides state-of-the-art computational solutions to enable the global efforts of drug discovery, translational medicine and tailored therapeutics at the post genomic era.

We study the genetics base of complex diseases and develop novel algorithms, data analysis methods, simulation models and tools for drug discovery, biomarkers identification, epigenetics research, population stratification and prediction of dose response.

ICS integrative analyzes solutions, and biological interpretations of complex multi-dimensional data are applied in various therapeutic areas such as Oncology, Diabetes, Neuroscience and Cardiovascular diseases.

As an ICS team member with strong analytical and scientific insight, you will have a global impact on the future of personalized medicine: 'The Right Drug, at The Right Dose for The Right Patient at The Right Time'!

Lilly Singapore is expanding and the ICS group is looking for candidates in the following positions:

- **Bioinformatics Manager**
- **Sr. Statistical Geneticist**
- **Sr. Bioinformatics Scientist**
- **Sr. Cheminformatics Scientist**
- **Principal Statistician**
- **Scientific Liaison**

The successful candidates will work closely with their bioinformatics, statistics and software engineering peers at ICS and will collaborate with biologists, chemists, geneticists and physicians at Eli Lilly. We work closely with Lilly System Biology and Drug Discovery Research teams at Singapore as well as with the Discovery Informatics organization and the Global Discovery Statistics group in Europe and USA.

Minimum requirements:

- Ph.D. in Statistical Genetics/Bioinformatics/ Computational Biology/Biostatistics/Biophysics/ Cheminformatics or a related discipline
- 3 years' post-graduation experience
- Background in Oncology / Diabetes / Cardiovascular Neuroscience
- Statistics: SAS/R/S-Plus/Partek
- OS: Unix/Linux, Windows
- Databases: Oracle/SQL/mySQL
- Scripting: Perl, Shell

Preferred Experience:

- Industry experience in Biotech/Phamaceutical/Drug Discovery
- Experience in the analysis of large data sets such as microarrays, sequencing, proteomics and imaging data
- Strong publications record
- Demonstrated learning agility
- Excellent communication and multidisciplinary collaborative skills

For more information and online application, please visit **www.lscdd.lilly.com.sg/lscdd/careers**.

www.lscdd.lilly.com.sg

Lilly

Answers That Matter.

NIAID
NATIONAL INSTITUTE OF ALLERGY AND INFECTIOUS DISEASES

RESEARCH FELLOW

The National Institute of Allergy and Infectious Diseases (NIAID), a major research component of the National Institutes of Health (NIH) and the Department of Health and Human Services, is recruiting for a Research Fellow. The position will be available in the Molecular Pathology Section of the Laboratory of Immunopathology, and scientists with a M.D., Ph.D., or D.V.M. are eligible. The research activity involves (1) studies of the roles played by CTCF in imprinting, X chromosome inactivation, and the organization of transcriptional domains; and (2) analyses of BORIS expression and function in gametogenesis and stem/progenitor cells, in response to infectious agents, as well as the consequences of aberrant expression in cancers. This full-time research position offers a unique opportunity to work on investigations that range from basic molecular biology to studies of gene-manipulated mice in a collaborative environment, and provides excellent training for scientists who plan a career in molecular biology, infectious disease and cancer research.

Research Fellow applicants should have three or more years of relevant post-doctoral experience; the salary range is $44,180 - $108,319. A full package of benefits (including retirement, health, life and long term care insurance, Thrift Savings Plan participation, etc.) is available. Applicants with an M.D. degree are eligible for the NIH Loan Repayment Program. Applicants should send their curriculum vitae, a letter of interest, and names and addresses of three (3) references to Victor Lobanenkov, Twinbrook I, Room 1417, 5640 Fishers Lane, Rockville, MD 20892, FAX: (301)-402-0077, email: vlobanenkov@niaid.nih.gov

For further information about NIAID and available job opportunities, please visit:
http://healthresearch.niaid.nih.gov/dl

Director, Division of Pharmacotherapies and Medical Consequences of Drug Abuse

National Institute on Drug Abuse • Department of Health and Human Services • National Institutes of Health

The National Institute on Drug Abuse (NIDA) at the National Institutes of Health (NIH) is seeking a senior-level scientist with expertise in medications development and the conduct of clinical trials who will bring significant experience to operate in an intellectually challenging Federal biomedical research institution engaged in a national research program to understand the biomedical and social causes and consequences of drug addiction throughout the world.

This is a scientific executive position that offers a unique and challenging opportunity for the right individual to direct an extramural scientific program of national and international scope within NIDA.

The position entails providing leadership in the development of new medications for the treatment of addictive disorders. To accomplish this mission, the division (1) plans and directs studies to identify, evaluate, and develop new medications for Food and Drug Administration (FDA) review and approval; (2) develops and administers a national program of basic and clinical pharmaceutical research, conducted at academic settings, to develop innovative immunological and pharmacological treatment approaches; (3) supports training in the preclinical and clinical sciences; (4) collaborates with the pharmaceutical industry and other Federal medications development programs (e.g., National Institute on Alcohol Abuse and Alcoholism) to facilitate medications development for addictive disorders; and (5) works closely with the FDA to assure that the research designs to show efficacy are evaluated and approved in the most expeditious manner.

The successful candidate will possess an M.D. and/or Ph.D. degree, have knowledge of neuropharmacology and clinical research, and have experience in medications development. The candidate should also possess knowledge on addiction medicine and the neuroscience of addiction. Managerial experience in medications development in the biotechnology or pharmaceutical sectors, or Federal service for at least 5 years is highly desirable. The individual must also have demonstrated ability to manage personnel, budgets, and timelines across multiple fiscal years.

Application Process: Salary is commensurate with experience; a full package of Federal Government benefits is available, including retirement, health and life insurance, long-term care insurance, leave, and retirement savings plan (401K equivalent). Send your application package, including: CV, bibliography, and two letters of recommendation to the National Institutes of Health, Attn: Stephanie Jones, Office of Human Resources; 2115 East Jefferson St., Room 2D-204, Rockville, Maryland 20853, or e-mail jones17@mail.nih.gov; phone: 919-541-7913. For further information on the position, please contact the search committee chair: Barry Hoffer, M.D., by e-mail: bhoffer@intra.nida.nih.gov, or phone: 443-740-2463. Your application package must be received by March 15, 2009. All information provided by applicants will remain confidential and will not be released outside the NIDA search process without a signed release from candidates.

NIH encourages the application and nomination of qualified women, minorities, and individuals with disabilities.
HHS and NIH are Equal Opportunity Employers.

drugabuse.gov

U.S. Department of Health and Human Services
NATIONAL INSTITUTES OF HEALTH
NIDA NATIONAL INSTITUTE ON DRUG ABUSE

WWW.NIH.GOV

Department of Health and Human Services
National Institutes of Health
National Cancer Institute
Division of Cancer Treatment and Diagnosis
Translational Research Program

Announcement Number: **NCI-09-303083-DH**
Supervisory Medical Officer, GS-602-15

Position: **Associate Director, Translational Research Program,**
Division of Cancer Treatment and Diagnosis

The National Cancer Institute (NCI) is responsible for stimulating and supporting scientific discovery and its application to achieve a future when all cancers are uncommon and easily treated. We are seeking a highly energetic and creative individual to head its Translational Research Program (TRP) within the Division of Cancer Treatment and Diagnosis (DCTD).

The mission of the Translational Research Program (TRP) is to integrate scientific advancements in the understanding of the biology of human cancer with the development of new interventions for the prevention, diagnosis, and treatment of cancer patients or populations at risk for cancer, by fostering broad interdisciplinary investigations that focus on bringing discoveries from the laboratory to the clinic, and coordinating resources of the National Cancer Institute with those of academia, industry, and non-profit organizations/foundations to reduce cancer incidence, morbidity and mortality, to extend survival, and to increase the quality of life of cancer patients.

This is accomplished by:

- Planning, advising, coordinating, evaluating, and supporting the Specialized Programs of Research Excellence (SPOREs), which use the P50 grant funding mechanism, to translate novel scientific discoveries from the laboratory and/or population studies to the clinic for testing in humans with cancer, to determine the biological basis for clinical observations, and to use specimens from clinical studies to determine correlations between biomarkers and outcomes in patients.
- Encouraging and facilitating collaborations between SPOREs, Cancer Centers, other NCI/NIH funded mechanisms and programs, and outside organizations, to increase cross-fertilization of ideas, leverage resources, reduce duplication, and ensure access of resources to projects and investigators.
- Establishing high-quality organ-specific tumor specimen banks to provide research resources for the cancer research community.
- Maintaining the Developmental Research Program and Career Development Program of the SPOREs to promote high risk/high payoff projects and to ensure the develop ment of promising researchers new to translational research.
- Supporting research in high incidence cancers as well as in rare cancers.
- Collaborating with patient advocates who support translational science in cancer.

The Translational Research Program will have approximately 10 employees and supports an operations budget and the SPOREs grant portfolio. The program is located in Rockville, Maryland.

Qualifications Required: Candidates must have an M.D./D.O. degree and a current U.S. medical license. Board Certification or eligibility in Medical or Pediatric Oncology/Hematology, or Pathology is highly desirable. Candidates should be internationally recognized as an expert in the field of oncology with extensive experience in the conduct of translational research, including prior and/or current expertise in translational laboratory-based research. Understanding of and experience in clinical research, including knowledge and understanding of the science and regulatory issues related to clinical trials is also required. The selectee will perform clinical duties at least ten percent of the time which will involve direct patient care or work incident to patient care. Other qualifications include a demonstrated acumen for strategic plan development, implementation, evaluation; analysis of objectives and outcomes; management of financial and human resources; and implementation of EEO principles. The candidate must also have the ability to communicate clearly and effectively both in writing and orally, skill in establishing and maintaining effective collaborative relationships with other health care professionals and scientists within and outside the organization, and demonstrated experience providing managerial leadership to other professional staff including coordination of work and evaluation of output. Knowledge of NIH/NCI grant and contract mechanisms and processes is extremely desirable. Appointments are limited to U.S. citizens.

Salary and Benefits: Total annual compensation will be commensurate with education and experience. Various incentives may apply in individual circumstances, based on experience and expertise. A recruitment incentive/bonus and relocation expenses may also be available to the selectee. Full Federal benefits including health and life insurance options, retirement, paid holidays, vacation and sick leave will be provided.

How to apply: To obtain the mandatory application requirements and other necessary information, please visit: **http://jobsearch.usajobs.opm.gov/a9nih.asp ,Vacancy Announcement number, NCI-09-303083-DH**. For more information on applying, please contact **Ms. Mary Lou Weathers at (301) 402-5059, email: weatherm@mail.nih.gov** .

APPLICATIONS MUST BE RECEIVED BY FEBRUARY 27, 2009.

Max Planck Institute for Demographic Research

Directors: Prof. James W. Vaupel – Prof. Joshua R. Goldstein

www.demogr.mpg.de

The Max Planck Institute for Demographic Research (MPIDR) seeks to recruit a

Research Scientist

to conduct research for the Laboratory of Demographic Data. Qualified demographers, sociologists, statisticians, and other scientists with a research background in the social sciences are invited to apply. We intend to fill the position as soon as possible.The duration of the contract will initially be limited to three years. The salary is paid according to qualification and in accordance with the rules of federal employees in Germany, up to level 14 TVöD.

The successful applicant must have completed Ph.D. degree in demography or a related field. He or she must have a proven record of scientific work on population change in Europe or other industrialized societies as well as proficiency in demographic methods and computer applications.

The work will include processing and analyzis of demographic data on fertility and family dynamics. The position requires practical skills in handling demographic data, expertise in statistical analysis and relevant packages. Fluency in English is essential.

The Max Planck Society is committed to employing more handicapped Individuals and especially encourages them to apply. The Society wishes to increase the share of women in areas where they are underrepresented, and strongly encourages women to apply.

Applications should include a CV with a statement of academic interests and relevant experience, a list of publications, two recommendations, and contact details of two referees.

Please send all materials by 20th of January 2009 to the:

MAX-PLANCK-GESELLSCHAFT

Max Planck Institute for Demographic Research
Attn. Edelgard Katke
Konrad-Zuse-Str. 1, 18057 Rostock, Germany
Email: katke@demogr.mpg.de

The University of Texas at Austin
invites applications and nominations for the position of

Dean
John A. and Katherine G. Jackson School of Geosciences
Effective September 1, 2009

The Jackson School serves to organize and oversee one of the largest geoscience programs in the country. The School (www.jsg.utexas.edu) is in the initial implementation phase of its strategic plan "Changing the World of Geosciences." With an endowment of over $450 million, the school provides an unprecedented opportunity for its leader to have a major impact on the field of geoscience well into the future. The school includes the Department of Geological Sciences, the Institute for Geophysics, and the Bureau of Economic Geology and employs approximately 50 full-time faculty and 100 research scientists. The department currently serves approximately 300 undergraduate majors and more than 180 graduate students.

We seek a visionary leader with proven scientific and administrative skills who will work with the faculty and research scientists to develop the Jackson School to its full potential as one of the world's top institutions in the geosciences and who will represent the School effectively to the University administration, to the state and national political leadership, and to the public. At UT Austin, all academic deans report to the Executive Vice President and Provost of the university.

Preferred qualifications include: (1) creative leadership capable of creating synergy within the school and interfacing with other programs within the university; (2) distinguished scholarship, with a strong research record and experience in academia, including teaching; (3) administrative experience that demonstrates vision, managerial ability, and communication skills; and (4) commitment to balancing academic and research excellence with the diverse broader missions of units within the school.

Applications and nominations should include a letter describing the applicant's qualifications and potential interest in the position. Applicants should also include a description of relevant experience and accomplishments, curriculum vitae, and the names and addresses of six references (references will not be contacted without the candidate's permission). Send applications and nominations to: **Dr. David Hillis, Chair, Dean Selection Committee, Section of Integrative Biology, 1 University Station C0930, University of Texas at Austin, Austin, Texas 78712-0253.** Review of applications will begin on **January 20, 2009**, but applications will be accepted until the position is filled.

The University of Texas at Austin is an Affirmative Action/Equal Employment Employer. All qualified applicants will receive consideration for employment without regard to race, color, religion, sex, national origin, disability, age, citizenship status, Vietnam era or special disabled veteran's status, or sexual orientation. This is a security sensitive position; background check on selected applicant is required.

Dean
College of Science

Purdue University invites applications and nominations for the position of Dean of the College of Science.

Established in 1869, Purdue is Indiana's land-grant university, a comprehensive educational and research institution which is a member of the prestigious American Association of Universities (AAU). The West Lafayette campus, located one hour north of Indianapolis and two hours south of downtown Chicago, has ten colleges with an enrollment of 39,000 students. The College of Science is made up of seven departments: Biological Sciences, Chemistry, Computer Science, Earth and Atmospheric Sciences, Mathematics, Physics, and Statistics. In addition, there are numerous interdisciplinary programs. The College has 304 faculty and 403 staff; and it enrolls approximately 2,740 undergraduate students and 1,012 graduate students.

The Dean's primary role is to provide vision and leadership in the College and to foster a culture supportive of the College's interdisciplinary and core missions, both internally and externally to the broader academic community, through excellence in learning, discovery, and engagement. The Dean reports directly to the provost and joins with the College's department heads, faculty, other deans, vice presidents, and the president, to assure that learning activities of the highest quality flourish at all levels.
An affinity for fund raising resulting in the ability to secure flexible support for the many programs of the College is an important responsibility of the Dean.

As chief academic and administrative officer of the College, the Dean actively represents the College to a variety of constituencies internal and external to the University.

The successful candidate will: • have a preeminent scientific record commensurate with the caliber of scholars the College expects to attract to Purdue; and, • be an effective communicator; • have a commitment to undergraduate and graduate education; • be an enthusiastic leader in developing resources; • be an excellent administrator with a proven record of vision and leadership resulting in the ability to achieve specific goals, set priorities, and allocate resources; • have substantial experience with the national research funding environment, understand the changing economic climate and how it impacts the college, and understand the political climate in a Research I university; • be sensitive to all the constituencies served by the University and be able to articulate and advocate the goals of the College; • have an effective voice and a demonstrated commitment to cultural and ethnic diversity and gender equity.

Qualified candidates will have credentials appropriate for a tenured full professorship and demonstrated excellence in administration. Purdue is committed to providing a named or distinguished professorship if appropriate.

Applications should include a cover letter that addresses the above criteria and a full CV, and should be sent to: **Jerry H. Baker, Baker and Associates LLC, 10 Glenlake Parkway, South Tower, Suite 140, Atlanta, GA 30328; jbaker@baasearch.com**. Screening will begin on **January 15, 2009** and will continue until the position is filled.

The College of Science website can be accessed at **www.science.purdue.edu** for information about the College.

Purdue University is an Equal Opportunity/ Equal Access/Affirmative Action Employer fully committed to achieving a diverse workforce.

Department of Biotechnology
Ministry of Science and Technology
Government of India

Executive Director (1 Post)
Deans (3 Posts)
National Agri-Food Biotechnology Institute (NABI)

Chief Executive Officer (1 Post)
Food Bioprocessing Unit (FBPU)

To be located at the knowledge City Sector 81, Mohali, Punjab

The Department of Biotechnology, Ministry of Science & Technology, Government of India is establishing an Agri-food cluster comprising National Agri-food Biotechnology Institute (NABI) and a Food Bioprocessing Unit (FBPU) in the ambience of an Agri-food Biotechnology Park in the Knowledge City, Sector 81, Mohali, Punjab. The goal of NABI will be to serve as a Centre of Excellence in inter-disciplinary science, translational science and product development with focus on agribiotechnology, food science technology, nutrition sciences and nutraceuticals. It will also train world-class human resource in these areas. The FBPU will act as a real-time interface between laboratory scale testing and large scale manufacture, linking R&D with a GMP production facility, and clinical testing for safety and validation of nutritional/ health benefits. It and will also serve as an incubator for start-up companies. The immediate neighbours for the agri-food cluster in the Knowledge City are: Indian Institute of Science Education and Research (established by the Ministry of HRD) and Institute of Nano-Science & Technology (being set up by the Department of Science & Technology, Government of India)

Applications are invited from Indian citizens including non-resident Indians with outstanding and proven track record in science, technology and innovation in areas related to this inter-disciplinary institute.The posts offer the chance to set up, and then to lead new inter-disciplinary programmes and development of teams and infrastructure and foster collaboration with industry, medical, engineering, agricultural and food institutions. There will also be exciting opportunities for oversight of extramural activities including support to research resource units in other regional institutions.

Requirement for Executive Director and Deans (NABI):

Qualifications
- Masters Degree in biological, engineering sciences or medical sciences.
- PhD or equivalent degree in an area relevant to the institute's objectives and goals.

Excellence
- Scientific publications.
- Creation of IP or technologies.

Experience
- Responsible position of work in any R&D/ planning/ academic/scientific institution/ organization/ industry for 15 years for Executive Director and 10 years for Deans.
- Innovation leadership and inter-disciplinary research.

Requirement for Chief Executive Officer (FBPU):

Qualifications
- Masters Degree in biological or engineering sciences. Food Technologists will be preferred.
- PhD or equivalent degree in an area relevant to the unit's objectives and goals.

Excellence
- Creation of IP or technologies.
- Experience in technology transfer.
- Scientific publications.

Experience
- Setting up and management of industry/ pilot plant units for 15 years.
- Understanding and management of innovation and inter-disciplinary projects.
- 15 years of experience in a responsible position of work in any R&D/planning/academic/scientific institution/ organization/ industry.

The applicant should not be above 55 years of age but age relaxation may be allowed for exceptional candidates. The appointment will be on a contract basis for a period of 5 years, which will be extendable for a further term subject to a maximum age limit of 60 years after internal and external review at the end of 4 years.

Other pertinent details of NABI & FBPU including salary and allowances as well as application formats can be downloaded from DBT website: **www.dbtindia.nic.in**. Applications should be forwarded to Dr. Rajesh Kapur, Advisor, Department of Biotechnology, Ministry of Science & Technology, Block-2, CGO Complex, Lodhi Road, New Delhi - 110 003, India.

The last Date for Receipt of Applications is 03.02.2009

Postdoctoral Research Position: Anthropogenic Climate Change

The Program in Science, Technology, and Environmental Policy at the Woodrow Wilson School of Public and International Affairs at Princeton University invites applications for postdoctoral Research Associates for research on anthropogenic climate change under the direction of **Professor Michael Oppenheimer**. General areas of interest include impacts and vulnerability of human and natural systems, and domestic and international policy frameworks aimed at fostering greenhouse gas emission mitigation and adaptation.

Recent research in this program has focused on: the vulnerability of coral reefs, the nitrogen cycle and its response to climate variability and change, paleoclimatic studies of the behavior of earth's ice sheets and sea level and implications for the future, the impacts of sea level rise on the coastal zone, the human responses to climate impacts including migration, the application of climate modeling to the foregoing problems, energy policy including the appropriate role for bio-fuels, the role of uncertainty and learning in decision making on problems of global change, and various aspects of emissions trading. This research is motivated by an interest in climate policy on all time scales and particularly, the means to implement Article 2 of the UNFCCC ("avoiding dangerous anthropogenic interference with the climate system"). Potential applicants are encouraged to explore papers and research projects described at: **http://www.princeton.edu/step/people/faculty/michael-oppenheimer/**.

Applicants should have a strong background in one or more of the areas above and an interest in attacking problems from a multidisciplinary perspective, including the exploration of implications for public policy. Research is often carried out in collaboration with natural and social scientists in the Woodrow Wilson School, as well as Princeton's Department of Geosciences, the Atmosphere and Ocean Sciences Program, the Department of Ecology and Evolutionary Biology, and NOAA's Geophysical Fluid Dynamics Laboratory.

The initial appointment will be for one year, with the possibility of renewal.

The Postdoctoral Research Associate's position is open to all regardless of citizenship, but requires a completed doctorate in a relevant area of environmental science and does not support work towards the completion of a degree. The research associate position will be eligible for salary and full employee benefits in accordance with Princeton University guidelines. Applicants should send a CV and a cover letter describing their areas of expertise and interest via email to Charles Crosby at **ccrosby@princeton.edu**. The search begins immediately and continues until the position is filled. Please submit materials by **January 20th , 2009**. For information about applying to Princeton and voluntarily self-identifying, please link to **http://www.princeton.edu/dof/about_us/dof_job_openings/**.

Princeton University is an Equal Opportunity Employer and complies with applicable EEO and Affirmative Action regulations.

EVMS
Eastern Virginia Medical School

Faculty Position
Department of Microbiology and Molecular Cell Biology

Applications are invited for a tenure-track position at the level of Assistant Professor in the Department of Microbiology and Molecular Cell Biology at Eastern Virginia Medical School, located in the dynamic and growing community of Hampton Roads, Virginia. Appointees will join a strong faculty focused in the areas of cancer biology, proteomics, virology and immunology. Applicants in the areas of chromatin remodeling, developmental biology, epigenetic gene regulation and/or DNA recombination as applied to cancer biology or infectious diseases will be given special consideration. Investigators with a translational focus or ongoing research funding are strongly encouraged to apply.

Applicants should send a curriculum vitae, three references and a description of future research to:

Edward M. Johnson, Ph.D.
Chairman, Department of Microbiology and Molecular Cell Biology
Eastern Virginia Medical School
700 West Olney Road
Norfolk, VA 23501

EVMS is an Equal Opportunity, Affirmative Action Employer, and drug free workplace.

At Monsanto, our talented employees are contributing to our success as a global leader in agriculture. By delivering exceptional results in one of the world's most important industries, we are creating solutions that improve productivity in farming while reducing the impact on our environment.

We are looking for a talented individual for the following position in **Chesterfield, MO**:

SCIENTIST – Immunoassay Development

PhD in Biochemistry, Immunochemistry or Biotechnology with 3 or more years of laboratory experience in immunoassay or other type of protein assay development required.

Responsible for identification and evaluation of new enabling technologies and potential collaborations that will provide new understanding and approaches for more efficient protein assays.

To view a more complete and detailed job description of this exciting position, please visit our website at **www.monsanto.com** and to apply online select **requisition # mons-00009951**. We offer very competitive salaries and an extensive benefits package.

The life of any plant starts with a seed. Within the right environment it grows to become something amazing. At Monsanto, our philosophy is the same – we are committed to helping individuals progress in careers with unlimited potential.

The world, re-imagined

Imagine your world at Monsanto by visiting us on our website,
www.monsanto.com/careers

Monsanto is an equal opportunity employer who values diversity.

MONSANTO imagine®

Weill Cornell Medical College

Faculty Position
Director
Appel Institute for Alzheimer's Research

Weill Cornell Medical College is currently undergoing a major expansion of its research program including the construction of a new research building. As part of this expansion we are seeking a Director to establish a new institute; The Appel Institute for Alzheimer's Research. The goal of the Institute, consistent with the donor's wishes, is to better understand the mechanisms behind this disease and to develop treatments leading to a cure.

Candidates should have an outstanding record of productivity in basic or clinical research with a major program likely to impact Alzheimer's research. The recruited faculty will be provided with generous support and space as part of this initiative. In addition to medical student teaching, candidates will participate in the Graduate School of Medical Sciences Program which includes faculty from the Weill Cornell Medical College and the Sloan-Kettering Institute, and in the Tri-Institutional MD-PhD Program and the Training Program in Chemical Biology, which also include faculty from The Rockefeller University. Applications should include a curriculum vitae and a statement of research interests. Applications should be sent electronically to: **hmlander@med.cornell.edu** (**Dr. Harry Lander, Associate Dean for Research Administration, Weill Cornell Medical College, 1300 York Avenue, New York, NY 10021**). All applications will be treated confidentially.

EEO/AA/M/F/D/V

Better thinkers;
Better futures

Founded in 1919, AUC's campus has moved to a new, state-of-the-art campus in New Cairo beginning Fall Semester, 2008. AUC's degree programs are accredited by the Commission on Higher Education of the Middle States Association of Colleges and Schools; Engineering programs are accredited by ABET and the Management program is accredited by AACSB. For more information visit our website at www.aucegypt.edu.

The normal teaching load is three courses per semester and English is the language of instruction. For expatriates, benefits include housing, annual round-trip air travel for appointee and qualifying dependents, plus schooling for the equivalent of up to two children at Cairo American College. In view of AUC's protocol agreement with the Egyptian government, which requires specific proportions of Egyptian, U.S., and third-country citizen faculty, at this time preference will be given to qualified applicants who are U.S. citizens.

Application Instructions:
All applicants must submit the following documents via online.

a) A current C.V.
b) A letter of interest
c) A completed AUC Personal Information Form (PIF)
d) Please ask three referees familiar with your professional background to send reference letters directly to our office in New York or to the Office of the Provost.

The American University in Cairo is an Equal Opportunity and Affirmative Action Employer.

THE AMERICAN UNIVERSITY IN CAIRO

BIOINFORMATICS (BIOINORM-1-09)

Job Description: The School of Sciences and Engineering has launched a new interdisciplinary Master of Science degree in Biotechnology. The School is inviting applications for a tenure-track faculty position at any professorial level in Bioinformatics, beginning September 2009.

Requirements: The candidate must hold a doctoral level degree with an educational background in biology and computer science. The successful candidate may be a biologist with advanced degrees in information technology or a computer scientist specialized in information technology with advanced degrees in Biology. The candidate should have a strong track record of teaching and research in the areas of bioinformatics, in particular, computational aspects of molecular structure, bioperl, and simulation of biological and complex structures.

Additional Information: The faculty slot could be housed in either the Biology Department or the Department of Computer Science and Engineering. He/she is also expected to lead research activities in bioinformatics and to collaborate with the Yousef Jameel Science and Technology Research Center at AUC.

COMPARATIVE ANATOMY AND PHYSIOLOGY (BIOL-1-09)

Job Description: The Department of Biology invites applications for a tenure-track faculty position at any professorial level in the area of comparative anatomy and physiology, beginning September 2009. Highly motivated individuals with commitment to undergraduate and graduate education will be expected to teach introductory and upper level courses in the undergraduate biology program, including, but not limited to, comparative anatomy, invertebrate and vertebrate physiology, human physiology, and developmental biology. Preference would be given to applicants with experience in premedical advising.
The successful candidate is expected to advise undergraduate and graduate students in their research thesis and develop an internationally recognized research program using vertebrate or invertebrate model systems to address fundamental questions in biology, including, but not limited to, cell signaling, morphogenesis, and symbiosis between organisms. The Department of Biology is committed to collaborative, interdisciplinary education and research. Toward this end, the department has recently established advanced molecular biology laboratory, and a cutting-edge genomics facility, including a high-through DNA sequencer and high performance computational system. The successful applicant is encouraged to utilize and expand the current facilities.

Requirements: The candidate must hold a doctoral degree.

Additional Information: Deadline of applications is January 15, 2009. Review of applications will start immediately. One-, two- or three-year appointment, subject to mutual agreement will begin September 2009. Renewal of an appointment depends upon institutional needs and/or the appointee's performance. When applying, include teaching philosophy and a short description of intended research with letter of interest.

MARINE BIOLOGY (BIOL-2-09)

Job Description: The Department of Biology invites applications for a tenure-track faculty position at any professorial level with specialization in marine biology, beginning September 2009. Highly motivated individuals with commitment to undergraduate and graduate education will be expected to teach introductory and upper level courses in the undergraduate biology program, including, but not limited to, marine ecology (focusing on the Red Sea), marine biology, and environmental biology.
The successful candidate is expected to advise undergraduate and graduate students in their research thesis and develop an internationally recognized research program to address fundamental questions in the field of marine and/or environmental biology. The Department of Biology is committed to collaborative, interdisciplinary education and research. Toward this end, the department has recently established an advanced molecular biology laboratory, marine biology station at El Gouna, Red Sea, and a cutting-edge genomics facility, including high-throughput DNA sequencer and high performance computational system. The successful applicant is encouraged to utilize and expand the current facilities. Applicants who may take advantage of the unique geographic location in proximity of the Red Sea are particularly encouraged.

Requirements: The candidate must hold a doctoral degree.

Additional Information: Deadline of applications is January 15, 2009. Review of applications will start immediately.
One-, two- or three-year appointment, subject to mutual agreement will begin September 2009. Renewal of an appointment depends upon institutional needs and/or the appointee's performance. When applying, include teaching philosophy and a short description of intended research with letter of interest.

http://aucegypt.interviewexchange.com

Science Careers is the catalyst for your ambition.

Visit our ENHANCED WEBSITE!

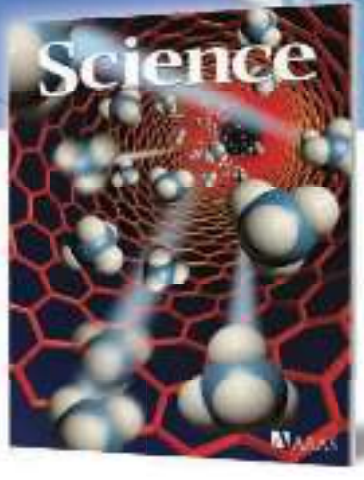

Promoting your ambition is what we do. We're your catalyst for connecting with the industry's top employers. We're the experts and source for accessing the latest and most relevant career information across the globe.

Our newly designed website offers a set of tools that help you discover career opportunities and your personal potential. Whether you're seeking a new job, career advancement in your chosen field, or ways to stay current on industry trends, *Science* Careers is your catalyst for an accelerated future.

Your Future Awaits.

Improved Website Features:

- Relevant Job E-mail Alerts
- Improved Resume Uploading
- Content Specific Multimedia Section
- Facebook Profile

Job Search Functionality:

- Save and Sort Jobs
- Track Your Activity
- Search by Geography
- Enhanced Job Sorting

Science Careers
From the Journal *Science* AAAS

ScienceCareers.org

Child Health Institute of New Jersey

DIRECTOR, CHILD HEALTH INSTITUTE OF NEW JERSEY

UMDNJ-Robert Wood Johnson Medical School (RWJMS) is currently recruiting a Director for the Child Health Institute of New Jersey (CHINJ). We seek a visionary leader who can successfully integrate basic and clinical research initiatives, thereby building a robust translational scientific program. The ideal candidate should be well-grounded in the field of child health, have demonstrated experience in building and integrating a strong clinical and scientific program, and possess strong leadership skills required to recruit and lead a diverse group of investigators (PhD, MD/PhD, and MD) whose academic and/or clinical careers are focused on child health, pediatric diseases and normal and abnormal development in human or model systems. Excellence forged via these scientific and clinical collaborations will allow the Child Health Institute to assume a statewide and national leadership position to address unmet pediatric needs. Located on a prominent and collaborative medical school campus in New Brunswick, NJ, CHINJ offers 54,000 square feet of laboratory, core facilities, and conference and office space, located directly adjacent to clinic space housing an expanding pediatric practice.

The CHINJ offers a unique opportunity to foster scientific and clinical collaboration and will empower UMDNJ-Robert Wood Johnson Medical School in its continued leadership role in the clinical programs at New Brunswick hospitals. The new Institute will add focus and coherence to the UMDNJ-RWJMS Centers of Excellence, all of which pursue development-related studies, without having explicit missions in this area. Current centers of excellence include the core Transgenic and Gene Targeting Facility, the Cancer Institute of New Jersey (CINJ), the Center for Advanced Biotechnology and Medicine (CABM), the Environmental and Occupational Health Sciences Institute (EOHSI), the planned Cardiovascular Institute, as well as the Institute for the Study of Child Development in the Department of Pediatrics.

The Director will have an opportunity to recruit other Institute members critical for the development of programs that are broad-based across RWJMS and the local scientific community and be expected to promote collaborators within the School and the scientific communities at Rutgers and Princeton Universities and numerous pharmaceutical and biotechnology companies.

The Director will report directly to the Dean and will hold a position similar to a department chair. The new Institute is adjacent to the Bristol-Myers Squibb Children's Hospital at Robert Wood Johnson University Hospital, the medical school's principal teaching hospital, and with the PSE&G Children's Specialized Hospital create an international center of excellence in newborn and pediatric care and child health research.

Review of applications will begin immediately and will continue until the ideal candidate is chosen. Please send nominations and/or application, including a brief statement of the attributes and qualities of the individual, visions and strategic goals for building the Institute and curriculum vitae to: **Molly Gabel, MD, Chair of Search Committee, c/o Bonnie Baloga-Altieri, PhD, RN, Director, Administration, Office of the Dean, UMDNJ-Robert Wood Johnson Medical School, 125 Paterson Street, Suite 1400, New Brunswick, New Jersey 08903, Email: balogabl@umdnj.edu.** UMDNJ is an Affirmative Action/Equal Opportunity Employer. For more information, visit **www.umdnj.edu/hrweb**

UMDNJ
ROBERT WOOD JOHNSON MEDICAL SCHOOL
University of Medicine & Dentistry of New Jersey

MAX PLANCK INSTITUTE FOR CHEMICAL ECOLOGY

Outstanding Early-Career Scientist

The Max Planck Society announces an INDEPENDENT JUNIOR RESEARCH GROUP to be hosted at THE MAX PLANCK INSTITUTE FOR CHEMICAL ECOLOGY.

We seek an outstanding early-career scientist to lead an independent junior research group working in the area of chemically-mediated interactions among organisms. Candidates should have a record of internationally recognized research accomplishments. While there is no restriction on the precise area of research, it should complement and interact synergistically with the other groups and departments at the Institute. Current research focuses on the ecology, evolution, chemistry and biochemistry of interactions among plants, insects and microbes, as well as biodiversity-related topics.

The Institute offers a stimulating and interdisciplinary research environment with strong links to the Friedrich Schiller University, Jena, and the Leibniz Institute for Natural Product Research and Infection Biology. Ph.D. studies are coordinated by an International Max Planck Research School. The Institute provides state-of-the-art equipment, greenhouses and insect rearing facilities including laboratories for experimental work with transgenic plants and insects.

Funding for the group leader position (equivalent to an assistant professor) and associated support is guaranteed for five years with the possibility of extension for up to four additional years. The group will be provided with modern laboratory space, funds for positions for a post-doc, Ph.D. student and technical assistant, and an adequate budget for running costs.

To apply please register and upload (1) a CV including a list of publications, (2) one page summary of your scientific achievements and a two pages statement of your future research plans, and (3) up to three of your most important papers at:

http://www.ice.mpg.de

Also please arrange to have two letters of recommendation uploaded directly by your referees at the above webpage. The deadline for receiving applications is **December 31, 2008.** Please note that a symposium (scientific presentation of short listed candidates plus interviews) is planned in conjunction with the recruitment of a similar position at the MPI for Evolutionary Biology in Plön on **January 29/30, 2009.** Location: Max Planck Institute for Chemical Ecology, Jena, Germany.

The Max Planck Society is an equal opportunity employer, and is very interested in raising the proportion of women in areas where they are underrepresented. Thus applications from female scientists are especially encouraged.

Further information can be obtained from:

Prof. Jonathan Gershenzon, Managing Director
E-Mail: gershenzon@ice.mpg.de

Max Planck Institute for Chemical Ecology
Hans-Knöll-Straße 8
D-07745 Jena
Germany

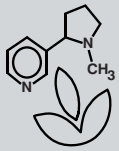

UNIVERSITY *of* CALIFORNIA, SAN DIEGO

SKAGGS SCHOOL *of* PHARMACY
and PHARMACEUTICAL SCIENCES

Faculty Positions in Pharmaceutical Sciences

The University of California, San Diego, Skaggs School of Pharmacy and Pharmaceutical Sciences (SSPPS) (Web: **http://pharmacy.ucsd.edu**) is initiating a new growth phase with the anticipated hiring of 6-8 basic scientists over the next 3-4 years. Only five years after the first Pharm. D. class was admitted, the SSPPS faculty already ranks in the top tier among pharmacy schools in NIH-supported research. In the coming year we are seeking exceptional faculty members for multiple tenure-track or tenured positions at the Assistant, Associate, or Full Professor levels in the area of pharmacology, pharmaceutical chemistry, and pharmaceutics. These individuals will play a lead role in enhancing our drug discovery efforts by complementing the existing strengths in natural products, neuro- and immunopharmacology, cancer chemotherapy, microbiology and virology, physiology and development, drug metabolism and disposition, proteomics and mass spectrometry, and NMR. Areas of particular interest include medicinal/synthetic chemistry, computer-aided and structure-based drug design, animal models of disease, molecular toxicology, cell biology, and structural biology. UCSD has a superb environment for collaborations, and strong linkages exist between the SSPPS and the Scripps Institution of Oceanography, Department of Chemistry and Biochemistry, Department of Pharmacology, Department of Cellular and Molecular Medicine, and Moores Comprehensive Cancer Center, and the various clinical departments in the School of Medicine. Opportunities abound for interaction with The Scripps Research Institute, Salk Institute, Burnham Institute, and La Jolla Institute of Allergy and Immunology as well as nearly 400 local pharmaceutical and biotechnology groups. Outstanding laboratory space is available in the new Pharmaceutical Sciences Building, located within the Health Sciences Center at UCSD. In addition to vigorous pursuit of innovative research programs, successful candidates will team teach in courses for Ph.D., Pharm.D., and M.D. students.

Candidates are expected to have a strong track record of scientific and academic achievements demonstrated by publication record and grant funding appropriate to rank, combined with documented skills in teaching. Letters of recommendation should provide evaluation of the candidate's high academic caliber for this faculty position. Salary and appointment level will be commensurate with qualifications and experience and based on published UC pay scales for the Health Sciences.

To apply, send a detailed resume/curriculum vitae, a statement of research plans, and names and addresses of at least three references to the **Chair, Search Committee for Pharmaceutical Sciences, c/o Cynthia Barlow, Human Resource Manager, Skaggs School of Pharmacy and Pharmaceutical Sciences MC 0657, University of California, San Diego, 9500 Gilman Drive, La Jolla, CA 92093-0657**. E-mail: **ssppsapo@ucsd.edu**. Please reference advertisement **#SSPPS1108SCI**.

Review of applications will begin **January 1, 2009** and will continue until the respective positions are filled.

UCSD is an Affirmative Action/Equal Opportunity Employer committed to excellence through diversity.

Max Planck Institute for Demographic Research

Directors: Prof. James W. Vaupel – Prof. Joshua R. Goldstein

www.demogr.mpg.de

The Max Planck Institute for Demographic Research is seeking to expand further its quantitative, interdisciplinary activities in the field of

Evolutionary Biodemography / Comparative Life History Analysis

by making appointments at the

PhD, Post-Doc, and Research Scientist levels.

The research program focuses on understanding how evolution can shape age-specific mortality in tandem with age-specific fertility and other aspects of the life-history. We aim to tackle these issues by synthesizing quantitative insights from diverse disciplines including demography, life history biology, ecology, mathematics, statistics and actuarial science. As well as considering flexible, open appointments for strong candidates with appropriate backgrounds and relevant interests, the institute will make specific appointments of comparative life history biologists, phylogenetic and demographic analysts, database developers, mathematical theoreticians, programmers and statisticians to develop the

AgeLife Project,

a collaborative international network to advance understanding of lifespan and age-specific demography by comparing a wide range of organisms across the tree of life. Successful candidates will complement an existing interdisciplinary research team of more than 20 scientists and support staff within the institute. Those in the AgeLife project will have links with other partners in the network, but will principally be based in Rostock. Information about the institute, our work in Evolutionary Biodemography, and the AgeLife project can be found at www.demogr.mpg.de/agelife.

Applications should be addressed to Executive Director Prof. James W. Vaupel and should include a CV with a statement of academic interests and relevant experience, details of all qualifications including grades, a list of any publications, and the contact details of 3 referees. All material should be e-mailed to: appl-agelife@demogr.mpg.de. Review of applications will begin on 15th February 2009. We will consider applications received before the end of March. PhD positions will typically start in early September 2009, and other positions will start as soon as possible after appointment. PhD and postdoc appointments are made on doctoral and postdoctoral stipends respectively, and Research Scientist positions are on TVöD 13.

The Max Planck Society wishes to increase the share of women in areas where they are underrepresented, and strongly encourages women to apply.

The Max Planck Society is committed to employing more handicapped individuals and especially encourages them to apply.

MAX-PLANCK-GESELLSCHAFT

UNIVERSITY OF SASKATCHEWAN

Assistant Professor in Biochemistry

The Department of Biochemistry invites applications for a tenure-track position at the level of Assistant Professor. Candidates must have a Ph.D. with at least 2 years of post-doctoral experience. The successful applicant is expected to establish a strong, independent and externally funded research program in biochemistry, preferably in a research area related to metabolism, gene expression, lipid and carbohydrate biochemistry or the biochemical basis of diseases. An interest and/or experience in bioinformatics would be an asset. In addition, participation in teaching of both the undergraduate medical and biochemistry curricula will be required. The successful applicant will have a broad range of collaborative possibilities on campus with scientists in other departments and colleges, including the Canadian Light Source (**www.cls.usask.ca**) and the Saskatchewan Structural Sciences Centre (**www.usask.ca/sssc**).

Please submit both electronic and signed hard copies of the application, including curriculum vitae; a detailed statement on research interests and of previous teaching experience in a single PDF document to: **Dr. R.L. Khandelwal, Head, Department of Biochemistry, College of Medicine, University of Saskatchewan, 107 Wiggins Road, Saskatoon, SK S7N 5E5 Canada; Email: ramji.khandelwal@usask.ca; Phone: (306) 966-4368; Fax: (306) 966-4390**.

Applicants should also arrange for three confidential letters of reference to be sent separately to the same address. The closing date for receipt of applications is **February 1, 2009**. The effective date for appointment is between April 1, 2009 and July 1, 2009.

All qualified candidates are encouraged to apply. However, Canadian citizens and permanent residents will be given priority. The University of Saskatchewan is committed to Employment Equity. Members of Designated Groups (women, aboriginal people, people with disabilities and visible minorities) are encouraged to self-identify on their applications.

AMERICAN SOCIETY FOR MICROBIOLOGY

POSTDOCTORAL POSITIONS AVAILABLE

AMERICAN SOCIETY FOR MICROBIOLOGY AND COORDINATING CENTER FOR INFECTIOUS DISEASES

2009 POSTDOCTORAL RESEARCH PROGRAM

Up to ten positions will be awarded for full-time research on infectious diseases which cause significant public health problems. Fellows will perform research in residence at one of the laboratories of the the Centers for Disease Control and Prevention (CDC). CDC operates laboratories in Atlanta, GA, Ft. Collins, CO, Anchorage, AK, and San Juan, Puerto Rico.

Eligible fields of study include:

- **Bacterial and Mycotic Diseases**
- **Viral and Rickettsial Infections**
- **Nosocomial Infections**
- **HIV/AIDS**
- **Vector-borne Infectious Diseases**
- **Sexually Transmitted Diseases**
- **Parasitic Diseases**

Positions are limited to individuals who either earned their doctorate degree (Ph.D., Sc.D., M.D., D.V.M., or D.D.S.) or have completed a primary residency within three years of their proposed start date. The program provides an annual stipend for two years, up to $500 relocation expenses, up to $3,000 health care benefits package and up to $2,000 for professional development. The fellowship is for 2 years.

The application deadline is **January 15, 2009**. For more information, visit: **http://www.asm.org/Education/index.asp?bid=15497**. The brochure and application are available on line.

ASM
American Society for Microbiology

CDC/NCID
Centers for Disease Control and Prevention/National Center for Infectious Diseases

The UC Davis Genome Center integrates experimental and computational approaches to address key problems at the forefront of genomics. The Center is housed in a new research building with state-of-the-art computational and laboratory facilities and currently comprises 14 experimental and computational faculty. These faculty are developing an internationally recognized program in genomics and computational biology at Davis, building on and enhancing the unique strengths and unmatched breadth of the life sciences on the UC Davis campus.

The Genome Center invites applications for tenure-track faculty positions in all areas of genomics with emphasis on next-generation proteomics and statistical genomics involving animal, plant or microbial systems. Applicants interested in genomic approaches to human diseases and investigators employing large-scale, technology-driven approaches that complement existing strengths at UC Davis are particularly encouraged to apply. Candidates should be strongly motivated by the biological importance of their research and should value the opportunity to work in close collaboration with other groups and disciplines.

Candidates may be at any academic level. At the senior level, we invite applications from prominent scientists with distinguished records of research, teaching, and leadership in genomics. At the junior level, we invite applications from candidates whose accomplishments in innovative research and commitments to teaching demonstrate their potential to develop into the future leaders in these fields.

These positions require a Ph.D. or equivalent. Appointments will be at the Assistant, Associate or Full Professor level in an appropriate academic department in any of six schools, or colleges. The position will remain open until filled. For fullest consideration, applicants should submit a letter of application, a curriculum vitae, statements of research and teaching interests, and the names of at least five references to the Genome Center Web site **www.genomecenter.ucdavis.edu** by **January 15, 2009**.

The University of California is an Affirmative Action/Equal Opportunity Employer.

9 Senior Research Positions at Swedish Universities

The Swedish Research Council announces nine Senior Research Positions within natural and engineering sciences. The positions are intended for scientists who have obtained a Ph.D., where the date of exam, with a few exceptions, is not older than ten years prior to the end of the application period. The primary obligation of Senior Research Position appointees is to conduct research. The positions are financed for a maximum of six years.

There is one position each within the following areas:

- Advanced scattering techniques
- Ecological genetics
- Enzymology
- Experimental soft matter physics
- Multiscale modelling in fluid mechanics or material mechanics
- Integrated geophysics of the lithospheric mantle
- Inorganic synthesis
- Parallel computation methods and architectures
- Theoretical modelling of molecular catalytic processes

The proposal must be approved by a Swedish host university or other Swedish host higher education institution.

Apply at www.vr.se no later than February 11, 2009
Application form and instructions can be found at www.vr.se/english

Vetenskapsrådet

RUSH UNIVERSITY MEDICAL CENTER

CHAIRPERSON
DEPARTMENT OF BIOCHEMISTRY

Rush Medical College of Rush University Medical Center is seeking a Chairperson for the Department of Biochemistry. The Department currently has fourteen full time faculty members whose main research focuses on connective tissue biochemistry and pathophysiology. The Department is a member of the Rush Arthritis and Orthopedics Institute that brings together world renowned physicians and scientists whose focus is on the musculoskeletal system providing clinical care, education and research. The Institute combines the strengths of the Departments of Orthopedic Surgery, Anatomical Sciences and Cell Biology, Biochemistry and the Section of Rheumatology in the Department of Internal Medicine.

The Department of Biochemistry has strong research support with 4 endowed chairs and an NIH training grant that has supported twelve postdoctoral fellows over the past twelve years. The Department also has a strong graduate program, responsibility for teaching medical students and participates in academic administration and community service.

Candidates should be nationally recognized research scientists in one or more of the connective tissue disciplines: pathobiochemistry, genetics or regenerative medicine. They should have a scholarly research track record, as well as a translational research interest, history of external funding and qualify for appointment at a senior academic rank. Nominations or letters of interest that include a curriculum vitae should be sent to:

Julie Karstrand, Director of Physician Services
Rush University Medical Center
Armour Academic Facility, Suite 202
600 South Paulina Street
Chicago, IL 60612
or preferably via email to
Julie_Karstrand@Rush.edu

CV's should be submitted no later **March 31, 2009**.

RUSH IS AN EQUAL OPPORTUNITY/AFFIRMATIVE ACTION EMPLOYER.

POSTDOCTORAL POSITIONS

Xenopus Development,
Transgenic Mouse Generation, Genetics

The Hormel Institute, University of Minnesota,
Austin, MN 55912

Postdoctoral positions are available beginning January 1, 2009 at The Hormel Institute, a research branch of the University of Minnesota, located in Austin, MN. Successful candidates have the opportunity to work in a variety of research positions in the Cellular and Molecular Biology Group (**Dr. Zigang Dong** and **Dr. Ann M. Bode**) or Stem Cells and Cancer Group (**Dr. Rebecca Morris**) at The Hormel Institute.

Postdoctoral positions are available to study the role of histone, MAPKs and other kinase affecting Xenopus development process. Applicants should have experience with injection into frog embryos and some manipulation of embryonic tissue. Postdoctoral positions are also available for transgenic mouse generation and applicants should have experience in mouse embryonic stem cell culture.

Postdoctoral position is available requiring experience in genetics, linkage analysis, SNP chips, and human and mouse genome databases, and additional training in molecular biology, mouse models, and gene characterization. Postdoctoral position is also available requiring training in molecular biology, cloning, mouse model development, advanced microscopy methods such as FISH, immunohistochemistry, and histology.

A Ph.D. in genetics, molecular biology, cellular development, biochemistry, pharmacy, biology or related fields is required.

Please apply on-line at the University of Minnesota employment home page **www.umn.edu/ohr/employment**. For **Xenopus and Transgenic Mouse positions**, please reference Requisition Number **#158283** and for the **Genetics positions**, please reference Requisition Number **#158962** or **#158963**. For any position, please e-mail your curriculum vitae to: **ambode@hi.umn.edu**.

The University of Minnesota is committed to the policy that all persons shall have equal access to its programs, facilities, and employment without regard to race, color, creed, religion, national origin, sex, age, marital status, disability, public assistance status, veteran status, or sexual orientation.

Max Planck Institute for Metals Research

Stuttgart / Germany

MAX-PLANCK-GESELLSCHAFT

PhD / Post-Doc position

Interface-solvent interactions in colloidal dispersions: molecular structure and (femtosecond) dynamics

The project: Nanoscopic colloidal systems are a key component in many areas of science and technology. The physical and chemical properties of such systems are mainly determined by their interfacial properties. Although a clear picture sometimes exists of processes occurring on the macro- and microscopic length and time scale, the underlying molecular picture is not understood. The reason for this gap in knowledge is that the surrounding medium forms an impenetrable barrier to most molecular probes.
Recent developments in the area of nonlinear optics have led to novel nonlinear light scattering methods with which understanding on the molecular scale can be obtained. In this project the question of how interfaces influence the chemical and physical properties of nanoscopic particles in solution will be tackled by applying femtosecond (time-resolved) second-order nonlinear optical methods in combination with other techniques, such as IR spectroscopy and dynamic light scattering.

About the group: The work will be carried out in the Independent Research Group "Spectroscopy of Biointerfaces" at the Max-Planck Institute for Metals Research, Stuttgart, Germany. Available equipment includes a high power femtosecond infrared laser system with tunable infrared laser pulses (800 nm – 20 microns), an IR spectrometer, light scattering equipment and preparation laboratories. The institute has excellent technical staff and workshops. Some of our projects can be found on our website: http://www.mf.mpg.de/en/abteilungen/roke/ index.html

The candidate: The successful candidate will have a MSc or PhD degree in physics or chemistry, ideally with experience in nonlinear (time-resolved) spectroscopic techniques and experience with working with femtosecond laser systems.

Terms of employment: The position is for 2 years (Post-Doc/TVöD EG 13) or 3 years (PhD/TVöD EG 13/2) as of now.

The Max Planck Society is committed to employ more handicapped individuals and espacially encourages them to apply. The Max Planck Society seeks to increase the number of women in these areas where they are underrepresented and therfore explicitly women to apply.

Application
Please send a CV (including a publication list and the names of 2 potential references) with a cover letter to:

Max-Planck-Institute Stuttgart
Gemeinsame Verwaltung
Heisenbergstraße 1
70569 Stuttgart
ballmann@vw.mpi-stuttgart.mpg.de
For further information please contact Dr. S. Roke,
fon: 0049-711-689-3679/-3660, email: roke@mf.mpg.de

top employers post jobs on *Science* Careers.

We've got **Careers** down to a **Science**.

With thousands of job postings from 9 out of 10 top employers, *Science* Careers connects you to exceptional career opportunities across the globe. We know the industry and have the resources to prove it. Whether your path is R&D, tenure track, bioprocessing, or lab management, *Science* Careers is dedicated to matching qualified scientists with the industry's top employers. Drop by **www.ScienceCareers.org** and begin searching jobs today.

Science Careers

From the journal *Science* AAAS

www.ScienceCareers.org

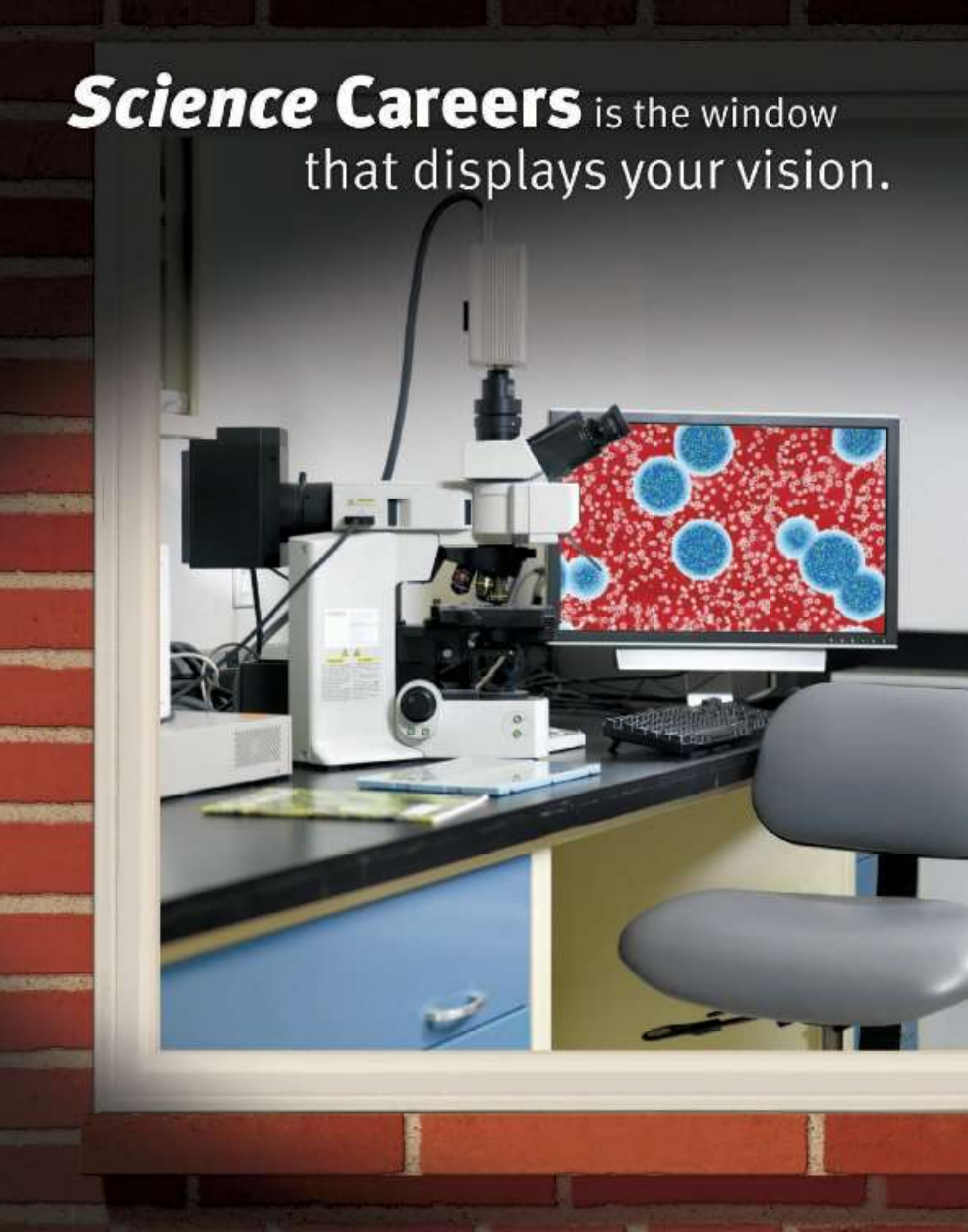
Science Careers is the window
that displays your vision.

Visit our ENHANCED WEBSITE!

Revealing your vision to employers is our job. We're your source for connecting with top employers in industry, academia, and government. We're the experts and entry point to the latest and most relevant career information across the globe.

Our newly designed website offers a set of tools that reveal career opportunities and your personal potential. Whether you're seeking a new job, career advancement in your chosen field, or ways to stay current on industry trends, *Science* Careers is your window to a limitless future.

Improved Website Features:

- Relevant Job E-mail Alerts
- Improved Resume Uploading
- Content Specific Multimedia Section
- Facebook Profile

Job Search Functionality:

- Save and Sort Jobs
- Track Your Activity
- Search by Geography
- Enhanced Job Sorting

Your Future Awaits.

Science Careers

From the journal *Science* AAAS

ScienceCareers.org

POSITIONS OPEN

The University of Utah
Moran Eye Center

The University of Utah's Department of Ophthalmology seeks **TENURE-TRACK FACULTY** (Ph.D., M.D., M.D./Ph.D.) with research interests in the genetics of human ocular disease, especially retinal disease.

All research will be based in the new John Moran Eye Center. The University of Utah offers a rich academic environment with strong professional training programs in medicine, neuroscience, molecular biology, bioengineering, and computer sciences. Successful candidates will be expected to be active in professional education and demonstrate strong extramural funding history.

Applicants should send their curriculum vitae, a statement of research interests, and names and contact information for three references to **e-mail: julee.lamothe@hsc.utah.edu.** Applications will be accepted until a suitable candidate is identified.

The University of Utah is an Equal Opportunity Affirmative Action Employer and encourages applications from women and minorities and provides reasonable accommodations to the known disabilities of applicants and employees.

Two **POSTDOCTORAL POSITIONS** are available January 2, 2009, in the newly established laboratory of **Dr. Arie Horowitz** at the Department of Molecular Cardiology of the Cleveland Clinic Lerner Research Institute and the Department of Molecular Medicine in the Cleveland Clinic Lerner College of Medicine of Case Western Reserve University. The Horowitz laboratory focuses on molecular mechanisms of blood vessel sprouting and guidance, using state-of-the-art cell and molecular biology approaches (see *Circ. Res.* **103:**e71-e79, published online, and **103:**710-16, 2008). Applicants are required to have a background in vascular biology and to be skilled in modern cell and molecular biology techniques. Applicants are expected to demonstrate familiarity with Dr. Horowitz's recent publications and to explain their interest in joining his laboratory. Successful candidates will receive a competitive salary and excellent benefits.

Preference will be given to candidates who (1) received their Doctorates in the last three years; (2) are independent; (3) are driven towards the establishment of scientific maturity and an academic career; (4) enjoy collaborative research; and (5) have strong communication skills in spoken and written English.

Please e-mail curriculum vitae and the names and contact information of at least three references to **e-mail: destefs@ccf.org.** Applications received before January 15, 2009, will receive full consideration.

TENURE-TRACK ASSISTANT PROFESSOR
Animal Physiology

The Department of Biology, University of Wisconsin-Stevens Point, offers a tenure-track, nine-month faculty position in animal physiology at the Assistant Professor level, beginning August 2009. Teaching obligations include animal physiology to biology and natural resource majors; a senior seminar; and an upper-level course in specialty. Research involving undergraduates, and Department service and student advising are part of this position. A Ph.D. in animal physiology or equivalent, and teaching and research experience are required. Experience is exemplified by publications, grants, evidence of teaching excellence, and/or postdoctoral work.

The Department encourages applicants from underrepresented groups, and those with experience teaching underrepresented students.

Include curriculum vitae, statements of teaching philosophy and research interests, three letters of recommendation, and undergraduate and graduate transcripts. Send application materials to**: Dr. C. Yahnke, Chair, Biology Department, University of Wisconsin-Stevens Point, Stevens Point, WI 54481.** Review begins 16 February 2009, and continues until filled. For more information, **telephone: 715-346-2455; fax: 715-346-3624; e-mail: cyahnke@uwsp.edu.**

Affirmative Action/Equal Opportunity Employer.

EKU

Three Tenure-Track 9-Month Appointments

EASTERN KENTUCKY UNIVERSITY

The Department of Biological Sciences at EKU is accepting applications for **three tenure-track, 9-month appointments**, to begin August 15, 2009. Each position requires a Ph.D. from a regionally accredited or internationally recognized institution and, for each, candidates must have a strong record of research accomplishments and must provide evidence of excellent teaching and communication skills. The typical teaching load for these positions is 12 hours per semester, with possibility of reassigned time with extramural funding. For more information on these positions, please review the full job descriptions and qualification requirements on EKU's online employment system. **All applicants must apply via this system at jobs.eku.edu. (Botanist position, please search requisition 0604563; Vertebrate Morphologist or Physiologist position, search 0604567; Aquatic Invertebrate Zoologist position, search 0604564).** Review of applications will begin on January 14, 2009 for each of these positions and will continue until the positions are filled.

Offers of employment are contingent upon completion of a satisfactory background check and educational credential verification. Eastern Kentucky University is an EEO/AA institution that values diversity in its faculty, staff, and student body. In keeping with this commitment, the University welcomes applications from diverse candidates and candidates who value diversity.

Kentucky UNBRIDLED SPIRIT

Academia Sinica
Taipei, Taiwan

Positions for Postdoctoral Fellows

Academia Sinica (AS) seeks outstanding applicants for postdoctoral fellow positions at its individual research institutes and centers. Postdoctoral Fellowship Program at AS offers unique research opportunities for individuals to engage in frontier research projects that will further advance their research careers.

With an annual budget of more than US $350 millions, AS has a substantial number of world-class researchers in addition to its state-of-the-art facilities. As the most eminent research institution in Taiwan, currently AS has about 600 postdoctoral fellows working in areas of mathematics and physical sciences, life sciences, and humanities and social sciences. We welcome international applicants with records of excellence. The deadline of application is March 1st, 2009. **Applicant must first find a corresponding researcher to sponsor his/her application. Please go to the Academia Sinica web site http://aao.sinica.edu.tw/pfjob-e.html to find out details about the application process and various research opportunities available.**

THE UNIVERSITY OF TEXAS SOUTHWESTERN MEDICAL CENTER

ASSISTANT PROFESSORS: The Department of Orthopaedic Surgery invites outstanding scientists with Ph.D., M.D., or equivalent degrees to apply for tenure-track assistant professor positions. Candidates who use innovative mechanical, molecular biological or computational methods with important applications to musculoskeletal related systems, ranging from individual genes and proteins to cells and organs are encouraged to apply. However, the scientific excellence of the candidates is more important than the specific area of research.

This position is part of the continuing growth of the Department at one of the country's leading academic medical centers and will be supported by significant laboratory space, competitive salaries, and exceptional startup packages. The University of Texas Southwestern Medical Center is the scientific home to four Nobel Prize laureates, 17 members of the National Academy of Sciences and 19 members of the Institute of Medicine. UT Southwestern conducts more than 3,500 research projects annually totaling more than $350 million.

Applicants should submit curriculum vitae, a brief statement of research plans, and arrange to have three letters of reference sent to: **Joseph Borrelli, Jr., MD c/o Kathy Stroud (kathy.stroud@utsouthwestern.edu), Department of Orthopaedic Surgery, 1801 Inwood Road, WA4.312, Dallas, TX 75390-8883**.

UT Southwestern strongly encourages applications from women, minorities, and people with physical challenges. An Equal Opportunity Employer

---

CTC
centro tecnológico da carne

CTC, a technological center within the food industry located in Galicia (Spain), with its research mainly focused on the technological transfer together with the advice and the professional training to the companies related to this sector, seeks to fill the position of

Food Authenticity Area Coordinator

Candidates are expected to have a PhD and further research on innovation within the food quality/safety field, have wide experience in the management of multicultural and multidisciplinary teams.

Salary range: 40,000-50,000€
Online applications accepted at the IMAN Program:
www.programaiman.eu
Application deadline: 15th February 2009.

iman

POSITIONS OPEN

GROUP LEADER, BIOINFORMATICS/ SYSTEMS BIOLOGY
University of Bergen, Norway

The Computational Biology Unit (CBU) at the University of Bergen is searching for an additional Group Leader in the field of computational biology/bioinformatics.

Please send your curriculum vitae, your ten most relevant publications, and a detailed statement of research interests to **Prof. Inge Jonassen (e-mail: inge.jonassen@bccs.uib.no), Head of CBU.** The evaluation of applications will commence on 4 January 2009, and will continue until a suitable candidate is found.

To read a full-text version of this ad please visit the following **website: http://melding.uib.no/doc/ledige_stillinger/1226666905.html.**

ASSISTANT PROFESSOR, BIOCHEMISTRY
Marshall University

The Department of Chemistry at Marshall University is seeking to fill a nine-month, tenure-track position at the Assistant Professor level. Qualified applicants will have a Ph.D. and preferably postdoctoral or equivalent experience in any area of experimental biochemistry. The new hire will teach biochemistry at the undergraduate and Master's level. The appointee is expected to have a strong commitment to excellence in teaching and research. For more information about our Department and University, please visit **website: http://www.marshall.edu/chemistry.**

All candidates must send current curriculum vitae, statements of research plans and teaching philosophy, copies of all transcripts, and have three letters of reference sent to: **Chemistry Search Committee, Department of Chemistry, Marshall University, Huntington, WV 25755.** Electronic/faxed applications cannot be accepted. The review of applicants will begin immediately and continue until the position is filled. *Marshall University is the recipient of an NSF ADVANCE grant and the U.S. Labor Department's EVE Award for its Affirmative Action Employment Opportunity Programs.*

ASSISTANT PROFESSOR of RESEARCH
Cardiovascular Physiology and Genomics

A faculty position at the Assistant Professor level (nontenure research track) is available to study molecular basis of cardiovascular diseases. Experience and publications in molecular cardiovascular medicine are required. Applicants must have Ph.D./M.D. and a minimum of two years of postdoctoral experience. Competitive salary, fringe benefits, and grant opportunities. Significant research experience with at least three of the following is preferred: vascular biology, gene therapy, signal transduction, molecular biology, genomics, stem cell biology, protein chemistry, or proteomics. Send detailed curriculum vitae and names of three references to: **Dr. Zhongjie Sun, Department of Physiology, University of Oklahoma Health Science Center, U.S.A. E-mail: zhongjie-sun@ouhsc.edu.**

Two **POSTDOCTORAL POSITIONS** are available within the Department of Molecular and Cellular Biochemistry. Qualified candidates will study mechanisms by which hSWI/SNF chromatin remodelers and protein arginine methyltransferases epigenetic modifiers affect short and long term silencing of chromatin, and how aberrations in expression of these chromatin modifiers impact growth of leukemia and lymphoma cells. Interested candidates should have a strong background in biochemistry, cellular, and molecular biology, and should send their curriculum vitae and three letters of recommendation to **e-mail: sif.1@osu.edu.**

POSITIONS OPEN

POSTDOCTORAL FELLOW
The Center for Cardiovascular Research
Department of Biochemistry and Molecular Biology
Saint Louis University School of Medicine

Saint Louis University, a Catholic, Jesuit institution dedicated to student learning, research, health care, and service, is seeking applicants for a Postdoctoral Fellow in the Edward A. Doisy Department of Biochemistry and Molecular Biology and Center for Cardiovascular Research, beginning in the winter of 2009. A Postdoctoral position is now available in the laboratory of **Dr. David Ford.** Successful candidates are expected to have a Ph.D. degree in life sciences with a special emphasis on cardiovascular physiology and/or biochemistry. Projects using in vivo and isolated heart models to research dynamic alterations in metabolomes and signaling pathways in metabolic and cardiovascular diseases are available in the laboratory. NIH standards will be used in setting the pay scale.

Interested candidates must submit a cover letter, application, and current curriculum vitae to **website: http://jobs.slu.edu** (position number 20080679).

Saint Louis University is an Affirmative Action, Equal Opportunity Employer, and encourages nominations and applications from women and minorities.

POSTDOCTORAL POSITIONS
DNA Chips and Infectious Diseases

Positions available as part of a Weill Cornell Medical College - National Institute of Allergy and Infectious Diseases-funded Collaborative Project Grant for development of comprehensive DNA chip, capillary array, assays to distinguish bacterial, protozoan, and viral food, and waterborne pathogens from common pathogens employing high throughput screening platforms using microbial signature profiles as well as identifying human susceptibility or resistance single nucleotide polymorphisms. Applicant should have a Ph.D or M.D. with substantial research experience, preferably in infectious diseases, molecular biology, genomics, bioinformatics, DNA arrays, liquid-handling robotics, and/or automation in DNA and PCR technology. Competitive salary commensurate with experience. Send curriculum vitae and names of three references to: **Dr. Linnie Golightly, Division of International Medicine and Infectious Diseases, Room A421, Weill Cornell Medical College, 1300 York Avenue, New York, NY 10065. Fax: 212-746-8675. E-mail: lgolight@med.cornell.edu.** Or: **Prof. Francis Barany, Program Director, Department of Microbiology, P.O. Box 62, Weill Cornell Medical College, 1300 York Avenue, New York, NY 10065. Fax: 212-746-7983. E-mail: barany@med.cornell.edu.**

Equal Opportunity Employer.

POSTDOCTORAL FELLOWSHIPS

The Geophysical Laboratory, Carnegie Institution of Washington, invites applications for Postdoctoral Fellowships. The Geophysical Laboratory emphasizes interdisciplinary experimental and theoretical research in fields spanning geoscience, microbiology, chemistry, and physics. The Laboratory supports world-class facilities in high-pressure research; organic, stable isotope and biogeochemistry; mineral physics and petrology; and astrobiology. Please see **website: http://www.gl.ciw.edu/employment/postdoctoral_positions** for information on the application process. Also, see **website: http://www.gl.ciw.edu/** for a listing of personnel, current research interests, major facilities, and application information.

Completed applications for Carnegie Fellowships should be submitted by January 26, 2009, to: **Russell J. Hemley, Director, Geophysical Laboratory, 5251 Broad Branch Road, NW, Washington, DC 20015-1305 U.S.A.**

The Geophysical Laboratory is an Equal Opportunity Employer.

POSITIONS OPEN

John Jay College of Criminal Justice, City University of New York, invites applicants for two **TENURE-TRACK POSITIONS** in its Department of Sciences.

For more information, go to **website: http://www.jjay.cuny.edu/jobs.**

A **POSTDOCTORAL POSITION** in corneal innate immunity and in diabetic wound healing is available at the Kresge Eye Institute, Wayne State University School of Medicine. Our laboratory uses a variety of approaches to study the underlying mechanisms and to develop unique therapies for microbial keratitis and for diabetic keratopathy. A commitment for two to three years is expected with salary commensurate with experience. Please e-mail curriculum vitae, statement of research interest, and three names of reference to **e-mail: fyu@med.wayne.edu.**

POSTDOCTORAL FELLOW POSITION, University of Alabama at Birmingham, to study proteomics in kidney disease (*J. Biol. Chem.* **281:**39681-92, 2006; *J. Clin. Invest.* **112:**209-221, 2003). Ph.D. in biochemistry and minimum of two years of experience in proteomics during or after Ph.D. are required. Experience in kidney disease is not necessary. E-mail curriculum vitae and summary of research experience to: **Sumant S. Chugh, M.D.,** at **e-mail: chugh@uab.edu.**

MARKETPLACE